



University
of Glasgow

Trenaman, Anna Louise (2012) *Trypanosoma brucei BRCA2 in the regulation of genome stability and DNA repair*. PhD thesis.

<http://theses.gla.ac.uk/3256/>

Copyright and moral rights for this thesis are retained by the author

A copy can be downloaded for personal non-commercial research or study, without prior permission or charge

This thesis cannot be reproduced or quoted extensively from without first obtaining permission in writing from the Author

The content must not be changed in any way or sold commercially in any format or medium without the formal permission of the Author

When referring to this work, full bibliographic details including the author, title, awarding institution and date of the thesis must be given

Trypanosoma brucei BRCA2 in the
regulation of genome stability and DNA
repair

Anna Louise Trenaman

BSc (Hons) MRes

Submitted in fulfilment of the requirements for the
Degree of Doctor of Philosophy

Wellcome Trust Centre for Molecular Parasitology
Institute of Infection, Immunity and Inflammation
College of Medical Veterinary and Life Sciences
University of Glasgow

March 2012

Abstract

Trypanosoma brucei is a protistan parasite of mammals that evades its host's immune responses by antigenic variation, which in *T. brucei* involves the periodic switching of the Variant Surface Glycoprotein (VSG) coat to antigenically distinct variants. The *T. brucei* genome contains a huge archive of silent VSG genes that are expressed from specialised expression sites, only one of which is actively transcribed at any one time. Copying of silent VSG genes into the active expression site has been shown to occur by homologous recombination, as mutation of the *RAD51* recombinase and a distantly related gene, *RAD51-3*, impairs this process. *BRCA2* is a protein that binds and regulates the function of Rad51 during homologous recombination. Mutation of *BRCA2* in bloodstream form *T. brucei* leads to increased sensitivity to DNA damaging agents, and impairments in homologous recombination, *RAD51* subnuclear foci formation and VSG switching, suggesting that it too acts in recombination-repair and antigenic variation. Beyond these phenotypes, an accumulation of putative gross chromosomal rearrangements in the megabase chromosomes of the *T. brucei* genome and a novel replication phenotype were also observed, and the basis of both these processes was unclear. *T. brucei* *BRCA2* is highly unusual relative to orthologues in other eukaryotes, as the protein contains an expansion in the number of *RAD51*-binding BRC repeat motifs, which are arranged in a tandem repeat array that has not been observed elsewhere.

In order to examine the function of *BRCA2* in the maintenance of genome stability in *T. brucei*, *brca2* homozygous mutants were generated in procyclic form TREU 927 and Lister 427 cells. Analysis of genomic stability by Southern blotting and pulsed field agarose gel electrophoresis revealed that *BRCA2*'s function in the maintenance of genome stability appears to be either bloodstream form-specific, or plays a more substantial role in this life cycle stage. To examine the function of the BRC repeat expansion, cell lines containing variants of *BRCA2* with reduced numbers of BRC repeats were generated, expressed in *brca2* homozygous mutants and phenotype analysis carried out. Growth and DNA repair were restored by the expression of virtually all variants, suggesting the BRC repeat expansion is not an adaptation for general genome maintenance, though the repair activity of a variant with a

single BRC repeat appeared to differ between bloodstream and procyclic form parasites. In contrast to this, a striking correlation between BRC repeat number and the regulation of RAD51 subnuclear dynamics was observed, showing that the BRC array expansion has important functional significance.

GST pull-down analysis was used to examine the domains of *T. brucei* BRCA2 that interact with RAD51, revealing an extent of interaction not apparent in BRCA2 orthologues in other organisms. This complexity of interaction was further analysed by immunolocalisation of BRCA2 and RAD51, before and after DNA damage, which showed potentially dynamic co-localisation of the two repair factors. Finally, a putative interaction between *T. brucei* BRCA2 and CDC45 was tested both *in vitro* and *in vivo*, but could not be validated, suggesting it does not provide an explanation for the replication defects observed in bloodstream form *brca2*^{-/-} mutant cells. All of the analyses above shed light on the function of the BRCA2 protein in the regulation of homologous recombination in *T. brucei*.

Table of contents

Abstract	2
Table of contents	4
List of figures	9
List of tables	14
Acknowledgements	15
Author's declaration	16
List of abbreviations	17
Chapter 1: Introduction	21
1.1 General Introduction to <i>Trypanosoma brucei</i>	22
1.1.1 Phylogeny of <i>Trypanosoma</i>	22
1.1.2 Disease, symptoms and treatment	23
1.1.3 The life cycle of <i>T. brucei</i>	25
1.1.4 The genome of <i>T. brucei</i>	27
1.1.5 Transcription and translation in <i>T. brucei</i>	29
1.2 Antigenic variation	30
1.2.1 Antigenic variation in <i>T. brucei</i>	31
1.2.2 The Variant Surface Glycoprotein.....	32
1.2.3 VSG expression sites	34
1.2.4 VSG switching mechanisms	35
1.2.4.1 Transcriptional switching	36
1.2.4.2 Recombinational switching.....	37
1.3 DNA repair.....	40
1.3.1 Double strand break repair	41
1.3.2 Non-homologous end joining.....	42
1.3.2.1 Micro-homology mediated end joining.....	44
1.3.3 Homologous recombination.....	44
1.3.4 Mechanism of homologous recombination	45
1.3.4.1 Single-strand annealing.....	47
1.3.4.2 Break-induced replication.....	48
1.3.4.3 Gene conversion	48
1.3.4.4 Synthesis-dependent strand annealing	49
1.3.5 The role of homologous recombination in replication	50
1.4 BRCA2.....	51
1.4.1 The discovery of BRCA2	51
1.4.2 The structure of BRCA2	52
1.4.2.1 The BRC repeats.....	52
1.4.2.2 Rad51 binding at the BRCA2 C-terminus.....	55
1.4.2.3 Rad51 binding in the context of full-length BRCA2.....	56
1.4.2.4 The BRCA2 DNA binding domain	57
1.4.2.5 The BRCA2 nuclear localisation signals.....	59
1.4.3 The function of BRCA2 in homologous recombination	59
1.4.4 BRCA2 interacting proteins	61
1.4.5 Functions of BRCA2 in the Fanconi Anaemia pathway	63
1.5 DNA repair in other organisms	64
1.5.1 Homologous recombination in <i>Caenorhabditis elegans</i>	64
1.5.2 Homologous recombination in <i>Ustilago maydis</i>	65
1.5.3 DNA repair in <i>T. brucei</i>	66
1.5.3.1 <i>T. brucei</i> BRCA2	68
1.6 Rad51	72

1.7	Aims of this thesis.....	74
Chapter 2: Methods and materials	75	
2.1	Trypanosome culture	76
2.1.1	Trypanosome strains	76
2.1.2	Trypanosome growth.....	76
2.1.2.1	Stabilate preparation and retrieval.....	77
2.1.3	Stable, clonal transformation of trypanosomes.....	77
2.1.4	Re-cloning of polyclonal trypanosome populations.....	78
2.2	Isolation of material from trypanosomes	79
2.2.1	Isolation of genomic DNA	79
2.2.2	Genomic plug preparation	80
2.2.3	Isolation of RNA.....	80
2.2.4	Protein extraction.....	80
2.2.4.1	For SDS-PAGE separation.....	80
2.2.4.2	For co-immunoprecipitation.....	81
2.2.5	Aqueous fractionation	81
2.3	Phenotype analysis.....	82
2.3.1	<i>In vitro</i> growth and doubling time.....	82
2.3.2	DNA damage sensitivity	82
2.3.2.1	Hydroxyurea damage	83
2.3.2.2	Phleomycin damage.....	83
2.3.2.3	Methyl methanesulphonate damage	84
2.3.3	Fluorescent Activated Cell Sorting Analysis	84
2.4	Microscopy	84
2.4.1	Cell cycle analysis	84
2.4.2	Immunolocalisation.....	85
2.5	Molecular biology techniques	86
2.5.1	Primer design	86
2.5.2	Polymerase Chain Reaction	87
2.5.2.1	PCR purification	88
2.5.3	Site-directed mutagenesis	88
2.5.4	Reverse Transcription Polymerase Chain Reaction	88
2.5.5	Quantitative Real-Time Polymerase Chain Reaction.....	89
2.5.6	Restriction digest.....	89
2.5.7	Phosphatase treatment	90
2.5.8	DNA fragment purification	90
2.5.9	DNA fragment blunting	90
2.6	Cloning	90
2.6.1	T4 DNA ligase	90
2.7	Transformation of <i>E. coli</i>	91
2.7.1	<i>E. coli</i> colony screening.....	91
2.7.2	DNA extraction from <i>E. coli</i>	92
2.7.3	Ethanol precipitation of DNA	92
2.8	Electrophoresis.....	92
2.8.1	DNA electrophoresis.....	92
2.8.2	Pulsed field agarose gel electrophoresis.....	92
2.8.2.1	Ethidium bromide staining of pulsed field agarose gels.....	93
2.8.3	Protein electrophoresis.....	93
2.9	Blotting.....	94
2.9.1	Southern blotting	94
2.9.2	Western blotting.....	94
2.10	Radiolabelling and hybridisation of DNA probes.....	95

2.10.1	Probe manufacture by random primer labelling of DNA	95
2.10.2	Hybridisation and detection of radiolabelled DNA probes.....	95
2.11	Western blot detection	96
2.11.1	Hybridisation and detection of antibodies	96
2.11.2	Anti-BRCA2 Antiserum	97
2.12	<i>In vivo</i> co-immunoprecipitation	97
2.13	<i>In vitro</i> Glutathione S-Transferase pull-down.....	98
2.14	Bioinformatics	99

Chapter 3: The function of *T. brucei* BRCA2 in the maintenance of genome

stability.	100
3.1	Introduction.....	101
3.2	Generation of <i>BRCA2</i> gene disruption mutants in PCF TREU 927 <i>T. brucei</i>	102
3.2.1	<i>BRCA2</i> gene deletion constructs.....	102
3.2.2	Generation of <i>BRCA2</i> mutants in PCF TREU 927 <i>T. brucei</i>	103
3.2.3	Confirmation of <i>BRCA2</i> mutants by PCR	104
3.2.4	Confirmation of <i>BRCA2</i> mutants by Southern analysis	105
3.2.5	Confirmation of <i>BRCA2</i> mutants by western analysis	107
3.3	Phenotypic analysis of PCF TREU 927 <i>BRCA2</i> mutants.....	108
3.3.1	Analysis of <i>in vitro</i> growth	108
3.3.2	Analysis of DNA damage sensitivity	109
3.3.3	Analysis of the cell cycle.....	114
3.3.4	Analysis of RAD51 focus formation	117
3.3.5	Analysis of genomic stability in PCF TREU 927 <i>BRCA2</i> mutants .	121
3.4	Analysis of the timescale of genomic rearrangements in BSF Lister 427 <i>BRCA2</i> mutants.....	131
3.5	Generation of <i>BRCA2</i> gene disruption mutants in PCF Lister 427 <i>T. brucei</i>	133
3.5.1	Generation of <i>BRCA2</i> mutants in PCF Lister 427 <i>T. brucei</i>	134
3.5.2	Confirmation of <i>BRCA2</i> mutants by PCR	134
3.5.3	Confirmation of <i>BRCA2</i> mutants by Southern analysis	135
3.5.4	Attempt at confirmation of <i>BRCA2</i> mutants by western analysis ...	136
3.6	Phenotypic analysis of PCF Lister 427 <i>BRCA2</i> mutants.....	137
3.6.1	Analysis of <i>in vitro</i> growth	137
3.6.2	Analysis of DNA damage sensitivity	138
3.6.3	Confirmation of the DNA damage sensitivity of PCF Lister 427 <i>BRCA2</i> mutants	141
3.6.4	Analysis of genomic stability in PCF Lister 427 <i>BRCA2</i> mutants...	142
3.7	Summary	147

Chapter 4: The function of the BRCA2 BRC repeat expansion in *T. brucei*.151

4.1	Introduction.....	152
4.2	Complementation of PCF TREU 927 <i>brca2</i> ^{-/-} mutant with variants of <i>BRCA2</i> with reduced numbers of BRC repeats.....	153
4.2.1	Generation of constructs containing variants of <i>BRCA2</i> with reduced numbers of BRC repeats	153
4.2.2	Generation of re-expresser cell lines in PCF TREU 927	156
4.2.3	Confirmation of re-expresser cell lines by PCR	157
4.2.4	Confirmation of re-expresser cell lines by Southern analysis	158
4.2.5	Attempt at confirmation of re-expresser cell lines by western analysis	159

4.2.6	Analysis of <i>BRCA2</i> mRNA levels in re-expresser cell lines by quantitative RT-PCR	160
4.3	Phenotypic analysis of PCF TREU 927 <i>BRCA2</i> re-expresser cell lines	163
4.3.1	Analysis of <i>in vitro</i> growth	163
4.3.2	Analysis of DNA damage sensitivity	164
4.3.3	Analysis of RAD51 focus formation	168
4.3.4	Analysis of the sub-cellular distribution of RAD51 by aqueous fractionation	172
4.4	Complementation of PCF Lister 427 <i>brca2</i> ^{-/-} mutants with variants of <i>BRCA2</i> with reduced numbers of BRC repeats	175
4.4.1	Generation of re-expresser cell lines in PCF Lister 427	175
4.4.2	Analysis of <i>BRCA2</i> mRNA levels in re-expresser cell lines by quantitative RT-PCR	177
4.5	Phenotypic analysis of PCF Lister 427 <i>BRCA2</i> re-expresser cell lines	179
4.6	Complementation of BSF Lister 427 <i>brca2</i> ^{-/-} mutants with variants of <i>BRCA2</i> with reduced numbers of BRC repeats	183
4.6.1	Generation of re-expresser cell lines in BSF Lister 427	183
4.6.2	Confirmation of re-expresser cell lines by PCR	184
4.6.3	Confirmation of re-expresser cell lines by Southern analysis	184
4.6.4	Attempt at confirmation of re-expresser cell lines by western analysis	185
4.6.5	Analysis of <i>BRCA2</i> mRNA levels in re-expresser cell lines by quantitative RT-PCR	186
4.7	Phenotypic analysis of BSF Lister 427 <i>BRCA2</i> re-expresser cell lines.	188
4.7.1	Analysis of <i>in vitro</i> growth	188
4.7.2	Analysis of DNA damage sensitivity	189
4.7.3	Analysis of RAD51 focus formation	192
4.8	Summary	197
Chapter 5: Analysis of <i>BRCA2</i>-RAD51 interactions.....		201
5.1	Introduction	202
5.2	<i>In vitro</i> GST pull-down	203
5.2.1	Generation of bacterial fusion protein over-expression constructs	204
5.2.2	Generation of co-expressing bacterial cultures	209
5.2.3	GST pull-down using co-expressing bacterial cultures	209
5.3	Co-immunolocalisation of RAD51 and <i>BRCA2</i>	216
5.3.1	Endogenous C-terminal epitope tagging strategy	216
5.3.2	Generation of C-terminal 12myc tagged <i>BRCA2</i> cell line	218
5.3.3	Co-immunolocalisation of <i>BRCA2</i> and RAD51	218
5.3.4	Analysis of the sub-cellular distribution of <i>BRCA2</i> by aqueous fractionation	224
5.4	Summary	225
Chapter 6: Does <i>T. brucei</i> <i>BRCA2</i> interact with <i>CDC45</i>?		231
6.1	Introduction	232
6.2	<i>In vivo</i> co-immunoprecipitation	235
6.2.1	Endogenous C-terminal epitope tagging strategy	235
6.2.2	Generation of a <i>CDC45</i> ^{+/+} mutant cell line in PCF TREU 927 <i>T. brucei</i>	236
6.2.3	Generation of C-terminal 12myc tagged <i>CDC45</i> ^{+/+} cell line	239
6.2.4	Co-immunoprecipitation using the <i>CDC45</i> ^{+/+} 12myc tagged cell line	240

6.2.5	Generation of C-terminal double-tagged cell lines in PCF TREU 927 <i>T. brucei</i>	241
6.2.6	Confirmation of C-terminal double-tagged cell lines	242
6.2.7	Co-immunoprecipitation using C-terminal double-tagged cell lines.....	243
6.2.8	Co-immunoprecipitation after exposure to DNA damage	244
6.2.8.1	Confirmation of DNA damage.....	246
6.2.9	Endogenous N-terminal epitope tagging strategy.....	247
6.2.10	Generation of N-terminal double-tagged cell lines in PCF TREU 927 <i>T. brucei</i>	250
6.2.11	Co-immunoprecipitation using N-terminal double-tagged cell lines.....	251
6.3	<i>In vitro</i> GST pull-down	253
6.3.1	Generation of bacterial protein over-expression constructs.....	253
6.3.2	Generation of co-expressing bacterial cultures	254
6.3.3	GST pull-down using co-expressing bacterial cultures	254
6.4	Summary	257
Chapter 7: Discussion		259
7.1	Introduction.....	260
7.2	<i>T. brucei</i> BRCA2 functions in the maintenance of genome stability in the bloodstream form only.....	261
7.3	The BRC repeat expansion is critical for RAD51 subnuclear dynamics.....	264
7.4	Interactions between <i>T. brucei</i> BRCA2 and RAD51 are unusually extensive.	266
7.5	<i>T. brucei</i> BRCA2 does not bind CDC45.....	269
Appendices.....		271
Appendix 1: <i>BRCA2</i> gene sequence		272
Appendix 2: Alignment of <i>ingi</i> retrotransposons in TREU 927.....		279
Appendix 3: Tree of TREU 927 VSGs.....		280
Appendix 4: Alignment of TREU 927 VSG family members		281
VSG family 1		281
VSG family 2.....		281
VSG family 3.....		282
VSG family 4.....		282
List of references		283

List of figures

Figure 1-1 A phylogenetic tree of the six supergroups that have been proposed within the kingdom eukarya.....	23
Figure 1-2 The life cycle of <i>T. brucei</i>	27
Figure 1-3 A parasitaemic profile of a <i>T. brucei</i> infection in a cow.....	32
Figure 1-4 The Variant Surface Glycoprotein (VSG).....	33
Figure 1-5 The chromosomal location of silent VSG arrays in <i>T. brucei</i> strain TREU 927.....	34
Figure 1-6 A schematic representation of a generic bloodstream expression site.....	35
Figure 1-7 <i>In situ</i> transcriptional VSG switching.....	37
Figure 1-8 VSG switching utilises silent VSG genes from different genome locations.....	39
Figure 1-9 Mosaic VSG formation by segmental gene conversion.....	39
Figure 1-10 Telomere reciprocal exchange resulting in a VSG switching event.....	40
Figure 1-11 Pathways of eukaryotic DNA double strand break repair.....	42
Figure 1-12 The core proteins involved in non-homologous end joining.....	44
Figure 1-13 The proteins involved in the early stages of eukaryotic homologous recombination.....	47
Figure 1-14 Holliday junction resolution.....	49
Figure 1-15 A representation of human BRCA1 and BRCA2 proteins showing their functional domains and interacting proteins.....	52
Figure 1-16 Proposed model for the role of the BRCA2 BRC repeats in DSB repair.....	60
Figure 1-17 Proposed model for role of the BRCA2 C-terminal Rad51-binding motif during DNA replication.....	61
Figure 1-18 A schematic representation of <i>T. brucei</i> BRCA2 and its putative functional domains.....	70
Figure 1-19 Representation of the number of BRC repeats in BRCA2 proteins from trypanosomatids and other eukaryotes.....	70
Figure 1-20 Multiple sequence alignment of the BRC repeats from trypanosomatids and humans.....	71
Figure 1-21 Alignment of the C-terminal DNA/DSS1-binding domains of BRCA2.....	71
Figure 1-22 C-terminal alignment around a CDK phosphorylation site in human BRCA2.....	72
Figure 3-1 <i>BRCA2</i> gene deletion constructs.....	103
Figure 3-2 Confirmation of PCF TREU 927 <i>BRCA2</i> mutants by PCR.....	105
Figure 3-3 Confirmation of PCF TREU 927 <i>BRCA2</i> mutants by Southern analysis.....	106
Figure 3-4 Confirmation of PCF TREU 927 <i>BRCA2</i> mutants by western analysis.....	108
Figure 3-5 Analysis of <i>in vitro</i> growth of PCF TREU 927 <i>BRCA2</i> mutants.....	109
Figure 3-6 A representative survival curve for PCF TREU 927 <i>BRCA2</i> mutants exposed to MMS.....	112
Figure 3-7 A representative survival curve for PCF TREU 927 <i>BRCA2</i> mutants exposed to phleomycin.....	112
Figure 3-8 EC50 values of PCF TREU 927 <i>BRCA2</i> mutants exposed to MMS.....	113
Figure 3-9 EC50 values of PCF TREU 927 <i>BRCA2</i> mutants exposed to phleomycin.....	113
Figure 3-10 The cell cycle of procyclic form <i>T. brucei</i>	115
Figure 3-11 Cell cycle analysis of PCF TREU 927 <i>BRCA2</i> mutants.....	116
Figure 3-12 DNA content of 'others' in PCF TREU 927 <i>brca2</i> ^{-/-} mutants.....	116

Figure 3-13 Examples of zoids in PCF TREU 927 <i>brca2</i> ^{-/-} mutants.....	117
Figure 3-14 Graphical representation of RAD51 focus formation in PCF TREU 927 <i>BRCA2</i> mutants exposed to phleomycin.....	119
Figure 3-15 Representative images of RAD51 focus formation in PCF TREU 927 <i>BRCA2</i> mutants exposed to phleomycin.....	120
Figure 3-16 Western analysis of RAD51 in PCF TREU 927 <i>BRCA2</i> mutants exposed to phleomycin.	121
Figure 3-17 Screening PCF TREU 927 <i>BRCA2</i> mutant re-clones by PCR.....	122
Figure 3-18 The location of <i>ingi</i> retrotransposons in the subtelomeres of TREU 927 chromosome 9.	124
Figure 3-19 Analysis of genomic stability of PCF TREU 927 <i>BRCA2</i> mutants by Southern analysis using DNA probes against <i>ingi</i> retrotransposons.....	124
Figure 3-20 Analysis of the suitability of <i>ingi</i> DNA probes for detection of genomic instability in BSF Lister 427 <i>BRCA2</i> mutants.	125
Figure 3-21 Analysis of genomic stability of PCF TREU 927 <i>BRCA2</i> mutants by Southern analysis using DNA probes against <i>VSGs</i>	128
Figure 3-22 Analysis of genomic stability of PCF TREU 927 <i>BRCA2</i> mutants by pulsed field agarose gel electrophoresis.....	130
Figure 3-23 Screening BSF Lister 427 <i>brca2</i> ^{-/-} mutant re-clones by PCR.....	132
Figure 3-24 Analysis of genomic stability of BSF Lister 427 <i>BRCA2</i> mutants by Southern analysis using a DNA probe against <i>VSG121</i>	133
Figure 3-25 Confirmation of PCF Lister 427 <i>BRCA2</i> mutants by PCR.....	135
Figure 3-26 Confirmation of PCF Lister 427 <i>BRCA2</i> mutants by Southern analysis.	136
Figure 3-27 Analysis of <i>in vitro</i> growth of PCF Lister 427 <i>BRCA2</i> mutants.....	137
Figure 3-28 A representative survival curve for PCF Lister 427 <i>BRCA2</i> mutants exposed to MMS.	139
Figure 3-29 A representative survival curve for PCF Lister 427 <i>BRCA2</i> mutants exposed to phleomycin.	139
Figure 3-30 EC50 values of PCF Lister 427 <i>BRCA2</i> mutants exposed to MMS.	140
Figure 3-31 EC50 values of PCF Lister 427 <i>BRCA2</i> mutants exposed to phleomycin.....	140
Figure 3-32 Analysis of <i>in vitro</i> growth of PCF Lister 427 <i>BRCA2</i> mutants exposed to MMS.	142
Figure 3-33 Screening PCF Lister 427 <i>brca2</i> ^{-/-} mutant re-clones by PCR.	143
Figure 3-34 Analysis of genome stability of PCF Lister 427 <i>BRCA2</i> mutants by Southern analysis using a DNA probe against <i>VSG121</i>	143
Figure 3-35 Screening PCF Lister 427 <i>brca2</i> ^{-/-} mutant re-clones by PCR.	144
Figure 3-36 Analysis of genomic stability of PCF Lister 427 <i>BRCA2</i> mutants by Southern analysis using a DNA probe against <i>VSG121</i>	145
Figure 3-37 Analysis of genomic stability of PCF Lister 427 <i>BRCA2</i> mutants by pulsed field agarose gel electrophoresis.....	146
Figure 4-1 A diagram of the 7 <i>BRC</i> variant domain of <i>T. brucei</i> <i>BRCA2</i> generated by DNA synthesis.....	154
Figure 4-2 Cloning strategy used for the assembly of the <i>pRM482::BRC</i> variant re-expresser constructs.....	155
Figure 4-3 <i>pRM482::BRC</i> re-expression constructs.....	156
Figure 4-4 Confirmation of PCF TREU 927 <i>BRCA2</i> re-expresser cell lines by PCR.	157
Figure 4-5 Confirmation of PCF TREU 927 <i>BRCA2</i> re-expresser cell lines by Southern analysis.	159
Figure 4-6 Attempt at confirmation of PCF TREU 927 <i>BRCA2</i> re-expresser cell lines by western analysis.	160

Figure 4-7 Testing PCF TREU 927 <i>BRCA2</i> re-expresser RT-PCR reactions by PCR.	162
Figure 4-8 Quantitative RT-PCR analysis of the PCF TREU 927 <i>BRCA2</i> re-expresser cell lines.	162
Figure 4-9 Analysis of <i>in vitro</i> growth of the PCF TREU 927 <i>BRCA2</i> re-expresser cell lines.	163
Figure 4-10 A representative survival curve for PCF TREU 927 <i>BRCA2</i> re-expresser cell lines exposed to MMS.....	166
Figure 4-11 A representative survival curve for PCF TREU 927 <i>BRCA2</i> re-expresser cell lines exposed to phleomycin.....	166
Figure 4-12 EC50 values of PCF TREU 927 <i>BRCA2</i> re-expresser cell lines exposed to MMS.	166
Figure 4-13 EC50 values of PCF TREU 927 <i>BRCA2</i> re-expresser cell lines exposed to phleomycin.	167
Figure 4-14 Graphical representation of RAD51 focus formation in PCF TREU 927 <i>BRCA2</i> re-expresser cell lines exposed to phleomycin.....	169
Figure 4-15A Representative images of RAD51 focus formation in PCF TREU 927 <i>BRCA2</i> re-expresser cell lines exposed to phleomycin.....	170
Figure 4-16 Western analysis of RAD51 in PCF TREU 927 <i>BRCA2</i> re-expresser cell lines exposed to phleomycin.....	172
Figure 4-17 Aqueous fractionation of PCF TREU 927 <i>BRCA2</i> re-expresser cell lines exposed to phleomycin.....	174
Figure 4-18 Confirmation of PCF Lister 427 <i>BRCA2</i> re-expresser cell lines by PCR.	176
Figure 4-19 Confirmation of PCF Lister 427 <i>BRCA2</i> re-expresser cell lines by Southern analysis.	177
Figure 4-20 Testing PCF Lister 427 <i>BRCA2</i> re-expresser RT-PCR reaction products by PCR.....	178
Figure 4-21 Quantitative RT-PCR analysis of the PCF Lister 427 <i>BRCA2</i> re-expresser cell lines.	178
Figure 4-22 Analysis of <i>in vitro</i> growth of the PCF Lister 427 <i>BRCA2</i> re-expresser cell lines.	179
Figure 4-23 A representative survival curve for PCF Lister 427 <i>BRCA2</i> re-expresser cell lines exposed to MMS.....	181
Figure 4-24 A representative survival curve for PCF Lister 427 <i>BRCA2</i> re-expresser cell lines exposed to phleomycin.....	181
Figure 4-25 EC50 values of PCF Lister 427 <i>BRCA2</i> re-expresser cell lines exposed to MMS.....	182
Figure 4-26 EC50 values of PCF Lister 427 <i>BRCA2</i> re-expresser cell lines exposed to phleomycin.	182
Figure 4-27 Confirmation of BSF Lister 427 <i>BRCA2</i> re-expresser cell lines by PCR.	184
Figure 4-28 Confirmation of BSF Lister 427 <i>BRCA2</i> re-expresser cell lines by Southern analysis.	185
Figure 4-29 Attempt at confirmation of BSF Lister 427 <i>BRCA2</i> re-expresser cell lines by western analysis.	186
Figure 4-30 Testing BSF Lister 427 <i>BRCA2</i> re-expresser RT-PCR reaction products by PCR.....	187
Figure 4-31 Quantitative RT-PCR analysis of the BSF Lister 427 <i>BRCA2</i> re-expresser cell lines.	187
Figure 4-32 Analysis of <i>in vitro</i> growth of the BSF Lister 427 <i>BRCA2</i> re-expresser cell lines.	188

Figure 4-33 A representative survival curve for BSF Lister 427 BRCA2 re-expresser cell lines exposed to MMS.....	190
Figure 4-34 A representative survival curve for BSF Lister 427 BRCA2 re-expresser cell lines exposed to phleomycin.....	190
Figure 4-35 EC50 values of BSF Lister 427 BRCA2 re-expresser cell lines exposed to MMS.....	191
Figure 4-36 EC50 values of BSF Lister 427 BRCA2 re-expresser cell lines exposed to phleomycin.....	191
Figure 4-37 Graphical representation of RAD51 focus formation in BSF Lister 427 BRCA2 re-expresser cell lines exposed to phleomycin.....	194
Figure 4-38A Representative images of RAD51 focus formation in BSF Lister 427 BRCA2 re-expresser cell lines exposed to phleomycin.....	195
Figure 4-39 Western analysis of RAD51 in BSF Lister 427 BRCA2 re-expresser cell lines exposed to phleomycin.....	197
Figure 5-1 GST pull-down strategy.....	204
Figure 5-2 Construct used for N-terminal GST tagging of RAD51 for over-expression in <i>E. coli</i>	207
Figure 5-3 Construct used for N-terminal His tagging of BRCA2 variants for over-expression in <i>E. coli</i>	207
Figure 5-4 A schematic diagram of the His-tagged BRCA2 variant proteins over-expressed in <i>E. coli</i>	208
Figure 5-5 Sequence alignment of putative PhePP motifs from BRCA2 orthologues.....	209
Figure 5-6 GST pull-down analysis of the interactions between RAD51 and the N-terminal domain of BRCA2.....	211
Figure 5-7 GST pull-down analysis of the interactions between RAD51 and the C-terminal domain of BRCA2.....	215
Figure 5-8 Construct used for C-terminal 12myc tagging of <i>T. brucei</i> BRCA2....	217
Figure 5-9 Strategy for C-terminal 12 myc tagging of <i>T. brucei</i> proteins at their endogenous loci.....	217
Figure 5-10 Confirmation of expression of C-terminal 12myc tagged BRCA2 by western analysis.....	218
Figure 5-11 Representative images of BRCA2 and RAD51 localisation in PCF TREU 927 <i>T. brucei</i> exposed to phleomycin for 5 hours.....	221
Figure 5-12 Representative images of BRCA2 and RAD51 localisation in PCF TREU 927 <i>T. brucei</i> exposed to phleomycin for 24 hours.....	222
Figure 5-13 Representative images of BRCA2 and RAD51 localisation in PCF TREU 927 <i>T. brucei</i> in the absence of DNA damage.....	223
Figure 5-14 Western analysis of BRCA2 12myc and RAD51 in PCF TREU 927 <i>T. brucei</i> after exposure to phleomycin.....	224
Figure 5-15 Aqueous fractionation of PCF TREU 927 BRCA2 12myc tagged cell line exposed to phleomycin.....	225
Figure 5-16 A representation of BRCA2 orthologues showing their functional domains and interacting proteins.....	230
Figure 6-1 Construct used for C-terminal 12myc tagging of <i>T. brucei</i> CDC45....	236
Figure 6-2 CDC45 gene deletion construct.....	237
Figure 6-3 Confirmation of PCF TREU 927 CDC45-/+ mutant cell lines by PCR.....	238
Figure 6-4 Confirmation of expression of C-terminal 12myc tagged CDC45-/+ by western analysis.....	239
Figure 6-5 Co-immunoprecipitation analysis of the interaction between CDC45 12myc and BRCA2.....	240

Figure 6-6 Confirmation of co-expression of C-terminal epitope tagged proteins in PCF TREU 927 <i>T. brucei</i> .	243
Figure 6-7 Co-immunoprecipitation analysis of the interaction between BRCA2 and CDC45, and between BRCA2 and RAD51.	244
Figure 6-8 Co-immunoprecipitation analysis of the interaction between BRCA2 and CDC45, and BRCA2 and RAD51 after exposure to hydroxyurea.	245
Figure 6-9 Co-immunoprecipitation analysis of the interaction between BRCA2 and CDC45, and BRCA2 and RAD51 after exposure to MMS.	246
Figure 6-10 Flow cytometry profiles of propidium iodide-stained cells after exposure to hydroxyurea.	247
Figure 6-11 Constructs used for N-terminal epitope tagging of <i>T. brucei</i> proteins.	249
Figure 6-12 Strategy for N-terminal epitope tagging of <i>T. brucei</i> proteins at their endogenous loci.	250
Figure 6-13 Confirmation of co-expression of N-terminal epitope tagged proteins in PCF TREU 927 <i>T. brucei</i> .	251
Figure 6-14 Co-immunoprecipitation analysis of the interaction between BRCA2 and CDC45, and BRCA2 and RAD51.	252
Figure 6-15 Construct used for N-terminal GST tagging of CDC45 for over-expression in <i>E. coli</i> .	254
Figure 6-16 GST pull-down analysis of the interactions between CDC45 and BRCA2.	256

List of tables

Table 2-1 List of oligonucleotide primers used in this thesis.....	87
Table 2-2 List of primary antiserum used in this thesis.....	97
Table 2-3 List of secondary antiserum used in this thesis.....	97
Table 3-1 <i>In vitro</i> population doubling times of PCF TREU 927 <i>BRCA2</i> mutants.	109
Table 3-2 Statistical analysis of Alamar Blue results.....	114
Table 3-3 RAD51 focus formation in PCF TREU 927 <i>BRCA2</i> mutants exposed to phleomycin.....	118
Table 3-4 BLASTn hits for the five <i>VSG</i> DNA probes.....	127
Table 3-5 <i>In vitro</i> population doubling times of PCF Lister 427 <i>BRCA2</i> mutants.	138
Table 3-6 Statistical analysis of Alamar Blue results.....	141
Table 4-1 <i>In vitro</i> population doubling times of PCF TREU 927 <i>BRCA2</i> re- expresser cell lines.....	164
Table 4-2 Statistical analysis of Alamar Blue results.....	167
Table 4-3 RAD51 focus formation in PCF TREU 927 <i>BRCA2</i> re-expresser cell lines exposed to phleomycin.....	169
Table 4-4 <i>In vitro</i> population doubling times of PCF Lister 427 <i>BRCA2</i> re- expresser cell lines.....	180
Table 4-5 Statistical analysis of Alamar Blue results.....	183
Table 4-6 <i>In vitro</i> population doubling times for BSF Lister 427 <i>BRCA2</i> re- expresser cell lines.....	189
Table 4-7 Statistical analysis of Alamar Blue results.....	192
Table 4-8 RAD51 focus formation in BSF Lister 427 <i>BRCA2</i> re-expresser cell lines exposed to phleomycin.....	194
Table 5-1 Quantification of the localisation of <i>BRCA2</i> and <i>RAD51</i> in PCF TREU 927 <i>T. brucei</i> before and after exposure to phleomycin.....	220

Acknowledgements

I would firstly like to thank my mother, without the emotional support and encouragement extended over the last four years I would never have succeeded.

I would also like to thank Richard McCulloch, not only for the inspiration for this thesis and guidance throughout, but also for the stimulating tea time discussions that have enriched my life.

I also extend my thanks to all members of the Barry and McCulloch labs, past and present that I have had the pleasure of working with and also colleagues in WTCMP, especially Alex for help with fixing administrative problems.

Lastly I wish to thank Bill, Darren and Olwyn for giving me this opportunity to undertake this PhD, the students of the four-year Wellcome Trust PhD programme for stimulating Annual Retreats and finally The Wellcome Trust for financial support.

Author's declaration

I declare that this thesis and the results presented within are entirely my own work except where otherwise stated. No part of this thesis has been previously submitted for a degree at any university.

Anna Trenaman

List of abbreviations

ADP	adenosine diphosphate
ApoL1	apolipoprotein A1
ATM	ataxia telangiectasia mutated
ATP	adenosine triphosphate
ATR	ataxia telangiectasia and Rad3-related protein
BER	base excision repair
BES	bloodstream <i>VSG</i> expression site
BIR	break induced replication
<i>BLE</i>	bleomycin resistance gene
bp	base-pairs
BSA	bovine serum albumin
<i>BSD</i>	blasticidin-S-deaminase gene
BSF	bloodstream form
BVSG	bloodstream variant surface glycoprotein
cAMP	cyclic adenosine monophosphate
CDC	cell division cycle
CDK	cyclin dependent kinase
cDNA	complementary DNA
CIP	alkaline phosphatase (calf intestinal)
CMG	CDC45-MCM-GINS complex
DAPI	4', 6-diamidino-2-phenylindole
dATP	deoxyadenosine triphosphate
DBD	DNA-binding domain
DGC	directional gene cluster
dH ₂ O	distilled water
DIC	differential interference contrast
DNA	deoxyribonucleic acid
dNTP	deoxyribonucleotide triphosphate
DSB	double strand break
dsDNA	double-stranded DNA
DTT	1, 4-dithiothreitol
EDTA	ethylenediaminetetraacetic acid
ES	<i>VSG</i> expression site
<i>ESAG</i>	expression site associated gene
ESB	expression site body
EtBr	ethidium bromide
FA	fanconi anaemia
FACS	fluorescence activated cell sorting

FBA	fractionation buffer A
FCS	foetal calf serum
FITC	fluorescein isothiocyanate
GCR	gross chromosomal rearrangement
gDNA	genomic DNA
GPI	glycosylphosphatidylinositol
<i>GPI</i>	<i>glucose 6-phosphate isomerase gene</i>
GST	glutathione S-transferase
HA	influenza haemagglutinin epitope
HAT	human african trypanosomiasis
HCL	hydrochloric acid
HJ	holliday junction
HMI	Hirumi's modified Iscove's medium
HR	homologous recombination
HTH	helix-turn-helix motif
HU	hydroxyurea
IPTG	isopropyl- β -D-thiogalactopyranoside
kb	kilobase-pairs
kDa	kilo-dalton
kDNA	kinetoplast DNA
LB	Luria-Bertani
LMP	low melting point
Mb	megabase-pairs
MBq	mega becquerels
MCM	minichromosome maintenance
MMEJ	micro-homology mediated end joining
MMR	mismatch repair
MMS	methyl methanesulphonate
MOPS	3-(N-morpholino) propanesulfonic acid
MRN	Mre11-Rad50-Nbs1 (in mammals)
mRNA	messenger RNA
MRX	Mre11-Rad50-Xrs2 (in yeast)
MVR	minisatellite variant repeat
MVSG	metacyclic variant surface glycoprotein
Myc	c-myc epitope
NDS	agarose plug buffer
<i>NEO</i>	<i>neomycin phosphotransferase gene</i>
NER	nucleotide excision repair
NHEJ	non-homologous end joining
NLS	nuclear localisation signal
OB	oligonucleotide/oligosaccharide- binding

ORF	open reading frame
PAGE	polyacrylamide gel electrophoresis
PARP	poly ADP-ribose polymerase
PBS	phosphate buffered saline
PCF	procyclic form
PCNA	proliferating cell nuclear antigen
PCR	polymerase chain reaction
PIKK	phosphatidylinositol 3-kinase-related kinase
PolyA	polyadenylate
<i>PUR</i>	puromycin-N-acetyltransferase gene
qRT-PCR	quantitative real time polymerase chain reaction
RNA	ribonucleic acid
RNA pol I	RNA polymerase I
RNA pol II	RNA polymerase II
RNA pol III	RNA polymerase III
RPA	replication protein A
RT	reverse transcriptase
RT-PCR	reverse transcriptase polymerase chain reaction
ROS	reactive oxygen species
SCR	sister chromatid recombination
SDM	semi-defined medium
SDS	sodium dodecyl sulphate
SDSA	synthesis-dependent strand annealing
SIF	stumpy induction factor
SL	spliced leader
SOB	super optimal broth
SOC	SOB supplemented with glucose
SRA	serum resistance-associated gene
SSA	single-strand annealing
SSB	single-stranded DNA binding protein
SSC	saline sodium citrate buffer
ssDNA	single-stranded DNA
TAE	tris/ acetic acid/ EDTA buffer
TB1/10E	tris/ boric acid/ 1/10 EDTA buffer
TBE	tris/ boric acid/ EDTA buffer
TDB	trypanosome dilution buffer
TES	N-[tris (hydroxymethyl) methyl]-2-aminoethanesulfonic acid
TLB	trypanosome lysis buffer
TLF	trypanolytic factor
TREU	Trypanosomiasis Research Edinburgh University
UTR	untranslated region

UV	ultraviolet
<i>vlp</i>	variable large protein
VSG	variant surface glycoprotein
<i>vsp</i>	variable small protein
VSP	variant surface protein
WHO	world health organisation
WLB	wash/lysis buffer
ZM	Zimmerman post fusion medium
ZMG	ZM supplemented with glucose

Chapter 1: Introduction

1.1 General Introduction to *Trypanosoma brucei*

1.1.1 Phylogeny of *Trypanosoma*

Recent advances in molecular phylogenetics have allowed the division of Eukaryotes into five supergroups: *Excavata*, *Chromalveolata*, *Archaeplastida*, *Amoebozoa* and *Opisthokonta* (Adl *et al.*, 2005; Hampl *et al.*, 2009). This new grouping places many protistan parasites, including members of the genera *Trypanosoma*, *Leishmania*, *Trichomonas* and *Giardia*, in the *Excavata* supergroup (Figure 1-1; Dacks, Walker, and Field, 2008). *Trypanosoma* belong to the family *Trypanosomatidae*, which contains at least nine genera, including *Leishmania*. Trypanosomatids are members of the order *Kinetoplastidae*, which are characterised by the possession of a complex catenated network of mitochondrial DNA circles organised in a disc-like structure called the kinetoplast (Lukes *et al.*, 2002). Kinetoplastids are members of the phylum *Euglenozoa*. Thus, the taxonomic ranks for *Trypanosoma* are as follows: supergroup, *Excavata*; phylum, *Euglenozoa*; order, *Kinetoplastidae*; family, *Trypanosomatidae* and genus, *Trypanosoma* (Simpson, Stevens, and Lukes, 2006). Much of our understanding of fundamental molecular biology in eukaryotes comes from studies of yeasts, metazoa and plants. Relative to this, less work has considered protozoan organisms, though it is clear that many key processes, such as transcription and mitochondrial biology, are diverged (i.e. extensive *trans*-splicing, multigene transcription units, kinetoplast DNA structure and extensive mRNA editing). Given these aspects of divergence, it is of interest to consider whether the processes that control genome stability display similar divergence, either because of evolutionary distance or because of the needs of a parasitic lifestyle. In this regard, *Trypanosoma* are a key organism of study, as extensive tools for genetic manipulation are available.

The genus *Trypanosoma* includes both American and African trypanosome species. *Trypanosoma cruzi* is an intracellular parasite of mammals, which causes Chagas disease in South America. In contrast, members of the African Salivarian branch of trypanosomes are extracellular parasites of mammals mainly found in sub-saharan Africa, and include *Trypanosoma congolense*, *Trypanosoma vivax* and *Trypanosoma brucei*, which cause Human African Trypanosomiasis

(HAT; also called Sleeping Sickness) in humans and Nagana in domestic cattle and horses.

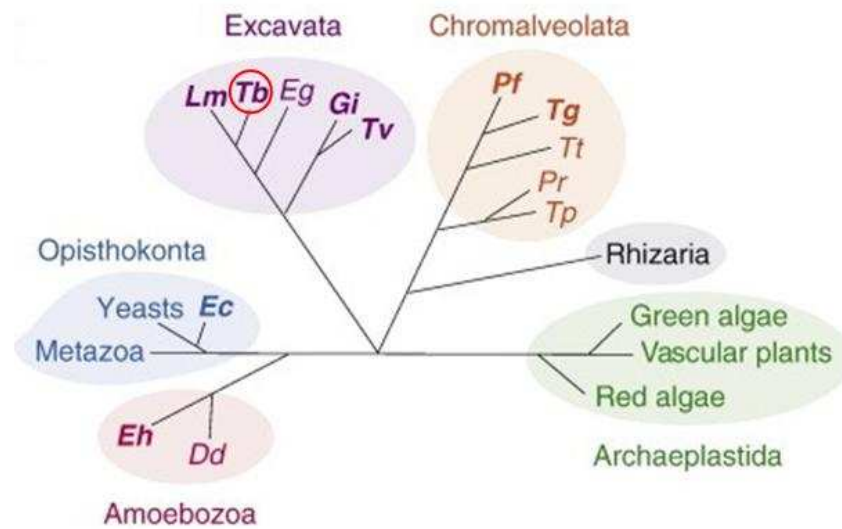


Figure 1-1 A phylogenetic tree of the six supergroups that have been proposed within the kingdom eukarya.

The supergroups are named and indicated by shaded lozenges. Taxon supergroups are colour-coded and parasitic taxa are in bold. *Trypanosoma brucei* is indicated by a red circle. Taxa represented are Dd; *Dictyostelium discooidium*, Ec; *Encephalitozoon cuniculi*, Eg; *Euglena gracilis*, Eh; *Entamoeba histolytica*, Gi; *Giardia intestinalis*, Lm; *Leishmania major*, Pf; *Plasmodium falciparum*, Pr; *Phytophthora ramorum*, Tb; *Trypanosoma brucei*, Tg; *Toxoplasma gondii*, Tp; *Thalassiosira pseudonana*, Tt; *Tetrahymena thermophila* and Tv; *Trichomonas vaginalis*. Figure reproduced from Dacks, Walker, and Field, 2008.

1.1.2 Disease, symptoms and treatment

Trypanosoma brucei is the only African trypanosome that infects humans, and is divided into three morphologically identical sub-species: *T. b. brucei*, *T. b. gambiense* and *T. b. rhodesiense*. These sub-species classifications are based on geographical distribution, host specificity and the course of infection in humans. *T. b. brucei* is unable to establish human infections, in part because it is susceptible to lysis by apolipoprotein L1 (ApoL1), a component of trypanolytic factor (TLF) found in human serum (Pays *et al.*, 2006). *T. b. brucei* infects domestic cattle and horses causing the wasting disease Nagana. *T. b. gambiense* and *T. b. rhodesiense* have developed resistance to human trypanolysis; in *T. b. rhodesiense* through the expression of the serum resistance-associated (SRA) gene (Xong *et al.*, 1998; Oli *et al.*, 2006), and in *T. b. gambiense* through SRA-independent resistance to lysis by ApoL1 and, in some strains, reduced uptake of TLF (Kieft *et al.*, 2010; Capewell *et al.*, 2011). The clinical course of HAT differs depending on which of these sub-species is involved (Turner *et al.*, 2004). *T. b. gambiense* causes a chronic form of HAT in west and central Africa, whereas *T.*

b. rhodesiense causes a more acute form of the disease in east and southern Africa (Hoare, 1973).

African trypanosomes are extracellular parasites, which proliferate in the tissue fluids and bloodstream of their mammalian host. The early-stage of the disease is characterised by fever, anaemia, lack of appetite and wasting caused by inflammation and necrosis within the capillaries of major organs (Vickerman, 1985). If the infection is allowed to progress, the parasites eventually cross the blood brain barrier. This late-stage infection is characterised by motor and sensory disorders, sleep disturbances, followed by seizures and finally coma. If untreated, Human African Trypanosomiasis is always fatal (Barrett *et al.*, 2003; Sternberg, 2004; Barrett *et al.*, 2007).

In 1995, the World Health Organisation (WHO) estimated that 60 million people were at risk of HAT, with an estimated 300,000 new cases per year, with fewer than 30,000 cases diagnosed and treated (WHO, 1995). In 2004, a review of the figures on HAT showed the number of new reported cases falling to 17,616 with an estimated cumulative rate of between 50,000 and 70,000 cases (WHO, 2004), and this decrease is thought to be due to increased control.

Only four drugs are registered for the treatment of HAT, and all are associated with side effects and an increasing rate of treatment failure (Barrett *et al.*, 2003; Kennedy, 2004). Pentamidine is used for the treatment of early-stage *T. b. gambiense* infections and is a diamidine compound. Some of the observed side effects include nephrotoxicity and pancreatic damage. Suramin is a colourless analog of the trypanocidal dye trypan blue and is used for the treatment of early-stage *T. b. rhodesiense* infections. Some of the observed side effects are heavy proteinuria, exfoliative dermatitis, severe diarrhoea and prolonged high fever. Melarsoprol is an organic arsenical compound that has the ability to enter the central nervous system, making it a suitable drug for treating late-stage cases of *T. b. gambiense* and *T. b. rhodesiense* infections. Fatalities have been known to occur in ~ 8% of cases with this treatment, but the most common side effects include headache, tremor, slurring of speech and convulsions. Finally, eflornithine is used for the treatment of both early- and late-stage *T. b. gambiense* infections. It is an ornithine derivative that acts by inhibiting the enzyme ornithine decarboxylase, which is involved in polyamine synthesis in

trypanosomes. The most common side effects include diarrhoea, anaemia, leukopenia, and convulsions. In 2009, the WHO added the combination therapy of eflornithine and nifurtimox, which is used to treat American Trypanosomiasis (Chagas disease), to its list of essential medicines. This has reduced the duration of eflornithine monotherapy and, hopefully, the onset of drug resistance.

1.1.3 The life cycle of *T. brucei*

T. brucei is transmitted between mammals by the tsetse fly (*Glossina sp*) (Cross, 2001; Steverding, 2008), and employs a complex life cycle to allow development within both the mammalian host and fly vector. These organisms provide contrasting environments and the parasite has evolved several distinct life cycle stages adapted to their respective hosts (Figure 1-2). Two main types of life cycle stage have been identified: replicative stages and transmission stages. Replicative stage parasites include the long slender bloodstream form, the procyclic form and the epimastigote form, and their role is to establish and maintain infections in their respective environments (Barry and McCulloch, 2001). Transmission stage parasites include the short stumpy bloodstream form and the metacyclic form. These are pre-adapted to their destination host, but have a finite half-life if not transmitted as they are non-replicative, cell cycle arrested forms (e.g. short stumpy cells lie in G₀ phase; Matthews and Gull, 1997).

When an infective tsetse fly takes a blood meal from a mammalian host, it deposits metacyclic form cells below the skin (Vickerman, 1985). Cells of this life cycle stage develop in the salivary glands of the tsetse fly and express a Metacyclic Variant Surface Glycoprotein (MVSG) coat (Tetley *et al.*, 1987), which serves to protect against the mammalian host's innate immune system (section 1.2.1), and also to hide invariant surface molecules from the host's immune surveillance. In the mammal these non-dividing metacyclic form cells differentiate into long slender bloodstream form parasites, which can proliferate by cell division whilst moving from the site of deposition to the bloodstream (Vickerman, 1985; Matthews and Gull, 1994; Matthews, Ellis, and Paterou, 2004). In the long slender bloodstream form cells the MVSG coat is replaced by Bloodstream Variant Surface Glycoproteins (BVSGs), which involves expression of the VSG gene from a distinct genomic location and enables the trypanosome

population to evade eradication by the host immune system to establish and maintain an infection by a process called antigenic variation (section 1.2.1). In the bloodstream, long slender cells can differentiate into a short stumpy bloodstream form. This occurs in a density dependent manner due to the accumulated secretion of a low molecular weight factor, termed stumpy induction factor (SIF), from the long slender bloodstream form trypanosomes. SIF induces growth arrest through a cyclic adenosine monophosphate (cAMP) signalling pathway (Vassella *et al.*, 1997). Short stumpy form trypanosomes are pre-adapted to the tsetse fly environment with metabolic changes that allow them to switch from the glucose energy source in the mammalian bloodstream to the proline energy source found in the tsetse fly midgut (Hendriks *et al.*, 2000). Once ingested by a tsetse fly, the short stumpy form cells differentiate into replicative procyclic form cells that express a procyclin protein coat on their surface. The precise function of the procyclin coat is unknown, though it is thought to protect against trypanocidal factors in the tsetse fly midgut (Roditi and Liniger, 2002). The procyclic form cells move to the alimentary tract where they proliferate by cell division before differentiating into mesocyclic form cells, which migrate into the tsetse fly salivary glands (Roditi and Liniger, 2002). Once in the salivary glands, mesocyclic form cells undergo an asymmetrical cell division, producing a large daughter cell (that appears to be discarded) and a small daughter cell, which is the progenitor of the epimastigote form that attaches to the salivary gland wall and multiplies by cell division (Van den Abbeele *et al.*, 1999; Fenn and Matthews, 2007). It is here that genetic exchange is thought to occur in the life cycle, including between different *T. brucei* strains and sub-species, though it appears to be non-obligatory (Tait and Turner, 1990; Gibson and Stevens, 1999; Gibson *et al.*, 2008). Analysis of fluorescently tagged meiosis-specific proteins has allowed the recent identification of the meiotic stage of *T. brucei* within the tsetse fly (Peacock *et al.*, 2011). This morphologically distinct dividing epimastigote form, present in the salivary glands, was identified due to strong expression of meiosis-specific proteins in the nucleus (Peacock *et al.*, 2011). When the epimastigote form cells detach from the salivary gland wall they differentiate into metacyclic form cells and are ready to be transmitted to another mammalian host. The life cycle is then complete.

In the laboratory, two replicative stages of *T. brucei* are able to be maintained and manipulated in culture; these are the procyclic form of the parasite, which replicates in the tsetse fly midgut, and the long slender bloodstream form of the parasite, which replicates in the blood and tissue fluids of the mammalian host (Brun and Schonemberger, 1979; Hirumi and Hirumi, 1989). Some laboratory strains, which have been termed monomorphic, have lost the ability to differentiate from the long slender bloodstream form to the short stumpy form, undermining the natural route of transmission through the fly. Other strains, which retain this ability to differentiate are termed pleomorphic (Wijers and Willett, 1960; Matthews and Gull, 1994).

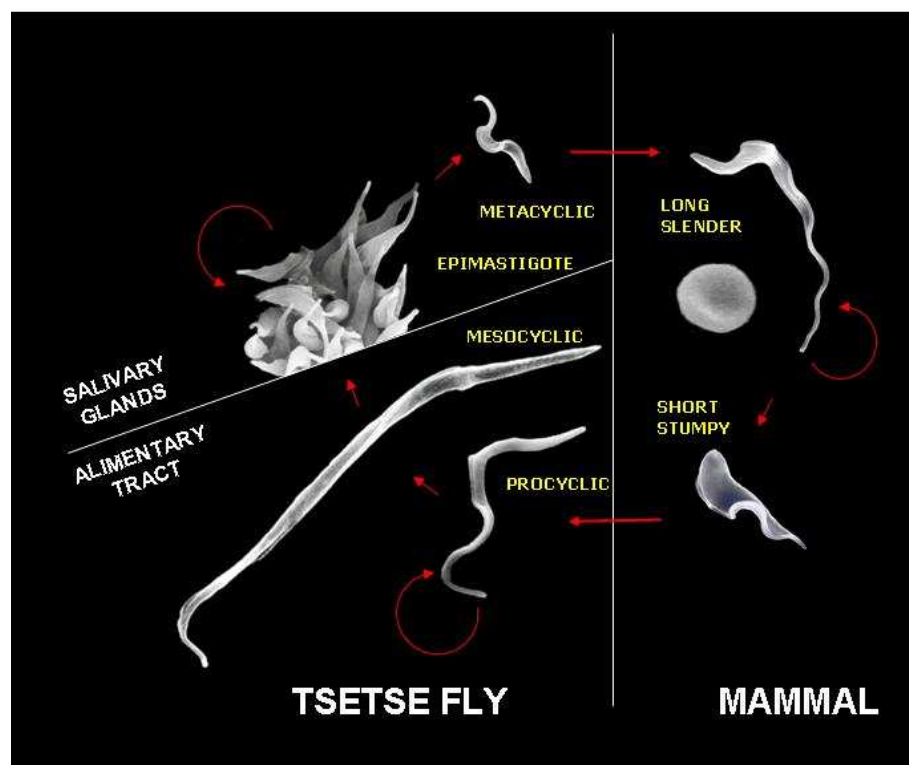


Figure 1-2 The life cycle of *T. brucei*.

The different life cycle stages shown are scanning electron micrographs, reproduced to scale. An erythrocyte is shown next to the long slender bloodstream stage for comparison. Curved arrows depict stages capable of replication, whereas straight arrows represent differentiation and progression through the life cycle. The host organism and the name of the life cycle stage are indicated. Figure reproduced from Barry and McCulloch, 2001.

1.1.4 The genome of *T. brucei*

In 2005, the project to sequence the megabase-sized chromosome DNA of *T. brucei* was completed (Berriman *et al.*, 2005) using the genome of the *T. brucei* strain TREU (Trypanosomiasis Research Edinburgh University) 927/4. The nuclear genome of *T. brucei* contains 11 megabase chromosomes that range in size from

~ 0.9 Mb to ~ 5.7 Mb and are named from 1-11 in order of increasing size; their total size is ~ 26 Mb (Berriman *et al.*, 2005; Hertz-Fowler, Renauld, and Berriman, 2007) The megabase chromosomes contain 9068 predicted genes that include ~ 900 pseudogenes and ~ 1700 *T. brucei*-specific genes (Berriman *et al.*, 2005).

The *T. brucei* megabase chromosomes have been divided into three domains. The central core contains most of the housekeeping genes, which are mainly transcribed by RNA polymerase II (RNA Pol II) as multigene transcription units. A proximal subtelomeric region is also defined that is largely composed of transcriptionally silent arrays of tandemly repeated units of *variant surface glycoprotein (VSG)* gene cassettes; interspersed with this are retrotransposon and retrotransposon-associated sequences, and some expression site-associated genes (*ESAGs*). Finally, there is a distal subtelomeric region that contains *MVSG* and *BVSG* expression sites (*ESs*), which are RNA Pol I transcription units that are the sole locations in which *VSGs* are expressed (Hertz-Fowler, Renauld, and Berriman, 2007). It is predicted that up to 55% of the *T. brucei* megabase chromosomes are devoted to subtelomeres, containing ~ 10% of the total predicted gene repertoire (Callejas *et al.*, 2006; Hertz-Fowler, Renauld, and Berriman, 2007). Since the majority of this subtelomeric repertoire is *VSG* and *VSG*-associated genes and sequences involved in the evasion of host immune destruction, this illustrates the importance of antigenic variation to trypanosome survival (section 1.2.1; Barry and McCulloch, 2001; Marcello and Barry, 2007).

The *T. brucei* nucleus also contains intermediate- and mini-chromosomes (Melville *et al.*, 1998; El Sayed *et al.*, 2000), which appear to have evolved to expand the *VSG* repertoire. In most strains, there are between 1 and 5 intermediate-chromosomes, of 200-900 kb in size, and numerous (~ 100) mini-chromosomes of 30-150 kb in size (Melville *et al.*, 1998; Melville *et al.*, 2000; El Sayed *et al.*, 2000; Alsford *et al.*, 2003; Wickstead, Ersfeld, and Gull, 2004). The intermediate-chromosomes contain *VSG* expression sites in the subtelomeres and a core sequence consisting of many copies of a 177 bp repeat sequence (Wickstead, Ersfeld, and Gull, 2004). The mini-chromosomes also contain many copies of the 177 bp repeats, arranged in a large repetitive palindrome, as well as a repertoire of silent subtelomeric *VSG* genes (Wickstead, Ersfeld, and Gull, 2004). It has been suggested that the 177 bp repeat sequences function in the

maintenance of mini- and intermediate-chromosomes through mediating replication (Weiden *et al.*, 1991).

Comparison of different *T. brucei* isolates revealed considerable chromosome size polymorphisms between isolates and also between diploid chromosome homologs within a single isolate (Melville *et al.*, 1998; Melville, Gerrard, and Blackwell, 1999; Melville *et al.*, 2000). This variation in chromosome size is also observed in other kinetoplastid parasites, including *Leishmania*, *Trypanosoma cruzi* and also *Plasmodium*, although not to the same extent as observed in *T. brucei* (Janse, 1993; Henriksson *et al.*, 1995; Wincker *et al.*, 1996). This variation in chromosome and genome size has been attributed, in part, to expansion in the many arrays of tandemly repeated gene families (Melville *et al.*, 2000; Melville, Gerrard, and Blackwell, 1999). The expansion of gene families in this manner is thought to be a mechanism to increase gene expression levels and therefore the level of protein, due to the lack of transcriptional regulation found in *T. brucei* (section 1.1.5; Ivens *et al.*, 2005; Callejas *et al.*, 2006). However, the major size variation appears to arise due to changes in the number and organisation of VSGs in the subtelomeric arrays (Callejas *et al.*, 2006), and this cannot be driven by gene expression as these sequences are not normally transcribed at these locations.

Analysis of the genome sequences of *T. brucei*, *T. cruzi* and *L. major* (also known as the TriTryps) has revealed a striking conservation of gene order (synteny), despite high levels of divergence at the sequence level and major differences in chromosome numbers and size (Melville *et al.*, 1998; Melville, Gerrard, and Blackwell, 1999; Melville *et al.*, 2000; Ghedin *et al.*, 2004; El Sayed *et al.*, 2005). The presence of retrotransposon-like elements at the few sites of genome rearrangements observed, suggests a role for retrotransposons in shaping the genomes of these kinetoplastid organisms (Ghedin *et al.*, 2004).

1.1.5 Transcription and translation in *T. brucei*

The housekeeping genes contained in the central core of the megabase chromosomes of *T. brucei* are arranged in directional gene clusters (DGCs), separated by so-called strand switch regions. All genes in a DGC are transcribed polycistronically from a single promoter, leading to a lack of control over the

transcription of most individual genes (Kooter *et al.*, 1987; El Sayed *et al.*, 2003; Berriman *et al.*, 2005). In contrast to bacteria, the co-transcribed genes in *T. brucei* are not generally functionally related (Clayton, 2002). A single pre-mRNA is thought to be generated from each DGC and requires post-transcriptional modification to generate mature mRNA ready for translation. In *trans*-splicing, a 'spliced leader' (SL) RNA is fused to the 5' end of each mRNA (Gunzl, 2010), creating a cap structure that appears unique to kinetoplastids and consists of 7-methylguanosine and 4 methylated nucleotides (Bangs *et al.*, 1992). The addition of a polyadenylated (PolyA) tail to the 3' end of the mRNA appears to occur in a co-ordinated reaction with *trans*-splicing, producing mature mRNA (Clayton, 2002). The RNA polymerases utilised by trypanosomes for transcription are also unusual. In most eukaryotes, transcription is carried out by 3 types of RNA polymerase: RNA pol I generates rRNA, RNA pol II produces mRNA, and RNA pol III yields tRNA (Rutter *et al.*, 1976; Tamura *et al.*, 1996; Cramer, 2002), although additional small RNAs are also produced by RNA pol II and III. In *T. brucei*, RNA pol II is primarily responsible for the transcription of housekeeping genes (Devaux *et al.*, 2006). Uniquely, a small number of protein-encoding genes are transcribed by RNA pol I, including the VSG expression site and procyclin genes (Navarro and Gull, 2001; Gunzl *et al.*, 2003), and this is thought to be an adaptation to allow the high level of transcription required for these abundant proteins (Gunzl *et al.*, 2003).

1.2 Antigenic variation

The survival of pathogens within a host relies on the successful evasion of host immune responses and many adaptations to allow persistence and enhanced transmission of pathogens have been observed. The invasion of host cells allows parasites, such as members of the genera *Toxoplasma* and *Leishmania*, an environment safe from immune surveillance in which to replicate (Sibley, 2004). Parasites that do not invade host cells, such as *T. brucei*, are constantly exposed to host immune defences and may use antigenic variation to evade host immune responses. Antigenic variation involves periodic changes in the antigens exposed on the pathogen surface to antigenically distinct variants, thus altering their appearance to the host immune system (Barbour and Restrepo, 2000; Zambrano-Villa *et al.*, 2002).

Antigenic variation is observed in a diverse array of pathogens with a wide variety of underlying mechanisms. For instance, *Giardia lamblia*, the causative agent of Giardiasis, utilises a transcriptional control mechanism to switch expression between a repertoire of 150 genes that encode the Variant Surface Protein (VSP) (Mowatt, Aggarwal, and Nash, 1991; Kulakova *et al.*, 2006). In contrast, some members of the genus *Borrelia* use a mechanism of gene conversion by recombination to switch their surface lipoprotein antigens, called variable large protein (*vlp*) and variable small protein (*vsp*) (Zhang *et al.*, 1997). *B. hermsii* has been found to contain approximately 60 silent genes present on episomes, and gene conversion between fragments of *vlp* and *vsp* genes utilise this genetic material (Dai *et al.*, 2006). However, in *B. burgdorferi* homologous recombination does not play a role in antigenic variation as mutation of the RecA recombinase enzyme in this organism does not impair infection rates (Liveris *et al.*, 2008).

1.2.1 Antigenic variation in *T. brucei*

T. brucei was the first organism discovered to undergo antigenic variation as a means of escaping the host immune system (Vickerman, 1978; Borst, 1986; Greaves and Borst, 1987) and remains one of the best-studied examples of this process (reviewed in Borst, 2002; Figueiredo, Cross, and Janzen, 2009; Morrison, Marcello, and McCulloch, 2009; Horn and McCulloch, 2010; Rudenko, 2010). Infections with *T. brucei* are characterised by waves of parasitaemia (Figure 1-3). In part, these waves are due to the formation of non-replicating short stumpy cells at high parasite densities (MacGregor *et al.*, 2011), however another major contributing factor is antigenic variation of the major surface antigen, the VSG (McCulloch, 2004). The production of specific antibodies against the VSG surface coat leads to the destruction of those parasites. The avoidance of complete parasite elimination is due to a sub-population of parasites that have switched to a new, antigenically distinct VSG and will be temporarily rendered invisible to the immune system, and so escape immune destruction to re-populate the host organism (Morrison *et al.*, 2005). Nevertheless, as these VSG-expressing cells outgrow, they too will be targeted for immune killing. Thus, antigenic variation succeeds by the continual switching to new VSGs, keeping the parasites 'one step ahead' of the host immune response.

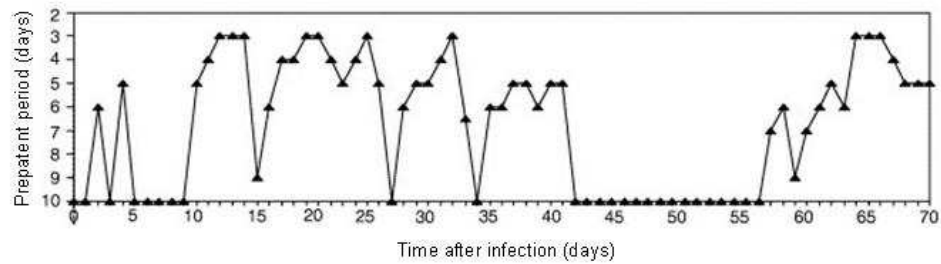


Figure 1-3 A parasitaemic profile of a *T. brucei* infection in a cow.

The x-axis follows the timeline of infection, from days 0-70. The parasitaemic profile of the cow was plotted as measured by the prepatent period in days (y-axis), from inoculating 0.2 ml cattle blood into an immunosuppressed mouse to achieve a parasitaemia of $1 \times 10^{8.1}$ trypanosomes.ml⁻¹, a measure that is approximately proportional to the parasite density in the cow. Figure reproduced from Morrison *et al.*, 2005.

1.2.2 The Variant Surface Glycoprotein

In the mammalian host, 5×10^6 dimers (10^7 copies) of a VSG form a densely packed coat on the parasite surface that performs multiple protective functions (Figure 1-4; Cross, 1975). Firstly, the tightly packed VSG coat shields invariant surface molecules, such as receptors and transport channels, from immune recognition (Ziegelbauer and Overath, 1993; Chung, Carrington, and Field, 2004; Schwede *et al.*, 2011). Secondly, it protects the parasite from the host's innate and adaptive immune responses, not simply by antigenic variation but also due to modulation of these immune responses, the mechanism of which is incompletely understood (Leppert, Mansfield, and Paulnock, 2007; Paulnock, Freeman, and Mansfield, 2010). Lastly, antibody binding to VSG molecules leads to rapid internalisation and degradation of the antibody and recycling of the VSG back to the cell surface (Engstler *et al.*, 2007). VSG proteins are anchored to the parasite membrane by a glycosylphosphatidylinositol (GPI) anchor at their C-terminus, which is buried in the coat and is more conserved than the surface exposed and highly antigenic N-terminus (Blum *et al.*, 1993; Ferguson, 1999; Schwede *et al.*, 2011).

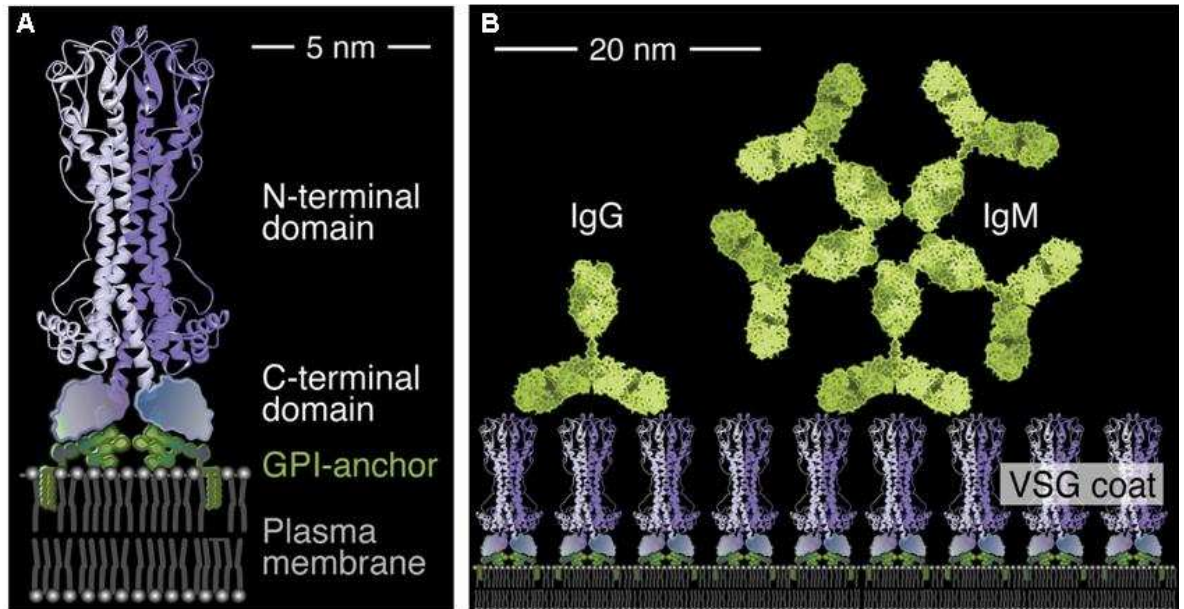


Figure 1-4 The Variant Surface Glycoprotein (VSG).

(A) The structure of a VSG homodimer (monomers in light blue and purple) that is attached to the *T. brucei* plasma membrane by a glycosylphosphatidylinositol (GPI) anchor. (B) A schematic representation of the cell surface of bloodstream form *T. brucei* showing the densely packed VSG coat bound by IgG and IgM molecules (drawn to scale). Figure reproduced from Engstler *et al.*, 2007.

The *T. brucei* genome contains ~ 1600 non-expressed VSG genes located in subtelomeric tandem arrays in the megabase-chromosomes, containing between 3 and ~ 250 VSG genes and pseudogenes (Figure 1-5; Berriman *et al.*, 2005). VSGs are effectively the only genes found on the mini-chromosomes, and are located immediately adjacent to the telomere (Williams, Young, and Majiwa, 1982; Wickstead, Ersfeld, and Gull, 2004). The gene archives used for antigenic variation are commonly found at subtelomeric locations, as observed in *Pneumocystis carinii* (Keely *et al.*, 2005) and *Plasmodium falciparum* (Scherf, Figueiredo, and Freitas-Junior, 2001). It is thought that this is because the subtelomeric environment allows for greater ectopic recombination than elsewhere in linear chromosomes (Barry *et al.*, 2003).

VSG genes have a basic ‘cassette’ organisation, comprising in total between 3 and 4 kb of sequence: one or more 70 bp repeat sequences are normally found at the 5’ flank of the cassette, followed downstream by so-called ‘co-transposed sequence’ upstream of the VSG open reading frame (ORF), which is then flanked by 3’ sequence with limited sequence homology between cassettes (Liu *et al.*, 1983). The genome sequencing project of *T. brucei* revealed that the majority of VSG genes are defective in some way: only 7% were found to be fully functional, 9% were atypical, 66% are full-length pseudogenes (with frame shifts and/or in-

frame stop codons) and 18% are gene fragments (Berriman and Harris, 2004; Marcello and Barry, 2007). Initially, it was thought that there was no organisation of *VSG* genes according to sequence similarity (Berriman *et al.*, 2005). However, a more recent study has found that approximately 550 *VSG*s exist in high-identity subfamilies of pairs, triplets and quadruplets, which are thought to be important in mosaic gene formation (section 1.2.4.2; Marcello and Barry, 2007). This process is a form of antigenic variation that utilises the vast archive of *VSG* pseudogenes and gene fragments to create antigenically novel *VSG* variants (Marcello and Barry, 2007). Indeed, the use of mosaic gene formation may be the predominant form of antigenic variation in other pathogens such as *Borrelia sp*, *Neisseria sp* and *Anaplasma sp* (Zhang and Norris, 1998; Hamrick *et al.*, 2001; Brayton *et al.*, 2002).

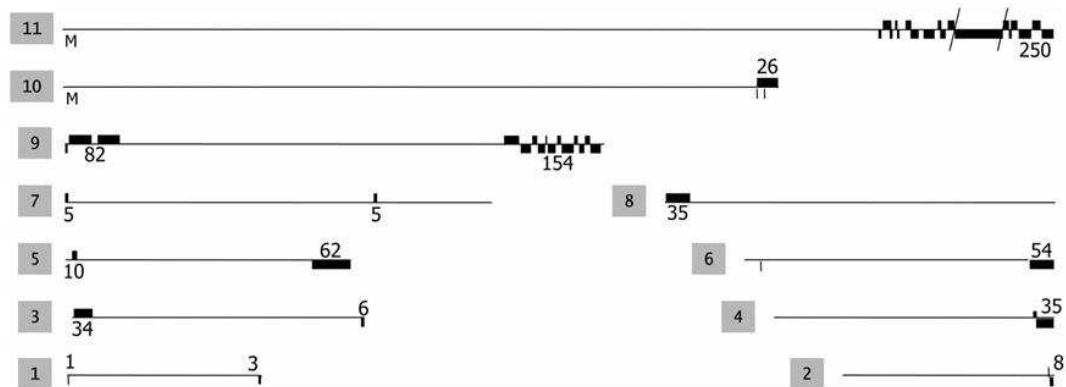


Figure 1-5 The chromosomal location of silent *VSG* arrays in *T. brucei* strain TREU 927. The assembled megabase chromosomes are represented by horizontal lines, with the chromosome number in a grey box to the left of each chromosome. Arrays of *VSG*s are depicted by black blocks; the orientation of sets of *VSG*s is shown by the position of the box above or below the line. The provisional number of *VSG*s in each array is shown. Breaks in contiguation in chromosome 11 are represented by oblique lines. Figure reproduced from Barry *et al.*, 2005.

1.2.3 *VSG* expression sites

A pre-requisite for the success of antigenic variation is that a single *VSG* is expressed at any one time, from a specialised polycistronic transcription unit called a *VSG* expression site (ES) (Figure 1-6; Pays *et al.*, 2001). At least 10 bloodstream expression sites (BESs) are thought to exist, located at the subtelomeres of the megabase- and intermediate-chromosomes (Becker *et al.*, 2004; Hertz-Fowler *et al.*, 2008; Young *et al.*, 2008). BESs vary hugely in size, from 40-100 kb, but have a conserved structure. The *VSG* gene is invariably located closest to the telomere (Berriman *et al.*, 2002), and upstream are the 70

bp repeats, which can be present in large arrays containing hundreds of copies. Located further upstream of these repeats lie between 8 and 12 expression site associated genes (*ESAGs*) and pseudogenes (Berriman *et al.*, 2002; Hertz-Fowler *et al.*, 2008; Young *et al.*, 2008). *ESAGs* 6 and 7 are the only *ESAGs* to have been found in every BES analysed to date and encode two subunits of the transferrin receptor which is required for iron uptake from the host (Schell *et al.*, 1991; Berriman *et al.*, 2002). Transcription of the active BES is carried out by RNA pol I from a single upstream promoter (Gunzl *et al.*, 2003). The parasite employs multiple mechanisms to ensure that only a single BES is actively transcribed at any one time and accumulating evidence suggests that multiple epigenetic phenomena may be involved in maintaining transcriptionally silent chromatin at inactive BESs (Rudenko, 2010; Horn and McCulloch, 2010).

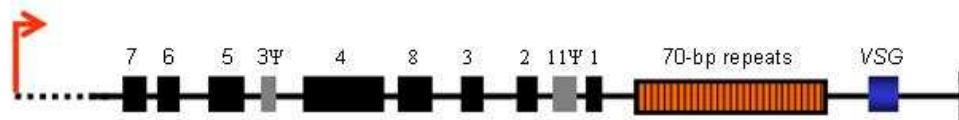


Figure 1-6 A schematic representation of a generic bloodstream expression site. The diagram shows an example of a *T. brucei* Lister 427 bloodstream expression site and indicates the variant surface glycoprotein (*VSG*, blue box) and expression-site associated genes (*ESAG* 1, 2, 3, 4, 5, 6, 7, 8, black boxes) separated by a region of 70 bp repeats (orange boxes). Also shown are the promoter (red arrow), telomeric repeat region (vertical black line), and pseudo-*ESAGs* (Ψ , grey boxes). Figure adapted from Hertz-Fowler *et al.*, 2008.

1.2.4 *VSG* switching mechanisms

Antigenic variation relies on the periodic switching of the surface antigen to an antigenically distinct variant. In *T. brucei* this is achieved by utilising the multiplicity of the BESs and also the vast archive of silent *VSG* genes and pseudogenes. *VSG* switching is spontaneous and occurs at a rate of about 10^{-2} to 10^{-3} switches per cell per generation in isolates recently recovered from hosts (pleomorphic cells; Lamont, Tucker, and Cross, 1986; Turner and Barry, 1989), but at a reduced rate in lab-adapted strains (monomorphic cells, 10^{-5} to 10^{-6} ; Turner, 1997). *VSG* switches appear to operate in a hierarchy; telomeric *VSGs* are activated earliest in infections, followed by intact subtelomeric *VSGs* and, lastly, pseudogenes are recombined to form mosaic *VSGs* (Thon *et al.*, 1990; Marcello and Barry, 2007; Morrison, Marcello, and McCulloch, 2009). The mechanisms that underlie this ordering strategy remain unknown (Capbern *et*

al., 1977;Morrison *et al.*, 2005), and we have only a partial picture of the mechanisms that drive VSG switching.

1.2.4.1 Transcriptional switching

Only one BES is actively transcribed at any one time, but because there may be up to 20 BESs, each containing a different VSG gene, switching to the expression of a new VSG can occur by turning off transcription of the active BES and activating a previously silent BES (Figure 1-7). This is termed transcriptional, or *in situ*, switching and is thought to occur by epigenetic mechanisms (Rudenko, 2010;Horn and McCulloch, 2010). However, this only allows access to a repertoire of approximately 20 VSG genes, which would rapidly become exhausted during the course of an infection. *In situ* switching is not thought to contribute significantly in pleomorphic cell lines (Robinson *et al.*, 1999), though it is thought to be the dominant switching mechanism in lab-adapted monomorphic cell lines (Barry, 1997). Mutation of a number of genes has been shown to result in the loss of singular ES transcription (Rudenko, 2010), and two genes, *DOT1B* and *Cohesin*, have been implicated in the switch between a silent and inactive BES (Figueiredo, Janzen, and Cross, 2008;Landeira *et al.*, 2009;Frederiks *et al.*, 2010). However, the trigger for such a switch, and the mechanisms that are thought to co-ordinate this process are unknown (Chaves *et al.*, 1998). Though a putative subnuclear site for BES transcription, termed the Expression Site Body (ESB), was described 10 years ago (Navarro and Gull, 2001), the nature of this entity remains obscure.

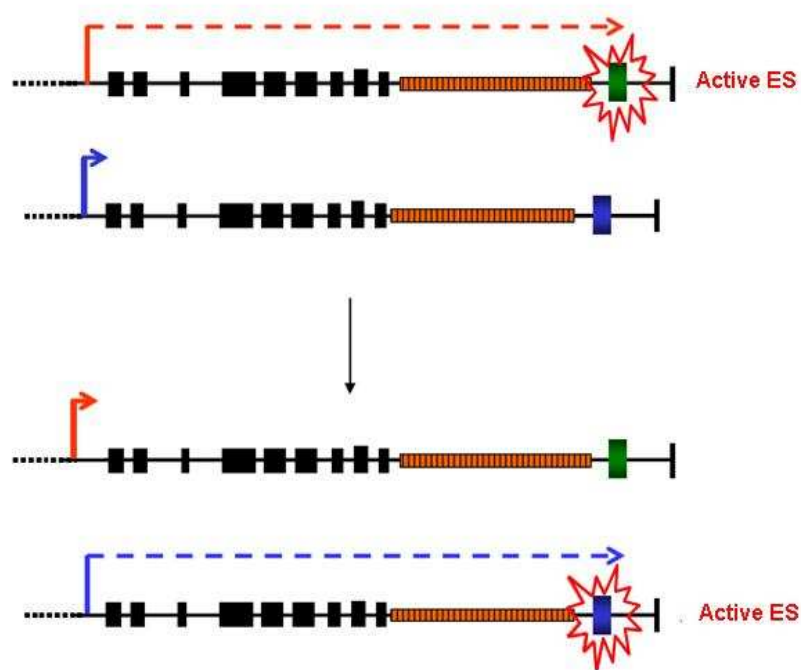


Figure 1-7 *In situ* transcriptional VSG switching.

An *in situ* transcriptional VSG switching event occurs when the active expression site (red dashed arrow) is transcriptionally switched off and a previously silent expression site (blue dashed arrow) is transcriptionally switched on. This results in the expression of the green VSG being switched off and the initiation of the expression of the blue VSG. Also shown are expression site associated genes (ESAG, black boxes), 70 bp repeats (orange boxes), promoter (red and blue arrows), and telomeric repeat region (vertical black line). Figure adapted from Rachel Dobson, PhD Thesis, 2009.

1.2.4.2 Recombinational switching

The most common form of VSG switching requires DNA recombination events. Such recombinational switching involves the movement of a VSG from a silent location in the genome into the active BES, replacing the existing VSG gene (Robinson *et al.*, 1999). There are three different pathways of recombinational switching all putatively utilising homologous recombination (HR). HR is commonly used by organisms to generate diversity in surface antigens, including *Candida albicans*, *Borrellia sp* and *Neisseria sp* (Palmer and Brayton, 2007).

The first recombinational pathway is gene conversion and involves copying a silent VSG gene from the megabase subtelomeric arrays, from a silent BES or from the telomere of a mini-chromosome, into the active BES where it replaces the existing, previously expressed, VSG (Figure 1-8). The amount of sequence copied is variable, but generally extends from the 70 bp repeats to homology in the 3' end of the VSG ORF, although this can extend into the 3' untranslated region (UTR) and beyond into the telomere (Liu *et al.*, 1983; Michels *et al.*, 1983; Timmers *et al.*, 1987; Matthews *et al.*, 1990). In monomorphic cell lines,

gene conversion reactions between BESs can utilise homology from at least 6 kb upstream of the *VSG*, beyond the 70 bp repeats (Lee and Van der Ploeg, 1987). Though *VSG* gene conversion commonly utilises the 70 bp repeats, the deletion of these sequences does not inhibit *VSG* switching (McCulloch, Rudenko, and Borst, 1997; Boothroyd *et al.*, 2009).

The second recombinational pathway is mosaic gene conversion and, as previously mentioned, allows the use of the vast archive of *VSG* pseudogenes and gene fragments to form novel *VSG* variants (Figure 1-9). Mosaic *VSG* genes are assembled using multiple segmental gene conversion reactions, and are distinct from the above conversions of intact *VSG*s because the reaction relies on regions of homology within *VSG* ORFs, rather than flanking homology. Mosaic *VSG* genes generally form and are expressed later in infections, perhaps because the reaction is less efficient (Thon *et al.*, 1990; Barbet and Kamper, 1993; Marcello and Barry, 2007). Indeed, it is not clear where the novel *VSG*s are formed, though they must eventually be moved to the BES.

The final recombinational pathway is telomere reciprocal exchange and involves a simple cross-over event between two telomeric *VSG*s, where the chromosome ends containing the active BES and a silent telomeric *VSG* (in an ES or mini-chromosome) are simply exchanged with no loss of DNA sequence (Figure 1-10). This pathway is thought to occur less commonly, as it is limited to telomeric *VSG*s (Pays *et al.*, 1985; Shea *et al.*, 1986).

Our understanding of the mechanisms of *VSG* switching by recombination stems primarily from the generation and analysis of *T. brucei* mutants in homologues of genes that have been implicated in HR. These are discussed below (section 1.5.3), but the broad conclusion is that *VSG* switching exploits HR, rather than being a specialised, parasite-specific reaction. Nonetheless, a number of questions remain. One question that has recently attracted attention is how the reaction is initiated. It has been suggested that a double strand break in the region of the BES 70 bp repeats forms a trigger for HR (Liu *et al.*, 1983; Boothroyd *et al.*, 2009). However, how such a break might form is unclear, and it is surprising that the deletion of the 70 bp repeats does not then impair *VSG* switching (McCulloch, Rudenko, and Borst, 1997). Another question surrounds mosaic *VSG* formation and whether it is a related reaction to intact

VSG gene conversion. The assays that have been used to examine the impact of gene mutation on VSG switching only detect early VSG switch events (McCulloch, Rudenko, and Borst, 1997; Kim and Cross, 2010), and no study has asked if mosaic VSG formation is similarly impaired.

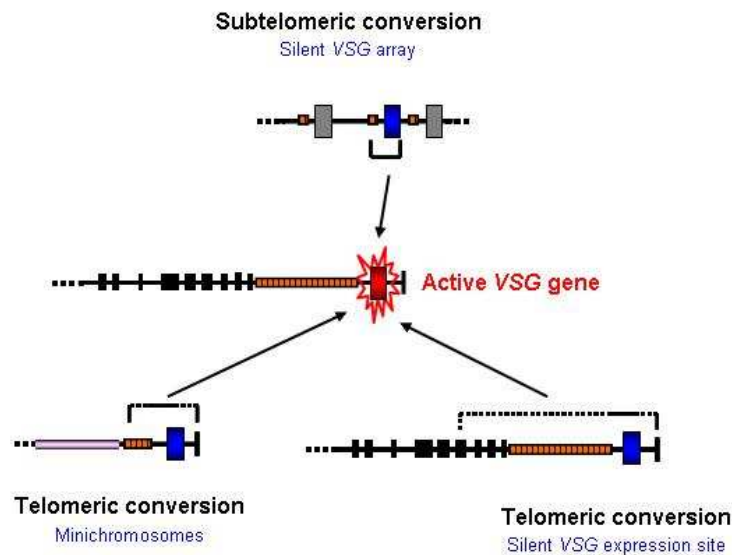


Figure 1-8 VSG switching utilises silent VSG genes from different genome locations. A silent VSG gene (blue boxes) is copied by homologous recombination into the active expression site replacing the existing active VSG (red box). Donor VSGs can come from subtelomeric silent VSG arrays, telomeric mini-chromosomal VSGs or one of the other silent VSG expression sites. Brackets indicate the amount of sequence copied, with dashes indicating variation in the amount of sequence that may be copied. Also shown are expression site associated genes (black boxes), 70 bp repeats (orange boxes), telomeric repeat region (vertical black line). Figure adapted from Rachel Dobson, PhD Thesis, 2009.

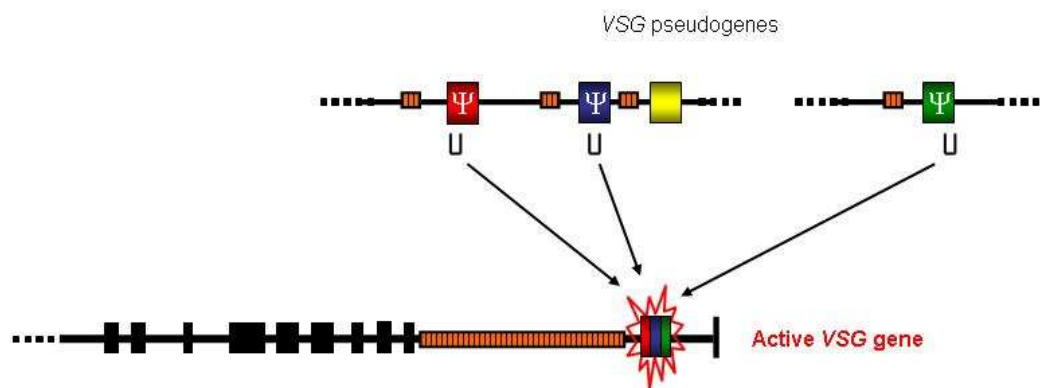


Figure 1-9 Mosaic VSG formation by segmental gene conversion. A new mosaic VSG gene (red, blue and green box) is formed by segmental gene conversion from a number of VSG pseudogenes (Ψ , red, blue and green boxes). Brackets indicate the extent of sequence copied. Also shown are expression site associated genes (black boxes), 70 bp repeats (orange boxes), and telomeric repeat region (vertical black line). Figure adapted from Rachel Dobson, PhD Thesis, 2009.

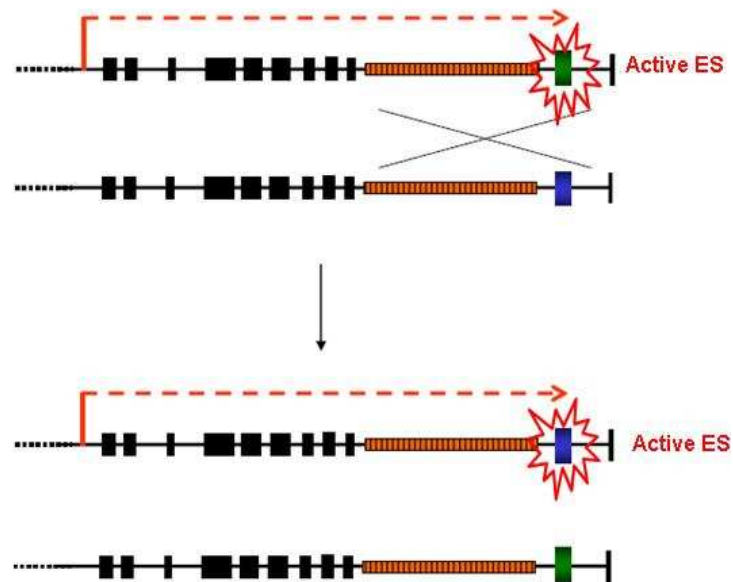


Figure 1-10 Telomere reciprocal exchange resulting in a VSG switching event. Telomere reciprocal exchange occurs when homologous recombination (crossed lines) between two BESs (shown, top) or an active BES and a silent mini-chromosomal VSG (not shown) leads to the simple switching of the VSG and/or surrounding sequences. The previously silent VSG (blue box) recombines into the active expression site (red dashed arrow). There is no loss of DNA during this cross-over event and both VSGs are retained. Also shown are expression site associated genes (black boxes), 70 bp repeats (orange boxes), promoter (red arrow), and telomeric repeats (vertical black line). Figure adapted from Rachel Dobson, PhD Thesis, 2009.

1.3 DNA repair

Genomes encode the information required to produce all cellular components within the structure of nucleic acid molecules. DNA and RNA allow this information to be stored, transferred between generations and read to allow protein production. Maintenance of the sequence fidelity of the genome is therefore of utmost importance. Many endogenous and exogenous agents, as well as the intrinsic instability of DNA molecules and the complex processes it undergoes, have the ability to cause damage to DNA (Kuzminov, 1995). The consequences of DNA damage include DNA fragmentation and rearrangement, which in multi-cellular organisms can lead to cancer and ultimately death (Khanna and Jackson, 2001). It is therefore desirable, at least in most settings, that DNA damage is repaired as swiftly as possible without the loss of genome fidelity. Given the diversity of DNA damage, many different mechanisms of DNA repair exist. These mechanisms may be broadly divided into two groups; those that join broken DNA molecules by repairing phosphodiester bonds at strand breaks, and those that use excision mechanisms to remove damaged bases or strands. Three main pathways of excision repair have been described: mismatch

repair (MMR), base excision repair (BER) and nucleotide excision repair (NER). All three mechanisms have two common properties; the use of a nuclease(s) to remove the damaged bases and a DNA polymerase(s) and ligase(s) to fill in the resulting gap and repair the DNA backbone. The specific proteins used in the three pathways differ greatly and, as these processes are not closely related to the subject of this thesis, they will not be discussed further.

1.3.1 Double strand break repair

Amongst the lesions that break the phosphodiester backbone of DNA molecules, those in which both strands are cleaved, termed DNA double strand breaks (DSBs), are considered particularly genotoxic. DSBs arise frequently during DNA replication and can also be induced by ionising radiation, mutagenic chemicals and free radicals. Repair of DSBs occurs primarily by two independent mechanisms; non-homologous end joining (NHEJ) and homologous recombination (HR) (Figure 1-11). These two pathways of DSB repair are conserved in most eukaryotes. However, NHEJ appears to be favoured in mammalian cells, whilst HR is favoured by lower eukaryotes (Liang *et al.*, 1998). There are a number of determinants that have been shown to affect repair pathway choice, including the cell cycle stage at which the DNA damage occurs, the position of the DSB along the chromosome and the nature of the DNA substrate (Kass and Jasin, 2010; Symington and Gautier, 2011; Xu and Price, 2011), however the precise mechanism remains to be elucidated.

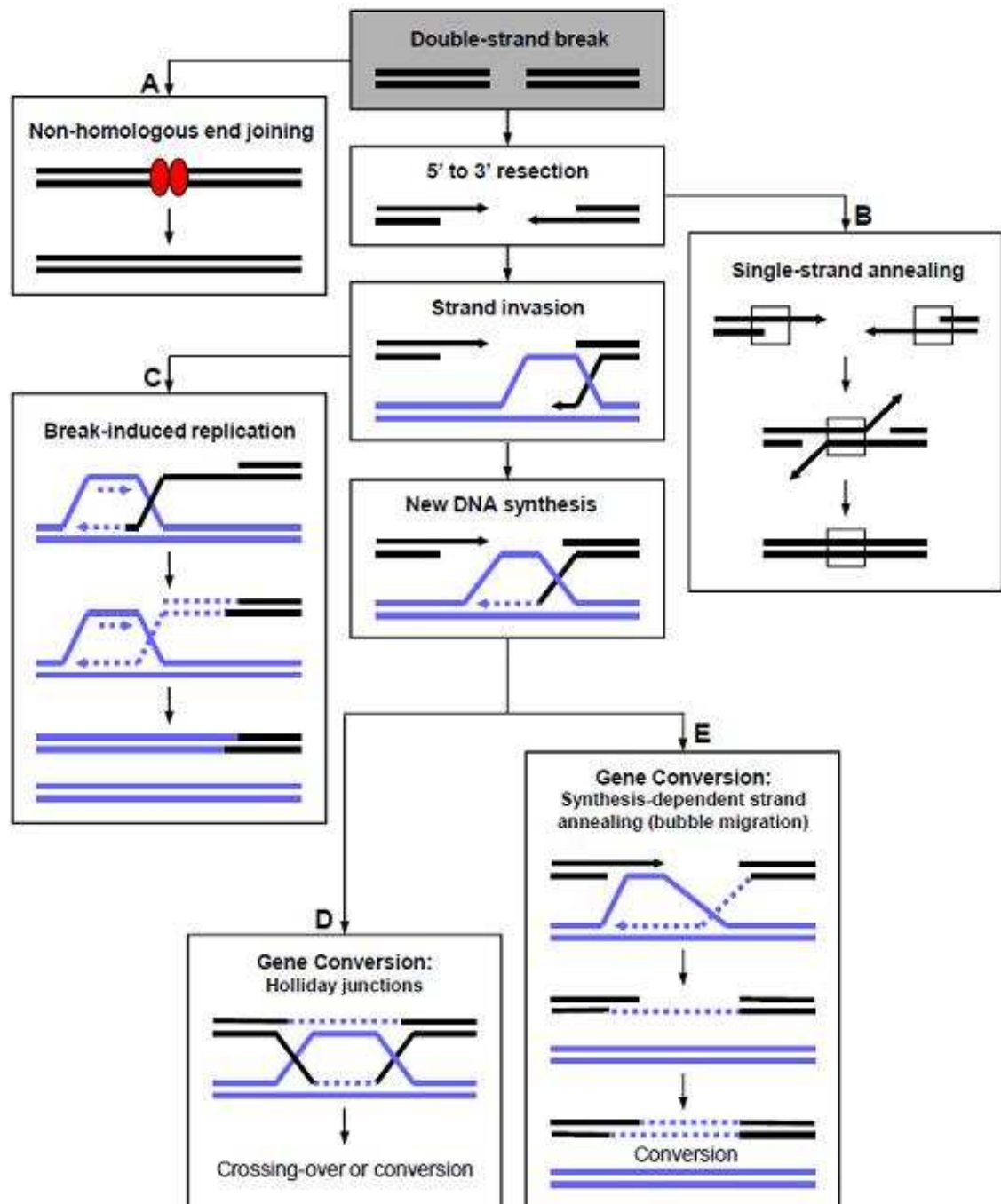


Figure 1-11 Pathways of eukaryotic DNA double strand break repair.

The two main pathways of eukaryotic DSB repair; non-homologous end joining (A), and homologous recombination (B - E). DNA containing a DSB is represented by black lines, intact duplex DNA by blue lines, newly synthesised DNA by dashed lines, and NHEJ machinery by red circles. (B) Single-strand annealing (SSA) occurs where the boxes indicate sequence homology, (C) Break-induced replication (BIR), and (D-E) Gene conversion. Figure adapted from Jo Bell, PhD thesis, 2002.

1.3.2 Non-homologous end joining

Non-homologous end joining involves the repair of a DSB by re-ligation of the DNA ends and frequently results in changes in the DNA sequence at the site of the DSB through loss or addition of sequence. No sequence homology is required for NHEJ to occur and therefore NHEJ acts on a wide variety of DSB substrates

(Lieber *et al.*, 2008;Lieber, 2010). The core proteins that carry out NHEJ consist of; the Ku heterodimer (Ku70 and Ku80), the catalytic subunit DNA-PKcs, and the DNA ligase IV-XRCC4 complex (Figure 1-12). The Ku heterodimer forms a DNA end-binding complex that recognises and binds, with high affinity, to both ends of the DSB, forming a bridge and leading to recruitment of other NHEJ factors. DNA-PKcs is the first factor to be recruited, and there is some evidence to suggest that (auto-) phosphorylation plays a role in the interaction of DNA-PKcs at the DSB (Smith and Jackson, 1999;Dobbs, Tainer, and Lees-Miller, 2010). However, this phosphorylation is not essential as some eukaryotes, including yeast, lack a homolog of DNA-PKcs (Critchlow and Jackson, 1998;Featherstone and Jackson, 1999;Parsons *et al.*, 2005). DNA-PKcs is a member of the phosphatidylinositol 3-kinase-like kinase (PIKK) family that includes ATM and ATR, which are also involved in the response to DNA damage (Smith and Jackson, 1999). The next factor to be recruited is the DNA ligase complex consisting of DNA ligase IV and the XRCC4 protein, a ligase IV-interacting protein (Sibanda *et al.*, 2001). The gaps in the DNA are ligated together and the break is repaired. It has been shown that NHEJ is the main pathway in V(D)J recombination, which creates diversity among the immunoglobulin and T cell receptor genes found in the mammalian immune system (Xu *et al.*, 2005). To date, no evidence for NHEJ has emerged from studies of DNA repair in *T. brucei* and related kinetoplastids (Conway *et al.*, 2002b;Glover, McCulloch, and Horn, 2008). Indeed, there is no bioinformatic evidence for the existence of DNA ligase IV or XRCC4 (Burton *et al.*, 2007), though each Ku subunit is present (Conway *et al.*, 2002a;Janzen *et al.*, 2004).

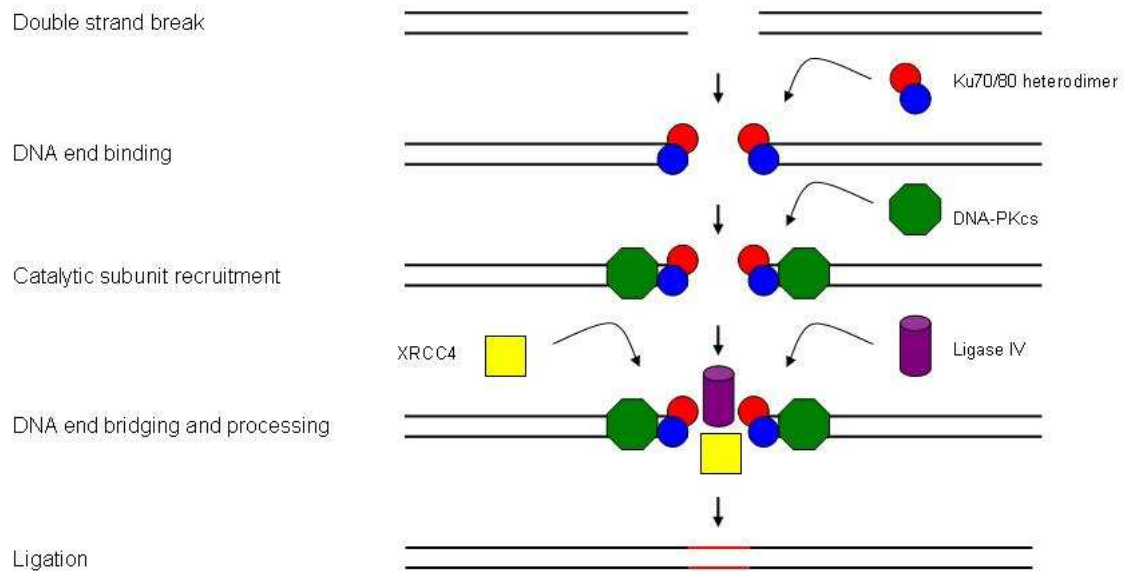


Figure 1-12 The core proteins involved in non-homologous end joining. Black lines represent duplex DNA. Following a DSB the Ku70/80 heterodimer (red and blue circles) binds to the DNA ends and recruits the catalytic subunit of the DNA protein kinase (DNA-PKcs, green octagon). The DNA ligase IV – XRCC4 complex (purple cylinder and yellow square) is recruited to complete the ligation reaction. Figure adapted from Claire Hartley, PhD Thesis, 2008.

1.3.2.1 Micro-homology mediated end joining

A number of reports have shown a distinct form of DSB end-joining that is mediated by short, ~ 5-25 bp stretches of sequence homology (Decottignies, 2007). This pathway was thought to act as a backup to classical NHEJ (Nussenzweig and Nussenzweig, 2007), but has been shown to play a prominent role in Ig class switch recombination in B cells (Yan *et al.*, 2007) and cancer development (Zhu *et al.*, 2002). The micro-homology mediated end joining (MMEJ) pathway is independent of core NHEJ factors, such as Ku70 and Ku80, but the precise proteins involved are as yet unknown (McVey and Lee, 2008), meaning it is unclear if it is distinct from NHEJ or HR, or uses aspects of both pathways. Nonetheless, MMEJ has been described in *T. brucei* both *in vivo* and *in vitro* (Conway *et al.*, 2002b; Burton *et al.*, 2007; Glover, McCulloch, and Horn, 2008; Glover, Jun, and Horn, 2011), and may have assumed the role of NHEJ, though until catalytic factors can be identified its functional significance is hard to define.

1.3.3 Homologous recombination

Homologous recombination involves the repair of a DSB by utilising the homologous sequence of an unbroken DNA molecule as a template and therefore

generally conserves the sequence fidelity of the genome. HR is conserved in all organisms, from bacteria to humans (Cromie, Connelly, and Leach, 2001), and is more complex than NHEJ, involving multiple sub-pathways and a greater number of factors. HR has been shown to repair DSBs resulting from stalled or collapsed replication forks (section 1.3.5) and exposure to DNA damaging agents (Petermann and Helleday, 2010; Symington and Gautier, 2011). It also has a role in the exchange of genetic material during meiosis, creating genetic diversity (Ehmsen and Heyer, 2008), and in antigenic variation of pathogens such as *T. brucei* (Vickerman, 1978). HR can be split into a number of different mechanisms, including single-strand annealing (Figure 1-11B), break-induced replication (Figure 1-11C) and gene conversion (Figure 1-11D and E). These mechanisms appear quite different, and appear to employ subtly differing catalytic components, but share the use of a homologous template and the same catalytic steps of pre-synapsis, synapsis and post-synapsis (Hamatake, Dykstra, and Sugino, 1989; San Filippo, Sung, and Klein, 2008; Holthausen, Wyman, and Kanaar, 2010). HR in eukaryotes requires a large number of proteins known as the Rad52 epistasis group, which include the proteins Rad50, Rad51, Rad52, Rad54, Rad55, Rad57, Rad59, Mre11 and Xrs2 (Symington, 2002). Rad51 is a recombinase enzyme and acts by forming a helical nucleoprotein filament on single-stranded DNA (ssDNA) to facilitate HR (section 1.6). Rad51 is functionally and structurally conserved with RecA and RadA in bacteria and archaea, respectively. The other members of the Rad52 epistasis group appear to promote Rad51 activity, acting either upstream or downstream of the formation of the Rad51 nucleoprotein filament (Symington, 2002).

1.3.4 Mechanism of homologous recombination

The proteins involved in the early stages of HR in eukaryotes are displayed in Figure 1-13. In pre-synapsis, the DSB is recognised and the DNA ends are resected by exonucleases to reveal 3' ssDNA overhangs which allow the binding of the recombinase (Rad51/RadA/RecA in eukaryotes/archaea/bacteria, respectively) with the aid of cofactors. DNA end resection is carried out by the RecBCD complex in bacteria, the MRX complex in yeast (comprising of Mre11, Rad50 and Xrs2) and the MRN complex in mammals (comprising of Mre11, Rad50 and Nbs1) (Paull, 2010; Longhese *et al.*, 2010; Symington and Gautier 2011). These complexes all have helicase and nuclease activity and are responsible for

the production of 3' ssDNA overhangs that can be thousands of bases long (White and Haber, 1990; Sun, Treco, and Szostak, 1991). In eukaryotes, the ssDNA overhangs are coated with replication protein A (RPA), a homologue of the bacterial ssDNA-binding protein (SSB). These proteins have wider roles in the cell than simply acting in HR, but protect the ssDNA from nucleases and also remove any secondary structure which is inhibitory to nucleoprotein filament formation (Sugiyama, Zaitseva, and Kowalczykowski, 1997). Cofactors involved in the loading of the recombinase onto the ssDNA overhangs must first remove RPA/SSB from the ssDNA (Sung, 1997a; Sung, 1997b). Rad52 has been shown to carry out this function in yeast and mammals (Sung, 1997a; Benson, Baumann, and West, 1998), however, Rad52 is absent from *D. melanogaster*, *C. elegans* and *T. brucei*. Evidence exists that the breast cancer susceptibility protein BRCA2 can carry out this role (section 1.4). Most eukaryotes express multiple Rad51-related proteins, often called Rad51 paralogues, which aid Rad51 function and are required for recombinational DNA repair (Thacker, 2005; Lin *et al.*, 2006). Yeast utilise a complex of Rad55 and Rad57 to help nucleate the Rad51 nucleoprotein filament on ssDNA (Hays, Firmenich, and Berg, 1995; Sung, 1997b). Mammals contain five Rad51 paralogues, which form two distinct complexes, the precise functions of which have not yet been ascertained (Suwaki *et al.*, 2011). In *T. brucei*, four RAD51 paralogues are found, each of which acts in HR and influences the subnuclear mobility of RAD51 (Proudfoot and McCulloch, 2005; Dobson *et al.*, 2011). In addition, at least three of the RAD51 paralogues have been shown to interact and therefore presumably form a complex or complexes (Dobson *et al.*, 2011), but the evolutionary relationship between these proteins and those present in yeast and mammals remains unclear.

Once the DNA-recombinase nucleoprotein filament has been assembled synapsis, or strand exchange, occurs. This involves the invasion of a homologous duplex DNA molecule by the broken DSB end(s) and the formation of a displacement-loop (D-loop) structure at the point of base-pairing. Strand invasion is aided by Rad54, a double-stranded DNA (dsDNA)-dependent ATPase, which is a member of the Swi2/Snf2 family of chromatin remodelling factors (Heyer *et al.*, 2006; Mazin *et al.*, 2010) Rad54 uses the energy released from the hydrolysis of ATP to supercoil and separate the strands of the homologous DNA template and stabilise the nucleoprotein filament (Heyer *et al.*, 2006; Mazin *et al.*, 2010). DNA synthesis

occurs following the formation of the D-loop structure using the 3' DSB end as a primer and the homologous strand as a template (Paques and Haber, 1999; Holmes and Haber, 1999). The second 3' end of the DSB can also invade the D-loop in a process called second end capture, this can lead to the formation of a four-branched DNA structure called a Holliday Junction (HJ) (Holliday, 1964).

In post-synapsis the resolution of the strand exchange intermediate takes place. Cleavage of the HJ is carried out, at least in humans, by a recently discovered resolvase, GEN1 (Ip *et al.*, 2008; Rass *et al.*, 2010), and yields either a crossover product (section 1.3.4.3) or a non-crossover product (gene conversion; section 1.3.4.4).

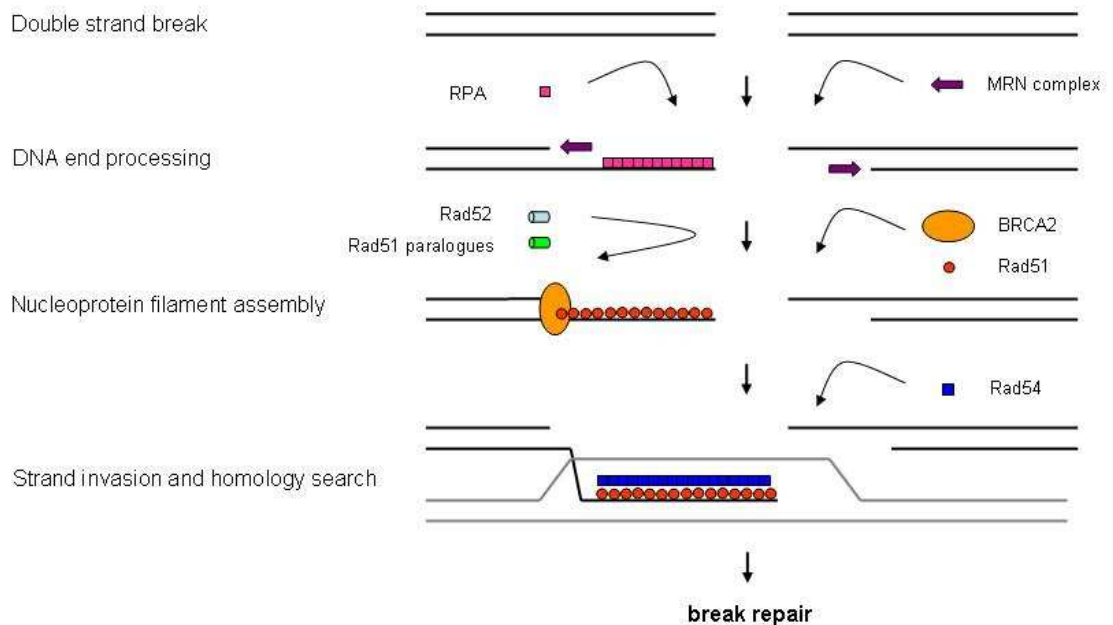


Figure 1-13 The proteins involved in the early stages of eukaryotic homologous recombination.

Black lines represent duplex DNA and grey lines represent intact duplex DNA used as a template for repair. Following a DSB the 5' ends of the DSB are resected with the aid of the MRN complex (purple arrow) to form 3' ssDNA tails. The ssDNA tails become coated with RPA (pink squares). The loading of the Rad51 (red circles) nucleoprotein filament is aided by Rad52 (light blue cylinder), the Rad51 paralogues (green cylinder) and BRCA2 (orange oval). The filament then actively 'scans' the genome for homologous sequences in a 'strand invasion' process that is aided by Rad54 (dark blue squares). Following this, one tail invades the homologous DNA duplex forming a displacement (D)-loop, which is then extended by DNA synthesis (not shown). Figure adapted from Claire Hartley, PhD Thesis, 2008.

1.3.4.1 Single-strand annealing

Single-strand annealing (Figure 1-11B) occurs on repetitive DNA sequences and is a Rad51-independent HR pathway, which usually involves the loss of some genetic material (Paques and Haber, 1999). Following the formation of a DSB,

the 5' ends are resected to expose complementary regions within the 3' strands flanking the break site. These complementary sequences are able to anneal to each other, eliminating the need for a strand exchange step. The 3' non-homologous ends are excised and DNA synthesis and ligation complete the repair. Annealing of the complementary sequences is facilitated by accessory proteins: Rad52 can act in this way in *H. sapiens*, *U. maydis* and *S. cerevisiae* (Sugiyama, New, and Kowalczykowski, 1998;Kojic *et al.*, 2008;Feng *et al.*, 2011;Liu and Heyer, 2011), and BRCA2 homologues (section 1.4) in *U. maydis* and *C. elegans*, which lacks a Rad52 homologue, have also been shown to function in the SSA pathway (Petalcorin *et al.*, 2006;Mazloum, Zhou, and Holloman, 2007).

1.3.4.2 Break-induced replication

Break-induced replication (Figure 1-11C) involves invasion by only one end of the DSB and can occur by both Rad51-dependent and Rad51-independent mechanisms (McEachern and Haber, 2006;Llorente, Smith, and Symington, 2008). Once DNA resection has occurred the 3' ssDNA overhang invades a homologous chromosome. Following this, a replication fork is established and the chromosome is copied for long distances, even to the chromosome end. Rad51-dependent BIR is much more efficient than Rad51-independent, but requires a longer length of homologous substrate (Davis and Symington, 2004;Malkova *et al.*, 2005).

1.3.4.3 Gene conversion

Gene conversion allows the transfer of genetic material from one DNA molecule to its homologue in a uni-directional manner, and is the most common mechanism of HR in DSB repair (Chen *et al.*, 2007). Gene conversion occurs most frequently between newly replicated sister chromatids, in which settings it is genetically silent. However, it can also occur between two allelic chromosomes, and between homologous sequences on different chromosomes (Chen *et al.*, 2007). If an HJ is formed following the formation of the strand exchange intermediate(Figure 1-11D), the product generated from resolution of this HJ depends on the orientation of strand cleavage (Figure 1-14): a non-crossover product results from cleavage of the HJ along the one axis and results in gene conversion; if the strands are cleaved along different axes, a non-crossover

product is generated. This model for DSB repair predicts that HJ resolution would lead to an equal number of crossover and non-crossover events. However, this is not the case, as mitotic recombination events result in an extremely low occurrence of crossover events (Esposito, 1978; Haber and Hearn, 1985; Kupiec and Petes, 1988). To account for this, the synthesis-dependent strand annealing (SDSA) model was proposed (section 1.3.4.4; Nassif *et al.*, 1994; Paques and Haber, 1999).

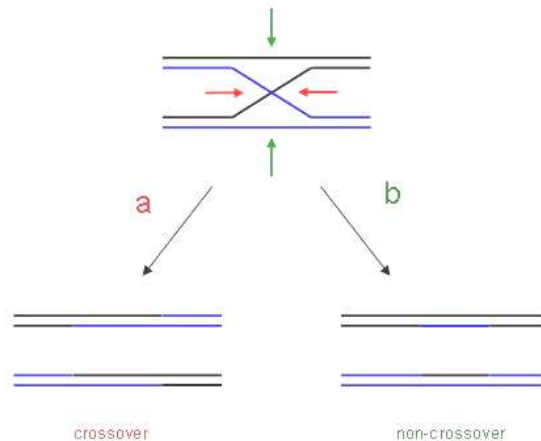


Figure 1-14 Holliday junction resolution.

A schematic representation of the two possible products formed following Holliday junction resolution. A crossover product occurs when cleavage of both strands of the HJ occurs along the same axis (a, red arrows) and a non-crossover event occurs when cleavage of the HJ occurs in different axes (b, green arrows). Figure adapted from Rachel Dobson, PhD Thesis, 2009.

1.3.4.4 Synthesis-dependent strand annealing

In this model (Figure 1-11E), only one 3' strand invades the homologous DNA template, while the other strand remains unengaged (Nassif *et al.*, 1994). Following DNA polymerisation, the newly synthesised strand is then displaced from the template and anneals to the previously unengaged 3' strand by a second strand annealing step, allowing repair of the DSB (Haber *et al.*, 2004; Ira, Satory, and Haber, 2006). The products that arise from this process are predominantly non-crossover. However, modification of the pathway can lead to crossover events (Ferguson and Holloman, 1996).

1.3.5 The role of homologous recombination in replication

As already mentioned, HR has been shown to be involved in the repair of stalled replication forks that are often associated with genome rearrangements (Michel *et al.*, 2007;Nagaraju and Scully, 2007;Budzowska and Kanaar, 2009;Petermann and Helleday, 2010;Branzei and Foiani, 2010). Replication forks may stall and collapse for a variety of reasons, including damage to DNA replication substrates, DNA-bound proteins blocking replication progression, DNA secondary structures and transcription. HR is implicated in at least three pathways of replication fork re-start or repair. Firstly, trans-lesion synthesis uses error-prone DNA polymerases to by-pass a DNA lesion and enables the progression of replication across the lesion (Prakash, Johnson, and Prakash, 2005). The DNA lesion remains (called a daughter strand gap) and may be repaired using the sister chromatid as a template in an HR mechanism called sister chromatid recombination (SCR) (Scully, Puget, and Vlasakova, 2000;Michel *et al.*, 2004;Nagaraju and Scully, 2007). Secondly, template switching may occur when a stalled replication fork switches to using the nascent daughter strand as a replication template. HR is implicated in this process that often leads to complex genome rearrangements, such as observed in yeast and *U. maydis* (Lambert *et al.*, 2005;Mazloum and Holloman, 2009;Lambert *et al.*, 2010). Finally, the HR proteins Rad51 and BRCA2 have been shown to play multiple roles during DNA replication, including maintaining replication fork progression (Daboussi *et al.*, 2008), stabilisation of stalled replication forks (Lomonosov *et al.*, 2003), protection against degradation of nascent DNA (Hashimoto *et al.*, 2010;Schlachter *et al.*, 2011), direct processing of stalled replication forks into DSBs (Michel *et al.*, 2004), and reversal of stalled replication forks to allow replication re-start without the occurrence of DNA damage (Michel *et al.*, 2001). *brca2* mutant phenotypes, which include an accumulation of gross chromosomal rearrangements and extensive chromosomal abnormalities (section 1.4;Patel *et al.*, 1998;Yu *et al.*, 2000), point to a failure in replication fork rescue by HR (Michel, Ehrlich, and Uzest, 1997;Seigneur *et al.*, 1998;Chen and Kolodner, 1999).

The repair of DNA structures created during replication has been proposed to occur during the G2 gap phase of the cell cycle, prior to entry into mitosis and

after S-phase and the completion of DNA replication (Su, Bernal, and Venkitaraman, 2008). Microscopically visible focal accumulations containing Rad51, BRCA1, BRCA2 and PCNA (proliferating cell nuclear antigen) form in undamaged S-phase mammalian cells where they are proposed to be repair centres for broken replication forks (Tashiro *et al.*, 1996; Scully *et al.*, 1997; Chen *et al.*, 1998). However, the formation of these Rad51 replication-coupled repair foci does not require BRCA2 or the Rad51 paralogues (Tarsounas, Davies, and West, 2004). The multiple pathways for the bypass and removal of DNA-template lesions, and for the restart of stalled replication forks, highlights the importance of such mechanisms to ensure that DNA replication is completed faithfully every cell cycle (Michel *et al.*, 2004).

1.4 BRCA2

1.4.1 The discovery of BRCA2

Breast cancer is one of the most common causes of cancer-related deaths in women and approximately 10% of individuals who develop the disease are genetically predisposed to it (Nathanson, Wooster, and Weber, 2001). The first breast cancer susceptibility gene, *BRCA1*, was identified in 1990 by linkage analysis and positional mapping (Hall *et al.*, 1990). However, a failure to assign all cases of breast cancer to a mutation in *BRCA1* led to the search for a second breast cancer susceptibility gene and, in 1995, *BRCA2* was identified (Wooster *et al.*, 1994; Wooster *et al.*, 1995). The products of both these genes function in the maintenance of genome stability through HR (Moynahan *et al.*, 1999; Xia *et al.*, 2001; Moynahan, Pierce, and Jasin, 2001). However, they are remarkably different proteins, most notably in terms of their size and the proteins with which they interact (Figure 1-15). The following sections will focus on the BRCA2 protein, which is the subject of this thesis.

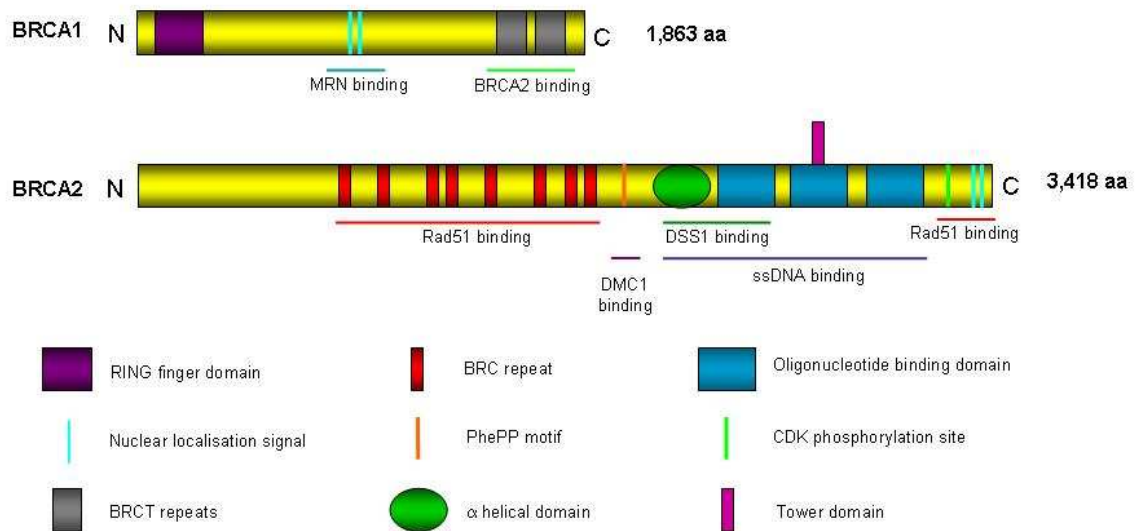


Figure 1-15 A representation of human BRCA1 and BRCA2 proteins showing their functional domains and interacting proteins.

Both proteins are large polypeptides (1,863 and 3,418 amino acids, respectively) that interact with each other and with several other proteins. BRCA1 interacts with BRCA2 and the MRN (Mre11/Rad50/Nbs1) complex. The RING finger domain, nuclear localisation signals (NLSs) and BRCA1 C-terminal (BRCT) domains are indicated. Similarly, BRCA2 interacts with BRCA1, Rad51 (the HR recombinase), DMC1 (the meiosis-specific recombinase), and DSS1. The eight BRC repeats, the PhePP motif that interacts with DMC1, the DNA/DSS1-binding domain (alpha-helical domain, oligonucleotide-binding (OB) domains and tower domain) that interacts with ssDNA and DSS1, and the C-terminal NLSs and CDK phosphorylation site are indicated. Figure adapted from West, 2003.

1.4.2 The structure of BRCA2

The human BRCA2 protein is a large polypeptide, 3418 amino acid residues in length, and initial investigations revealed no obvious similarities with other published protein sequences (Wooster *et al.*, 1995). Further investigation revealed that BRCA2 contains several key motifs, including eight BRC repeats, a DNA binding domain (DBD) and two nuclear localisation signals (NLSs).

1.4.2.1 The BRC repeats

A series of eight degenerate BRC repeat motifs were discovered in the central third of BRCA2, encoded by exon 11 (Bork, Blomberg, and Nilges, 1996). These repeated motifs are highly conserved at the sequence level between mammalian BRCA2 proteins (Lo *et al.*, 2003). However, a remarkable degree of divergence exists between the eight BRC repeats within a single BRCA2 homologue (Figure 1-20), suggesting that they may have evolved to achieve different functions (Bork, Blomberg, and Nilges, 1996; Bignell *et al.*, 1997; Pellegrini and Venkitaraman, 2004). The BRC repeat motif is approximately 30 amino acid residues in length and separated by linker regions that vary in size from 60 to

300 amino acids, which show no sequence conservation (Bork, Blomberg, and Nilges, 1996; Bignell *et al.*, 1997).

The phenotypes of *brca2*^{-/-} mutants in mammalian cells include early embryonic lethality, severe growth retardation, impaired cell division and sensitivity to ionising radiation, indicating the essential function of this protein (Sharan *et al.*, 1997; Ludwig *et al.*, 1997; Suzuki *et al.*, 1997). A major breakthrough occurred when it was discovered that BRCA2 binds Rad51, the HR recombinase (Sharan *et al.*, 1997; Chen *et al.*, 1998; Marmorstein, Ouchi, and Aaronson, 1998). In mammalian cells, it was observed that after the induction of DNA damage BRCA2 and Rad51 co-localise to form mega-Dalton structures observed microscopically as foci, and that these Rad51 foci fail to form in the absence of BRCA2 (Yuan *et al.*, 1999; Tarsounas, Davies, and West, 2003). An interaction between BRCA2 and monomeric Rad51 was confirmed to occur at the BRC repeats, and six or eight of the BRC repeats have been reported to bind Rad51 *in vitro*, depending on the assay used (co-immunoprecipitation or yeast 2-hybrid; Wong *et al.*, 1997; Chen *et al.*, 1998; Marmorstein, Ouchi, and Aaronson, 1998). A possible explanation for the differences in Rad51 binding observed is that the level of sequence diversity across the BRC repeats could produce binding sites with a range of affinities for Rad51 (Pellegrini and Venkitaraman, 2004). Indeed, this theory is supported by the fact that although all BRC repeats have the ability to bind Rad51 *in vitro*, some bind with a stronger affinity than others (see below; Chen *et al.*, 1998; Esashi *et al.*, 2005; Thorslund, Esashi, and West, 2007; Carreira and Kowalczykowski, 2011).

The elucidation of the X-ray crystal structure of human BRC repeat 4 bound to the core domain of Rad51 led to the identification of a seven amino acid motif (F-TASGK) located within the BRC repeat that is critical for making hydrophobic and hydrophilic interactions with Rad51 (Pellegrini *et al.*, 2002). These residues are conserved in all of the eight BRC repeats in human BRCA2 and form a BRC repeat sequence fingerprint (Pellegrini *et al.*, 2002; Lo *et al.*, 2003). Point mutations within the BRC repeat fingerprint are associated with an increased susceptibility to breast and ovarian cancers and have been shown to be sufficient to disrupt the binding of Rad51 to the BRC repeat motif (Chen *et al.*, 1999), indicating the importance of this motif in the regulation of Rad51 by BRCA2 (Gayther *et al.*, 1997; Davies *et al.*, 2001; Pellegrini *et al.*, 2002; Tal,

Arbel-Goren, and Stavans, 2009;Ochiai *et al.*, 2011). Further analysis has identified a second structural domain of the BRC repeat, within an alpha-helical context, that is also essential for the interaction with Rad51 (Rajendra and Venkitaraman, 2010). Additionally, it has been shown that an oligomerisation motif in Rad51 exists at the subunit-subunit interface (section 1.6), which has been shown to function in the assembly of Rad51 into multimeric filament and ring forms (Pellegrini *et al.*, 2002;Shin *et al.*, 2003). It is thought that the BRC repeat mimics this oligomerisation motif using a β -hairpin structure and so regulates the assembly of Rad51 filaments onto DNA (Pellegrini *et al.*, 2002;Lo *et al.*, 2003;Shin *et al.*, 2003;Nomme *et al.*, 2008).

A recent paper has systematically analysed Rad51 binding by each of eight peptides corresponding to the BRC repeats *in vitro* and showed that there are two categories of BRC repeat in human BRCA2 (Figure 1-16;Carreira and Kowalczykowski, 2011). The first category, consisting of BRC repeats 1 to 4, bind with high affinity to monomeric Rad51, reduce its ATPase activity, and maintain the recombinase in an active ATP-bound state until required (Carreira *et al.*, 2009;Carreira and Kowalczykowski, 2011). In addition, members of this category of BRC repeats limit the assembly of Rad51 onto dsDNA and have the ability to remove RPA from ssDNA, thereby promoting nucleation onto ssDNA (Davies *et al.*, 2001;Galkin *et al.*, 2005;San Filippo *et al.*, 2006;Shivji *et al.*, 2009;Carreira *et al.*, 2009). BRC4 has also been shown to disrupt Rad51-dsDNA nucleoprotein filaments when present in molar excess of Rad51 (Davies *et al.*, 2001;Tarsounas, Davies, and West, 2004;Davies and Pellegrini, 2007;Esashi *et al.*, 2007). The second category of BRC repeats, consisting of BRC repeats 5 to 8, bind free Rad51 with low affinity but bind to Rad51-ssDNA filaments with high affinity and function to stabilise these filaments through a reduction in ATP hydrolysis by Rad51, thereby promoting nascent filament growth (Galkin *et al.*, 2005;Carreira *et al.*, 2009;Carreira and Kowalczykowski, 2011). It is thought that the two groups of BRC repeats co-operate in order to bring about delivery of monomeric Rad51 to the site of DNA damage, facilitate efficient filament nucleation preferentially onto ssDNA whilst impeding nucleation on dsDNA and the propagation of filament growth through binding and stabilisation, thereby stimulating DNA strand exchange.

The requirement for eight copies of the BRC repeat motif observed in human BRCA2 was originally postulated to be an adaptation to deliver sufficient Rad51 molecules to the sites of DNA damage, thereby allowing efficient repair (Pellegrini and Venkitaraman, 2004). However, experiments in *brca2* mutant cell lines expressing a single BRC repeat fused to the ssDNA-binding domain of RPA70 showed a partial reversal of the *brca2* phenotype with substantially improved HR and DNA repair, suppression of genome instability and restoration of Rad51 focus formation after DNA damage, indicating that BRCA2 with a single BRC repeat can function in HR to some extent (Saeki *et al.*, 2006). Also, BRCA2 orthologues in *Caenorhabditis elegans* and *Ustilago maydis* function with a single BRC repeat (section 1.5.1 and 1.5.2, respectively; Kojic *et al.*, 2002; Martin *et al.*, 2005). The additional BRC repeats could simply be indicative of the necessity for greater control of HR in the putatively more complex biological systems acting in mammals. However, if correct, there are exceptions to this rule, most notably the *T. brucei* homologue of BRCA2 that is predicted to contain up to fifteen BRC repeats (section 1.5.3.1; Lo *et al.*, 2003; Hartley and McCulloch, 2008).

1.4.2.2 Rad51 binding at the BRCA2 C-terminus

Human BRCA2 has also been shown to bind Rad51 at an extreme C-terminal motif, encoded by exon 27, that is highly conserved in mammalian BRCA2 and distinct from the BRC repeat motif (Mizuta *et al.*, 1997; Sharan *et al.*, 1997; Esashi *et al.*, 2005; Esashi *et al.*, 2007; Davies and Pellegrini, 2007). This C-terminal motif has the ability to bind Rad51 in its oligomerised heptameric ring form, and also Rad51-DNA nucleoprotein filament form, by binding at the interface between two Rad51 monomers. In both settings BRCA2 binding functions to stabilise the Rad51 multimeric forms (Davies and Pellegrini, 2007; Esashi *et al.*, 2007). This C-terminal Rad51 binding motif is phosphorylated by unknown cyclin-dependent kinases (CDKs) at Serine 3291 (S3291), and this phosphorylation functions to abrogate the interaction of the C-terminal binding domain with Rad51 (Esashi *et al.*, 2005). The extent of S3291 phosphorylation was shown to decrease after the induction of DNA damage by ionising radiation (Esashi *et al.*, 2005), and to increase as cells progress from G2 to M phase. Thus, it was postulated S3291 phosphorylation allows BRCA2 to regulate Rad51-dependent HR to ensure completion of DNA repair before entry into mitosis. In addition, induced DNA damage results in increased BRCA2-Rad51 interaction via

the C-terminal motif, and perhaps overcomes cell-cycle regulation to allow dephosphorylation of S3291, Rad51 filament binding and stabilisation, thereby stimulating HR-mediated repair of DNA damage (Lord and Ashworth, 2007). Cancer-associated mutations in BRCA2 occur at S3291 and residue 3292, which could disrupt the regulation of Rad51 by this C-terminal motif (McAllister *et al.*, 2002; Donoho *et al.*, 2003; Esashi *et al.*, 2005). The binding and stabilisation of Rad51 nucleoprotein filaments by the C-terminus of BRCA2 and was initially thought to protect against filament disassembly by BRC repeat 4 (Davies and Pellegrini, 2007; Esashi *et al.*, 2007). However, in light of the role of a subset of the BRC repeats in the stabilisation of Rad51-ssDNA nucleoprotein filaments, the function of the C-terminal Rad51-binding domain has been re-investigated. Recent work has suggested that this C-terminal Rad51-binding motif is dispensable for DNA repair by HR as a derivative of chicken BRCA2 with the C-terminal CDK phosphorylation site mutated to mimic the constitutive presence of a phosphate group (and therefore unable to bind Rad51) did not show any detectable DNA repair or recombination defects (Ayoub *et al.*, 2009). However, the disassembly of Rad51 foci after the induction of DNA damage was shown to be impaired and linked to a delay in the onset of mitosis (Ayoub *et al.*, 2009). The finding that this CDK phosphorylation site mutant is capable of supporting DNA repair and HR is consistent with earlier work that showed the C-terminus of mammalian BRCA2, encompassing all residues downstream of the most C-terminal BRC repeat, can be replaced with RPA and still function in these processes (Saeki *et al.*, 2006); it was not determined if cells expressing such a fusion protein display mitosis defects. Very recent work has also indicated that the C-terminal Rad51-binding domain of human BRCA2 may be critical for the protection of stalled replication forks from degradation (Schlachter *et al.*, 2011), and may function through the stabilisation of Rad51 nucleoprotein filaments on nascent ssDNA (Figure 1-17; Hashimoto *et al.*, 2010).

1.4.2.3 Rad51 binding in the context of full-length BRCA2

The large size of the human BRCA2 protein had precluded the purification of the full-length polypeptide until 2010, when three labs published the purification of BRCA2 by three distinct methods (Jensen, Carreira, and Kowalczykowski, 2010; Liu *et al.*, 2010; Thorslund *et al.*, 2010). Initial experiments *in vitro* demonstrate that BRCA2 binds approximately six Rad51 molecules (Liu *et al.*,

2010;Jensen, Carreira, and Kowalczykowski, 2010), directs the nucleation of Rad51 filaments onto ssDNA in preference over dsDNA (Thorslund *et al.*, 2010;Liu *et al.*, 2010;Jensen, Carreira, and Kowalczykowski, 2010), and stimulates the displacement of RPA by the Rad51 filament (although a direct interaction with RPA was not observed;Liu *et al.*, 2010;Jensen, Carreira, and Kowalczykowski, 2010). A role for DSS1 (section 1.4.2.4) in the stimulation of BRCA2-mediated Rad51 binding to RPA-covered ssDNA was also observed (Liu *et al.*, 2010). BRCA2 was also shown to stabilise active ATP-bound Rad51-ssDNA nucleoprotein filaments by reducing the ATPase activity of Rad51 (Jensen, Carreira, and Kowalczykowski, 2010), and thus stimulates DNA strand exchange (Thorslund *et al.*, 2010;Liu *et al.*, 2010;Jensen, Carreira, and Kowalczykowski, 2010). No DNA polarity preference was detected, with nucleation on both 3' and 5' ssDNA tails observed, indicating a possible function for BRCA2 in daughter strand gap repair during replication (Jensen, Carreira, and Kowalczykowski, 2010). In support of this, a binding requirement for the junction between ss- and dsDNA was not detected (Jensen, Carreira, and Kowalczykowski, 2010), and binding to replication fork structures was observed *in vitro* (Thorslund *et al.*, 2010). Unlike the *U. maydis* and *C.elegans* orthologues of BRCA2 (section 1.5.1 and 1.5.2), the ability of human BRCA2 to anneal ssDNA-RPA complexes was not detected (Jensen, Carreira, and Kowalczykowski, 2010). Uniquely, both monomeric and dimeric forms of BRCA2 were observed by electron microscopy (Thorslund *et al.*, 2010).

1.4.2.4 The BRCA2 DNA binding domain

The region of human BRCA2 downstream of the BRC repeats has been shown to bind a small, highly acidic protein named DSS1, which is mutated in split hand/split foot syndrome (Crackower *et al.*, 1996;Marston *et al.*, 1999). The co-expression of DSS1 and the C-terminal domain of mouse and rat BRCA2 (~ 800 amino acids) allowed the elucidation of the X-ray crystal structure of the C-terminal domain of BRCA2 bound to DSS1 (Yang *et al.*, 2002). Structures were determined with and without bound ssDNA, revealing five distinct domains in the C-terminal region of BRCA2. The first domain is 190 amino acids in size and consists mainly of α helices (α -helical domain). This is followed by three oligonucleotide/oligosaccharide-binding folds (OB1, OB2 and OB3), which are structurally similar to the OB fold present in most ssDNA binding proteins.

Protruding from OB2 is a 130-amino acid insertion that adopts a tower-like structure (tower domain), consisting of a pair of long anti-parallel helices that support a three-helix bundle, which contains a helix-turn-helix motif (HTH). This HTH motif is similar to the DNA-binding domains of bacterial site-specific recombinases. ssDNA was observed bound to the OB2 and OB3 domains and the presence of the HTH motif analogous to that of bacterial site-specific recombinases led to the prediction that the BRCA2 DNA/DSS1-binding domain would bind dsDNA, as well as ssDNA. Indeed, when the DNA binding preferences of the BRCA2 DNA/DSS1-binding domain were investigated, it was shown to bind with high affinity to ssDNA, presumably through the three OB folds, and a role for the tower domain in binding to dsDNA was observed, although with much lower affinity (San Filippo *et al.*, 2006). In light of these data, it was proposed that BRCA2 could be responsible for targeting Rad51 to the ssDNA/dsDNA junction at the sites of processed DSBs, and in the removal of RPA from ssDNA to facilitate Rad51 nucleoprotein filament formation (Yang *et al.*, 2002; Pellegrini and Venkitaraman, 2004).

Experiments to investigate the function of this conserved C-terminal DBD were performed with CAPAN-1 cells, which have lost one BRCA2 allele and the remaining allele contains a frame-shift that causes premature termination of translation leading to a truncated BRCA2 lacking the entire C-terminal DBD (Goggins *et al.*, 1996). CAPAN-1 cells are sensitive to DNA damage, have lost the ability to form Rad51 foci and display chromosome instability (Abbott, Freeman, and Holt, 1998; Yuan *et al.*, 1999). Analysis of the repair of an I-SceI induced DSB lead to the discovery that homology-directed DNA repair was defective in this cell line (Moynahan, Pierce, and Jasin, 2001). Culturing of CAPAN-1 cells in the presence of Poly ADP-ribose polymerase (PARP) inhibitors, a breast cancer therapy that causes lethality in *brca2* null cells (Helleday, 2011), lead to the occasional resistant clones arising. These resistant cells were active in homology-directed repair of DSBs, proficient at Rad51 focus formation and recovered chromosome stability, all in the absence of the DBD of BRCA2 (Edwards *et al.*, 2008). Coupled with the findings from experiments in which the BRC repeat region of BRCA2 was fused to the RPA70 ssDNA binding domain, leading to attenuation of the *brca2*^{-/-} phenotype, this indicates that the DBD is to some extent expendable for DNA repair (Saeki *et al.*, 2006). As mentioned

previously, the BRC repeats of BRCA2 seem to possess an inherent preference for facilitating Rad51 nucleation on ssDNA over dsDNA (Carreira and Kowalczykowski, 2011), the molecular basis of which has not yet been elucidated.

1.4.2.5 The BRCA2 nuclear localisation signals

Antibodies against human BRCA2 show it to be localised to the nucleus (Bertwistle *et al.*, 1997). Characterisation of the rat and mouse homologues of BRCA2 lead to the discovery of two nuclear localisation signals (NLSs) at the extreme C-terminus of the protein, which are characterised by a positively charged core peptide unit of KKRR (McAllister *et al.*, 1997;Spain *et al.*, 1999;McAllister *et al.*, 2002). Investigation of the localisation of the smallest known cancer-associated truncation of BRCA2, which removes 224 amino acids from the C-terminal of the protein (including the two NLSs), demonstrated this protein to be cytoplasmically located, indicating that the two NLSs are functional and that translocation to the nucleus is required for the normal function of BRCA2 in HR (Spain *et al.*, 1999;Davies *et al.*, 2001).

1.4.3 The function of BRCA2 in homologous recombination

The phenotypes of *brca2* null mice demonstrate a critical function for BRCA2 in the regulation of homology directed repair of DSBs, and the maintenance of genome stability (Sharan *et al.*, 1997;Ludwig *et al.*, 1997;Suzuki *et al.*, 1997;Connor *et al.*, 1997;Patel *et al.*, 1998;Yu *et al.*, 2000;Moynahan, Pierce, and Jasin, 2001;Holloman, 2011). Summaries of current understanding of the roles provided by BRCA2 in promoting genome stability via Rad51 are shown in Figure 1-16 and Figure 1-17. It is thought that the BRC repeats of mammalian BRCA2 provide mediator functions for Rad51 during homology-directed repair of DSBs (Holloman, 2011;Carreira and Kowalczykowski, 2011). Specifically, BRC repeats 1-4 bind monomeric Rad51 and initiate Rad51 filament nucleation on ssDNA, which is then extended by BRC repeats 5-8 through stabilisation of the nascent filaments and facilitation of filament growth, therefore promoting DNA strand exchange (Figure 1-16;Carreira and Kowalczykowski, 2011). The C-terminal Rad51-binding site, though dispensable, may play a role in the

regulation of this activity, linking it to cell cycle progression, with CDK phosphorylation of Serine3291 disrupting Rad51 binding and hastening the disassembly of the Rad51 filament (Ayoub *et al.*, 2009; Holloman, 2011). Alternatively, or perhaps in addition, the C-terminus of BRCA2 may play a critical role in the protection of stalled replication forks from degradation (Figure 1-17), via stabilisation of Rad51 filaments on nascent DNA via the BRCA2 C-terminal Rad51-binding domain, regulation of which is achieved by CDK phosphorylation of Serine3291 (Holloman, 2011; Schlacher *et al.*, 2011). What seems unclear is how this latter role for the BRCA2 C-terminus, which is not proposed to lead to HR (Schlacher *et al.*, 2011), can be reconciled with the explicitly HR-promoting role of previous models of BRCA2 function.

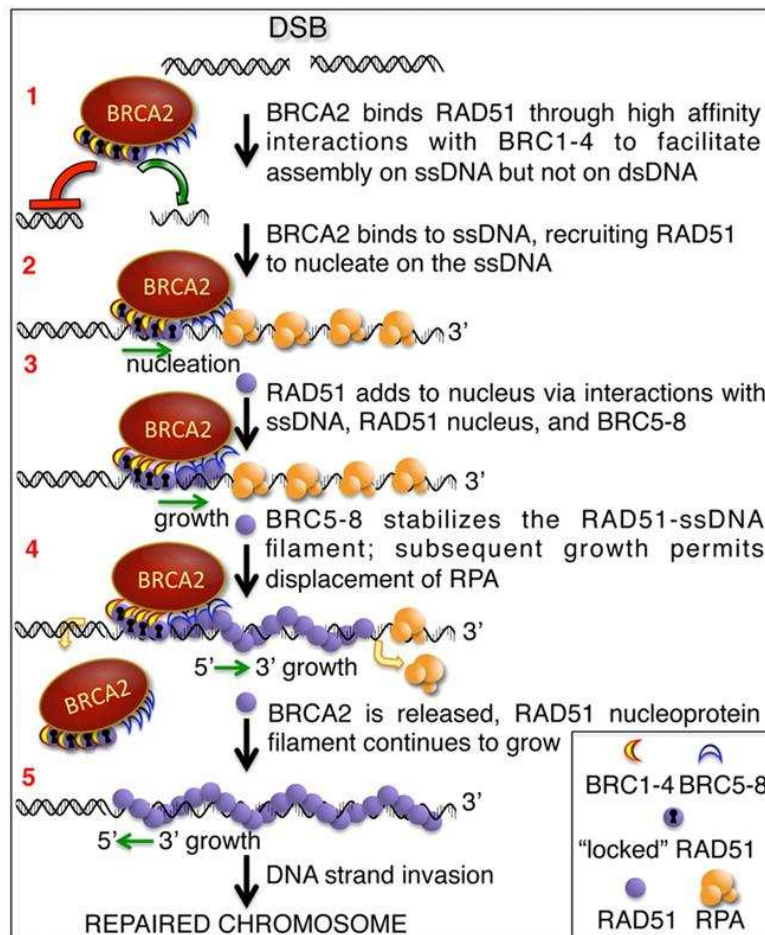


Figure 1-16 Proposed model for the role of the BRCA2 BRC repeats in DSB repair. Upon formation of a DSB (top), the dsDNA is resected to generate ssDNA tails. (1) BRC repeats 1-4 (yellow crescents) bind monomeric Rad51 (blue circles) and enhance binding to ssDNA ("locked" Rad51, 2). The binding of BRCA2 directs Rad51 onto the ssDNA of a processed DSB and restricts assembly onto the dsDNA nearby. "Locked" Rad51 nucleates onto ssDNA and BRC repeats 5-8 (blue crescents) stabilise the nascent nucleoprotein filament by limiting ATP hydrolysis by Rad51 (3). The subsequent growth of the Rad51 nucleoprotein filament displaces RPA (yellow circles) from the ssDNA. At this point, BRCA2 can be released from the DNA to promote Rad51 nucleation at another DSB (4). The Rad51 filament continues to grow from the BRCA2-stabilised nucleus to form the ATP-bound

nucleoprotein filament capable of homologous DNA pairing (5). Figure reproduced from Carreira and Kowalczykowski, 2011.

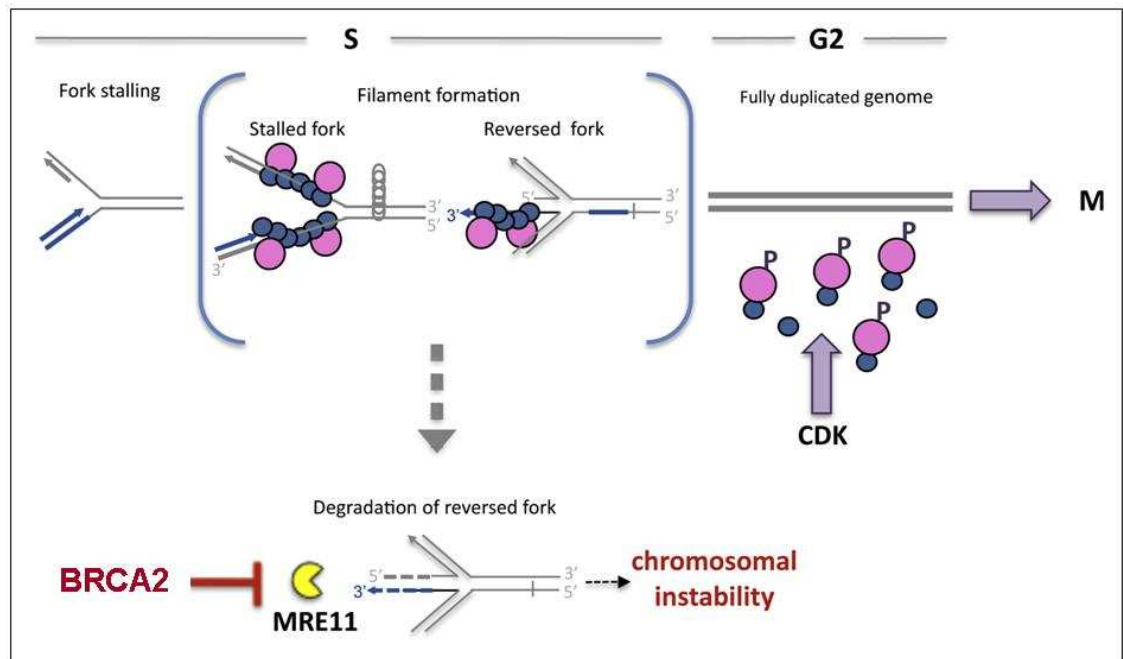


Figure 1-17 Proposed model for role of the BRCA2 C-terminal Rad51-binding motif during DNA replication.

In S-phase, BRCA2 (pink circle) stabilises Rad51 filaments (blue circles) on ssDNA at stalled replication forks, thereby preventing fork reversal. Alternatively, stabilised filaments directly protect a reversed fork. Once the replication stall is removed, genome duplication can proceed until completed. BRCA2 is then no longer required for fork protection, and CDK phosphorylation of the BRCA2 C-terminus allows Rad51 filaments to dissociate and progression into M phase is initiated. In the absence of BRCA2, nascent strands of the stalled fork are unprotected and degraded, possibly by Mre11 (yellow pacman), leading to chromosomal instability. Figure reproduced from Schlacher *et al.*, 2011.

1.4.4 BRCA2 interacting proteins

Mammalian BRCA2 has been shown to interact with a large number of proteins, the first of which to be described was BRCA1, and these two proteins co-localise in subnuclear foci following DNA damage (Chen *et al.*, 1998). As mentioned above, the C-terminal DNA-binding domain of BRCA2 also binds DSS1, a small highly acidic protein that is mutated in split hand/split foot syndrome (Crackower *et al.*, 1996). DSS1 is required for recombinational repair but its mechanism of action remains to be elucidated (Marston *et al.*, 1999;Kojic *et al.*, 2003;Gudmundsdottir *et al.*, 2004). The X-ray crystal structure determined of the C-terminal ~ 800 residues of BRCA2 showed that DSS1 binds BRCA2 in an extended conformation, interacting with the α -helical, OB1 and OB2 domains (Yang *et al.*, 2002). The interaction between these two proteins has also been

observed *in vitro* with full-length purified BRCA2, and DSS1 has been shown to stimulate Rad51 binding to RPA covered ssDNA (Liu *et al.*, 2010).

A 2 MDa BRCA2-containing complex was isolated in 2001, within which a structural DNA binding component was identified and named BRCA2-associated factor 35 (BRAF35; Marmorstein *et al.*, 2001). Since then, BRAF35 (also called HMG20b) has been identified as a member of the high-motility group of non-sequence specific DNA-binding proteins (Wang *et al.*, 1998; Sumoy *et al.*, 2000; Marmorstein *et al.*, 2001; Lee *et al.*, 2011), and a novel function for BRAF35 in facilitating the completion of cytokinesis via an interaction with BRCA2 has been proposed (Lee *et al.*, 2011).

BRCA2 has also been shown to be part of the Fanconi Anaemia (FA) pathway (section 1.4.5), where it interacts with FANCD2 and FANCG (Hussain *et al.*, 2003; Hussain *et al.*, 2004). BRCA2 function has also been shown to require the protein PALB2/FANCN, another component of the FA pathway (Xia *et al.*, 2006; Xia *et al.*, 2007), and PALB2 has been demonstrated to co-purify with full-length BRCA2 (Thorslund *et al.*, 2010).

Human BRCA2 is required for meiotic recombination, and this function is thought to be mediated by its interaction with the meiosis-specific recombinase, DMC1 (Bishop *et al.*, 1992). DMC1 is a closely related paralogue of Rad51 found widely in eukaryotes, capable of promoting strand exchange in similar ways to the mitotic recombinase (Masson and West, 2001). Human BRCA2 binds DMC1 at a conserved motif called the PhePP motif (KVFVPPFK) that is located downstream of the BRC repeats (Thorslund, Esashi, and West, 2007). This PhePP motif is distinct from the BRC repeats and promotes specific interactions with DMC1, but not with Rad51 (Thorslund, Esashi, and West, 2007). BRCA2 and DMC1 co-localise in nuclear foci during meiotic recombination (Bishop, 1994; Tarsounas *et al.*, 1999), and purified full-length BRCA2 has been shown to interact with DMC1 *in vitro* (Jensen, Carreira, and Kowalczykowski, 2010).

1.4.5 Functions of BRCA2 in the Fanconi Anaemia pathway

Fanconi anaemia is an autosomal recessive disorder characterised by bone marrow failure, compromised genome stability, and a predisposition to cancer (D'Andrea and Grompe, 2003;D'Andrea, 2010). FA is a highly complicated and heterogeneous disease caused by mutations in 13 genes, whose products include FANCA, FANCB, FANCC, FANCD1, FANCD2, FANCE, FANCF, FANCG, FANCI, FANCL, FANCM and FANCN, each of which have been demonstrated to function in the FA pathway although their precise roles remain unclear (Joenje and Patel, 2001;Meetei *et al.*, 2005;Levitus, Joenje, and de Winter, 2006;Smogorzewska *et al.*, 2007). The hallmark phenotype of FA cells is hypersensitivity to DNA cross-linking agents, and this lead to the implication of homology-directed DNA repair in the FA pathway (Grompe and D'Andrea, 2001;Joenje and Patel, 2001). The breast cancer susceptibility proteins have been demonstrated to play integral roles in the FA pathway, indeed in 2002 it was concluded that FANCD1 and BRCA2 are one and the same (Howlett *et al.*, 2002). This was due to the observation that cell lines defective in FANCD1 carry bi-allelic mutations in BRCA2 (Howlett *et al.*, 2002), coupled with the discovery that BRCA2 can complement for the defect in FANCD1 cell lines (Howlett *et al.*, 2002). BRCA1 is known to be required for the efficient foci formation of FANCD2 (Garcia-Higuera *et al.*, 2001;Vandenberg *et al.*, 2003), and BRCA2 interacts with FANCD2 and FANCN (Hussain *et al.*, 2004;Reid *et al.*, 2007;Xia *et al.*, 2007). Of the remaining proteins, it is known that FANCA, FANCB, FANCC, FANCE, FANCF, FANCG, FANCL and FANCM interact to form a multi-subunit nuclear complex. This core complex is known to play multiple roles within the FA pathway, an example of which is found following exposure to DNA damage, when the FA core complex monoubiquitylates FANCD2, causing it to re-locate to subnuclear foci with BRCA1 and Rad51 (Garcia-Higuera *et al.*, 2001;Taniguchi and D'Andrea, 2006). Here, FANCD2 is thought to promote the loading of BRCA2/FANCD1 into chromatin complexes, facilitating the assembly of Rad51 foci and thereby promoting HR (Wang, Andreassen, and D'Andrea, 2004;Hussain *et al.*, 2004).

1.5 DNA repair in other organisms

The DNA repair systems in *Caenorhabditis elegans*, *Ustilago maydis* and *Trypanosoma brucei* have been characterised and provide an interesting comparison with the extensively studied system in mammals. DNA repair in these organisms is described with particular emphasis placed on homology-directed repair and the BRCA2 orthologues. In some respects, the streamlined machinery of HR in these systems may provide insights into the minimum requirements for DNA repair.

1.5.1 Homologous recombination in *Caenorhabditis elegans*

A BRCA2-related protein, CeBRC-2, was discovered in *C. elegans* from a yeast two-hybrid screen of Rad51 interacting partners (Martin *et al.*, 2005). CeBRC-2 is a polypeptide, 394 amino acids in length, and contains a single BRC repeat, a single oligonucleotide binding (OB) domain (with similarity to the OB domains present in the ssDNA binding protein RPA) and two NLS motifs. CeBRC-2 was demonstrated to interact directly with monomeric CeRad51 via the single BRC repeat motif present and bind preferentially to ssDNA, in an interaction thought to be important for Rad51 filament nucleation onto ssDNA at the site of DNA damage (Martin *et al.*, 2005; Petalcorin *et al.*, 2006; Petalcorin *et al.*, 2007). *in vitro* analysis of CeBRC-2 demonstrated an ability to stimulate D-loop formation by CeRad51 and, unusually for a BRCA2 orthologue, to promote DNA single-strand annealing (Petalcorin *et al.*, 2006). The lack of a detectable Rad52 homologue in this organism may provide an explanation for this unusual annealing function of CeBRC-2 (Liu and Heyer, 2011). The single BRC repeat of CeBRC-2 has also been shown to stabilise Rad51-DNA filaments via interaction with the Rad51 N-terminal domain and may function to promote filament propagation (Petalcorin *et al.*, 2007).

Mutants that contain an N-terminal truncated variant of Cebr-2, lacking the OB domain, display embryonic lethality and meiotic recombination defects (Martin *et al.*, 2005). Formation of CeRad51 foci at the sites of DSBs is dependent on CeBRC-2 and suggests a requirement for CeBRC-2 for the repair of DSBs by HR (Martin *et al.*, 2005). Complementation studies in mammalian cells demonstrate

that CeBRC-2 is able to bind directly to mammalian Rad51 and also restore the formation of Rad51 foci formation after DNA damage in *brca2*^{-/-} cells (Min *et al.*, 2007). Analysis of differences between the phenotypes of CeRad51 and CeBRC-2 mutant cells suggested a role for CeBRC-2 in promoting the use of an alternative repair pathway in the absence of CeRad51. CeBRC-2 mutants form DNA damage foci in the absence of CeRad51 and the abnormal chromosomal aggregates that form in CeBRC-2 mutants can be rescued by blocking NHEJ (Martin *et al.*, 2005).

1.5.2 Homologous recombination in *Ustilago maydis*

The yeast-like fungus *Ustilago maydis* is extremely resistant to killing by ionising radiation (Holliday *et al.*, 1971; Resnick, 1978). The homologous recombination system in this organism is unusual in containing both a Rad51 orthologue and Rec2, an evolutionarily divergent Rad51-paralogue (Rubin, Ferguson, and Holloman, 1994). Rec2 has inherent homologous pairing and DNA strand transfer activity, unlike Rad51 paralogues in other systems (Bennett and Holloman, 2001). *U. maydis* Rad51 and Rec2 appear to have non-redundant roles in DNA repair, as mutation of either gene results in radiation sensitivity (Ferguson *et al.*, 1997). Rad51 and Rec2 have been shown to interact with each other, and in response to DNA damage both Rad51 and Rec2 form intra-nuclear foci thought to be the sites of active recombinational repair (Kojic, Thompson, and Holloman, 2001). Rad51 foci formation is dependent on Rec2 or Brh2 (see below); however, Rec2 foci can form in response to DNA damage in the absence of Rad51 and Brh2 (Kojic *et al.*, 2006).

A screen for DNA repair-defective mutants in *U. maydis* identified a BRCA2 orthologue, Brh2 (Kojic *et al.*, 2002). *U. maydis* Brh2 is also a simplified version of mammal BRCA2, being 1,075 amino acids in length and containing a single BRC repeat. Brh2 contains two NLSs, and a highly conserved DBD at the C-terminus consisting of a small alpha-helical domain, two OB domains and a tower domain. *brh2* mutant cells have the same phenotype as *rad51* mutant cells, with defects in allelic recombination, meiosis, gap repair and repair of ionising radiation damage (Bennett and Holloman, 2001; Kojic *et al.*, 2002). However, genomic instability and the accumulation of gross chromosomal rearrangements were additionally observed in *brh2* mutants (Kojic *et al.*, 2002). Interactions between

Brh2 and Rad51 were shown to occur at the single BRC repeat motif and also an extreme C-terminal motif thought to be analogous to the C-terminal Rad51-binding motif in mammalian BRCA2 (Kojic *et al.*, 2002;Kojic *et al.*, 2005), though no sequence homology can be found. *In vitro* experiments have shown that Brh2 nucleates Rad51 filament formation at a dsDNA/ssDNA junction, promotes filament elongation and thereby stimulates DNA recombination (Yang *et al.*, 2005;Mazloun, Zhou, and Holloman, 2007). *U. maydis* Brh2 is unusual in that the N-terminal domain, containing the single BRC repeat, was shown to be sufficient for rescue of the *brh2* mutant phenotype (Zhou, Kojic, and Holloman, 2009). However, the discovery of an additional DNA-binding domain, that was not identifiable by sequence analysis, explained this result (Zhou, Kojic, and Holloman, 2009). Deletion of this non-canonical N-terminal DNA-binding domain creates a requirement for Rad52 for DNA repair activity (Kojic *et al.*, 2011). Brh2 also possesses inherent DNA annealing activity and an ability to perform second end capture; these functions are thought to enable the single-strand annealing and synthesis-dependent strand-annealing pathways in this highly radiation resistant organism (Mazloun, Zhou, and Holloman, 2007;Mazloun, Zhou, and Holloman, 2008;Mazloun and Holloman, 2009). Brh2 has additionally been shown to promote template-switching reactions that enable recombinational bypass of lesions that occur during DNA replication (Mazloun and Holloman, 2009).

1.5.3 DNA repair in *T. brucei*

Many genes involved in DNA repair mechanisms have been identified in *T. brucei*, most notably RAD51, BRCA2, MRE11, DMC1, KU70/KU80 and four RAD51 paralogues. *T. brucei* contains homologues of the KU70 and KU80 proteins, which have been shown to function in telomere maintenance in this organism (Conway *et al.*, 2002a;Janzen *et al.*, 2004). However, evidence of NHEJ has not been obtained and the apparent absence of the key DNA ligase IV and XRCC4 proteins may be a possible explanation for this (Burton *et al.*, 2007). Mutation of the MRE11 homologue identified in *T. brucei* has been shown to cause retarded growth, impaired HR, an accumulation of gross chromosomal rearrangements and increased sensitivity to DNA damaging agents (but not MMS). Despite this, evidence for a role in antigenic variation was not seen (Tan, Leal, and Cross, 2002;Robinson *et al.*, 2002). *T. brucei* DMC1 has been identified as a close homologue of RAD51, which groups with DMC1 from other eukaryotes in

phylogenetic analysis (Proudfoot and McCulloch, 2006). Consistent with this, mutation of DMC1 does not result in any detectable changes in DNA repair, recombination or antigenic variation in bloodstream form cells, which grow exclusively by mitotic division (Proudfoot and McCulloch, 2006). The likelihood that *T. brucei* DMC1 contributes to the meiotic genetic exchange that has been recorded in the tsetse fly (Tait and Turner, 1990; Gibson and Stevens, 1999) is consistent with evidence that expression of the protein appears limited to a previously unidentified meiotic life cycle stage in the tsetse salivary glands (Peacock *et al.*, 2011), though experiments to show that mutation of the gene impairs this process are lacking. Mutation of the RAD51 homologue identified in *T. brucei* has been shown to cause retarded growth, sensitivity to DNA damaging agents, impaired homologous recombination and antigenic variation, with down-regulation of both *in situ* and transcriptional VSG switching observed (McCulloch and Barry, 1999). However, VSG switches were still observed, so alternative, RAD51-independent mechanisms for VSG switching must exist. After the induction of DNA damage *T. brucei* RAD51 is detected in clearly visible subnuclear foci (Proudfoot and McCulloch, 2005). The levels of RAD51 expression upon the induction of DNA damage in *T. brucei* do not increase, in contrast to the up-regulation observed in other closely related organisms, including *T. cruzi* (Regis-da-Silva *et al.*, 2006) and *L. major* (McKean *et al.*, 2001). *T. brucei* contains four RAD51 paralogues (RAD51-3, RAD51-4, RAD51-5 and RAD51-6), which is an unusually large repertoire among protists (Dobson *et al.*, 2011). Each of the four paralogues has been systematically mutated and all have been shown to cause impaired DNA repair and homologous recombination. However, only one paralogue (RAD51-3) has been shown to impair VSG switching (Proudfoot and McCulloch, 2005; Dobson *et al.*, 2011). RAD51-3 and RAD51-4 have been shown to interact with each other *in vivo*, and interactions between RAD51-3 and RAD51-6, and RAD51-4 and RAD51-6 have been detected *in vitro* (Dobson *et al.*, 2011). As mentioned previously (section 1.3.2.1), micro-homology mediated end joining has been demonstrated to play a significant, secondary role to HR in DNA repair in trypanosomes (Conway *et al.*, 2002b; Burton *et al.*, 2007; Glover, McCulloch, and Horn, 2008), and may yet prove to play an important role in genome evolution and antigenic variation in this organism (Glover, Jun, and Horn, 2011).

1.5.3.1 *T. brucei* BRCA2

The *T. brucei* homologue of BRCA2 (predicted 1,649 amino acids) was identified by BLAST searching the *T. brucei* genome sequence with the sequence of the human BRCA2 polypeptide (Lo *et al.*, 2003; Hartley and McCulloch, 2008). The most striking feature of *T. brucei* BRCA2 was the prediction of the presence of 15 BRC repeat motifs from the genome sequence of TREU 927 (Figure 1-18). This number of BRC repeat motifs is a remarkable expansion that is particularly noticeable as BRCA2 proteins in other trypanosomatids contain between 1 and 3 BRC repeats, which is more reminiscent of other unicellular organisms (Figure 1-19). The BRC repeats of *T. brucei* BRCA2 display sequence conservation with BRC repeats from other organisms, and the sequence fingerprint residues identified as critical for Rad51 binding demonstrate this conservation (Figure 1-20; Lo *et al.*, 2003). However, the organisation of the BRC repeats is unlike that seen in multiple BRC repeat BRCA2 homologues in other organisms. In contrast with the sequence divergence of the 8 individual BRC repeats of mammalian BRCA2, all but the most C-terminal BRC repeat in *T. brucei* BRCA2 are identical in sequence. In addition, whereas the human BRC repeats are dispersed throughout the middle third of the polypeptide, the *T. brucei* BRC repeats are arranged as a near perfect array close to the N-terminus, with the intervening, non-BRC repeat sequences near-perfectly conserved between repeat units. Only one other organism is known to contain a BRCA2 with close to this number of BRC repeats: *Trichomonas vaginalis* (14 predicted BRC repeats; data not shown). However, here the BRC repeats are not so closely conserved relative to each as those in *T. brucei*, and the inter-BRC repeat sequences are not conserved.

T. brucei BRCA2 displays considerable conservation in the region containing the DSS1/DNA-binding domain present in mammalian BRCA2 proteins. Amongst these motifs, the α -helical and OB domains 1 and 2 are remarkably conserved, and even the more C-terminal tower domain and OB domain 3, though less conserved, appear recognisable (Figure 1-21; Claire Hartley, PhD Thesis, 2008). Downstream of this DBD is a C-terminal extension, absent in *U. maydis* Brh2 and in *A. thaliana* BRCA2 (Figure 1-22), which shows limited overall sequence homology with human BRCA2. Nevertheless, within this domain a serine residue is positionally conserved adjacent to a proline and therefore bears a

resemblance to the C-terminal CDK phosphorylation site present at Serine 3291 in mammalian BRCA2 proteins: in *T. brucei* BRCA2 this would correspond with Serine 1523 (Figure 1-22; Claire Hartley, PhD Thesis, 2008). The same motif, if functional, appears conserved also in *T. cruzi*, but not in *L. major*. Three putative NLS motifs have been proposed in *T. brucei* BRCA2 (Claire Hartley, PhD Thesis, 2008), two upstream of the BRC repeats and a single, bipartite sequence present downstream of the last BRC repeat. A divergent PhePP motif may also be present just downstream of the bipartite NLS (section 5.2.1).

brca2^{-/-} mutants in bloodstream form Lister 427 *T. brucei* cells display DNA repair phenotypes characterised by retarded growth, increased DNA damage sensitivity, impaired homologous recombination, impaired localisation of RAD51 to subnuclear foci after DNA damage, and impaired antigenic variation. Interestingly, an accumulation of putative gross chromosomal rearrangements (GCRs) were observed after prolonged passaging (Hartley and McCulloch, 2008), and also a replication phenotype that is manifest as an increase in the number of cells with aberrant DNA configurations, as measured by DAPI staining and counting of individual cells. Further analysis of these 'others' showed they are mainly 1N0K and 2N1K cells, suggesting progression through cytokinesis before the completion of mitosis. Consistent with this was an observed increase in the number of 2N2K cells in which the two nuclei were visibly connected, rather than being separate in the cell (Claire Hartley, PhD Thesis, 2008).

In an attempt to determine the function of the BRC repeat expansion in *T. brucei* BRCA2, *brca2*^{-/-} mutant cells were complemented with a variant of BRCA2 containing a single BRC repeat (the divergent C-terminal repeat), which restored the growth, replication, and VSG switching phenotypes to wild-type levels, but not the recombination, DNA damage sensitivity, or RAD51 foci formation defects (Hartley and McCulloch, 2008; Claire Hartley, PhD Thesis, 2008). The *brca2*^{-/-} mutant cells were also complemented with a variant of BRCA2 containing the BRC repeat domain fused to the *T. brucei* RPA50 subunit that is homologous to the 70 kDa RPA-1 of eukaryotes, in a recapitulation of successful experiments in mammalian and *U. maydis* cells (Kojic *et al.*, 2005; Saeki *et al.*, 2006). This led to the restoration of the DNA repair and recombination phenotypes and to the conclusion that the C-terminal DBD was not required for DNA repair, as seen in other organisms. However, the

replication phenotype was not complemented, leading to the conclusion that the C-terminal domain of BRCA2 is critical for replication progression, though the basis for this was unclear (Claire Hartley, PhD Thesis, 2008). This C-terminal domain of BRCA2 has been suggested to interact *in vitro* with part of the *T. brucei* homologue of CDC45 (Oyola, Bringaud, and Melville, 2009), which is a protein essential for the initiation and progression of DNA replication (Chapter 6; Zou, Mitchell, and Stillman, 1997). The BRC repeats of *T. brucei* BRCA2 have also been suggested to interact with RAD51 and the four RAD51 paralogues by yeast 2-hybrid, with a single BRC repeat sufficient for binding to RAD51-3 and RAD51-5 (Hall *et al.*, 2011), although the function of these interactions, not seen to date in any other organism, remains to be elucidated.

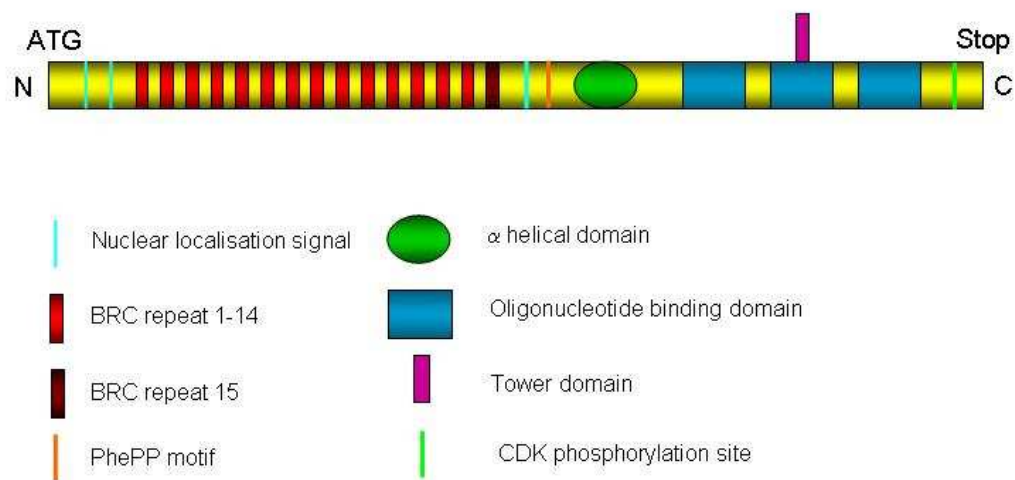


Figure 1-18 A schematic representation of *T. brucei* BRCA2 and its putative functional domains.

The diagram represents the predicted functional domains of *T. brucei* BRCA2, including the BRC repeats 1-14 (red bars), BRC repeat 15 (dark red bar), NLS (light blue bar), PhePP motif (orange bar), alpha helical domain (green oval), OB domains (blue boxes), tower domain (purple box), and putative CDK phosphorylation site (light green bar). Figure adapted from Claire Hartley, PhD Thesis, 2008.

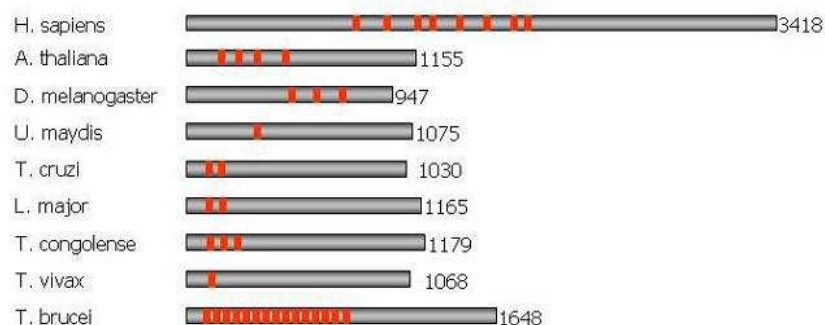


Figure 1-19 Representation of the number of BRC repeats in BRCA2 proteins from trypanosomatids and other eukaryotes.

BRC repeat motifs are displayed (red bars), and their position within the BRCA2 polypeptides are shown. Protein sizes in amino acid residues are indicated. Figure reproduced from Hartley and McCulloch, 2008.

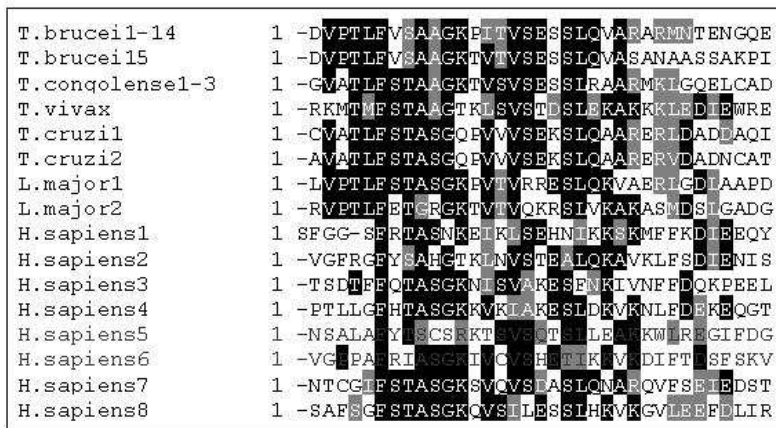


Figure 1-20 Multiple sequence alignment of the BRC repeats from trypanosomatids and humans.
 The polypeptide sequences of the BRC repeats were taken from *T. brucei*, *T. congolense*, *T. vivax*, *T. cruzi* and *H. sapiens*. Residues that are identical in greater than 50% of the sequences are shaded in black and similarly conserved residues shaded in grey. Figure reproduced from Claire Hartley, PhD Thesis, 2008.

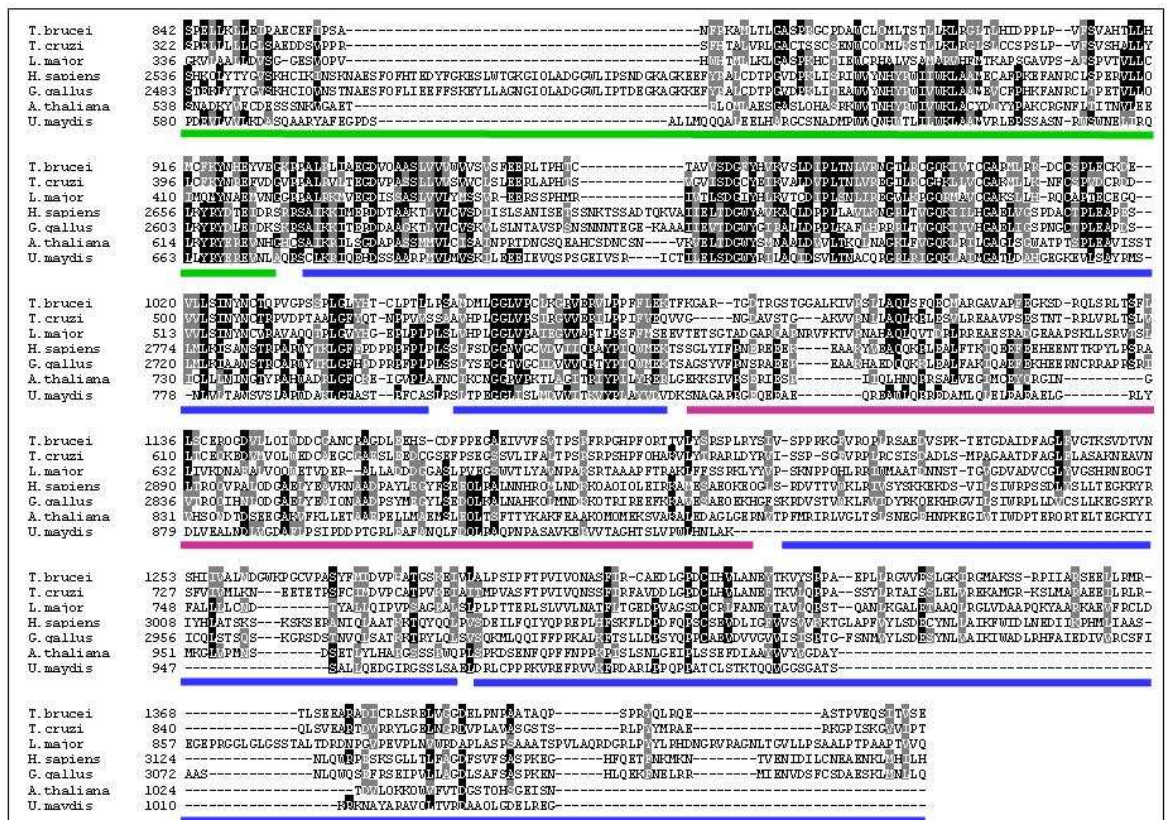
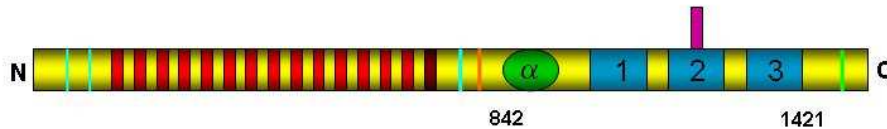


Figure 1-21 Alignment of the C-terminal DNA/DSS1-binding domains of BRCA2.
 Multiple sequence alignment of the C-terminal DNA/DSS1-binding domains of the BRCA2 proteins from *T. brucei*, *T. cruzi*, *L. major*, *H. sapiens*, *G. gallus*, *A. thaliana* and *U. maydis*. Residues that are identical in at least 50% of the proteins are shaded in black and similarly conserved residues are shaded in grey. The coloured blocks within the alignment represent the corresponding domains in the diagram of BRCA2 shown above. Figure adapted from Claire Hartley, PhD Thesis, 2008.

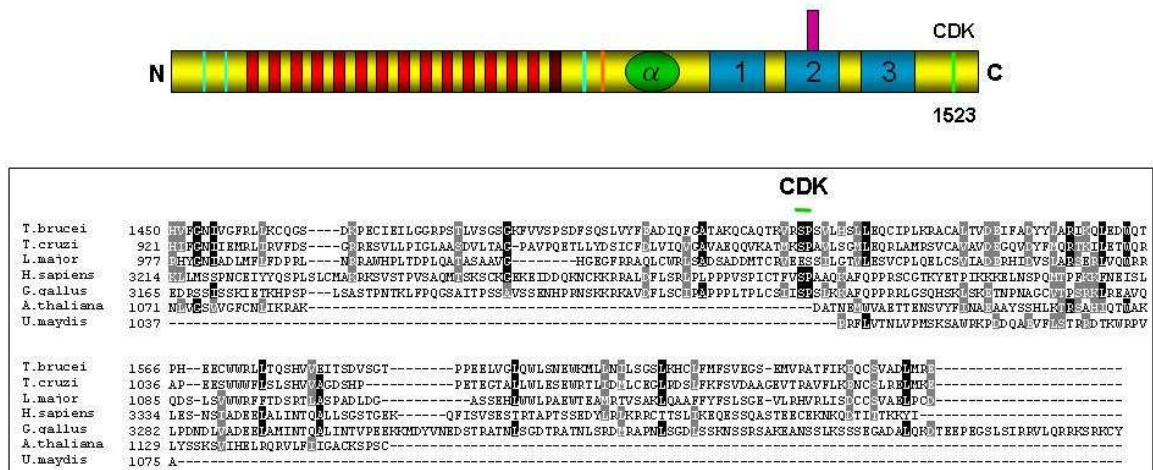


Figure 1-22 C-terminal alignment around a CDK phosphorylation site in human BRCA2. Multiple sequence alignment of the C-terminus of the BRCA2 proteins from *T. brucei*, *T. cruzi*, *L. major*, *H. sapiens*, *G. gallus*, *A. thaliana* and *U. maydis*. Residues that are identical in at least 50% of the proteins are shaded in black and similarly conserved residues are shaded in grey. The putative CDK phosphorylation site is highlighted (CDK). Figure adapted from Claire Hartley, PhD Thesis, 2008.

1.6 Rad51

Rad51, the eukaryotic HR recombinase (Radding, 1991; Sung, 1994; Sung and Robberson, 1995), appears to be one of only a small number of proteins that are universally conserved, with orthologues named RecA and RadA found in bacteria and archaea, respectively (Ogawa *et al.*, 1993). This implies that HR is an essential process for the propagation of all living cells. Human Rad51 is a protein of 37 kDa that possesses a core domain, termed the RecA-fold, which contains Walker A and B motifs that are responsible for ATP binding and hydrolysis (Walker *et al.*, 1982). In the absence of DNA, Rad51 forms inactive heptameric ring structures (Shin *et al.*, 2003). In the presence of DNA, Rad51 forms a highly ordered right-handed nucleoprotein filament (Benson, Stasiak, and West, 1994). Interactions between Rad51 monomers are thought to occur via an oligomerisation motif located at the subunit interface (Shin *et al.*, 2003). The Rad51 nucleoprotein filament forms with equal affinity on ss- and dsDNA, with a stoichiometry of 3 - 4 bp per protein (Benson, Stasiak, and West, 1994). DNA in the nucleoprotein filament is under-wound and extended by ~ 50% relative to B-form DNA (Ogawa *et al.*, 1993; Arata *et al.*, 2009). These Rad51 nucleoprotein filaments are active and possess DNA pairing, strand invasion and strand exchange activities (Shinohara, Ogawa, and Ogawa, 1992; Baumann and West, 1997), which are stimulated by RPA, through removal of secondary structure in

the ssDNA tail (McIlwraith *et al.*, 2000), and by Ca^{2+} , through a reduction in the ATPase activity of Rad51 thereby maintaining the filament in an active, stable state (Bugreev and Mazin, 2004; Chi *et al.*, 2006). No intrinsic polarity preference for DNA has been observed, and filaments form on both the 3' and 5' ssDNA tails produced by the processing of a DSB (McIlwraith *et al.*, 2000). Rad51 nucleoprotein filament assembly occurs in two steps: nucleation and growth. 2 - 5 Rad51 monomers are required to form a stable nucleation event and growth occurs *in vitro* to a finite length (Van der Heijden *et al.*, 2007; Mine *et al.*, 2007; Hilario *et al.*, 2009). It is thought that *in vivo* Rad51 filaments are made up of many small fragments arising from multiple nucleation events, and the highly dynamic and flexible nature of this Rad51 filament is thought to facilitate strand exchange (Galletto *et al.*, 2006). Filament disassembly after the completion of strand exchange requires Rad54, an ATP-dependant DNA translocase, and also the hydrolysis of ATP by Rad51 (Amitani, Baskin, and Kowalczykowski, 2006; Li *et al.*, 2007).

When bacteria are exposed to DNA damage, expression of the bacterial recombinase (RecA) is induced to increase more than 15 fold in an 'SOS response' (Little and Mount, 1982; Walker, 1984; Janion, 2008); mammalian cells do not exhibit such an induction (Tarsounas, Davies, and West, 2004; Michel, 2005), but it is common in eukaryotes as diverse as yeast and *T. cruzi* (Regis-da-Silva *et al.*, 2006; Putnam, Jaehnig, and Kolodner, 2009), suggesting mammals may be the exception. When DNA damage is detected, Rad51 and other repair proteins that are normally diffuse throughout the nucleus (Haaf *et al.*, 1995; Scully *et al.*, 1997) are rapidly relocated and concentrated into subnuclear complexes that are microscopically detected as foci. This creates an effect whereby the local concentration of repair enzymes is increased, forming what is considered a repair centre (Tarsounas, Davies, and West, 2004; Lisby and Rothstein, 2009), the precise composition and function of which remains unknown. Studies of the nuclear localisation and dynamics of mammalian Rad51 have identified three pools of Rad51; a large mobile pool of Rad51 exists alongside two smaller, relatively immobile pools, one bound by BRCA2 and the other self-associated in oligomeric heptamers (Essers *et al.*, 2002; Yu *et al.*, 2003).

1.7 Aims of this thesis

The initial aim of this thesis was to further investigate the role of BRCA2 in the regulation of genome stability in *T. brucei*, with particular focus on the genetic dissection of the chromosomal rearrangements observed in *brca2*^{-/-} mutants and the function of the unusual BRC repeat expansion.

A second aim of this thesis was to define the interactions between *T. brucei* BRCA2 and RAD51 in the hope this would shed further light on the mechanism of the regulation of homology-directed DNA repair by BRCA2 in this organism.

Finally, the putative function for *T. brucei* BRCA2 in the repair of stalled replication forks was further investigated, focusing on the proposed interaction with CDC45.

Chapter 2: Methods and materials

2.1 Trypanosome culture

2.1.1 Trypanosome strains

The bloodstream form (BSF) *T. brucei* strain used in this thesis is Lister 427 (Rudenko *et al.*, 1996; McCulloch, Rudenko, and Borst, 1997). This is a monomorphic strain, which usually only displays the long slender BSF cells. The switching frequency of the VSG being expressed is approximately 10^{-6} - 10^{-7} switches/cell/generation (Lamont, Tucker, and Cross, 1986; Turner, 1997). The procyclic form (PCF) *T. brucei* strains used in this thesis are Lister 427 and TREU (Trypanosomiasis Research Edinburgh University) 927 (Turner *et al.*, 1990).

2.1.2 Trypanosome growth

BSF cell density was determined microscopically using a Bright-Line haemocytometer (Hausser Scientific). In a 10 μ l aliquot of culture, the number of parasites under a 1 mm square area (0.1 μ l volume) was counted and multiplied by 10^4 to obtain the number of cells. ml^{-1} of culture. *In vitro* growth of BSF cells was carried out at 37°C in a humidified 5% CO₂ incubator using HMI-9 growth medium (Hirumi and Hirumi, 1989) supplemented with 20% (v/v) heat-inactivated foetal calf serum (FCS; Sigma) and 1% (v/v) penicillin/streptomycin (Sigma). The population doubling time of this strain is approximately 8 hours (Proudfoot and McCulloch, 2006). To keep a working culture of BSF cell lines, cells were passaged three times weekly by the addition of 20 μ l of a culture grown to a density of $\sim 4 \times 10^6$ cells. ml^{-1} to 1.5 ml HMI-9 medium in a 24-well plate. BSF cultures were grown in petri dishes in volumes of up to 25 mls to obtain large numbers of cells.

PCF cell density was determined using a Z2 Coulter Particle Count and Size Analyzer (Beckman Coulter) according to manufacturer's instructions.

Background counts due to particles in the culture medium were subtracted from readings of cell dilutions into IsoFlow Sheath Fluid (Beckman Coulter), typically of 1:1000. Output is given in cells. ml^{-1} of culture. *In vitro* growth of PCF cells was carried out at 27°C using a derivative of semi-defined medium (SDM-79; Brun and Schonenberger, 1979) supplemented with 10% (v/v) heat-inactivated FCS (Sigma) and 0.2% (v/v) Haemin (Sigma; diluted from 2 mg. mL^{-1} solution in 0.2 M

NaOH). The population doubling time of the PCF is approximately 10 hours. To keep a working culture of PCF cell lines, cells were passaged three times weekly by addition of 1 ml of a culture grown to a density of $\sim 4 \times 10^7$ cells.ml⁻¹ to 9 mls SDM-79 medium in a vented 25 cm² tissue culture flask. PCF cultures were grown in vented 75 cm² tissue culture flasks in volumes of up to 100 mls to obtain large numbers of cells.

2.1.2.1 Stabilate preparation and retrieval

For the long term storage of trypanosomes, stabilates were prepared by the addition of 100 µl of sterile 100% glycerol to 900 µl of culture grown to a density of $\sim 2 \times 10^6$ cells.ml⁻¹ (BSF) or $\sim 8 \times 10^6$ cells.ml⁻¹ (PCF). These 1 ml aliquots were placed in 1.2 ml cryotubes (Nunc), before being wrapped in cotton wool, frozen slowly at - 80 °C overnight and then transferred to liquid nitrogen storage. For retrieval of stabilates from liquid nitrogen storage, frozen cells were defrosted at 37 °C (BSF) or 27 °C (PCF), and placed in 10 mls HMI-9 growth medium (BSF) or 5 mls SDM-79 growth medium (PCF) overnight; cells were then passaged normally as described above.

2.1.3 Stable, clonal transformation of trypanosomes

BSF cells were grown to a density of $\sim 2 \times 10^6$ cells.ml⁻¹ and centrifuged at room temperature for 10 minutes at 583 x g. The cells were re-suspended in Zimmerman post-fusion medium (ZM; 5 M NaCl, 1 M KCl, 1 M Na₂HPO₄, 1 M KH₂HPO₄, 1 M MgOAc, 0.2 M CaCl₂) supplemented with 1 M D-glucose (ZMG), at a concentration of 1×10^8 cells.ml⁻¹. 5×10^7 cells per transformation were electroporated in 500 µl ZMG at 1.5 kV and 25 µF capacitance using a BioRad Gene Pulser II. Approximately 5 µg of purified DNA in a maximum volume of 10 µl, that had been restriction digested and ethanol precipitated was routinely used for transformations. After electroporation, cells were placed in 10 mls HMI-9 for 24 hours before being subjected to antibiotic selection. The recovered cells were centrifuged at room temperature for 10 minutes at 583 x g and re-suspended in HMI-9 supplemented with the appropriate antibiotics at a concentration of 5×10^5 cells.ml⁻¹. $1-2 \times 10^7$ cells were plated out in 1.5 ml aliquots over two 24 well plates. Transformants were counted after 7-10 days by looking at the plates using a light microscope (Leitz) and counting the number of

wells that contained growing cells. The population of cells in a well should have descended from a single transformant, and could therefore be considered as clonal, so long as less than 80% of the wells contain living cells (Wickstead, Ersfeld, and Gull, 2003). Typically six clones were chosen and expanded for further analysis.

PCF cells were grown to a density of $\sim 8 \times 10^6$ cells.ml⁻¹ and centrifuged at room temperature for 10 minutes at 583 x g. The cells were re-suspended in Zimmerman post-fusion medium (ZM; 5 M NaCl, 1 M KCl, 1 M Na₂HPO₄, 1 M KH₂HPO₄, 1 M MgOAc, 0.2 M CaCl₂), at a concentration of 1×10^8 cells.ml⁻¹. 5×10^7 cells per transformation were electroporated twice in 500 μ l ZM at 1.5 kV and 25 μ F capacitance using a BioRad Gene Pulser II. Approximately 5 μ g of purified DNA in a maximum volume of 10 μ l, that had been restriction digested and ethanol precipitated was routinely used for transformations. After electroporation, cells were placed in 10 mls of SDM-79 for 24 hours before being subjected to antibiotic selection. The recovered cells were diluted to concentrations of 10^3 , 10^4 , 10^5 and 10^6 cells in 20 mls of conditioned media (75% (v/v) SDM-79, 10% (v/v) FCS, 15% (v/v) SDM-79 conditioned by growth of wild-type PCF cells to $\sim 8 \times 10^6$.ml⁻¹, centrifuged and filter sterilised to remove trypanosomes) supplemented with the appropriate antibiotics, and plated out over four 96-well plates (175 μ l per well). Transformants were counted after 10-14 days by looking at the plates under a light microscope (Leitz) and counting the number of wells that contained growing cells. The population of cells in a well should have descended from a single transformant, and could therefore be considered as clonal, so long as less than 20% of the wells contain living cells. Typically six clones were chosen and expanded for further analysis.

2.1.4 Re-cloning of polyclonal trypanosome populations

After prolonged passaging of trypanosome cultures, clonal populations were obtained by re-cloning the cell cultures prior to further analysis. BSF cells were grown to a density of $\sim 2 \times 10^6$ cells.ml⁻¹ before plating out cells in two 24 well plates on HMI-9 supplemented with the appropriate antibiotics at a concentration of ~ 12 cells per plate. Clones typically emerged after 7-10 days and were counted by looking at the number of wells containing living cells using a light microscope (Leitz). The population of cells in a well should have

descended from a single cell, and could therefore be considered as clonal, so long as less than 80% of the wells contain living cells (Wickstead, Ersfeld, and Gull, 2003). Typically six clones were selected and expanded for further analysis.

PCF cells were grown to a density of $\sim 8 \times 10^6$ cells.ml⁻¹ before plating out cells in four 96 well plates on conditioned media supplemented with the appropriate antibiotics at concentrations of 10^3 , 10^4 , 10^5 and 10^6 cells per plate. Clones typically emerged after 10-14 days and were counted by looking at the number of wells containing living cells using a light microscope (Leitz). The population of cells in a well should have descended from a single cell, and could therefore be considered as clonal, so long as less than 20% of the wells contain living cells. Typically six clones were selected and expanded for further analysis.

2.2 Isolation of material from trypanosomes

2.2.1 Isolation of genomic DNA

Genomic DNA (gDNA) was prepared using the DNeasy Blood and Tissue kit (Qiagen). 10 mls of BSF grown to a density of $\sim 4 \times 10^6$ cells.ml⁻¹ or 5 mls of PCF grown to a density of $\sim 2 \times 10^7$ cells.ml⁻¹ were harvested by centrifugation at 1620 x g for 10 minutes at room temperature, washed with 1 ml PBS, before DNA extraction according to manufacturer's protocol.

Genomic DNA that was to be subsequently used for restriction digestion and Southern blot analysis was prepared using the Gentra Puregene cell kit (Qiagen). 50 mls of BSF grown to a density of $\sim 4 \times 10^6$ cells.ml⁻¹ or 20 mls of PCF grown to a density of $\sim 2 \times 10^7$ cells.ml⁻¹ were harvested by centrifugation at 1620 x g for 10 minutes at room temperature. Cell pellets were washed twice with 1 ml PBS before DNA extraction according to manufacturer's protocol. The concentration of gDNA extracted was quantified using a spectrophotometer (Eppendorf) to measure the absorbance at 260nm, typically using a dilution of 1 μ l of gDNA into 49 μ l of dH₂O.

2.2.2 Genomic plug preparation

Each genomic agarose plug prepared for the work in this thesis contained $\sim 1 \times 10^8$ PCF cells. PCF cells were grown to a density of $\sim 8 \times 10^6$ cells.ml⁻¹, centrifuged at 2500 x g for 5 minutes at room temperature and washed twice in 25 mls of cold Trypanosome Dilution Buffer (TDB; 120 mM NaCl, 1.2 mM KH₂PO₄, 30 mM TES, 40 mM NaH₂PO₄, 5 mM NaHCO₃, 5 mM KCl, 10 mM D-Glucose, 1 μ M MgSO₄.7H₂O). The pellet was then re-suspended in 50 μ l TDB and warmed at 37°C for 2 minutes, before adding an equal volume of pre-warmed 1.4% Hi-strength Low Melting Point (LMP) agarose (Biogene) made with dH₂O. This mixture was swirled to mix before filling disposable plug moulds (BioRad) with 100 μ l of the agarose/trypanosome solution and leaving for 15 minutes at room temperature to set. Plug moulds were submerged in ice cold NDS buffer, pH 9.0 (0.5 M EDTA, 10 mM Tris and 34.1 mM lauroyl sarcosine) for 10 minutes at 4°C. The agarose plugs were then removed from the moulds, incubated in 1 ml NDS buffer, pH 9.0 containing 1 mg.ml⁻¹ proteinase K (Invitrogen) at 50°C for ~ 24 hours and then transferred into 1 ml NDS buffer, pH 8.0 containing 1 mg.ml⁻¹ proteinase K at 50°C for ~ 24 hours. The plugs were finally transferred into 1 ml NDS buffer, pH 8.0 for storage at 4°C indefinitely.

2.2.3 Isolation of RNA

2×10^7 BSF or PCF cells from cultures grown to densities of $\sim 2 \times 10^6$ cells.ml⁻¹ and $\sim 8 \times 10^6$ cells.ml⁻¹ respectively, were centrifuged at 583 x g for 10 minutes at room temperature. Cell pellets were washed once with 1ml PBS. Cell pellets were stored at -80°C until required. Total RNA was extracted using the RNeasy mini kit (Qiagen) according to manufacturer's instructions. On-column DNase treatment (Qiagen) was carried out according to manufacturer's instructions for RNA to be subsequently used for qRT-PCR (section 2.5.5).

2.2.4 Protein extraction

2.2.4.1 For SDS-PAGE separation

25 mls of BSF cells grown to a density of $\sim 4 \times 10^6$ cells.ml⁻¹, or 10 mls of PCF cells grown to a density of $\sim 2 \times 10^7$ cells.ml⁻¹, were harvested by centrifugation at 1620 x g for 10 minutes at room temperature and washed once with 1 ml PBS.

The pellet was re-suspended in SDS-PAGE sample buffer (0.5 M Tris-HCL, pH 6.8, 20% Glycerol, 10% SDS, 5% 2-mercaptoethanol, 0.1% (w/v) bromophenol blue, 170 mM DTT) to a concentration of 5×10^8 cells.ml⁻¹. Protein extracts were denatured at 98 °C for 5 minutes prior to electrophoretic separation (section 2.8.3).

2.2.4.2 For co-immunoprecipitation

3×10^8 PCF cells from a culture grown to a density of $\sim 8 \times 10^6$ cells.ml⁻¹ were centrifuged at 1620 x g for 10 minutes at room temperature. The cell pellet was washed twice with 1 ml PBS prior to resuspension in 500 µl Trypanosome Lysis Buffer (TLB; 20 mM Tris-HCl (pH 8.0), 400 mM NaCl, 1 mM EDTA, 0.5% Nonidet P-40, 10% Glycerol, 1 mM DTT, 1 x Complete EDTA-free Protease Inhibitor Cocktail (Roche)). Cell suspensions were frozen at - 80 °C until required. Frozen cell suspensions were defrosted on ice and then lysed by vortexing for 30 seconds at high speed before incubation on ice for 30 minutes. Cell debris was pelleted by centrifugation at 20,000 x g for 20 minutes at 4 °C. The supernatant was transferred to a clean eppendorf and used immediately for experiments (section 2.12).

2.2.5 Aqueous fractionation

Aqueous fractionation was performed to separate the soluble nuclear and cytoplasmic proteins from *T. brucei* as described in Zeiner *et al.*, (2003). 5×10^8 PCF cells from a culture grown to a density of $\sim 8 \times 10^6$ cells.ml⁻¹ were centrifuged at 1620 x g and washed twice in 5 ml ice cold Fractionation Buffer A (FBA; 150 mM sucrose, 20 mM KCl, 3 mM MgCl₂, 20 mM HEPES-KOH (pH 7.9), 1 mM DTT, and 1 x Complete EDTA-free Protease Inhibitor Cocktail (Roche)). The cell pellet was re-suspended in 1 ml of FBA and 0.2% Nonidet P-40 (Calbiochem) was added. The cell suspension was passed through a 26-gauge syringe needle three times. The suspension was centrifuged at 20,000 x g for 10 minutes at 4 °C. The supernatant was separated and centrifuged again at 20,000 x g at 4 °C. This supernatant contains the soluble cytoplasmic proteins. The cell pellet was re-suspended in 500 µl of FBA and passed through a 26-gauge syringe needle 15 times. The suspension was centrifuged at 20,000 x g at 4 °C for 10 minutes. The

supernatant was removed and the pellet re-suspended in 500 μl of FBA. This suspension contains the soluble nuclear proteins.

2.3 Phenotype analysis

2.3.1 *In vitro* growth and doubling time

In vitro growth analysis was carried out on BSF cells by inoculating 2 ml cultures with 5×10^4 cells. ml^{-1} , from a culture grown to a density of $\sim 2 \times 10^6$ cells. ml^{-1} . The numbers of cells were counted at 24, 48, and 72 hours subsequently using a Bright-Line haemocytometer (Hausser Scientific).

For PCF cells, a 2 ml culture was inoculated with 5×10^5 cells. ml^{-1} , from a culture grown to a density of $\sim 8 \times 10^6$ cells. ml^{-1} . The numbers of cells were counted at 24, 48, and 72 hours subsequently using a Z2 Coulter particle count and size analyzer (Beckman Coulter).

Three repetitions of each cell line were carried out and the results plotted on a semi-logarithmic scale. The doubling time for the cell populations were calculated by comparing the cell count in mid-log phase using the following equation: $\text{Time Elapsed} \div (3.3 \times \text{Log} [\text{Cell count at the end of time elapsed} \div \text{Cell count at the beginning}])$, where the time elapsed is in hours, and the cell count is in cells. ml^{-1} . All population doubling times calculated in this thesis were determined using cell counts obtained between 24 and 48 hours.

2.3.2 DNA damage sensitivity

The sensitivity of trypanosomes to DNA damaging agents can be analysed using the Alamar Blue assay (Raz *et al.*, 1997; Onyango, Burri, and Brun, 2000). Alamar Blue (resazurin sodium salt; Sigma) is a blue-coloured, non-fluorescent compound. However, in actively metabolising cells, resazurin is reduced to resorufin, which is pink and highly fluorescent (Raz *et al.*, 1997; O'Brien *et al.*, 2000). Cells were grown to a density of $\sim 2 \times 10^6$ cells. ml^{-1} (BSF) or $\sim 8 \times 10^6$ cells. ml^{-1} (PCF). First, the 96 well plate (Nunc) was prepared; 100 μl of the corresponding media was added to all wells except for the first column. To the first column, 200 μl of the stock of MMS or phleomycin were added (0.01% and 4

$\mu\text{g.ml}^{-1}$ respectively for BSF or 0.08% and $32 \mu\text{g.ml}^{-1}$ respectively for PCF). A two-fold serial dilution was made by taking 100 μl from the first column and mixing it with the next column. Then 100 μl from the second column was added to the third column and mixed, and so on until the last column to which no drug was added. To each row, 100 μl of cells at a density of $2 \times 10^5 \text{ cells.ml}^{-1}$ (BSF) or $5 \times 10^5 \text{ cells.ml}^{-1}$ (PCF) were added, except for the last row which was left with no cells as a background control. These cells were allowed to grow for 48 hours at their respective normal culture temperatures, after which 20 μl of 0.125 mg.ml^{-1} resazurin sodium salt (Sigma) in PBS was added. This was then incubated for 24 hours and the plate read by a spectrophotometer using filters of 540 nm excitation and 590 nm emission (Wallac Envision, 2102 Multi-label reader) and the data analysed using Microsoft Office Excel and GraphPad Prism4. In Excel, average background counts with no cells added were subtracted from all values and percentage survival was calculated relative to no drug controls. In GraphPad, these data were transformed using $X=\text{Log}(X)$ and nonlinear regression (curve fitting) was then performed. EC50 values relative to the wild type cell line in each case were plotted with 95% confidence intervals.

2.3.2.1 Hydroxyurea damage

Hydroxyurea (HU) inhibits ribonucleotide reductase, an enzyme involved in deoxyribonucleotide triphosphate (dNTP) synthesis and thereby causes a stall in DNA replication (Hofer *et al.*, 1997). PCF cells grown to a density of $\sim 4 \times 10^6 \text{ cells.ml}^{-1}$ were treated with 0.3 mM HU for 16 hours (2 cell cycles). The effect of HU was confirmed by FACS analysis of cells (section 2.3.3; Forsythe, McCulloch, and Hammarton, 2009).

2.3.2.2 Phleomycin damage

Phleomycin is a group of copper-containing antibiotic peptides of the bleomycin family first isolated from *Streptomyces verticillus*. It has been shown to inhibit DNA synthesis by blocking the activity of DNA polymerase and inducing the formation of DNA double strand breaks (Falaschi and Kornberg, 1964; Reiter, Kelley, and Milewski, 1972). PCF cells grown to a density of $\sim 4 \times 10^6 \text{ cells.ml}^{-1}$ were treated with 1-2 $\mu\text{g.ml}^{-1}$ phleomycin for 18-24 hours, as indicated. BSF

cells grown to a density of $\sim 1 \times 10^6$ cells.ml⁻¹ were treated with 0.25-1 $\mu\text{g.ml}^{-1}$ phleomycin for 18 hours, as indicated.

2.3.2.3 Methyl methanesulphonate damage

Methyl methanesulphonate (MMS) is an alkylating agent that methylates DNA to produce methylated purines at the 7' position of guanine residues and the 3' position of adenine residues (Brookes and Lawley, 1961;Reiter *et al.*, 1967). PCF cells grown to a density of $\sim 4 \times 10^6$ cells.ml⁻¹ were treated with MMS as indicated.

2.3.3 Fluorescent Activated Cell Sorting Analysis

For fluorescent activated cell sorting (FACS) analysis, 1×10^6 cells from a culture of PCF cells grown to a density of $\sim 8 \times 10^6$ cells.ml⁻¹ were pelleted by centrifugation at 583 x g for 10 minutes at room temperature, washed once with 1 ml PBS and re-suspended in cold 70% methanol (v/v) in PBS. The cells were fixed by incubation at 4°C overnight. After fixation, cells were washed in 10 ml of ice cold PBS, re-suspended in 1 ml of PBS containing 10 $\mu\text{g.ml}^{-1}$ propidium iodide (Sigma) and 10 $\mu\text{g.ml}^{-1}$ RNase A (Sigma), and incubated at 37°C for 45 minutes. FACS was performed with a Becton Dickinson FACSCalibur using detector FL2-A and an AmpGain value of 1.75.

2.4 Microscopy

2.4.1 Cell cycle analysis

In order to analyse the cell cycle, cells were prepared for microscopy by DAPI staining (4, 6-diamidino-2-phenylindole; Vector Laboratories). DAPI stain binds preferentially to dsDNA and fluoresces under UV light, allowing the DNA content of fixed cells to be analysed. 100 μl of BSF cells grown to a density of $\sim 2 \times 10^6$ cells.ml⁻¹ or 50 μl of PCF cells grown to a density of $\sim 8 \times 10^6$ cells.ml⁻¹ were spread thinly on a microscope slide and allowed to air dry. Cells were fixed by immersion in methanol at room temperature for 10 minutes. Slides were allowed to air dry before placing two drops of vectashield with DAPI (1.5 $\mu\text{g.ml}^{-1}$; Vector Laboratories) onto the slide, positioning a coverslip and sealing the slide with clear nail varnish. Differential interface contrast (DIC) was used to visualise

intact cells and UV (461 nm) to visualise DAPI using a Zeiss Axioskop microscope. Cells were counted according to the number of nuclei and kinetoplasts they contained. Cells in G1 phase of the cell cycle contain 1 nucleus and 1 kinetoplast (1N1K). Kinetoplast division then occurs resulting in cells with 1 nucleus and 2 kinetoplasts (1N2K). After this, the nucleus divides leading to cells containing 2 nuclei and 2 kinetoplasts (2N2K). Completion of cytokinesis forms two daughter cells in G1 phase, containing 1 nucleus and 1 kinetoplast (1N1K). Any cells that were observed not to be in these cell cycle phases were noted as being aberrant cell types and were described as 'others'.

2.4.2 Immunolocalisation

Endogenously expressed epitope-tagged proteins were visualised by immunolocalisation using a microscope. 5×10^5 PCF cells from a culture grown to a density of $\sim 8 \times 10^6$ cells.ml⁻¹, or 5×10^6 BSF cells from a culture grown to a density of $\sim 2 \times 10^6$ cells.ml⁻¹, were centrifuged at 735 x g for 5 mins and washed in 1 ml ice cold PBS. The cell pellet was re-suspended in 50 μ l ice cold PBS before being spread thinly on a silane prep glass slide (Sigma) and allowed to air dry. Cells were fixed by soaking in cold methanol for 15 minutes. Excess methanol was washed off by submersion in ice cold PBS twice before blocking in 2% FCS in PBS for 1 hour to overnight. Primary antibodies (Table 2-2) were diluted to the required concentration in 2% FCS in PBS and incubated on the slide for 1 hour. Excess antibody was washed off with 2% FCS in PBS and the procedure repeated with the secondary Alexa Fluor-conjugated antibody (Invitrogen, Table 2-3). The slides were washed for the final time in ice cold PBS and dried to remove excess liquid. One drop of DAPI (Vector laboratories) was added to the slide and a coverslip positioned and sealed with clear nail varnish. A FITC (520 nm) filter was used to visualise Alexa Fluor 488 conjugated antibodies, a Rhodamine (673 nm) filter was used to visualise Alexa Fluor 594 conjugated antibodies, differential interface contrast (DIC) was used to visualise intact cells and UV (461 nm) was used to visualise DAPI using a Zeiss Axioskop microscope. High resolution images were obtained with a Deltavision confocal microscope using the same slides. De-convolution was carried out and flattened projections of the resulting image slices obtained using softWoRx Explorer (Applied Precision) are shown.

2.5 Molecular biology techniques

2.5.1 Primer design

Gene sequences were downloaded from GeneDB (www.genedb.org) using the gene accession number. Sequences were viewed in CLC Genomics Workbench 4 (CLC Bio). Primers were designed using the web-based programme Primer 3 (<http://frodo.wi.mit.edu/primer3/>). Restriction sites were added to the 5' end of the primer along with an additional three cytosine bases at the 5' terminus to allow efficient restriction digest of PCR products. Start and stop codons were added or removed as required and care was taken to ensure coding sequences remained in-frame with fusion tags after cloning. Mutagenesis primers were designed with the base pairs to be altered in the centre and 15 to 20 base pairs of flanking complementary sequence. Primers for qRT-PCR were designed using the Applied Biosystems qRT-PCR primer design programme. All oligonucleotides used in this thesis were synthesised by Eurofins MWG Operon (www.eurofinsdna.com) and are listed in Table 2-1. Appendix 1 displays the location of all primers within the *T. brucei* BRCA2 gene.

No	Sequence	Restriction sites	
1	CCC ACTAGT GCTGATACACTTT CACCGTG	<i>SpeI</i>	
2	CCC CTCGAG CTACGGGTGCTGCATCGCCA	<i>XhoI</i>	
3	CCC CTCGAG GCTACTGTGTCTTCTCGGAC	<i>XhoI</i>	
4	CCCG GATCC CAACCGCACGTGCGTCTGGTACT	<i>BamHI</i>	
5	CCC AAGCTT GGCGGGAGCTTCCAGACGATGTG	<i>HindIII</i>	
6	CCCT CTAGAG CGCCCGCCAGCGAGGGAGT	<i>XbaI</i>	
16	CCC CTCGAG CTATTCTCGCATAAGATCAGCG	<i>XhoI</i>	
32	CCC AAGCTT GAAGTGAAAGTTTGTAGTGTCC	<i>HindIII</i>	
33	CCCT CTAGAT TCTCGCATAAGATCAGCG	<i>XbaI</i>	
37	CCC CTCGAG GTTGAAGTGAGGGGTGGTTAGC	<i>XhoI</i>	
40	CCCT CGCGAGGATCC CAACCGCACGTGCGTCTG	<i>NruI</i>	<i>BamHI</i>
41	CCCT CGCGAGATATC AAAACATAGATTACGCACACAC	<i>NruI</i>	<i>EcoRV</i>
42	CCCT CTAGAG GACATTGTCATTGCTGTAG	<i>XbaI</i>	
43	CTCAAACCAAGGTAAGAGCTCCTTCCGTGCTTCAT		
44	ATGAAGCACGGAAGGAGCTTACCTTGGTTTGAG		
45	CAAAACAATGCGCTCAAACCAAGGTAAGAGAACCTTCCGTGCTTCAT		
46	ATGAAGCACGGAAGGTTCTTACCTTGGTTTGAGCGCATTGTTTTG		
48	ATACTTGTTTGCCGACACTGC		
49	TCGAGGACCTTAAATCCTCTACC		
51	CCCG GATCC ATCCAAGCTAGCAAGAAAGC	<i>BamHI</i>	
59	CGCTAATCAGCATGAAGTCG		
75	CCCG GATCC CACAAGTGCAGCACGTACCTTAAGC	<i>BamHI</i>	
76	CCC CTCGAG CTATTCTGAAACCGTAATACTCTGC	<i>XhoI</i>	
86	CTTTGTGCGAGCTGATGC		
87	CGTCCGGTGCTTTTCCTG		
88	AGGGTGAAACCCTCACACAG		
89	CTTTGCAGAGACAGCTCGTG		
91	CCCG GATCC CGCTAAGAATAAAGGAGCGGTTGC	<i>BamHI</i>	

93	CCC <u>GGATCC</u> CAGCCACAAAAAGGAAGAC	<i>Bam</i> HI	
94	CCC <u>CTCGAG</u> CTATGTACGTGGCGTCCTCTTC	<i>Xho</i> I	
97	TTGAAGCAGCGAACAAAGAC		
98	TGCCCTTGTAGACCTATGC		
99	ACACTCGCAGCAATCCAAG		
100	AAAAAGCAGCAGCATTCAAC		
101	TTAGAGAGCGGAACCAAAGC		
102	GCAGATAGCTGCTGCTAGGG		
103	CAAGGTGCCACCCTTAAATG		
104	CCTTTTGTGCCTTGTCTTG		
112	CCC <u>ACTAGT</u> AGCCACAAAAAGGAAGAC	<i>Spe</i> I	
113	CCCT <u>TCTAGA</u> CTCTTGGCCATTTTCAGTCCCG	<i>Xba</i> I	
114	CCCT <u>TCTAGA</u> AATTCACATCTGCGCTTGTTG	<i>Xba</i> I	
115	CCC <u>GGATCC</u> ATAATCAGAATTTGACTTCCG	<i>Bam</i> HI	
116	CCC <u>ACTAGT</u> AACACTCGCACCAAAAATAAG	<i>Spe</i> I	
117	CCC <u>GGTACC</u> TTCTCAGCCTTTGCCTCAC	<i>Kpn</i> I	
118	CCC <u>GGTACC</u> ACCGAAGTGTGCCTTTTGTG	<i>Kpn</i> I	
119	CCC <u>GGATCC</u> CCCCTGGTATACGCGTTAAG	<i>Bam</i> HI	
129	CCC <u>GGATCC</u> GCTGATACACTTTCACCGTG	<i>Bam</i> HI	
130	CCC <u>CTCGAG</u> TCAGCGCCCGCCAGCGAG	<i>Xho</i> I	
133	AAGCGGTGCACCTAACTGAC		
138	GCTGCCTTCCGCTATGGAT		
139	CCACTCGCCCTTTCAAACAA		
140	ATGGCCAAGCCTTTGTCTC		
141	TTAGCCCTCCCACACATAACC		
142	TGGGGAGCAAAGATGAAAAC		
143	CCGTTGCCATAACGGGTCCC		
144	ATGACCGAGTACAAGCCC		
145	TCAGGCACCGGGCTTGCG		
146	TAACCTTTACAACAGAGCGCACAACTTAA		
147	CGCTGGCTGTGGTGCTCAGAATCATGCAGA		
150	CAGGAGGATCGTTCGGCACCTTGCG		
151	CATGCGCCTGTGGTTCAGCATAGC		
152	CC <u>CTCGAG</u> GACATGACATTTCTTGACCC	<i>Xho</i> I	
153	CCT <u>CGCGAGGATCC</u> ATAATCAGAATTTGACTTCCG	<i>Nru</i> I	<i>Bam</i> HI
154	TACGGAGTCCATTGTACCTG		
155	TTCAGGCTGGCCAATGCG		

Table 2-1 List of oligonucleotide primers used in this thesis.

Primer numbers referred to throughout the text are shown, as are the oligonucleotide sequences and restriction sites. Base pairs to be mutated during site-directed mutagenesis are indicated by underline.

2.5.2 Polymerase Chain Reaction

Template DNA used for polymerase chain reactions (PCRs) was typically 0.025 µg of gDNA prepared using DNeasy Blood and Tissue kit (Qiagen; section 2.2.1) or 0.025 ng of circular plasmid prepared by QIAprep spin miniprep kit (Qiagen; section 2.7.2).

For diagnostic PCR reactions *Taq* DNA polymerase (New England Biolabs [NEB]) was used, typically in a reaction of 25 µl containing 0.1 µM 5' primer, 0.1 µM 3' primer, 1 x ThermoPol Buffer (NEB), 200 µM dNTPs (Invitrogen), 0.5 Units of *Taq* DNA polymerase (NEB), and dH₂O to 25 µl. PCRs were conducted in a Robocycler

(Stratagene) with typical conditions of 95°C for 5 minutes, followed by 25 to 30 cycles of 95°C for 1 minute, 50-60°C for 1 minute, 72°C for 1 minute per kb of expected product, and a final cycle of 72°C for 10 minutes.

For PCR reactions where low error rates were required the high fidelity Phusion DNA polymerase (Finnzymes) was used, typically in a reaction of 50 µl containing 0.5 µM 5' primer, 0.5 µM 3' primer, 1 x Phusion High Fidelity (HF) buffer (Finnzymes), 200 µM dNTPs (Invitrogen), 1 Unit of Phusion DNA polymerase (Finnzymes), and dH₂O to 50 µl. PCRs were conducted in a Robocycler (Stratagene) with typical conditions of 98°C for 5 minutes, followed by 30 to 35 cycles of 98°C for 1 minute, 50-60°C for 1 minute, 72°C for 1 minute per kb of expected product, and a final cycle of 72°C for 10 minutes.

2.5.2.1 PCR purification

Specific PCR products required for cloning were routinely cleaned up using the QIAquick PCR purification kit (Qiagen) according to the manufacturer's protocol.

2.5.3 Site-directed mutagenesis

Site-directed mutagenesis was carried using KOD hot start DNA polymerase (Novagen). Circular plasmid containing the sequence to be mutated was used as a template for a 50 µl PCR reaction containing 0.3 µM 5' primer, 0.3 µM 3' primer, 1 x KOD buffer (Novagen), 0.2 mM dNTPs (Invitrogen), 1.5 mM MgSO₄, 1 Unit of KOD DNA polymerase (Novagen), and dH₂O to 50 µl. PCRs were conducted in a Robocycler (Stratagene) with typical conditions of 95°C for 5 mins, followed by 18 to 20 cycles of 95°C for 30 seconds, 50-60°C for 30 seconds, 70°C for 1 minute per kb of plasmid. Template DNA was restriction digested with *DpnI* (Promega) for ~ 3 hours prior to transformation into *E. coli* (section 2.7). Plasmid DNA was extracted from *E. coli* colonies (section 2.7.2) and screened by sequencing (Eurofins MWG Operon).

2.5.4 Reverse Transcription Polymerase Chain Reaction

Reverse Transcription PCR (RT-PCR) was carried out on 2 µg of the total RNA extracted from trypanosomes (section 2.2.3) in order to produce the cDNA required for quantitative real-time PCR (qRT-PCR; section 2.5.4). The

SuperScript First Strand Reverse Transcription kit (Invitrogen) was used according to manufacturer's protocol. Random hexameric primers (Invitrogen) were used and controls without reverse transcriptase were prepared for each sample. cDNA was stored at - 20°C until required. PCR was carried out on the plus and minus RT cDNA samples generated in order to test for gDNA contamination. Primers for *DNA polymerase I* (150 and 151; Table 2-1) were used to amplify from the products of the cDNA reactions and the absence of PCR product from the minus RT samples confirms the absence of gDNA contamination.

2.5.5 Quantitative Real-Time Polymerase Chain Reaction

qRT-PCR was carried out on the cDNA samples generated by RT-PCR (section 2.5.4). qRT-PCR primers against the gene of interest were used together with qRT-PCR primers against an endogenous control gene (*tubulin*, 154 and 155). Power SYBR Green PCR master mix (Applied Biosystems) was used to set up the qRT-PCR reactions in a volume of 25 µl in a Micro Amp optical 96-well reaction plate (Applied Biosystems) before sealing with clear adhesive film (Applied Biosystems). Reactions were carried out in quadruplicate so that outliers could be discarded prior to data analysis. Plates were frozen at - 20°C until required. qRT-PCR was carried out on a 7500 Real Time PCR System machine (Applied Biosystems) using the standard cycling conditions and data was analysed using the 7500 System Software (Applied Biosystems).

2.5.6 Restriction digest

PCR products and plasmids for cloning were routinely digested by specific restriction endonucleases. A typical digest for cloning contained 2 µg of DNA, 1 x buffer specific to restriction enzyme (NEB), 100 µg.ml⁻¹ BSA (NEB), up to 10 Units of restriction endonuclease enzyme (NEB) and dH₂O to 50 µl. Reactions were incubated for 2 hours to overnight at 37°C. A typical digest for plasmid screening contained 0.25 µg of DNA, 1 x buffer specific to restriction enzyme (NEB), 100 µg.ml⁻¹ BSA (NEB), up to 2 Units of restriction endonuclease enzyme (NEB) and dH₂O to 20 µl. Reactions were incubated for 1 hour at 37°C.

2.5.7 Phosphatase treatment

Restriction digests of plasmid backbones subsequently required for ligation reactions were treated with Alkaline Phosphatase (Calf Intestinal; CIP [NEB]) in order to remove the 5' phosphate groups from the cut DNA ends and so prevent vector re-circularisation during ligation. 5 Units of CIP (NEB) was added to restriction digestion reactions and incubated for a further 30 minutes at 37°C prior to DNA purification.

2.5.8 DNA fragment purification

PCR reactions yielding non-specific products and plasmid restriction digests were separated by DNA electrophoresis (section 2.8.1) and visualised on a UV transilluminator. The product of interest was excised using a scalpel blade and purified using a QIAquick gel extraction kit (Qiagen) according to the manufacturer's protocol.

2.5.9 DNA fragment blunting

The blunting of sticky ends produced from restriction digestion was carried out using T4 DNA polymerase (NEB) in a 20 µl reaction containing 10 µl of gel extracted insert DNA, 1 x T4 DNA ligase buffer (NEB), 1.5 Units of T4 DNA polymerase, 0.2 mM dNTPs, 100 µg.ml⁻¹ BSA (NEB) and dH₂O to 20 µl. Reactions were incubated at 37°C for 1 hour before heat inactivation of the T4 DNA polymerase at 75°C for 10 minutes. Ligation reactions were set up directly with the resulting insert DNA.

2.6 Cloning

2.6.1 T4 DNA ligase

Insert fragments for cloning were prepared by PCR followed by PCR purification (section 2.5.2.1) or DNA fragment purification from an agarose gel (section 2.5.8). Vector backbones were prepared by restriction digest, Phosphatase treatment and DNA fragment purification. The concentration of insert and vector DNA was determined by measuring the absorbance at 260 nm using a spectrophotometer (Eppendorf). The volume of insert and vector DNA in a

ligation reaction was determined by using the equation: $[(\text{ng vector} \times \text{kb insert}) / \text{kb vector}] \times \text{ratio insert/vector} = \text{ng insert}$. Ligation reactions were carried out in a volume of 20 μl typically containing 100 ng vector, 1 x T4 DNA ligase buffer (NEB), 400 Units T4 DNA ligase (NEB), the correct volume of insert and dH_2O to 20 μl . Reactions were incubated at room temperature for one hour to overnight prior to transformation into *E. coli* (section 2.7).

2.7 Transformation of *E. coli*

All *E. coli* growth was carried out in Luria-Bertani broth ([LB; 5 g yeast extract (Formedium), 10 g tryptone (Formedium), 10 g NaCl in 1 L dH_2O pH 7.0 (NaOH)] and 20 g agar (Formedium) was added if plates were required). For cloning, 10 μl of ligation or 10 ng of circular plasmid was added to a 100 μl aliquot of chemically competent DH5 α *E. coli* (Invitrogen). After incubation on ice for 15 minutes the cells were subjected to heat shock at 42 °C for 45 seconds after which they were cooled on ice for 5 minutes. 250 μl of super optimal broth (SOB) with added glucose (SOC; 20 g tryptone, 5 g yeast extract, 0.5 g NaCl, 10 ml 1 M MgCl_2 , 10 ml 1 M MgSO_4 , 10 ml 2 M glucose in 1 L dH_2O) was added and cells allowed to recover in a shaking incubator at 37 °C for one hour. Cells were spread on plates containing the appropriate antibiotic for the plasmid transformed. To allow single colonies to grow overnight at 37 °C, typically 100 μl of cells transformed with a ligation were plated, and only 20 μl of cells transformed with a circular plasmid were plated.

2.7.1 *E. coli* colony screening

E. coli colonies transformed with ligation reactions were routinely screened for the insert of interest by PCR. Colonies were picked using a pipette tip and inoculated into 20 μl of dH_2O . 2 μl of this solution was used as a template for a PCR reaction (section 2.5.2) using primers specific to the vector insert required. Colonies containing the correct insert were inoculated into 5 ml LB containing the appropriate antibiotic in a universal vial (Greiner) and DNA extracted (section 2.7.2). *E. coli* colonies transformed with circular plasmid were picked using a pipette tip and placed in 5 ml LB containing the appropriate antibiotic in a universal vial and grown overnight in a shaking incubator at 37 °C. DNA was extracted as below (section 2.7.2).

2.7.2 DNA extraction from *E. coli*

Plasmid DNA was extracted from 5 ml overnight cultures of *E. coli* using the QIAprep spin miniprep kit (Qiagen) according to the manufacturer's protocol.

2.7.3 Ethanol precipitation of DNA

In preparation for transformation into trypanosomes, DNA was cleaned and concentrated by ethanol precipitation after restriction digestion. One tenth of the total volume of 3 M sodium acetate (pH 5.2) was added along with three times the total volume of 100% ethanol. The solution was then incubated at -20°C for one hour to overnight, after which the DNA was centrifuged at 20,000 x g for 30 minutes at 4°C. The DNA pellet was washed with 1 ml of 70% ethanol and re-centrifuged for one minute. The pellet was air dried for 10 minutes and re-suspended in the required volume of dH₂O.

2.8 Electrophoresis

2.8.1 DNA electrophoresis

Standard DNA separations were performed on 1.0% UltraPure agarose (Invitrogen) gels made with 1 x TAE buffer (40 mM Tris, 19 mM acetic acid, 1 mM EDTA) and containing 1 x SYBRSafe (Invitrogen). The separations were run in 1 x TAE buffer at 100 V for ~ 30 minutes. 1 kb DNA ladder (NEB) was used as a size marker and apparatus was supplied by BioRad. Separating gDNA restriction digests for Southern blot analysis was carried out as above except they were electrophoresed at ~ 30 V overnight. Small DNA products of 500 bp or less was separated on 2% agarose gels as above. DNA gels were visualised and photographed using a GelDoc (BioRad) machine using UV light with a SYBRSafe filter.

2.8.2 Pulsed field agarose gel electrophoresis

Prior to electrophoretic separation, the pulsed field agarose gel electrophoresis apparatus (CHEF-DR III, BioRad) was cleaned by the circulation of 2 litres of 0.1% SDS for 1 hour at 20°C. The tank was then rinsed by circulating dH₂O for 1 hour at 20°C, and once by circulating the electrophoresis buffer 1 x TB1/10E (90 mM

Tris, 90 mM boric acid, 2 mM EDTA) for 1 hour at 15°C. Gels were electrophoresed in 2 litres of buffer, which was circulated in the tank for at least 30 minutes at 15°C before the gel was run. Separations of megabase-chromosomes were conducted using 1.2% agarose (Seakem LE). Agarose was dissolved in 150 mls of electrophoresis buffer, and 140 mls used to prepare a gel using the tray provided with the pulsed field agarose gel electrophoresis system, keeping the remainder at 37°C. After the agarose gel had set, the comb was removed, agarose genomic plugs placed into the wells, and the wells sealed with the remaining agarose. The agarose genomic plugs had been prepared by a minimum of three rounds of dialysis for a minimum of 1 hour in the appropriate electrophoresis buffer. Gels were electrophoresed at 15°C with an included angle of 120°, and 2.5 V.cm⁻¹ for 144 hours with an initial switch time of 1400 seconds and final switch time of 700 seconds for the separation of megabase-chromosomes.

2.8.2.1 Ethidium bromide staining of pulsed field agarose gels

Chromosomes were visualised by placing agarose gels in 200 mls of electrophoresis buffer containing 4 µl ethidium bromide (EtBr) at 10 µg.ml⁻¹ and placing on a rocking table for ~ 30 minutes. They were then de-stained in dH₂O for ~ 30 minutes, or until they could be visualised clearly by UV illumination.

2.8.3 Protein electrophoresis

Protein samples were fractionated either on NuPAGE Novex Bis-Tris 10% mini gels (Invitrogen) or NuPAGE Novex Tris-Acetate 3-8% mini gels (Invitrogen). The gels were electrophoresed at 200 Volts in 1 x MOPS SDS running buffer (Invitrogen) or 1 x Tris-Acetate SDS running buffer (Invitrogen) respectively, in the XCell *SureLock* Mini-Cell (Invitrogen). Proteins were visualised directly by Coomassie staining; gels were placed in Coomassie stain solution (0.25 g Coomassie brilliant blue R (Sigma) in 90 ml of methanol: water (1:1, v/v) and 10 mls glacial acetic acid), and placed on a rocker for 1 hour to overnight. Visualisation of protein bands was achieved by placing the gels in destaining solution (10% glacial acetic acid, 40% methanol) for 1-3 hours and viewing on a light box.

2.9 Blotting

2.9.1 Southern blotting

Agarose gels to be Southern blotted were photographed on a UV transilluminator alongside a ruler parallel to the gel in order to allow calculation of the sizes of fragments hybridised by radioactively labelled DNA. To depurinate the DNA, the gel was soaked in 125 mM HCl for 15 minutes and then rinsed with dH₂O. The DNA was then denatured by placing the gel in denaturation solution (0.5 M NaOH, 1.5 M NaCl) for 30 minutes. Following rinsing with dH₂O, the gel was placed in neutralisation solution (1 M Tris base, 1.5 M NaCl, 186 mM HCl) for 30 minutes. The gel was rinsed again in dH₂O, before rinsing in 20 x SSC transfer buffer (3 M NaCl, 300 mM NaOAc). The DNA was subsequently transferred to a nylon membrane (Hybond XL, Amersham Biosciences) by overnight capillary blotting (Sambrook, Fritsch, and Maniatis, 1989) using 20 x SSC transfer buffer. Following transfer, the DNA was cross-linked to the membrane twice using the auto-crosslink setting on a UV Stratalinker (Stratagene).

Pulsed field gels were Southern blotted essentially as described above, but with slightly different wash treatments due to the chromosomes being tightly bound within the agarose. After ethidium bromide staining, the chromosomes were nicked by soaking the gels twice in 125 mM HCl for 30 minutes. After rinsing in dH₂O the chromosomes were denatured by soaking in denaturation solution twice for 1 hour. The treatment then resumed as the protocol above, apart from the capillary blotting, which was usually performed for at least 96 hours with the addition of extra transfer buffer after 48 hours.

2.9.2 Western blotting

Western blotting of protein gels was carried out using the Mini Trans-Blot Cell (Bio-Rad). Gels, Hybond ECL nitrocellulose membrane (Amersham), foam and filter paper (BioRad) were equilibrated in transfer buffer (0.19 M Glycine, 0.025 M Tris base, 20% methanol), before assembling the gel sandwich. The sandwich consisted of the gel and the nitrocellulose membrane, surrounded by filter paper and foam, sandwiched between plastic cassettes. An ice block was placed

alongside the cassette to prevent overheating. Transfer was carried out by electrophoresing at 100 Volts for 2 hours.

2.10 Radiolabelling and hybridisation of DNA probes

2.10.1 Probe manufacture by random primer labelling of DNA

The DNA fragments used for probe manufacture were specific PCR products amplified as described previously (section 2.5.2), separated on an agarose gel and purified using the QIAquick gel extraction kit (section 2.5.8). Radio-labelling of these fragments was performed using the Prime It II kit (Stratagene). 25 ng of DNA was mixed with 10 μl random oligonucleotide primers (27 OD units. ml^{-1}) and dH_2O in a final reaction volume of 36 μl . The DNA was denatured by incubation at 95°C for 5 minutes. 10 μl of 5 x dATP primer buffer, 3 μl of $\alpha^{32}\text{P}$ -labelled dATP (~0.74 MBq; Perkin Elmer) and 1 μl Klenow DNA polymerase (5 U. μl^{-1}) was added and the reaction incubated at 37°C for 5 minutes. The reaction was stopped by the addition of 2 μl of stop mix (Stratagene). The probes were then purified from any unincorporated nucleotides by size exclusion chromatography using illustra Probe Quant G-50 Micro columns (GE Healthcare) according to the manufacturer's protocol. After purification, the probes were denatured at 95°C for 5 minutes before hybridisation.

2.10.2 Hybridisation and detection of radiolabelled DNA probes

Nylon membranes blotted with DNA were placed in a hybridisation tube (Hybaid) with ~ 50 mls of pre-warmed 0.5 M Church Gilbert solution (342 mM Na_2HPO_4 , 158 mM NaH_2PO_4 , 7% (w/v) SDS, 1 mM EDTA) and pre- hybridised for a minimum of 1 hour typically at 60°C in a rotating hybridisation oven. The denatured, radiolabelled probe was then added to the Church Gilbert solution in the hybridisation tube and allowed to hybridise to the blot overnight typically at 60°C in a rotating hybridisation oven. Following hybridisation, the membrane was washed in a rotating hybridisation oven with 50 mls of 2 x SSC, 0.1% SDS for 15 minutes typically at 60°C and then 50 mls of 0.2 x SSC, 0.1% SDS for another

15 minutes. After washing, the membranes were sealed in plastic and exposed to a Storage Phosphor screen (GE Healthcare) at room temperature for 1-72 hours (depending on the strength of the signal). The Storage Phosphor screen was then visualised using a Typhoon 8610 phosphorimager (Molecular Dynamics). Washes were repeated as necessary. To strip nylon membranes of hybridised probe DNA, membranes were placed in a heat-proof container with boiling stripping buffer (0.1% SDS, 0.4 M NaOH). After incubation for 10 minutes the solution was poured off and the procedure repeated. Successful stripping was checked by exposure to a Storage Phosphor screen for 24 hours and visualisation using a Typhoon 8610.

2.11 Western blot detection

2.11.1 Hybridisation and detection of antibodies

Nitrocellulose membranes blotted with protein were placed in blocking buffer (PBS, 5% Milk (Marvel), 0.1% Tween 20 (Sigma)), for 1 hour to overnight, on a rocker. Membranes were rinsed in blocking buffer before placing in blocking buffer containing the primary antibody (Table 2-2) for 1 hour. Membranes were rinsed three times in PBST (PBS, 0.1% Tween 20 (Sigma)) for 10 minutes, before placing in blocking buffer containing the secondary antibody (Table 2-3) for 1 hour. In this thesis, all secondary antibodies used for western blot were horseradish peroxidase conjugated. Membranes were rinsed three times in PBST for 10 minutes before applying the SuperSignal West Pico Chemiluminescent Substrate (Pierce). The substrate was applied to the membrane and placed in the dark for 5 minutes before exposing the membrane to an X-ray film (Kodak) for 5 seconds to overnight. X-ray films were visualised by developing in a Kodak M-35-M X-omat processor. To strip the nitrocellulose membranes of bound antibodies, membranes were placed in a container with 10 mls of Restore Western Blot Stripping Buffer (Pierce) and rocked for 30 minutes. Successful stripping was checked by applying SuperSignal West Pico Chemiluminescent Substrate (Pierce) to the membrane and exposing it to an X-ray film. Membranes were finally rinsed in PBST before being re-probed as above.

Name	Host animal	Company/Laboratory	Dilution
Anti-BRCA2	Chicken	Covalab	1:200
Anti-RAD51	Rabbit	R. McCulloch	1:500-1000
Anti-NOG1	Rabbit	M. Parsons	1:5000
Anti-OPB1	Sheep	J. Mottram	1:1000
Anti-Myc	Mouse	Millipore	1:7000
Anti-HA	Mouse	Sigma	1:10000
Anti-His	Mouse	Sigma	1:750
Anti-GST	Mouse	Novagen	1:10000

Table 2-2 List of primary antiserum used in this thesis.

Name	Conjugation	Company/Laboratory	Dilution
Anti-Chicken	HRP	Invitrogen	1:200
Anti-Rabbit	HRP	Molecular Probes	1:500
Anti-Sheep	HRP	Santa Cruz	1:5000
Anti-Mouse	HRP	Invitrogen	1:1000
Anti-Rabbit Alexa Fluor 594	Alexa Fluor 594	Invitrogen	1:7000
Anti-Myc Alexa Fluor 488	Alexa Fluor 488	Invitrogen	1:7000

Table 2-3 List of secondary antiserum used in this thesis.

2.11.2 Anti-BRCA2 Antiserum

Two peptide antigens corresponding to amino acids 105-ARARMNTENGQEST-118 and 1556-RIKQLEDWQTPHEEC-1570 were inoculated into two chickens with complete Freund's adjuvant at day 0 and with incomplete Freund's adjuvant at days 14, 28 and 63 (Covalab). The final bleeds (day 90) from the two chickens were subjected to affinity purification using the two peptides and the resultant antisera was pooled. This is referred to as anti-BRCA2 antiserum.

2.12 *In vivo* co-immunoprecipitation

Protein was extracted from PCF cells as above (section 2.2.4.2). A 50 µl aliquot of protein extract was taken as an input sample and frozen in SDS-PAGE sample buffer until required. The remaining protein extract was split into two eppendorfs, ~ 250 µl each. To this was added 50 µl of 50% bead slurry. Beads (Anti-Myc agarose (Millipore) and Anti-HA agarose (Roche)) were prepared by washing twice with 1 ml Trypanosome Lysis Buffer (TLB) with centrifugation at 5,000 x g for 1 minute at 4°C and adding an equal volume of TLB to make up to a 50% slurry. Samples were incubated with end-over-end rotation at 4°C for 1 hour. Beads were pelleted by centrifugation at 5,000 x g for 1 minute at 4°C and washed 5 times with 1 ml TLB. 100 µl of SDS-PAGE sample buffer was added and

the sample boiled for 5 minutes at 98°C prior to separation on an SDS-PAGE gel and western blotting.

2.13 *In vitro* Glutathione S-Transferase pull-down

Glutathione S-Transferase (GST) pull-down studies in *E. coli* were carried out as co-expression studies, with two complementary plasmids (pGEX-4T-3 (GE healthcare) and pRSF-1b (Novagen)) transformed into the same bacterial cell line. For each experiment fresh transformations of Rosetta2 BL21 (Novagen) chemically competent *E. coli* were prepared. A single colony was picked from the transformation plate, inoculated into 5 ml LB containing the appropriate antibiotics and grown at 37°C overnight in a shaking incubator. 1 ml of culture was diluted into 50 ml LB containing the appropriate antibiotics in a 250 ml conical flask and grown at 37°C until an OD₆₀₀ nm of ~ 0.5 was reached whereupon protein expression was induced by the addition of isopropyl-β-D-thiogalactopyranoside (IPTG; Melford) at a final concentration of 1 mM. Once induced, flasks were transferred to a shaking incubator at 25°C and grown overnight. Cells were harvested by centrifugation at 3750 x g for 20 minutes at 4°C. Cell pellets were re-suspended in 5 ml ice cold Wash/Lysis Buffer (WLB; 1 mM DTT (Melford), 0.1% (v/v) NP-40, 13 Units.ml⁻¹ DNase1 (Invitrogen), 1 x Complete EDTA-free Protease Inhibitor Cocktail (Roche) in PBS) by vortexing. Cells were subjected to a cycle of freeze thaw at - 80°C prior to sonication on ice for 4 cycles of 10 seconds sonication with 20 seconds rest between pulses using a Soniprep 150 (MSE). Insoluble material was removed by centrifugation at 20,000 x g for 20 minutes at 4°C. A 100 µl aliquot of supernatant (input) was frozen in SDS-PAGE sample buffer until required.

100 µl of bead slurry (Glutathione Sepharose HP (GE Healthcare)) per cell extract was prepared by washing twice with 5 ml WLB at 500 x g for 2 minutes at 4°C. After washing beads, were re-suspended in 10 volumes of WLB and 1 ml of bead slurry added to each cell extract. After incubation with end-over-end rotation at 4°C for 1 hour beads were pelleted by centrifugation at 500 x g for 2 minutes at 4°C and the supernatant carefully removed. Beads were washed five times with 5 ml WLB. To elute bound proteins, beads were incubated with 500 µl elution buffer (50 mM Tris-HCL (pH 8.0), 200 mM NaCl, 20 mM reduced glutathione (Sigma), 0.1% NP-40, 1 mM DTT) for 1 hour with end-over-end

rotation at 4°C. Beads were pelleted at 500 x g for 2 minutes at 4°C and elution buffer removed to a clean eppendorf. A 100 µl aliquot (elution) was frozen in SDS-PAGE sample buffer until required.

2.14 Bioinformatics

Gene sequences were downloaded from GeneDB (www.genedb.org) and viewed in CLC Genomics Workbench (CLC Bio). Sequence alignments were carried out and trees generated using CLC Genomics workbench. BLASTn search of the *T. brucei* TREU 927 genome sequence was carried out using the facility at www.genedb.org.

Chapter 3: The function of *T. brucei* BRCA2 in the maintenance of genome stability.

3.1 Introduction

Previous studies on *brca2*^{-/-} mutants generated in *T. brucei* bloodstream form (BSF) cells in strain Lister 427 demonstrated that they display a genomic instability phenotype, detectable by an accumulation of visible karyotype changes in the megabase chromosomes (Hartley and McCulloch, 2008), which may correspond with gross chromosomal rearrangements (GCRs) observed in *brca2*^{-/-} mutants in other organisms (see below; Yu *et al.*, 2000; Kojic *et al.*, 2002; Ko, Lee, and Lee, 2008). At least some of the genome rearrangements in *T. brucei* BSF *brca2*^{-/-} mutant cells appear to arise due to deletions within the subtelomeric *VSG* arrays, as evidenced by the loss of members of the *VSG121* gene family after prolonged passaging (Hartley and McCulloch, 2008). However, in the absence of a genome-wide annotation of the *VSG* repertoire in *T. brucei* Lister 427, indicating their chromosomal locations, it has not been possible to determine how widely affected the *VSG* arrays are by mutation of *BRCA2*. Interestingly, no rearrangements were observed in the intermediate or mini-chromosomes and, as these chromosomes do not harbour *VSG* arrays, this lends support to the idea that the karyotype changes may be limited to, or at least most severely evident as, changes within the *VSG* arrays. This genomic instability phenotype has not been observed in *rad51*^{-/-} mutants in *T. brucei*, though the experimental procedures adopted were not equivalent to the *brca2*^{-/-} mutant analysis: here, *rad51*^{-/-} clones were examined after prolonged passaging and isolation of *VSG* switch variants (McCulloch and Barry, 1999), and also after transformation to measure recombination events and characterise the recombinants (McCulloch and Barry, 1999). A very similar genomic instability phenotype is, however, observed in *mre11*^{-/-} mutants (section 1.5.3; Robinson *et al.*, 2002). The function of *BRCA2* in the maintenance of genome integrity has been well documented in mammals and *Ustilago maydis* (Moynahan, Pierce, and Jasin, 2001; Kojic *et al.*, 2002), and it is possible that this is a function that is conserved in the trypanosomatids. However, where GCRs in these organisms are manifest as chromosome deletions and translocations, deletion appeared to predominate in *T. brucei brca2*^{-/-}, and *mre11*^{-/-}, mutants. Whether this is because *BRCA2* plays subtly different roles in *T. brucei*, or is due to differences in genome composition, is unknown.

This chapter aims to understand the precise genetic modifications that occur during the genome rearrangements observed in *T. brucei brca2*^{-/-} mutants. In order to achieve this, it was decided to mutate *BRCA2* in the genome strain of *T. brucei*, TREU 927. The availability of the complete genome sequence for this strain, including annotation of > 800 VSGs (Marcello and Barry, 2007), should allow the dissection of the rearrangements at the sequence level, with a focus on the subtelomeric VSG archive. TREU 927 is a pleomorphic strain of *T. brucei*, and although gene mutants have been described in the BSF (van Deursen *et al.*, 2001), due to the difficulties associated with the prolonged passaging of these cells, it was decided to analyse *brca2*^{-/-} mutants in the procyclic form (PCF) cells of this strain.

3.2 Generation of *BRCA2* gene disruption mutants in PCF TREU 927 *T. brucei*

3.2.1 *BRCA2* gene deletion constructs

Homozygous mutants of *BRCA2* were generated in PCF TREU 927 *T. brucei* using a classical gene deletion strategy where the entire *BRCA2* open reading frame (ORF) is removed. The *BRCA2* gene deletion constructs that were used, $\Delta BRCA2::BSD$ and $\Delta BRCA2::PUR$, are displayed in Figure 3-1 (gift, Claire Hartley). These constructs contain regions of the 5' and 3' un-translated regions (UTR) flanking the *BRCA2* ORF cloned into pBluescript (Stratagene) and used as targeting sequence to enable homologous recombination and replacement of the entire *BRCA2* ORF with antibiotic resistance cassettes, following transformation. To allow selection of constructs that have integrated into the genome, one of two antibiotic resistance cassettes was cloned between the flanks. The *blasticidin* (*BSD*) and *puromycin* (*PUR*) resistance cassettes each contain processing signals derived from *actin* and *tubulin* intergenic sequences flanking the antibiotic resistance ORFs to allow RNA *trans*-splicing and polyadenylation, respectively. For transformation, the $\Delta BRCA2::BSD$ and $\Delta BRCA2::PUR$ constructs were excised from pBluescript by restriction digestion with *Xho*I and *Xba*I, the digested DNA was then ethanol precipitated and approximately 5 μ g of the resuspended DNA was used for each transformation.

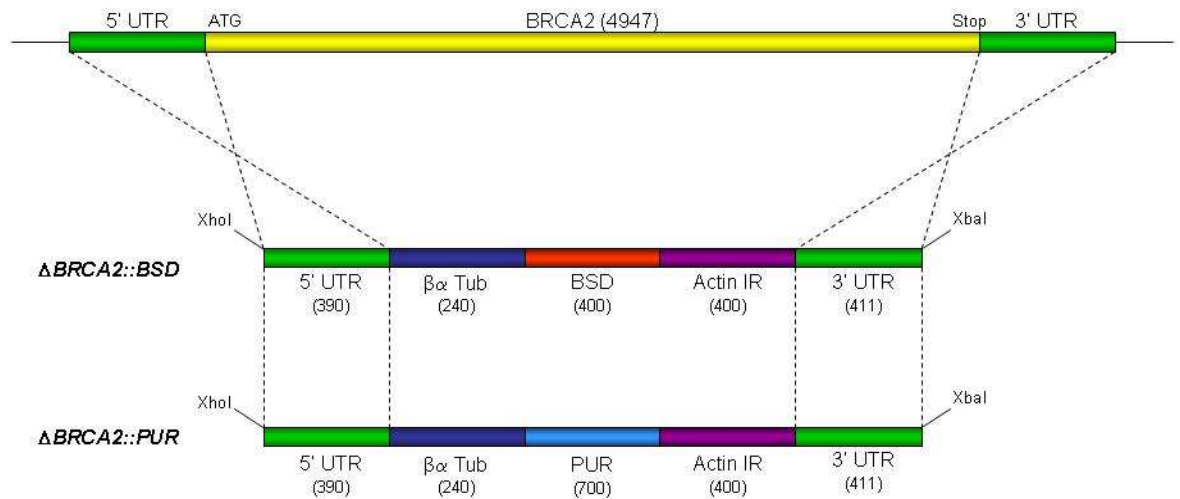


Figure 3-1 *BRCA2* gene deletion constructs.

Restriction maps of the constructs used for the deletion of *BRCA2* are shown, relative to the *BRCA2* ORF (top). Sizes of the individual components are shown (bp), and are not drawn to scale. Constructs were cloned into the pBluescript plasmid and excised using the *XhoI* and *XbaI* restriction sites shown. 5' UTR and 3' UTR correspond to un-translated regions upstream and downstream of the *BRCA2* ORF, respectively. $\beta\alpha$ Tub: $\beta\alpha$ tubulin intergenic region. Actin IR: actin intergenic region. BSD: blasticidin resistance ORF. PUR: puromycin resistance ORF.

3.2.2 Generation of *BRCA2* mutants in PCF TREU 927 *T. brucei*

Two separate transformations were carried out in order to generate two independent *BRCA2* heterozygous (-/+) cell lines using the Δ *BRCA2*::*BSD* and Δ *BRCA2*::*PUR* constructs. To do this, wild-type PCF TREU 927 (WT 927) cells were transformed using the protocol described in section 2.1.3 and antibiotic resistant transformants were selected by placing cells on SDM-79 media (GIBCO) supplemented with 10 $\mu\text{g}.\text{ml}^{-1}$ blasticidin (Calbiochem) or 1 $\mu\text{g}.\text{ml}^{-1}$ puromycin (Sigma). The generation of *BRCA2*-/+ mutants was confirmed by PCR analysis performed on genomic DNA extracted from six blasticidin resistant clones and six puromycin resistant clones. Two independent *BRCA2*-/+ mutant clones were chosen (-/+ *BSD* and -/+ *PUR*; Figure 3-2B) and subsequently transformed with the complementary *BRCA2* gene deletion construct in order to generate independent *BRCA2* homozygous (-/-) mutant cell lines. Antibiotic resistant transformants were selected with 5 $\mu\text{g}.\text{ml}^{-1}$ blasticidin and 0.5 $\mu\text{g}.\text{ml}^{-1}$ puromycin.

3.2.3 Confirmation of *BRCA2* mutants by PCR

The generation of *brca2*^{-/-} mutants was initially confirmed by PCR performed on genomic DNA extracted from seven putative *-/- BSD-PUR* transformant clones and eight putative *-/- PUR-BSD* transformant clones. PCR was performed using primers specific to the *BSD* (primers 140 and 141) and *PUR* (primers 144 and 145) resistance ORFs, and also a 1.2 kb region of the *BRCA2* ORF (primers 48 and 49). The location of the primers and expected sizes of the PCR products are displayed in Figure 3-2A. The sequences of all primers used in this thesis are displayed in Table 2-1 and their location if within the *BRCA2* gene sequence can be found in Appendix 1.

The agarose gel in Figure 3-2B demonstrates the presence of the *BSD* and *PUR* resistance ORFs in all of the putative *brca2*^{-/-} mutant clones. Some of these clones still retained the *BRCA2* ORF, and produced a PCR product with the primers specific to part of the *BRCA2* ORF; whether these had integrated the second knockout construct into an unknown genomic location, or were triploid for the *BRCA2* locus or chromosome, is unknown. These ‘incorrect’ clones were discarded. Apart from these, a number of clones were apparent (five *-/- BSD-PUR*, and at least one *-/- PUR-BSD*; indicated by ‘*’ in Figure 3-2B) that failed to amplify a PCR product using the primers specific to part of the *BRCA2* ORF, and had integrated both the *BSD* and *PUR* resistance cassettes. Two of these putative *brca2*^{-/-} mutant clones, from distinct *BRCA2*^{-/+} antecedents (and thus independently derived), were selected for further analysis (from now on, referred to as *-/- BSD-PUR* and *-/- PUR-BSD*).

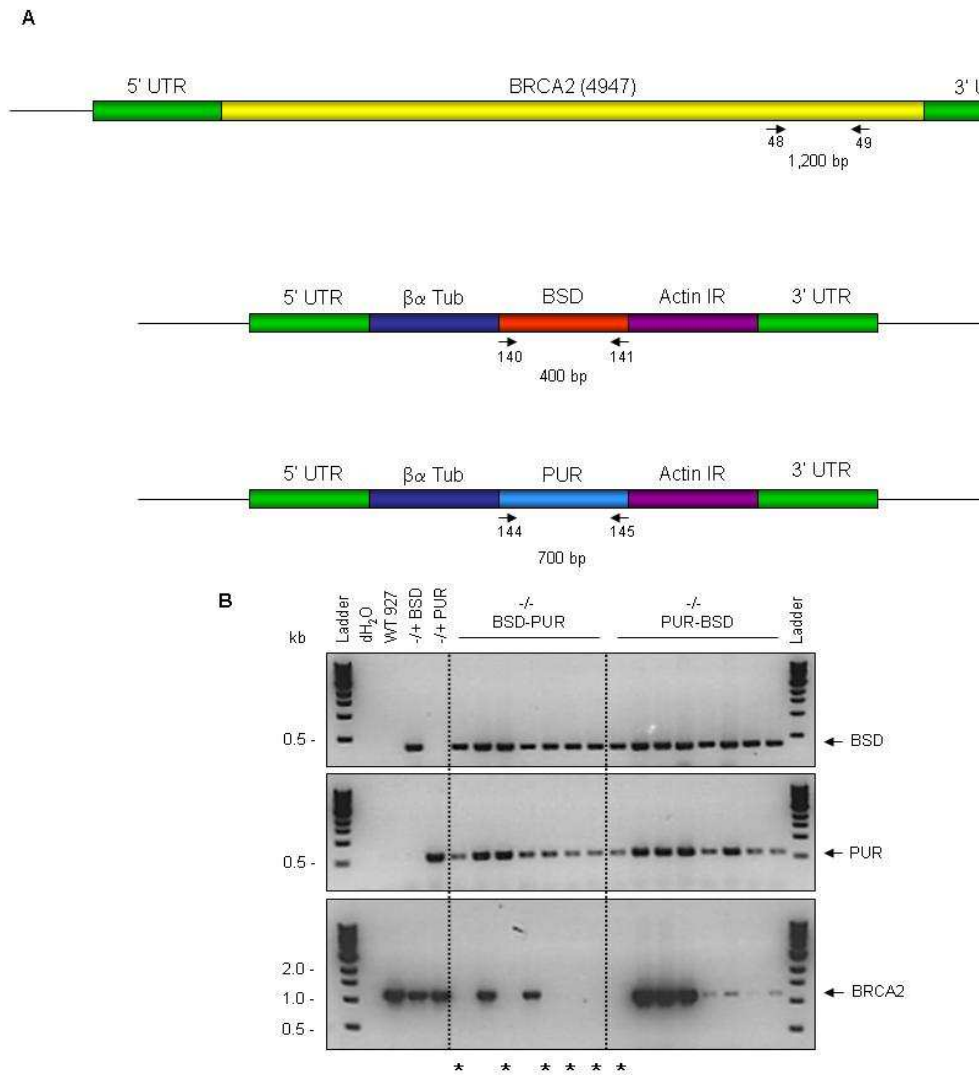


Figure 3-2 Confirmation of PCF TREU 927 *BRCA2* mutants by PCR.

(A) Primers used to amplify part of the *BRCA2* ORF, and the *BSD* and *PUR* resistance ORFs are indicated (black arrows), with the expected sizes of the resulting PCR products shown (bp). (B) An agarose gel of the PCR products obtained using the primers, described above, and genomic DNA extracted from wild-type TREU 927 (WT 927), *BRCA2* heterozygous (-/+), and putative *brca2* homozygous (-/-) mutant cell lines. The two independent *BRCA2*-/+ mutants are indicated by -/+ *BSD* and -/+ *PUR*, and the putative *brca2*-/- mutants derived from these are indicated by -/- *BSD-PUR* and -/- *PUR-BSD*, respectively. Distilled water (dH₂O) was used as a negative control. The PCR products produced from the *BSD*, *PUR* and *BRCA2* ORFs are indicated (black arrows), and size markers are shown (Ladder, kb). ‘*’ indicates *brca2*-/- mutants that are confirmed by PCR.

3.2.4 Confirmation of *BRCA2* mutants by Southern analysis

To confirm the generation of two independent *brca2*-/- mutant cell lines, Southern analysis was performed. Genomic DNA extracted from wild-type TREU 927, -/+ and -/- *BRCA2* mutant cell lines was digested with *Sac*II and *Hind*III, separated by electrophoresis on a 1% agarose gel, Southern blotted and hybridised at 60°C with a DNA probe generated by PCR-amplification with the primers 152 and 153, corresponding with the 5' UTR of the *BRCA2* ORF (the

region included in the gene deletion constructs). The location of primers, predicted restriction enzyme recognition sites and expected DNA fragment sizes in this approach are displayed in Figure 3-3A.

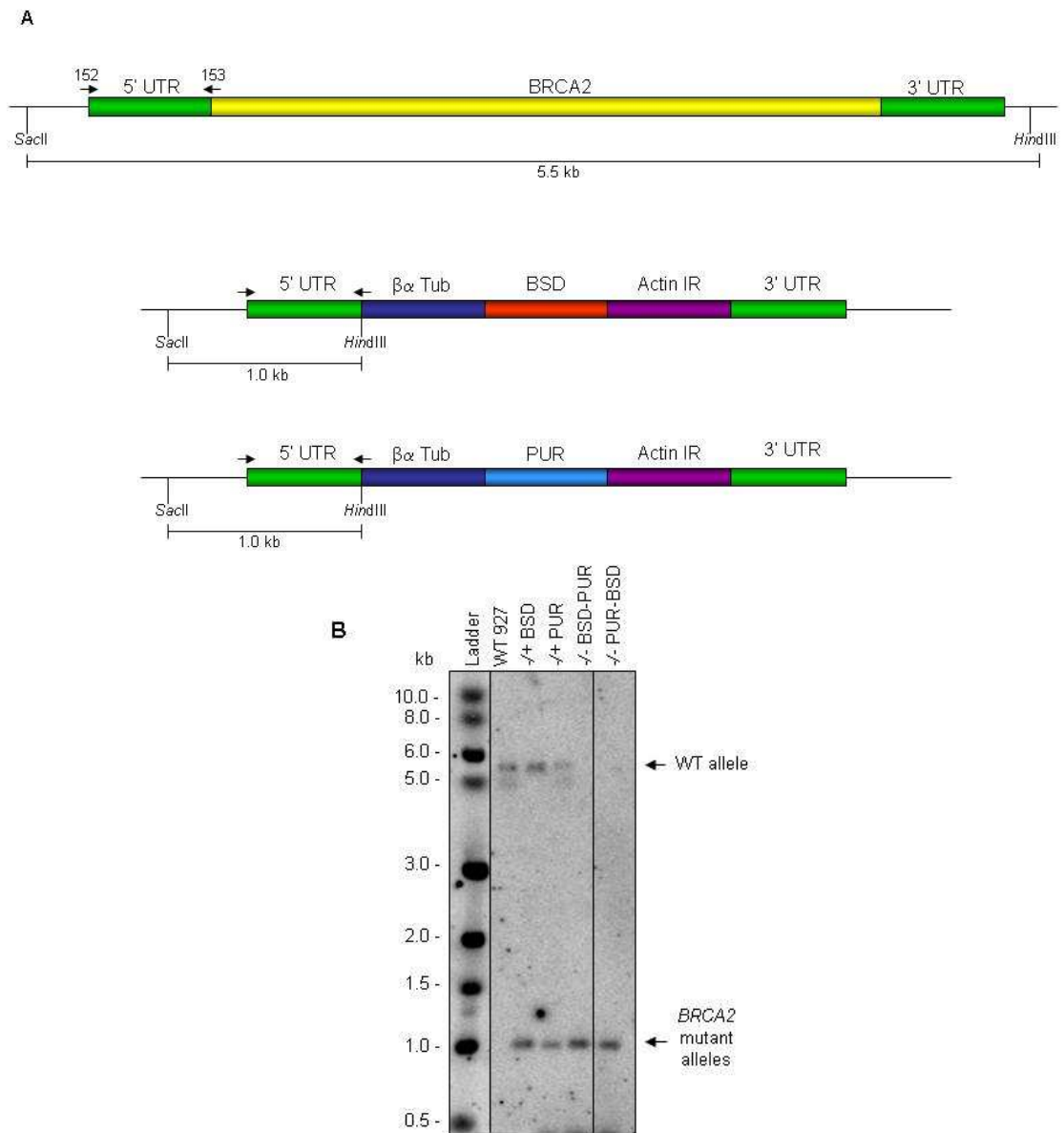


Figure 3-3 Confirmation of PCF TREU 927 *BRCA2* mutants by Southern analysis. (A) Restriction maps showing the expected products of restriction digestion, Southern blotting and hybridisation with the 5' UTR of the *BRCA2* ORF (black arrows indicate the primers used to PCR-amplify this as a DNA probe). The restriction sites are indicated, with the expected restriction fragment sizes shown (kb). (B) 5 μ g of genomic DNA extracted from wild-type TREU 927 (WT 927), *-/+* and *-/-* *BRCA2* mutant cell lines was digested with *SacI* and *HindIII* before being separated by electrophoresis on an agarose gel. The DNA was Southern blotted before being hybridised with a DNA probe against the 5' UTR of the *BRCA2* ORF. The bands produced from the WT allele and the *BRCA2* mutant alleles are indicated (black arrows), and size markers are shown (Ladder, kb).

The Southern blot in Figure 3-3B demonstrates that the intact *BRCA2* ORF exists in wild-type TREU 927 cells. In this strain no allelic size variation is detectable at this gene locus, as observed in wild-type BSF Lister 427 cells where the two

alleles of *BRCA2* possess different numbers of BRC repeat motifs (Hartley and McCulloch, 2008). The *BRCA2*^{-/+} mutants have one *BRCA2* allele replaced with either a *BSD* or *PUR* resistance cassette. In the putative *brca2*^{-/-} mutants, there was no evidence for the presence of an intact *BRCA2* ORF, suggesting both alleles of the gene were deleted, one replaced by the *BSD* cassette and the other replaced by the *PUR* cassette (though these cannot be distinguished in this Southern approach, Figure 3-2B shows that each antibiotic resistance ORF is present).

3.2.5 Confirmation of *BRCA2* mutants by western analysis

In order to try and detect BRCA2 protein in *T. brucei*, antiserum was raised in chickens against two peptides that were synthesised based on the predicted *T. brucei* BRCA2 polypeptide (section 2.11.2). One peptide corresponded with the BRC repeat domain (amino acids 105 to 118), and the second was derived from the C-terminus of the protein (amino acids 1556 to 1570). A number of attempts at western blot analyses were performed (data not shown), using whole cell extracts from PCF *T. brucei* cells. This revealed that, on occasion, a band of the size expected for *T. brucei* BRCA2 was observed (176 kDa); however, in all cases, significant numbers of further bands were seen, presumably reflecting non-specific binding of the antiserum to other *T. brucei* proteins, and in many cases the 176 kDa band expected for BRCA2 was not seen. Despite the lack of reproducibility of this antiserum, confirmation of the *brca2*^{-/-} mutants by western blot was attempted multiple times using total protein extract from wild-type TREU 927, ^{-/+} and ^{-/-} *BRCA2* mutant cell lines, which was separated by SDS-PAGE on a 3-8% Tris-Acetate gel, blotted and probed with anti-BRCA2 antiserum at a dilution of 1:200. The clearest result of these experiments is displayed in Figure 3-4.

The western blot in Figure 3-4 suggested that BRCA2 protein was visible at approximately the expected size (176 kDa) in the wild-type and two *BRCA2*^{-/+} mutant cell lines, and was absent in the two *brca2*^{-/-} mutant cell lines. A non-specific protein band is visible at ~ 58 kDa and, if this is considered as a protein loading control, demonstrates approximately equal loading of cell extracts from the five cell lines.

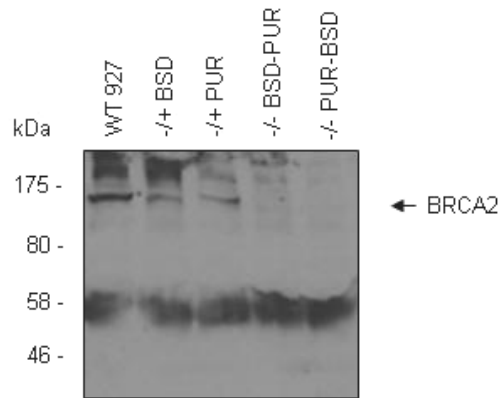


Figure 3-4 Confirmation of PCF TREU 927 *BRCA2* mutants by western analysis. Total protein extracts from wild-type TREU 927 (WT 927), *-/+* and *-/-* *BRCA2* mutant cell lines were separated by SDS-PAGE and western blotted before being probed with anti-*BRCA2* antiserum (1:200 dilution). The band of the size expected for the *BRCA2* protein is indicated (black arrow), and size markers are shown (kDa).

3.3 Phenotypic analysis of PCF TREU 927 *BRCA2* mutants

3.3.1 Analysis of *in vitro* growth

brca2^{-/-} mutants in BSF Lister 427 *T. brucei* display an increased population doubling time (approximately 2-fold) when compared to wild-type BSF Lister 427 cells (Claire Hartley, PhD Thesis, 2008). To determine if the same phenotype is observed in PCF TREU 927 *brca2*^{-/-} mutant cells, *in vitro* growth was analysed. 2 ml cultures were inoculated at a density of 5×10^5 cells.ml⁻¹ and counted using a Coulter Counter (Beckman) at 24, 48 and 72 hours subsequently. The average counts from three experimental repetitions are plotted in Figure 3-5, and extrapolated doubling times (calculated as detailed in section 2.3.1) are displayed in Table 3-1.

From the growth curves and doubling times displayed it is apparent that disruption of a single *BRCA2* allele has no discernible effect on the growth of *BRCA2*^{-/+} cells when compared to wild-type cells. However, the *brca2*^{-/-} mutants display a slight retardation in growth as evidenced by an increase in doubling time from the wild-type value of ~ 11 hours to between 13 and 19 hours for the two mutant cell lines. This is an increase in doubling time that is less than the observed 2-fold increase of *brca2*^{-/-} mutants in BSF Lister 427 cells (Hartley and McCulloch, 2008).

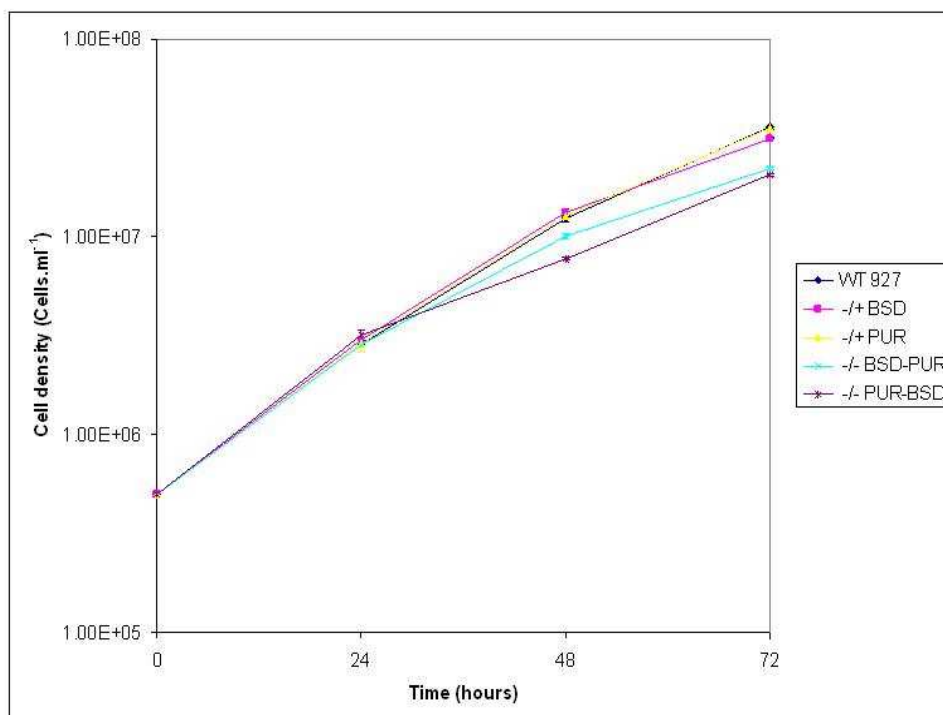


Figure 3-5 Analysis of *in vitro* growth of PCF TREU 927 *BRCA2* mutants. 2 ml cultures of wild-type TREU 927 (WT 927), *-/+* and *-/-* *BRCA2* mutant cell lines were inoculated at 5×10^5 cells.ml⁻¹ and cell densities counted 24, 48, and 72 hours subsequently are shown. Values are averaged from the counts from three experimental repetitions, and vertical lines indicate standard deviation.

Cell line	Doubling time (hours)
WT 927	10.98
-/+ BSD	10.82
-/+ PUR	11.29
-/- BSD-PUR	13.13
-/- PUR-BSD	18.70

Table 3-1 *In vitro* population doubling times of PCF TREU 927 *BRCA2* mutants. The mean doubling time for wild-type TREU 927 (WT 927), *-/+* and *-/-* *BRCA2* mutant cell lines is displayed, in hours, and was calculated from the data displayed in Figure 3-5.

3.3.2 Analysis of DNA damage sensitivity

brca2^{-/-} mutants in BSF Lister 427 display increased sensitivity to DNA damaging agents, including methyl methanesulphonate (MMS) and phleomycin, when compared to wild-type BSF Lister 427 cells (Hartley and McCulloch, 2008). MMS is an alkylating agent that methylates DNA to produce methylated purines at the 7' position of guanine residues and the 3' position of adenine residues (Brookes and Lawley, 1961; Reiter *et al.*, 1967). Phleomycin is a group of copper-containing antibiotic peptides of the bleomycin family first isolated from *Streptomyces verticillus*. Phleomycin has been shown to inhibit DNA synthesis by blocking the

activity of DNA polymerase and inducing the formation of DNA double strand breaks (Falaschi and Kornberg, 1964; Reiter, Kelley, and Milewski, 1972). In order to determine the sensitivity of the PCF TREU 927 *brca2*^{-/-} mutant cell lines to these DNA damaging agents, the Alamar Blue assay was used. Alamar Blue (resazurin sodium salt; Sigma) is a blue-coloured, non-fluorescent compound. However, in actively metabolising cells, resazurin is reduced to resorufin, which is pink and highly fluorescent (Raz *et al.*, 1997; O'Brien *et al.*, 2000). Monitoring the reduction of Alamar Blue can be achieved by measuring the production of fluorescent resorufin with a spectrophotometer (Wallac Envision) using filters of 540 nm excitation and 590 nm emission. By plotting the extent of fluorescence against log drug concentration, and performing nonlinear regression on these data, a sigmoidal survival curve was generated. Calculation of EC50, the drug concentration that causes 50% cell death, allows the metabolic capacity of the cells to be quantified, and provides an indirect assessment of cell growth or survival.

The Alamar blue assay was set up as detailed in section 2.3.2 with wild-type TREU 927, *-/+* and *-/-* *BRCA2* mutant cell lines. The extent of fluorescence for each cell line was plotted graphically over the range of log drug concentrations (for representative examples see Figure 3-6 and Figure 3-7). From this, EC50s were determined from each individual plot and then average EC50s (plus 95% confidence intervals) were calculated from the three experimental repetitions. The mean EC50s for each cell line were then plotted relative to the wild-type EC50, which was taken as 100% (Figure 3-8 and Figure 3-9). Data was presented in this way due to the fact that between experimental repetitions variation in the absolute EC50 values was observed despite the patterns of relative sensitivity between the cell lines being essentially equivalent.

The survival curves displayed in Figure 3-6 and Figure 3-7 are representative of the three experimental repetitions performed. These data demonstrate that as the concentration of DNA damaging agent increases the fluorescence, and therefore the percentage of surviving cells that are actively reducing Alamar blue to fluorescent resorufin, reduces until the concentration at which all cells are killed is reached. It is apparent that the *brca2*^{-/-} cell lines display reduced survival in the presence of both MMS and phleomycin, when compared to wild-type cells. The *BRCA2*^{-/+} *PUR* cell line appeared to demonstrate survival that is

intermediate between the wild-type and *brca2*^{-/-} cell lines for both DNA damaging agents and the *BRCA2*^{-/+} BSD cell line shows survival essentially equivalent to wild-type cells. The extrapolated EC50 values (graphs displayed in Figure 3-8 and Figure 3-9) support the graphical observations. In Figure 3-8, measuring sensitivity to MMS, the disruption of a single *BRCA2* allele in the *BRCA2*^{-/+} BSD cell line does not detectably alter the sensitivity of the cell line to MMS, when compared to wild-type cells. In the same assay, the *BRCA2*^{-/+} PUR cells appeared to have a lower EC50, suggesting they had increased sensitivity to MMS, though this was not statistically significant (see below). In Figure 3-9, measuring sensitivity to phleomycin, the *BRCA2*^{-/+} PUR cell line again appeared to be more sensitive than wild-type cells (though not significantly, see below), while the *BRCA2*^{-/+} BSD cells were more resistant to this damaging agent (although not significantly). Why single gene disruptions of *BRCA2* potentially display such changes is unclear. Irrespective of this, both *brca2*^{-/-} mutants displayed a greater sensitivity to both DNA damaging agents.

To evaluate the above data, the EC50 values of the wild-type TREU 927, ^{-/+} and ^{-/-} *BRCA2* mutant cell lines were compared using student's T-tests, and the results of this are displayed in Table 3-2. The statistical analyses largely confirm the graphical observations. No statistical difference in the calculated EC50 values was observed between wild-type cells and *BRCA2*^{-/+} mutants ($p > 0.05$) for both DNA damaging agents. However, the *BRCA2*^{-/+} BSD cell line was statistically different to all cell lines analysed ($p \leq 0.05$) after phleomycin treatment, apart from wild-type. A statistically significant difference was found between wild-type cells and both *brca2*^{-/-} mutants ($p \leq 0.05$) after MMS treatment, and one of the *brca2*^{-/-} mutants (*PUR*-*BSD*; $p \leq 0.05$) after phleomycin treatment.

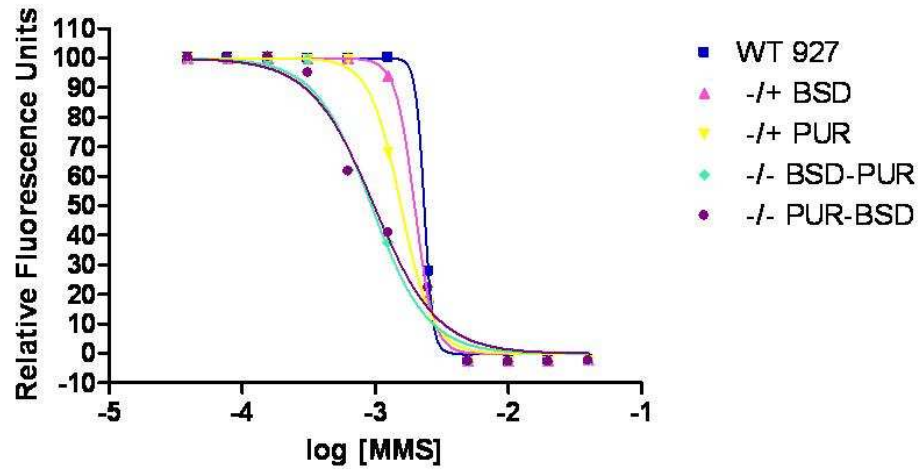


Figure 3-6 A representative survival curve for PCF TREU 927 *BRCA2* mutants exposed to MMS.

The extent of fluorescence for each cell line (WT, *-/+* and *-/-*), obtained using the Alamar blue assay, is plotted against the log of MMS concentrations. Nonlinear regression was performed and fitted curves are shown for each cell line.

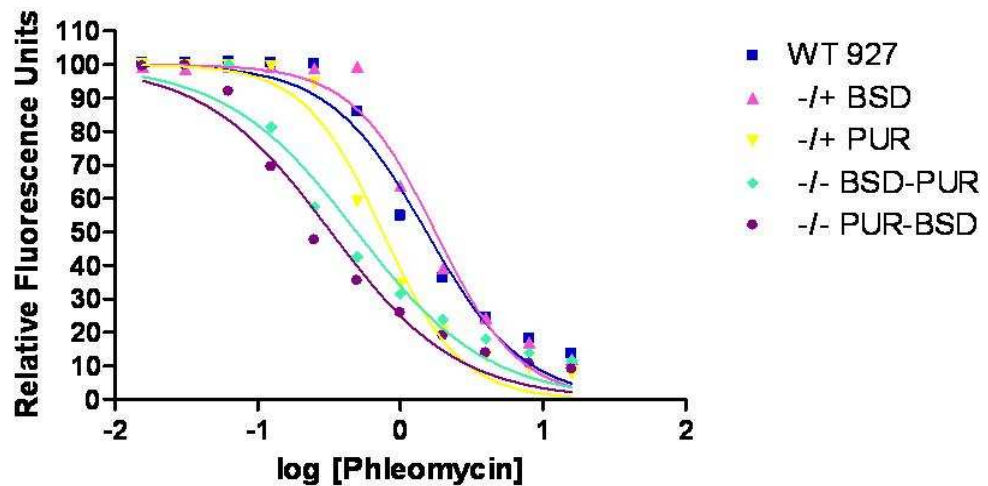


Figure 3-7 A representative survival curve for PCF TREU 927 *BRCA2* mutants exposed to phleomycin.

The extent of fluorescence for each cell line (WT, *-/+* and *-/-*), obtained using the Alamar blue assay, is plotted against the log of phleomycin concentrations. Nonlinear regression was performed and fitted curves are shown for each cell line.

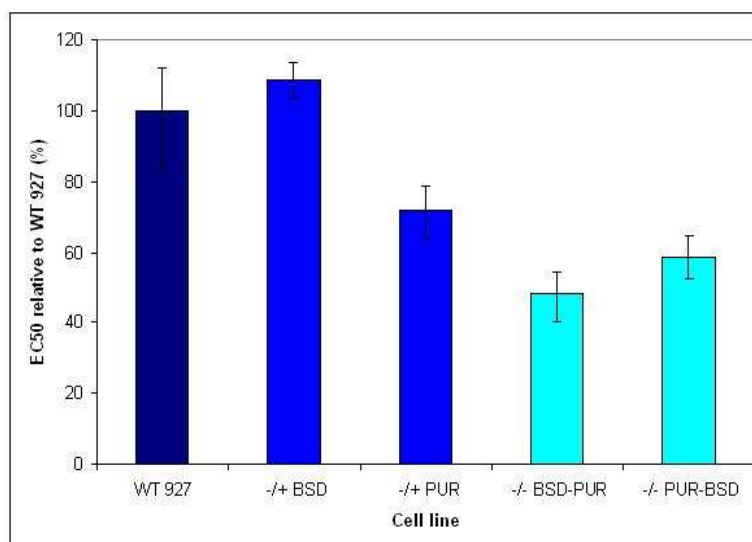


Figure 3-8 EC50 values of PCF TREU 927 *BRCA2* mutants exposed to MMS. Wild-type TREU 927 (WT 927), *-/+* and *-/-* *BRCA2* mutant cell lines were placed in serially decreasing amounts of MMS and allowed to grow for 48 hours, before the addition of Alamar Blue. After a further 24 hours, the reduction of Alamar Blue was measured by the amount of fluorescent resorufin generated. EC50 values are the mean from three experimental repetitions expressed as a percentage relative to wild-type and bars indicate 95% confidence intervals.

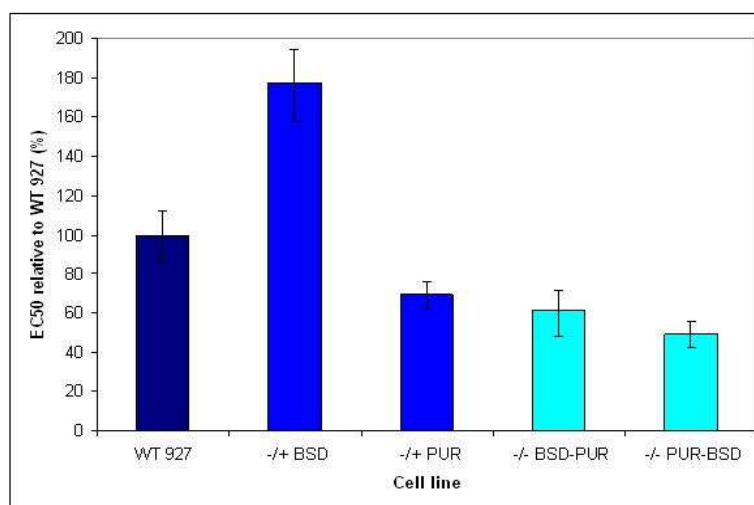


Figure 3-9 EC50 values of PCF TREU 927 *BRCA2* mutants exposed to phleomycin. Wild-type TREU 927 (WT 927), *-/+* and *-/-* *BRCA2* mutant cell lines were placed in serially decreasing amounts of phleomycin and allowed to grow for 48 hours, before the addition of Alamar Blue. After a further 24 hours, the reduction of Alamar Blue was measured by the amount of fluorescent resorufin generated. EC50 values are the mean from three experimental repetitions expressed as a percentage relative to wild-type and bars indicate 95% confidence intervals.

A

	-/+ BSD	-/+ PUR	-/- BSD-PUR	-/- PUR-BSD
WT 927	0.6581	0.0670	0.0237	0.0356
-/+ BSD		0.0749	0.0256	0.1006
-/+ PUR			0.0012	0.4048
-/- BSD-PUR				0.4699

B

	-/+ BSD	-/+ PUR	-/- BSD-PUR	-/- PUR-BSD
WT 927	0.1294	0.0975	0.0787	0.0259
-/+ BSD		0.0332	0.0139	0.0335
-/+ PUR			0.4069	0.0944
-/- BSD-PUR				0.4637

Table 3-2 Statistical analysis of Alamar Blue results.

P values are shown for student's T-tests comparing the mean EC50 values of wild-type TREU 927 (WT 927), +/- and -/- *BRCA2* mutant cell lines grown in the presence of MMS (A) or phleomycin (B). Areas shaded in yellow indicate a significant difference ($P \leq 0.05$). No correction has been made for simultaneous multiple comparisons.

3.3.3 Analysis of the cell cycle

brca2-/- mutants in BSF Lister 427 display an unusual replication phenotype consistent with the initiation of cytokinesis prior to the completion of nuclear DNA replication (Claire Hartley, PhD Thesis, 2008), which is not seen in other DNA repair mutants, most notably *rad51*-/- (McCulloch and Barry, 1999). The cell cycle stage of kinetoplasts can be easily defined by visualising the DNA content of fixed cells by DAPI staining. In addition to staining the nuclear DNA (nDNA), the mitochondrial DNA of kinetoplasts is also visible following DAPI staining, as it is organised in a concentrated collection of mini- and maxi-circle DNAs within an organelle called the kinetoplast (and hence is called kinetoplast DNA; kDNA) (Lukes *et al.*, 2002). The kinetoplast divides slightly ahead of the nucleus in the *T. brucei* cell cycle, and therefore allows the cell cycle stage of individual cells within an unsynchronised population to be determined by their N-K ratio (Figure 3-10; McKean, 2003).

Following fixation and DAPI staining (section 2.4.1), cells were counted according to the number of nuclei and kinetoplasts they contained. Cells in the G1 and S phases of the cell cycle contain 1 nucleus and 1 kinetoplast (1N1K). Cells in the G2 phase of the cell cycle contain 1 nucleus and 2 kinetoplasts (1N2K), as kinetoplast division precedes nuclear division. Following this, the nucleus divides and generates cells with 2 nuclei and 2 kinetoplasts (2N2K). Such

cells are in the M, mitotic, phase of the cell cycle. Cytokinesis subsequently generates two 1N1K cells in G1 phase, re-starting the cell cycle. Any cells that were observed not to conform to these standard configurations were noted as being aberrant cell types and were described as ‘others’. The data from the cell cycle analysis of the PCF TREU 927 *BRCA2* mutant cell lines is displayed in Figure 3-11.

These data demonstrate that the mutation of one *BRCA2* allele has no discernible effect on the distribution of cell cycle stages. In contrast, the *brca2*^{-/-} mutants showed an accumulation in the number of ‘others’ and a concomitant decrease in the number of 1N1K cells, when compared to wild-type cells. The DNA content of these ‘others’ was further analysed (Figure 3-12) and the majority (66%) were observed to be anucleate cells (primarily 0N1K; zoids) (Figure 3-13). This was subtly different from the distribution of ‘others’ observed in the BSF Lister 427 *brca2*^{-/-} mutants (Claire Hartley, PhD thesis, 2008): though increased numbers of 0N1K cells were seen in the BSF, these did not predominate to the same extent, and the ‘others’ were more evenly split between cells with raised kDNA (primarily 0N1K and 0N2K) and raised nDNA content (primarily 1N0K and 2N1K). In addition, in the BSF mutants an increase in the number of 2N2K cells with attached nuclei were seen, which were not observed here in the PCF. Oyola *et al.*, (2009) observed that upon deletion of *BRCA2* in PCF Lister 427 *T. brucei* cells approximately 80% of the total cell population presented a ‘nundu’ phenotype, characterised by a round, swollen DAPI-stained structure situated approximately in the middle of the cell body. No cells with this ‘nundu’ morphology were observed in this work.

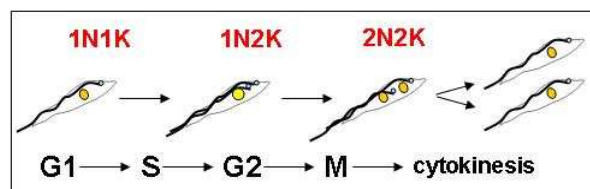


Figure 3-10 The cell cycle of procyclic form *T. brucei*.

The diagram shows the replication and division of the nucleus and kinetoplast during the *T. brucei* cell cycle. During the G1 and S phases of the cell cycle *T. brucei* contains 1 nucleus and 1 kinetoplast (1N1K). Kinetoplast division occurs in G2 phase of the cell cycle before nuclear division, resulting in cells containing 1 nucleus and 2 kinetoplasts (1N2K). Nuclear mitosis (M) leads to cells having 2 nuclei (2N2K), and occurs prior to cytokinesis, which generates two progeny containing 1N1K, which will restart the cell cycle. G1 and G2 represent cell cycle growth phases. Diagram reproduced from Hammarton, 2007.

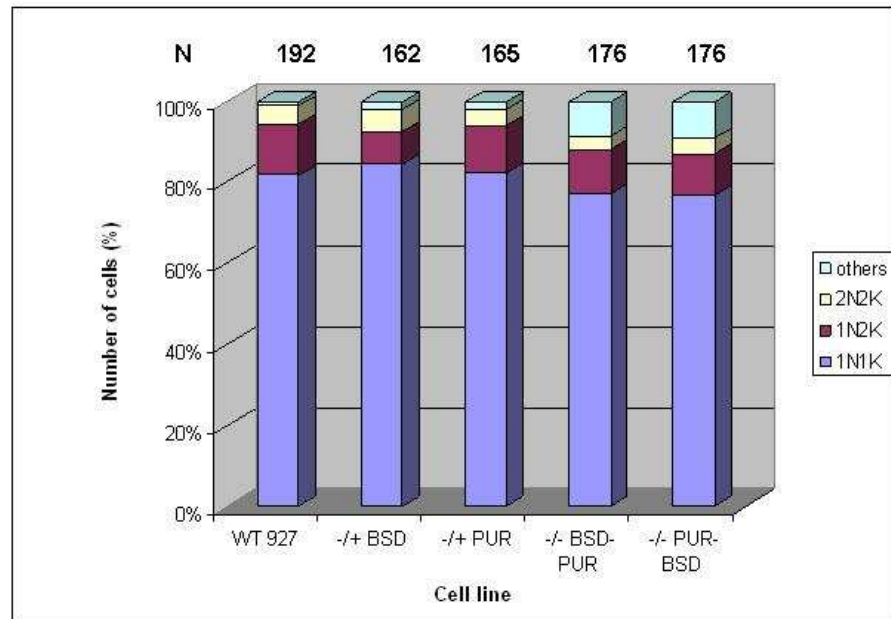


Figure 3-11 Cell cycle analysis of PCF TREU 927 *BRCA2* mutants.

The DNA content of wild-type TREU 927 (WT 927), *-/+* and *-/-* *BRCA2* mutant cell lines were visualised by DAPI staining of fixed cells. The numbers of cells with 1 nucleus and 1 kinetoplast (1N1K), 1 nucleus and 2 kinetoplasts (1N2K), 2 nuclei and 2 kinetoplasts (2N2K), and cells that do not fit into the expected classifications (others), were counted and represented by their count as a percentage of the total cells counted (N).

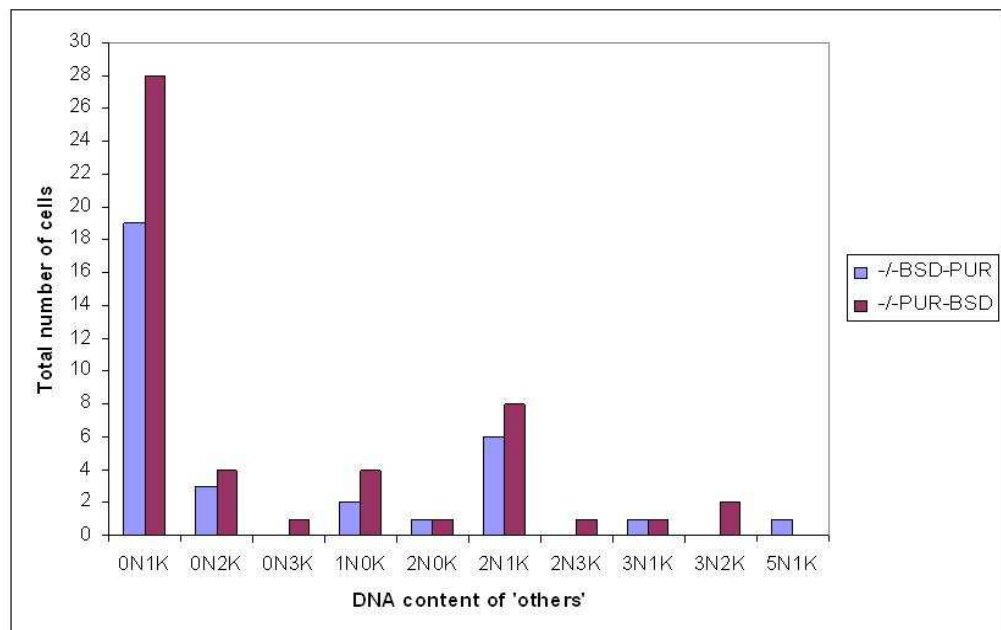


Figure 3-12 DNA content of 'others' in PCF TREU 927 *brca2*^{-/-} mutants.

Total numbers of cells that do not fit into the expected classifications (others) are represented for the PCF TREU 927 *brca2*^{-/-} mutants. The DNA content is displayed as the number of nuclei (N) and the number of kinetoplasts (K).

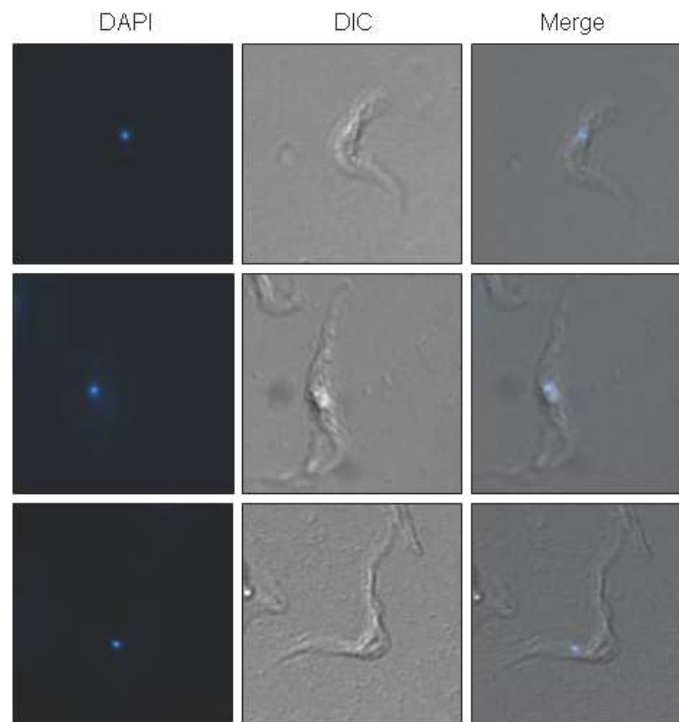


Figure 3-13 Examples of zoids in PCF TREU 927 *brca2*^{-/-} mutants. Each cell is shown after staining with DAPI (DAPI) and in differential interface contrast (DIC). Merged images of DAPI and DIC cells are also shown (Merge).

3.3.4 Analysis of RAD51 focus formation

brca2^{-/-} mutants in BSF Lister 427 *T. brucei* display a marked deficiency in the ability to form RAD51 foci after DNA damage (Proudfoot and McCulloch, 2005; Glover, McCulloch, and Horn, 2008; Hartley and McCulloch, 2008). To date, the localisation of RAD51 in response to DNA damage in PCF cells has not been examined, and so the ability of the PCF TREU 927 *BRCA2* mutant cell lines to form RAD51 foci was analysed. Cells were treated with phleomycin (1 $\mu\text{g}\cdot\text{ml}^{-1}$ for 18 hours) before being fixed onto slides and probed with anti-RAD51 antiserum at a dilution of 1:1000 and visualised with Alexa Fluor 594 conjugated anti-rabbit antiserum (1:7000 dilution, Invitrogen); DNA was visualised with DAPI, and control cells without phleomycin treatment were similarly examined. The number of RAD51 foci present in the nucleus of the cells were counted for at least 200 cells per cell line and represented as a percentage of the total number of cells counted in Table 3-3 and plotted graphically (Figure 3-14).

Representative images of cells are displayed in Figure 3-15.

In the absence of DNA damage RAD51 foci were seen in ~ 2% of cells (data not shown; examples are depicted in Figure 3-15). The small numbers of RAD51 foci that are seen in the wild-type TREU 927, *-/+* and *-/-* *BRCA2* mutant cell lines

without phleomycin treatment may be due to repair at sites of stalled replication forks, as these foci have been suggested to be able to form in the absence of BRCA2 (Tarsounas, Davies, and West, 2004). After the induction of DNA damage, the number of wild-type and *BRCA2*^{-/+} cells containing no detectable RAD51 foci reduced to ~ 25% (Figure 3-14, Table 3-3). These data demonstrate that the wild-type and *BRCA2*^{-/+} cell lines are efficient at forming RAD51 foci following DNA damage. This response is quantitatively very similar to that described in BSF *T. brucei* (Proudfoot and McCulloch, 2005; Hartley and McCulloch, 2008; Glover, McCulloch, and Horn, 2008), where 70-80% of cells formed foci after the same treatment and most cells, like the PCF cells analysed here, had 1-2 detectable foci, although some had more. The *brca2*^{-/-} mutant cell line appeared to have almost completely lost the ability to form RAD51 foci after the induction of DNA damage, as almost no foci were visible (only 2 cells had a detectable focus out of the 212 analysed). This may, in fact, be a more severe defect than observed in BSF cells, where up to 4% of *brca2*^{-/-} cells display RAD51 foci (Hartley and McCulloch, 2008), though it would be preferable to analyse greater numbers of cells, and it cannot be excluded that there is greater background fluorescence in the BSF cells with this anti-RAD51 antiserum possibly causing greater apparent foci.

		Number of cells with RAD51 foci (%)						
		0	1	2	3	4	>4	N
Cell line	WT 927	25.9	23.1	19.3	17.0	8.1	6.6	347
	^{-/+} BSD	25.3	30.8	17.0	12.6	6.3	8.0	364
	^{-/-} BSD-PUR	99.1	0.9	0.0	0.0	0.0	0.0	212

Table 3-3 RAD51 focus formation in PCF TREU 927 *BRCA2* mutants exposed to phleomycin. Wild-type TREU 927 (WT 927), ^{-/+} and ^{-/-} *BRCA2* mutant cell lines were treated with 1 µg.ml⁻¹ phleomycin for 18 hours and the number of cells with a specific number of subnuclear RAD51 foci formed (0, 1, 2, 3, 4, > 4) were counted and are represented as a percentage of the total cells counted (N). Boxes shaded in light yellow contain foci, whilst boxes shaded in bright yellow contain the highest percentage of foci.

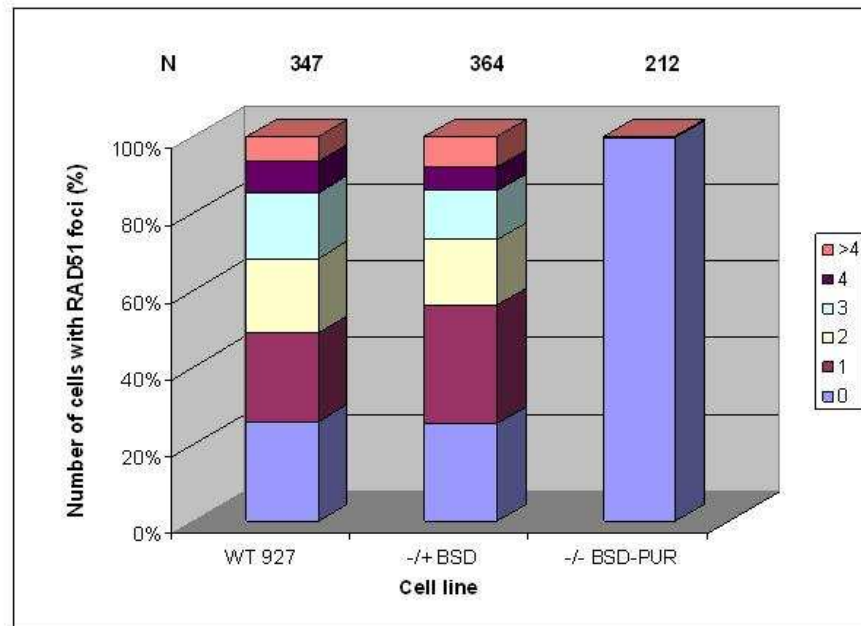


Figure 3-14 Graphical representation of RAD51 focus formation in PCF TREU 927 *BRCA2* mutants exposed to phleomycin. Wild-type TREU 927 (WT 927), *-/+*, and *-/-* *BRCA2* mutant cell lines were treated with $1 \mu\text{g}\cdot\text{ml}^{-1}$ phleomycin for 18 hours and the number of cells with a specific number of subnuclear RAD51 foci formed (0, 1, 2, 3, 4, > 4) were counted and are represented as a percentage of the total cells counted (N).

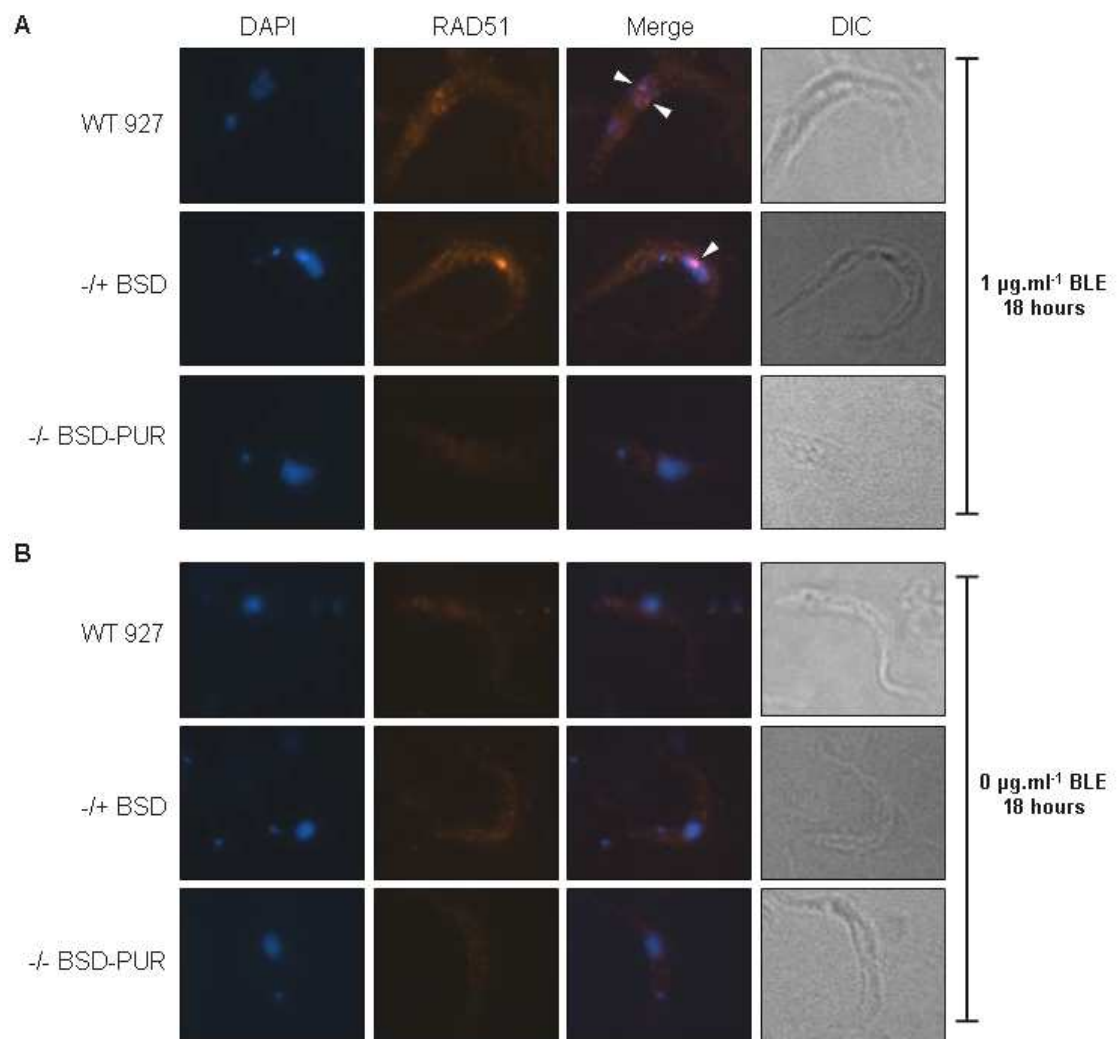


Figure 3-15 Representative images of RAD51 focus formation in PCF TREU 927 *BRCA2* mutants exposed to phleomycin.

(A) Images of wild-type TREU 927 (WT 927) +/- and -/- *BRCA2* mutant cell lines after phleomycin treatment ($1 \mu\text{g}\cdot\text{ml}^{-1}$ for 18 hours). Images were similarly prepared from cells without phleomycin treatment (B). White arrows indicate RAD51 foci. Each cell is shown in differential interface contrast (DIC), after staining with DAPI (DAPI) and after hybridisation with anti-RAD51 antiserum (1:1000 dilution) and secondary hybridisation with Alexa Fluor 594 conjugated anti-rabbit antiserum (RAD51, 1:7000 dilution). Merged images of DAPI and RAD51 cells are also shown (Merge).

To ensure that the observed differences in RAD51 foci were not due simply to a difference in the levels of RAD51 in the *brca2*^{-/-} cells, or that they could be accounted for by a loss of RAD51 up-regulation after phleomycin treatment, western analysis was carried out. Total protein was extracted from cells before and after the same regime of phleomycin treatment as employed above and separated by SDS PAGE on a 10% Bis-Tris gel. After blotting, the gel was probed with anti-RAD51 antiserum at a dilution of 1:500. The blot was then stripped (section 2.11.1) and re-probed with anti-OPB1 antiserum (1:1000 dilution) to ensure equal protein loading levels. The western blot in Figure 3-16 demonstrates that the levels of RAD51 protein remain constant after phleomycin

treatment in wild-type, and *BRCA2*^{-/+} cell lines, and are unchanged in the *brca2*^{-/-} cells. Thus, *BRCA2* is not a determinant of RAD51 stability and the recombinase expression levels are not detectably upregulated by phleomycin damage, unlike RAD51 in the related parasites *T. cruzi* and *L. major* (McKean *et al.*, 2001; Regis-da-Silva *et al.*, 2006).

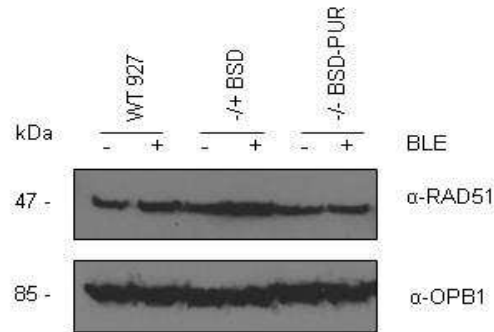


Figure 3-16 Western analysis of RAD51 in PCF TREU 927 *BRCA2* mutants exposed to phleomycin.

Total protein extracts from wild-type TREU 927 (WT 927), ^{-/+}, and ^{-/-} *BRCA2* mutant cell lines were separated by SDS PAGE and western blotted before being probed with anti-RAD51 antiserum (1:500 dilution). '-' indicates protein extracts prepared without phleomycin treatment and '+' indicates protein extracts prepared after phleomycin treatment (1 μg.ml⁻¹ BLE for 18 hours). The blots were stripped and re-probed with anti-OPB1 antiserum (1:1000 dilution) as a loading control. Size markers are shown (kDa).

3.3.5 Analysis of genomic stability in PCF TREU 927 *BRCA2* mutants

After prolonged passaging (~ 290 generations) *brca2*^{-/-} mutants in BSF Lister 427 *T. brucei* display genomic instability, detectable by an accumulation of visible karyotype changes in the megabase chromosomes, at least some of which arise due to deletions within the *VSG* arrays (Hartley and McCulloch, 2008). In order to examine these rearrangements in more detail, the *brca2*^{-/-} mutant cell lines generated here, in PCF TREU 927, were grown for ~ 380 generations before analysis of genomic stability by examination of the molecular karyotype in multiple clones generated from passaged populations.

After prolonged passaging, the wild-type TREU 927, ^{-/+} *BSD* and ^{-/-} *BSD-PUR* *BRCA2* mutant cell lines were re-cloned as described in section 2.1.4 and a total of eight clones were chosen for analysis. The *brca2*^{-/-} clones were checked by PCR, using the primers described in Figure 3-2A, to ensure that they remained homozygous mutants, in order to exclude the possibility that cross-contamination with either wild-type or *BRCA2*^{-/+} cells had occurred during the

prolonged passaging, as these would likely have a growth advantage. The agarose gel in Figure 3-17 demonstrates that the *BRCA2* ORF remained absent from the six *brca2*^{-/-} mutant clones, and that both the *BSD* and *PUR* ORFs were present in each.

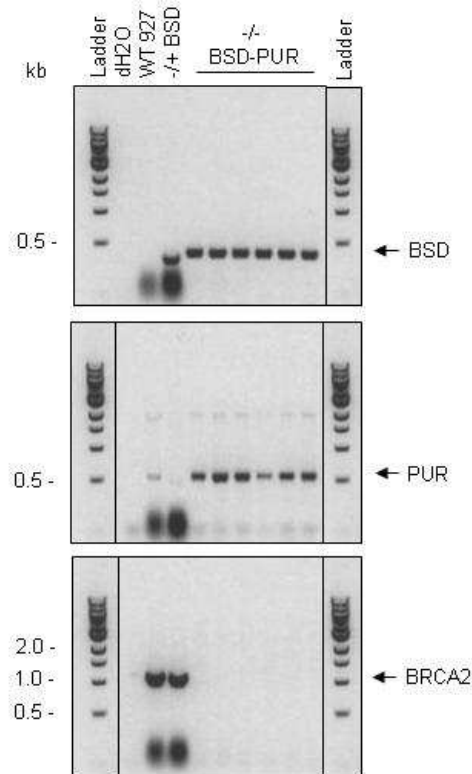


Figure 3-17 Screening PCF TREU 927 *BRCA2* mutant re-clones by PCR. An agarose gel of PCR products obtained using the primers, described in Figure 3-2A, and genomic DNA extracted from wild-type TREU 927 (WT 927), *-/+* and *-/-* *BRCA2* mutant clonal cell lines grown for ~ 380 generations. Distilled water (dH₂O) was used as a negative control. The PCR products produced from the *BSD*, *PUR* and *BRCA2* ORFs are indicated (black arrows), and size markers are shown (Ladder, kb).

Southern analysis was then performed using DNA probes designed to hybridise to multiple members of the *ingi* retrotransposon family. Retrotransposons constitute the most abundant mobile genetic element described in the genome of *T. brucei*, consisting of up to ~ 5% of the haploid genome (Berriman *et al.*, 2005). The *ingi* retrotransposon is 5.25 kb in size and composed of a 4.7 kb fragment bordered by two separate halves of the ribosomal mobile element (RIME) (Kimmel, Olemioyoi, and Young, 1987; Murphy *et al.*, 1987). If functional, it encodes a 1,657 amino acid protein containing a central reverse transcriptase domain, a C-terminal DNA-binding domain and an N-terminal apurinic/apyrimidinic (AP)-like endonuclease domain (Murphy *et al.*, 1987; Olivares, Alonso, and Lopez, 1997). The *T. brucei* genome contains ~ 115

copies of the *ingi* retrotransposon with only three intact copies that potentially code for functional retrotransposition machinery (Bringaud *et al.*, 2004; Berriman *et al.*, 2005; Bringaud *et al.*, 2008). *Ingi* retrotransposons are autonomous, which means that they encode for their own transposition. It was originally thought that they were randomly distributed throughout the genome, but it is now known that they show a relative site-specificity for insertion (Bringaud *et al.*, 2004). The majority of *ingi* retrotransposons contain a ~ 12 bp direct repeat sequence upstream that is thought may be the recognition site of the *ingi*-encoded endonuclease (Bringaud *et al.*, 2004). The distribution of retrotransposons in the *T. brucei* genome has been analysed and it was discovered that they are over-represented in strand-switch regions (113 elements per Mb), compared to coding regions (1.8 elements per Mb) and subtelomeric regions (26.7 elements per Mb) (Bringaud *et al.*, 2007; Bringaud *et al.*, 2008). *Ingi* retrotransposons in the subtelomeres are interspersed between *VSG* genes located in the silent *VSG* arrays (Figure 3-18; Berriman *et al.*, 2005).

The rationale behind using the *ingi* DNA probes was that it was considered they may provide a more complete picture of genetic changes in the genome, and more specifically within the subtelomeres, than could be obtained by designing DNA probes for a large number of individual *VSG* genes. 77 of the most complete *ingi* sequences extracted from the TREU 927 genome sequence were aligned (Appendix 2) and two DNA probes were designed against relatively conserved regions, named *INGI-1* and *INGI-2*, and amplified by PCR using primers 86 and 87, and 88 and 89, respectively. The eight clonal cell lines analysed in Figure 3-17 were used for this analysis. Genomic DNA was extracted from each, digested with *Xho*I or *Hind*III, separated by electrophoresis on a 1% agarose gel, Southern blotted and hybridised at 60°C with the *ingi* DNA probes.

The Southern blots in Figure 3-19 demonstrate that this approach revealed no obvious *ingi* rearrangements in the six *brca2*^{-/-} mutant clones, as the complex banding patterns closely resembled each other and that seen in the single wild-type and *BRCA2*^{-/+} clones used for comparison. Though this may indicate an absence of *ingi*-associated rearrangements, it is possible that the complexity of the banding pattern masked any subtle changes.

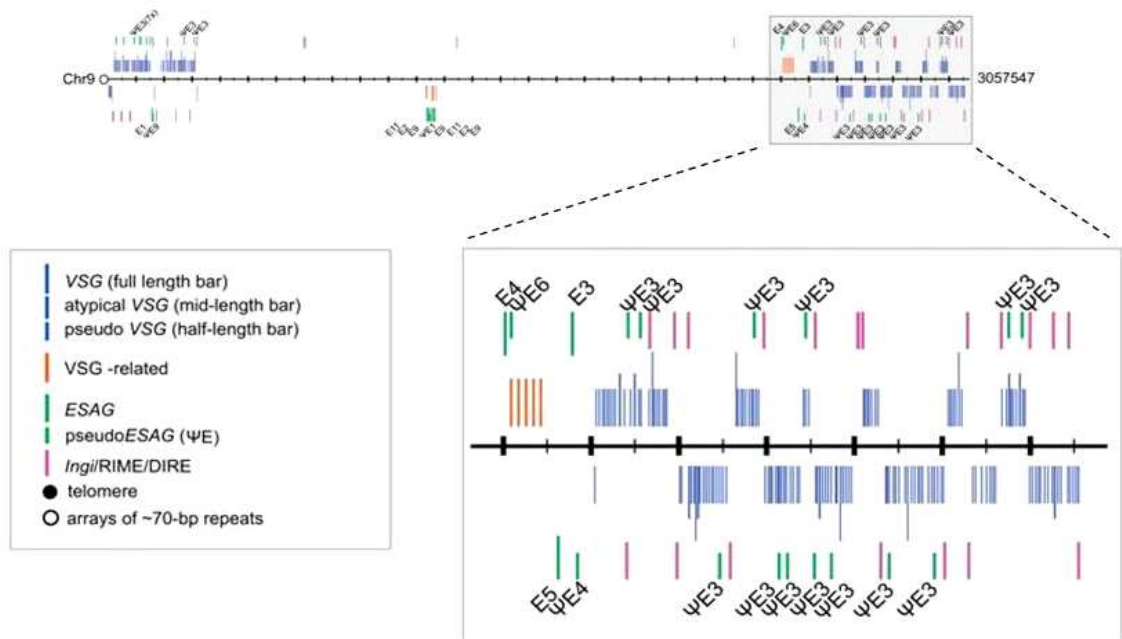


Figure 3-18 The location of *ingi* retrotransposons in the subtelomeres of TREU 927 chromosome 9.

The location of VGSs (blue), ESAGs (green) and *ingi* retrotransposons (purple) are shown for the subtelomere of chromosome 9. Reproduced from Berriman *et al.*, 2005.

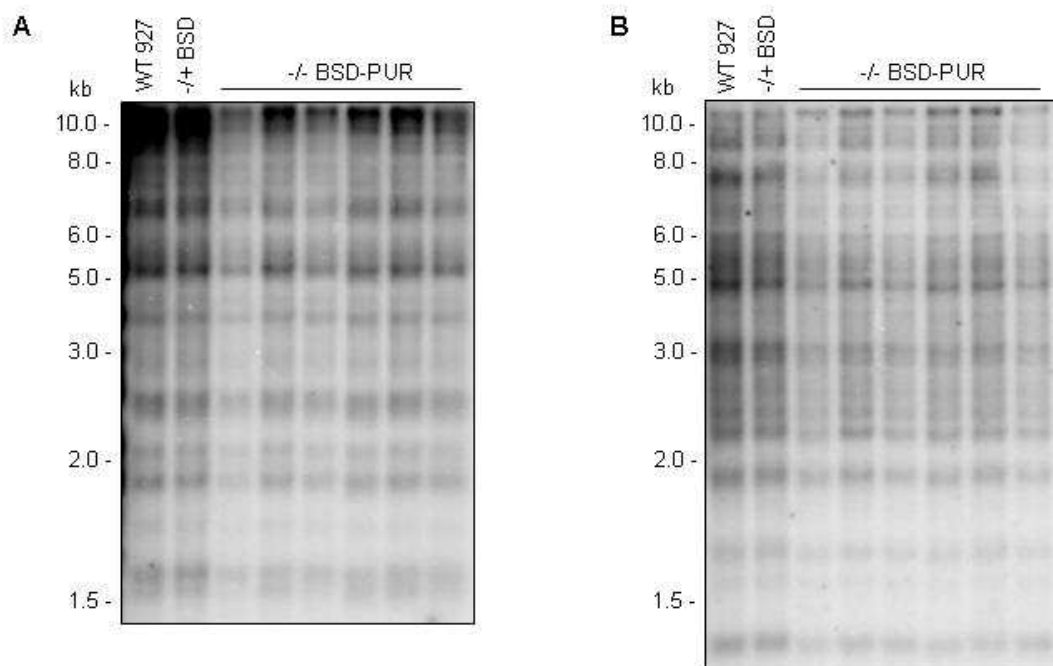


Figure 3-19 Analysis of genomic stability of PCF TREU 927 *BRCA2* mutants by Southern analysis using DNA probes against *ingi* retrotransposons.

5 μ g of genomic DNA extracted from wild-type TREU 927 (WT 927), *-/+* and *-/-* *BRCA2* mutant clones was digested with *Xho*I (A) or *Hind*III (B), before being separated by electrophoresis on an agarose gel. The DNA was Southern blotted before being hybridised with a DNA probe against *ingi* (*INGI-1* (A) or *INGI-2* (B)). Size markers are shown (kb). The clones analysed in Figure 3-17 were used for this analysis and grown for \sim 380 generations.

In order to test whether the *ingi* DNA probes are suitable for detecting the putative GCRs predicted for *T. brucei brca2*^{-/-} mutants, the *INGI-1* probe was used to hybridise at 60°C to a Southern blot of genomic DNA from BSF Lister 427 *brca2*^{-/-} mutants that had undergone passaging and cloning, and where genome rearrangements had been predicted by the loss of members of the *VSG121* family (section 3.4; Hartley and McCulloch, 2008). The Southern blot in Figure 3-20 reveals a similarly complex banding pattern as seen in the PCF TREU 927 cells that, again, does not provide clear evidence for GCRs. As such, we can conclude that the *ingi* DNA probes are unsuitable for monitoring the genomic instability previously described in BSF Lister 427 *brca2*^{-/-} mutants.

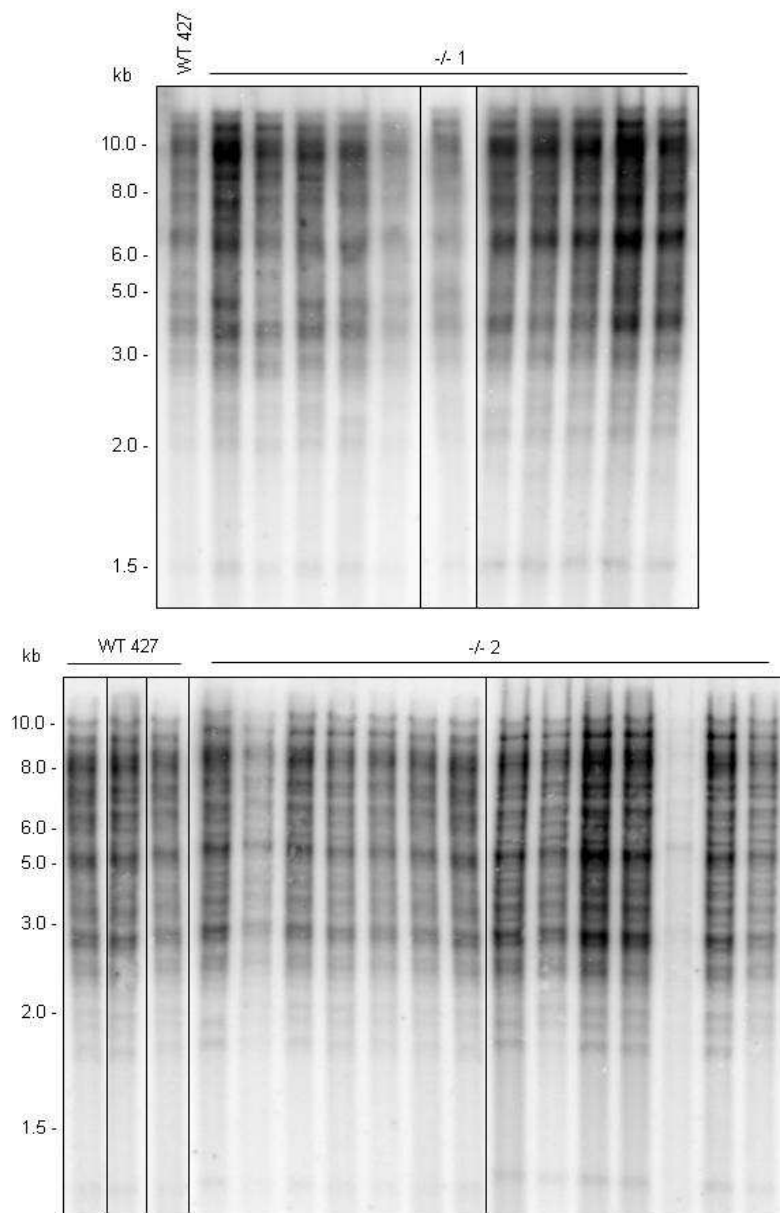


Figure 3-20 Analysis of the suitability of *ingi* DNA probes for detection of genomic instability in BSF Lister 427 *BRCA2* mutants.

5 µg of genomic DNA extracted from wild-type Lister 427 (WT 427) and *brca2*^{-/-} mutant clones (-/-1 or -/-2) was digested with *Xmn*I, before being separated by electrophoresis on an agarose gel. The DNA was Southern blotted before being hybridised with a DNA probe against *ingi* (*INGI-1*). Size markers are shown (kb). The clones analysed in section 3.4 were used for this analysis and grown for ~ 150 generations.

In order to ask if genome rearrangements occur in the *brca2*^{-/-} TREU 927 PCF mutants, DNA probes were next designed to analyse specific VSGs within the VSG arrays in these cells. VSG protein sequences from TREU 927 were aligned and a tree generated (Appendix 3). Four VSG families were identified containing between 5 and 6 relatively closely related members. The VSG genes of these families were aligned (Appendix 4) and primers were designed to amplify DNA probes that should hybridise to regions conserved within these VSG family members. BLASTn searches of the *T. brucei* TREU 927 genome were carried out using the DNA probe sequences and the results are detailed in Table 3-4. Five DNA probes were designed, named VSG1 to VSG5, and amplified using primers 97 and 98, 99 and 100, 101 and 102, and 103 and 104, and 102 and 133, respectively. The eight clonal cell lines analysed in Figure 3-17 were used for this analysis. Genomic DNA was extracted, digested with *Hind*III, separated by electrophoresis on a 1% agarose gel, Southern blotted and hybridised at 50°C with the VSG1 or VSG2 DNA probes. These Southern blots were then stripped and re-probed with the VSG3 or VSG4 DNA probes.

The Southern blots in Figure 3-21 provide no evidence for karyotype changes in the *brca2*^{-/-} mutant cells, as the banding patterns of the six *brca2*^{-/-} mutant clones closely resemble each other, and that seen in the wild-type and *BRCA2*^{-/+} mutant clones used for comparison. The Southern blot in Figure 3-21A was hybridised with the VSG1 probe that binds predominantly to two restriction fragments of ~ 8.5 kb and ~ 10 kb in size. These bands are visible in the wild-type and *BRCA2*^{-/+} cell lines, and are maintained at the same size in all six *brca2*^{-/-} mutant clones analysed. The Southern blot in Figure 3-21B was hybridised with the VSG2 probe which displays a much more complex banding pattern, with predominant restriction fragments visible at ~ 1.7 kb, ~ 2.7 kb and ~ 8.0 kb. These bands are present, at the same size, in all clones analysed. The Southern blot in Figure 3-21C was hybridised with the VSG3 probe which again binds predominantly to two restriction fragments of ~ 5.0 kb and ~ 2.0 kb in size that are present at the same size in all the clones analysed. The final Southern blot in Figure 3-21D was hybridised with the VSG4 probe and displays two

restriction fragments at ~ 1.5 kb and ~ 5.0 kb that are again maintained in size across all the clones analysed. Thus, for each VSG analysed, there is no sign of gene loss, or of rearrangements that would lead to changes in restriction digest patterns.

Probe name	BLASTn hits (Gene ID)	Expect values	Identity (%)
VSG1	Tb09.244.0140	1.6e-111	99
	Tb09.244.1850	1.9e-101	94
	Tb11.57.0026	1.3e-100	94
	Tb09.244.1750	0.081	57
VSG2	Tb08.27P2.610	2.0e-86	100
	Tb09.244.0660	2.4e-59	85
	Tb08.27P2.260	3.6e-23	68
	Tb927.10.16450	2.8e-22	68
	Tb11.09.0006	4.7e-22	66
	Tb09.v2.0360	1.2e-19	66
	> 50 hits		
VSG3	Tb08.27P2.530	3.9e-103	100
	Tb927.5.5160	3.6e-75	86
	Tb09.244.0270	0.46	55
	Tb11.57.0088	7	62
VSG4	Tb08.244.1310	4.4e-83	96
	Tb11.20.0004	4.2e-73	90
	Tb927.4.5460	1.8e-71	89
	Tb927.3.5850	2.2e-07	56
VSG5	Tb927.5.5160	5.4e-110	97
	Tb08.27P2.530	3.9e-81	84
	Tb09.244.0490	0.21	58

Table 3-4 BLASTn hits for the five VSG DNA probes.

The five DNA probes designed were subjected to BLASTn search of the *T. brucei* TREU 927 genome and the Gene IDs of the hits returned are shown with their Expect values and percentage identities.

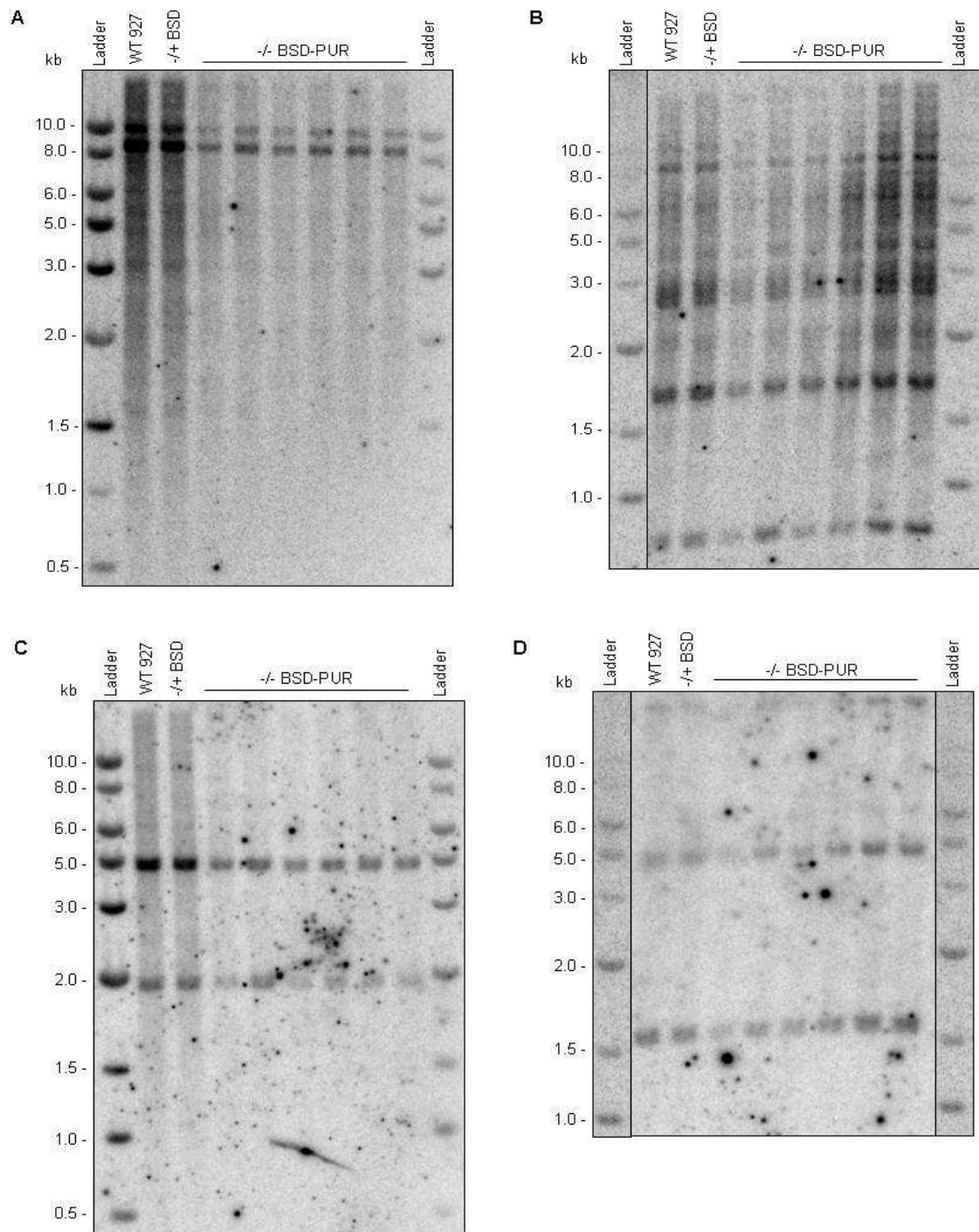


Figure 3-21 Analysis of genomic stability of PCF TREU 927 *BRCA2* mutants by Southern analysis using DNA probes against VSGs. 5 μ g of genomic DNA extracted from wild-type TREU 927 (WT 927), +/- and -/- *BRCA2* mutant clones was digested with *HindIII* before being separated by electrophoresis on an agarose gel. The DNA was Southern blotted before being hybridised with DNA probes against VSG1 (A), VSG2 (B), VSG3 (C) or VSG4 (D). Size markers are shown (Ladder, kb). The clones analysed in Figure 3-17 were used for this analysis and grown for ~ 380 generations.

In order to assay more globally for any genome rearrangements, the molecular karyotype of the intact chromosomes in the eight clonal cell lines was analysed by pulsed field agarose gel electrophoresis. Genomic plugs containing 1×10^8 cells of each of the clones derived from the passaged populations were made as detailed in section 2.2.2 and the intact chromosomes were separated by electrophoresis on a 1.2% agarose gel using conditions detailed in section 2.8.2.

The ethidium bromide-stained pulsed field agarose gel in Figure 3-22A shows the expected karyotype of *T. brucei* TREU 927 (Melville *et al.*, 1998), and little evidence for rearrangements in the *brca2*^{-/-} mutant clones after prolonged passaging. Unlike in BSF Lister 427 *brca2*^{-/-} mutants (Melville *et al.*, 2000; Hartley and McCulloch, 2008), substantial reductions in the size of the megabase chromosomes, visible as faster migrating bands, were not seen in this analysis. Southern blotting of the pulsed field agarose gel was next used to allow specific chromosomes to be visualised. DNA probes against VSGs predicted to reside on chromosome 5 (*VSG5*, primers 102 and 133; see Table 3-4) and chromosome 9 (*VSG1*, primers 97 and 98), and against *Glucose-6-phosphate isomerase* (*GPI*, primers 142 and 143), which is located on chromosome 1, were amplified by PCR, and hybridised at 50°C to the pulsed field agarose gel Southern blot (Figure 3-22B, C and D). For each DNA probe, hybridisation to a chromosome of the expected size was seen in each *brca2*^{-/-} mutant clone, suggesting no loss of the complete genes. In addition, there was no evidence in any of the clones for significant reduction (or increase) in the size of chromosomes when compared to wild-type and *BRCA2*^{-/+} mutant clones, suggesting that large-scale genome rearrangements had not occurred.

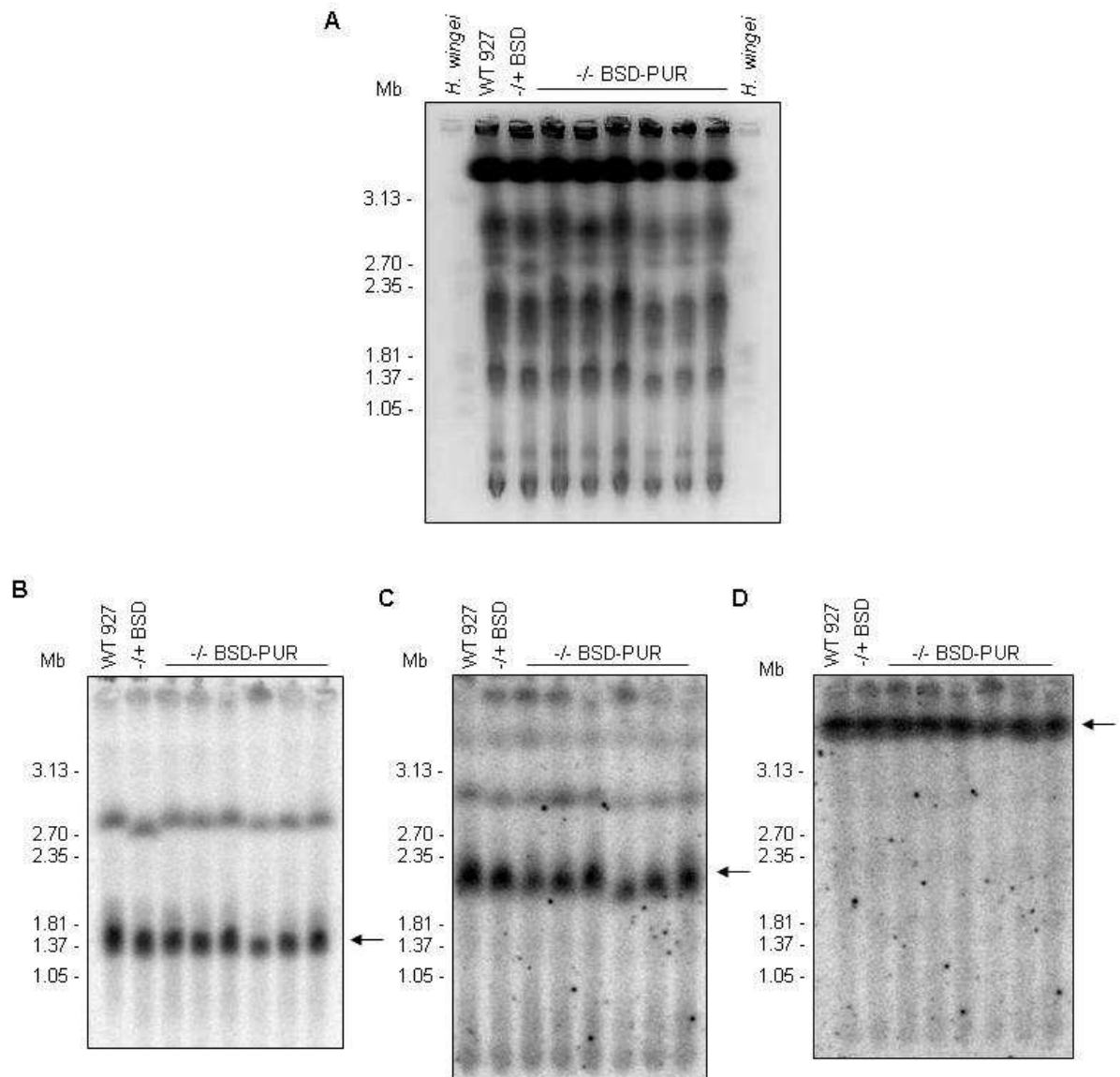


Figure 3-22 Analysis of genomic stability of PCF TREU 927 *BRCA2* mutants by pulsed field agarose gel electrophoresis. (A) Ethidium bromide-stained pulsed field agarose gel electrophoresis separation of intact genomic DNA from wild-type TREU 927 (WT 927), *-/+* and *-/-* *BRCA2* mutant clones. Lanes containing marker DNA molecules are indicated: *H. wingei*. The clones analysed in Figure 3-17 were used for this analysis and grown for ~ 380 generations. (B-D) Southern blots of the pulsed field agarose gel electrophoresis separation of intact genomic DNA from wild-type TREU 927 (WT 927), *-/+* and *-/-* *BRCA2* mutant clones. The Southern blot was hybridised sequentially with DNA probes against *GPI* (*Glucose-6-phosphate isomerase*, B), *VSG5* (C) and *VSG1* (D). The chromosomes probed for are indicated (black arrows), and size markers are shown (Mb).

Taken together, the above data suggest that *brca2*-/- mutants in PCF TREU 927 do not display equivalent levels of putative GCRs to those seen in BSF Lister 427 *brca2*-/- mutants, even after more extensive passaging. These data could indicate a function for BRCA2 in the maintenance of genome stability that is restricted to the BSF of *T. brucei*. However, an alternative explanation for this could be found in the differences in the relative size or composition of the VSG

arrays in the TREU 927 and Lister 427 strains. Karyotype analysis has suggested that the genome size of TREU 927 is amongst the smallest of the *T. brucei* strains examined (Melville *et al.*, 1998). Microarray analysis suggests that the larger size of the genome in Lister 427 is accounted for by significantly larger numbers of VSGs in the subtelomeres of the megabase chromosome (Callejas *et al.*, 2006). Assuming that the *brca2*^{-/-} GCRs observed in Lister 427 are concentrated in the VSG-containing subtelomeres, the putatively smaller VSG repertoire of TREU 927 may mean that these rearrangements are less frequent or less detectable. Another plausible explanation is that the composition of the VSG arrays in the strain Lister 427 may contribute to the accumulation of putative GCRs in BSF Lister 427 *brca2*^{-/-} mutants, as a large number of families of VSGs exist containing multiple members with very high sequence similarity (Boothroyd *et al.*, 1982; Carrington *et al.*, 1991). The VSG array of the strain TREU 927 does not contain families of VSGs with large numbers of similar genes (Marcello and Barry, 2007) and therefore may be less prone to the homologous recombination reactions that may lead to an accumulation of GCRs.

3.4 Analysis of the timescale of genomic rearrangements in BSF Lister 427 *BRCA2* mutants

The timeline over which the putative GCRs occur in the *brca2*^{-/-} mutants in BSF Lister 427 is unknown. Analysis was conducted only after ~ 290 generations of growth and revealed rearrangements in the *VSG121* gene family (Hartley and McCulloch, 2008), which contains five closely related VSG genes, one located at the telomere and the other four likely to be located in subtelomeric arrays. Two independent BSF Lister 427 *brca2*^{-/-} mutants were generated previously (-/-1 and -/-2; Hartley and McCulloch, 2008), and were recovered from frozen storage after passaging for ~ 140 generations. To ask if genome rearrangements are detectable after this amount of growth, 23 clones of these mutants were generated, as described in section 2.1.4, and grown for a minimal further number of generations (~ 10) until sufficient genomic DNA could be recovered for Southern analysis. The clones were checked by PCR, using primers described in Figure 3-2A, to check the genetic status of the *brca2*^{-/-} cells. The agarose gel in Figure 3-23 demonstrates that the *BRCA2* ORF remained absent from the 23 *brca2*^{-/-} mutant clones.

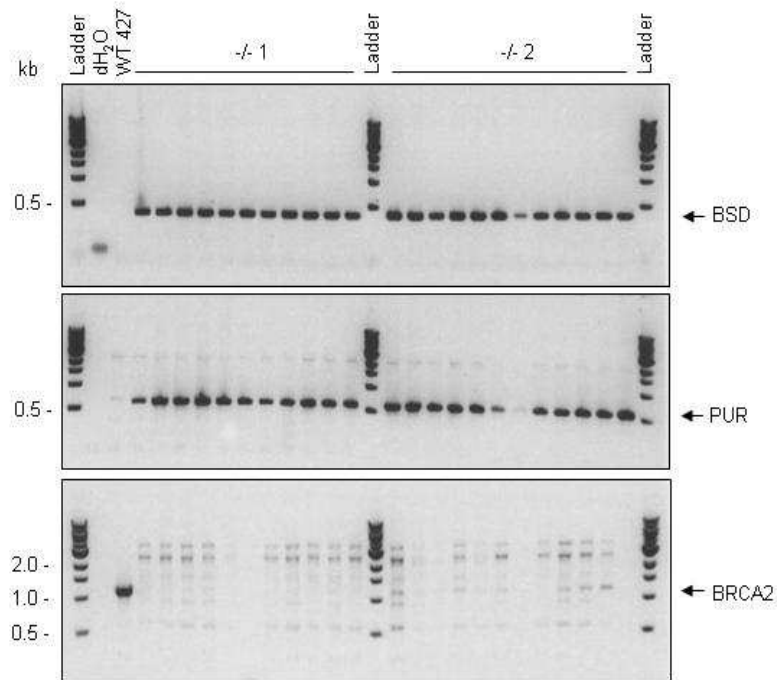


Figure 3-23 Screening BSF Lister 427 *brca2*^{-/-} mutant re-clones by PCR.

An agarose gel of the PCR products obtained using the primers, described in Figure 3-2A, and genomic DNA extracted from wild-type Lister 427 (WT 427) and *brca2*^{-/-} mutant clonal cell lines. Distilled water (dH₂O) was used as a negative control. The PCR products produced from the *BSD*, *PUR* and *BRCA2* ORFs are indicated (black arrows), and size markers are shown (Ladder, kb).

Southern analysis was then performed using a DNA probe specific to a region conserved in all five members of the *VSG121* family. Genomic DNA was extracted, digested with *XmnI*, separated by electrophoresis on a 1% agarose gel, Southern blotted and hybridised at 60°C with the DNA probe for *VSG121*, generated by PCR with primers 146 and 147. The Southern blot in Figure 3-24 demonstrates that loss of *VSG121* occurs at an earlier time-point than thought previously (Hartley and McCulloch, 2008). As expected, five copies of *VSG121* are present in wild-type BSF Lister 427 clones. However, in the majority of *brca2*^{-/-} mutant clones analysed (16 out of 22) one or more copies of *VSG121* had been lost, consistent with the presence of putative GCRs that result in the loss of non-essential genetic material. The telomeric copy of *VSG121* varies in size, presumably due to varying length of the telomere in some clones (lanes 1, 13, 17 and 24; Van der Ploeg, Liu, and Borst, 1984), but was never lost suggesting that such chromosomal rearrangements infrequently affect telomeres.

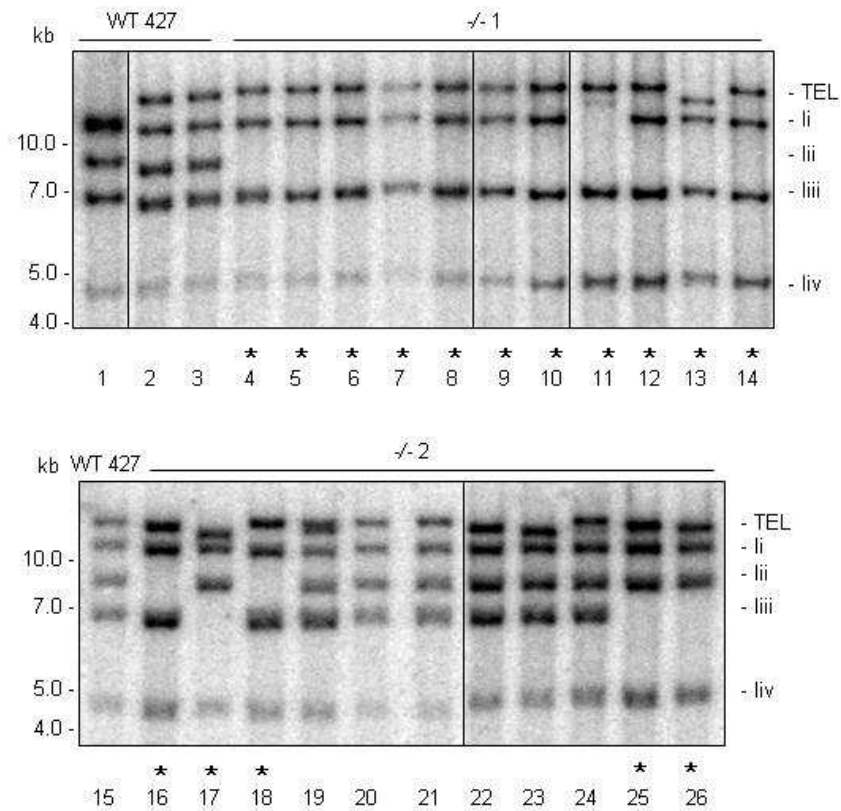


Figure 3-24 Analysis of genomic stability of BSF Lister 427 *BRCA2* mutants by Southern analysis using a DNA probe against *VSG121*. 5 μ g of genomic DNA extracted from wild-type Lister 427 (WT 427) and *brca2*^{-/-} mutant clones was digested with *Xmn*I, before being separated by electrophoresis on an agarose gel. The DNA was Southern blotted before being hybridised with a DNA probe against *VSG121*. One telomeric (TEL) gene and four genes that are likely to be present in subtelomeric arrays (li, lii, liii and liv) are shown. “*” indicates clones in which an internal gene copy has been lost. Size markers are shown (kb). The clones analysed in Figure 3-23 were used for this analysis and grown for ~ 150 generations.

3.5 Generation of *BRCA2* gene disruption mutants in PCF Lister 427 *T. brucei*

In order to test further the possibility that the function of *BRCA2* in maintaining genomic integrity is limited to the BSF parasites, homozygous mutants of *BRCA2* were generated in PCF cells in the Lister 427 strain using the same strategy described in section 3.2.1. Ideally, *BRCA2* mutants would also have been generated in BSF TREU 927 *T. brucei*, but as this strain is pleomorphic it was considered that the generation of homozygous mutants would be problematic, as would maintenance in culture during the passaging needed to reveal karyotype changes. In order to circumvent some of these difficulties it was attempted to transmit the PCF TREU 927 *brca2*^{-/-} mutants generated here through the tsetse fly vector (Craig Lapsley), however no visible metacyclic form trypansomes

were observed in tsetse fly saliva and therefore infection of mammals and isolation of BSF TREU 927 *brca2*^{-/-} mutants was not possible.

3.5.1 Generation of *BRCA2* mutants in PCF Lister 427 *T. brucei*

Two separate transformations were carried out in order to generate two independent *BRCA2*^{-/+} cell lines using the $\Delta BRCA2::BSD$ and $\Delta BRCA2::PUR$ gene deletion constructs (Figure 3-1). Wild-type PCF Lister 427 (WT 427) cells were transformed and antibiotic resistant transformants were selected by placing cells on SDM-79 media supplemented with 10 $\mu\text{g}.\text{ml}^{-1}$ blasticidin or 1 $\mu\text{g}.\text{ml}^{-1}$ puromycin. Two independent *BRCA2*^{-/+} clones were chosen (^{-/+} *BSD* and ^{-/+} *PUR*; Figure 3-25) and subsequently transformed with the complementary *BRCA2* gene deletion construct in order to generate two independent *brca2*^{-/-} mutant cell lines. Antibiotic resistant transformants were selected with 5 $\mu\text{g}.\text{ml}^{-1}$ blasticidin and 0.5 $\mu\text{g}.\text{ml}^{-1}$ puromycin.

3.5.2 Confirmation of *BRCA2* mutants by PCR

The generation of *brca2*^{-/-} mutants was initially confirmed by PCR performed on genomic DNA extracted from the putative *brca2*^{-/-} cell lines (six ^{-/-} *BSD-PUR* clones and six ^{-/-} *PUR-BSD* clones were chosen). PCR was performed using primers specific to the *BSD*, *PUR* and *BRCA2* ORFs as described in section 3.2.3 and Figure 3-2A.

The agarose gel in Figure 3-25 demonstrates the presence of the *BSD* and *PUR* resistance ORFs in all but one (*BSD-PUR*) of the putative *brca2*^{-/-} mutants. As seen in *brca2*^{-/-} mutants in PCF TREU 927, a number of these clones still retained the *BRCA2* ORF, producing a PCR product with the primers to amplify part of the *BRCA2* ORF. These 'incorrect' clones were discarded and two independent *brca2*^{-/-} mutant clones were selected from the clones that failed to amplify a PCR product using these primers (indicated by '*' in Figure 3-25). The two independent *brca2*^{-/-} mutant clones chosen were referred to as ^{-/-} *BSD-PUR* and ^{-/-} *PUR-BSD*.

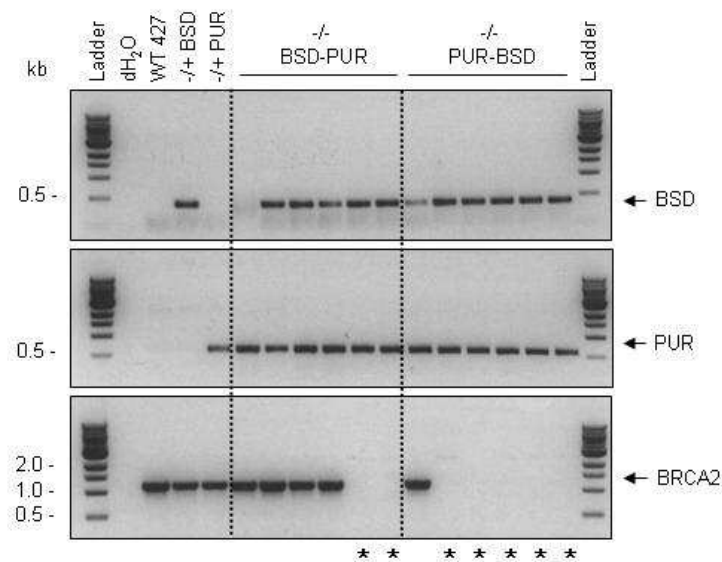


Figure 3-25 Confirmation of PCF Lister 427 *BRCA2* mutants by PCR.

An agarose gel of the PCR products, obtained using the primers, described in Figure 3-2A, and genomic DNA extracted from wild-type Lister 427 (WT 427), *BRCA2* heterozygous (-/+) and putative *brca2* homozygous (-/-) mutant cell lines. The two independent *BRCA2*^{-/+} mutants are indicated by -/+ *BSD* and -/+ *PUR*, and the putative *brca2*^{-/-} mutants derived from these are indicated by -/- *BSD-PUR* and -/- *PUR-BSD*, respectively. Distilled water (dH₂O) was used as a negative control. The PCR products produced from the *BSD*, *PUR* and *BRCA2* ORFs are indicated (black arrows), and size markers are shown (Ladder, kb). '*' indicates *brca2*^{-/-} mutants that are confirmed by PCR.

3.5.3 Confirmation of *BRCA2* mutants by Southern analysis

To confirm the generation of two independent *brca2*^{-/-} mutant cell lines, Southern analysis was performed as described in section 3.2.4. The only difference was that the genomic DNA extracted was digested with *Sac*II and *Stu*I prior to Southern blotting to enable the differentiation between the *BSD* and *PUR* alleles. The location of primers, predicted restriction enzyme recognition sites and expected DNA fragment sizes are displayed in Figure 3-26A.

The Southern blot in Figure 3-26B demonstrates that the intact *BRCA2* ORF exists in wild-type Lister 427 cells as two allelic size variants, and these have been shown to vary in the number of BRC repeat motifs they encode (Hartley and McCulloch, 2008). In each *BRCA2*^{-/+} mutant, a distinct *BRCA2* allele was replaced with either a *BSD* or *PUR* resistance cassette. In neither *brca2*^{-/-} mutant could an intact *BRCA2* ORF be detected, and instead both alleles of the gene were deleted, one replaced by a *BSD* cassette and the other replaced by a *PUR* cassette.

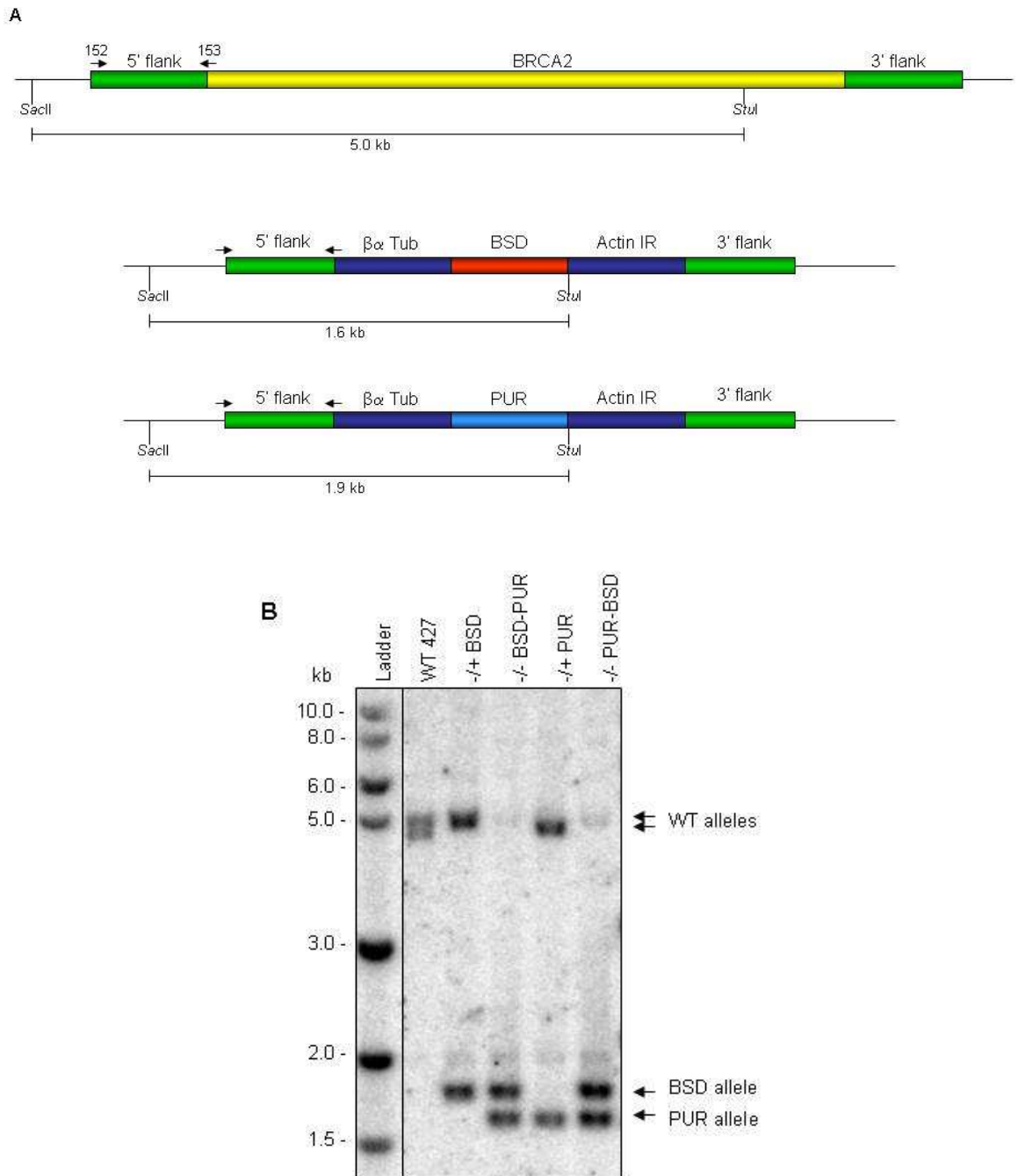


Figure 3-26 Confirmation of PCF Lister 427 *BRCA2* mutants by Southern analysis. (A) Restriction maps showing the expected products of restriction digestion, Southern blotting and hybridisation with the 5' UTR of the *BRCA2* ORF (black arrows indicate the primers used to PCR-amplify this as a DNA probe). The restriction sites are indicated, with the expected restriction fragment sizes shown (kb). (B) 5 μ g of genomic DNA extracted from wild-type Lister 427 (WT 427), *-/+* and *-/-* *BRCA2* mutant cell lines was digested with *SacII* and *StuI* before being separated by electrophoresis on an agarose gel. The DNA was Southern blotted before being hybridised with a DNA probe against the 5' UTR of the *BRCA2* ORF. The bands produced from the WT alleles and the *BRCA2* mutant alleles are indicated (black arrows), and size markers are shown (Ladder, kb).

3.5.4 Attempt at confirmation of *BRCA2* mutants by western analysis

Attempts at confirmation of the absence of expression of *BRCA2* in the PCF Lister 427 *brca2*^{-/-} cells by western blot using anti-*BRCA2* antiserum was

performed multiple times, including with the addition of 5% chicken serum (Sigma) in the blocking solution to reduce non-specific binding of the antibody. The result of these attempts was inconclusive due to the extensive nature of the non-specific binding of the antiserum and, therefore, is not displayed.

3.6 Phenotypic analysis of PCF Lister 427 *BRCA2* mutants

3.6.1 Analysis of *in vitro* growth

The *in vitro* growth of the PCF Lister 427 *BRCA2* mutant cell lines was analysed and the average counts from three experimental repetitions are plotted in Figure 3-27, and extrapolated doubling times are displayed in Table 3-5.

From the growth curves and doubling times displayed it is apparent that disruption of a single *BRCA2* allele has no discernible effect on the growth of *BRCA2*-/+ cell lines when compared to wild-type cells. However, the *brca2*-/- mutants display a very slight retardation in growth as evidenced by a slight increase in the doubling time from the wild-type value of ~ 11 hours to ~ 13 hours for the mutants. This minor growth impairment appears to be even slighter than that observed for the PCF TREU 927 *brca2*-/- cells (section 3.3.1).

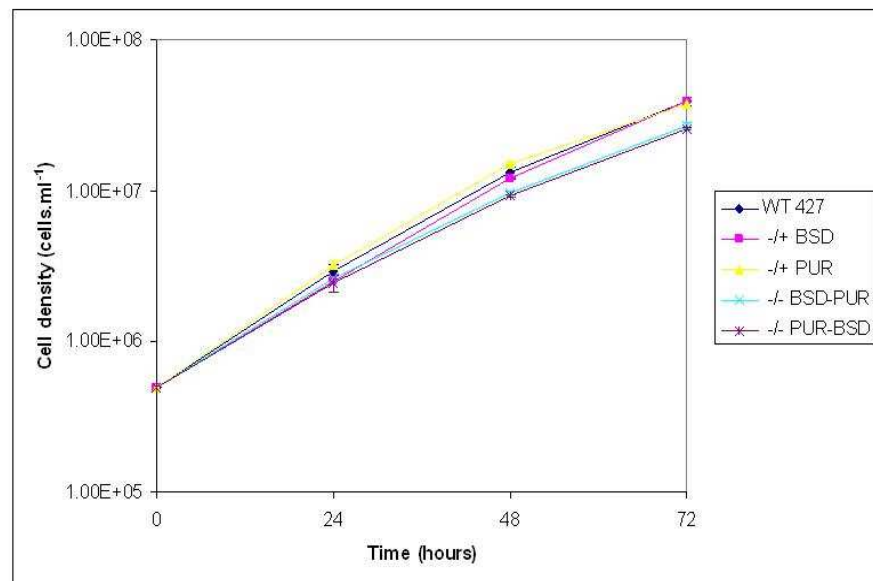


Figure 3-27 Analysis of *in vitro* growth of PCF Lister 427 *BRCA2* mutants. 2 ml cultures of wild-type Lister 427 (WT 427), -/+ and -/- *BRCA2* mutant cell lines were inoculated at 5×10^5 cells.ml⁻¹ and cell densities counted 24, 48, and 72 hours subsequently are shown. Values are averaged from the counts from three experimental repetitions, and vertical lines indicate standard deviation.

Cell line	Doubling time (hours)
WT 427	11.19
-/+ BSD	10.50
-/+ PUR	10.75
-/- BSD-PUR	12.77
-/- PUR-BSD	12.54

Table 3-5 *In vitro* population doubling times of PCF Lister 427 *BRCA2* mutants. The mean doubling time for wild-type Lister 427 (WT 427), -/+ and -/- *BRCA2* mutant cell lines is displayed, in hours, and was calculated from the data displayed in Figure 3-27.

3.6.2 Analysis of DNA damage sensitivity

The Alamar blue assay was used to determine the sensitivity of the PCF Lister 427 *BRCA2* mutant cell lines to the DNA damaging agents MMS and phleomycin. The Alamar blue assay was set up with wild-type Lister 427, -/+ and -/- *BRCA2* mutant cell lines. The extent of fluorescence for each cell line was plotted graphically over the range of log drug concentrations (for representative examples see Figure 3-28 and Figure 3-29). From this, EC50s were determined from each individual plot and then average EC50s (plus 95% confidence intervals) were calculated from the three experimental repetitions. The mean EC50s for each cell line were then plotted relative to the wild-type EC50, which was taken as 100% (Figure 3-30 and Figure 3-31).

The survival curves displayed in Figure 3-28 and Figure 3-29 are representative of the three experimental repetitions performed. These data demonstrate that as the concentration of DNA damaging agent increases the fluorescence, and therefore the percentage of surviving cells that are actively reducing Alamar blue to fluorescent resorufin reduces, until the concentration at which all cells are killed is reached. It is apparent that the *brca2*-/- cell lines display reduced survival in the presence of both compounds, when compared to wild-type cells. The *BRCA2*-/+ cell lines display survival that is essentially equivalent to wild-type cells, except for the *BRCA2*-/+ PUR cell line that appears to show a slightly greater survival in the presence of phleomycin (although not significantly, see below), perhaps similar to the differences in damage sensitivity seen previously for a *BRCA2*-/+ mutant cell line in PCF TREU 927 (section 3.3.2). The graphs of relative EC50 values displayed in Figure 3-30 and Figure 3-31 support the graphical observations and demonstrate that the disruption of a single *BRCA2*

allele has no discernible effect on the sensitivity of the *BRCA2*^{-/+} cell lines to the DNA damage caused by either compound when compared to wild-type cells. In contrast, the *brca2*^{-/-} mutants appeared to display a slightly greater sensitivity to both DNA damaging agents, though this was very slight and was markedly less than the *brca2*^{-/-} mutants in PCF TREU 927 (section 3.3.2)

To evaluate the above data the EC₅₀ values of the wild-type Lister 427, ^{-/+} and ^{-/-} *BRCA2* mutant cell lines were analysed using student's T-tests and the results of this are displayed in Table 3-6. The statistical analyses confirm the graphical observations. No statistical difference was observed between wild-type, ^{-/+} or ^{-/-} *BRCA2* mutant cells ($p > 0.05$) for both DNA damaging agents, underlining that the *brca2*^{-/-} mutants display at best only a slight phenotype of increased DNA damage sensitivity.

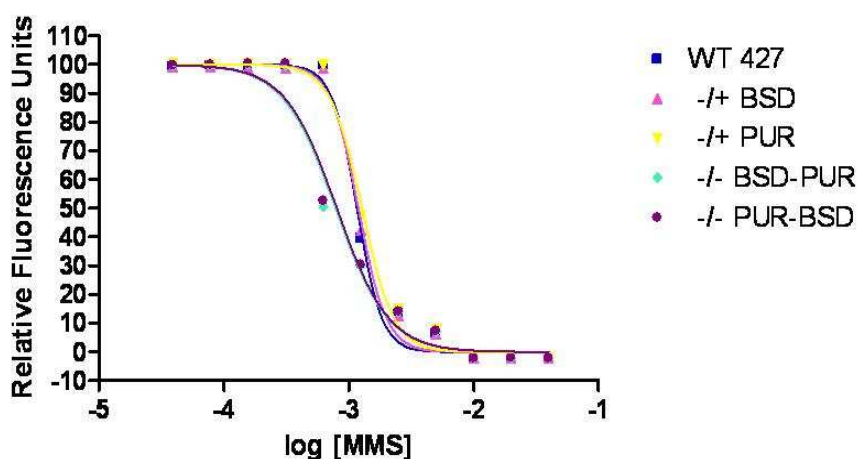


Figure 3-28 A representative survival curve for PCF Lister 427 *BRCA2* mutants exposed to MMS.

The extent of fluorescence for each cell line (WT, ^{-/+} and ^{-/-}) obtained using the Alamar blue assay is plotted against the log of MMS concentrations. Nonlinear regression was performed and fitted curves are shown for each cell line.

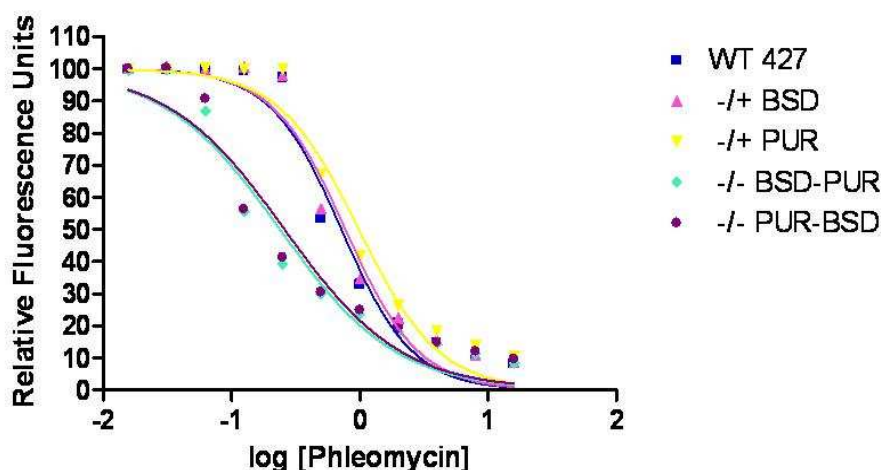


Figure 3-29 A representative survival curve for PCF Lister 427 *BRCA2* mutants exposed to phleomycin.

The extent of fluorescence for each cell line (WT, *-/+* and *-/-*) obtained using the Alamar blue assay is plotted against the log of phleomycin concentrations. Nonlinear regression was performed and fitted curves are shown for each cell line.

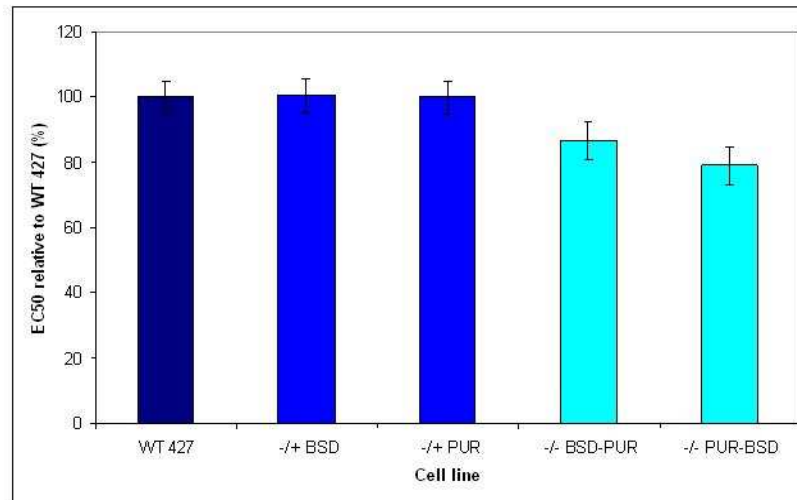


Figure 3-30 EC50 values of PCF Lister 427 *BRCA2* mutants exposed to MMS. Wild-type Lister 427 (WT 427), *-/+* and *-/-* *BRCA2* mutant cell lines were placed in serially decreasing amounts of MMS and allowed to grow for 48 hours, before the addition of Alamar Blue. After a further 24 hours, the reduction of Alamar Blue was measured by the amount of fluorescent resorufin generated. EC50 values are the mean from three experimental repetitions expressed as a percentage relative to wild-type and bars indicate 95% confidence intervals.

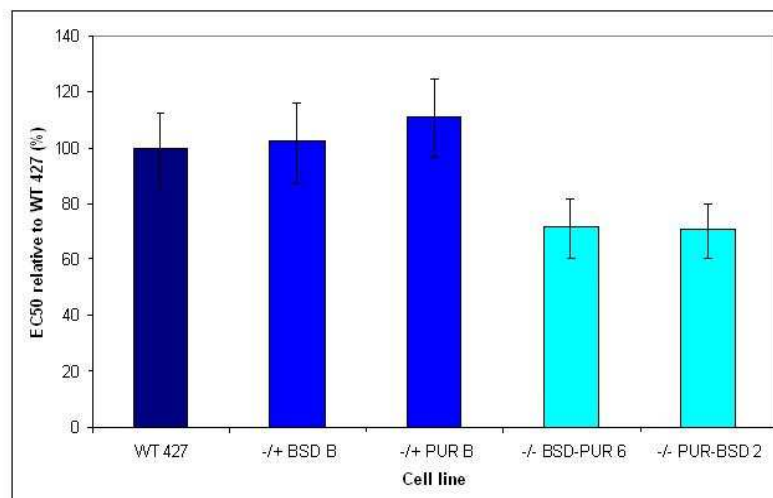


Figure 3-31 EC50 values of PCF Lister 427 *BRCA2* mutants exposed to phleomycin. Wild-type Lister 427 (WT 427), *-/+* and *-/-* *BRCA2* mutant cell lines were placed in serially decreasing amounts of phleomycin and allowed to grow for 48 hours, before the addition of Alamar Blue. After a further 24 hours, the reduction of Alamar Blue was measured by the amount of fluorescent resorufin generated. EC50 values are the mean from three experimental repetitions expressed as a percentage relative to wild-type and bars indicate 95% confidence intervals.

A

	-/+ BSD	-/+ PUR	-/- BSD-PUR	-/- PUR-BSD
WT 427	0.8547	0.9950	0.3205	0.1964
-/+ BSD		0.8829	0.3838	0.2405
-/+ PUR			0.4851	0.2884
-/- BSD-PUR				0.5277

B

	-/+ BSD	-/+ PUR	-/- BSD-PUR	-/- PUR-BSD
WT 427	0.3766	0.4461	0.3297	0.5040
-/+ BSD		0.5049	0.2950	0.4573
-/+ PUR			0.3394	0.4248
-/- BSD-PUR				0.9726

Table 3-6 Statistical analysis of Alamar Blue results.

P values are shown for student's T-tests comparing the mean EC50 values of wild-type Lister 427 (WT 427), +/- and -/- *BRCA2* mutant cell lines grown in the presence of MMS (A) or phleomycin (B). Areas shaded in yellow indicate a significant difference ($P \leq 0.05$). No correction has been made for simultaneous multiple comparisons.

3.6.3 Confirmation of the DNA damage sensitivity of PCF Lister 427 *BRCA2* mutants

Due to the lack of statistical significance associated with the DNA damage sensitivity of the two PCF Lister 427 *brca2*-/- mutant cell lines, it was decided to analyse the *in vitro* growth of these cells in the presence of MMS in order to confirm the results of the Alamar blue assay. 2 ml cultures were inoculated at 5×10^5 cells.ml⁻¹ in SDM-79 media supplemented with 0.0004% MMS and counted at 24, 48 and 72 hours subsequently. The average counts from three repetitions are plotted in Figure 3-32.

From the growth curve displayed it is apparent that the disruption of a single *BRCA2* allele has no discernible effect on the growth of the cells in the presence of MMS, when compared to wild-type cells. However, the *brca2*-/- mutant cells display a visible retardation in growth after 48 hours, indicating that disruption of *BRCA2* results in an increase in the DNA damage sensitivity of the mutant cell lines. For all the cells, the rate of growth was reduced by the presence of MMS, but this growth retardation was more pronounced for the *brca2*-/- mutants

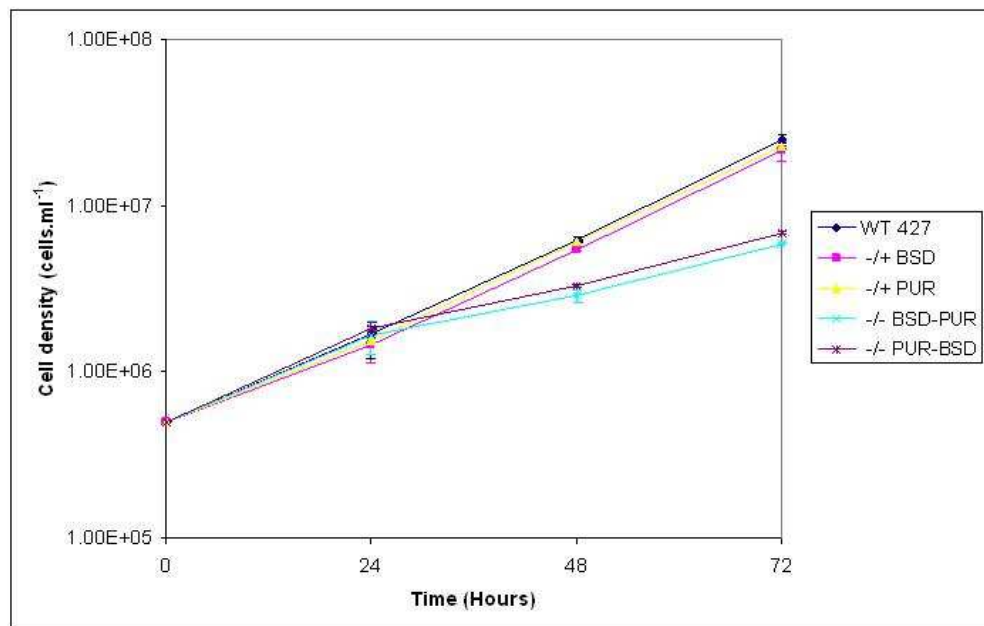


Figure 3-32 Analysis of *in vitro* growth of PCF Lister 427 *BRCA2* mutants exposed to MMS. 2 ml cultures of wild-type Lister 427 (WT 427), -/+ and -/- *BRCA2* mutant cell lines were inoculated at 5×10^5 cells.ml⁻¹ in media supplemented with 0.0004% MMS, and cell densities counted 24, 48, and 72 hours subsequently are shown. Values are averaged from the counts from three experimental repetitions, and vertical lines indicate standard deviation.

3.6.4 Analysis of genomic stability in PCF Lister 427 *BRCA2* mutants

After prolonged passaging (~ 290 generations) *brca2*-/- mutants in BSF Lister 427 *T. brucei* display evidence for putative GCRs, including gene deletions within the subtelomeric *VSG* arrays (Hartley and McCulloch, 2008). Data displayed in section 3.4 demonstrates that these rearrangements can occur earlier than previously thought (~ 150 generations), and provided a timescale over which analysis of the genomic stability of the *brca2*-/- mutants generated in PCF Lister 427 should be considered. The *brca2*-/- mutants in PCF Lister 427 were initially grown for ~ 80 generations before analysis of genomic stability by examination of the molecular karyotype.

Wild-type Lister 427, -/+ and -/- *BRCA2* mutant polyclonal cell lines were re-cloned and a total of 19 clones were chosen for analysis. PCR using primers described in Figure 3-2A was carried out to check the genetic status of the *brca2*-/- cells. The agarose gel in Figure 3-33 demonstrates that the *BRCA2* ORF remained absent from the 12 *brca2*-/- mutant clones.

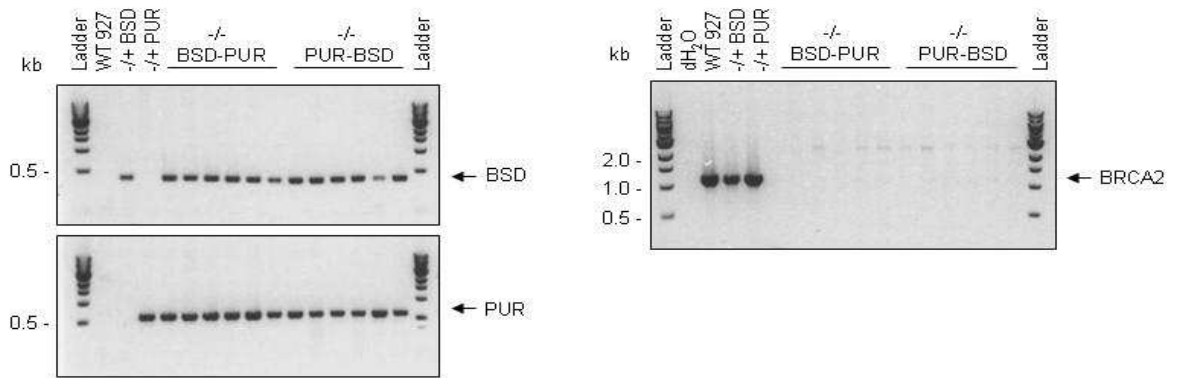


Figure 3-33 Screening PCF Lister 427 *brca2*^{-/-} mutant re-clones by PCR.

An agarose gel of the PCR products obtained using the primers, described in Figure 3-2A, and genomic DNA extracted from wild-type Lister 427 (WT 427), *-/+* and *-/-* *BRCA2* mutant clonal cell lines. Distilled water (dH₂O) was used as a negative control. The PCR products produced from the *BSD*, *PUR* and *BRCA2* ORFs are indicated (black arrows), and size markers are shown (Ladder, kb).

Southern analysis was then performed using a DNA probe against members of the *VSG121* family as described in section 3.4. The Southern blot in Figure 3-34 demonstrates that no loss of *VSG121* was detectable after ~ 80 generations of growth in PCF Lister 427 *brca2*^{-/-} mutant cells. As expected, five copies of *VSG121* were present in wild-type and *BRCA2*^{-/+} clones. However, five copies of *VSG121* were also present in all of the *brca2*^{-/-} mutant clones analysed, indicating the absence of genome rearrangements affecting the *VSG* arrays. Indeed in the *brca2*^{-/-} mutant clone in lane 6 a further copy of *VSG121* had been generated, by an unknown mechanism, and this cell line now contains a sixth copy of the gene. Such gene duplication has not been observed before, only gene loss. As seen before, the telomeric copy of *VSG121* varied in size but was never lost.

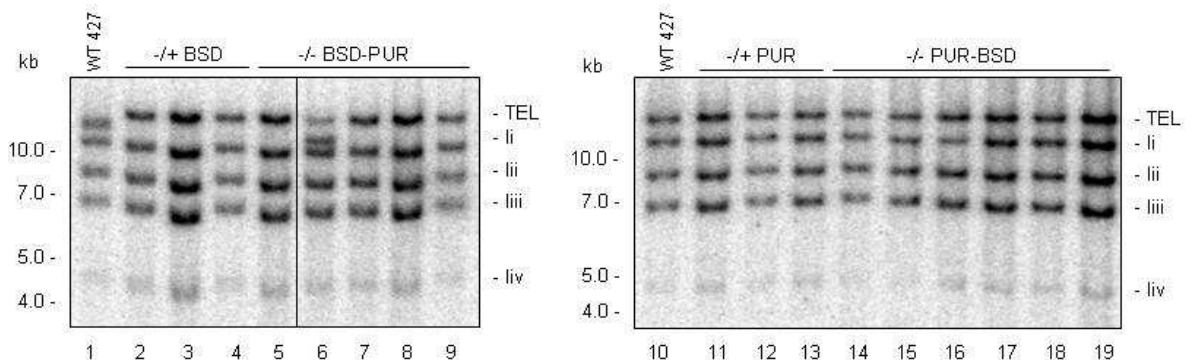


Figure 3-34 Analysis of genome stability of PCF Lister 427 *BRCA2* mutants by Southern analysis using a DNA probe against *VSG121*.

5 µg of genomic DNA extracted from wild-type Lister 427 (WT 427), *-/+* and *-/-* *BRCA2* mutant clones was digested with *Xmn*I before being separated by electrophoresis on an agarose gel. The DNA was Southern blotted before being hybridised with a DNA probe against

VSG121. One telomeric (TEL) gene and four genes that are likely to be present in subtelomeric arrays (li, lii, liii and liv) are shown. Size markers are shown (kb). The clones analysed in Figure 3-33 were used for this analysis and grown for ~ 80 generations.

Because of the discrepancy between the number of passages used here and the ~ 150 generations after which extensive loss of *VSG121* was seen in Lister 427 *brca2*^{-/-} mutants (section 3.4), the *BRCA2* mutants in PCF Lister 427 were grown for a longer period of time and subsequently re-cloned at ~ 230 generations growth. Clones were generated from the wild-type Lister 427, ^{-/+} and ^{-/-} *BRCA2* mutant polyclonal cell lines and a total of 24 clones were chosen for analysis. PCR using primers described in Figure 3-2A was again carried out to confirm the absence of *BRCA2* ORF in the *brca2*^{-/-} clones; and Figure 3-35 demonstrates that the *BRCA2* ORF remained absent from the 15 *brca2*^{-/-} mutant clones.

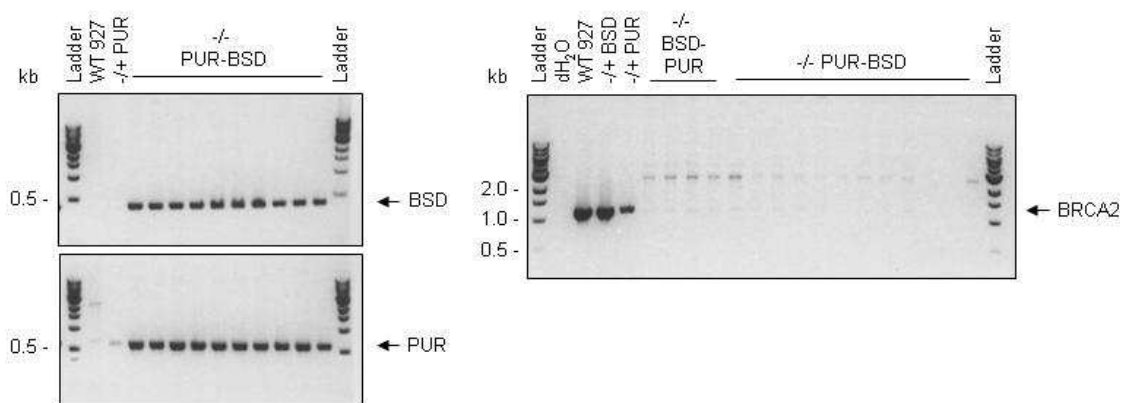


Figure 3-35 Screening PCF Lister 427 *brca2*^{-/-} mutant re-clones by PCR.

An agarose gel of the PCR products obtained using the primers, described in Figure 3-2A, and genomic DNA extracted from wild-type Lister 427 (WT 427), ^{-/+} and ^{-/-} *BRCA2* mutant clonal cell lines. Distilled water (dH₂O) was used as a negative control. The PCR products produced from the *BSD*, *PUR* and *BRCA2* ORFs are indicated (black arrows), and size markers are shown (Ladder, kb).

Southern analysis was then performed using a DNA probe against members of the *VSG121* family, as described in section 3.4. The Southern blot in Figure 3-36 demonstrates that no loss of *VSG121* was detectable in PCF Lister 427 *brca2*^{-/-} mutants, even after ~ 230 generations of growth. The wild-type Lister 427 clones in lanes 1, 10 and 11 appeared to have duplicated *VSG121* and contain a sixth copy of the gene, as seen for one *brca2*^{-/-} clone at ~ 80 generations (Figure 3-34, lane 6). As seen before, the telomeric copy of *VSG121* varied in size, quite considerably in lane 22, but was never lost.

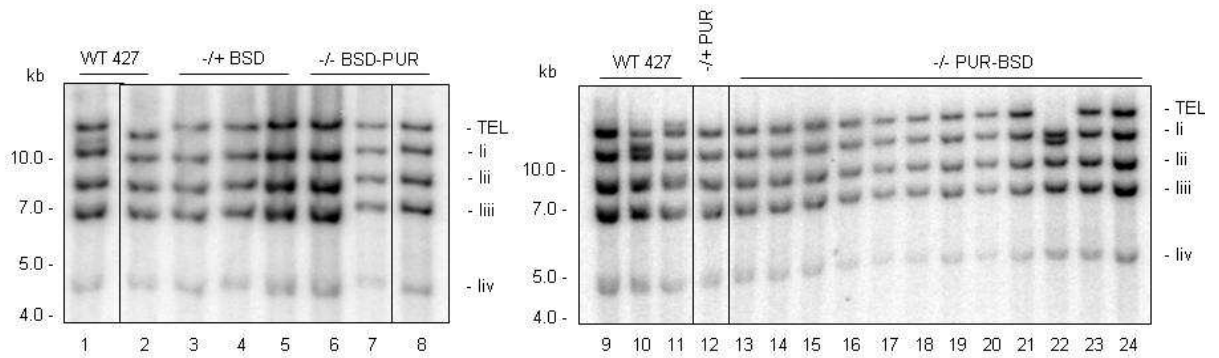


Figure 3-36 Analysis of genomic stability of PCF Lister 427 *BRCA2* mutants by Southern analysis using a DNA probe against *VSG121*. 5 μ g of genomic DNA extracted from wild-type Lister 427 (WT 427), *-/+* and *-/-* *BRCA2* mutant clones was digested with *XmnI* before being separated by electrophoresis on an agarose gel. The DNA was Southern blotted before being hybridised with a DNA probe against *VSG121*. One telomeric (TEL) gene and four genes that are likely to be present in subtelomeric arrays (li, lii, liii and liv) are shown. Size markers are shown (kb). The clones analysed in Figure 3-35 were used for this analysis and grown for ~ 230 generations.

In order to confirm the putative absence of genome rearrangements, the molecular karyotype of a number of the clones analysed in Figure 3-36 was carried out by pulsed field agarose gel electrophoresis. Genomic plugs containing 1×10^8 cells were made and the intact chromosomes were separated by electrophoresis on a 1.2% agarose gel.

The ethidium bromide-stained pulsed field agarose gel in Figure 3-37A shows the expected karyotype of *T. brucei* Lister 427 (Melville *et al.*, 2000) and indicates the absence of clear GCRs in the *brca2**-/-* mutants after prolonged passaging. Unlike in BSF Lister 427 *brca2**-/-* cells, where considerable size variation was evident in the chromosomes between 1.05-3.13 Mbps, there was a notable uniformity in size of the chromosomes in the different PCF Lister 427 *brca2**-/-* clones and relative to the wild-type and *BRCA2**-/+* clones. Only in the *brca2**-/-* clone in lane 12 did there appear to be a detectable change, with loss of signal for a band of ~ 2.35 Mb.

A Southern blot was next prepared from the pulsed field agarose gel and hybridised with DNA probes against *VSG121* and *Glucose-6-phosphate isomerase* (*GPI*), which is located on chromosome 1, which were amplified by PCR. The Southern blots in Figure 3-37B and Figure 3-37C, demonstrate chromosomes at the expected sizes for *GPI* and *VSG121* in the strain Lister 427 (Melville *et al.*, 2000; Hartley and McCulloch, 2008). As observed in the ethidium bromide-stained pulsed field agarose gel, the *brca2**-/-* mutant clone in lane 12 contains the only

detectable change in karyotype, and appeared to have lost genetic material leading to a reduction in size of the chromosome that harbours both *GPI* and at least one of the *VSG121* family genes. As only a small number of wild-type and *BRCA2*^{-/+} clones were analysed for genomic stability in this manner, it is possible that the rearrangement in the single *brca2*^{-/-} clone in lane 12 is simply due to changes in chromosome sequences as previously observed after prolonged passaging of *T. brucei* (Anneli Cooper, PhD, Thesis 2010).

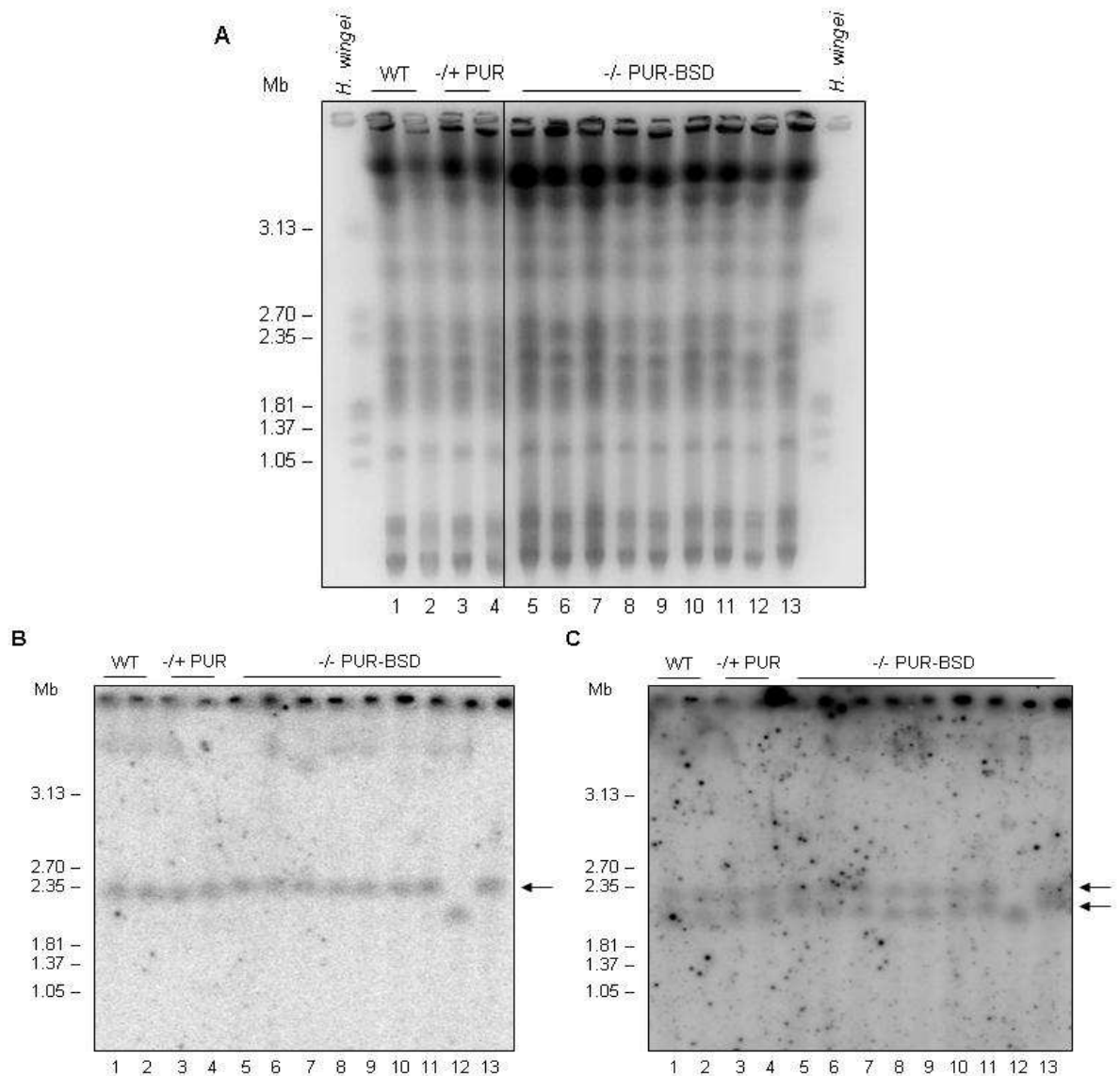


Figure 3-37 Analysis of genomic stability of PCF Lister 427 *BRCA2* mutants by pulsed field agarose gel electrophoresis.

(A) Ethidium bromide-stained pulsed field agarose gel electrophoresis separation of intact genomic DNA from wild-type Lister 427 (WT 427), +/- and -/- *BRCA2* mutant clones. Lanes containing marker DNA molecules are indicated: *H. wingei*. The clones analysed in Figure 3-35 were analysed here and grown for ~ 230 generations. **(B-C)** Southern blots of the pulsed field agarose gel electrophoresis separation of intact genomic DNA from wild-type Lister 427 (WT 427), +/- and -/- *BRCA2* mutant clones. The Southern blot was hybridised sequentially with DNA probes against *GPI* (*Glucose-6-phosphate isomerase*, B) and *VSG 121* (C). The chromosomes probed for are indicated (black arrows), and size markers are shown (Mb).

3.7 Summary

In this work, it has been shown that BRCA2 provides a role in the repair of DNA damage and in the subnuclear relocalisation of RAD51 after damage in PCF *T. brucei*, which was only previously examined in BSF cells. Despite this, the growth impairment and DNA damage sensitivity phenotypes of the PCF *brca2*^{-/-} mutants generated here are slighter than those observed for the BSF *brca2*^{-/-} mutants generated previously (Hartley and McCulloch, 2008). Why this might be is unclear, especially as the extent to which the PCF cells formed detectable subnuclear RAD51 foci is very comparable to that of the BSF cells (Hartley and McCulloch, 2008). One possible explanation is that BRCA2 plays an additional role in the BSF life cycle stage, or that it performs dual functions in both life cycle stages but one of these is more pronounced in the BSF. What this function might be is unclear from these data, but perhaps BRCA2's role in general repair of DNA damage is distinct from another role in the maintenance of genome stability. If this stability function required a greater proportion of the available BRCA2 in the BSF, then less BRCA2 might be available for general repair and mutation of *BRCA2* in the BSF stage would then have a much greater impact on the general well being of the cells, manifested as a larger growth defect and greater sensitivity to exogenously added DNA damaging agents. For this proposed dual function of BRCA2, perhaps specific to BSF cells, to be true, it supposes that the levels of BRCA2 available for DNA repair may be higher in PCF cells, and we have no further evidence for this. It is also not obvious why the levels of BRCA2 could not simply be life cycle stage regulated. The only known functions of BRCA2 are to aid RAD51-mediated HR (O'Donovan and Livingston, 2010; Holloman, 2011), so it seems likely that any such dual function for BRCA2 would be manifest through RAD51. In this regard, it would be intriguing to analyse the levels of RAD51 and BRCA2 proteins in the two life cycle stages and also to generate and analyse *rad51*^{-/-} mutants in PCF cells to see if the phenotypes of this mutation are comparable in PCF and BSF cells. It is not clear whether the observation that *T. brucei* RAD51 levels do not respond to DNA damage, as they do in *T. cruzi* and *L. major* (McKean *et al.*, 2001; Regis-da-Silva *et al.*, 2006), may be related to this. What is clear though, is that RAD51 is able to be relocalised efficiently to induced DNA damage in both PCF and BSF cells (Hartley and McCulloch, 2008).

A major issue that would need to be addressed in the above hypothesis is the nature of the putative dual roles for BRCA2. An obvious possibility is a function in VSG switching, which may only occur in the BSF where the VSG ES are actively transcribed (Horn and McCulloch, 2010; Rudenko, 2010). Why this should differ from general repair by HR is unknown. An alternative is that BRCA2 contributes to the maintenance of the subtelomeres, which may have features (such as chromatin structure) that differ between the two life cycle stages, rendering them more prone to instability in the BSF. This is clearly a possibility, as it would explain the observed differences in genome instability described here (see below). Nonetheless, we cannot discount more trivial explanations for the differences in growth and repair in BRCA2 mutants in BSF and PCF cells. For instance, it may be that differences in underlying doubling times of the two life cycle stages in culture simply mean that the assays employed here provide less discrimination in the PCF, which divide more slowly. It is also possible that the PCF cells experience increased oxidative damage, due to the greater mitochondrial metabolism in PCF cells relative to BSF cells (Bienen *et al.*, 1991; Hajduk *et al.*, 1992; Fang and Beattie, 2003) that is likely to yield higher levels of reactive oxygen species, which can damage DNA (Kryston *et al.*, 2011). Alternatively, previous work has suggested that cell cycle checkpoints differ in PCF and BSF cells (Hammarton, 2007), and it may then be that DNA damage is recognised, signalled or repaired differently.

The observed replication phenotype in BSF *brca2*^{-/-} mutant cells, consistent with the initiation of cytokinesis prior to the completion of DNA replication, manifests as an accumulation of cells with aberrant DNA configurations (Hartley and McCulloch, 2008). Analysis of the cell cycle in the TREU 927 PCF *brca2*^{-/-} mutants generated here revealed an accumulation of zoids (anucleate cells) and this may be due to differences in the cell cycle checkpoints between the two life cycle forms; with PCF cells lacking the mitosis to cytokinesis checkpoint that is present in BSF cells (Hammarton *et al.*, 2003; Hammarton, 2007), allowing PCF cells that have not replicated their nuclear DNA (1N2K) to proceed through cytokinesis generating progeny containing 1N1K and 0N1K DNA content (Woodward and Gull, 1990). It is also possible that BRCA2 plays a more central role in replication progression and/or re-start in the BSF, and this could account

for the reduction in the severity of the *brca2*^{-/-} mutant phenotypes in the PCF Lister 427 and TREU 927 strains.

This work reveals a clear life cycle stage difference in genome stability, which is more marked than the repair differences discussed above. It is shown that the genomic instability phenotype observed in Lister 427 BSF *brca2*^{-/-} mutant cells cannot be detected in the same *brca2*^{-/-} mutants generated here in PCF cells of both TREU 927 and Lister 427 strains. This surprising finding appears to indicate a function of BRCA2 in the maintenance of genome stability that is a BSF-specific phenomenon. The differences in the size and composition of the subtelomeric VSG arrays in the two strains, TREU 927 and Lister 427, do not appear to account for the absence of putative GCRs in the TREU 927 PCF *brca2*^{-/-} mutants generated here, as the Lister 427 PCF *brca2*^{-/-} mutants also generated do not display putative GCRs after prolonged passaging. Though any rearrangements in PCF *brca2*^{-/-} mutant cells may require a longer period of growth before accumulating to a level that is detectable, the increased population doubling times of this life cycle stage have been taken into account when estimating generation times. Thus, the lack of rearrangements in the PCF cells cannot be accounted for simply by growth rate differences. In fact, the genome rearrangements observed in the BSF *brca2*^{-/-} mutant cells have been detected at an earlier time point (~ 150 generations) than previously examined, and significantly earlier than the PCF analyses. The original aim of this chapter was to map the genomic rearrangements at the DNA sequence level using the assembled genome sequence of strain TREU 927. Due to the absence of genome rearrangements in the PCF *brca2*^{-/-} mutants generated here, this aim could not be carried out. Completion of the assembly of the Lister 427 genome, in particular the subtelomeres of the megabase chromosomes, and the design of a microarray to allow whole genome hybridisation would allow the genetic dissection of the rearrangements observed in BSF Lister 427 *brca2*^{-/-} mutants. In the absence of these data, we can only speculate about the reasons for these life cycle differences.

The basis of this function for BRCA2 in the maintenance of genome stability in the BSF may be differences in the chromatin structure between the two life cycle stages (Schlimme *et al.*, 1993; Burri *et al.*, 1994), possibly due to the requirement for antigenic variation and VSG expression in the BSF only (Hughes

et al., 2007;Figueiredo, Janzen, and Cross, 2008;Stanne and Rudenko, 2010;Figueiredo and Cross, 2010). In this regard, there is some evidence to suggest that these rearrangements may be specifically targeted to VSGs. The large karyotype changes that occur in BSF *brca2*^{-/-} mutants, that lead to the loss of copies of *VSG121*, do not detectably encompass the *ingi* retrotransposon families (or at least the families analysed here). Many of these *ingi* retrotransposons are located in strand switch regions, and some are distributed throughout the VSG arrays in the subtelomeres of the megabase chromosomes. This builds upon previous work showing that the intermediate- and mini-chromosomes, which do not harbour VSG arrays, are not affected by loss of BRCA2 (Hartley and McCulloch, 2008). Perhaps, then, the rearrangements are even more VSG-localised than previously thought

Chapter 4: The function of the BRCA2 BRC repeat expansion in *T. brucei*.

4.1 Introduction

The BRCA2 protein in *T. brucei* contains an unusual number and arrangement of the RAD51-binding motif, the BRC repeat, which distinguishes it from BRCA2 proteins in other species. The human BRCA2 protein contains eight BRC repeats (Figure 1-15), all of which have been shown to bind Rad51 in either monomer or nucleoprotein filament forms (Wong *et al.*, 1997;Carreira and Kowalczykowski, 2011). The BRC repeats have been demonstrated to have different affinities for binding Rad51 due to the variation in amino acid sequence that is apparent across the eight BRC repeats (Chen *et al.*, 1998;Pellegrini and Venkitaraman, 2004;Esashi *et al.*, 2005;Thorslund, Esashi, and West, 2007;Carreira and Kowalczykowski, 2011). The BRC repeats are spread across the central third of the BRCA2 protein, with spacer regions between repeats varying from between 60 and 100 amino acids in length, and showing no sequence conservation (Bork, Blomberg, and Nilges, 1996;Bignell *et al.*, 1997). In contrast to this, the BRCA2 protein identified in *T. brucei* is unusual in containing an expansion in the number of BRC repeats; up to 15 BRC repeat motifs were predicted from the TREU 927 genome sequence, and Southern and minisatellite variant repeat (MVR) mapping shows that, while this number is variable both between strains and between alleles within a strain, BRCA2 always has greater than 8 BRC repeats (Lo *et al.*, 2003;Hartley and McCulloch, 2008). If it is assumed that a given *BRCA2* allele encodes fifteen BRC repeats, sequence analysis revealed that the 14 most N-terminal motifs are identical in amino acid sequence, while the sequence of the most C-terminal motif is slightly diverged in the last 11 amino acids. In addition, the BRC repeat motifs are arranged across the N-terminal half of the *T. brucei* BRCA2 protein and exist in a perfect tandem repeated array, with exactly 9 amino acids separating each repeat from the next and showing complete conservation (Hartley and McCulloch, 2008). This unusual BRC repeat expansion and arrangement appears largely unique to *T. brucei* (Figure 1-19). Amongst kinetoplastid parasites, BRCA2 proteins in *T. cruzi* and *Leishmania sp.* each possess 2 non-identical BRC repeats, while the African trypanosomes *T. vivax* and *T. congolense* contain 1 and 3 BRC repeats, respectively (Hartley and McCulloch, 2008). In other protists, 1-2 BRC repeats appear the norm, though larger numbers are found in apicomplexan parasites and in *Trichomonas vaginalis* (6-8 and 14, respectively), though here the repeats do not show the

same level of sequence uniformity or array organisation (Hartley and McCulloch, 2008;Lo *et al.*, 2003). Indeed, only in *T. congolense* are the repeats arranged like the *T. brucei* tandem repeat array, albeit in a truncated form.

It has been postulated that this expansion in BRC repeat number in *T. brucei* BRCA2 could be an adaptation for the elevated rates of homologous recombination required by *T. brucei* in order to carry out antigenic variation efficiently. However, this appears not to be the case, or at least to be too simplistic a hypothesis. In BSF Lister 427 *brca2*^{-/-} mutant cells the re-expression of variants of *BRCA2* from *T. brucei* and *T. vivax* containing only a single BRC repeat restored observed *VSG* switching frequencies to wild-type levels (Hartley and McCulloch, 2008), indicating that 15 BRC repeats are not a requirement for efficient antigenic variation in *T. brucei*, at least as measured by the *VSG* switching assay employed. Despite this, expression of these *BRCA2* variants in BSF *brca2*^{-/-} cells did cause detectable impairment in two aspects of homologous recombination: homology-directed integration of transformed DNA constructs, and re-organisation of RAD51 into detectable subnuclear foci following phleomycin-induced DNA damage (Hartley and McCulloch, 2008).

This chapter aims to characterise the function of the BRC repeat expansion in *T. brucei* BRCA2 further, by investigating the phenotype of *T. brucei* cells expressing a number of variants of BRCA2 with reduced numbers of BRC repeats. Full-length BRCA2 was re-expressed in the *brca2*^{-/-} mutant cell lines in the same manner as the BRC variants, in order to determine whether or not the phenotypic defects observed were due to loss of *BRCA2* (Chapter 3), and not the result of secondary mutation(s).

4.2 Complementation of PCF TREU 927 *brca2*^{-/-} mutant with variants of *BRCA2* with reduced numbers of BRC repeats

4.2.1 Generation of constructs containing variants of *BRCA2* with reduced numbers of BRC repeats

Constructs to enable the re-expression of variants of *BRCA2* with reduced numbers of BRC repeats were generated. Re-expression constructs containing

the full-length *BRCA2* gene (cloned from Lister 427 and estimated to contain 12 BRC repeats) and a variant containing the single, most C-terminal, degenerate BRC repeat motif were generated previously (gift, Claire Hartley). Multiple attempts to create variants of *BRCA2* with reduced numbers of BRC repeats by PCR have failed (data not shown), and therefore the required BRC variant domains of *BRCA2* were synthesised. The synthesised DNA contained the 216 bp of the *BRCA2* ORF from the ATG start codon to the start of the first BRC repeat sequence, followed by 3, 6 or 9 ‘normal’ BRC repeats, then followed by the degenerate BRC repeat and finally 277 bp of sequence extending down to a unique *MfeI* restriction site (2473 bp; Figure 4-1). These *BRC* variant domains of *BRCA2* differ from each other only in the number of BRC repeats, since each conserved repeat is identical, and were called *4BRC*, *7BRC* and *10BRC*, respectively. A restriction digestion-based cloning approach was then used to assemble the re-expresser constructs by adding the variant BRC repeat domains to the *BRCA2* ORF sequence downstream of *MfeI*, avoiding problematic PCR-amplification across the BRC repeat sequences. The variant *BRC* repeat domains were synthesised with *EcoRV* and *XhoI* sites at the 5’ and 3’ ends, respectively, to allow direct cloning into pBluescript. The 2,473 bp C-terminal domain of *BRCA2*, from the unique *MfeI* restriction site downstream to the stop codon, was excised from an existing construct (pRSF1b *BRCA2* C-term, section 5.2.1) using the restriction endonucleases *MfeI* and *XhoI*. This C-terminal *BRCA2* DNA fragment was then cloned into the pBluescript *BRC* variant constructs using the *MfeI* and *XhoI* restriction sites. To create *pRM482::BRC* re-expression constructs (see below), the whole assembly of each variant was then excised from pBluescript by digestion with *EcoRV* and *XhoI*, and blunt cloned into pRM482 (gift, Richard McCulloch) prepared by *EcoRV* restriction digestion. The cloning strategy is displayed in Figure 4-2.

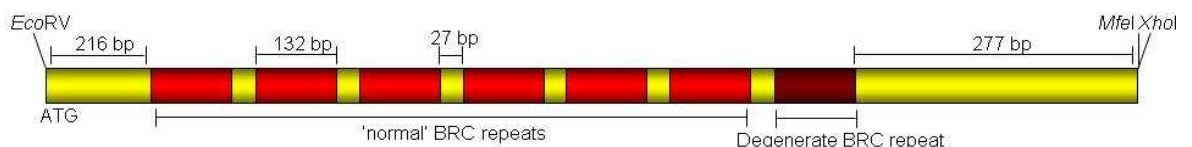


Figure 4-1 A diagram of the *7BRC* variant domain of *T. brucei BRCA2* generated by DNA synthesis. Indicated are the sequence motifs present including; 6 ‘normal’ BRC repeats (red boxes), the C-terminal degenerate BRC repeat (dark red box), the start (ATG), and the restriction sites used for cloning. The sizes of the component parts are shown (bp). *4BRC* and *10BRC* variant domains are not shown, but differ from *7BRC* only in possessing 3 and 9 ‘normal’ BRC repeat-encoding sequences, respectively.

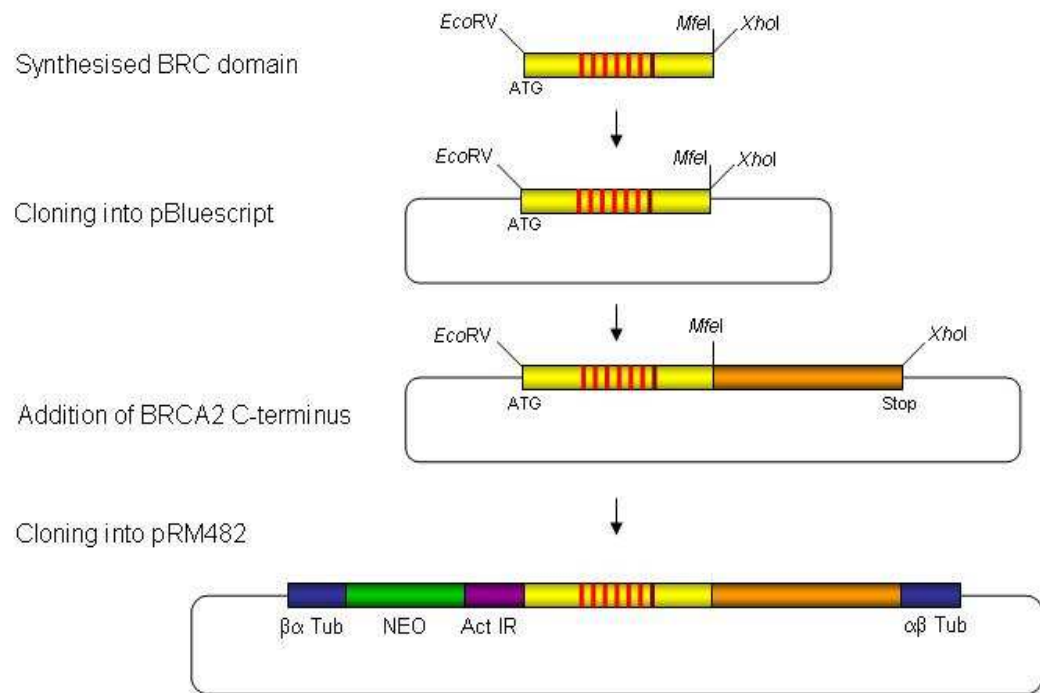


Figure 4-2 Cloning strategy used for the assembly of the *pRM482::BRC* variant re-expresser constructs.

The synthesised BRC repeat variants (top, yellow; only 7BRC is shown) were initially cloned into pBluescript using *EcoRV* and *XhoI* restriction sites. The C-terminus of *BRCA2* (orange) was prepared by restriction digestion with *MfeI* and *XhoI*, from an existing construct, and was ligated into the pBluescript-BRC construct directly downstream of the BRC variant insert. The whole insert was then excised using *EcoRV* and *XhoI*, and ligated into pRM482 (bottom) prepared by *EcoRV* digestion.

pRM482 is a construct that allows re-expression of a gene from the *tubulin* array in *T. brucei* (Figure 4-3), where it is transcribed initially as part of the endogenous transcript. The mature mRNA produced contains non-endogenous 5' and 3' UTRs derived from *trans*-splicing via an upstream *actin* intergenic sequence and polyadenylation from a downstream *tubulin* intergenic sequence. As such, the level of mRNA produced, and its stability, is likely to be altered relative to endogenous *BRCA2*. Nevertheless, re-expression by this strategy was successful for *BRCA2* in BSF Lister 427 *brca2*^{-/-} *T. brucei* leading to significant reversion of recombination and RAD51 foci impairment phenotypes (Hartley and McCulloch, 2008). pRM482 contains regions derived from *tubulin* intergenic sequences flanking the entire insert in pBluescript that provide targeting sequences to enable homologous recombination and replacement of an α *tubulin* ORF with the construct following transformation. To allow selection of constructs that have integrated into the genome, pRM482 contains the G418 antibiotic resistance cassette (*NEO*) containing processing signals derived from *tubulin* and *actin* intergenic sequences flanking the antibiotic resistance ORF. For transformation, the *pRM482::BRC* constructs were excised from pBluescript

by restriction digestion with *Xho*I and *Xba*I, the digested DNA was then ethanol precipitated and approximately 5 μ g of the resuspended DNA was used for each transformation.

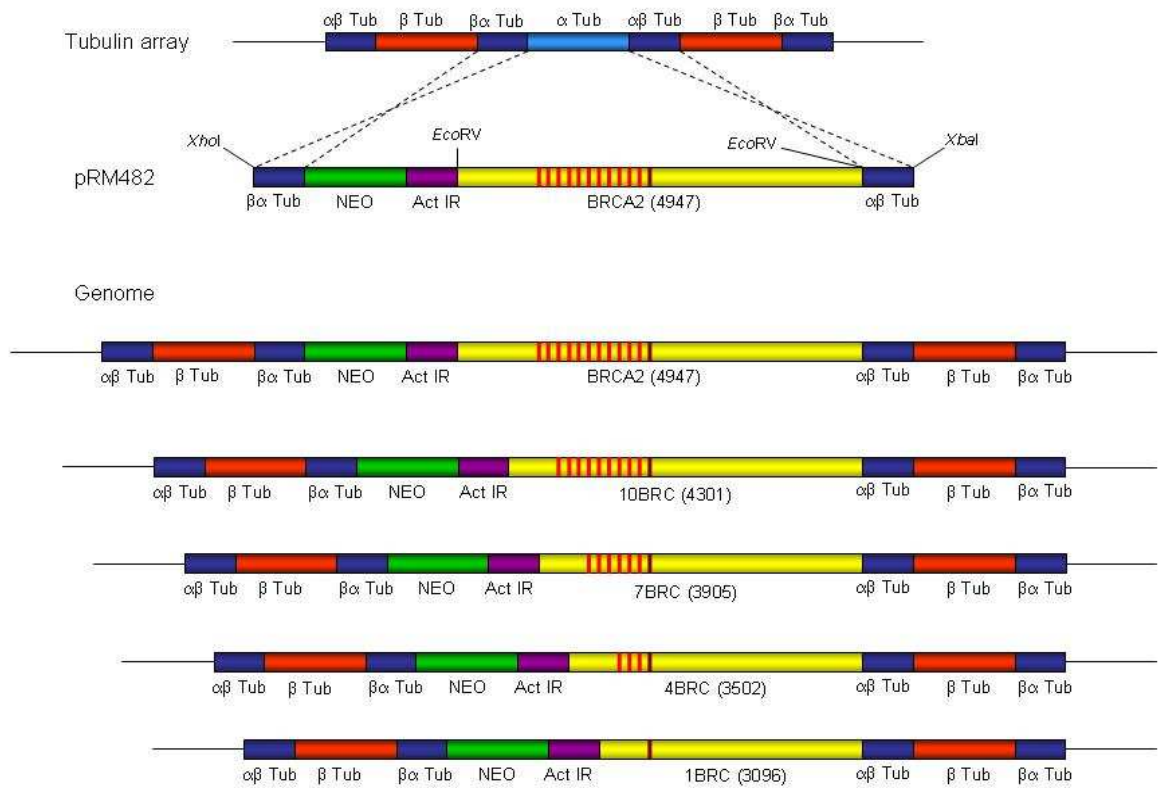


Figure 4-3 *pRM482::BRC* re-expression constructs. The full-length *BRCA2* ORF and four *BRC* variant ORFs (*1BRC*, *4BRC*, *7BRC* and *10BRC*) were cloned into an *EcoRV* site between the *actin* (*Act IR*) and *αβ tubulin* (*αβ Tub*) intergenic sequences of the plasmid *pRM482*, which contains the antibiotic resistance cassette for G418 (*NEO*). The construct is flanked with *tubulin* intergenic regions (*βα Tub* and *αβ Tub*) that allow integration by homologous recombination into the *tubulin* array (top), replacing an *α tubulin* ORF. Sizes of the *BRC* variants are shown (bp), and are not drawn to scale. Full-length *BRCA2* is shown with 12 *BRC* repeats, as it is cloned from Lister 427 cells and estimated to contain 12 *BRC* repeats.

4.2.2 Generation of re-expresser cell lines in PCF TREU 927

Transformations were carried out in order to generate five re-expresser cell lines in PCF TREU 927 *brca2*^{-/-} cells (section 3.2) containing full-length *BRCA2*, and variants of *BRCA2* with 1, 4, 7 and 10 *BRC* repeats using the *pRM482::BRC* re-expresser constructs (section 4.2.1). To do this, PCF TREU 927 *brca2*^{-/-} *BSD-PUR* mutant cells were transformed and antibiotic resistant transformants were selected by placing cells on SDM-79 media supplemented with 20 μ g.ml⁻¹ G418 (Sigma).

4.2.3 Confirmation of re-expresser cell lines by PCR

The generation of *BRCA2* re-expresser cell lines was initially confirmed by PCR performed on genomic DNA extracted from putative re-expresser clones resulting from the five transformations. PCR was performed using primers specific to the *BSD* and *PUR* resistance ORFs, and also a 1.2 kb region of the *BRCA2* ORF. The location of the primers and expected sizes of the PCR products are displayed in Figure 4-4A.

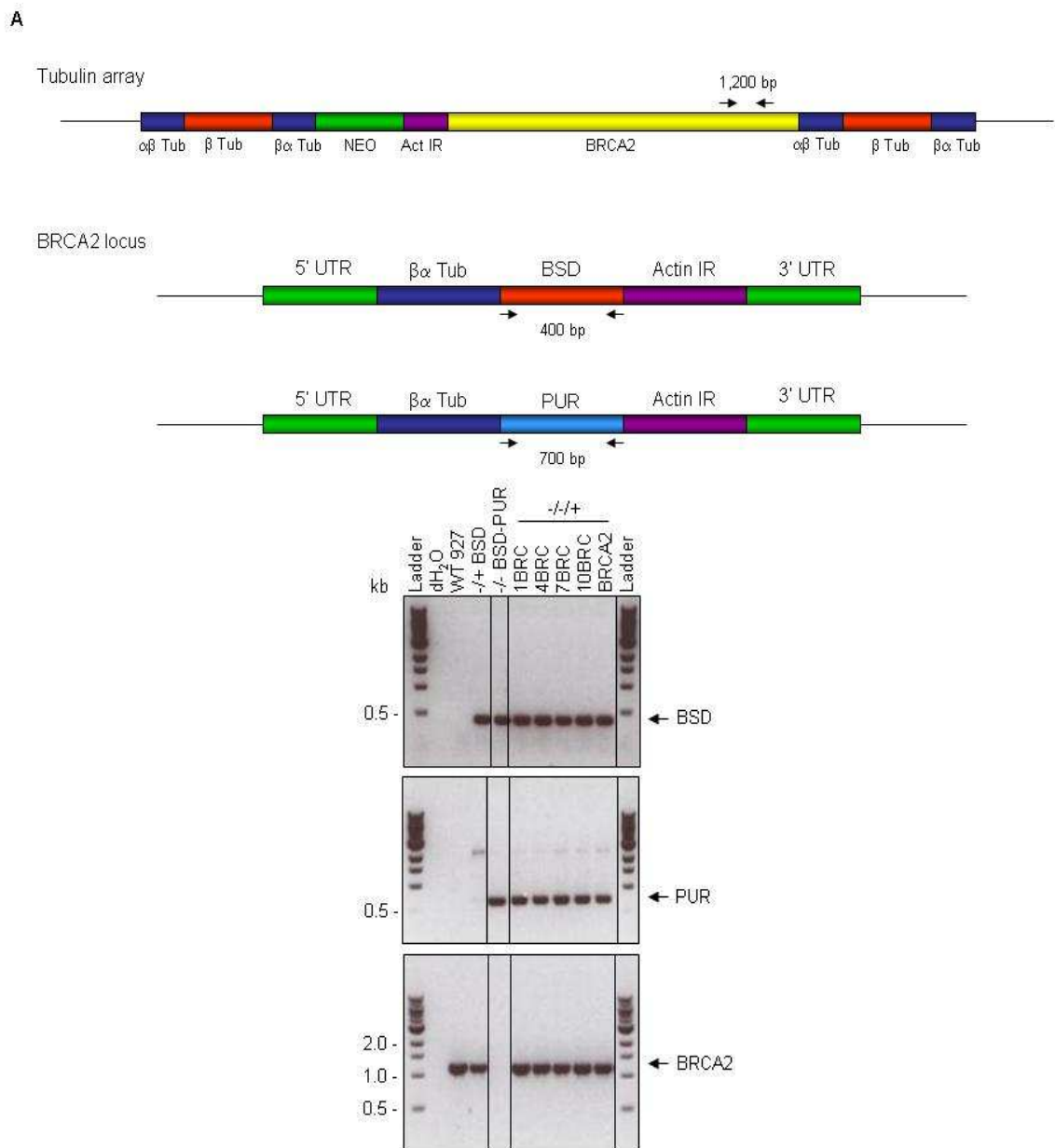


Figure 4-4 Confirmation of PCF TREU 927 *BRCA2* re-expresser cell lines by PCR. (A) Primers used to amplify part of the *BRCA2* ORF, and the *BSD* and *PUR* resistance ORFs, are indicated (black arrows), with the expected sizes of the resulting PCR products shown (bp). (B) An agarose gel of the PCR products obtained using the primers, described above, and genomic DNA extracted from wild-type TREU 927 (WT 927), +/- and -/- *BRCA2* mutant, and putative *BRCA2* re-expresser (-/-+) cell lines. Distilled water (dH₂O) was used as a

negative control. The PCR products produced from the *BSD*, *PUR* and *BRCA2* ORFs are indicated (black arrows), and size markers are shown (Ladder, kb).

The agarose gel in Figure 4-4B demonstrates the presence of the *BSD* and *PUR* resistance ORFs in all of the putative re-expresser cell lines. All five clones analysed here produced a PCR product with the primers specific to part of the *BRCA2* ORF, indicating they have integrated the re-expression construct. The five re-expresser cell lines selected for further analysis are referred to as; *-/-/+ 1BRC*, *-/-/+ 4BRC*, *-/-/+ 7BRC*, *-/-/+ 10BRC* and *-/-/+ BRCA2*.

4.2.4 Confirmation of re-expresser cell lines by Southern analysis

To confirm the generation of re-expresser cell lines, Southern analysis was performed. Genomic DNA extracted from wild-type TREU 927, *brca2*^{-/-} mutant and the five re-expresser (*-/-/+*) cell lines was digested with *Hind*III, separated by electrophoresis on a 1% agarose gel, Southern blotted and hybridised at 60°C with a DNA probe generated by PCR-amplification with the primers 48 and 49, corresponding to a 1.2 kb region of the *BRCA2* ORF. The location of primers, predicted restriction enzyme recognition sites and expected DNA fragment sizes in this approach are displayed in Figure 4-5A.

The Southern blot in Figure 4-5B demonstrates that the intact *BRCA2* ORF exists as a single size variant in wild-type TREU 927 cells and the *brca2*^{-/-} mutant cells no longer possess a *BRCA2* ORF (as described in section 3.2.4). The five re-expresser cell lines all contained a DNA fragment of the expected size for the *BRCA2 BRC* variants after integration and dependent on the number of BRC repeats, which indicates that they have integrated the *pRM482::BRC* constructs correctly into the *tubulin* array.

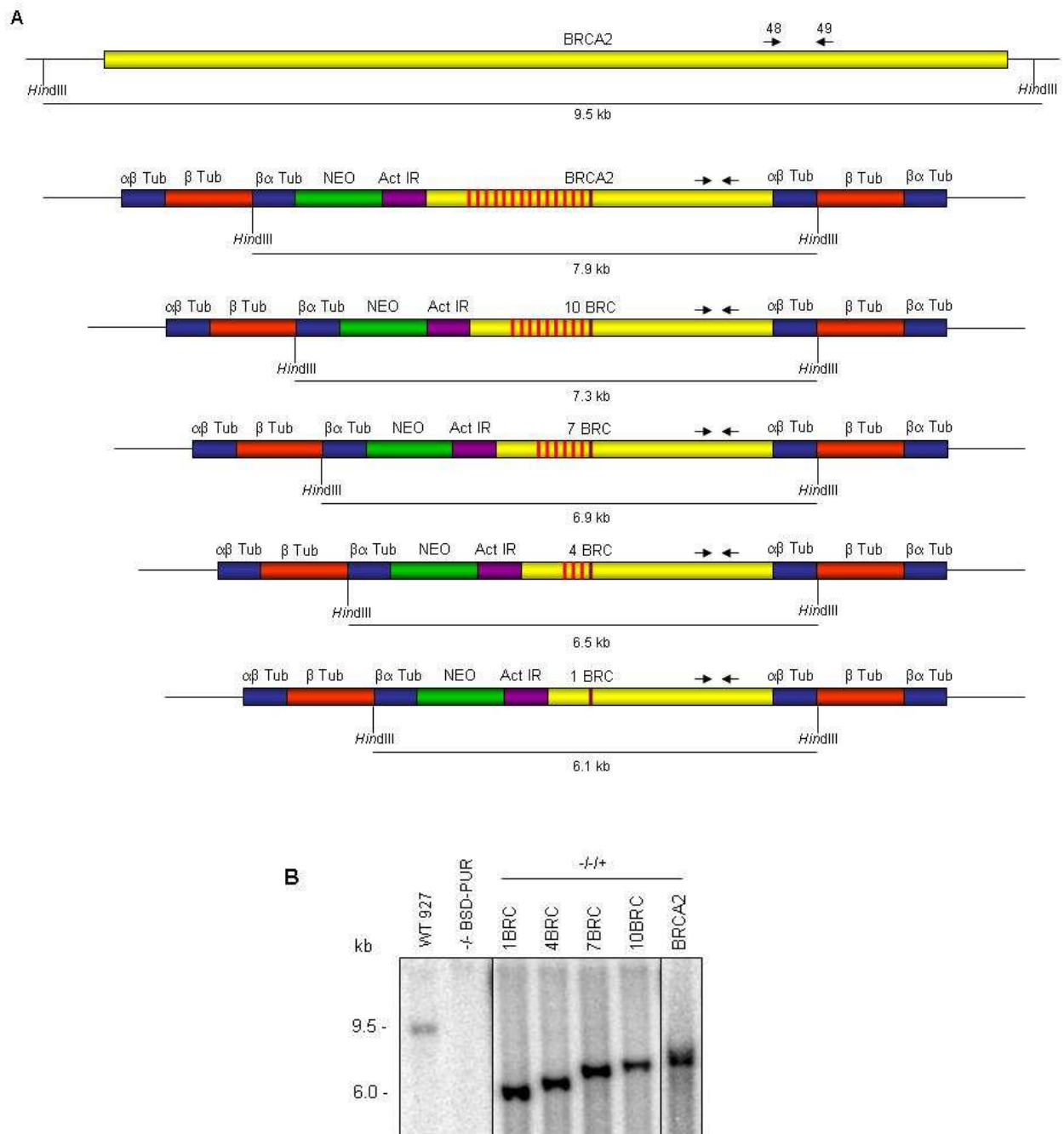


Figure 4-5 Confirmation of PCF TREU 927 *BRCA2* re-expresser cell lines by Southern analysis.

(A) Restriction maps showing the expected products of restriction digestion, Southern blotting and hybridisation with 1.2 kb of the *BRCA2* ORF (black arrows indicate the primers used to PCR-amplify this as a DNA probe). The restriction sites are indicated, with the expected restriction fragment sizes shown (kb). (B) 5 μ g of genomic DNA extracted from wild-type TREU 927 (WT 927), *brca2*^{-/-} mutant, and *BRCA2* re-expresser (-/-+) cell lines was digested with *Hind*III before being separated by electrophoresis on an agarose gel. The DNA was Southern blotted before being hybridised with a DNA probe against 1.2 kb of the *BRCA2* ORF. Size markers are shown (kb).

4.2.5 Attempt at confirmation of re-expresser cell lines by western analysis

Attempts at confirmation of the re-expression of the variants of *BRCA2* in the PCF TREU 927 *brca2*^{-/-} cells by western blot using anti-*BRCA2* antiserum were

performed multiple times, including with the addition of 5% chicken serum (Sigma) in the blocking solution to reduce non-specific binding of the antibody. The clearest result of these experiments is displayed in Figure 4-6.

The western blot in Figure 4-6 demonstrates a band visible at approximately the expected size (176 kDa) for the BRCA2 protein in the wild-type and *BRCA2*^{-/+} mutant cell lines, which was not present in the *brca2*^{-/-} cell line. Bands of the expected sizes for the BRCA2 BRC variants were not visible in the re-expresser cell lines. If the non-specific band visible at ~ 58 kDa is viewed as a loading control, it is apparent that although there was significant variation in the protein loading between the different cell lines, protein was detectable in all samples. This may suggest that the level of expression of the variants of BRCA2 is reduced relative to the endogenous locus and below the threshold of detection of the antiserum. However, one of the peptides recognised by the antiserum is the BRC repeat, and it is therefore possible the antiserum does not bind to the re-expressed variants as efficiently as full-length BRCA2.

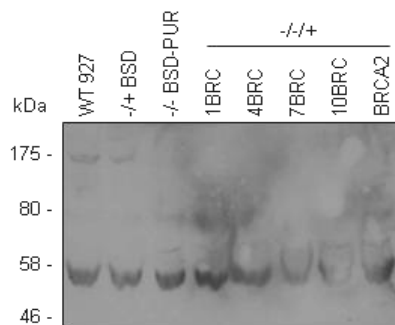


Figure 4-6 Attempt at confirmation of PCF TREU 927 BRCA2 re-expresser cell lines by western analysis.

Total protein extracts from wild-type TREU 927 (WT 927), ^{-/+} and ^{-/-} *BRCA2* mutant, and *BRCA2* re-expresser (^{-/-+}) cell lines were separated by SDS-PAGE and western blotted before being probed with anti-BRCA2 antiserum (1:200 dilution). Size markers are shown (kDa).

4.2.6 Analysis of *BRCA2* mRNA levels in re-expresser cell lines by quantitative RT-PCR

As the expression of the *BRCA2* variants could not be confirmed by western analysis, the mRNA levels were analysed by quantitative RT-PCR. Total RNA was extracted from wild-type TREU 927, *BRCA2*^{-/+} mutant and *BRCA2* re-expresser (^{-/-+}) cell lines, DNase treated and subsequently cDNA was synthesised by RT-PCR using the SuperScript First Strand Reverse Transcription Kit (section 2.5.4).

To confirm the absence of genomic DNA contamination in the extracted RNA, control cDNA reactions were performed without the addition of the reverse transcriptase (RT) enzyme. PCR analysis with primers specific for part of an endogenous gene, *DNA polymerase I (Poll; 150 and 151)*, was used to test for PCR-amplification of cDNA in RT plus and control RT minus samples. The agarose gel in Figure 4-7 demonstrates that cDNA had been generated successfully in all the RT plus samples, and that genomic DNA contamination was absent from all the RT minus samples, as no PCR product was visible.

Quantitative RT-PCR was carried out (section 2.5.5) on the cDNA produced in the RT plus samples using primers specific for part of an endogenous control gene, *tubulin* (154 and 155), and part of the *BRCA2* gene (138 and 139). Primer annealing was tested after the qRT-PCR reaction by running a dissociation curve step (data not shown), which confirmed that the primers were only producing a single product and were not producing primer dimers, which could adversely affect the results. The mRNA detected in this and subsequent qRT-PCR experiments (section 4.4.2 and section 4.6.5) cannot be absolutely confirmed to be *BRCA2* mRNA. Analysis of the *brca2*^{-/-} cell line, and the absence of a product could have provided further evidence that this is in fact *BRCA2* mRNA. In addition, electrophoretic separation of the PCR products would have allowed determination of the size of the product and sequencing of the product could have been carried out to absolutely confirm the amplification of *BRCA2* mRNA. However, the data in Figure 4-8 demonstrate that the *BRCA2*^{-/+} mutant cell lines have a ~ 50% reduced level of *BRCA2* mRNA when compared to wild-type cells, that is consistent with the deletion of a single *BRCA2* allele. However, the two different ^{-/+} cell lines analysed showed some inconsistency, with ~ 40% and ~ 60% reduction. It is possible that a different *BRCA2* allele has been deleted in each cell line, and the alleles show differences in levels of steady state mRNA, though these differences may simply reflect variation in the accuracy of qRT-PCR measurements. The five *BRCA2* re-expresser cell lines had varying levels of *BRCA2* mRNA, ranging from a ~ 20 - 60% reduced level when compared to wild-type cells. These variations may be real, and could reflect changes in mRNA due to the genes being expressed from variable locations within the *tubulin* array. Nevertheless, the data show a trend not dissimilar to the mRNA levels seen for ^{-/+} *BSD*, and suggest that this expression strategy generates *BRCA2* mRNA levels

close to those of a *BRCA2*^{-/+} mutant and slightly less than a wild-type cell line with two *BRCA2* alleles, consistent with integration of a single gene in each case.

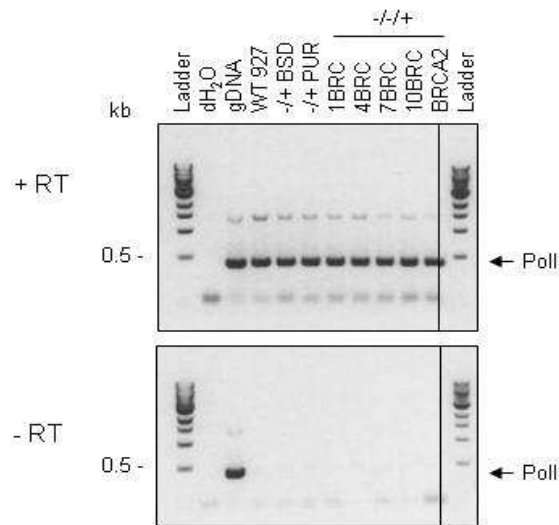


Figure 4-7 Testing PCF TREU 927 *BRCA2* re-expresser RT-PCR reactions by PCR. An agarose gel of the PCR products generated using primers specific to *DNA polymerase I* (*Poll*), amplified from cDNA generated by RT-PCR reactions containing reverse transcriptase (top, + RT). Control cDNA reactions were also analysed, lacking reverse transcriptase (bottom, - RT). Distilled water (dH₂O) was used as a negative control, and a genomic DNA sample (gDNA) as a positive control. Size markers are shown (Ladder, kb).

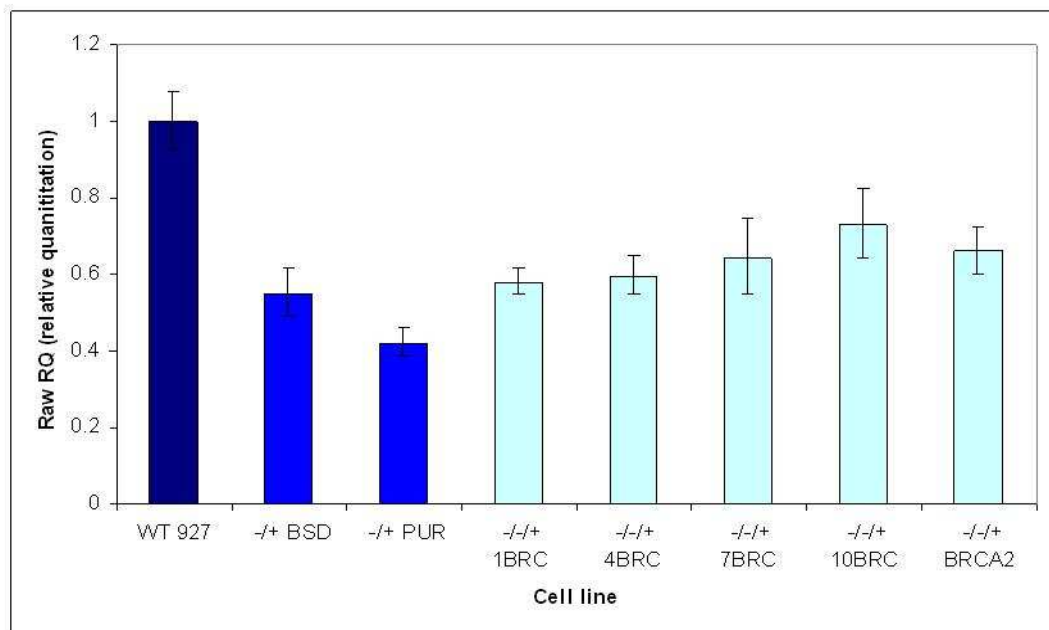


Figure 4-8 Quantitative RT-PCR analysis of the PCF TREU 927 *BRCA2* re-expresser cell lines.

Quantitative RT-PCR was carried out on cDNA generated from wild-type TREU 927 (WT 927), *BRCA2*^{-/+} mutant (*BSD* or *PUR*), and *BRCA2* re-expresser (*-/-+*) cell lines using primers specific for an endogenous control, *tubulin*, and *BRCA2*. All samples were normalised to the *tubulin* endogenous control and the level for *BRCA2* expressed relative to the WT 927 sample (which was set as one); values are the average quantification from four repetitions, and vertical lines indicate standard deviation.

4.3 Phenotypic analysis of PCF TREU 927 BRCA2 re-expresser cell lines

4.3.1 Analysis of *in vitro* growth

The *in vitro* growth of the PCF TREU 927 BRCA2 re-expresser cell lines was analysed in order to determine if variation in BRC repeat number correlates with the extent of the relatively minor growth impairment in TREU 927 *brca2*^{-/-} cells (section 3.3.1). In addition, the re-expression of full-length *BRCA2* allows us to determine if the impaired growth phenotype of the *brca2*^{-/-} cell line is due to loss of *BRCA2*, or might result from secondary mutations in the absence of a factor needed for repair of DNA damage. The average counts from three experimental repetitions are plotted in Figure 4-9, and extrapolated doubling times are displayed in Table 4-1.

From the growth curves and doubling times displayed it is apparent that the re-expression of *BRCA2* with 1, 4, 7 or 10 BRC repeats, or full-length *BRCA2*, restores growth of the *brca2*^{-/-} mutant cell line to essentially wild-type levels, with doubling times of between ~ 10.7 and ~ 11.3 hours for the re-expresser cell lines and ~ 11 hours for wild-type cells. It therefore appears that *BRCA2* with even a single BRC repeat is capable of supporting wild-type rates of growth, at least in culture.

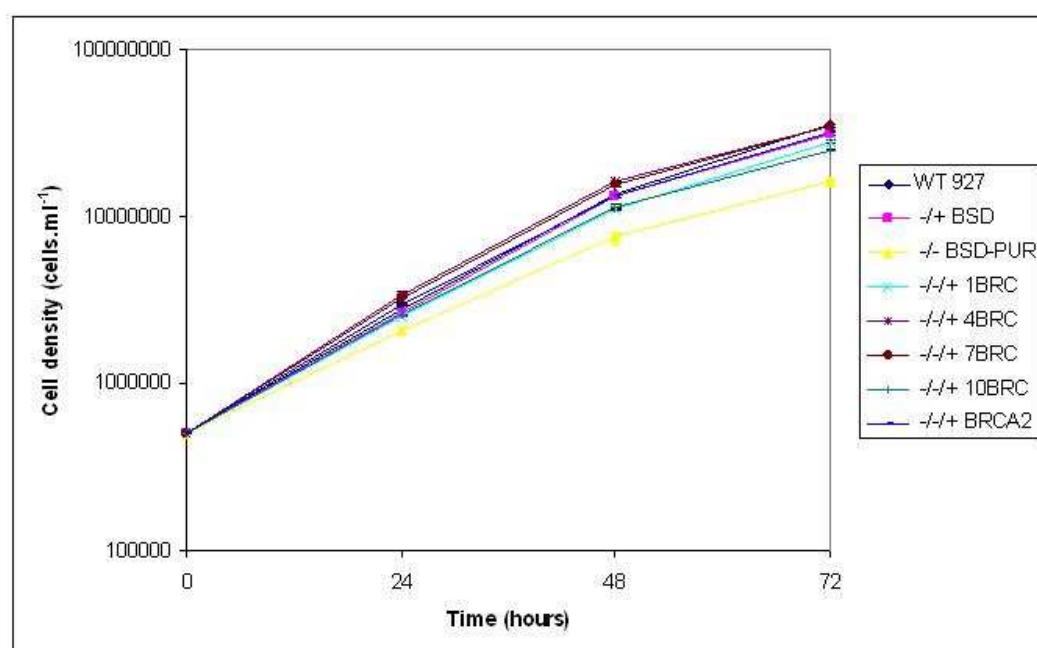


Figure 4-9 Analysis of *in vitro* growth of the PCF TREU 927 BRCA2 re-expresser cell lines.

2 ml cultures of wild-type TREU 927 (WT 927), *-/+* and *-/-* *BRCA2* mutant, and *BRCA2* re-expresser (*-/-/+*) cell lines were inoculated at 5×10^5 cells.ml⁻¹ and cell densities counted 24, 48, and 72 hours subsequently are shown. Values are averaged from the counts from three experimental repetitions, and vertical lines indicate standard deviation.

Cell line	Doubling time (hours)
WT 927	10.50
<i>-/+</i> BSD	10.38
<i>-/-</i> BSD-PUR	12.95
<i>-/-/+</i> 1BRC	11.35
<i>-/-/+</i> 4BRC	10.73
<i>-/-/+</i> 7BRC	10.68
<i>-/-/+</i> 10BRC	11.31
<i>-/-/+</i> <i>BRCA2</i>	11.27

Table 4-1 *In vitro* population doubling times of PCF TREU 927 *BRCA2* re-expresser cell lines.

The mean doubling time for wild-type TREU 927 (WT 927), *-/+* and *-/-* *BRCA2* mutant, and *BRCA2* re-expresser (*-/-/+*) cell lines is displayed, in hours, and was calculated from the data displayed in Figure 4-9.

4.3.2 Analysis of DNA damage sensitivity

The Alamar blue assay was used to determine the sensitivity of the PCF TREU 927 *BRCA2* re-expresser cell lines to the DNA damaging agents MMS and phleomycin. The Alamar blue assay was set up with wild-type TREU 927, *-/+* and *-/-* *BRCA2* mutant and *BRCA2* re-expresser (*-/-/+*) cell lines. The extent of fluorescence for each cell line was plotted graphically over the range of log drug concentrations (for representative examples see Figure 4-10 and Figure 4-11). From this, EC50s were determined from each individual plot and then average EC50s (plus 95% confidence intervals) were calculated from two experimental repetitions. The mean EC50s for each cell line were then plotted relative to the wild-type EC50, which was taken as 100% (Figure 4-12 and Figure 4-13).

The survival curves displayed in Figure 4-10 and Figure 4-11 are representative of the two repetitions performed. These data demonstrate that as the concentration of DNA damaging agent increases the fluorescence, and therefore the percentage of surviving cells that are actively reducing Alamar blue to fluorescent resorufin, reduces until the concentration at which all cells are killed is reached. It is apparent that the *brca2*-/- mutant cell line displayed reduced survival in the presence of both compounds (section 3.3.2), whilst the re-expression of *BRCA2* with 1, 4, 7, or 10 BRC repeats in this cell line restored

the reduced survival back to at least wild-type levels. Similarly, the full-length *BRCA2* re-expresser cell line also displayed levels of survival comparable to wild-type cells when exposed to both MMS and phleomycin. Indeed, in the presence of phleomycin, it could be argued that all the re-expresser cell lines displayed slightly increased survival compared to wild-type cells. The extrapolated EC50 values (graphs displayed in Figure 4-12 and Figure 4-13) confirm this, and also demonstrate that the re-expression of *BRCA2* with 1, 4, 7, or 10 BRC repeats or full-length *BRCA2* restored the increased sensitivity to MMS observed in the *brca2*^{-/-} cells back to approximately wild-type levels, with calculated EC50s being essentially equivalent. These data also appear to confirm that each re-expresser cell line, with the exception of 7BRC, displayed an increased (though not statistically significant, see below) resistance to phleomycin relative to wild-type and *BRCA2*^{-/+} cells, with EC50s between 50 and 100% higher than in wild-type cells. This increase has also been observed in BSF Lister 427 *brca2*^{-/-} cell lines re-expressing full-length *BRCA2* (Hartley and McCulloch, unpublished), though the basis for this phenomenon is unknown. Nevertheless, it is striking that the number of BRC repeats present in the re-expressed *BRCA2* variants does not correlate with an increase or decrease in sensitivity to DNA damage, with EC50s to both compounds and all variants being essentially equivalent.

To evaluate the above data further, the EC50 values of wild-type TREU 927, ^{-/+} and ^{-/-} *BRCA2* mutant and *BRCA2* re-expresser (^{-/-/+}) cell lines were compared using student's T-tests, and the results of this are displayed in Table 4-2. No statistical difference was observed between wild-type, ^{-/+}, ^{-/-} and *BRCA2* re-expresser cell lines ($p > 0.05$) for both DNA damaging agents. However, the lack of statistical significance may be due to the fact that only two experimental repetitions were performed, and further experiments may be needed to clarify if the observed trend for greater resistance to phleomycin is real. Indeed, though the *brca2*^{-/-} cells appeared more sensitive to MMS, this too was not seen to be statistically significant in these experiments, though it was in previous analysis (section 3.3.2).

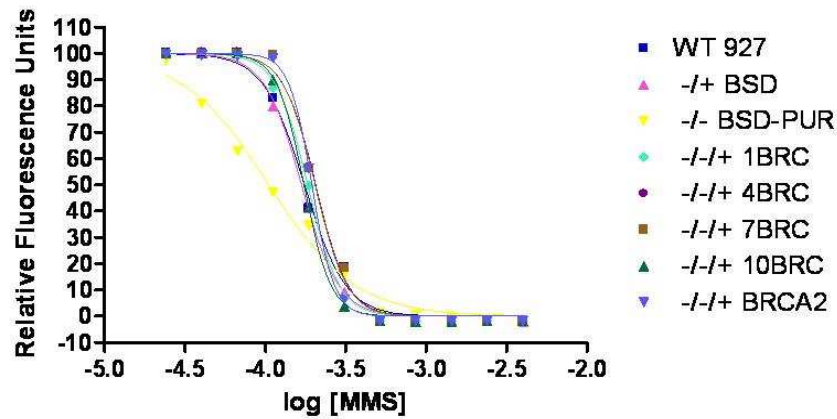


Figure 4-10 A representative survival curve for PCF TREU 927 BRCA2 re-expresser cell lines exposed to MMS.

The extent of fluorescence for each cell line (WT, $-/+$, $-/-$ and $-/-/+$) obtained using the Alamar blue assay is plotted against the log of MMS concentrations. Nonlinear regression was performed and fitted curves are shown for each cell line.

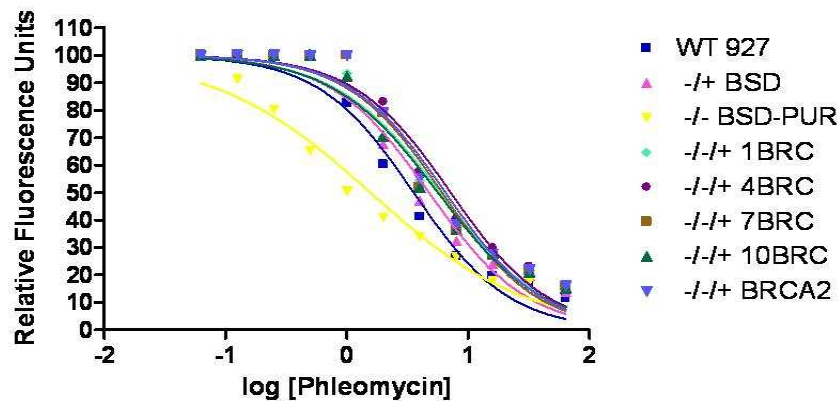


Figure 4-11 A representative survival curve for PCF TREU 927 BRCA2 re-expresser cell lines exposed to phleomycin.

The extent of fluorescence for each cell line (WT, $-/+$, $-/-$ and $-/-/+$) obtained using the Alamar blue assay is plotted against the log of phleomycin concentrations. Nonlinear regression was performed and fitted curves are shown for each cell line.

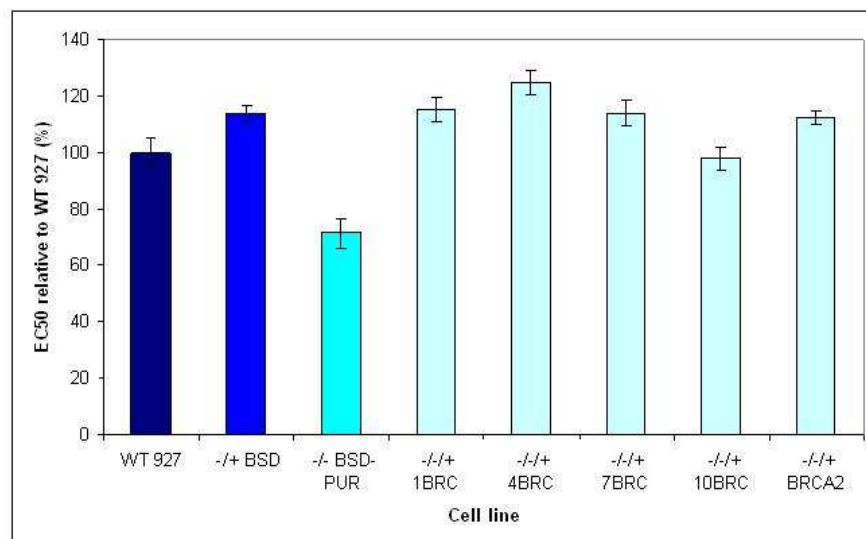


Figure 4-12 EC₅₀ values of PCF TREU 927 BRCA2 re-expresser cell lines exposed to MMS. Wild-type TREU 927 (WT 927), $-/+$ and $-/-$ BRCA2 mutant, and BRCA2 re-expresser ($-/-/+$) cell lines were placed in serially decreasing amounts of MMS and allowed to grow for 48 hours,

before the addition of Alamar Blue. After a further 24 hours the reduction of Alamar Blue was measured by the amount of fluorescent resorufin generated. EC50 values are the mean from two experimental repetitions expressed as a percentage relative to wild-type, and bars indicate 95% confidence intervals.

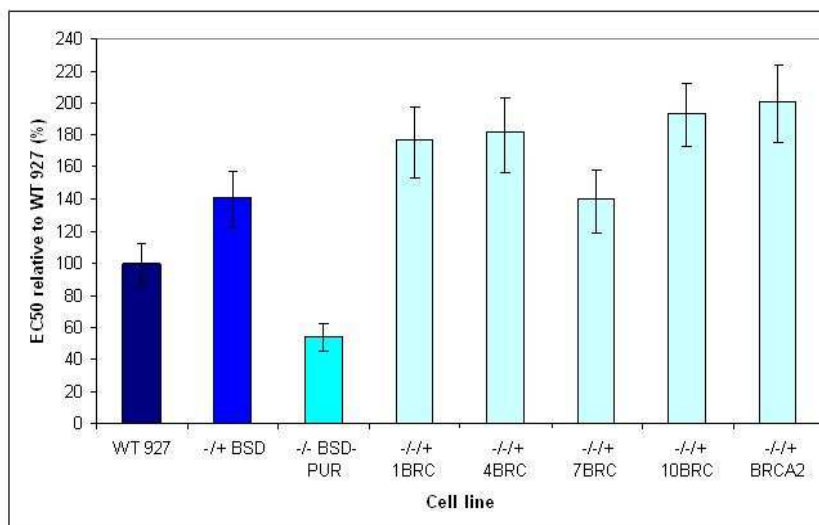


Figure 4-13 EC50 values of PCF TREU 927 BRCA2 re-expresser cell lines exposed to phleomycin.

Wild-type TREU 927 (WT 927), *-/+* and *-/-* BRCA2 mutant, and BRCA2 re-expresser (*-/+*) cell lines were placed in serially decreasing amounts of phleomycin and allowed to grow for 48 hours, before the addition of Alamar Blue. After a further 24 hours the reduction of Alamar Blue was measured by the amount of fluorescent resorufin generated. EC50 values are the mean from two experimental repetitions expressed as a percentage relative to wild-type, and bars indicate 95% confidence intervals.

A

	-/+ BSD	-/- BSD-PUR	-/+ 1BRC	-/+ 4BRC	-/+ 7BRC	-/+ 10BRC	-/+ BRCA2
WT 927	0.3145	0.0582	0.0903	0.2780	0.5779	0.8274	0.5129
-/+ BSD		0.0720	0.8832	0.6569	0.9924	0.4936	0.9600
-/- BSD-PUR			0.0696	0.1666	0.2872	0.2525	0.2316
-/+ 1BRC				0.4957	0.9404	0.2104	0.8231
-/+ 4BRC					0.9404	0.2104	0.0603
-/+ 7BRC						0.3390	0.8047
-/+ 10BRC							0.1934

B

	-/+ BSD	-/- BSD-PUR	-/+ 1BRC	-/+ 4BRC	-/+ 7BRC	-/+ 10BRC	-/+ BRCA2
WT 927	0.0769	0.0973	0.1064	0.1637	0.4262	0.2423	0.1694
-/+ BSD		0.0151	0.1396	0.3691	0.9799	0.3530	0.2295
-/- BSD-PUR			0.0306	0.1401	0.2696	0.1364	0.0880
-/+ 1BRC				0.9171	0.5592	0.6224	0.3488
-/+ 4BRC					0.1535	0.8725	0.7617
-/+ 7BRC						0.5805	0.4914
-/+ 10BRC							0.5985

Table 4-2 Statistical analysis of Alamar Blue results.

(A) P values are shown for student's T-tests comparing the mean EC50 values of wild-type TREU 927 (WT 927), *-/+* and *-/-* BRCA2 mutant, and BRCA2 re-expresser (*-/+*) cell lines grown in the presence of MMS (A) or phleomycin (B). Areas shaded in yellow indicate a significant difference ($P \leq 0.05$). No correction has been made for simultaneous multiple comparisons.

4.3.3 Analysis of RAD51 focus formation

The ability of PCF TREU 927 BRCA2 re-expresser cell lines to form RAD51 foci was next analysed in order to ask about the role of the BRC repeats and their expansion in RAD51 function. The numbers of RAD51 foci present in the nucleus of each of the cell lines that had been exposed to 1 $\mu\text{g}\cdot\text{ml}^{-1}$ phleomycin for 18 hours were counted for approximately 200 cells per cell line (Table 4-3) and plotted graphically (Figure 4-14). Representative images of cells are displayed in Figure 4-15A, and compared with control cells without phleomycin treatment in Figure 4-15B.

In the absence of DNA damage RAD51 foci were rarely seen (~ 2% of cells, Figure 4-15B), irrespective of the BRC repeat number or the presence or absence of intact, full-length BRCA2. As described previously (section 3.3.4), after the induction of DNA damage the number of wild-type and *BRCA2*-/+ cells containing no detectable RAD51 foci reduced to ~ 25%, with the majority of cells containing 1, 2 or 3 foci, while the *brca2*-/- mutant cells appeared to have lost the ability to form RAD51 foci. Comparing the re-expresser cell lines revealed a striking BRC repeat number-dependent increase in the ability to form RAD51 foci. The number of cells containing no RAD51 foci decreased as the BRC repeat number increased, with the full-length BRCA2 re-expresser cell line containing only 13% of cells with no detectable RAD51 foci, less than the ~ 25% of wild-type and *BRCA2*-/+ cells containing no RAD51 foci. The number of cells with detectable RAD51 foci increased as the BRC repeat number increased, though it appeared that under these experimental conditions the relative proportions of cells containing 1 or 2 RAD51 foci remained relatively constant as BRC repeat number increased, with the largest increases seen in the numbers of cells containing 3 or 4 RAD51 foci. Indeed, the *1BRC*, *4BRC* and *7BRC* re-expresser cell lines were markedly less efficient than wild-type or *BRCA2*-/+ cells at forming RAD51 foci, and it appears that ~ 10 BRC repeats are needed for the cells to respond equivalently. Overall, the correlation seen in this phenotype with BRC repeat number is quite distinct from the lack of correlation between BRC repeat number and cell survival after phleomycin treatment (section 4.3.2).

		Number of cells with RAD51 foci (%)						
		0	1	2	3	4	>4	N
Cell line	WT 927	25.9	23.1	19.3	17.0	8.1	6.6	347
	-/+ BSD	25.3	30.8	17.0	12.6	6.3	8.0	364
	-/- BSD-PUR	99.1	0.9	0.0	0.0	0.0	0.0	212
	-/+ 1BRC	55.4	20.9	15.2	5.4	1.3	1.8	388
	-/+ 4BRC	47.3	26.9	12.8	6.8	2.4	3.8	368
	-/+ 7BRC	36.5	26.9	18.7	11.4	5.0	1.4	219
	-/+ 10BRC	25.8	32.5	17.0	14.4	7.7	2.6	194
	-/+ BRCA2	13.6	27.2	27.7	15.7	11.5	4.2	191

Table 4-3 RAD51 focus formation in PCF TREU 927 BRCA2 re-expresser cell lines exposed to phleomycin.

Wild-type TREU 927 (WT 927), +/- and -/- BRCA2 mutant, and BRCA2 re-expresser (-/+) cell lines were treated with 1 $\mu\text{g}\cdot\text{ml}^{-1}$ phleomycin for 18 hours and the number of cells with a specific number of subnuclear RAD51 foci formed (0, 1, 2, 3, 4, > 4) were counted and are represented as a percentage of the total cells counted (N). Boxes shaded in light yellow contain foci, whilst boxes shaded in bright yellow contain the highest percentage of foci.

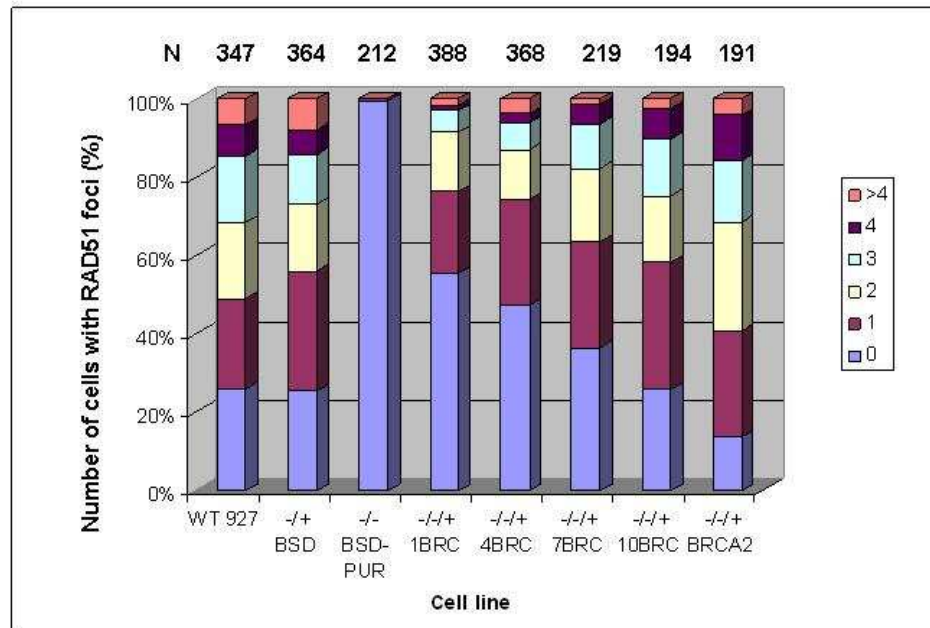


Figure 4-14 Graphical representation of RAD51 focus formation in PCF TREU 927 BRCA2 re-expresser cell lines exposed to phleomycin.

Wild-type TREU 927 (WT 927), +/- and -/- BRCA2 mutant, and BRCA2 re-expresser (-/+) cell lines were treated with 1 $\mu\text{g}\cdot\text{ml}^{-1}$ phleomycin for 18 hours and the number of cells with a specific number of subnuclear RAD51 foci formed (0, 1, 2, 3, 4, > 4) were counted and are represented as a percentage of the total cells counted (N).

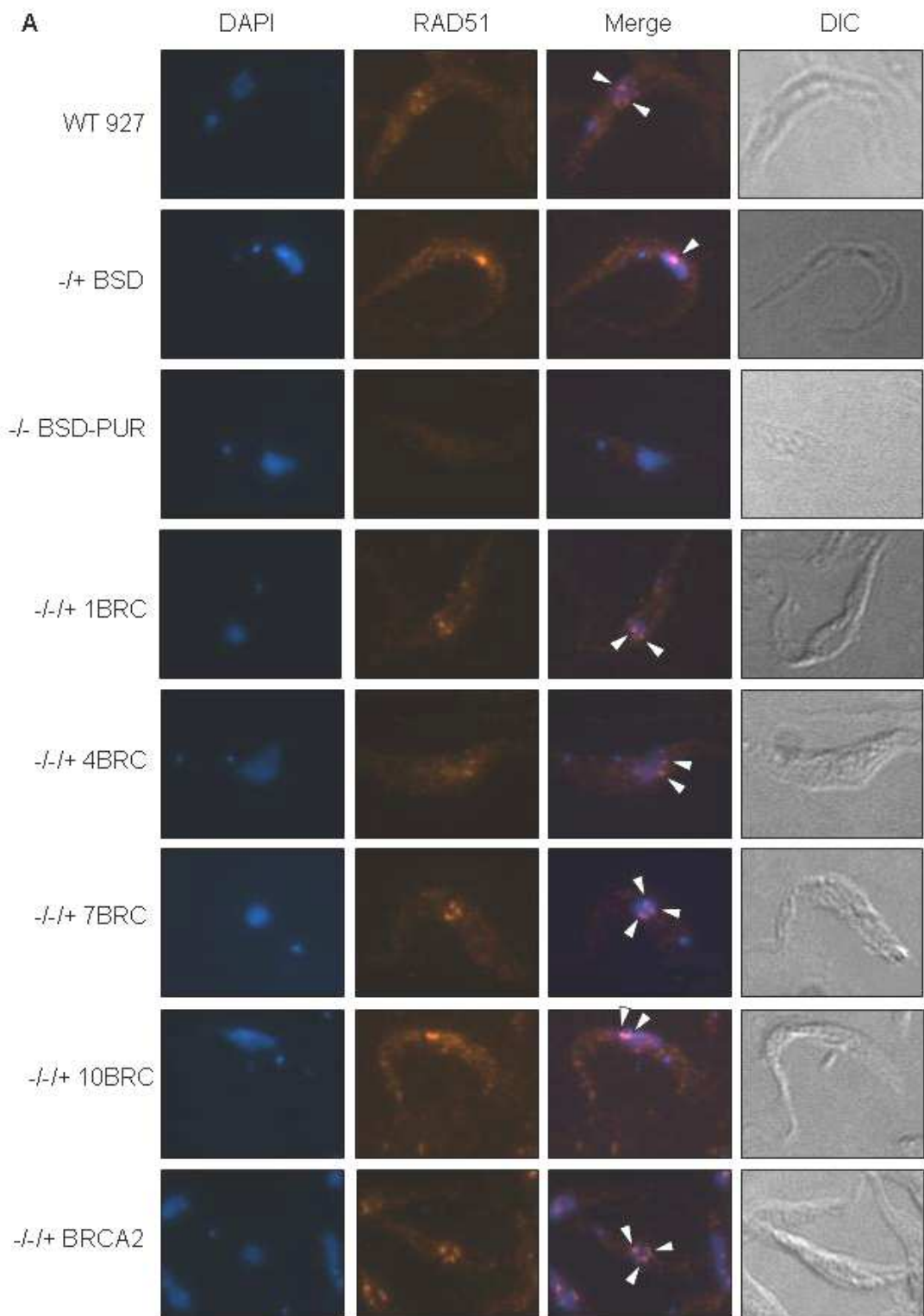


Figure 4-15A Representative images of RAD51 focus formation in PCF TREU 927 BRCA2 re-expresser cell lines exposed to phleomycin.

Images of wild-type TREU 927 (WT 927), *-/+* and *-/-* *BRCA2* mutant, and *BRCA2* re-expresser (*-/-/+*) cell lines after phleomycin treatment ($1 \mu\text{g}\cdot\text{ml}^{-1}$ for 18 hours). Each cell is shown in differential interface contrast (DIC), after staining with DAPI (DAPI) and after hybridisation with anti-RAD51 antiserum (1:1000 dilution) and secondary hybridisation with Alexa Fluor 594 conjugated anti-rabbit antiserum (1:7000 dilution, RAD51). Merged images of DAPI and RAD51 cells are also shown (Merge). White arrows indicate RAD51 foci.

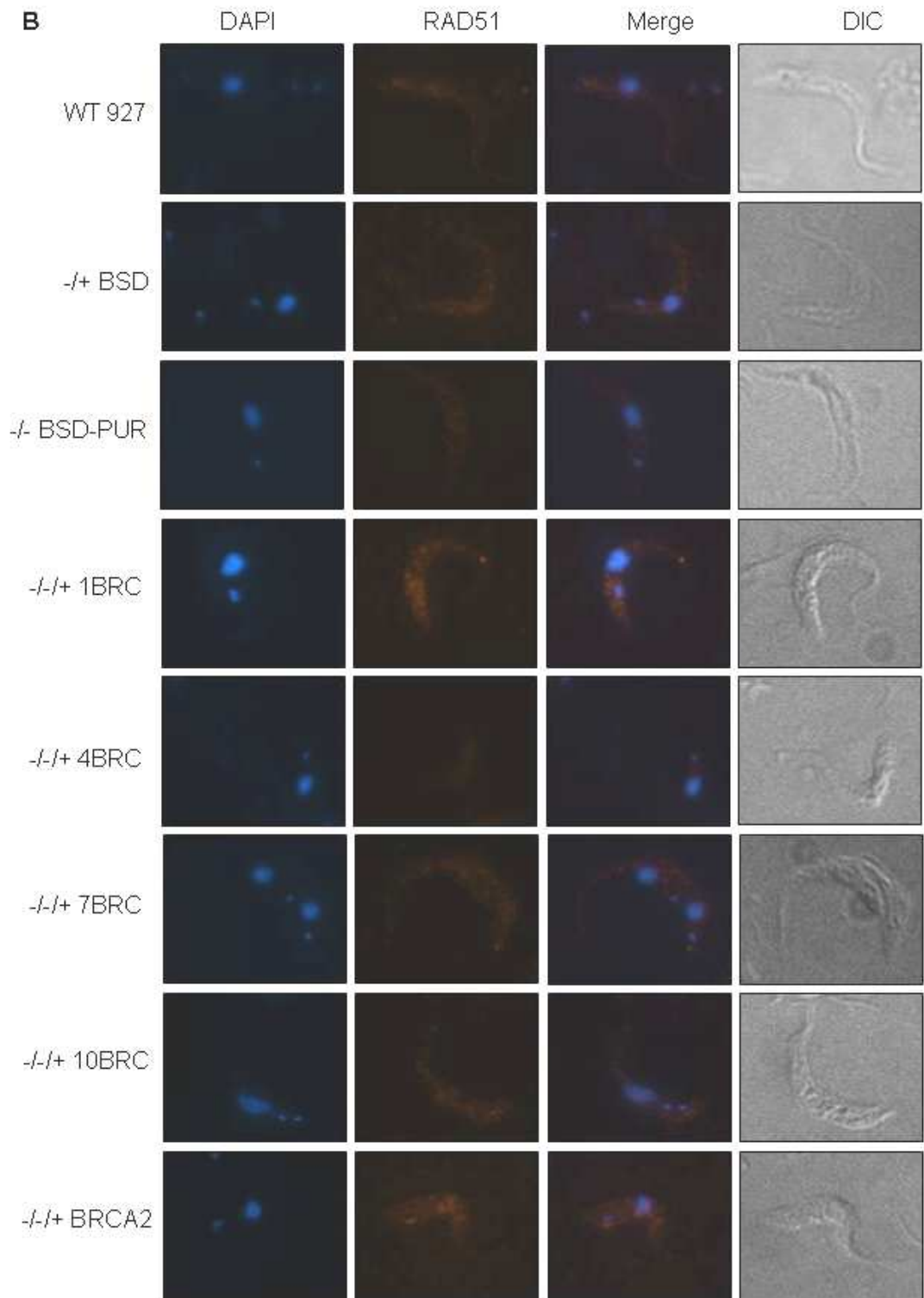


Figure 4-15B Representative images of RAD51 focus formation in PCF TREU 927 BRCA2 re-expresser cell lines.

Images of wild-type TREU 927 (WT 927), *-/+* and *-/-* BRCA2 mutant, and BRCA2 re-expresser (*-/-+*) cell lines without phleomycin treatment. Each cell is shown in differential interface contrast (DIC), after staining with DAPI (DAPI) and after hybridisation with anti-RAD51 antiserum (1:1000 dilution) and secondary hybridisation with Alexa Fluor 594 conjugated anti-rabbit antiserum (1:7000 dilution, RAD51). Merged images of DAPI and RAD51 cells are also shown (Merge).

To ensure that the observed differences in RAD51 focus formation were not due simply to a difference in the levels of RAD51 in the BRCA2 re-expresser cell lines after phleomycin treatment, western analysis was carried out. The western blot in Figure 4-16 demonstrates that the levels of RAD51 protein remain constant before and after phleomycin treatment in all cell lines.

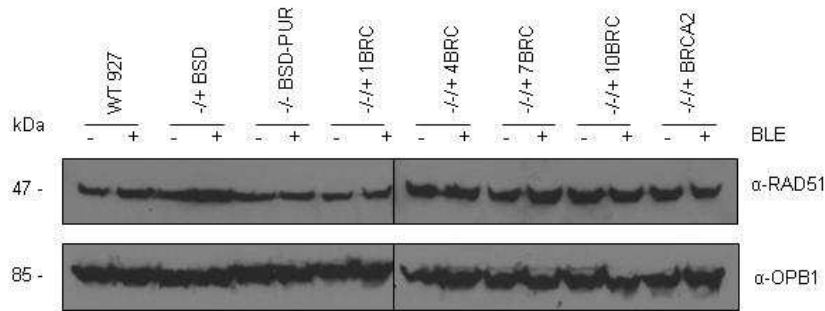


Figure 4-16 Western analysis of RAD51 in PCF TREU 927 BRCA2 re-expresser cell lines exposed to phleomycin.

Total protein extracts from wild-type TREU 927 (WT 927), *-/+* and *-/-* BRCA2 mutant, and BRCA2 re-expresser (*-/+*) cell lines were separated by SDS PAGE and western blotted before being probed with anti-RAD51 antiserum (1:500 dilution). '-' indicates protein extracts prepared without phleomycin treatment, and '+' indicates protein extracts prepared after phleomycin treatment ($1 \mu\text{g}\cdot\text{ml}^{-1}$ BLE for 18 hours). The blots were stripped and re-probed with anti-OPB1 antiserum (1:1000 dilution) as a loading control. Size markers are shown (kDa).

4.3.4 Analysis of the sub-cellular distribution of RAD51 by aqueous fractionation

A potential explanation for the above findings is that a primary function of the BRC repeats in BRCA2 is to sequester Rad51 until it is required for the repair of DNA double strand breaks, at which point it provides a means of transportation into the nucleus (Wong *et al.*, 1997; Chen *et al.*, 1998; Lord and Ashworth, 2007). In support of this, no nuclear localisation signal has been identified in *T. brucei* RAD51 to date and, in contrast to the clear subnuclear detection of RAD51 in foci following damage, the weaker signal detected by anti-RAD51 antiserum before damage appears to be distributed throughout the cell (Proudfoot and McCulloch, 2005; Hartley and McCulloch, 2008; Glover, McCulloch and Horn, 2008). In addition, BRCA2 contains three nuclear localisation signals in *T. brucei* (Figure 1-18), and evidence has been presented that BRCA2 carries out this nuclear transport of Rad51 in other organisms, as well as facilitating the loading of Rad51 onto the processed ssDNA tail and the formation of the nucleoprotein filament (Yuan *et al.*, 1999; Davies *et al.*, 2001; Venkitaraman, 2002). However, BRCA2-independent mechanisms of Rad51 transport have also been described

(Tarsounas, Davies, and West, 2003;Gildemeister, Sage, and Knight, 2009). The expansion in the number of BRC repeats in *T. brucei* could therefore be an adaptation to ensure the transport of sufficient RAD51 molecules into the nucleus and to the sites of DNA damage, perhaps to ensure general repair occurs efficiently whilst antigenic variation takes up a further requirement for RAD51 (see Chapter 3). In order to test this hypothesis, the distribution of RAD51 protein between the nucleus and the cytoplasm in the BRC variant re-expresser cell lines was analysed.

Aqueous fractionation was carried out on *T. brucei* whole cell extracts as detailed in section 2.2.5 (Zeiner, Sturm, and Campbell, 2003). Nuclear and cytoplasmic protein extracts were prepared from wild-type TREU 927, -/+ and -/- *BRCA2* mutant and *BRCA2* re-expresser (-/-/+) cell lines after phleomycin treatment ($1 \mu\text{g}.\text{ml}^{-1}$ for 18 hours), and control protein extracts without phleomycin treatment were similarly prepared. Protein extracts were separated by SDS-PAGE on 10% Bis-Tris gels before western blotting and probing sequentially with anti-RAD51 antiserum (1:500 dilution), anti-OPB1 antiserum (1:1000 dilution) and anti-NOG1 antiserum (1:5000 dilution). Blots were stripped between probings as described in section 2.11.1.

Anti-OPB1 antiserum (gift, Jeremy Mottram) was raised in sheep against *Leishmania major* recombinant oligopeptidase B and subsequently affinity-purified. Anti-NOG1 antiserum (gift, Marilyn Parsons) was raised in rabbits against *T. brucei* recombinant NOG1. OPB1 and NOG1 are proteins located in the cytoplasm and nucleolus of *T. brucei* cells, respectively, and were used to check that aqueous fractionation was successful (Park *et al.*, 2001;Munday *et al.*, 2011).

The western blots probed with NOG1 and OPB1 antiserum in Figure 4-17 demonstrate that the separation of nuclear and cytoplasmic proteins by aqueous fractionation was successful; OPB1 and NOG1 proteins were only present in the cytoplasmic and nuclear fractions, respectively. In all cell lines RAD51 was detected in both the nuclear and the cytoplasmic fractions, both before and after the induction of DNA damage. Notably, RAD51 was found in the nucleus in the *brca2*-/- cells, as also observed in mammalian cells (Orelli and Bishop, 2001;Yu *et al.*, 2003;Tarsounas, Davies, and West, 2003;Lee *et al.*,

2009;Gildemeister, Sage, and Knight, 2009). In addition, there was no strong evidence that the number of BRC repeats present in BRCA2 affects the relative amount of RAD51 in the nucleus and cytoplasm. In some cell lines there seemed to be a slight increase in the RAD51 concentration in the nucleus after the induction of DNA damage; for example, in the $-/+$ and $-/-$ BRCA2 mutants, and also the 4BRC and 7BRC re-expresser cell lines. It may be that this small increase is present in all nuclear extracts but is more easily detected in the western blots with either less total RAD51 present or a reduced X-ray film exposure time. As there was no evidence for the up-regulation of RAD51 expression after the induction of DNA damage in *T. brucei* (section 4.3.3), this increase, if real, may be due to a cellular re-distribution of RAD51. If correct, this is not inhibited by the deletion of BRCA2. The results presented in section 4.3.3 indicate that BRC repeat number is important for the ability to form RAD51 foci after DNA damage, and from these data it seems likely that this is a reflection of subnuclear dynamics, and not transport into the nucleus.

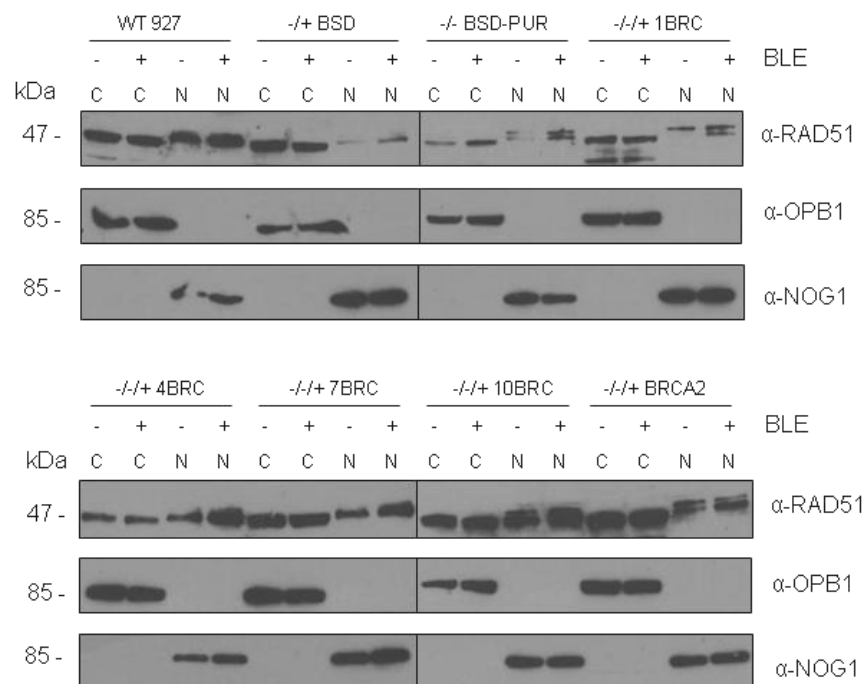


Figure 4-17 Aqueous fractionation of PCF TREU 927 BRCA2 re-expresser cell lines exposed to phleomycin.

Aqueous fractionation was performed to generate protein fractions enriched in soluble cytoplasmic proteins (C) and soluble nuclear proteins (N). Fractions were prepared from wild-type TREU 927 (WT 927), $-/+$ and $-/-$ BRCA2 mutant, and BRCA2 re-expresser ($-/+$) cell lines. '-' indicates fractions prepared without phleomycin treatment and '+' indicates fractions prepared after phleomycin treatment ($1 \mu\text{g}\cdot\text{ml}^{-1}$ BLE for 18 hours). Fractions were separated by SDS PAGE and western blotted before being sequentially probed, stripped and re-probed with anti-RAD51 antiserum (1:500 dilution), anti-OPB1 antiserum (1:1000 dilution) and anti-NOG1 antiserum (1:5000 dilution). Size markers are indicated (kDa).

4.4 Complementation of PCF Lister 427 *brca2*^{-/-} mutants with variants of *BRCA2* with reduced numbers of BRC repeats

4.4.1 Generation of re-expresser cell lines in PCF Lister 427

Given the potential differences in VSG archive size between Lister 427 and TREU 927 *T. brucei* strains, and the availability of PCF Lister 427 *brca2*^{-/-} mutants, the same strategy used to re-express the *BRC* variants described for TREU 927 (section 4.2) was adopted here with PCF Lister 427. To do this, PCF Lister 427 *brca2*^{-/-} *BSD-PUR* mutant cells were transformed with each of the *pRM482::BRC* re-expresser constructs (section 4.2.1) and antibiotic resistant transformants were selected by placing cells on SDM-79 media supplemented with 20 µg.ml⁻¹ G418. The generation of *BRCA2* re-expresser cell lines was initially confirmed by PCR performed on genomic DNA extracted from putative re-expresser clones resulting from the five transformations, as described in section 4.2.3. The agarose gel in Figure 4-18 demonstrates that the *BSD* resistance ORF was detected in the *1BRC*, *4BRC*, *10BRC* and full-length *BRCA2* putative re-expresser cell lines, while the *7BRC* cell line appeared to have lost the *BSD* resistance ORF by an unknown mechanism. The *PUR* resistance ORF was present in all of the putative re-expresser cell lines, and all five clones produced a PCR product with the *BRCA2* ORF primers, suggesting correct integration of the re-expression constructs. The five re-expresser cell lines are referred to as; *-/-/+ 1BRC*, *-/-/+ 4BRC*, *-/-/+ 7BRC*, *-/-/+ 10BRC* and *-/-/+ BRCA2*.

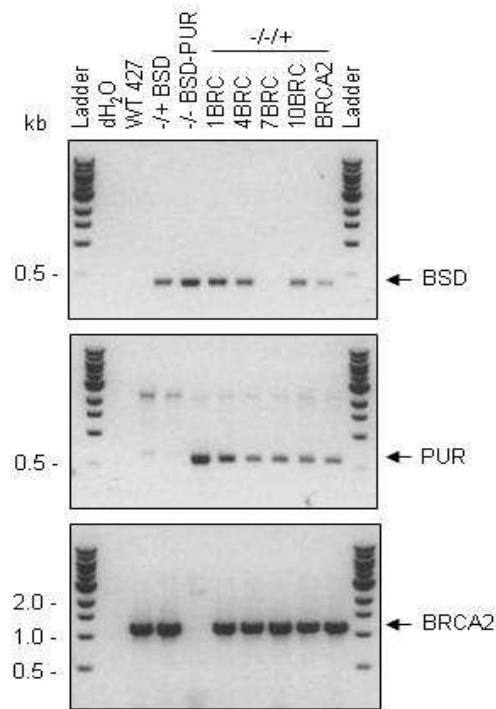


Figure 4-18 Confirmation of PCF Lister 427 *BRCA2* re-expresser cell lines by PCR. An agarose gel of the PCR products obtained using the primers, described in Figure 4-4A, and genomic DNA extracted from wild-type Lister 427 (WT 427), $-/+$ and $-/-$ *BRCA2* mutant, and putative *BRCA2* re-expresser ($-/-/+$) cell lines. Distilled water (dH_2O) was used as a negative control. The PCR products produced from the *BSD*, *PUR* and *BRCA2* ORFs are indicated (black arrows), and size markers are shown (Ladder, kb).

To confirm the generation of re-expresser cell lines, Southern analysis was performed as described in section 4.2.4. The Southern blot in Figure 4-19 demonstrates that the five re-expresser cell lines all contained a *BRCA2* DNA fragment of the expected size for the *pRM482::BRC* constructs correctly integrated into the *tubulin* array. The *7BRC* re-expresser line also displayed a DNA fragment corresponding in size to the larger wild-type allele of *BRCA2* (the alleles are of distinct sizes in this strain; section 3.5.3; Hartley and McCulloch, 2008). The reason for this is not known, but it shows that this clone is not equivalent in genetic composition to the other *BRC* variants, and the results from this cell line will be included from here on for illustrative purposes only.

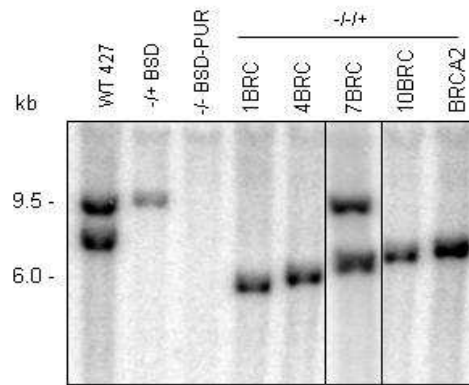


Figure 4-19 Confirmation of PCF Lister 427 *BRCA2* re-expresser cell lines by Southern analysis.

5 μ g of genomic DNA extracted from wild-type Lister 427 (WT 427), *-/+* and *-/-* *BRCA2* mutant, and *BRCA2* re-expresser (*-/-/+*) cell lines was digested with *HindIII* before being separated by electrophoresis on an agarose gel. The DNA was Southern blotted before being hybridised with a DNA probe against 1.2 kb of the *BRCA2* ORF. Restriction maps showing the expected products are displayed in Figure 4-5A, and size markers are shown (kb).

4.4.2 Analysis of *BRCA2* mRNA levels in re-expresser cell lines by quantitative RT-PCR

As the expression of the *BRCA2* variants cannot be confirmed by western analysis, the mRNA levels of the genes were analysed by quantitative RT-PCR as described in section 4.2.6. The agarose gel in Figure 4-20 shows the PCR products produced using primers specific for part of a control gene, *DNA polymerase I (Poli)*, used to demonstrate that cDNA has been amplified successfully in all the RT plus samples, and that genomic DNA contamination is absent from all the RT minus samples. The data in Figure 4-21 demonstrate that the *BRCA2*-*+/+* mutant cell lines have a ~ 50% reduced level of *BRCA2* mRNA when compared to wild-type levels, and four of the five re-expresser cell lines (*-/-/+ 1BRC*, *4BRC*, *10BRC* and *BRCA2*) have varying levels of *BRCA2* mRNA (from a ~ 10 - 40% reduced level compared to wild-type levels), but showed a consistent trend suggestive of a single copy gene. In contrast, the *7BRC* re-expresser cell line displayed a ~ 40% increased level in *BRCA2* mRNA when compared to wild-type levels. This is consistent with the presence of more than one *BRCA2* gene and confirms the suspicion that a wild-type *BRCA2* allele is still present in this cell line.

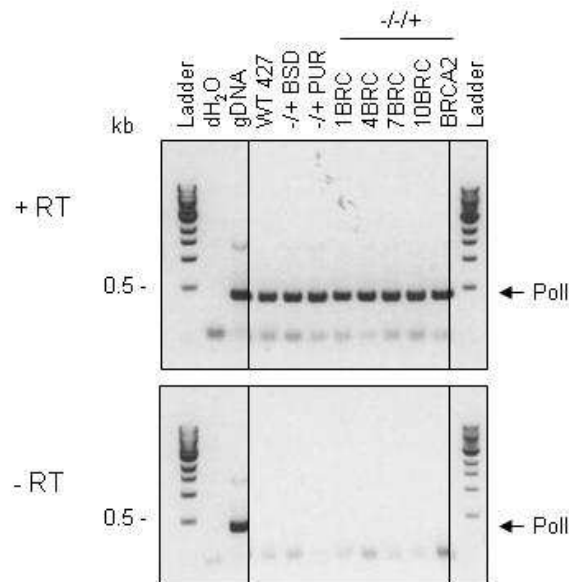


Figure 4-20 Testing PCF Lister 427 *BRCA2* re-expresser RT-PCR reaction products by PCR. An agarose gel of the PCR products generated using primers specific to *DNA polymerase I* (*Poll*), amplified from cDNA generated by RT-PCR reactions containing reverse transcriptase (top, + RT). Control reactions were also analysed, lacking reverse transcriptase (bottom, - RT). Distilled water (dH₂O) was used as a negative control and a genomic DNA sample (gDNA) as a positive control. Size markers are shown (Ladder, kb).

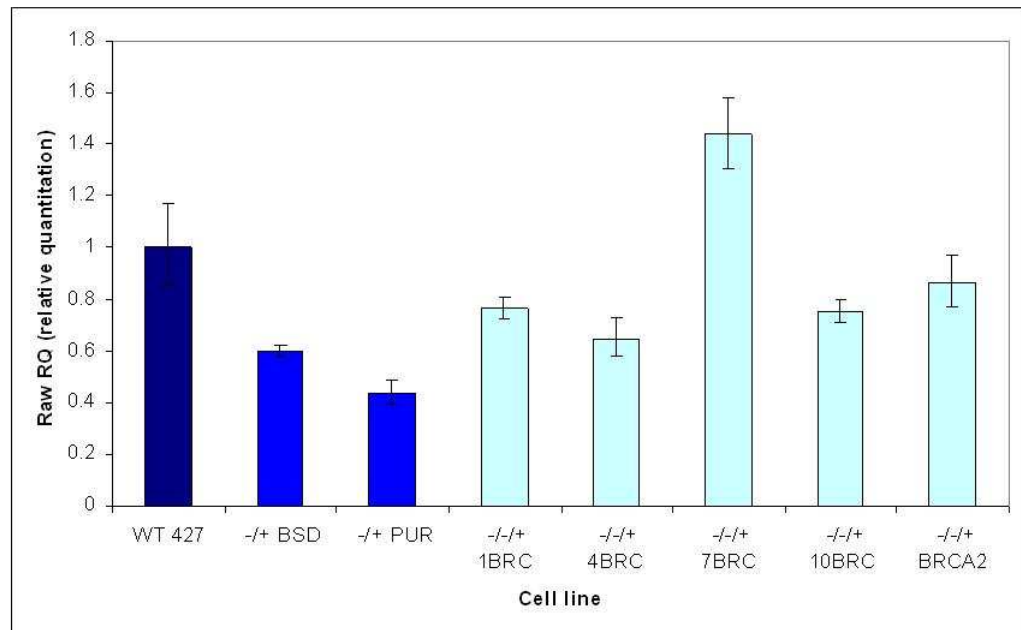


Figure 4-21 Quantitative RT-PCR analysis of the PCF Lister 427 *BRCA2* re-expresser cell lines.

Quantitative RT-PCR was carried out on cDNA generated from wild-type Lister 427 (WT 427), *BRCA2* $-/+$ mutant (*BSD* or *PUR*), and *BRCA2* re-expresser ($-/+$) cell lines using primers specific for an endogenous control, *tubulin*, and *BRCA2*. All samples were normalised to the *tubulin* endogenous control and the level for *BRCA2* expressed relative to the WT 427 sample (which was set as one); values are the average quantification from four repetitions and vertical lines indicate standard deviation.

4.5 Phenotypic analysis of PCF Lister 427 BRCA2 re-expresser cell lines

The *in vitro* growth of the PCF Lister 427 BRCA2 re-expresser cell lines was first analysed. These data are plotted in Figure 4-22, and extrapolated doubling times are displayed in Table 4-4. As seen previously, re-expression of *BRCA2* with 1, 4 or 10 BRC repeats, or full-length *BRCA2*, restored the growth of the *brca2*^{-/-} mutant cell line to essentially wild-type levels, with doubling times of ~ 10.5 hours for the re-expresser cell lines, ~ 11 hours for wild-type cells, and ~13 hours for the *brca2*^{-/-} cells. The 7BRC re-expresser displays an increased doubling time of ~ 9.6 hours, which is faster than that observed for wild-type cells.

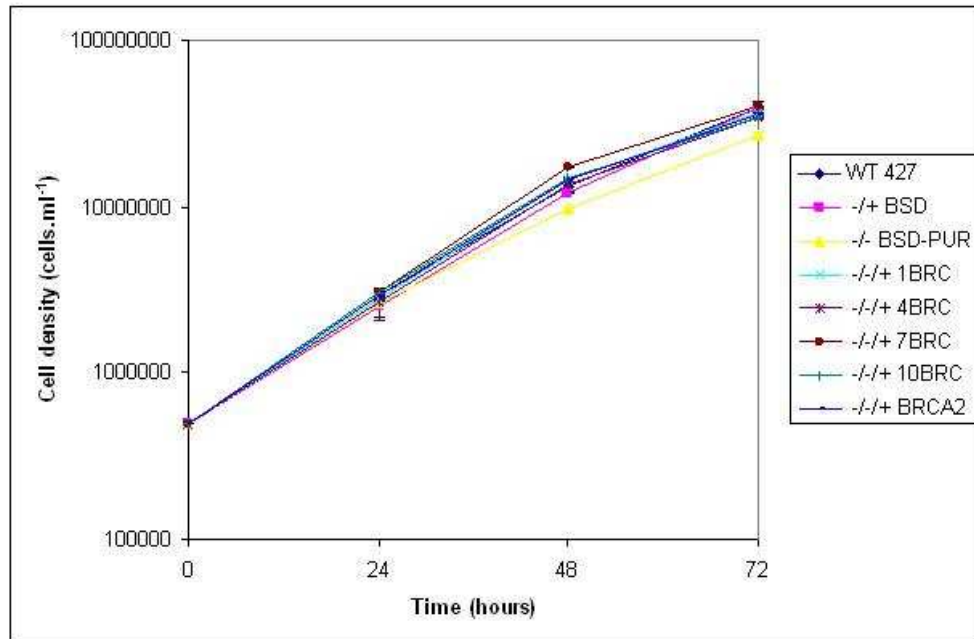


Figure 4-22 Analysis of *in vitro* growth of the PCF Lister 427 BRCA2 re-expresser cell lines. 2 ml cultures of wild-type Lister 427 (WT 427), *-/+* and *-/-* *BRCA2* mutant, and *BRCA2* re-expresser (*-/-+*) cell lines were inoculated at 5×10^5 cells.ml⁻¹ and cell densities counted 24, 48, and 72 hours subsequently are shown. Values are averaged from the counts from three experimental repetitions, and vertical lines indicate standard deviation.

Cell line	Doubling time (hours)
WT 427	11.19
-/+ BSD	10.50
-/- BSD-PUR	12.77
-/-+ 1BRC	10.22
-/-+ 4BRC	10.27
-/-+ 7BRC	9.65
-/-+ 10BRC	10.68
-/-+ BRCA2	10.45

Table 4-4 *In vitro* population doubling times of PCF Lister 427 BRCA2 re-expresser cell lines.

The mean doubling time for wild-type Lister 427 (WT 427), -/+ and -/- BRCA2 mutant, and BRCA2 re-expresser (-/-+) cell lines is displayed, in hours, from data displayed in Figure 4-22.

To measure sensitivity of these cell lines to DNA damage, the Alamar blue assay was set up with wild-type Lister 427, -/+ and -/- BRCA2 mutant, and BRCA2 re-expresser (-/-+) cell lines. Survival curves displayed in Figure 4-23 and Figure 4-24 are representative of the two repetitions performed, and show again that *brca2*-/- cell lines display reduced survival in the presence of both MMS and phleomycin, when compared to the wild-type and BRCA2-/+ cell lines. All the re-expresser cell lines displayed increased survival in the presence of both compounds, to levels above that of wild-type cells, and to essentially equivalent amounts. This is similar to that observed previously for TREU 927 PCF cells (section 4.3.2), but appears more marked in the Lister 427 PCF cells. The extrapolated EC50 values for MMS in Figure 4-25 is consistent with this: re-expression of BRCA2 with 1, 4, 7 or 10 BRC repeats or full-length BRCA2 restores the sensitivity to MMS observed in the *brca2*-/- cell line to values slightly above wild-type levels (10 - 20% increased). However, these data did not display statistical significance (Table 4-5). The EC50 data for phleomycin sensitivity, Figure 4-26, displays a more pronounced increase in survival, with EC50 values between 25% and 100% increased relative to wild-type cells. However, these were not seen as statistically significant differences (Table 4-5) between the wild-type cells and the 1BRC, 4BRC, 7BRC and full-length BRCA2 re-expresser cell lines ($p > 0.05$), though it was for the 10BRC re-expresser cell line ($p \leq 0.05$). Overall, the behaviour of the Lister 427 PCF cells is very comparable with the TREU 927 PCF cells, with the number of BRC repeats in the BRCA2 variants being indistinguishable in terms of their ability to support survival after DNA

damage, and even 1 BRC repeat being capable of reverting the small sensitivity of the *brca2*^{-/-} mutants. Given this, RAD51 foci formation was not examined.

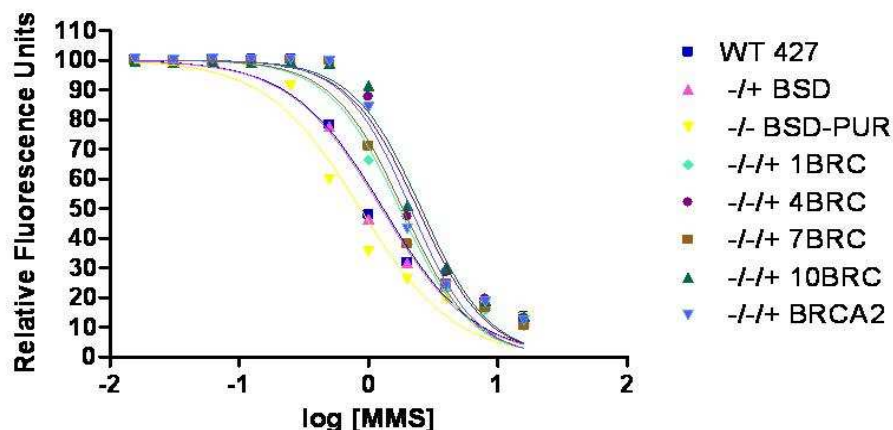


Figure 4-23 A representative survival curve for PCF Lister 427 BRCA2 re-expresser cell lines exposed to MMS.

The extent of fluorescence for each cell line (WT, *-/+*, *-/-* and *-/-+*) obtained using the Alamar blue assay is plotted against the log of MMS concentrations. Nonlinear regression was performed and fitted curves are shown for each cell line.

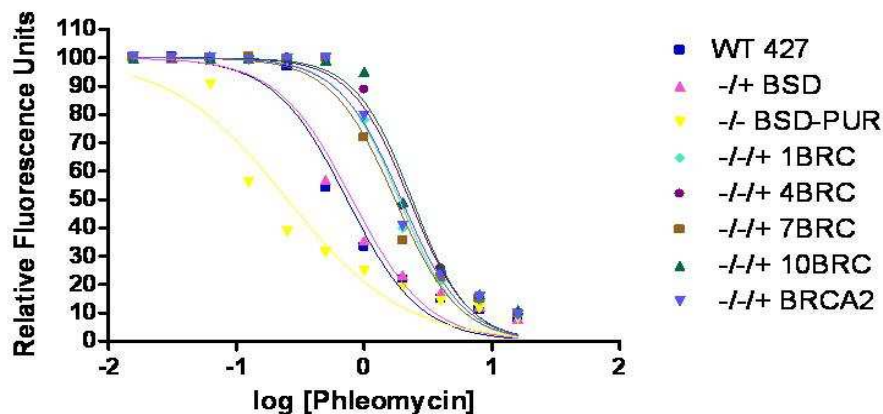


Figure 4-24 A representative survival curve for PCF Lister 427 BRCA2 re-expresser cell lines exposed to phleomycin.

The extent of fluorescence for each cell line (WT, *-/+*, *-/-* and *-/-+*) obtained using the Alamar blue assay is plotted against the log of phleomycin concentrations. Nonlinear regression was performed and fitted curves are shown for each cell line.

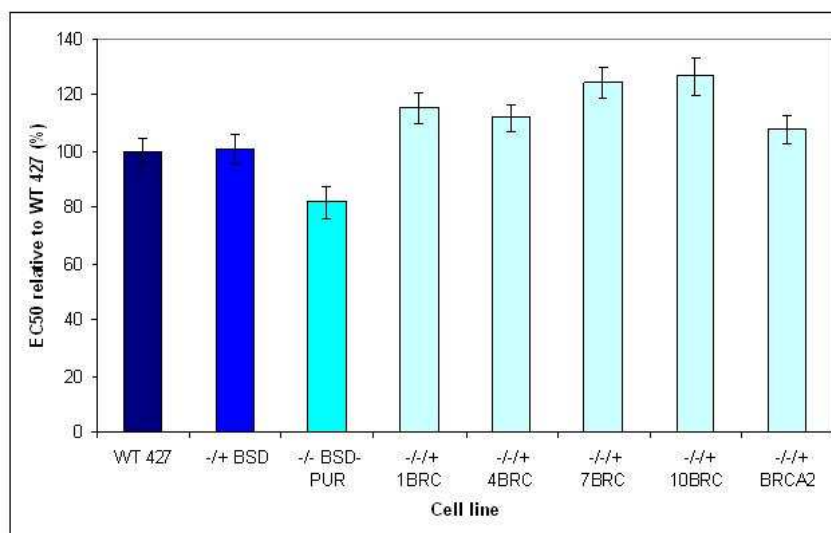


Figure 4-25 EC50 values of PCF Lister 427 BRCA2 re-expresser cell lines exposed to MMS. Wild-type Lister 427 (WT 427), *-/+* and *-/-* BRCA2 mutant, and BRCA2 re-expresser (*-/-+*) cell lines were placed in serially decreasing amounts of MMS and allowed to grow for 48 hours, before the addition of Alamar Blue. After a further 24 hours the reduction of Alamar Blue was measured by the amount of fluorescent resorufin generated. EC50 values are the mean from two experimental repetitions expressed as a percentage relative to wild-type and bars indicate 95% confidence intervals.

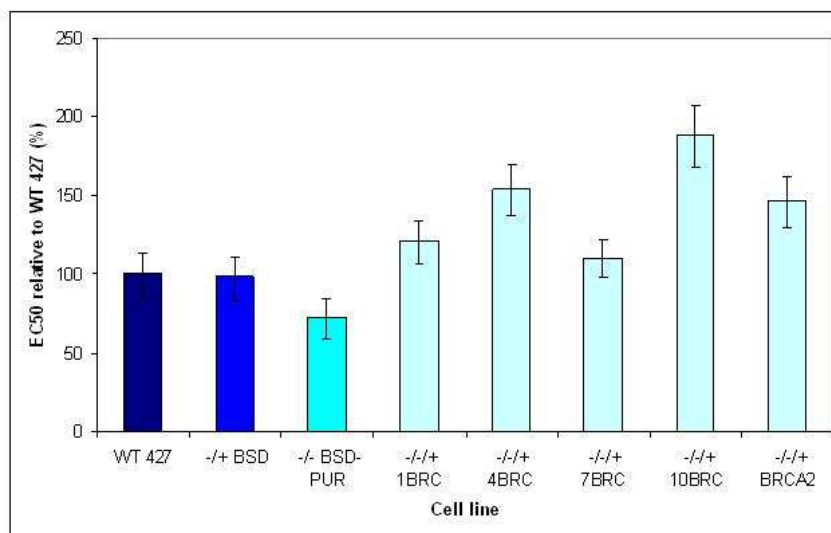


Figure 4-26 EC50 values of PCF Lister 427 BRCA2 re-expresser cell lines exposed to phleomycin. Wild-type Lister 427 (WT 427), *-/+* and *-/-* BRCA2 mutant, and BRCA2 re-expresser (*-/-+*) cell lines were placed in serially decreasing amounts of phleomycin and allowed to grow for 48 hours, before the addition of Alamar Blue. After a further 24 hours the reduction of Alamar Blue was measured by the amount of fluorescent resorufin generated. EC50 values are the mean from two experimental repetitions expressed as a percentage relative to wild-type and bars indicate 95% confidence intervals.

A

	-/+ BSD	-/- BSD-PUR	-/-/+ 1BRC	-/-/+ 4BRC	-/-/+ 7BRC	-/-/+ 10BRC	-/-/+ BRCA2
WT 427	0.8640	0.4427	0.6947	0.7758	0.5796	0.6806	0.8483
-/+ BSD		0.5040	0.7410	0.8131	0.6283	0.7107	0.8804
-/- BSD-PUR			0.2654	0.3393	0.2323	0.4091	0.3661
-/-/+ 1BRC				0.4359	0.0923	0.6586	0.1439
-/-/+ 4BRC					0.0834	0.5238	0.1527
-/-/+ 7BRC						0.9139	0.0209
-/-/+ 10BRC							0.4616

B

	-/+ BSD	-/- BSD-PUR	-/-/+ 1BRC	-/-/+ 4BRC	-/-/+ 7BRC	-/-/+ 10BRC	-/-/+ BRCA2
WT 427	0.0000	0.0000	0.2887	0.2075	0.7245	0.0264	0.1448
-/+ BSD		0.0000	0.2676	0.2009	0.6825	0.0258	0.1394
-/- BSD-PUR			0.1319	0.1400	0.3438	0.0201	0.0918
-/-/+ 1BRC				0.1518	0.5645	0.1290	0.0141
-/-/+ 4BRC					0.0686	0.3592	0.5032
-/-/+ 7BRC						0.2093	0.2072
-/-/+ 10BRC							0.2110

Table 4-5 Statistical analysis of Alamar Blue results.

P values are shown for student's T-tests comparing the mean EC50 values of wild-type Lister 427 (WT 427), +/- and -/- BRCA2 mutant, and BRCA2 re-expresser (-/-/+) cell lines grown in the presence of MMS (A) or phleomycin (B). Areas shaded in yellow indicate a significant difference ($P \leq 0.05$). No correction has been made for simultaneous multiple comparisons.

4.6 Complementation of BSF Lister 427 *brca2*-/- mutants with variants of *BRCA2* with reduced numbers of BRC repeats

4.6.1 Generation of re-expresser cell lines in BSF Lister 427

In Chapter 3, it was demonstrated that mutation of *BRCA2* appeared to have more profound consequences in BSF than in PCF cells, with visible chromosome rearrangements and more severe sensitivity to DNA damaging agents. To see if this may be a consequence of the *BRCA2* BRC repeat expansion being a selection for a BSF-specific process, the BRC variants were functionally examined in Lister 427 BSF *T. brucei* cells. As before (section 4.2), transformations were carried out in order to generate re-expresser cell lines in BSF Lister 427 *brca2*-/- cells (generated previously; *brca2*-/-1; Hartley and McCulloch, 2008) containing variants of *BRCA2* with 1, 4, 7 and 10 BRC repeats using the *pRM482::BRC* re-expresser constructs (section 4.2.1). Antibiotic resistant transformants were selected by placing cells on HMI-9 media supplemented with 2.5 $\mu\text{g.ml}^{-1}$ G418. The full-length *BRCA2* re-expresser BSF Lister 427 cell line generated previously (Hartley and McCulloch, 2008) was recovered from frozen storage.

4.6.2 Confirmation of re-expresser cell lines by PCR

PCR was performed on genomic DNA extracted from putative *BRCA2* re-expresser clones resulting from the four transformations, and also the full-length *BRCA2* re-expresser cell line, using primers specific to the *BSD*, *PUR* and *BRCA2* ORFs as described in section 4.2.3. The agarose gel in Figure 4-27 shows that the *BSD* and *PUR* resistance ORFs are present in all of the putative re-expresser cell lines, and that all five clones analysed here produced a PCR product with the primers specific to part of the *BRCA2* ORF. The cell lines are referred to as; *-/-/+ 1BRC*, *-/-/+ 4BRC*, *-/-/+ 7BRC*, *-/-/+ 10BRC* and *-/-/+ BRCA2*.

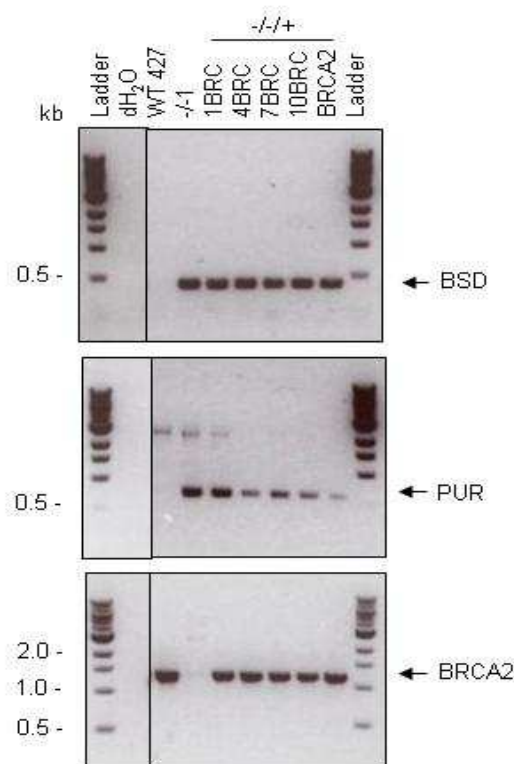


Figure 4-27 Confirmation of BSF Lister 427 *BRCA2* re-expresser cell lines by PCR. An agarose gel of the PCR products obtained using the primers, described in Figure 4-4A, and genomic DNA extracted from wild-type Lister 427 (WT 427), *brca2*^{-/-} mutant, and putative *BRCA2* re-expresser (*-/-/+*) cell lines. Distilled water (dH₂O) was used as a negative control. The PCR products produced from the *BSD*, *PUR* and *BRCA2* ORFs are indicated (black arrows), and size markers are shown (Ladder, kb).

4.6.3 Confirmation of re-expresser cell lines by Southern analysis

Southern analysis was next performed, as described in section 4.2.4, to check integration of the *pRM482::BRC* constructs. The Southern blot in Figure 4-28 demonstrates that the *BRCA2* ORF is present in two allelic size variants in wild-

type Lister 427 cells, as was seen for the PCF cells of this strain (section 3.5.3), and the *brca2*^{-/-} mutant cell line no longer possesses a *BRCA2* ORF, as previously observed (Hartley and McCulloch, 2008). The four re-expresser cell lines analysed here demonstrate a DNA fragment of the expected size for their BRC repeat variant *BRCA2* ORF, which indicates the constructs had integrated correctly into the *tubulin* array. The full-length *BRCA2* re-expresser cell line, which was generated previously and independently verified (Hartley and McCulloch, 2008), demonstrated a DNA fragment that was slightly smaller than expected, although this could be explained by irregularities in the electrophoresis separation of the genomic DNA due the presence of a large amount of DNA.

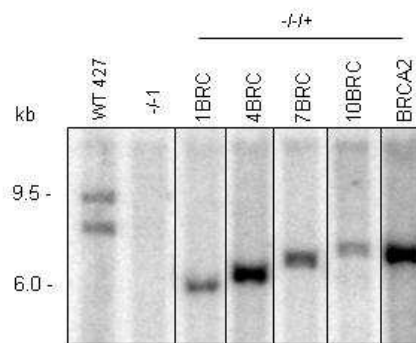


Figure 4-28 Confirmation of BSF Lister 427 *BRCA2* re-expresser cell lines by Southern analysis.

5 μ g of genomic DNA extracted from wild-type Lister 427 (WT 427), *brca2*^{-/-} mutant, and *BRCA2* re-expresser (-/-+) cell lines was digested with *Hind*III before being separated by electrophoresis on an agarose gel. The DNA was Southern blotted before being hybridised with a DNA probe against 1.2 kb of the *BRCA2* ORF. Restriction maps showing the expected fragment sizes are displayed in Figure 4-5A, and size markers are shown (kb).

4.6.4 Attempt at confirmation of re-expresser cell lines by western analysis

Multiple attempts were made at confirmation of the re-expression of the variants of *BRCA2* in the BSF Lister 427 *brca2*^{-/-} cells by western blot using anti-*BRCA2* antiserum, as before (section 4.2.5). The western blot in Figure 4-29 is the clearest of these experiments and demonstrates the presence of two faint bands at approximately the expected size for the *BRCA2* protein (176 kDa) in all cell lines, including the *brca2*^{-/-} mutant cell line, suggesting that it is not *BRCA2* but results from non-specific binding of the antiserum to other parasite proteins, such as also seen at ~ 58 kDa.

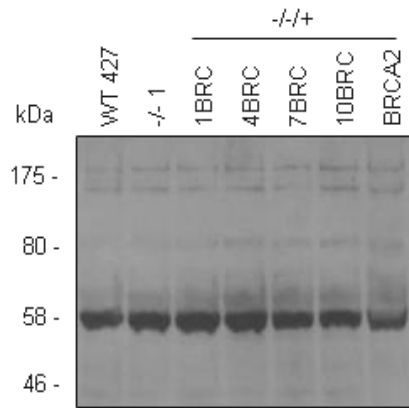


Figure 4-29 Attempt at confirmation of BSF Lister 427 BRCA2 re-expresser cell lines by western analysis.

Total protein extracts from wild-type Lister 427 (WT 427), *brca2*^{-/-} mutant, and BRCA2 re-expresser (-/-+) cell lines were separated by SDS-PAGE and western blotted before being probed with anti-BRCA2 antiserum (1:200 dilution). Size markers are shown (kDa).

4.6.5 Analysis of *BRCA2* mRNA levels in re-expresser cell lines by quantitative RT-PCR

As the western analysis was unsuccessful, *BRCA2* mRNA levels in the re-expresser cell lines were analysed by quantitative RT-PCR as described in section 4.2.6. The agarose gel in Figure 4-30 shows the PCR products produced using primers specific for part of a control gene, *DNA polymerase I (Poli)*, used to demonstrate that cDNA could be PCR-amplified successfully in all the RT plus samples, and that genomic DNA contamination was absent from all the RT minus samples. The qRT-PCR data in Figure 4-31 demonstrate greater variation of *BRCA2* mRNA levels in the five BSF re-expresser cell lines than was seen for either of the PCF analyses (sections 4.2.6 and 4.4.2). The -/-/+ 1BRC, 4BRC, 7BRC and 10BRC cell lines each displayed ~ 10 - 30% reduced levels compared with wild-type cells, which could be consistent with a lower copy number of the gene, but in all cases the level appeared higher than seen in PCF re-expresser cell lines, which was closer to 50% of wild-type (Figure 4-8 and Figure 4-21). Unusually, the full-length *BRCA2* re-expresser cell line displayed a ~ 20% increased level of *BRCA2* mRNA compared to wild-type cells, which could be more consistent with the presence of two copies of the *BRCA2* gene, which we cannot evaluate from the Southern data available. The reason for this increase is therefore not known, and nor is the reason for the increased *BRCA2* mRNA variation in BSF cells.

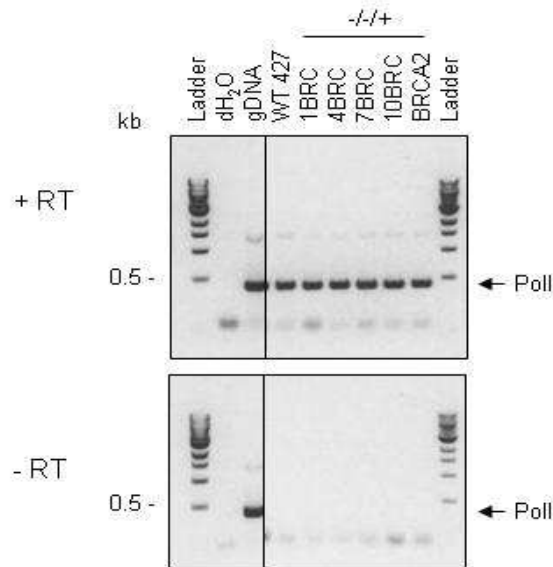


Figure 4-30 Testing BSF Lister 427 *BRCA2* re-expresser RT-PCR reaction products by PCR. An agarose gel of the PCR products generated using primers specific to *DNA polymerase I* (*Poll*), amplified from cDNA generated by RT-PCR reactions containing reverse transcriptase (top, + RT). Control reactions were also analysed, lacking reverse transcriptase (bottom, - RT). Distilled water (dH₂O) was used as a negative control and a genomic DNA sample (gDNA) as a positive control. Size markers are shown (Ladder, kb).

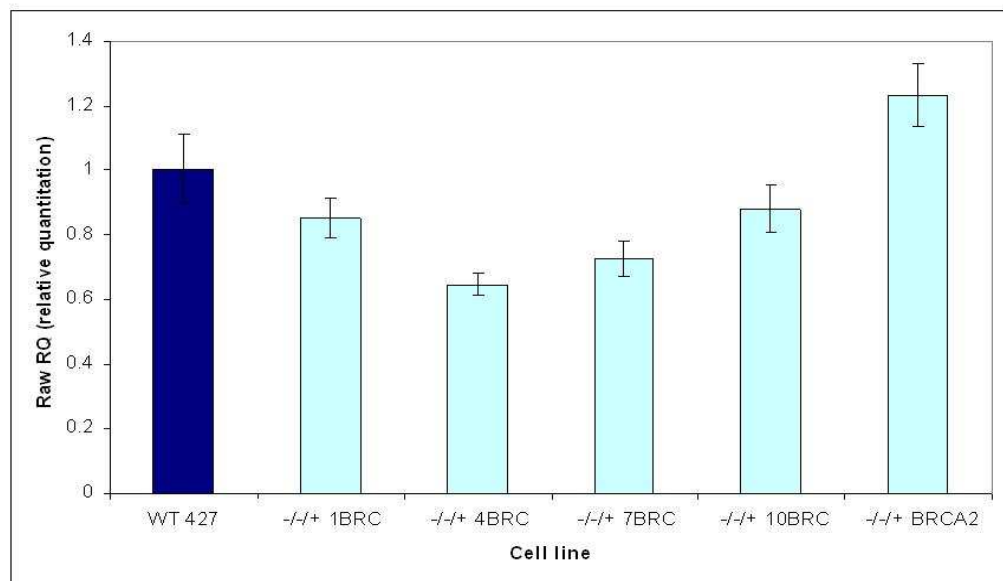


Figure 4-31 Quantitative RT-PCR analysis of the BSF Lister 427 *BRCA2* re-expresser cell lines.

Quantitative RT-PCR was carried out on cDNA generated from wild-type Lister 427 (WT 427) and *BRCA2* re-expresser (-/-+) cell lines using primers specific for an endogenous control, *tubulin*, and *BRCA2*. All samples were normalised to the *tubulin* endogenous control and the level for *BRCA2* expressed relative to the WT 427 sample (which was set as one); values are the average quantification from four repetitions and vertical lines indicate standard deviation.

4.7 Phenotypic analysis of BSF Lister 427 BRCA2 re-expresser cell lines

4.7.1 Analysis of *in vitro* growth

The *in vitro* growth of the BSF Lister 427 BRCA2 re-expresser cell lines was analysed, the results of which are plotted in Figure 4-32 and extrapolated doubling times displayed in Table 4-6. As described previously (Claire Hartley, PhD thesis, 2008), the BSF *brca2*^{-/-} mutants displayed substantial growth impairment relative to wild-type cells. Figure 4-32 clearly shows that the re-expression of *BRCA2* with 1, 4, 7 or 10 BRC repeats, or full-length *BRCA2*, restored the impaired growth of the *brca2*^{-/-} mutant cell line to levels above that observed for wild-type cells. The calculated doubling times were less clear with the values obtained for the re-expresser cell lines varying between ~ 11 to ~ 14.5 hours compared to the wild-type doubling time of ~ 10.5 hours, while *brca2*^{-/-} cells doubled in ~ 12.6 hrs. The reliability of these data could have been improved by measuring growth over a longer timescale using linear regression.

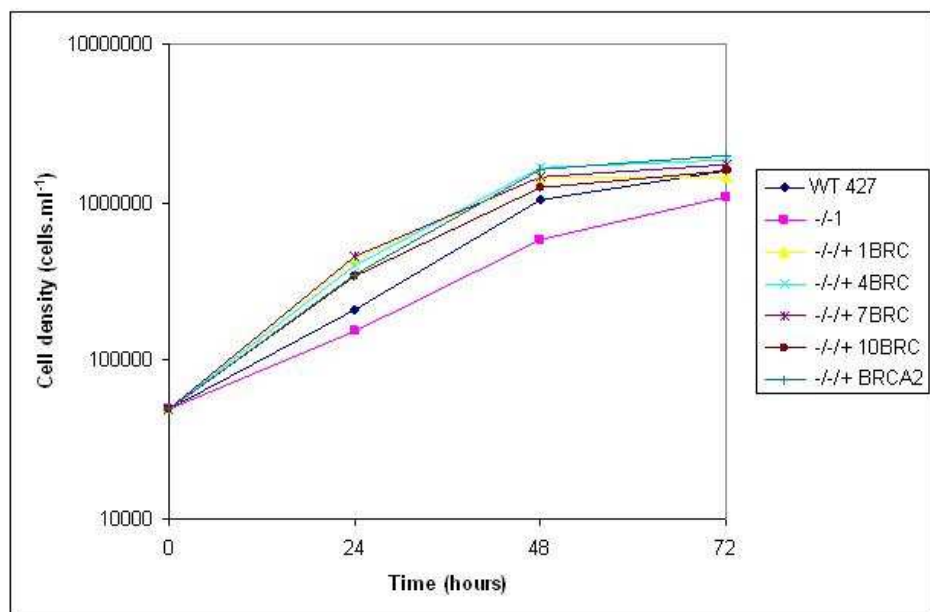


Figure 4-32 Analysis of *in vitro* growth of the BSF Lister 427 BRCA2 re-expresser cell lines. 2 ml cultures of wild-type Lister 427 (WT 427), *brca2*^{-/-} mutant, and BRCA2 re-expresser (-/-+) cell lines were inoculated at 5×10^4 cells.ml⁻¹ and cell densities counted 24, 48, and 72 hours subsequently are shown. Values are averaged from three experimental repetitions and vertical lines indicate standard deviation.

Cell line	Doubling time (hours)
WT 427	10.49
-/-1	12.64
-/-+ 1BRC	14.09
-/-+ 4BRC	11.79
-/-+ 7BRC	14.41
-/-+ 10BRC	13.05
-/-+ BRCA2	11.07

Table 4-6 *In vitro* population doubling times for BSF Lister 427 BRCA2 re-expresser cell lines.

The mean doubling time for wild-type Lister 427 (WT 427), *brca2*^{-/-} mutant, and BRCA2 re-expresser (-/-+) cell lines is displayed, in hours, and was calculated from the data displayed in Figure 4-32.

4.7.2 Analysis of DNA damage sensitivity

The Alamar blue assay was set up with wild-type Lister 427, *brca2*^{-/-} mutant and BRCA2 re-expresser (-/-+) cell lines. As before, the extent of fluorescence for each cell line was plotted graphically over the range of MMS and phleomycin concentrations (for representative examples see Figure 4-33 and Figure 4-34), and average EC50s (plus 95% confidence intervals) calculated from the three experimental repetitions were plotted relative to the wild-type EC50, which was taken as 100% (Figure 4-35 and Figure 4-36). From the survival curves, it was clear that BSF *brca2*^{-/-} mutants were significantly more sensitive to both DNA damaging agents, and this was confirmed by analysing the data with student's T-tests; displayed in Table 4-7. The re-expression of *BRCA2* with 1BRC repeat produced a cell line that alleviated some of the decreased survival observed in the *brca2*^{-/-} mutant cell line, but was still more sensitive than wild-type cells to both compounds. In contrast, the re-expression of *BRCA2* with 4, 7, or 10 BRC repeats, or re-expression of full-length *BRCA2*, restored survival of the *brca2*^{-/-} mutants to essentially wild-type levels. The extrapolated EC50 values displayed in Figure 4-35 and Figure 4-36 confirm these findings. The -/-+1BRC cell line displayed a 30% and 40% reduction in survival relative to wild-type cells for MMS and phleomycin, respectively, compared with a 70% and 80% reduction in survival for the *brca2*^{-/-} mutants. Furthermore, this increased sensitivity of the -/-+1BRC cells relative to wild-type cells was found to be statistically significant in both cases ($p \leq 0.05$, Table 4-7). The 4, 7 and 10 BRC repeat and full-length re-expresser cell lines displayed EC50 values essentially indistinguishable from the wild-type EC50, and no statistically significant differences were observed ($p > 0.05$).

Taken together, these data reveal a difference between BRCA2 function in BSF and PCF *T. brucei* cells. In both life cycle stages, reducing the number of BRC repeats in BRCA2 from 12-15 to 4, 7, 10 did not have any effect on sensitivity to DNA damaging agents. In contrast, whereas expression of a *BRCA2* variant with 1 BRC repeat (the divergent, C-terminal repeat) has no effect on DNA damage sensitivity in PCF cells, it displays significantly increased sensitivity in BSF cells.

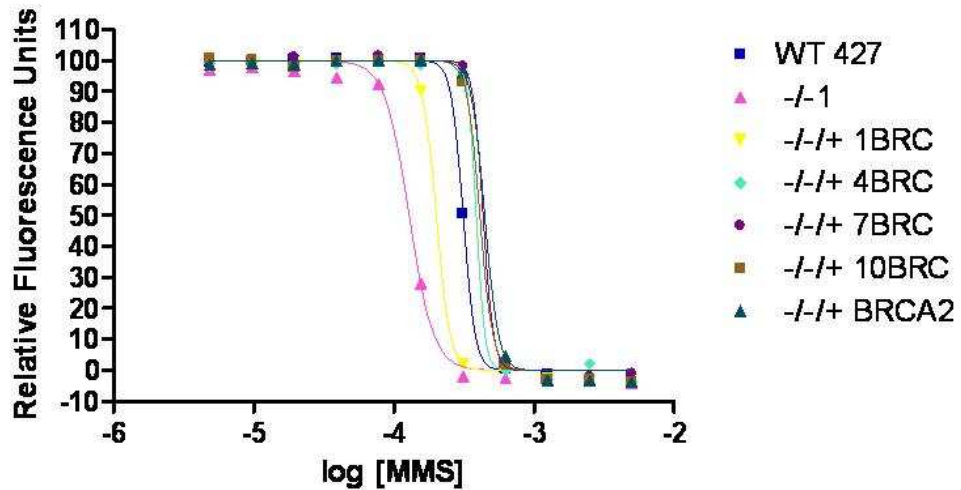


Figure 4-33 A representative survival curve for BSF Lister 427 BRCA2 re-expresser cell lines exposed to MMS.

The extent of fluorescence for each cell line (WT, *-/-* and *-/-+*) obtained using the Alamar blue assay is plotted against the log of MMS concentrations. Nonlinear regression was performed and fitted curves are shown for each cell line.

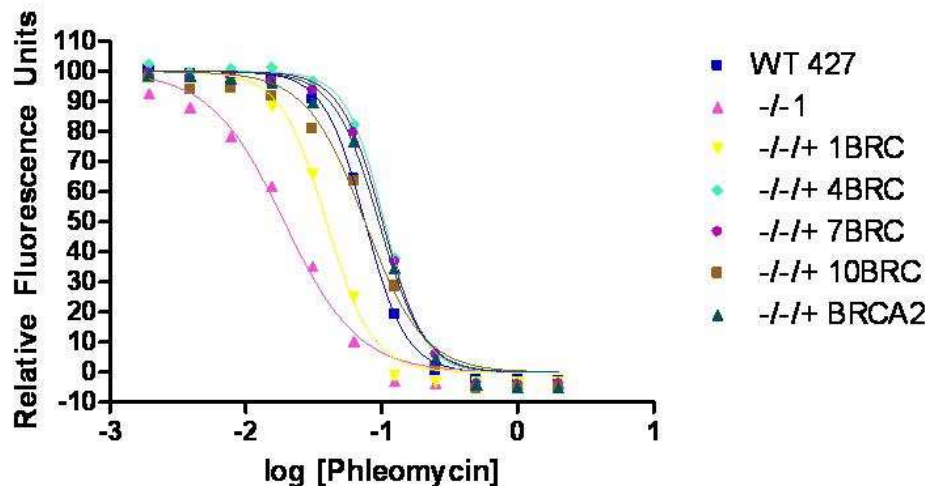


Figure 4-34 A representative survival curve for BSF Lister 427 BRCA2 re-expresser cell lines exposed to phleomycin.

The extent of fluorescence for each cell line (WT, *-/-* and *-/-+*) obtained using the Alamar blue assay is plotted against the log of phleomycin concentrations. Nonlinear regression was performed and fitted curves are shown for each cell line.

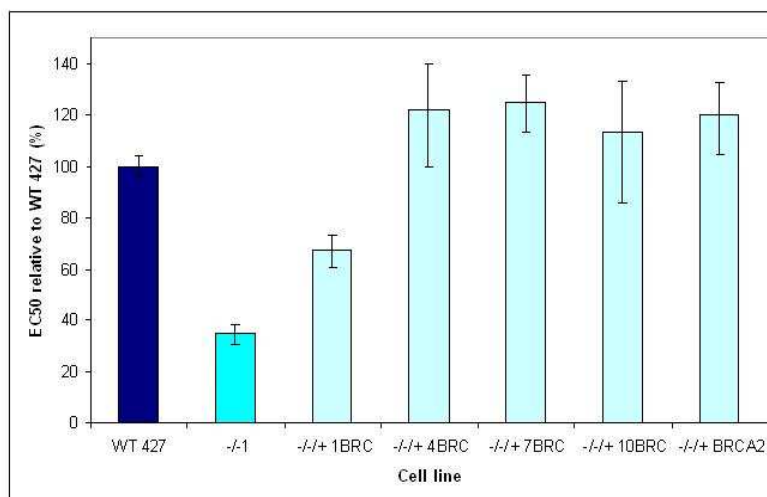


Figure 4-35 EC50 values of BSF Lister 427 BRCA2 re-expresser cell lines exposed to MMS. Wild-type Lister 427 (WT 427), *brca2*^{-/-} mutant, and BRCA2 re-expresser (-/-+) cell lines were placed in serially decreasing amounts of MMS and allowed to grow for 48 hours, before the addition of Alamar Blue. After a further 24 hours the reduction of Alamar Blue was measured by the amount of fluorescent resorufin generated. EC50 values are the mean from three experimental repetitions expressed as a percentage relative to wild-type and bars indicate 95% confidence intervals.

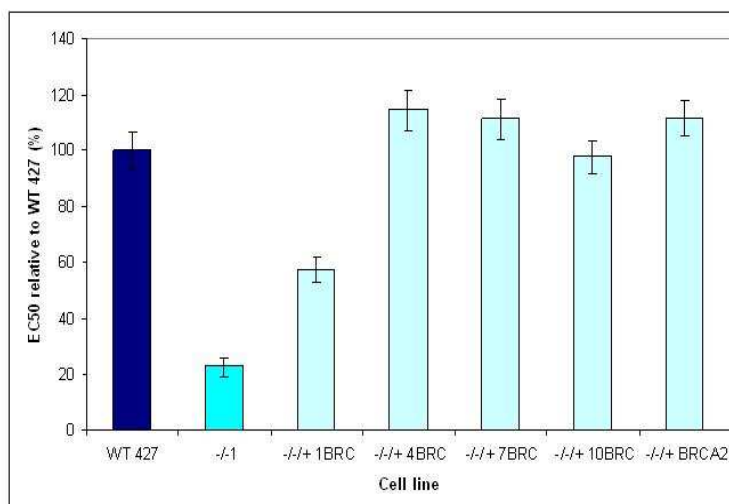


Figure 4-36 EC50 values of BSF Lister 427 BRCA2 re-expresser cell lines exposed to phleomycin. Wild-type Lister 427 (WT 427), *brca2*^{-/-} mutant, and BRCA2 re-expresser (-/-+) cell lines were placed in serially decreasing amounts of phleomycin and allowed to grow for 48 hours, before the addition of Alamar Blue. After a further 24 hours the reduction of Alamar Blue was measured by the amount of fluorescent resorufin generated. EC50 values are the mean from three experimental repetitions expressed as a percentage relative to wild-type and bars indicate 95% confidence intervals.

A

	-/-1	-/-+ 1BRC	-/-+ 4BRC	-/-+ 7BRC	-/-+ 10BRC	-/-+ BRCA2
WT 427	0.0016	0.0002	0.0894	0.0958	0.5691	0.3838
-/-1		0.0063	0.0034	0.0043	0.0444	0.0326
-/-+ 1BRC			0.0171	0.0207	0.1433	0.1015
-/-+ 4BRC				0.3017	0.5428	0.8703
-/-+ 7BRC					0.4007	0.6678
-/-+ 10BRC						0.0336

B

	-/-1	-/-+ 1BRC	-/-+ 4BRC	-/-+ 7BRC	-/-+ 10BRC	-/-+ BRCA2
WT 427	0.0004	0.0251	0.2347	0.5257	0.9449	0.5560
-/-1		0.0476	0.0107	0.0318	0.1090	0.0387
-/-+ 1BRC			0.0494	0.0948	0.2395	0.1017
-/-+ 4BRC				0.6928	0.4935	0.7801
-/-+ 7BRC					0.4529	0.9322
-/-+ 10BRC						0.3723

Table 4-7 Statistical analysis of Alamar Blue results.

P values are shown for student's T-tests comparing the mean EC50 values of wild-type Lister 427 (WT 427), *brca2*^{-/-} mutant, and BRCA2 re-expressor (-/-+) cell lines grown in the presence of MMS (A) or phleomycin (B). Areas shaded in yellow indicate a significant difference ($P \leq 0.05$). No correction has been made for simultaneous multiple comparisons.

4.7.3 Analysis of RAD51 focus formation

The ability of the BSF Lister 427 BRCA2 re-expressor cell lines to form RAD51 foci was next analysed. In this life cycle stage, the methanol fixation procedure used appears to result in greater background staining with the anti-RAD51 antiserum than is seen with formaldehyde fixation (Dobson *et al.*, 2011), but subnuclear foci were nevertheless detectable after 18 hrs growth in the presence of phleomycin; representative images of cells are displayed in Figure 4-38, and the numbers of RAD51 foci present in the nucleus of each cell line are shown in Table 4-8 and Figure 4-37. The *brca2*^{-/-} cells were analysed after growth in a reduced concentration of phleomycin ($0.25 \mu\text{g}\cdot\text{ml}^{-1}$) due to their increased sensitivity to this compound (section 4.3.2 and section 4.7.2).

In the absence of DNA damage clearly discernible RAD51 foci were rarely seen (~2% of cells), despite the greater amount of background staining (Figure 4-38B). After the induction of DNA damage with phleomycin, the number of wild-type cells containing no detectable RAD51 foci reduced to ~30%, a quantitatively similar response to that observed in PCF TREU 927 cells (section 4.3.3) and reported previously in Lister 427 BSF cells (Hartley and McCulloch, 2008). The BSF *brca2*^{-/-} mutant cell line had greatly reduced ability to form RAD51 foci

after the induction of DNA damage, as a single focus was detected in only 3.3% of cells. Again, this is a quantifiably similar finding to that described previously in the same mutants (Hartley and McCulloch, 2008). Though PCF TREU 927 *brca2*^{-/-} mutants appear even more impaired in RAD51 foci formation (only 0.9% displayed a detectable focus; Figure 4-14), it may be that this reflects the lesser background staining with anti-RAD51 antiserum in the tsetse fly stage. Hartley and McCulloch (2008) showed that BRCA2 with 1 BRC repeat is impaired in RAD51 foci formation in BSF cells, and these data confirm that finding; ~ 90% of the *1BRC* re-expresser cells contained no detectable foci after phleomycin treatment. The number of cells containing at least one detectable focus (~ 10%) appears greater than that observed for BSF Lister 427 *brca2*^{-/-} mutants, but remains a substantial impairment. Indeed, this impairment is more severe than that seen in the PCF TREU 927 *-/-/+1BRC* re-expresser cell line, where 45% of cells displayed RAD51 foci, consistent with the difference in phleomycin sensitivity detailed in the two cells lines (section 4.7.2).

The previous analysis of BRCA2 BRC repeat function in the contribution to RAD51 focus formation in BSF *T. brucei* was limited to BRCA2 variants with a single BRC repeat (Hartley and McCulloch, 2008). This work builds on that analysis by examining BRCA2 variants with increasing numbers of BRC repeats (4, 7 and 10) that are still reduced relative to full-length BRCA2, which has 12 BRC repeats in this *T. brucei* strain. Like the findings in TREU 927 PCF cells, a BRC-repeat number-dependent increase in the ability to form RAD51 foci was found. The number of cells containing no detectable RAD51 foci decreased as the BRC repeat number increased, with the full-length *BRCA2* re-expresser cell line containing ~ 30% of cells without RAD51 foci, which is essentially equivalent to wild-type cells. In contrast to TREU 927 PCF cells, where the *10BRC* variant re-expresser appeared to display an equivalent number and pattern of RAD51 foci to wild-type cells (Figure 4-14), here the *10BRC* variant did not respond to the same extent as wild-type cells (> 40% of cells did not display foci). Indeed, it is apparent that, overall, each BRC variant generates a greater proportion of cells with RAD51 foci in PCF cells compared with BSF. Moreover, the proportion of cells with larger numbers of RAD51 foci are consistently higher in PCF *BRC* variant re-expresser cell lines than in BSF *BRC* variants. Taken together, this appears to suggest that BRCA2 is more effective at re-distributing RAD51 to sites

of damage in PCF cells than in BSF cells, which may explain the difference in DNA damage sensitivities in the two life cycle stages (Chapter 3), both in wild-type cells and in BRC variant re-expresser cell lines (sections 4.3.2 and 4.7.2).

Cell line	Number of cells with RAD51 foci (%)						N
	0	1	2	3	4	>4	
WT 427	28.8	35.0	25.6	8.1	1.9	0.6	160
-/-1	96.7	3.3	0.0	0.0	0.0	0.0	182
-/-+ 1BRC	90.1	7.9	1.3	0.7	0.0	0.0	152
-/-+ 4BRC	64.3	20.0	13.6	1.4	0.7	0.0	140
-/-+ 7BRC	50.0	28.6	14.3	4.0	2.4	0.8	126
-/-+ 10BRC	42.5	26.0	20.5	8.7	1.6	0.8	127
-/-+ BRCA2	29.0	39.4	22.6	5.2	2.6	1.3	155

Table 4-8 RAD51 focus formation in BSF Lister 427 BRCA2 re-expresser cell lines exposed to phleomycin.

Wild-type Lister 427 (WT 427) and BRCA2 re-expresser (-/-+) cell lines were treated with 1 $\mu\text{g.ml}^{-1}$ phleomycin for 18 hours and the *brca2*^{-/-} mutant cell line was treated with 0.25 $\mu\text{g.ml}^{-1}$ phleomycin for 18 hours. The number of cells with a specific number of subnuclear RAD51 foci formed (0, 1, 2, 3, 4, > 4) were counted and are represented as a percentage of the total cells counted (N). Boxes shaded in light yellow contain foci, whilst boxes shaded in bright yellow contain the highest percentage of foci.

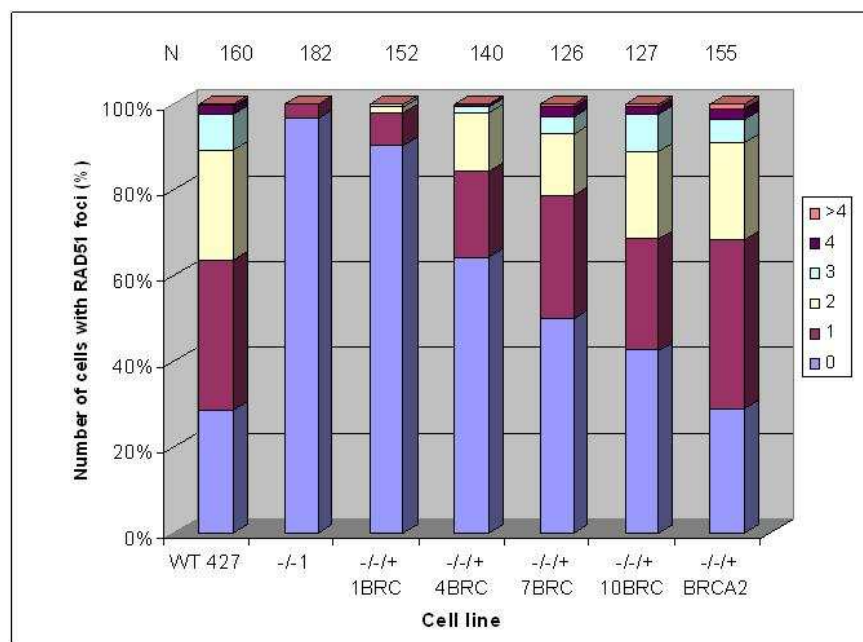


Figure 4-37 Graphical representation of RAD51 focus formation in BSF Lister 427 BRCA2 re-expresser cell lines exposed to phleomycin.

Wild-type Lister 427 (WT 427) and BRCA2 re-expresser (-/-+) cell lines were treated with 1 $\mu\text{g.ml}^{-1}$ phleomycin for 18 hours and the *brca2*^{-/-} mutant cell line was treated with 0.25 $\mu\text{g.ml}^{-1}$ phleomycin for 18 hours. The number of cells with a specific number of subnuclear RAD51 foci formed (0, 1, 2, 3, 4, > 4) were counted and are represented as a percentage of the total cells counted (N).

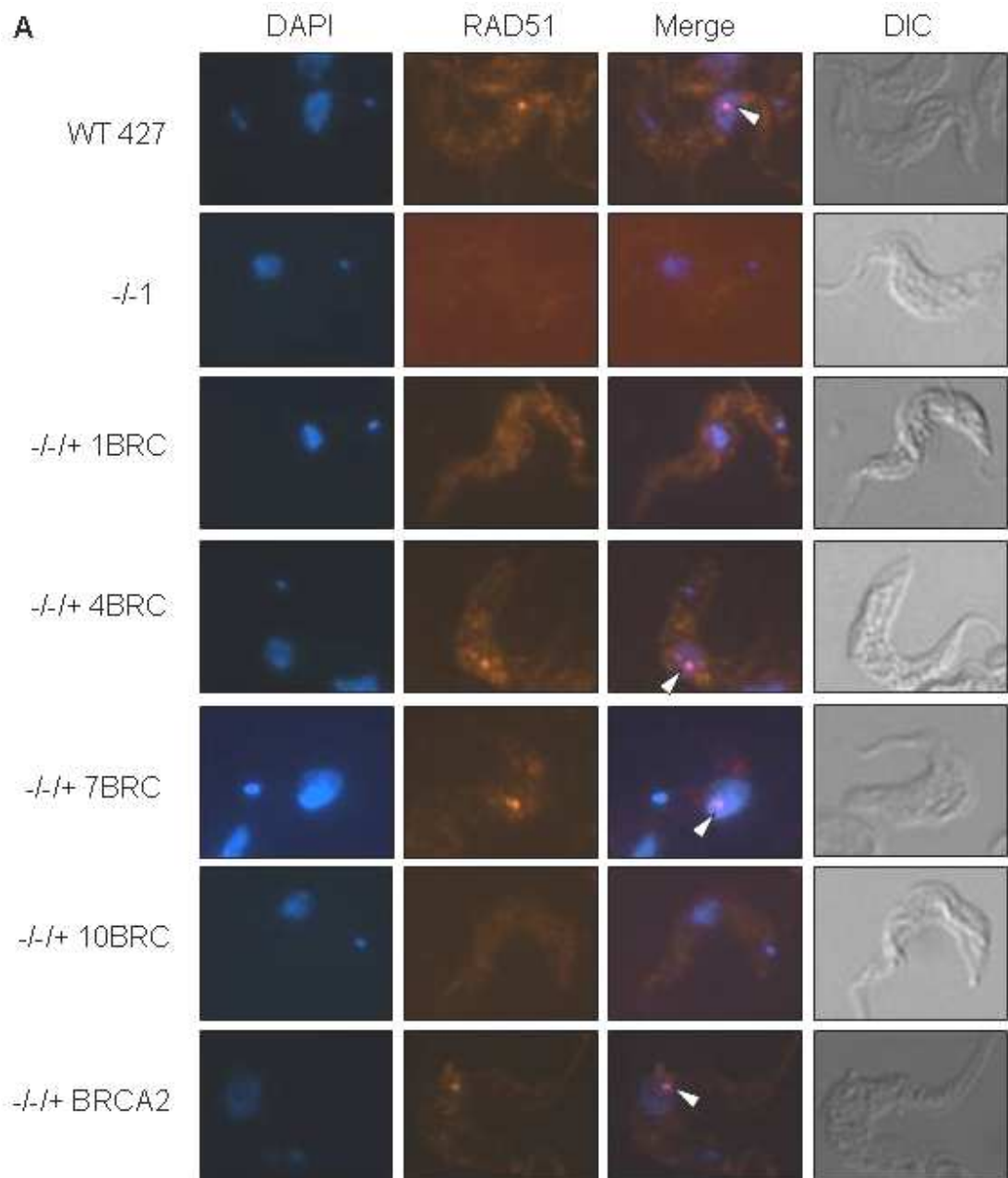


Figure 4-38A Representative images of RAD51 focus formation in BSF Lister 427 BRCA2 re-expresser cell lines exposed to phleomycin.

Images of wild-type Lister 427 (WT 427) and BRCA2 re-expresser (-/-+) cell lines after phleomycin treatment ($1 \mu\text{g}\cdot\text{ml}^{-1}$ BLE for 18 hours) and *brca2*^{-/-} mutant cell line after phleomycin treatment ($0.25 \mu\text{g}\cdot\text{ml}^{-1}$ BLE for 18 hours). Each cell is shown in differential interface contrast (DIC), after staining with DAPI (DAPI) and after hybridisation with anti-RAD51 antiserum (1:1000 dilution) and secondary hybridisation with Alexa Fluor 594 conjugated anti-rabbit antiserum (1:7000 dilution, RAD51). Merged images of DAPI and RAD51 cells are also shown (Merge). White arrows indicate RAD51 foci.

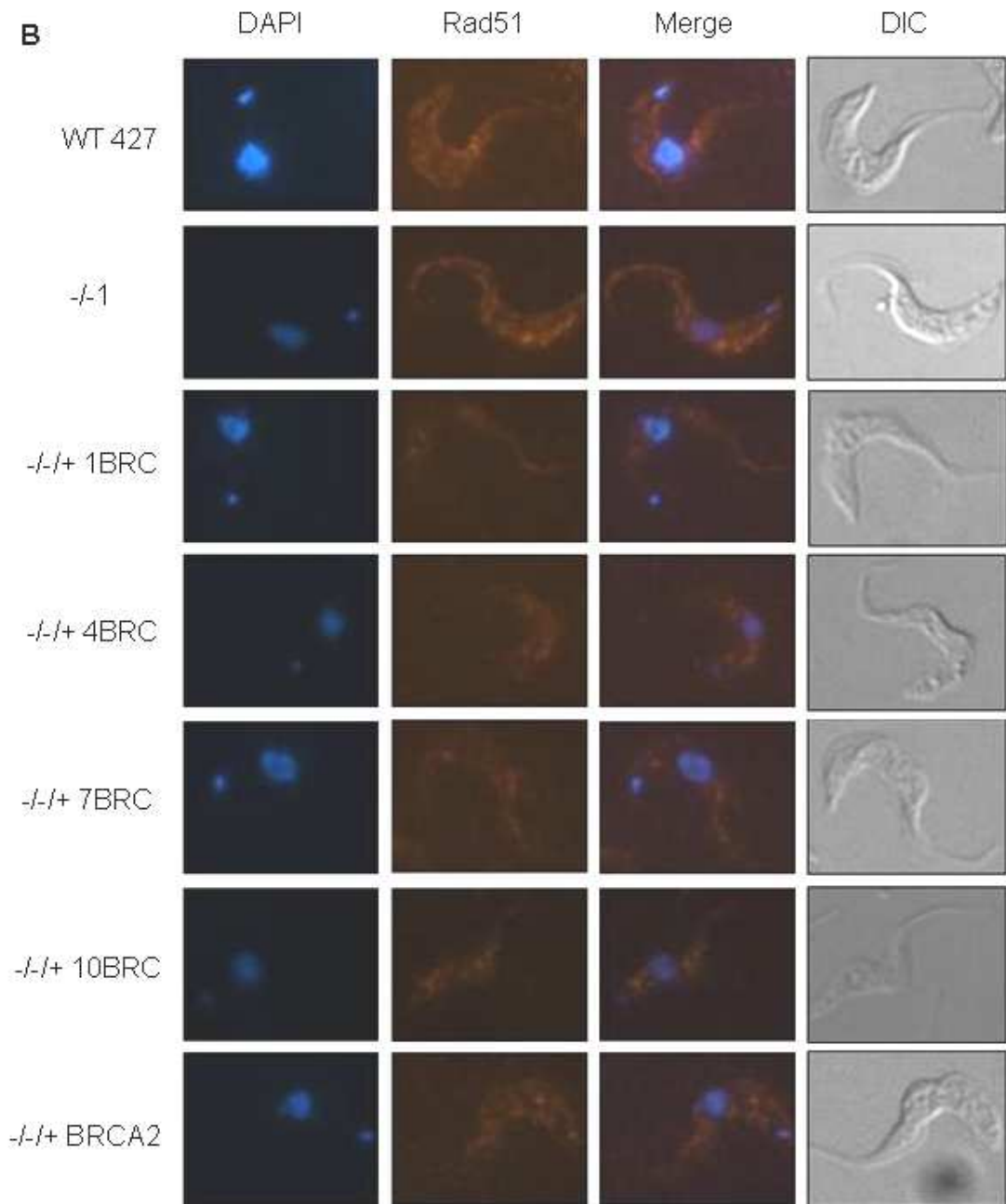


Figure 4-38B Representative images of RAD51 focus formation in BSF Lister 427 BRCA2 re-expresser cell lines.

Images of wild-type Lister 427 (WT 427), *brca2*^{-/-} mutant and BRCA2 re-expresser (^{-/-}+ cell lines without phleomycin treatment. Each cell is shown in differential interface contrast (DIC), after staining with DAPI (DAPI) and after hybridisation with anti-RAD51 antiserum (1:1000 dilution) and secondary hybridisation with Alexa Fluor 594 conjugated anti-rabbit antiserum (1:7000 dilution, RAD51). Merged images of DAPI and RAD51 cells are also shown (Merge).

Finally, to ensure that the observed differences in RAD51 foci formation are not due to differences in the levels of RAD51 in the BRCA2 re-expresser cell lines before or after phleomycin treatment, western analysis was carried out. As was seen in PCF cells, the western blot in Figure 4-39 demonstrates that the levels of RAD51 protein remain constant before or after phleomycin treatment in all cell lines.

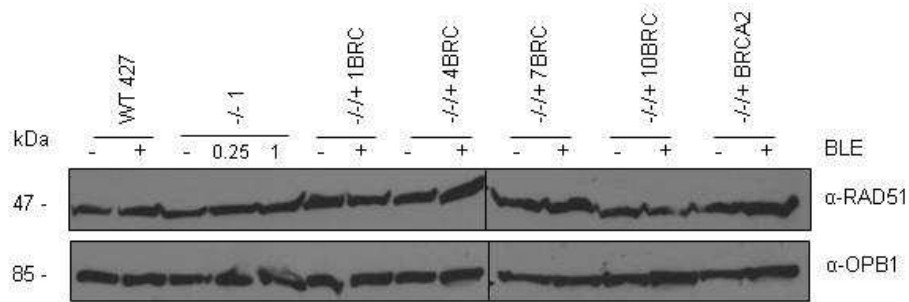


Figure 4-39 Western analysis of RAD51 in BSF Lister 427 BRCA2 re-expresser cell lines exposed to phleomycin.

Total protein extracts from wild-type Lister 427 (WT 427), *brca2*^{-/-} mutant and BRCA2 re-expresser (-/-+) cell lines were separated by SDS PAGE and western blotted before being probed with anti-RAD51 antiserum (1:500 dilution). '-' indicates protein extracts prepared without phleomycin treatment and '+' indicates protein extracts prepared after phleomycin treatment (1 $\mu\text{g}\cdot\text{ml}^{-1}$ BLE for 18 hours), except for the *brca2*^{-/-} mutant which was additionally treated with 0.25 $\mu\text{g}\cdot\text{ml}^{-1}$ BLE for 18 hours. The blots were stripped and re-probed with anti-OPB1 antiserum (1:1000 dilution) as a loading control. Size markers are shown (kDa).

4.8 Summary

The data presented in this chapter indicate that the phenotypes associated with the *brca2*^{-/-} mutants generated in the PCF TREU 927 and Lister 427 cells of *T. brucei* are due to the absence of BRCA2, and not a secondary mutation, as the re-expression of full-length BRCA2 in these cell lines restores the wild-type growth, DNA damage sensitivity and RAD51 foci formation phenotypes. This also confirms the data observed previously with the full-length BRCA2 re-expresser cell line generated in BSF Lister 427 *brca2*^{-/-} cells (Hartley and McCulloch, 2008).

Here, the importance of BRC repeat number in *T. brucei* BRCA2 has been systematically analysed by varying the number of BRC repeat motifs from 1 to 12 (the 'natural' repertoire); previously the function of a single BRC repeat was examined in *T. brucei* (Claire Hartley, PhD Thesis, 2008; Hartley and McCulloch, 2008). Indeed, in no other organism with BRCA2 possessing multiple BRC repeats has such an analysis been attempted. The data associated with the re-expression of variants of BRCA2 with varying numbers of BRC repeats reveals a number of things about BRCA2 function. Virtually all the BRC repeat variant re-expresser cell lines generated in all three strains demonstrated restored growth and DNA damage sensitivity when compared to the *brca2*^{-/-} mutant cell lines. The sole exception to this was the 1BRC re-expresser cell line in BSF Lister 427, which displayed greater DNA damage sensitivity than wild-type cells and all the other BRC variant expressers. Though the 1 BRC variant appeared less sensitive to DNA

damage than the parental *brca2*^{-/-1} cell line, it was still detectably repair-deficient, which is consistent with previous findings (Claire Hartley, PhD Thesis, 2008). The first thing these data show is that the strong growth impairment in BSF *brca2*^{-/-} mutants, and the weaker growth impairment in PCF mutants, is complemented irrespective of the BRC complement of BRCA2. This indicates that BRC repeat number is not a determinant of the role BRCA2 plays in promoting effective growth, and perhaps cell division or replication, in *T. brucei*. The second, more striking, finding is that these data demonstrate that it is not necessary for BRCA2 to have 12-15 BRC repeats in order to carry out efficient DNA damage repair in *T. brucei*. In the PCF re-expresser cell lines, a single BRC repeat is sufficient for maximal detectable levels of DNA repair, whereas 3 BRC repeats are required in BSF. An important caveat is that this finding is limited to the ability to repair damage to the extent measured by the assays adopted here, which is based on growth. More detailed analysis of lesion numbers, if this were possible, would be useful. Despite this, it is important to note that the BSF and PCF cells are not equivalent in terms of DNA repair; in Chapter 3 it was shown that PCF *brca2*^{-/-} mutants are less sensitive to DNA damage. Here, we show that the PCF cells expressing BRCA2 variants with reduced BRC repeat numbers form RAD51 foci after DNA damage more readily than the equivalent proteins in BSF, and greater numbers of foci are detected (see below). This could be an explanation as to why BRCA2 with a single BRC repeat is functional in DNA repair in PCF cells, but impaired in BSF cells.

Analysis of the ability of the re-expresser cell lines to form RAD51 foci demonstrated a striking concordance between BRC repeat number and the ability to form RAD51 subnuclear foci, in both life cycle stages. This is not because BRCA2 transports RAD51 to the nucleus (see below), but clearly demonstrates a functional and quantitative interaction between BRCA2 and RAD51. This is the first time that a biological process has been identified that is determined by multiple BRC repeats. However, the composition of these repair foci is unknown, in any organism (Lisby and Rothstein, 2009), as is the requirement for the multiple foci observed here during DNA repair (for instance, it is unclear if each foci represents a single site of DNA damage, or an accumulation of DNA breaks into a repair centre). These data require further verification, as a number of potential problems exist. For instance; the

detection threshold of RAD51 foci using fluorescence microscopy could be higher than expected, and therefore the absence of detectable foci may not necessarily correlate with the absence of RAD51-dependent DNA repair. It is also surprising that the sensitivity of the re-expresser cell lines to exogenous DNA damage does not display a BRC-repeat number dependence, as would be expected from the RAD51 foci formation data. However, the Alamar blue assay employed here is a secondary assay, which measures the metabolic capacity of the cells in the presence of DNA damaging agents, not directly the repair of the induced DNA damage, and could therefore be masking a more subtle phenotype revealed by the immunofluorescence.

These data also demonstrate the functionality of the 'degenerate' C-terminal BRC repeat, that was not clear from previous data (Claire Hartley, PhD Thesis, 2008), which showed that the 1BRC variant was deficient in HR and RAD51 focus formation. The demonstration that the 1BRC variant can support DNA repair, and to some extent RAD51 foci formation, in PCF cells shows that it is not degenerate, but can support RAD51-associated functions. It would be interesting to determine if there are differences in the mode and function of RAD51 binding between the conserved BRC repeats and the degenerate BRC repeat, as observed in mammalian BRCA2 where BRC 1 to 4 bind with high affinity to monomeric Rad51, bring about delivery to ssDNA at the site of DNA damage and facilitate efficient nucleation onto ssDNA, and BRC 5 to 8 bind to the nucleoprotein filament and stabilise it ensuring filament growth, thereby co-operating to bring about efficient DNA strand exchange (Carreira and Kowalczykowski, 2011). It would also be valuable to determine if the *T. brucei* 1BRC variant is capable of supporting HR in the PCF cells, since it is not in BSF cells (Hartley and McCulloch, 2008).

Aqueous fractionation indicates that RAD51 is found both in the nucleus and the cytoplasm of *brca2*^{-/-} cells to the same extent as in wild-type cells. This indicates that BRCA2 is either not responsible for nuclear transport of *T. brucei* RAD51, is one of a number of transporters, or that RAD51 mediates its own transport into the nucleus (Tarsounas, Davies, and West, 2003; Tarsounas, Davies, and West, 2004). In order to try and address this question further, site-directed mutants of the three putative *T. brucei* BRCA2 nuclear localisation signal sequences were generated, and re-expression in *brca2*^{-/-} mutant cells was

attempted (van den Hoek, Trenaman and McCulloch, data not shown). The supposition behind this analysis was that if BRCA2 was present, and able to bind RAD51, but unable to translocate to the nucleus this might reveal a transport function (for instance, alternate RAD51 transporters may be activated in the complete absence of BRCA2). For unknown reasons, these cell lines could not be generated, despite being based on precisely the same pRM482 re-expression system used here. It is possible that an 'untransportable' BRCA2 mutant acts in a dominant negative manner and leads to an impairment in DNA repair that is worse than a knockout of *brca2* or *rad51*, however an alternative approach will be required to investigate this further.

Chapter 5: Analysis of BRCA2- RAD51 interactions.

5.1 Introduction

In mammalian cells, it has been demonstrated that BRCA2 interacts directly with the Rad51 recombinase via multiple BRC repeat motifs, and also through a distinct C-terminal Rad51-binding motif (Wong *et al.*, 1997; Mizuta *et al.*, 1997; Chen *et al.*, 1998; Sharan *et al.*, 1997; Marmorstein, Ouchi, and Aaronson, 1998; Esashi *et al.*, 2005; Esashi *et al.*, 2007). Two classes of BRC repeat motifs have been described and it is proposed that they have evolved to promote Rad51 nucleation on single-stranded DNA resulting from the processing of a DSB and also to stabilise nascent Rad51-ssDNA filaments, facilitating propagation and thereby stimulating DNA strand exchange (Tarsounas, Davies, and West, 2003; Bugreev and Mazin, 2004; Esashi *et al.*, 2005; Esashi *et al.*, 2007; Shivji *et al.*, 2009; Carreira *et al.*, 2009; Carreira and Kowalczykowski, 2011). The first group of BRC repeats, consisting of repeats 1 to 4, bind with high affinity to monomeric Rad51 and reduce its ATPase activity, thereby maintaining Rad51 in an active ATP-bound state until required for filament nucleation (Carreira and Kowalczykowski, 2009; Carreira and Kowalczykowski, 2011). The second group, consisting of BRC repeats 5 to 8, bind free Rad51 with low affinity but bind to Rad51-ssDNA filaments with high affinity and function to stabilise them, thereby promoting filament growth (Galkin *et al.*, 2005; Carreira and Kowalczykowski, 2009; Carreira and Kowalczykowski, 2011). The BRCA2 C-terminal Rad51-binding motif is unrelated to the BRC repeat motif and, although highly conserved among vertebrate BRCA2 proteins, appears to be absent from BRCA2 orthologues in other taxa. The C-terminal motif binds and stabilises Rad51 in the multimeric filament, but not monomeric form (Davies and Pellegrini, 2007; Esashi *et al.*, 2007), and binding is cell cycle regulated by cyclin dependent kinase (CDK) phosphorylation of Serine3291 (Esashi *et al.*, 2005). Phosphorylation of Serine3291 in response to DNA damage inhibits binding by Rad51 at this site (Ayoub *et al.*, 2009). However, this C-terminal Rad51-binding motif appears to be dispensable for recombination and DNA repair; as a constitutively phosphorylated mutant that cannot bind Rad51 expressed in Chicken DT40 cells did not produce any detectable recombination or DNA repair defects (Ayoub *et al.*, 2009). A function for the C-terminal Rad51-binding motif in the protection of stalled replication forks from degradation has been described (Schlacher *et al.*,

2011) and may operate via stabilisation of Rad51 filaments on nascent DNA (Hashimoto *et al.*, 2010).

The BRCA2 orthologues identified in *C. elegans* and *U. maydis*, CeBRC-2 and Brh2 respectively, also demonstrate binding to Rad51, although with different mechanisms to that observed with mammalian BRCA2. *C. elegans* CeBRC-2 contains a single N-terminal BRC repeat that interacts directly with monomeric Rad51 (Martin *et al.*, 2005; Petalcorin *et al.*, 2006). No evidence of binding in the C-terminal region of CeBRC-2 has been found to date, though the region directly downstream of, and distinct from, the BRC repeat has been shown to bind Rad51 in filament form, inhibit ATP hydrolysis and so function to stabilise the nucleoprotein filament in a possibly analogous mechanism (Petalcorin *et al.*, 2007). *U. maydis* Brh2 also contains a single, N-terminal BRC repeat motif which binds monomeric Rad51 (Kojic *et al.*, 2002) and also a distinct C-terminal Rad51-binding domain, in the region downstream of the conserved DNA-binding domain (Kojic *et al.*, 2005). However, the N-terminal domain of Brh2 has been shown to rescue the *brh2-/-* mutant phenotype, and this was due to the presence of a non-canonical DNA-binding domain that was not identifiable from sequence data (Zhou, Kojic, and Holloman, 2009).

This chapter aims to investigate the interactions between *T. brucei* BRCA2 and RAD51, including during repair of DNA damage, using *in vitro* GST pull-down and *in vivo* co-immunolocalisation approaches. These data will allow us to ask if the mode of BRCA2-RAD51 interaction in *T. brucei* is conserved with that seen in other organisms, and should deepen our understanding of the regulation of RAD51-mediated homologous recombination by BRCA2.

5.2 *In vitro* GST pull-down

In vitro GST pull-down was performed order to define the domains of the *T. brucei* BRCA2 protein that mediate its interaction with RAD51 during DNA repair. This experiment was carried out using tagged fusion proteins co-expressed in *E. coli*, in an approach previously successful in detecting interactions between *T. brucei* RAD51 paralogue proteins (Dobson *et al.*, 2011). The GST pull-down strategy is displayed in Figure 5-1. GST-tagged RAD51 was expressed in *E. coli* and captured from whole cell lysates (input) using glutathione conjugated to

sepharose beads. After extensive washing, co-expressed His-tagged variants of BRCA2 that interacted with GST-RAD51 were detected in elution samples by western blot and hybridisation with anti-His antiserum.

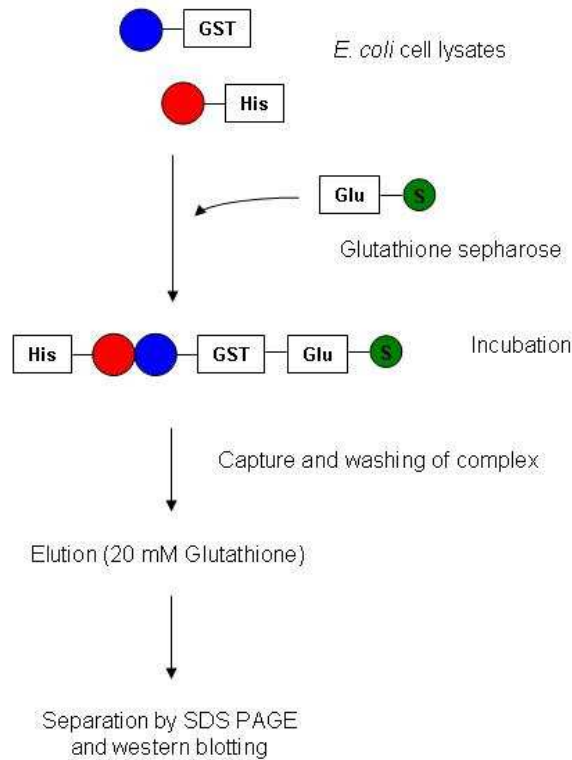


Figure 5-1 GST pull-down strategy.

GST RAD51 (GST, blue circle) and His BRCA2 variants (His, red circle) were co-expressed in *E. coli*. Whole cell lysates were prepared and incubated with Glutathione (Glu) conjugated to sepharose beads (S, green circle). Beads and bound protein complex were captured by centrifugation and washed extensively. His BRCA2 variants were detected after elution with 20 mM glutathione followed by SDS PAGE, blotting and hybridisation with anti-His antiserum.

5.2.1 Generation of bacterial fusion protein over-expression constructs

Two compatible bacterial protein over-expression constructs were used; pGEX-4T-3 (Amersham) and pRSF-1b (Novagen). *T. brucei* RAD51 was over-expressed in *E. coli* using the pGEX-4T-3 construct, which results in RAD51 being expressed as an N-terminal Glutathione S-Transferase (GST) fusion; the construct also contains an *ampicillin* (AMP) resistance cassette for selection (Figure 5-2). The pGEX-4T-3 construct containing the full-length *RAD51* gene was generated previously (gift, Chris Stockdale). Multiple variants of *T. brucei* BRCA2 were over-expressed in *E. coli* as N-terminal hexa-Histidine (His) fusions using the pRSF-1b construct; in each case, the constructs were maintained via a

kanamycin (*KAN*) resistance cassette for selection (Figure 5-3). The variants of BRCA2 (Figure 5-4) were generated by PCR using primers containing a *Bam*HI restriction site in the forward primer and an *Xho*I restriction site in the reverse primer to enable cloning into the pRSF-1b construct. The two empty vectors were used to express the His and GST tags (not fused to a protein) for control purposes.

The BRCA2 variants generated are grouped into the two ‘halves’ of the BRCA2 protein: the N-terminal and the C-terminal. The N-terminal half contains two putative nuclear localisation signal (NLS) sequences and the BRC repeat motifs; N-terminal BRCA2 variants were cloned with 1, 4, 7 or 10 BRC repeats, and were PCR-amplified using primers 93 and 94 from the *pRM482::BRC* re-expression constructs (section 4.2.1). The expressed BRC variant polypeptides were called His 1BRC, His 4BRC, His 7BRC and His 10BRC. The C-terminal half of BRCA2 contains all motifs present in the region downstream from the last BRC repeat motif. The His BRCA2 C-term variant contains this complete portion of the protein, including a putative PhePP motif (see below), the DNA/DSS1-binding domain (consisting of the alpha-helical domain, the three oligonucleotide-binding (OB) domains and the tower domain), and a putative CDK phosphorylation site at Serine1523 (section 1.4.2.4). This sequence was PCR-amplified from genomic DNA extracted from PCF TREU 927 cells using the primers 16 and 51. Site-directed mutagenesis (section 2.5.3) was then carried out on this construct to mutate the putative CDK phosphorylation site at Serine1523 to determine if the binding of RAD51 to the C-terminus of BRCA2 might be regulated by phosphorylation, as reported in mammalian cells (Mizuta *et al.*, 1997;Sharan *et al.*, 1997;Esashi *et al.*, 2005;Esashi *et al.*, 2007). The Serine residue at position 1523 was mutated to a Glutamine residue (Ser1523Glu) in order to mimic the presence of a phosphate group (using primers 45 and 46). As a control for any side effects due to manipulation of the Serine residue, an Alanine mutant (Ser1523Ala) was similarly generated (using primers 43 and 44). These variants were called His BRCA2 C-term Glu and His BRCA2 C-term Ala, respectively.

In order to determine if RAD51 binding localises to the region of BRCA2 downstream from the end of the DNA/DSS1-binding domain and containing the putative Serine1523 phosphorylation residue, truncated variants of His BRCA2 C-

term were constructed. Firstly, the His BRCA2 C-term variant was modified, using primers 51 and 76, to remove the sequence downstream from the end of the DNA/DSS1-binding domain, and this variant was called His BRCA2 DBD + PhePP. Secondly, the region downstream of the DNA/DSS1-binding domain was cloned, using primers 16 and 75, allowing the small, extreme C-terminus containing Serine1523 to be expressed as a fusion protein called His BRCA2 C-tail. To allow comparison with the Serine1523 mutants of His BRCA2 C-term, constructs were derived from each of the putative phosphorylation mutant variants described above (generating the proteins His BRCA2 C-tail Glu, and His BRCA2 C-tail Ala).

It has been previously reported that mammalian BRCA2 binds DMC1, the meiosis-specific recombinase, at a conserved motif called the PhePP motif (KVFVPPFK) that is located just downstream of the BRC repeats (Thorslund, Esashi, and West, 2007). GST pull-down experiments with a fragment of human BRCA2 corresponding to the PhePP motif did not demonstrate binding to Rad51 (Thorslund, Esashi, and West, 2007). However, both the *U. maydis* and *C. elegans* orthologues of BRCA2, Brh2 and CeBRC-2 respectively, display binding between a PhePP motif, albeit slightly diverged in sequence (Figure 5-5), and Rad51 (Petalcorin *et al.*, 2007;Kojic *et al.*, 2011). A sequence of substantial similarity (KPFVVPFA) was identified in *T. brucei* BRCA2 located immediately downstream of the central bi-partite NLS sequence at amino acids 764 to 771 (Figure 5-5). A function for *T. brucei* DMC1 in DNA repair has not been detected to date (Proudfoot and McCulloch, 2006), and due to the similarity between DMC1 and RAD51 (Proudfoot and McCulloch, 2005;Proudfoot and McCulloch, 2006), it was considered that this putative DMC1-binding site might be capable of binding RAD51. In order to test this, the His BRCA2 DBD + PhePP variant was modified, using primers 76 and 91, to remove the putative DMC1/RAD51-binding site to create His BRCA2 DBD - PhePP.

Finally, in order to test if the DNA/DSS1-binding domain interacts with RAD51, expression of a variant of BRCA2 consisting of the DNA/DSS1-binding domain was attempted. In mammalian cells, this region has been shown to interact with DSS1, a small, highly acidic protein which is mutated in split hand/split foot syndrome (Crackower *et al.*, 1996;Marston *et al.*, 1999), but there has been no

evidence for interaction with Rad51 to date. Unfortunately, expression of the *T. brucei* BRCA2 DNA/DSS1-binding domain in *E. coli* was unable to be detected.

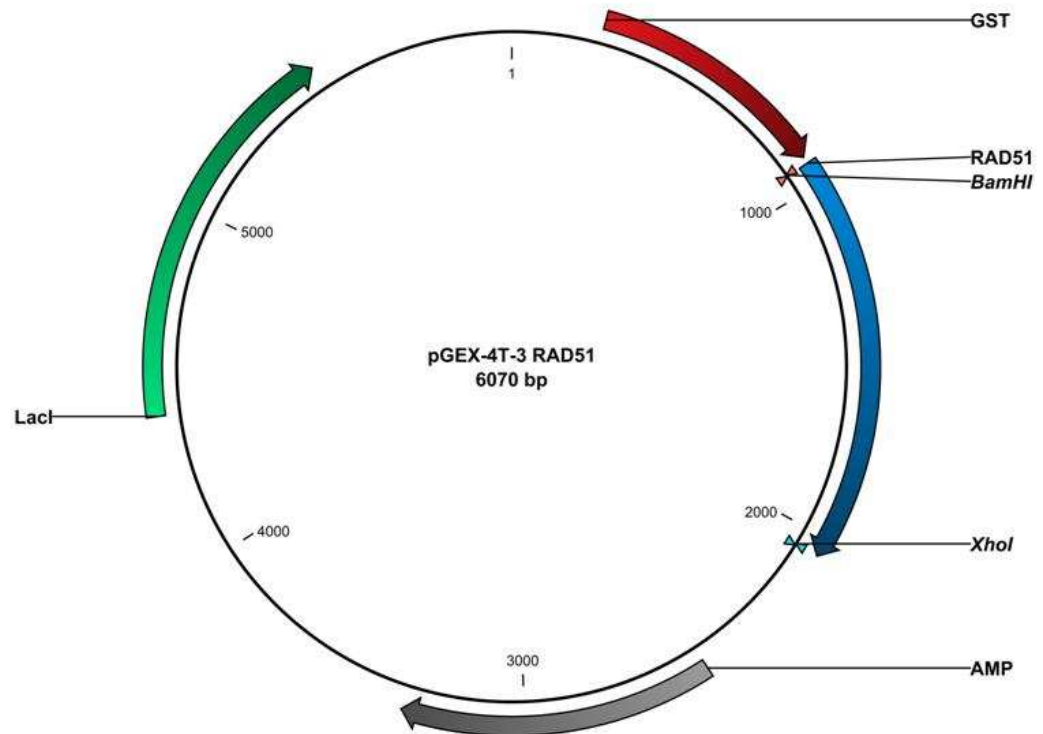


Figure 5-2 Construct used for N-terminal GST tagging of RAD51 for over-expression in *E. coli*. The *RAD51* ORF (blue) was cloned into *Bam*HI and *Xho*I restriction sites downstream of the GST tag (red). *AMP*: ampicillin resistance ORF (grey). *LacI*: lac repressor ORF (green). Sizes are shown (bp).

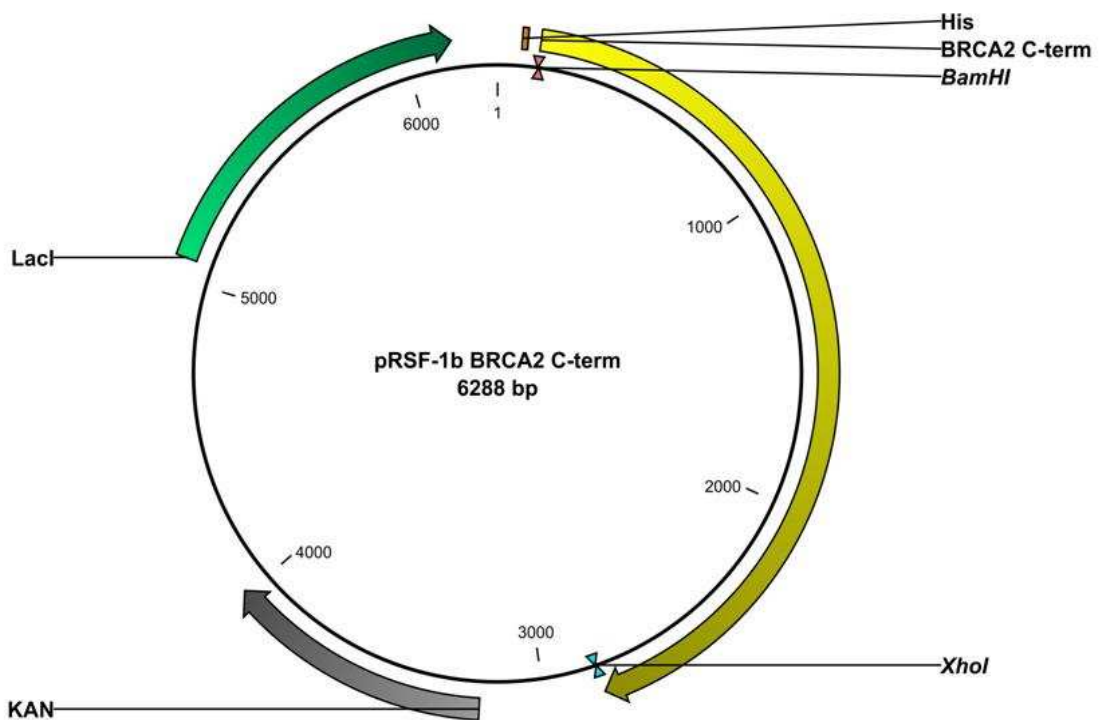


Figure 5-3 Construct used for N-terminal His tagging of BRCA2 variants for over-expression in *E. coli*.

The *BRCA2* variant ORFs (yellow, only *BRCA2* C-term is shown) were cloned into *Bam*HI and *Xho*I restriction sites downstream of the His tag (orange). *KAN*: *kanamycin* resistance ORF (grey). *Lact*: *lac* repressor ORF (green). Sizes are shown (bp).

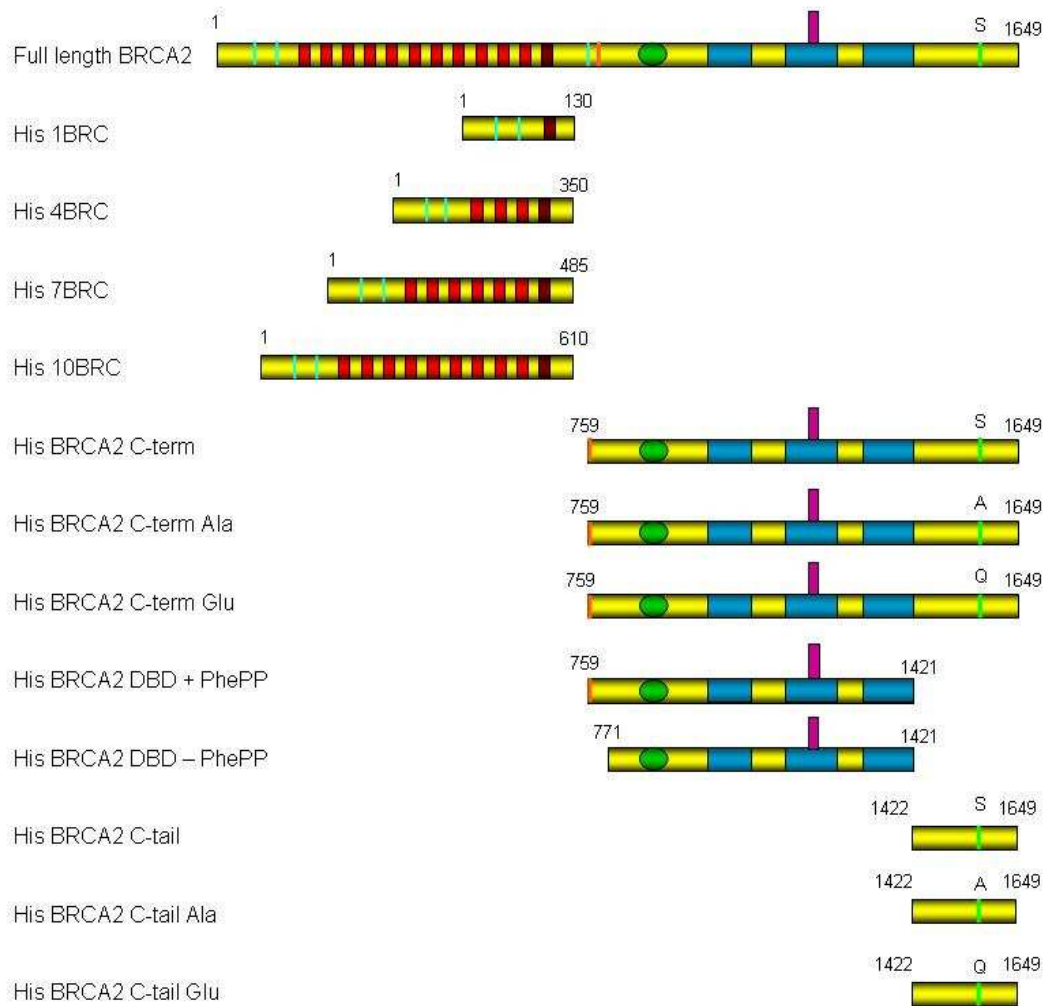


Figure 5-4 A schematic diagram of the His-tagged *BRCA2* variant proteins over-expressed in *E. coli*.

Full length *BRCA2* is shown (top) with protein domains indicated; nuclear localisation signals (light blue bars), 'normal' BRC repeats (red boxes), degenerate BRC repeat (dark red box), PhePP motif (orange bar), α helical domain (green oval), oligonucleotide binding domains (blue boxes), tower domain (purple bar) and putative CDK phosphorylation site (S, light green bar). The His-tagged *BRCA2* variants generated are shown with the domains present. Mutation of the putative CDK phosphorylation site is indicated; Ser1523Ala (A) and Ser1523Glu (Q), and amino acid positions are numbered.

Human	2404	KVVFVPPFK	2411
Ape	2404	KVVFVPPFK	2411
Mouse	2348	KVVFVPPFK	2356
Rat	2358	KVVFVPPFK	2365
Dog	2421	KVVFVPPFK	2428
Chicken	2353	KTFVPPFK	2360
At (A)	341	NSFVSPLW	348
Ce	83	SAFVSPFR	90
Um	486	PRFVTPFK	493
Tc	169	GCFVVPFA	176
Tb	764	KPFVVPFA	771

Figure 5-5 Sequence alignment of putative PhePP motifs from BRCA2 orthologues. BRCA2 from a variety of organisms; At (A): *Arabidopsis thaliana* BRCA2 homologue A. Ce: *Caenorhabditis elegans*. Um: *Ustilago maydis*. Tc: *Trypanosoma cruzi*. Tb: *Trypanosoma brucei*. Amino acids indicated in red are fully conserved in mammalian species. Figure adapted from Thorslund, Esashi, and West, 2007.

5.2.2 Generation of co-expressing bacterial cultures

Competent cells of the Rosetta2 *E. coli* bacterial strain (Novagen) were transformed with the constructs generated in section 5.2 to produce bacterial cultures co-expressing GST RAD51 and each of the His BRCA2 variants. Rosetta2 cells contain the pRare construct, which was maintained via a *chloramphenicol* (CHL) resistance cassette. Control cultures co-expressing GST RAD51 and the His tag alone (from construct pRSF-1b), His 10BRC and the GST tag alone (pGEX-4T-3), and His BRCA2 C-term and the GST tag alone were also generated to control for binding of the *T. brucei* proteins to the His or GST tags, rather than to each other. The competent *E. coli* cells were co-transformed, as detailed in section 2.7, with two constructs and selected on LB agar supplemented with 100 $\mu\text{g}.\text{ml}^{-1}$ ampicillin (Sigma), 50 $\mu\text{g}.\text{ml}^{-1}$ kanamycin (Sigma) and 34 $\mu\text{g}.\text{ml}^{-1}$ chloramphenicol (Sigma).

5.2.3 GST pull-down using co-expressing bacterial cultures

50 ml cultures of the bacterial cell lines were grown in LB media supplemented with antibiotics (see above) and protein expression induced with 1 mM IPTG as described in section 2.13. After growth for 16 hours at 25°C the bacterial cells were then harvested by centrifugation, lysed by sonication and the soluble proteins retained after the removal of insoluble cell debris by further

centrifugation as described in section 2.13; this is referred to as the input. GST and GST RAD51 were then recovered from the lysates using Glutathione conjugated to sepharose beads (Amersham) as described in section 2.13; protein recovered is referred to as the elution. The input and elution protein samples were separated by SDS PAGE on 10% Bis-Tris gels, western blotted and first probed with anti-His antiserum (Sigma) at a dilution of 1:750. The blots were then stripped and re-probed with anti-GST antiserum (Novagen) at a dilution of 1:10000. For unknown reasons the expressed GST-tagged RAD51 protein was not able to be detected by western blot in these conditions, despite the GST tag alone being detected (data not shown). Coomassie stained protein gels of the same elution samples showed clearly visible protein of the expected sizes for GST (28 kDa) and a prominent band at just under 80 kDa in size that is thought to be GST RAD51, for unknown reasons running at higher than its expected size of 67 kDa. Due to the problems with western blot detection, eluted GST RAD51 is shown as a coomassie-stained gel.

Interaction between RAD51 and the BRCA2 N-terminal BRC repeat region is shown in Figure 5-6. The western blot in Figure 5-6A shows the N-terminal BRCA2 variant input samples probed with anti-His antiserum and demonstrates the expression of His-tagged proteins at approximately the expected sizes for the His BRC variants; 1BRC (16 kDa), 4BRC (34 kDa), 7BRC (52 kDa) and 10BRC (66 kDa). The coomassie stained protein gel (Figure 5-6B) of the separated elution samples demonstrates that the GST and GST RAD51 proteins were successfully recovered by the GST pull-down approach. The western blot in Figure 5-6C shows the elution samples probed with anti-His antiserum and demonstrates the presence of only a very faint band corresponding to the His 10BRC variant (lane 4), which was not seen when 10BRC was co-expressed with GST alone (lane 5). This indicates that while 10BRC binds GST-RAD51, the 1BRC, 4BRC and 7BRC variants either do not bind, or bind so weakly that they cannot be detected under these experimental conditions. These data may indicate that binding between the BRC repeats of *T. brucei* BRCA2 and RAD51 is surprisingly weak and, at least in this experimental system, 10 BRC repeats must be present to detect this.

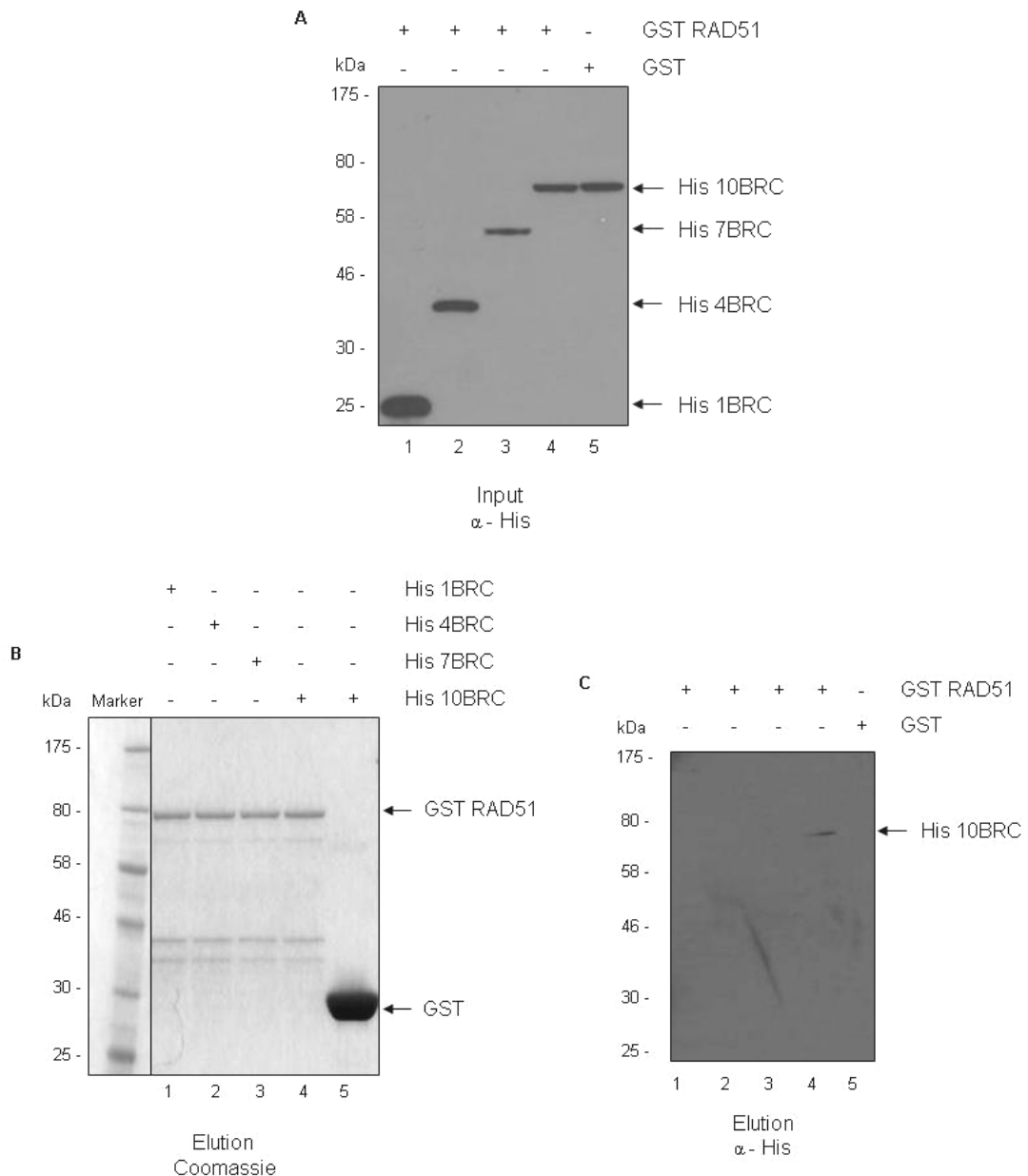


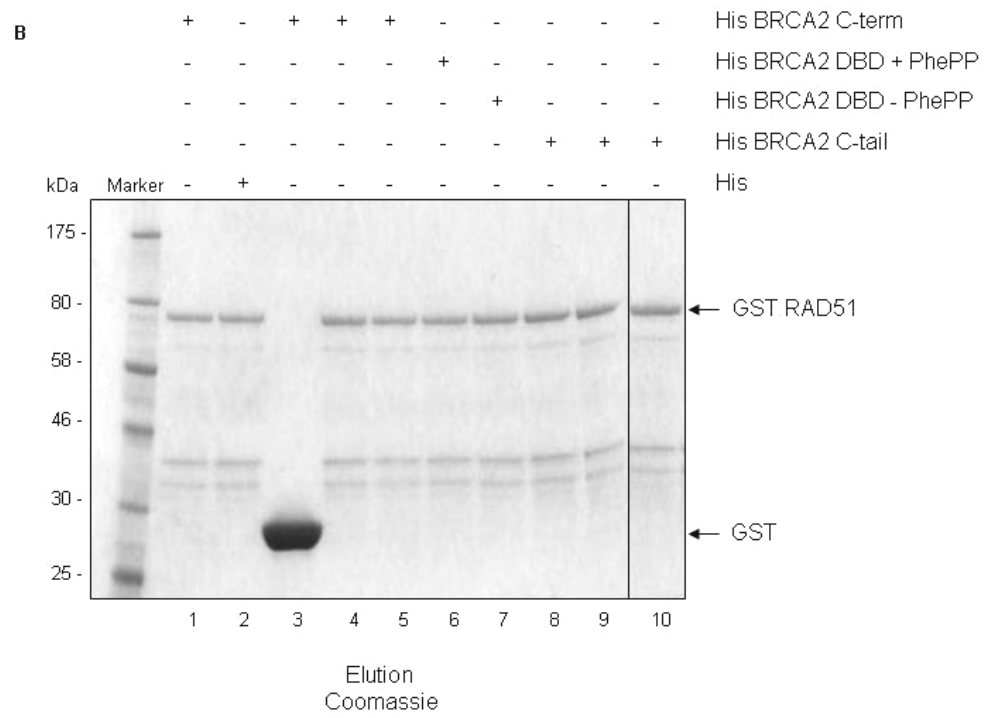
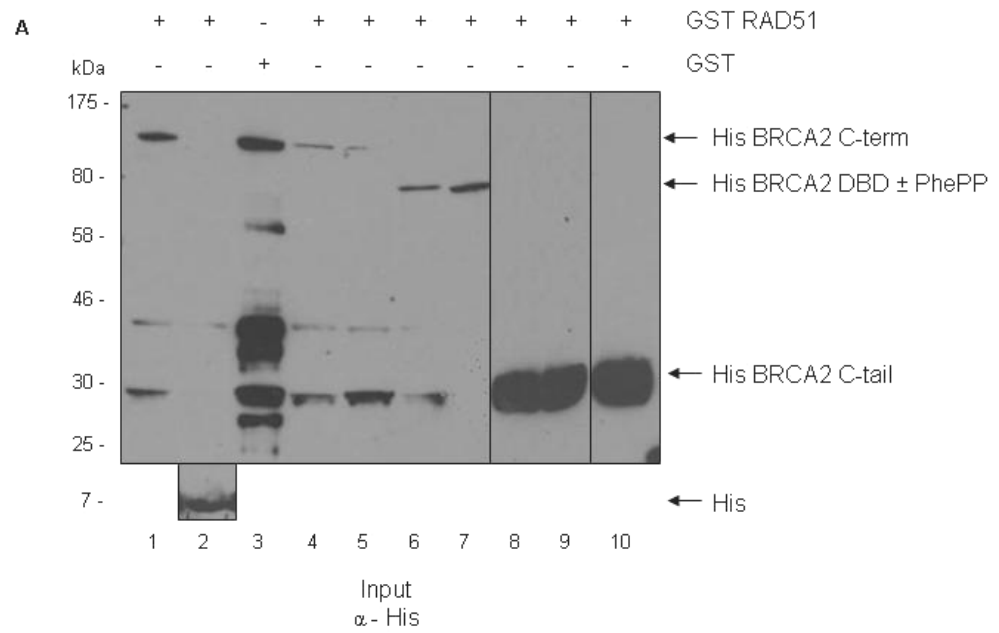
Figure 5-6 GST pull-down analysis of the interactions between RAD51 and the N-terminal domain of BRCA2.

(A) A western blot of the separated input samples probed with anti-His antiserum (1:750 dilution). His tagged proteins are indicated (black arrows), and the GST-tagged proteins that were co-expressed are indicated (top). (B) A coomassie stained gel of the separated elution samples showing GST RAD51 and the GST tag (black arrows). His-tagged proteins that were co-expressed are indicated (top). (C) A western blot of the separated elution samples probed with anti-His antiserum (1:750 dilution). GST-tagged proteins used for the pull-down are indicated (top). In each panel, size markers are shown (kDa).

Figure 5-7 shows analysis of interaction between RAD51 and the C-terminal BRCA2 variants. The western blot in Figure 5-7A shows input samples probed with anti-His antiserum and demonstrates expression of His-tagged proteins of the expected sizes for each of the variants; four His BRCA2 C-term variants (100 kDa; lanes 1, 3-5), His BRCA2 DBD + PhePP (75 kDa; lane 6), His BRCA2 DBD -

PhePP (73.5 kDa; lane 7), three His BRCA2 C-tail variants (28 kDa; lanes 8-10), and also the His tag (7 kDa; lane 2). The coomassie stained protein gel (Figure 5-7B) of the separated elution samples demonstrates the presence of the GST and GST RAD51 proteins, indicating they were successfully recovered by the GST pull-down approach. The western blot in Figure 5-7C shows the elution samples probed with anti-His antiserum to detect the His BRCA2 variants. The first control culture, where GST RAD51 was co-expressed with the His tag (lane 2), displayed some binding of the anti-His antiserum in the elution sample (see below). The second control culture, with His BRCA2 C-term co-expressed with GST did not display His tagged protein in the elution sample, indicating that no binding between the His BRCA2 C-term variant and GST has occurred (lane 3). Strong bands corresponding to each of the three His BRCA2 C-term variants were seen in each eluate (Figure 5-7C. lanes 1, 4-5). This indicates that all of the His BRCA2 C-term variants have bound to GST RAD51, irrespective of whether or not this was the wild-type sequence or the Ser1523Ala or Ser1523Glu mutants, indicating that RAD51 can bind *T. brucei* BRCA2 in the region downstream of the BRC repeats. Each of the His BRCA2 C-tail variants were also recovered by the GST pull-down (lanes 8-10), indicating that RAD51 can bind to the region C-terminal of the DNA/DSS1-binding domain. Though this appears analogous to Rad51-BRCA2 C-terminal interaction in mammals (Mizuta *et al.*, 1997;Sharan *et al.*, 1997;Esashi *et al.*, 2005;Esashi *et al.*, 2007;Davies and Pellegrini, 2007), the status of Serine1523 in *T. brucei* BRCA2 had no influence on RAD51 binding, suggesting binding to the C-tail region is not regulated by phosphorylation on this residue. Surprisingly, the His BRCA2 variant encompassing only the region between the BRC repeats and the C-tail (mainly composed of DNA/DSS1-binding domain) was also pulled down by GST RAD51 (lane 6), and this was unaffected by removal of the putative PhePP motif (lane 7). This suggests, firstly, that this PhePP motif is not a mediator of *T. brucei* RAD51 interaction and, secondly, that *T. brucei* BRCA2 possesses a binding site for RAD51 in the vicinity of the DNA/DSS1-binding domain that has not been observed in any other BRCA2 orthologue. Taken together, these data suggest that *T. brucei* RAD51 binds to at least two regions in the BRCA2 C-terminus downstream from the last BRC repeat: one region is found in or around the DNA/DSS1-binding domain, and the other in the poorly conserved C-tail. Thus, BRCA2-RAD51 interaction in *T. brucei* appears extensive, including these C-terminal regions and the BRC repeats.

As mentioned above, problems were encountered with the detection of the His tag alone due to its small size (7 kDa). The control input sample in Figure 5-7A (lane 2), with GST-RAD51 co-expressed with the His tag, shows a clearly visible band of the expected size for the His tag. In the corresponding elution sample in Figure 5-7C (lane 2) it appears that binding of the His antiserum was observed at just above the expected size for the His tag. Due to this, a coomassie stained gel of the input and elution samples containing GST-RAD51 co-expressed with the His tag were also analysed (Figure 5-7D). The input sample (lane 1) in Figure 5-7D shows the expression of a protein of the expected size for the His tag, and this band is not visible in the elution sample (lane 2), confirming that GST RAD51 has not bound to the His tag. In addition, no binding between the His tagged 1BRC, 4BRC and 7BRC variants of BRCA2 and GST RAD51 was detected in the previous experiment (Figure 5-6C lanes 1-3) and this acts as a negative control for this experiment also.



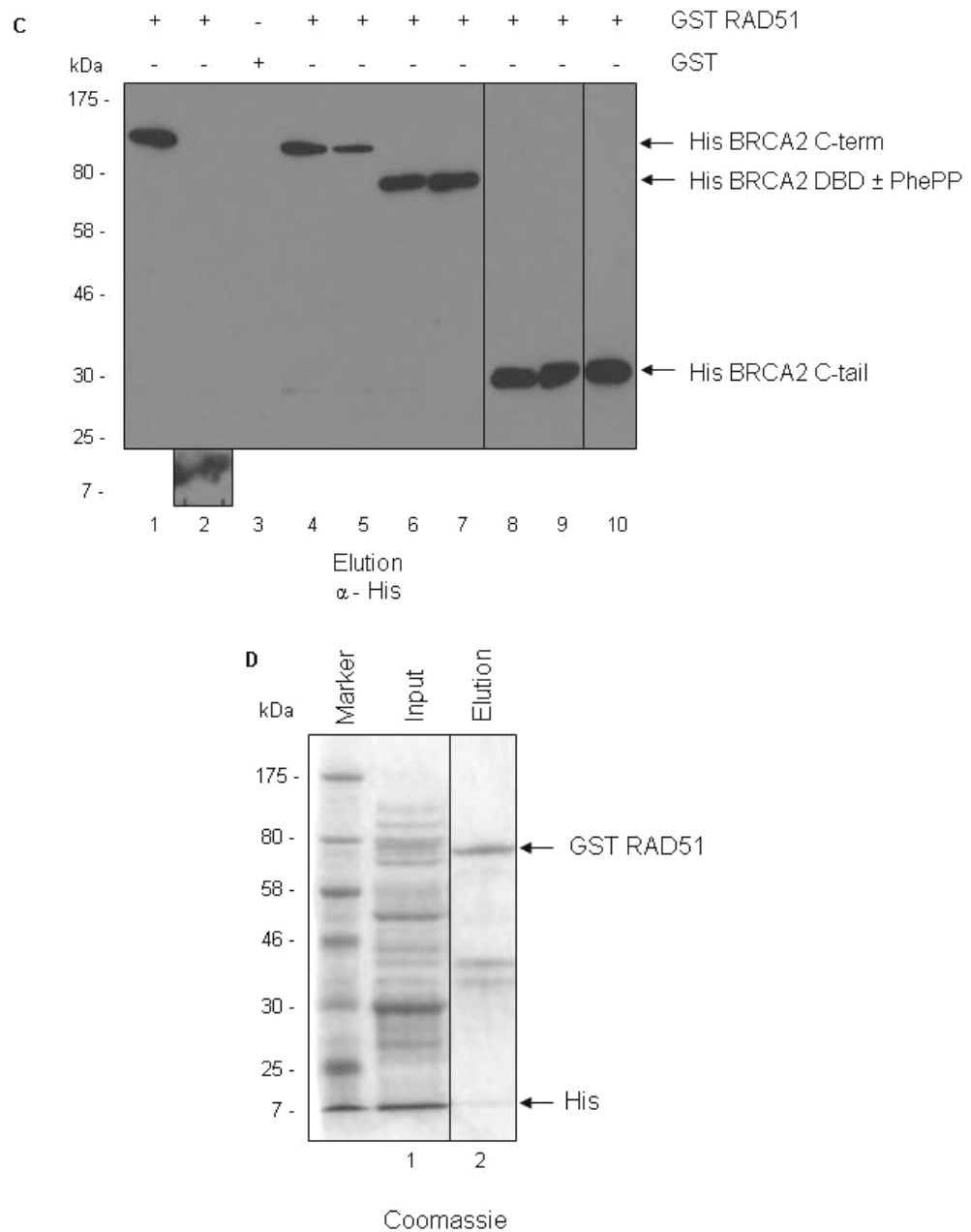


Figure 5-7 GST pull-down analysis of the interactions between RAD51 and the C-terminal domain of BRCA2.

(A) A western blot of the separated input samples probed with anti-His antiserum (1:750 dilution). His tagged proteins are indicated (black arrows), and the GST-tagged proteins that were co-expressed are indicated (top). (B) A coomassie stained gel of the separated elution samples showing GST Rad51 and the GST tag (black arrows). His-tagged proteins that were co-expressed are indicated (top). Lanes 4 and 9 contain the Ser1523Ala mutants, and lanes 5 and 10 the Ser1523Glu mutants. (C) A western blot of the separated elution samples probed with anti-His antiserum (1:750 dilution). GST-tagged proteins used for the pull-down are indicated (top). (D) A coomassie stained gel of the separated input and elution samples from GST Rad51 co-expressed with the His tag (black arrows). In each panel, size markers are shown (kDa).

5.3 Co-immunolocalisation of RAD51 and BRCA2

The GST pull-down analysis above indicates extensive BRCA2-RAD51 interaction *in vitro*. However, it does not tell us how the proteins might interact in the cell and in response to DNA damage. For this reason, co-immunolocalisation using epitope tagged BRCA2 and anti-RAD51 antiserum was carried out in order to investigate the cellular localisation of BRCA2 and RAD51 before and after the induction of DNA damage, and to test for co-localisation. Though a number of *T. brucei* factors, including BRCA2 and RAD51 paralogues (Hartley and McCulloch, 2008; Dobson *et al.*, 2011), have been shown to influence the ability of RAD51 to form subnuclear foci after damage, it is not clear if the proteins physically interact in these putative repair structures. Epitope tagged BRCA2 was used in this approach due to the lack of reproducibility and specificity of the anti-BRCA2 antiserum. A tag consisting of twelve copies of the c-myc epitope was added to the C-terminus of BRCA2 in PCF TREU 927 cells in a strategy previously used for PTP tagging and purification of *T. brucei* proteins (Schimanski, Nguyen, and Gunzl, 2005).

5.3.1 Endogenous C-terminal epitope tagging strategy

A construct (pNAT^{x12myc}) that enables the fusion of a C-terminal 12myc epitope tag at the endogenous loci of a gene of interest was modified to target *BRCA2* (Figure 5-8; Alsford and Horn, 2008). The strategy to enable the C-terminal tagging of *T. brucei* proteins at their endogenous loci is displayed in Figure 5-9. The C-terminal epitope tagging construct uses a region of the 3' end of the ORF to enable homologous recombination and integration into the genome. Selection of clones is enabled by the presence of a *blastocidin* (*BSD*) resistance cassette flanked by *tubulin* and *actin* processing sequences. After integration of the construct, endogenous upstream gene sequences are used for RNA *trans*-splicing, while the downstream integrated *BSD* cassette provides polyadenylation signals for the tagged gene, meaning that the 3' UTR is non-endogenous. For *BRCA2*, a 491 bp region of the 3' end of the *BRCA2* ORF was amplified by PCR using primers 32 and 33, which contained *HindIII* and *XbaI* restriction sites, respectively. The PCR-amplified region includes all ORF sequence up to, but omitting the stop codon to allow translational read-through into the epitope tag. This region also contains a unique restriction site (*SphI*) to allow linearisation of

the construct prior to transformation. The DNA fragment was cloned into the construct upstream of the epitope tag using the *Hind*III and *Xba*I restriction sites. For transformation, the construct was linearised by restriction digestion with *Sph*I, the digested DNA was then ethanol precipitated and approximately 5 µg of the resuspended DNA was used for each transformation.

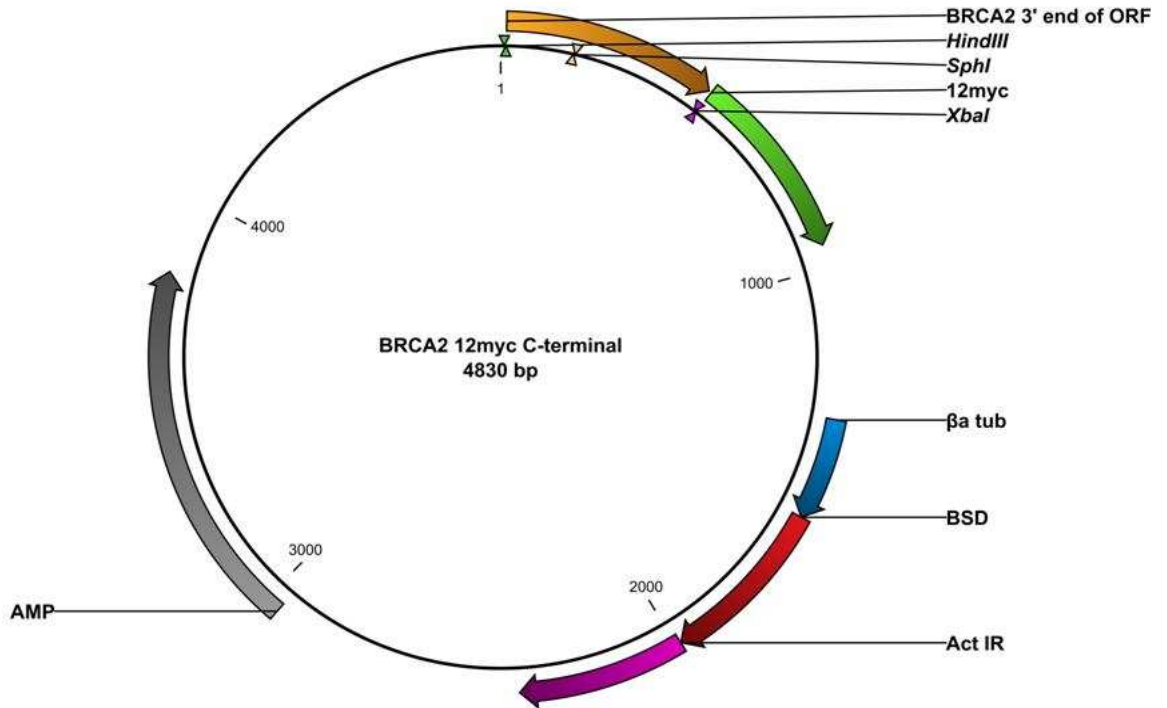


Figure 5-8 Construct used for C-terminal 12myc tagging of *T. brucei* BRCA2. 491 bp of the 3' end of the *BRCA2* ORF (orange) containing a unique restriction site (*Sph*I) was cloned into *Hind*III and *Xba*I restriction sites. The 12myc epitope tag (green) consists of 12 tandemly repeated copies of the c-myc epitope. The *BSD* resistance cassette is shown (red) flanked by the *tubulin* ($\beta\alpha$ Tub, blue) and *actin* (Act IR, purple) intergenic sequences. *AMP*: Ampicillin resistance ORF (grey). Sizes are shown (bp).

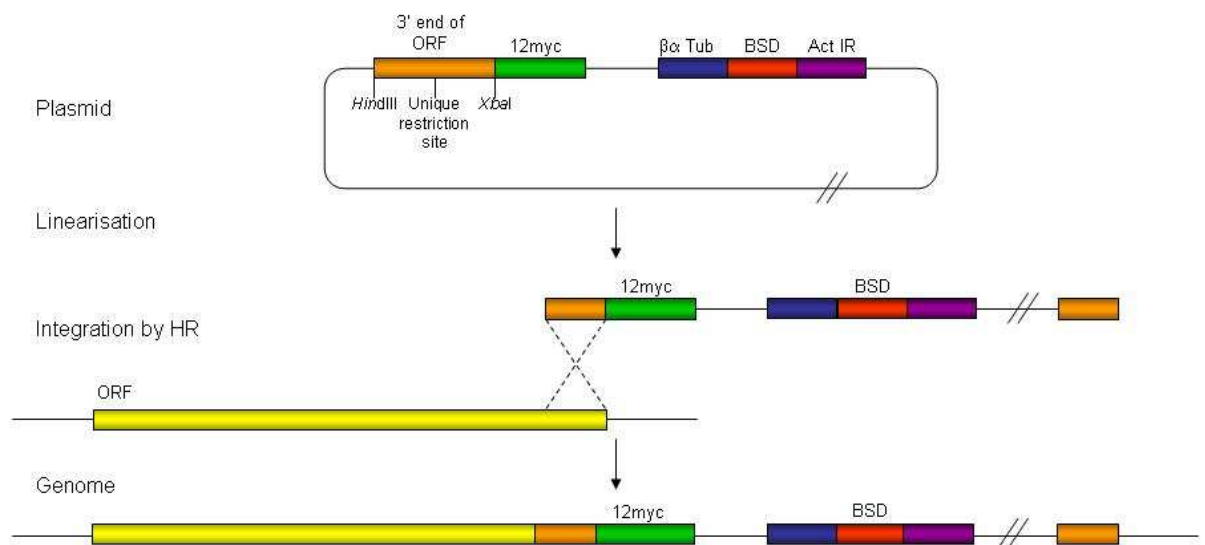


Figure 5-9 Strategy for C-terminal 12 myc tagging of *T. brucei* proteins at their endogenous loci.

A schematic of the C-terminal 12myc tagging construct, described in Figure 5-8, is shown (top). Linearisation of the construct using a unique restriction site, within the 3' end of the ORF (orange), allows integration into the genome by homologous recombination (HR). This produces the endogenous ORF fused with the C-terminal 12myc tag (green, bottom).

5.3.2 Generation of C-terminal 12myc tagged BRCA2 cell line

A transformation was carried out in order to generate a C-terminal 12myc tagged BRCA2 cell line. To do this, wild-type PCF TREU 927 cells were transformed with the BRCA2 12myc tagging construct and antibiotic resistant transformants were selected by placing cells on SDM-79 media supplemented with $10 \mu\text{g.ml}^{-1}$ blasticidin. The clones obtained from transformation were screened by western blot performed on total protein extracted from six blasticidin resistant clones. The total protein extracts were separated by SDS PAGE on a 3-8% Tris-Acetate gel before western blotting and probing with anti-myc antiserum at a dilution of 1:7000. The western blot in Figure 5-10 demonstrates that four of the six putative BRCA2 12myc cell lines contained a protein band of the expected size for BRCA2 12myc (193 kDa). One of these was taken forward for further analysis.

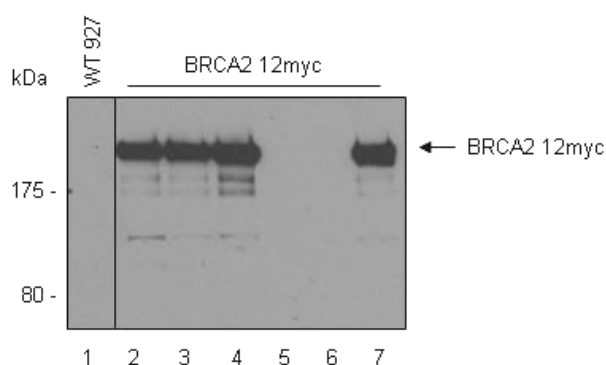


Figure 5-10 Confirmation of expression of C-terminal 12myc tagged BRCA2 by western analysis.

Total protein extract from wild-type TREU 927 (WT 927) and putative BRCA2 12myc tagged cell lines were separated by SDS-PAGE and western blotted before being probed with anti-myc anti-serum (1:7000 dilution). A band of the size expected for BRCA2 12myc tagged protein is indicated (black arrow), and size markers are shown (kDa).

5.3.3 Co-immunolocalisation of BRCA2 and RAD51

Fluorescence microscopy was performed (section 2.4.2) using the BRCA2 12myc cell line; anti-myc antiserum conjugated to Alexa Fluor 488 (1:7000 dilution, Invitrogen) was used to detect 12myc tagged BRCA2, and anti-RAD51 antiserum (1:1000 dilution), in conjunction with Alexa Fluor 594 conjugated anti-rabbit secondary antiserum (1:7000 dilution, Invitrogen), to detect RAD51. Cells were

treated with $2 \mu\text{g}\cdot\text{ml}^{-1}$ phleomycin and slides prepared 5 hours and 24 hours subsequently (Figure 5-11 and Figure 5-12, respectively). Control slides were similarly prepared without phleomycin treatment (Figure 5-13). Images were captured using a Zeiss Axioskop microscope with DAPI, DIC, Rhodamine and FITC filters. These images were used for quantification of the various categories of localisation observed (Table 5-1). The images presented in Figure 5-11, Figure 5-12 and Figure 5-13 were obtained from the same slides, but using a Deltavision confocal microscope (Volodymyr Nechyporuk-Zloy), and were subjected to deconvolution.

The localisation of BRCA2 in the absence of DNA damage appeared to be largely nuclear. In most cells (58 of 87), concentration of BRCA2 in multiple, discrete foci-like punctate structures was clearly visible, either around the nuclear periphery or throughout the nucleus (examples are shown in Figure 5-13). In a smaller, but still substantial number of cells (24 out of 87), BRCA2 localisation was less focal, either because staining was visible throughout the nucleus or because no clear subcellular staining was apparent. In a very small proportion of cells (~ 6%) BRCA2 was seen in peripheral nuclear 'rings' (see below). As has been seen previously (Chapter 3 and Chapter 4) in the absence of damage detectable RAD51 localisation was negligible (indeed, in this analysis, no RAD51 signal was detected).

After the induction of DNA damage, as has been described previously (Chapter 3 and Chapter 4) RAD51 formed clear subnuclear foci, the numbers of which increased between 5 and 24 hours (40% and 62% of total cells, respectively). The localisation of BRCA2 and RAD51 in these conditions can be broadly classified into several distinct types. Firstly, BRCA2 was seen much more frequently to be forming distinctive, generally continuous, rings around the edge of the DAPI stained DNA (Figure 5-11A and Figure 5-12A). The numbers of cells displaying this localisation increased with time, and in many cases no RAD51 foci were observed in these cells. When cells were seen with both RAD51 foci and BRCA2 rings, the RAD51 foci were observed in the nucleus within the BRCA2 ring (Figure 5-11B and Figure 5-12B), and the signals did not overlap. Secondly, there appeared to be little change, between 5 and 24 hours, in the numbers of cells with punctate BRCA2 rings around the DAPI stained DNA; again, these cells were seen both with and without the presence of subnuclear RAD51 foci (Figure 5-11C

and Figure 5-12C). Co-localisation was observed in ~ 50% of cells that had multiple BRCA2 and RAD51 foci, but in no cases was there complete co-localisation of all foci as observed in mammalian cells. Instead, it appeared that this colocalisation was essentially always between a single BRCA2 ‘focus’ that made up part of the punctate ring and a single RAD51 focus (Figure 5-11D and Figure 5-12D). Thirdly, BRCA2 was observed as focal accumulations spread throughout the nucleus, rather than being concentrated in the periphery (Figure 5-11E and Figure 5-12E). In some cases, however, predominantly peripheral foci were seen, with one or two more central foci (Figure 5-11B and D for examples), suggesting that the distinction between peripheral and subnuclear localisation, and perhaps also with rings, may be less clear-cut than presented here. Nevertheless, in the cells with BRCA2 subnuclear foci, some displayed no RAD51 foci, while others displayed both BRCA2 and RAD51 foci. Where BRCA2 and RAD51 foci were both present, most did not co-localise, though overlap in the signals between single BRCA2 and RAD51 foci were common (Figure 5-11F and Figure 5-12F).

A	Phleomycin ($\mu\text{g.ml}^{-1}$)	Time (hours)	BRCA2 rings	BRCA2 punctate rings	BRCA2 foci	Diffuse/no BRCA2	N
	0	0	5	28	30	24	87
	2	5	23	58	27	4	112
	2	24	40	77	49	4	170

BRCA2 rings					
B	Phleomycin ($\mu\text{g.ml}^{-1}$)	Time (hours)	RAD51 foci (no co-localisation)	RAD51 foci (co-localisation)	N
	0	0	0	0	0
	2	5	0	0	0
	2	24	28	0	28

BRCA2 punctate rings					
C	Phleomycin ($\mu\text{g.ml}^{-1}$)	Time (hours)	RAD51 foci (no co-localisation)	RAD51 foci (co-localisation)	N
	0	0	0	0	0
	2	5	19	15	34
	2	24	34	20	54

BRCA2 foci					
D	Phleomycin ($\mu\text{g.ml}^{-1}$)	Time (hours)	RAD51 foci (no co-localisation)	RAD51 foci (co-localisation)	N
	0	0	0	0	0
	2	5	4	6	10
	2	24	12	12	24

Table 5-1 Quantification of the localisation of BRCA2 and RAD51 in PCF TREU 927 *T. brucei* before and after exposure to phleomycin.

(A) Quantification of BRCA2 localisation without phleomycin treatment and after 5 or 24 hours growth in phleomycin ($2 \mu\text{g.ml}^{-1}$); cells in which BRCA2 localises in peripheral nuclear rings (BRCA2 rings), in more punctuate peripheral rings (BRCA2 punctate rings), in

subnuclear foci (BRCA2 foci), or where clear localisation of BRCA2 was not apparent (Diffuse/no BRCA2), are distinguished. Numbers indicate total number of cells observed and N indicates the total number of cells counted. Quantification of the number of cells that display RAD51 foci, and whether any of these foci co-localise with BRCA2; this is separated into cells with BRCA2 rings (B), BRCA2 punctate rings (C) and BRCA2 foci (D).

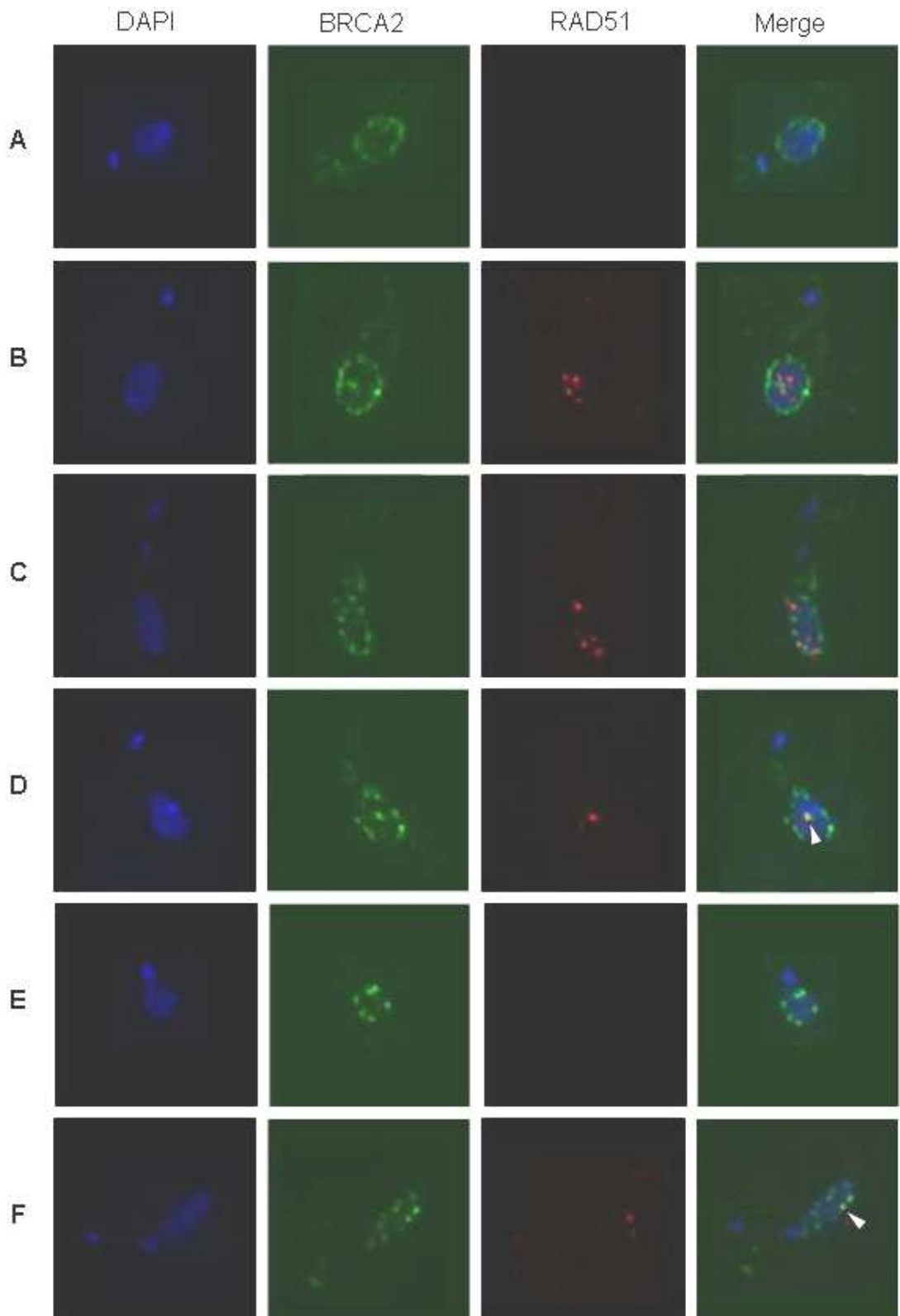


Figure 5-11 Representative images of BRCA2 and RAD51 localisation in PCF TREU 927 *T. brucei* exposed to phleomycin for 5 hours. Images of BRCA2 12myc cells after phleomycin treatment ($2 \mu\text{g}\cdot\text{ml}^{-1}$ BLE for 5 hours). Each cell is shown after staining with DAPI (DAPI), after hybridisation with anti-myc Alexa Fluor

488 conjugated antiserum (1:7000 dilution, BRCA2) and after hybridisation with anti-RAD51 antiserum (1:1000 dilution) and secondary hybridisation with Alexa Fluor 594 conjugated anti-rabbit antiserum (1:7000 dilution, RAD51). Merged images of DAPI, BRCA2 and RAD51 cells are also shown (Merge). White arrows indicate co-localisation between BRCA2 and RAD51. A: BRCA2 ring, B: BRCA2 ring with RAD51 foci, C: Punctate BRCA2 ring with RAD51 foci, D: Punctate BRCA2 ring with RAD51 co-localisation, E: BRCA2 foci, F: BRCA2 foci with RAD51 co-localisation.

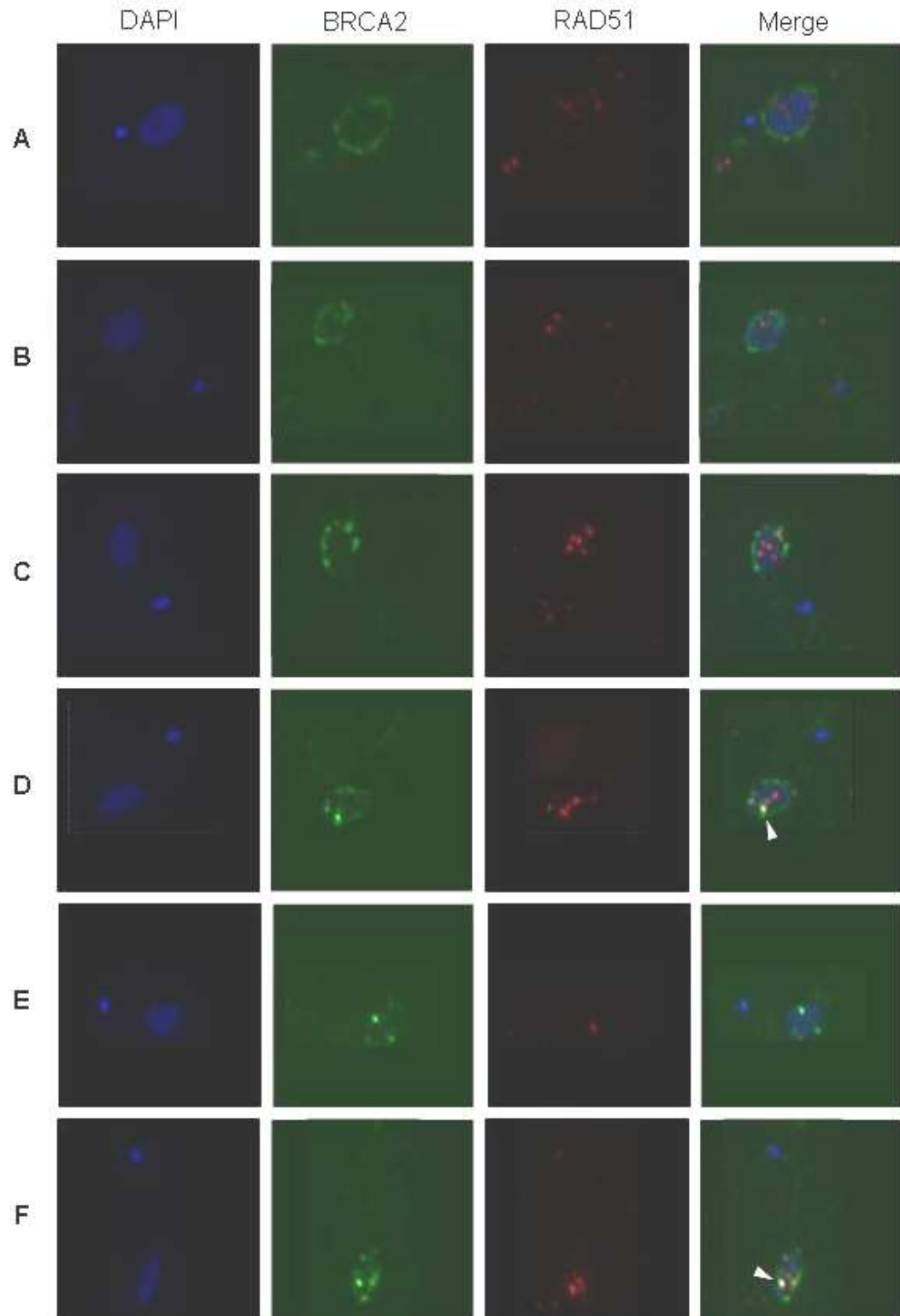


Figure 5-12 Representative images of BRCA2 and RAD51 localisation in PCF TREU 927 *T. brucei* exposed to phleomycin for 24 hours. Images of BRCA2 12myc cells after phleomycin treatment ($2 \mu\text{g}\cdot\text{ml}^{-1}$ BLE for 24 hours). Each cell is shown after staining with DAPI (DAPI), after hybridisation with anti-myc Alexa Fluor

488 conjugated antiserum (1:7000 dilution, BRCA2) and after hybridisation with anti-RAD51 antiserum (1:1000 dilution) and secondary hybridisation with Alexa Fluor 594 conjugated anti-rabbit antiserum (1:7000 dilution, RAD51). Merged images of DAPI, BRCA2 and RAD51 cells are also shown (Merge). White arrows indicate co-localisation between BRCA2 and RAD51. A: BRCA2 ring, B: BRCA2 ring with RAD51 foci, C: Punctate BRCA2 ring with RAD51 foci, D: Punctate BRCA2 ring with RAD51 co-localisation, E: BRCA2 foci, F: BRCA2 foci with RAD51 co-localisation.

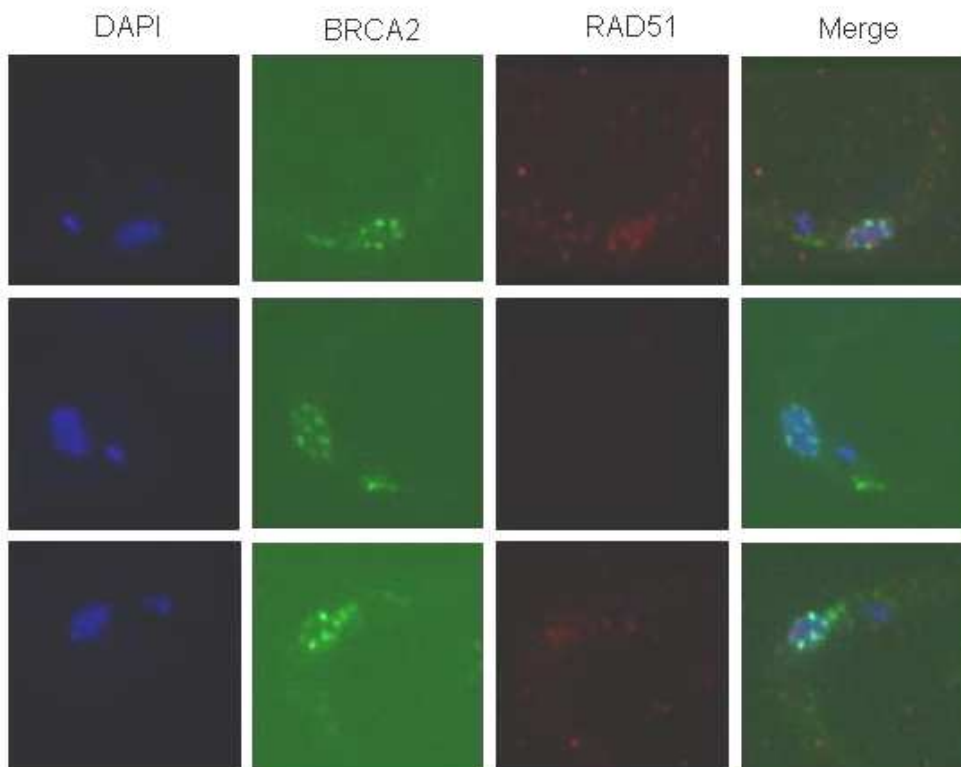


Figure 5-13 Representative images of BRCA2 and RAD51 localisation in PCF TREU 927 *T. brucei* in the absence of DNA damage.

Images of BRCA2 12myc cells without phleomycin treatment. Each cell is shown after staining with DAPI (DAPI), after hybridisation with anti-myc Alexa Fluor 488 conjugated antiserum (1:7000 dilution, BRCA2) and after hybridisation with anti-RAD51 antiserum (1:1000 dilution) and secondary hybridisation with Alexa Fluor 594 conjugated anti-rabbit antiserum (1:7000 dilution, RAD51). Merged images of DAPI, BRCA2 and RAD51 cells are also shown (Merge).

Having performed the above immunofluorescence, western analysis was next carried out in order to check that the differences in localisation observed were not simply due to changes in protein expression levels after DNA damage. Total protein extracts were prepared before and after phleomycin treatment ($2 \mu\text{g} \cdot \text{ml}^{-1}$ for 24 hours), separated by SDS PAGE on 3-8% Tris-Acetates gels and western blotted. The blot was probed with anti-myc antiserum (1:7000 dilution), anti-RAD51 antiserum (1:1000 dilution), and anti-OPB1 antiserum (1:1000 dilution) as a loading control. The blot was stripped between probings (section 2.11.1). The western blot in Figure 5-14 demonstrates that the levels of RAD51 and BRCA2 12myc remained constant after phleomycin treatment.

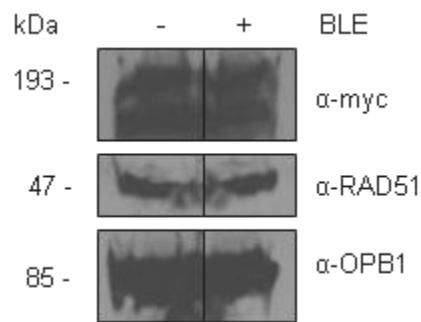


Figure 5-14 Western analysis of BRCA2 12myc and RAD51 in PCF TREU 927 *T. brucei* after exposure to phleomycin.

Total protein extracted from BRCA2 12myc tagged cells was separated by SDS PAGE and western blotted before being probed with anti-myc antiserum (1:7000 dilution) and anti-RAD51 antiserum (1:500 dilution). '-' indicates protein extracts prepared without phleomycin treatment, and '+' indicates protein extracts prepared after phleomycin treatment ($2 \mu\text{g.ml}^{-1}$ BLE for 24 hours). The blots were stripped and re-probed with anti-OPB1 antiserum (1:1000 dilution) as a loading control. Size markers are shown (kDa).

5.3.4 Analysis of the sub-cellular distribution of BRCA2 by aqueous fractionation

In order to examine further the subcellular distribution of BRCA2, aqueous fractionation was carried out on *T. brucei* whole cell extracts as detailed in section 2.2.5 (Zeiner, Sturm, and Campbell, 2003). Nuclear and cytoplasmic protein extracts were prepared from BRCA2 12myc cells after phleomycin treatment ($1 \mu\text{g.ml}^{-1}$ for 18 hours), and control protein extracts without phleomycin treatment were similarly prepared. Protein extracts were separated by SDS-PAGE on 3-8% Tris-Acetate gels before western blotting and probing sequentially with anti-myc antiserum (1:7000 dilution), anti-RAD51 antiserum (1:500 dilution), anti-OPB1 antiserum (1:1000 dilution) and anti-NOG1 antiserum (1:5000 dilution). Blots were stripped between probings as described in section 2.11.1. The western blot probed with NOG1 and OPB1 antiserum in Figure 5-15 demonstrates that the separation of nuclear and cytoplasmic proteins by aqueous fractionation was successful; OPB1 and NOG1 proteins were only present in the cytoplasmic and nuclear fractions, respectively. BRCA2 12myc was detected in both the nuclear and the cytoplasmic fractions, both before and after the induction of DNA damage. This is in agreement with the images obtained by fluorescence microscopy that were not subjected to deconvolution (data not shown) which show BRCA2 localised predominantly nuclearly in the formations discussed in section 5.3.3, but also present at low levels throughout the cytoplasm of the parasite. As seen previously (section 4.3.4), RAD51 was

detected in both nuclear and cytoplasmic fractions both with and without phleomycin treatment.

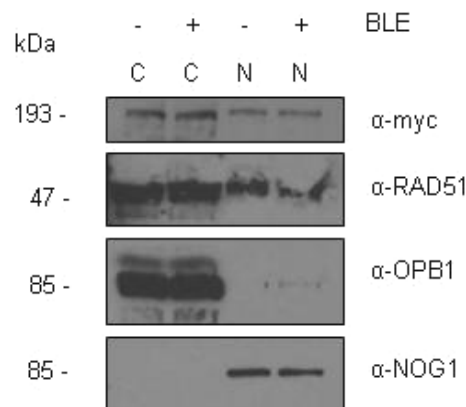


Figure 5-15 Aqueous fractionation of PCF TREU 927 BRCA2 12myc tagged cell line exposed to phleomycin.

Aqueous fractionation was performed to generate protein fractions enriched in soluble cytoplasmic proteins (C) and soluble nuclear proteins (N). Fractions were prepared from the BRCA2 12myc cell line. '-' indicates fractions prepared without phleomycin treatment and '+' indicates fractions prepared after phleomycin treatment ($1 \mu\text{g}\cdot\text{ml}^{-1}$ BLE for 18 hours). Fractions were separated by SDS PAGE and western blotted before being sequentially probed, stripped and re-probed with anti-myc antiserum (1:7000), anti-RAD51 antiserum (1:500 dilution), anti-OPB1 antiserum (1:1000 dilution) and anti-NOG1 antiserum (1:5000 dilution). Size markers are indicated (kDa).

5.4 Summary

The results from the *in vitro* GST pull-down experiment to identify the domains of *T. brucei* BRCA2 that interact with RAD51 are summarised in Figure 5-16, which also shows the protein interacting domains of BRCA2 orthologues from *H. sapiens*, *U. maydis* and *C. elegans*. Perhaps the most surprising finding from the GST pull-down analysis is that these data indicate that *T. brucei* RAD51 interaction with the N-terminal BRC repeat domain of BRCA2 is not observed until 10 BRC repeat motifs are present, at least in this experimental system. This is in direct contrast to *in vitro* observations with the BRC repeats of mammalian BRCA2, where a single repeat is sufficient to bind Rad51 (Wong *et al.*, 1997; Chen *et al.*, 1998; Carreira and Kowalczykowski, 2011), and the BRCA2 orthologues in *C. elegans* and *U. maydis* that only possess a single BRC repeat that is also sufficient to bind Rad51 and function in DNA repair (Figure 5-16; Kojic *et al.*, 2002; Martin *et al.*, 2005; Petalcorin *et al.*, 2006). However, it is hard to evaluate just how weak the observed binding of RAD51 to the BRC repeats of *T. brucei* BRCA2 is in comparison to the equivalent *in vitro* experiments performed with BRC repeat fragments of mammalian BRCA2 (Carreira and Kowalczykowski,

2011). It is possible that the *T. brucei* BRC repeats are simply poor at binding monomeric RAD51, and that *in vivo* they bind predominantly, or with higher affinity, to RAD51-ssDNA nucleoprotein filaments that may not be present in this experimental system. This is supported by the fact that the *T. brucei* BRC repeats most closely resemble the human BRC repeat 7 (with 48.6% similarity for the 'normal' *T. brucei* BRC repeat and 51.4% similarity for the 'degenerate' *T. brucei* BRC repeat), which is a member of the second group of human BRC repeats that are thought to bind with high affinity to Rad51 nucleoprotein filaments and function to stabilise them (Carreira and Kowalczykowski, 2011). If the BRC repeat expansion in *T. brucei* is an adaptation in order to bind with high affinity and stabilise RAD51-ssDNA nucleoprotein filaments, then it is possible that the perfect tandem repeat organisation of the array is critical in this function. The demonstration of binding of the BRC repeat array to RAD51 filaments using electrophoretic mobility shift assays (EMSAs) could be used to test this. It would also be interesting to investigate the DNA repair function of a variant of *T. brucei* BRCA2 with the BRC repeats dispersed, as in mammalian BRCA2. The BRC repeats of *T. brucei* BRCA2 have also been suggested to bind to the five RAD51 paralogues by yeast 2-hybrid analysis (Hall *et al.*, 2011), and these interactions were shown to be stronger than the observed interaction with RAD51 (Hall *et al.*, 2011). However, to date there is no report of an interaction between a BRCA2 orthologue and Rad51 paralogues in any other organism.

Binding of *T. brucei* RAD51 to the C-terminal domain of BRCA2 was observed with all of the BRCA2 variants tested here. RAD51 was shown to bind to the C-tail of BRCA2, the region downstream of the DNA/DSS1-binding domain, and this binding was not affected by mutation of a putative CDK phosphorylation site. RAD51 binding to this C-tail region may be analogous to the discrete C-terminal Rad51-binding site displayed by mammalian BRCA2 and *U. maydis* Brh2 (Esashi *et al.*, 2005; Kojic *et al.*, 2005; Esashi *et al.*, 2007). However, the mammalian Rad51-binding motif is not conserved across the BRCA2 orthologues, and notably not in *U. maydis*, so its functional significance outside mammals is unclear (Kojic *et al.*, 2005). Nonetheless, it would also be interesting to determine if *T. brucei* BRCA2 is indeed phosphorylated, how this phosphorylation changes throughout the cell cycle and the effect of phosphorylation on RAD51 binding (including at the C-terminus). It is highly likely that cell cycle-dependent phosphorylation is a

universal mechanism for the regulation of RAD51 binding and therefore function by BRCA2, as observed in mammalian cells (Esashi *et al.*, 2005; Ayoub *et al.*, 2009), due to the requirement of a homologous template that is most likely present after nuclear DNA replication has been completed. There is some evidence to suggest that the C-terminal Rad51-binding motif present in mammalian BRCA2 plays a critical role in replication by stabilising Rad51 filament formation on nascent DNA, preventing its degradation (Hashimoto *et al.*, 2010; Schlacher *et al.*, 2011). The mapping of the replication phenotype in *T. brucei* to the C-terminus of BRCA2 is consistent with this function (Claire Hartley, PhD Thesis, 2008) and a role for the observed multiple sites of RAD51 binding to the C-terminal region of BRCA2 in the maintenance of replication could be interesting to investigate.

T. brucei RAD51 was also shown to interact with a region of BRCA2 upstream of the C-tail, containing the DNA/DSS1-binding domain and including a putative DMC1 interaction motif (PhePP). Removal of this PhePP motif did not affect RAD51 binding, indicating that binding is occurring downstream of this motif, possibly within the DNA/DSS1-binding domain. DMC1 binding to the putative PhePP motif has not been demonstrated in *T. brucei*, and cannot be ruled out. However, the observed binding of Rad51 by the *U. maydis* orthologue of BRCA2 via the putative PhePP motif (Kojic *et al.*, 2011) does not appear to be conserved in *T. brucei* BRCA2. Further fine mapping of the interaction between RAD51 and the C-terminus of *T. brucei* BRCA2 is required to determine if indeed Rad51 binds to the DNA/DSS1-binding domain, which has not been detected to date in any organism. However, the possibility remains that an uncharacterised RAD51-binding domain exists in the region between the PhePP motif and the DNA/DSS1-binding domain.

The *in vivo* immunolocalisation of BRCA2 and RAD51 has produced a complex picture of the distribution of these proteins in *T. brucei*. BRCA2 appears to be a largely nuclearly located protein both before and after the induction of DNA damage, though subcellular fractionation does detect extra-nuclear protein. Focal accumulations of BRCA2 are clearly visible in the absence of DNA damage. However, once DNA damage has been induced a more complex distribution of BRCA2 is observed. Rings of BRCA2 around the DAPI stained DNA are observed more frequently, both 'smooth' and 'punctate' in nature, as well as BRCA2 foci

distributed throughout the nucleus and at the periphery. Co-localisation with RAD51 foci is observed, but at a much lower frequency than observed in mammalian cells (Mizuta *et al.*, 1997; Tarsounas, Davies, and West, 2003). However, BRCA2 and RAD51 do bind and interact with each other in *T. brucei*, as demonstrated by *in vivo* co-immunoprecipitation in Chapter 6 and the GST pull-down analysis here. RAD51 and BRCA2 localisation has been investigated in multiple systems. In mammalian cells multiple Rad51 foci are observed after DNA damage, the majority of which co-localise with BRCA2 (Mizuta *et al.*, 1997; Tarsounas, Davies, and West, 2003), which is similar to that observed in *Drosophila* (Brough *et al.*, 2008). Localisation of Rad51 in *C. elegans* is observed as multiple subnuclear foci during meiosis, and in *Cebrc-2* null mutants this localisation of Rad51 is dramatically reduced (Martin *et al.*, 2005). Bimolecular fluorescence complementation analysis in *C. elegans* using fluorescently labelled *Cebrc-2* and mammalian Rad51 indicates that *Cebrc-2* binds mammalian Rad51 and forms multiple discrete foci that increase in size after DNA damage (Min *et al.*, 2007). Co-localisation of Rad51 and Brh2 has not been studied in *U. maydis*, but the formation of Rad51 foci is observed after DNA damage in this organism, and is co-incident with the formation of Brh2 foci (Kojic *et al.*, 2006). The composition of DNA repair foci is not known, though it is assumed that they contain multiple copies of DNA repair factors and form a highly efficient DNA repair factory (Lisby and Rothstein, 2009). The relatively low occurrence of RAD51 and BRCA2 co-localisation in *T. brucei* when compared to mammalian cells could point to a role for BRCA2 in establishing the RAD51 foci and then moving away, leaving the RAD51 foci in place. It may also be consistent with BRCA2 acting in DNA damage and an additional role, as discussed in Chapter 4. The most striking observation from the immunolocalisation images are the ‘rings’ of BRCA2 that are observed in a small percentage of cells after DNA damage. It may be possible that this ring structure represents sites of replication located at the periphery of the nucleus (Elias *et al.*, 2002; Calderano *et al.*, 2011), or even binding to chromosome telomeres, which have been demonstrated to be located at the nuclear periphery (Chung *et al.*, 1990). A role in VSG switching can probably be discarded as this analysis was carried out in PCF cells that presumably do not undergo VSG switching.

Taken together, these data reveal a complex picture of *T. brucei* BRCA2 subnuclear behaviour, with a perhaps dynamic redistribution between general peripheral nuclear localisation and accumulation into more discrete foci both at the nuclear periphery and in the interior. Furthermore, this localisation shows surprisingly little overlap with RAD51, which is only seen in subnuclear foci after damage. In contrast to the extensive co-localisation seen between BRCA2 and RAD51 in the nuclei of mammals and *Drosophila* (Mizuta *et al.*, 1997; Tarsounas, Davies, and West, 2003; Brough *et al.*, 2008) after damage, here we see frequent examples where there is no such co-localisation. In addition, when *T. brucei* BRCA2 and RAD51 do localise it appears to be nearly always in a single focus amongst many foci.

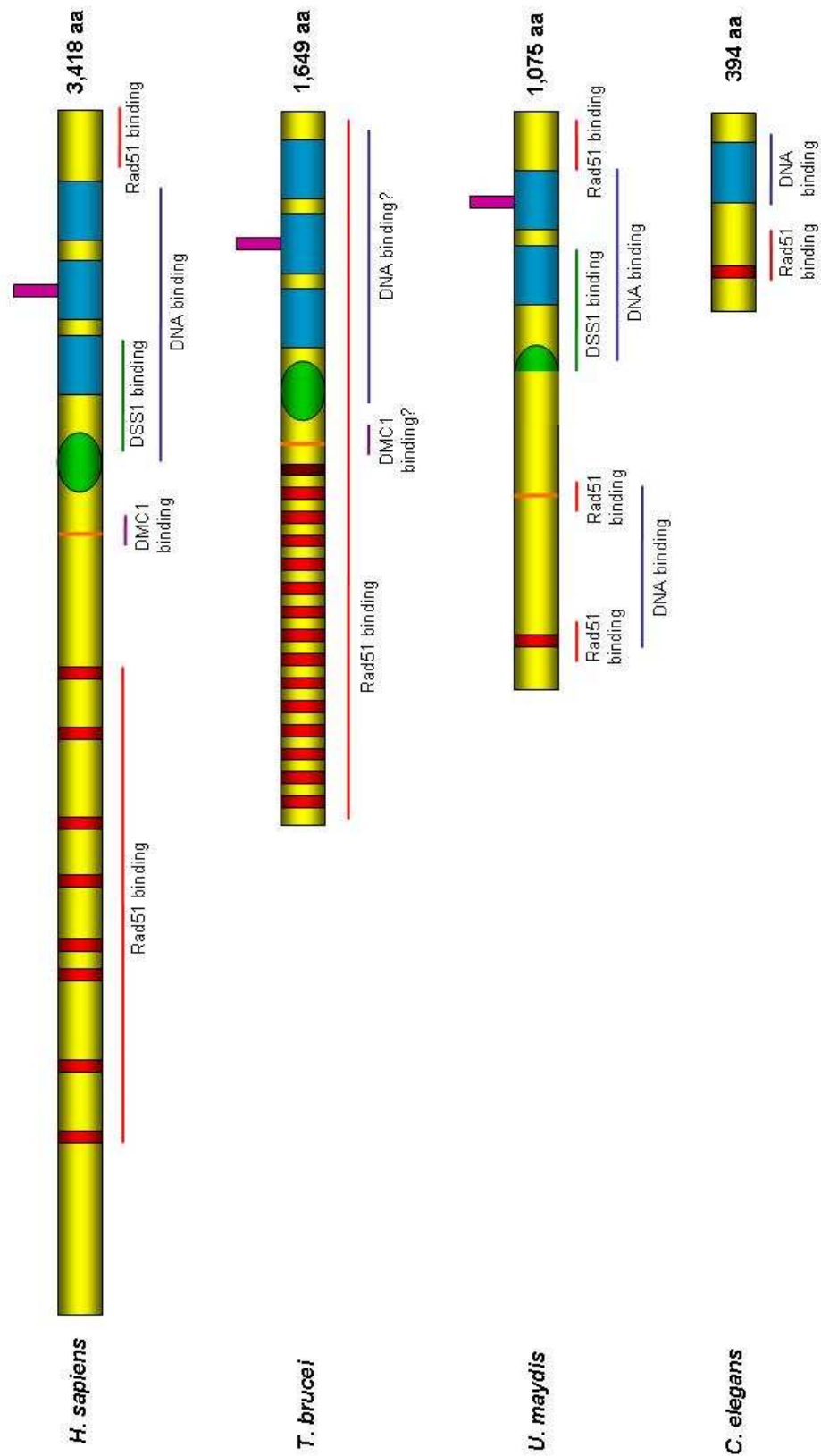


Figure 5-16 A representation of BRCA2 orthologues showing their functional domains and interacting proteins.

BRCA2 orthologues from *H. sapiens*, *T. brucei*, *U. Maydis* and *C. elegans* are shown with the protein domains indicated; BRC repeats (red bars), 'degenerate' BRC repeat (dark red bar), PhePP motif (orange line), alpha-helical domain (green oval/semi-circle), oligonucleotide-binding domain (blue box), and tower domain (purple bar). Interacting proteins and their sites of binding are indicated below the protein, and '?' indicates predicted binding sites. Not to scale.

Chapter 6: Does *T. brucei* BRCA2 interact with CDC45?

6.1 Introduction

In mammalian cells, it has been demonstrated that BRCA2 plays multiple roles to ensure faithful genome replication, although the precise mechanisms remain to be elucidated (Michel *et al.*, 2004; Nagaraju and Scully, 2007; Constanzo, 2011). A number of publications have begun to implicate BRCA2 in the maintenance of replication fork progression (Daboussi *et al.*, 2008), the stabilisation of DNA structures at stalled replication forks (Lomonosov *et al.*, 2003) and, in some cases, DNA replication directly (Michel *et al.*, 2001; Michel *et al.*, 2004). A function for the BRCA2 C-terminal Rad51-binding motif in the protection of stalled replication forks from degradation by Mre11 has been described (Schlacher *et al.*, 2011), and may operate via stabilisation of Rad51 filaments on nascent DNA (Hashimoto *et al.*, 2010). Mutation of the BRCA2 C-terminal CDK phosphorylation site at Serine 3291 to Alanine, which does not support Rad51 binding to this motif, was shown to be deficient in this protection function, despite being HR proficient (Schlacher *et al.*, 2011). Mutation of the equivalent C-terminal Rad51-binding motif in avian BRCA2, which also ablates Rad51 binding, has been demonstrated to link the observed faster disassembly of Rad51 subnuclear complexes to the early onset of mitosis, despite having no effect on HR-mediated DNA repair (Ayoub *et al.*, 2009). BRCA2 has also been shown to interact with BRAF35 (also called HMG20b), a member of the high-motility group of non-sequence specific DNA-binding proteins (Wang *et al.*, 1998; Sumoy *et al.*, 2000; Marmorstein *et al.*, 2001; Lee *et al.*, 2011). This interaction was localised to the BRC repeats of BRCA2, and BRAF35 displays the highest affinity for BRC repeat 5, a motif that binds poorly to Rad51 (Lee *et al.*, 2011; Carreira and Kowalczykowski, 2011). Depletion of *BRAF35* by *RNAi* delays and disrupts the completion of cell division by cytokinesis (Lee *et al.*, 2011) in a phenotype previously detected in *BRCA2*-deficient cells (Daniels *et al.*, 2004). Therefore, a novel function of BRAF35 in facilitating the completion of cytokinesis via an interaction with the BRC repeats of BRCA2 has been proposed (Lee *et al.*, 2011). A role for BRCA2 in facilitating the completion of cell division by cytokinesis has also been observed (Daniels *et al.*, 2004; Jonsdottir *et al.*, 2009; Vinciguerra *et al.*, 2010; Rowley *et al.*, 2011), though doubt has been cast due to the absence of hallmarks of a failure to complete cytokinesis in HeLa cells depleted of *BRCA2* by *RNAi* and a lack of BRCA2 localisation to cytokinetic structures (Lekomtsev *et*

al., 2010). BRCA2 has also been shown to associate with telomeres in mouse embryonic fibroblasts during the S and G2 phases of the cell cycle (Badie *et al.*, 2010), and is proposed to act in loading Rad51 to facilitate telomere replication and protection by capping (Badie *et al.*, 2010). Finally, in the highly radiation resistant fungus *U. maydis*, the BRCA2 orthologue Brh2 has been shown to promote template switching reactions that enable HR-mediated bypass of DNA replication blocking lesions (Mazloun and Holloman, 2009).

brca2^{-/-} mutants in BSF Lister 427 *T. brucei* display a replication phenotype that is not observed in other DNA repair mutants, most notably *rad51*^{-/-} (Claire Hartley, PhD Thesis, 2008), which is consistent with the initiation of cytokinesis prior to the completion of nuclear DNA replication (Claire Hartley, PhD Thesis, 2008). There is evidence to suggest that the C-terminal region of *T. brucei* BRCA2 may function in this replication role. Firstly, DAPI analysis of *brca2*^{-/-} cells in which the C-terminal region of BRCA2 in isolation was re-expressed suggested partial complementation of the replication defect observed in the *brca2*^{-/-} mutant cells, as the number of aberrant cells was more comparable with wild-type and full-length *BRCA2* re-expresser cell lines (Claire Hartley, PhD Thesis, 2008). Secondly, the re-expression of a variant of *BRCA2* consisting of the BRC repeat region fused to the RPA50 subunit continued to generate aberrant cells, indicating that C-terminal-specific functions underlie this replication phenotype (Claire Hartley, PhD Thesis, 2008). The publication of an observed interaction between the C-terminal domain of BRCA2 and a region of the *T. brucei* homologue of CDC45 (Oyola, Bringaud, and Melville, 2009), a protein essential for DNA replication (see below; Zou, Mitchell, and Stillman, 1997; Tercero, Labib, and Diffley, 2000), presented a possible novel mechanism for the involvement of BRCA2 in DNA replication. This publication did not explore this question, but perhaps the interaction with CDC45 allows homology-directed DNA repair of stalled replication forks in a mechanism to ensure that replication stalls are overcome in *T. brucei*.

CDC45 is a protein originally identified in *Saccharomyces cerevisiae* (Hardy, 1997) that is essential for the initiation and progression of DNA replication (Zou, Mitchell, and Stillman, 1997; Tercero, Labib, and Diffley, 2000). CDC45 localises to the nucleus (Hopwood and Dalton, 1996) and has been shown to bind to the minichromosome maintenance (MCM2-7) and GINS complexes to form the

replicative helicase, the CMG complex (CDC45-MCM-GINS; Aparicio, Ibarra, and Mendez, 2006; Aparicio *et al.*, 2009; Ilves *et al.*, 2010; Costa *et al.*, 2011). CDC45 is thought to play a critical role in firing assembled pre-replication complexes to allow the start of DNA replication (Zou, Mitchell, and Stillman, 1997), and has also been shown to move with replication forks, presumably functioning during fork progression (Aparicio, Weinstein, and Bell, 1997). The MCM2-7 proteins have weak DNA helicase activity on their own, and binding to CDC45 and GINS stimulates this helicase activity (Aparicio *et al.*, 2009; Ilves *et al.*, 2010; Costa *et al.*, 2011), allowing unwinding of DNA at the origin of replication. The components of the CMG complex have recently been identified in *T. brucei* and depletion of CDC45 by *RNAi* was observed to be lethal (Dang and Li, 2011). Further observations indicate that CDC45 is excluded from the nucleus after the completion of nuclear DNA replication (Dang and Li, 2011), and may suggest a possible role for CDC45 in a mechanism to prevent re-replication of nuclear DNA during the cell cycle in trypanosomes (Dang and Li, 2011).

Oyola *et al.*, (2009) used a *T. brucei* cDNA library in a yeast 2-hybrid screen to detect potential BRCA2 interactors. A homologue of *T. brucei* CDC45 was identified in approximately one-third of colonies analysed. Further yeast 2-hybrid analysis was carried out with the two 'halves' of BRCA2, and positive colonies were only obtained with the C-terminal half of BRCA2. The interaction was quantitatively much stronger than that observed with a positive control, and only a medium strength interaction was observed between BRCA2 and RAD51 using the same assay. Co-immunoprecipitation analysis was carried out using full-length BRCA2 over-expressed in *T. brucei* or the C-terminal half of BRCA2 over-expressed as a hexa-histidine fusion in *E. coli*. Interaction with a fragment of CDC45 (residues 371-523) over expressed in *E. coli* as a GST fusion was tested for and observed with both the full-length and the C-terminal fragment of BRCA2. The detection of this interaction between the C-terminal half of BRCA2 and CDC45 in *T. brucei* was interesting as a potential explanation for the replication phenotype observed in BSF *brca2*^{-/-} mutants (Hartley and McCulloch, 2008), and is consistent with the location of the replication phenotype to the C-terminus of BRCA2 (Claire Hartley, PhD Thesis, 2008).

This chapter aims to test the validity of the putative interaction between BRCA2 and CDC45 in *T. brucei*. Two approaches were taken. Firstly, the interaction was

investigated *in vivo* by co-immunoprecipitation using epitope-tagged proteins expressed from their endogenous loci in *T. brucei*. Secondly, *in vitro* GST pull-down was performed using fusion proteins over-expressed in *E. coli*. Both of these approaches have been used successfully to identify interacting proteins in *T. brucei* (Dobson *et al.*, 2011; Calvin Tiengwe, PhD Thesis, 2010), and GST pull-down was used to examine BRCA2-RAD51 interaction in this work (Chapter 5).

6.2 *In vivo* co-immunoprecipitation

The lack of antiserum against *T. brucei* CDC45 meant that in order to detect the presence of this protein a tag consisting of twelve copies of the c-myc epitope was added to the C-terminus in PCF TREU 927 cells, as described previously (section 5.3.1). This epitope tag allowed the immunoprecipitation of CDC45 using antiserum against the c-myc epitope.

6.2.1 Endogenous C-terminal epitope tagging strategy

The pNAT^{x12myc} construct, which enables the fusion of a C-terminal 12myc epitope tag at the endogenous loci of a gene of interest, was modified to target *CDC45* (Figure 6-1; Alford and Horn, 2008). The epitope tagging strategy is described in section 5.3.1. A 925 bp region of the 3' end of the *CDC45* ORF was PCR-amplified using primers 5 and 6, which contained *HindIII* and *XbaI* restriction sites, respectively, to allow cloning into the construct upstream of the epitope tag. The DNA fragment contained a unique restriction site (*EcoRV*) to allow linearisation prior to transformation. For transformation, the construct was linearised by restriction digestion, the digested DNA was then ethanol precipitated and approximately 5 µg of the resuspended DNA was used for each transformation.

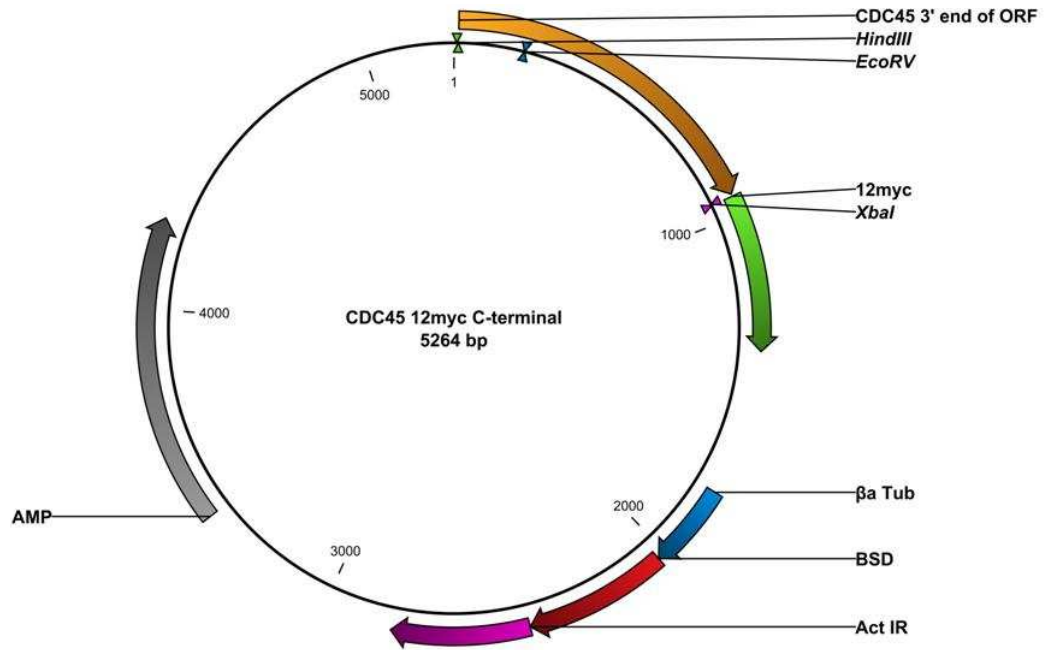


Figure 6-1 Construct used for C-terminal 12myc tagging of *T. brucei* CDC45. 925 bp of the 3' end of the *CDC45* ORF (orange) containing a unique restriction site (*EcoRV*) was cloned into *HindIII* and *XbaI* restriction sites. The 12myc epitope tag (green) consists of 12 tandemly repeated copies of the c-myc epitope. The *BSD* resistance cassette is shown (red) flanked by the *tubulin* (β a Tub, blue) and *actin* (Act IR, purple) intergenic sequences. *AMP*: Ampicillin resistance ORF (grey). Sizes are shown (bp).

6.2.2 Generation of a *CDC45*^{-/+} mutant cell line in PCF TREU 927 *T. brucei*

In order to confirm that the presence of the 12myc epitope tag was not interfering with the function of the CDC45 protein it was decided to generate the tagged cell line in a *CDC45* heterozygous (-/+) background, meaning that all of the CDC45 expressed would contain the epitope tag. CDC45 is an essential protein in mammals, *S. cerevisiae* and *Xenopus laevis* (Hardy, 1997; Zou, Mitchell, and Stillman, 1997; Mimura and Takisawa, 1998; Tercero, Labib, and Diffley, 2000; Aparicio *et al.*, 2009) and *RNAi* of *T. brucei* CDC45 in PCF cells leads to cell death (Dang and Li, 2011). Therefore the generation of the tagged cell line in a heterozygous background would confirm that the tagged protein is functional.

The *CDC45*^{-/+} mutant cell line was generated in PCF TREU 927 *T. brucei* using a classical gene knockout strategy where the entire *CDC45* ORF is removed. A *CDC45* knockout construct, Δ *CDC45*::*PUR* (Figure 6-2), was assembled. The construct contains regions of the 5' and 3' UTRs flanking the *CDC45* ORF cloned into pBluescript and used as targeting sequence to enable homologous

recombination and replacement of the entire *CDC45* ORF with an antibiotic resistance cassette following transformation. Primers were designed to amplify 503 bp of the 5' UTR and 526 bp of the 3' UTR flanking the *CDC45* ORF. The 5' UTR was amplified using primers 37 and 40, which contained *Xho*I and *Nru*I restriction sites, respectively. The 3' UTR was amplified using primers 41 and 42, which contained *Nru*I and *Xba*I restriction sites, respectively. The two DNA fragments were cloned into pBluescript in a three-way ligation using the *Xho*I, *Nru*I and *Xba*I restriction sites. To allow selection of the construct that has integrated into the genome a *puromycin* (*PUR*) resistance cassette, prepared by restriction digestion with *Nru*I from Δ *BRCA2*::*PUR* construct (section 3.2.1), was blunt cloned between the flanks using the *Nru*I restriction site. The *PUR* resistance cassette contained mRNA processing signals derived from *actin* and *tubulin* intergenic sequences, flanking the antibiotic resistance ORF, to allow RNA *trans*-splicing and polyadenylation, respectively. For transformation, the construct was excised from pBluescript by restriction digestion with *Xho*I and *Xba*I, the digested DNA was then ethanol precipitated and approximately 5 μ g of the resuspended DNA was used for transformation.

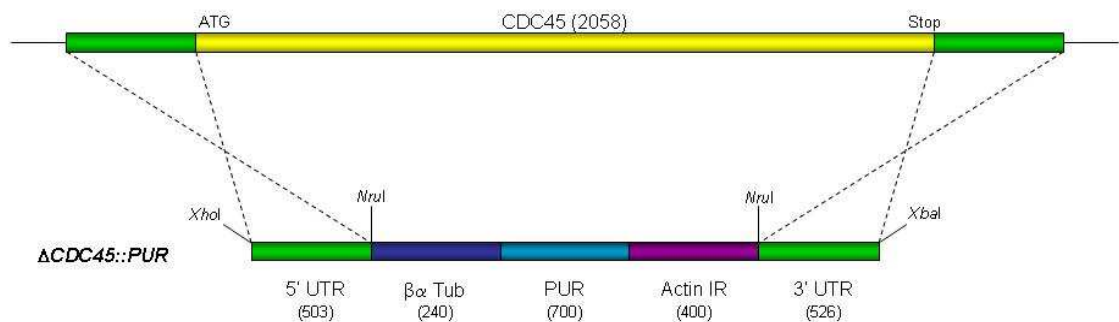


Figure 6-2 *CDC45* gene deletion construct.

Restriction map of the construct used for the deletion of *CDC45* is shown, relative to the *CDC45* ORF (top). Sizes of the individual components are shown (bp) and are not to scale. Constructs were cloned into pBluescript and excised using the *Xho*I and *Xba*I restriction sites shown. 5' UTR and 3' UTR correspond to un-translated regions upstream and downstream of the *CDC45* ORF, respectively. $\beta\alpha$ Tub: $\beta\alpha$ *tubulin* intergenic region, Actin IR: *Actin* intergenic region, *PUR*: *puromycin* resistance ORF.

A transformation was carried out in order to generate a *CDC45*^{-/+} mutant cell line using the Δ *CDC45*::*PUR* construct. To do this, PCF wild-type TREU 927 cells were transformed and antibiotic resistant transformants were selected by placing cells on SDM-79 media supplemented with 1 μ g.ml⁻¹ puromycin.

The generation of *CDC45*^{-/+} mutants was confirmed by PCR analysis performed on genomic DNA extracted from six puromycin resistant clones. PCR was performed using primers specific to the *PUR* resistance ORF (primers 144 and 145) in order to confirm that the cassette was integrated into the genome. Integration into the correct locus was checked by PCR using a forward primer specific to the *PUR* resistance ORF (primer 144) and a reverse primer located in the 3' UTR outside of the region cloned in the gene deletion construct (primer 59). The location of the primers and expected sizes of the PCR products are displayed in Figure 6-3A. The agarose gel in Figure 6-3B demonstrates the presence of the *PUR* resistance gene in all of the putative *CDC45*^{-/+} mutant clones analysed. The PCR with primers 144 and 59 demonstrates that in two cell lines (indicated by "*" in Figure 6-3B) the gene deletion construct has integrated in the correct location and replaced a *CDC45* ORF. The *CDC45*^{-/+} mutant clone chosen for further analysis is referred to as *CDC45*^{-/+} *PUR*.

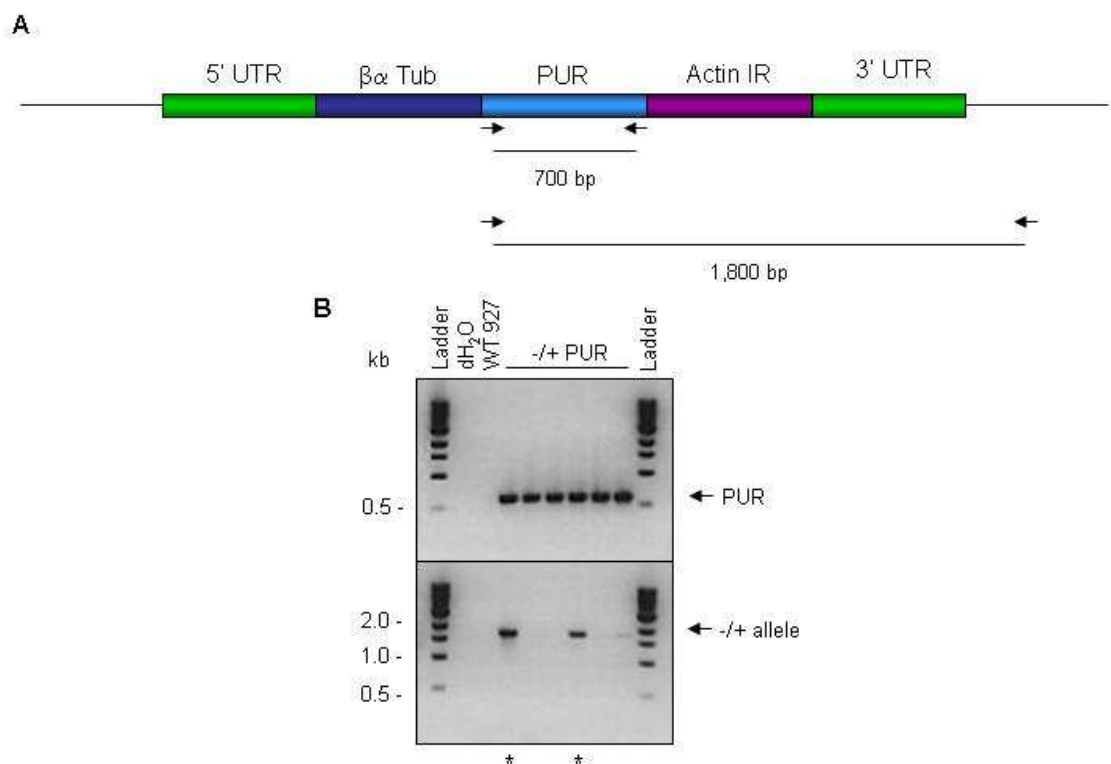


Figure 6-3 Confirmation of PCF TREU 927 *CDC45*^{-/+} mutant cell lines by PCR. (A) Primers used to amplify the puromycin resistance ORF (*PUR*), or a region spanning *PUR* and the *CDC45* 3'UTR, are indicated (black arrows), with the expected sizes of the resulting PCR products shown (bp). (B) An agarose gel of the PCR products obtained using the primers, described above, and genomic DNA extracted from wild-type TREU 927 (WT 927) and putative *CDC45*^{-/+} mutant cell lines. Distilled water (dH₂O) was used as a negative control. The PCR products produced from the *PUR* and *-/+* allele are indicated (black arrows), and size markers are shown (Ladder, kb). "*" indicates *CDC45*^{-/+} mutants that are confirmed by PCR.

6.2.3 Generation of C-terminal 12myc tagged *CDC45*-/+ cell line

A transformation was next carried out in order to generate a C-terminal 12myc tagged *CDC45* cell line in the *CDC45*-/+ background. To do this, the *CDC45*-/+ *PUR* cell line was transformed with the *CDC45* 12myc tagging construct (section 5.3.1) and antibiotic resistant transformants were selected by placing cells on SDM-79 media supplemented with 10 $\mu\text{g}\cdot\text{ml}^{-1}$ blasticidin and 0.5 $\mu\text{g}\cdot\text{ml}^{-1}$ puromycin. The clones obtained from transformation were screened by western blot performed on total protein extracted from six blasticidin and puromycin resistant clones. The total protein extracts were separated by SDS PAGE on a 3-8% Tris-Acetate gel before western blotting and probing with anti-myc antiserum (Millipore) at a dilution of 1:7000. The western blot in Figure 6-4 demonstrates that four of the six putative *CDC45*-/+ 12myc cell lines contain a protein band of the expected size (93 kDa) for *CDC45* 12myc. Also present is a smaller protein band, which could be a degradation product or a post-translationally modified *CDC45* variant (e.g. phosphorylated); it may also simply result from the antiserum binding to non-specific *T. brucei* proteins, though why then it would not be detected in wild-type cells is unclear. One of these clones was taken forward for further analysis. Given the efficiency of generating blasticidin and puromycin resistant cells that detectably express myc-tagged *CDC45*, and the fact that the cells display no gross growth rate changes (data not shown), it seems likely that the C-terminal epitope tag does not critically impair *CDC45* function. However, without checking for the presence of a wild-type *CDC45* allele, this remains to be confirmed.

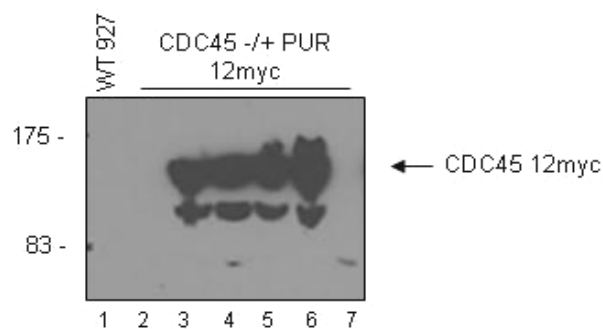


Figure 6-4 Confirmation of expression of C-terminal 12myc tagged *CDC45*-/+ by western analysis.

Total protein extract from wild-type TREU 927 (WT 927) and putative 12myc tagged *CDC45*-/+*PUR* cell lines, were separated by SDS-PAGE and western blotted before being probed with anti-myc antiserum (1:7000 dilution). The band predicted to correspond with the *CDC45* 12myc tagged protein is indicated (black arrow), and size markers are shown (kDa).

6.2.4 Co-immunoprecipitation using the *CDC45*-/+ 12myc tagged cell line

Co-immunoprecipitation using the *CDC45*-/+ 12myc tagged cell line, and wild-type TREU 927 cells as a control was next performed. Total protein was extracted (section 2.2.4.2) from cells; this is referred to as the input. Immunoprecipitation of CDC45 12myc was carried out using anti-myc antiserum conjugated to agarose beads (Millipore) as described in section 2.12; protein recovered is referred to as the elution. The input and elution protein samples were separated by SDS PAGE on 3-8% Tris-Acetate gels, western blotted and first probed with anti-BRCA2 antiserum at a dilution of 1:200. The blots were then stripped and re-probed with anti-myc antiserum at a dilution of 1:7000. The western blot in Figure 6-5 demonstrates that in both the wild-type TREU 927 and *CDC45*-/+ 12myc cell lines a band of the expected size for the BRCA2 protein (176 kDa) was present in the input samples (lanes 1 and 2). A band of the expected size for CDC45 12myc (93 kDa) was present only in the tagged cell line input (lane 2) and elution (lane 4). The elution samples demonstrate that CDC45 12myc was successfully immunoprecipitated from the tagged cell line (lane 4), and was not detectable in wild-type cells (lane 3). No BRCA2 protein was detected in the elution sample of either cell line, suggesting that an interaction was undetectable under these conditions. However, given the unreliable nature of the detection of BRCA2 with the anti-BRCA2 antiserum (see previous chapters), this could not be considered a definitive experiment.

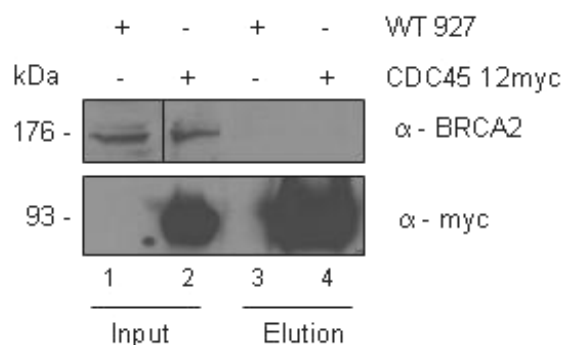


Figure 6-5 Co-immunoprecipitation analysis of the interaction between CDC45 12myc and BRCA2.

Total protein extracts from wild-type TREU 927 (WT 927) and *CDC45*-/+ 12myc cell lines were subjected to immunoprecipitation using anti-myc antiserum conjugated to agarose beads. Input and elution samples were separated by SDS-PAGE and western blotted before being probed with anti-myc antiserum (1:7000 dilution) and anti-BRCA2 anti-serum (1:200 dilution). Size markers are indicated (kDa).

6.2.5 Generation of C-terminal double-tagged cell lines in PCF TREU 927 *T. brucei*

In order to overcome the limitations of the anti-BRCA2 antiserum it was decided to generate cell lines in which both BRCA2 and CDC45 were epitope tagged at the C-terminus. A construct was assembled to allow the addition of a 6HA epitope tag to the C-terminus of BRCA2 at the endogenous locus in the *T. brucei* genome. This 6HA tagging construct was identical to the 12 myc tagging construct except the 12myc epitope tag was replaced with a 6HA epitope tag, and a *bleomycin* (*BLE*) resistance cassette was inserted in place of the *BSD* resistance cassette to allow selection of clones. The cloning of the section of the 3' end of the *BRCA2* ORF was carried out using the same strategy as for the *BRCA2* 12myc construct (section 5.3.1). Primers 32 and 33 were used to amplify 491 bp region at the 3' end of the *BRCA2* ORF containing a unique *SphI* restriction site.

It was also decided to create a positive control for the co-immunoprecipitation reaction and test for the functionality of interactions with the epitope tagged BRCA2 protein. It has been demonstrated that both mammalian and *T. brucei* BRCA2 and Rad51 interact strongly with each other *in vitro* (Chapter 5;Sharan *et al.*, 1997;Chen *et al.*, 1998;Marmorstein, Ouchi, and Aaronson, 1998). The generation of a *T. brucei* cell line with both BRCA2 and RAD51 C-terminally epitope tagged allowed this interaction to act as a positive control for the co-immunoprecipitation experiment. A construct to allow the addition of a 12myc epitope tag to the C-terminus of RAD51 at the endogenous locus in the *T. brucei* genome was generated previously (gift, Rachel Dobson) with a *blastidicin* (*BSD*) resistance cassette for selection (Figure 6-1). The unique site used for linearisation of this construct was *BlnI*. In a recent study (Dang and Li, 2011), endogenously tagged CDC45 with a C-terminal epitope tag consisting of 3 copies of the HA epitope was demonstrated to interact with the other two members of the CMG complex in *T. brucei*. This provides some evidence that C-terminal epitope tagging of CDC45 does not impair its ability to functionally interact with members of the CMG complex, albeit in a slightly different context to that used here. However, we cannot rule out that 12myc tagging of CDC45 somehow impairs functional interaction with BRCA2, or with other proteins, despite the fact that the *CDC45*^{+/-} 12myc cells grow normally (data not shown).

Because of the limitations in the availability of suitable resistance cassettes it was decided to generate the two double-tagged cell lines in wild-type PCF TREU 927 cells, as opposed to heterozygous backgrounds for all tagged proteins. This meant that half of the protein expressed in each cell line was epitope tagged as only one allele had the tagging construct integrated. The generation of the BRCA2 6HA tagged cell line was carried out by the transformation of wild-type PCF TREU 927 cells with the linearised BRCA2 6HA construct. Cells were selected on SDM-79 media supplemented with $15 \mu\text{g}\cdot\text{ml}^{-1}$ Zeocin (Invitrogen) and six of the resulting clones were chosen. BRCA2 6HA protein expression was confirmed by western blot (data not shown), prior to further transformation. One of these confirmed cell lines was then subjected to two transformations, with the linearised CDC45 12myc construct or the linearised RAD51 12myc construct. For each transformation, cells were selected on SDM-79 media supplemented with $10 \mu\text{g}\cdot\text{ml}^{-1}$ blasticidin and $10 \mu\text{g}\cdot\text{ml}^{-1}$ Zeocin, and six of the resulting clones were chosen from each transformation.

6.2.6 Confirmation of C-terminal double-tagged cell lines

The twelve putative double-tagged cell lines were subject to screening by western blot in order to confirm the expression of the two epitope tagged proteins in each. Total protein was extracted from wild-type TREU 927 and the twelve double-tagged cell lines and separated by SDS PAGE on 3-8% Tris-Acetate gels, western blotted and probed with anti-HA antiserum (Sigma) at a dilution of 1:10000. The blots were then stripped and re-probed with anti-myc antiserum (Millipore) at a dilution of 1:7000. The western blots in Figure 6-6 demonstrate that all twelve of the tested clones contained correctly expressed BRCA2 6HA tagged protein of the expected size (183 kDa). Half of the twelve clones also expressed a protein of the expected size for the myc-tagged variants; 55 kDa for RAD51 12myc, or 93 kDa for CDC45 12myc. One of each of the double-tagged cell lines was chosen for co-immunoprecipitation analysis.

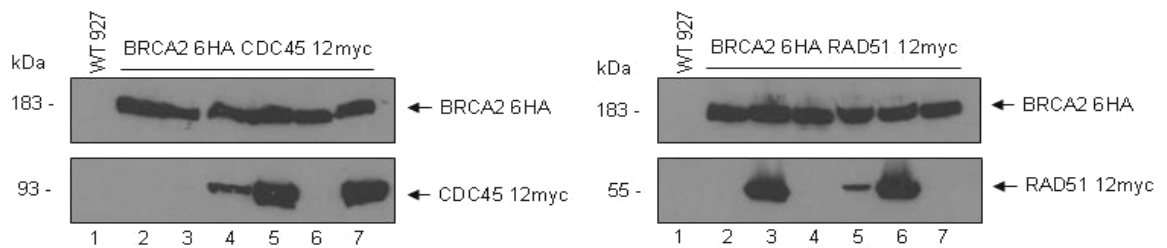


Figure 6-6 Confirmation of co-expression of C-terminal epitope tagged proteins in PCF TREU 927 *T. brucei*.

Total protein extracts from wild-type TREU 927 (WT 927) and the two putative double-tagged cell lines (BRCA2 6HA CDC45 12myc and BRCA2 6HA RAD51 12myc) were separated by SDS-PAGE and western blotted before being probed with anti-HA antiserum (1:10000 dilution, top). The blots were stripped and re-probed with anti-myc antiserum (1:7000 dilution, bottom). The bands produced by BRCA2 6HA, CDC45 12myc, and RAD51 12myc proteins are indicated (black arrows), and size markers are shown (kDa).

6.2.7 Co-immunoprecipitation using C-terminal double-tagged cell lines

Co-immunoprecipitation using the two C-terminal double-tagged cell lines, and wild-type TREU 927 cells as a control, was performed with anti-myc antiserum as described above (section 6.2.4). The co-immunoprecipitation experiment was additionally performed using anti-HA antiserum conjugated to agarose beads (Roche). The input and elution samples were separated by SDS PAGE on 3-8% Tris-Acetate gels, western blotted and probed with anti-HA antiserum at a dilution of 1:10000. The blot was then stripped and re-probed with anti-myc antiserum at a dilution of 1:7000.

The western blots in Figure 6-7 show analysis of interaction between BRCA2 and RAD51, and also BRCA2 and CDC45. The input samples demonstrate expression of tagged proteins of the expected size for the tagged cell lines analysed, but absent in wild-type cells. The elution samples demonstrate the successful immunoprecipitation of BRCA2 6HA by the anti-HA beads and either RAD51 12myc or CDC45 12myc by the anti-myc beads. An interaction between either RAD51 or CDC45 and BRCA2 could not be detected using the anti-HA immunoprecipitation, as evidenced by the blank anti-myc probed elution blot (Figure 6-7A). However, an interaction between BRCA2 and RAD51 was detected using the anti-myc immunoprecipitation of RAD51 12myc, as evidenced by the presence of a band consistent with BRCA2 6HA in the anti-HA probed elution blot (Figure 6-7B). In contrast, an interaction between CDC45 and BRCA2 was not detected. This could be because the proteins do not interact, or could result

from a variety of experimental reasons, the most probable of which is that such an interaction is not strong or abundant enough to survive the relatively harsh conditions during such a co-immunoprecipitation experiment.

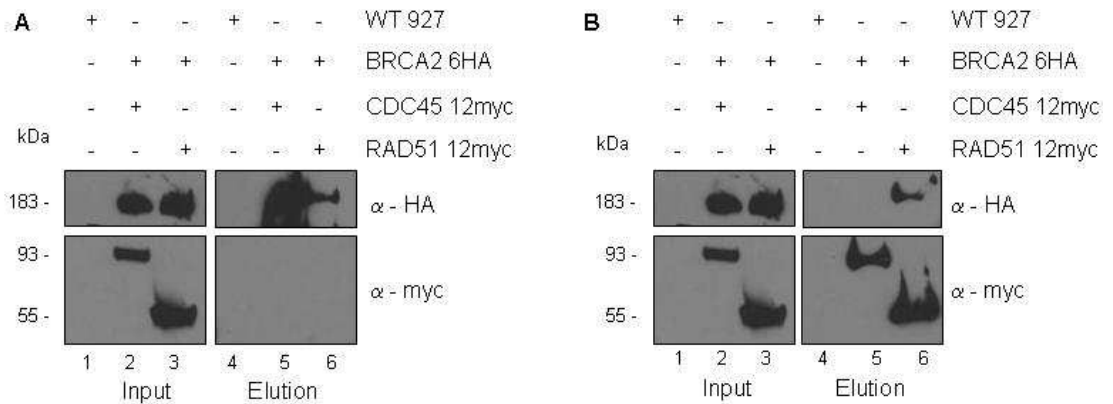


Figure 6-7 Co-immunoprecipitation analysis of the interaction between BRCA2 and CDC45, and between BRCA2 and RAD51.

Total protein extracts from wild-type TREU 927 (WT 927) and the double-tagged cell lines (BRCA2 6HA CDC45 12myc, and BRCA2 6HA RAD51 12myc) were immunoprecipitated using anti-HA antiserum (A) or anti-myc antiserum (B) conjugated to agarose beads. Input and elution samples were separated by SDS-PAGE and western blotted before being probed with anti-myc antiserum (1:7000 dilution) and anti-HA anti-serum (1:10000 dilution). Size markers are shown (kDa).

6.2.8 Co-immunoprecipitation after exposure to DNA damage

In order to try and increase the probability of detecting an interaction between CDC45 and BRCA2, it was decided to repeat the co-immunoprecipitation experiment with protein extracted after the cells had been treated with DNA damage. The rationale behind this was that BRCA2-CDC45 interaction *in vivo* may only occur in the presence of replication-blocking lesions, which are only present in low abundance during normal growth in culture. Two types of DNA damaging agent were therefore chosen; methyl methanesulphonate (MMS) and hydroxyurea (HU). MMS is a DNA alkylating agent and may form DNA replication fork barriers (Brookes and Lawley, 1961; Reiter *et al.*, 1967; Beranek, 1990; Sedgwick, 2004). *T. brucei* mutants of components of the homologous recombination machinery, *rad51*, *rad51-3*, *rad51-5* and *brca2*, all display increased sensitivity to MMS (McCulloch and Barry, 1999; Proudfoot and McCulloch, 2005; Hartley and McCulloch, 2008). HU acts by inhibiting ribonucleotide reductase, an enzyme involved in deoxyribonucleotide triphosphate (dNTP) synthesis, depleting the nucleotide pool and thereby stalling DNA replication (Hofer *et al.*, 1997). HU has been used to successfully

synchronise bloodstream *T. brucei* by causing an S-phase block (Forsythe, McCulloch, and Hammarton, 2009). Wild-type TREU 927 cells and the two double-tagged cell lines were treated with 0.002% MMS for 16 hours, or 0.3 mM HU for 16 hours, before protein was extracted as described in section 2.2.4.2. Immunoprecipitation using anti-myc antiserum conjugated to agarose beads and also anti-HA antiserum conjugated to agarose beads was carried out as described in section 6.2.4. The input and elution samples were separated by SDS PAGE on 3-8% Tris-Acetate gels, western blotted and probed with anti-HA antiserum at a dilution of 1:10000. The blot was then stripped and re-probed with anti-myc antiserum at a dilution of 1:7000.

The western blots in Figure 6-8 and Figure 6-9 show analysis of interaction between BRCA2 and RAD51, and also BRCA2 and CDC45, after DNA damage with HU and MMS, respectively. For both co-immunoprecipitation experiments performed, in the presence of MMS or HU, both results are essentially equivalent to each other, and to the data presented in Figure 6-7, in the absence of DNA damage and despite this increased amount of DNA damage from both treatments, an interaction between BRCA2 and CDC45 could still not be detected.

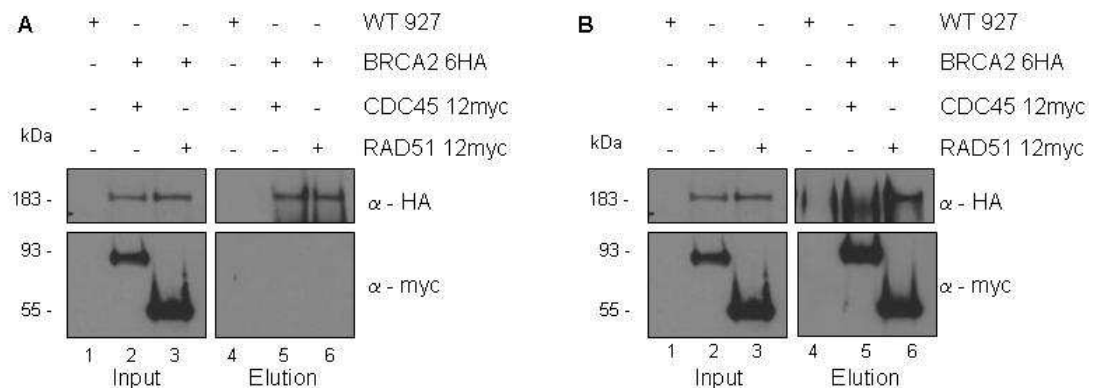


Figure 6-8 Co-immunoprecipitation analysis of the interaction between BRCA2 and CDC45, and BRCA2 and RAD51 after exposure to hydroxyurea.

Total protein extracts from wild-type TREU 927 (WT 927) and double-tagged cell lines (BRCA2 6HA CDC45 12myc and BRCA2 6HA RAD51 12myc) prepared after treatment with hydroxyurea (0.3 mM for 16 hours) were immunoprecipitated using anti-HA antiserum (A) or anti-myc antiserum (B) conjugated to agarose beads. Input and elution samples were separated by SDS-PAGE and western blotted before being probed with anti-myc antiserum (1:7000 dilution) and anti-HA anti-serum (1:10000 dilution). Size markers are indicated (kDa).

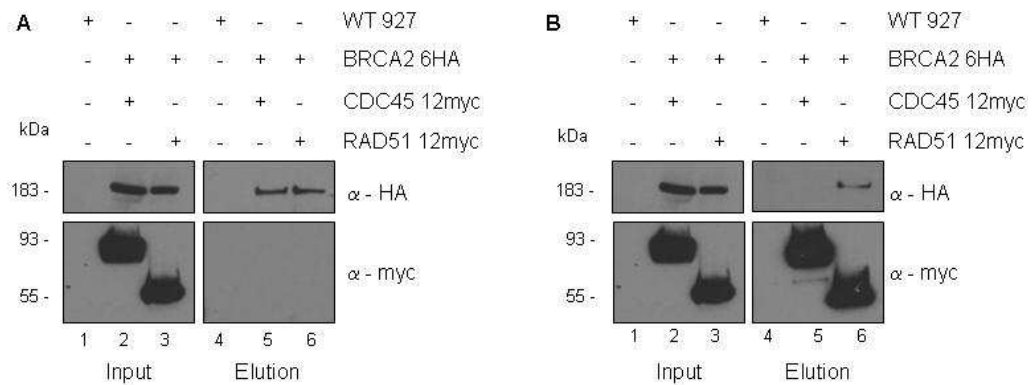


Figure 6-9 Co-immunoprecipitation analysis of the interaction between BRCA2 and CDC45, and BRCA2 and RAD51 after exposure to MMS.

Protein extracts from wild-type TREU 927 (WT 927) and double-tagged cell lines (BRCA2 6HA CDC45 12myc and BRCA2 6HA RAD51 12myc) prepared after treatment with MMS (0.002% for 16 hours) were immunoprecipitated using anti-HA antiserum (A) or anti-myc antiserum (B) conjugated to agarose beads. Input and elution samples were separated by SDS-PAGE and western blotted before being probed with anti-myc antiserum (1:7000 dilution) and anti-HA anti-serum (1:10000 dilution). Size markers are indicated (kDa).

6.2.8.1 Confirmation of DNA damage

In order to ensure that the above HU treatment resulted in replication stalling, the cells used for the immunoprecipitation were analysed, in parallel, for the distribution of cells in the various phases of the cell cycle. This was done by analysing DNA content by fluorescent-activated cell sorting (FACS) after propidium iodide-staining of the DNA of the cells. Samples from untreated wild-type PCF TREU 927, and from the two double-tagged cell lines treated with HU, were prepared as described in section 2.2.4.2, and a total of 10^4 cells were sorted using detector FL2-A. The FACS plots in Figure 6-10 show that the wild-type, non HU-treated, cell population gave a characteristic flow cytometry profile comprising two peaks; cells in the G1 phase of the cell cycle are represented by the peak at position 200, corresponding to 2C DNA content (C represents haploid DNA content); and cells with double DNA content (4C) are in G2 phase, M phase or cytokinesis and appear as a peak at position 400. S phase cells with intermediate DNA contents were detected between the two peaks (Chowdhury, Zhao, and Englund, 2008; Forsythe, McCulloch, and Hammarton, 2009). The double-tagged, HU-treated cell populations gave a flow cytometry profile characteristic of cells with an S-phase block, with the majority of cells present in a peak between the 200 and 400 position; this indicates that the treatment with HU caused stalling of replication and accumulation of cells in this cell cycle stage. As MMS is in more routine use in the laboratory during analysis

of the sensitivity of DNA repair mutants, it was deemed unnecessary to check its effectiveness in this experiment.

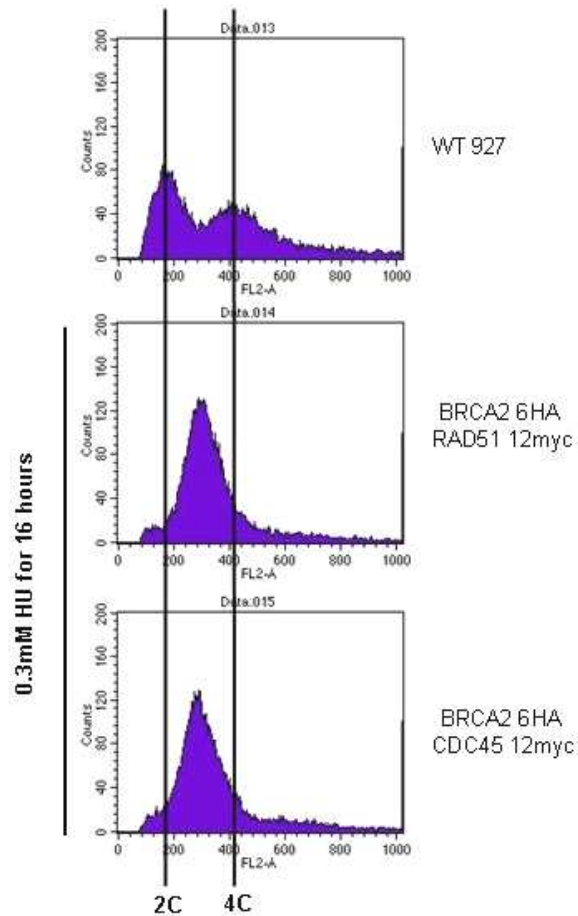


Figure 6-10 Flow cytometry profiles of propidium iodide-stained cells after exposure to hydroxyurea.

Histograms show propidium iodide-stained untreated wild-type TREU 927 (WT 927) and HU-treated (0.3 mM for 16 hours) double-tagged cell lines after flow cytometry analysis. The peaks corresponding with cells containing 2C and 4C DNA content are indicated.

6.2.9 Endogenous N-terminal epitope tagging strategy

It is possible that the presence of an epitope tag at the C-terminus of either or both of BRCA2 and CDC45 could interfere with the proposed interaction between the proteins, and this is the reason that an interaction could not be detected. It was therefore decided to use a construct that allows the addition of an epitope tag to the N-terminus of a gene to generate a second set of cell lines with proteins double-tagged, this time at the N-terminus.

Two constructs that enable the fusion of an N-terminal 12myc or 6HA epitope tag at the endogenous locus of a gene of interest were generated by modification of an existing construct containing a fluorescent protein and TY

epitope tag (pEnT6B; Kelly *et al.*, 2007). Maps of the two constructs are displayed in Figure 6-11, and the strategy to enable the N-terminal tagging of *T. brucei* proteins at their endogenous loci is displayed in Figure 6-12. The N-terminal epitope tagging construct uses a region of the 5' UTR immediately upstream of the ORF and also a region of the 5' end of the ORF to enable homologous recombination and integration into the genome. Selection of clones is enabled by the presence of a *BSD* resistance cassette in the 12myc construct and a *BLE* resistance cassette in the 6HA construct. The resistance ORFs are flanked by *tubulin* and *actin* processing sequences. After integration of the construct, endogenous downstream gene sequences provide polyadenylation signals for the tagged gene, while upstream sequences of the integrated resistance cassette are used for RNA *trans*-splicing, meaning that the 5' UTR is non-endogenous. For *BRCA2*, primers 112 and 113 were used to PCR-amplify 213 bp of the 5' end of the *BRCA2* ORF; the forward primer contained a *SpeI* restriction site and the reverse primer a unique restriction site (*XbaI*) to allow linearisation of the construct prior to transformation. Primers 114 and 115 were used to PCR-amplify 274 bp of the *BRCA2* 5' UTR; the forward primer contained the same unique restriction site (*XbaI*) and the reverse primer a *BamHI* restriction site. The DNA fragments were cloned into the 6HA tagging construct downstream of the epitope tag in a three-way ligation using the *SpeI*, *XbaI* and *BamHI* restriction sites. The same strategy was used to clone the sequences specific to *RAD51* and *CDC45* into the 12myc N-terminal tagging constructs. The primers used to amplify the respective 5' end of ORFs and 5' UTRs were; 116, 117 and 118, 119 for *RAD51*; and 1, 2 and 3, 4 for *CDC45*, and the unique restriction sites used were *KpnI* and *XhoI*, respectively. In this manner three constructs were assembled to enable the generation of N-terminally tagged *BRCA2* 6HA, *RAD51* 12myc and *CDC45* 12myc. For transformation, the constructs were linearised by restriction digest using the unique restriction enzymes, the digested DNA was then ethanol precipitated and approximately 5 µg of the resuspended DNA was used for each transformation.

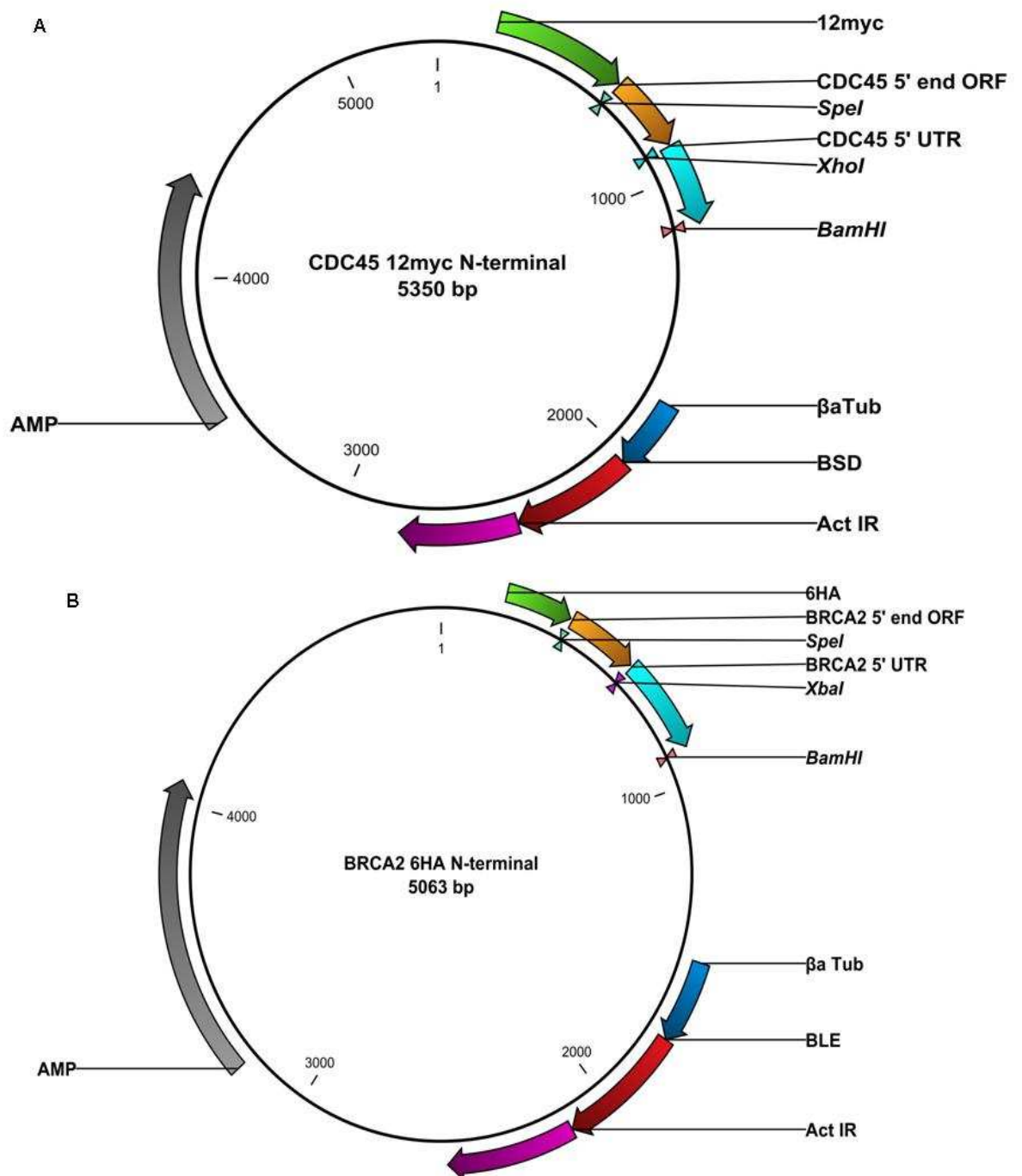


Figure 6-11 Constructs used for N-terminal epitope tagging of *T. brucei* proteins. (A) Construct used for the N-terminal 12myc tagging of CDC45 and RAD51 (only CDC45 is shown). 250 bp of the 5' end of the *CDC45* ORF (orange) and 272 bp of the 5' UTR (light blue) were cloned into the *SpeI* and *BamHI* restriction sites with a unique restriction site between (*XhoI*). The 12myc epitope tag (green) consists of 12 tandemly repeated copies of the c-myc epitope. (B) Construct used for the N-terminal 6HA tagging of BRCA2. 213 bp of the 5' end of the *BRCA2* ORF (orange) and 274 bp of the 5' UTR (light blue) were cloned into the *SpeI* and *BamHI* restriction sites with a unique restriction site between (*XbaI*). The 6HA epitope tag (green) consists of 6 copies of the HA epitope. In both maps, The *BSD* or *BLE* resistance cassette (red) is shown flanked by the *tubulin* (β a Tub, dark blue) and *actin* (Act IR, purple) intergenic sequences. *AMP*: Ampicillin resistance ORF. Sizes are shown (bp).

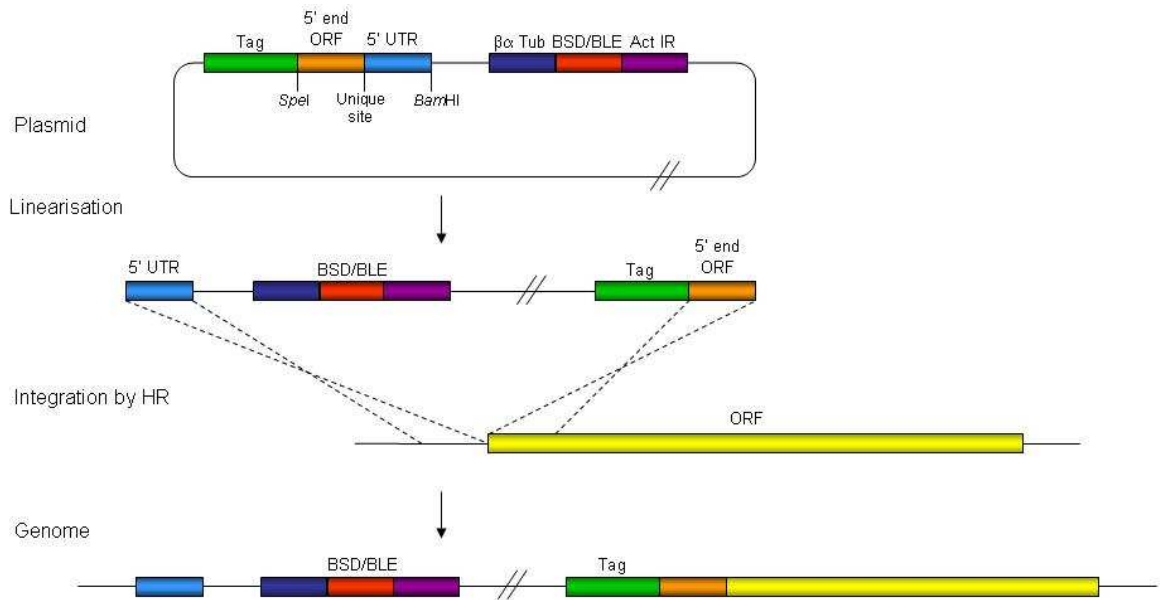


Figure 6-12 Strategy for N-terminal epitope tagging of *T. brucei* proteins at their endogenous loci.

A schematic of the N-terminal tagging constructs, described in Figure 6-11, is shown (top). Linearisation of the construct using a unique restriction site, between the 3' end of the ORF (orange) and the 5' UTR (light blue), allows integration into the genome by homologous recombination (HR). This produces the endogenous ORF fused with the N-terminal epitope tag (green, bottom).

6.2.10 Generation of N-terminal double-tagged cell lines in PCF TREU 927 *T. brucei*

Cell lines in which both BRCA2 and CDC45, and BRCA2 and RAD51 were epitope tagged at the N-terminus were generated as described in section 6.2.5. The generation of CDC45 12myc and RAD51 12myc tagged cell lines was carried out first by the transformation of wild-type PCF TREU 927 cells with linearised constructs. The expression of tagged protein was confirmed by western blot (data not shown). These two confirmed cell lines were then subjected to transformation with the linearised BRCA2 6HA construct and six clones were chosen from each transformation. The twelve putative double-tagged cell lines were subject to screening as described in section 6.2.6. The western blots in Figure 6-13 demonstrate that all of the tested clones expressed proteins of the expected size for CDC45 12myc or RAD51 12myc (93 kDa and 55 kDa, respectively) that were recognised by anti-myc antiserum. All of the twelve clones also expressed proteins recognised by anti-HA antiserum of the expected size for BRCA2 6HA (183 kDa).

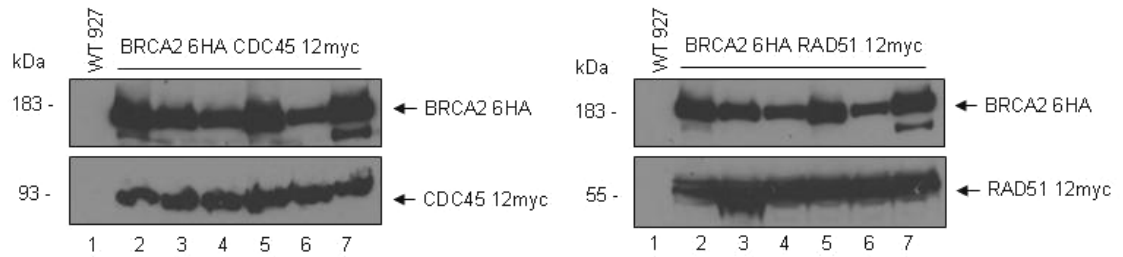


Figure 6-13 Confirmation of co-expression of N-terminal epitope tagged proteins in PCF TREU 927 *T. brucei*.

Total protein extracts from wild-type TREU 927 (WT 927) and the two putative double-tagged cell lines (BRCA2 6HA CDC45 12myc and BRCA2 6HA RAD51 12myc) were separated by SDS-PAGE and western blotted before being probed with anti-HA antiserum (1:10000 dilution, top). The blots were stripped and re-probed with anti-myc antiserum (1:7000 dilution, bottom). The bands produced by BRCA2 6HA, CDC45 12myc, and RAD51 12myc are indicated (black arrows), and size markers are shown (kDa).

6.2.11 Co-immunoprecipitation using N-terminal double-tagged cell lines

Co-immunoprecipitation using the two double-tagged cell lines, and wild-type TREU 927 cells as a control was performed, as described in section 6.2.7.

Additional controls were also performed to ensure that binding had not occurred between the epitope-tagged proteins and the antiserum-conjugated beads. Cell lines containing a single protein epitope-tagged at the N-terminus were subject to immunoprecipitation using antiserum conjugated to agarose beads that were specific to the epitope tag not present in the cell line analysed. For example, the single-tagged BRCA2 6HA cell line was subject to immunoprecipitation with anti-myc antiserum conjugated to agarose beads and the elution sample was probed with anti-HA antiserum in order to detect any non-specific binding of BRCA2 6HA to the anti-myc beads. The western blots in Figure 6-14 show analysis of interaction between BRCA2 and RAD51, and also BRCA2 and CDC45. The input samples in Figure 6-14A demonstrate expression of the tagged proteins of the expected size for the cell lines analysed. The elution samples in Figure 6-14B (anti-HA beads) demonstrate the successful immunoprecipitation of BRCA2 6HA (lanes 4 and 5, α -HA). However, interaction between either RAD51 or CDC45 and BRCA2 could not be detected, as the anti-myc probed elution blot was blank (lanes 4 and 5, α -myc). The control experiments with single tagged RAD51 12myc or CDC45 12myc cell lines also did not show any myc-tagged proteins in the elution samples (lanes 2 and 3, α -myc), indicating that there was no non-specific binding to the anti-HA beads. The elution samples in Figure 6-14C (anti-myc beads) demonstrate the successful immunoprecipitation of RAD51 12myc and

CDC45 12myc by the anti-myc beads (lanes 3 and 4, α -myc). A possible interaction between BRCA2 and RAD51 can be detected, as evidenced by the presence of a faint band of the expected size for BRCA2 6HA in the anti-HA probed elution blot (lane 4, α -HA), though there was considerable background, non-specific binding in this blot. An interaction between CDC45 and BRCA2 was not detected (lane 3, α -HA), but the background makes this difficult to be certain of. The control experiment with the single tagged BRCA2 6HA cell line showed small amounts of HA tagged proteins in the elution sample (lane 2, α -HA), indicating that there was some non-specific binding to the anti-myc beads in this experiment.

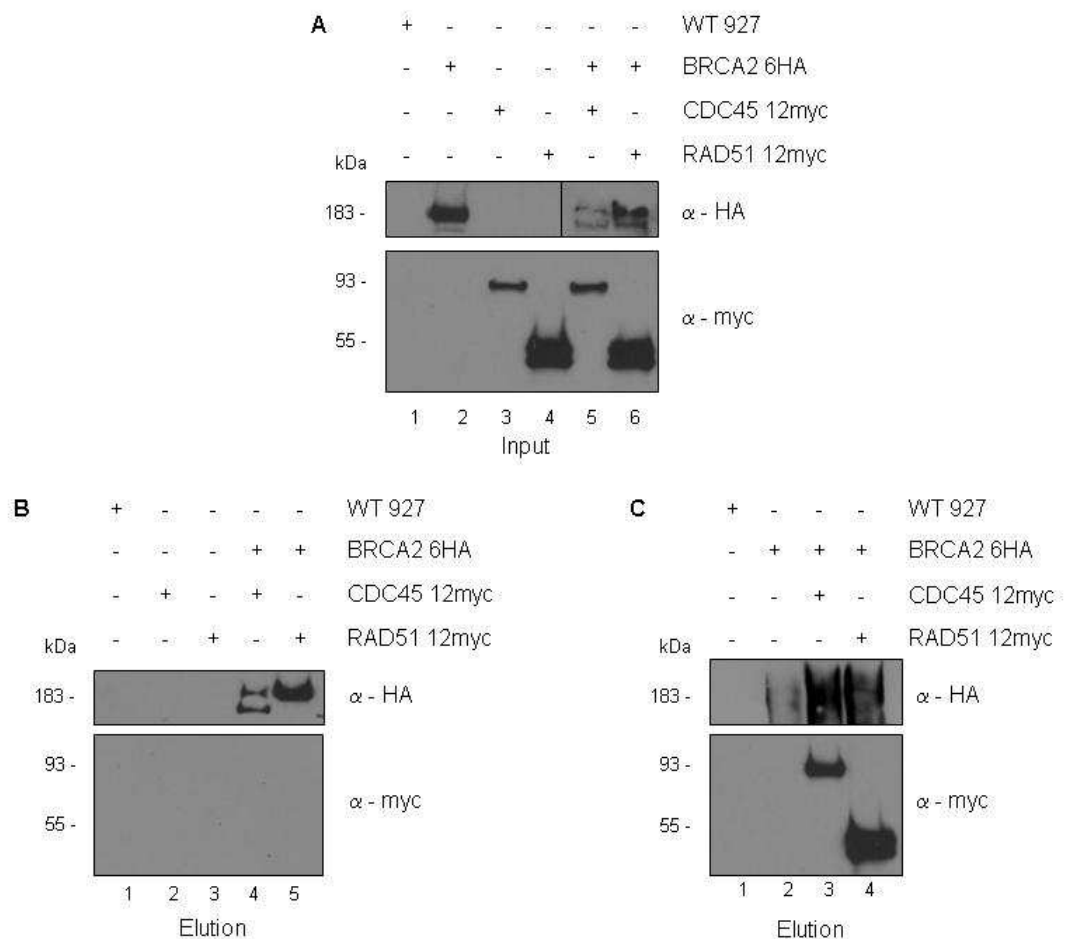


Figure 6-14 Co-immunoprecipitation analysis of the interaction between BRCA2 and CDC45, and BRCA2 and RAD51.

Total protein extracts from wild-type TREU 927 (WT 927) and double-tagged cell lines (BRCA2 6HA CDC45 12myc, and BRCA2 6HA RAD51 12myc) were immunoprecipitated using anti-HA antiserum (B) or anti-myc antiserum (C) conjugated to agarose beads. Input (A) and elution (B and C) samples were separated by SDS-PAGE and western blotted before being probed with anti-myc antiserum (1:7000 dilution) and anti-HA antiserum (1:10000 dilution). Size markers are shown (kDa).

6.3 *In vitro* GST pull-down

Given the lack of convincing evidence for BRCA2-CDC45 interaction *in vivo* from the above experiments, an attempt was next made to recapitulate the interaction between *T. brucei* BRCA2 and CDC45 observed in Oyola *et al.*, (2009). To do this, GST pull-down was carried out using proteins over-expressed in *E. coli*.

6.3.1 Generation of bacterial protein over-expression constructs

The co-expression of two tagged proteins from compatible bacterial over-expression constructs has successfully been used to detect interaction between *T. brucei* proteins previously (Chapter 5; Dobson *et al.*, 2011). The His BRCA2 C-term and His 10BRC expression constructs described in section 5.2.1 were used in conjunction with CDC45 over-expressed in *E. coli* using the pGEX-4T-3 construct. This results in CDC45 being expressed as an N-terminal Glutathione S-Transferase (GST) fusion; the plasmid also contains an *ampicillin* (AMP) resistance cassette for selection (Figure 6-15). The *CDC45* ORF was PCR-amplified using primers 129 and 130 that contained *Bam*HI and *Xho*I restriction sites, respectively, to allow cloning into pGEX-4T-3. The two empty vectors were used to express the His and GST tags (not fused to a protein) for control purposes.

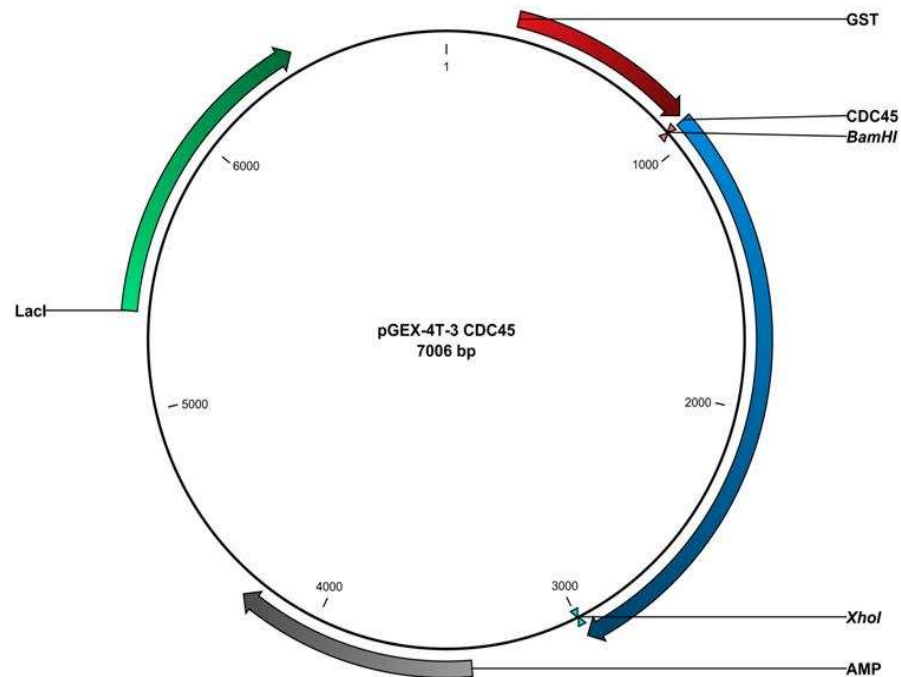


Figure 6-15 Construct used for N-terminal GST tagging of CDC45 for over-expression in *E. coli*. The *CDC45* ORF (blue) was cloned into the *Bam*HI and *Xho*I restriction sites downstream of the GST tag (red). *AMP*: ampicillin resistance ORF (grey). *Lact*: lac repressor ORF (green). Sizes are shown (bp).

6.3.2 Generation of co-expressing bacterial cultures

Competent cells of the Rosetta2 *E. coli* strain were transformed with the constructs generated in section 6.3.1 and 5.2 to produce five bacterial cultures. The first experimental culture contained the His BRCA2 C-term and GST CDC45. The three other cultures were controls, containing one of each of the expression constructs (His BRCA2 C-term, His 10BRC and GST CDC45) and the complementary empty vector, to control for binding of the *T. brucei* proteins to the His or GST tags. The competent *E. coli* cells were co-transformed with two plasmids and selected on LB agar supplemented with 100 $\mu\text{g}\cdot\text{ml}^{-1}$ ampicillin, 50 $\mu\text{g}\cdot\text{ml}^{-1}$ kanamycin and 34 $\mu\text{g}\cdot\text{ml}^{-1}$ chloramphenicol.

6.3.3 GST pull-down using co-expressing bacterial cultures

GST pull-down was carried out as described in section 5.2.3. For unknown reasons the expressed GST-tagged CDC45 protein was not able to be detected by western blot in these conditions, as previously encountered with GST RAD51 (section 5.2.3). For this reason eluted GST CDC45 is shown as a coomassie-stained gel. Analysis of interaction between BRCA2 and CDC45 is displayed in

Figure 6-16. The western blot in Figure 6-16A shows input samples probed with anti-His antiserum and demonstrates expression of His-tagged proteins of the expected sizes for the BRCA2 C-term (100 kDa), 10BRC (66 kDa) and His tag (7 kDa). Figure 6-16B shows a coomassie stained protein gel of the separated elution samples and demonstrates the presence of the GST (28 kDa) and GST CDC45 (104 kDa) proteins, indicating they were successfully recovered by the GST pull-down approach. The western blot in Figure 6-16C shows the elution samples probed with anti-His antiserum to detect the His-tagged BRCA2 variants: no signal was detected even with very long exposures (overnight), demonstrating that no His-tagged proteins were recovered. This indicates that the BRCA2 C-term and 10BRC proteins have not bound either GST (lanes 4 and 5) or GST CDC45 (lanes 2 and 3), and also that the His tag itself has not bound to GST CDC45 (lane 1), although some binding is observed. For this reason, a coomassie stained gel of the input and elution samples of the control culture co-expressing GST-CDC45 and the His tag is shown in Figure 6-16D, and demonstrates the presence of a protein of the expected size for the His tag (7 kDa) in the input sample, which is absent from the elution sample, confirming the GST CDC45 has not bound non-specifically to the His tag. In addition, no binding between either the His BRCA2 C-term or the His 10BRC variant of BRCA2 and GST RAD51 was detected (Figure 6-16C) and this acts as a negative control. From these experiments, interaction between *T. brucei* CDC45 and *T. brucei* BRCA2 is not apparent. This was tested for the BRC repeats, for which no such interaction might be predicted, and also for the C-terminal 'half' of the protein downstream of the BRC repeats, which has been suggested to mediate CDC45 binding (Oyola, Bringaud, and Melville, 2009).

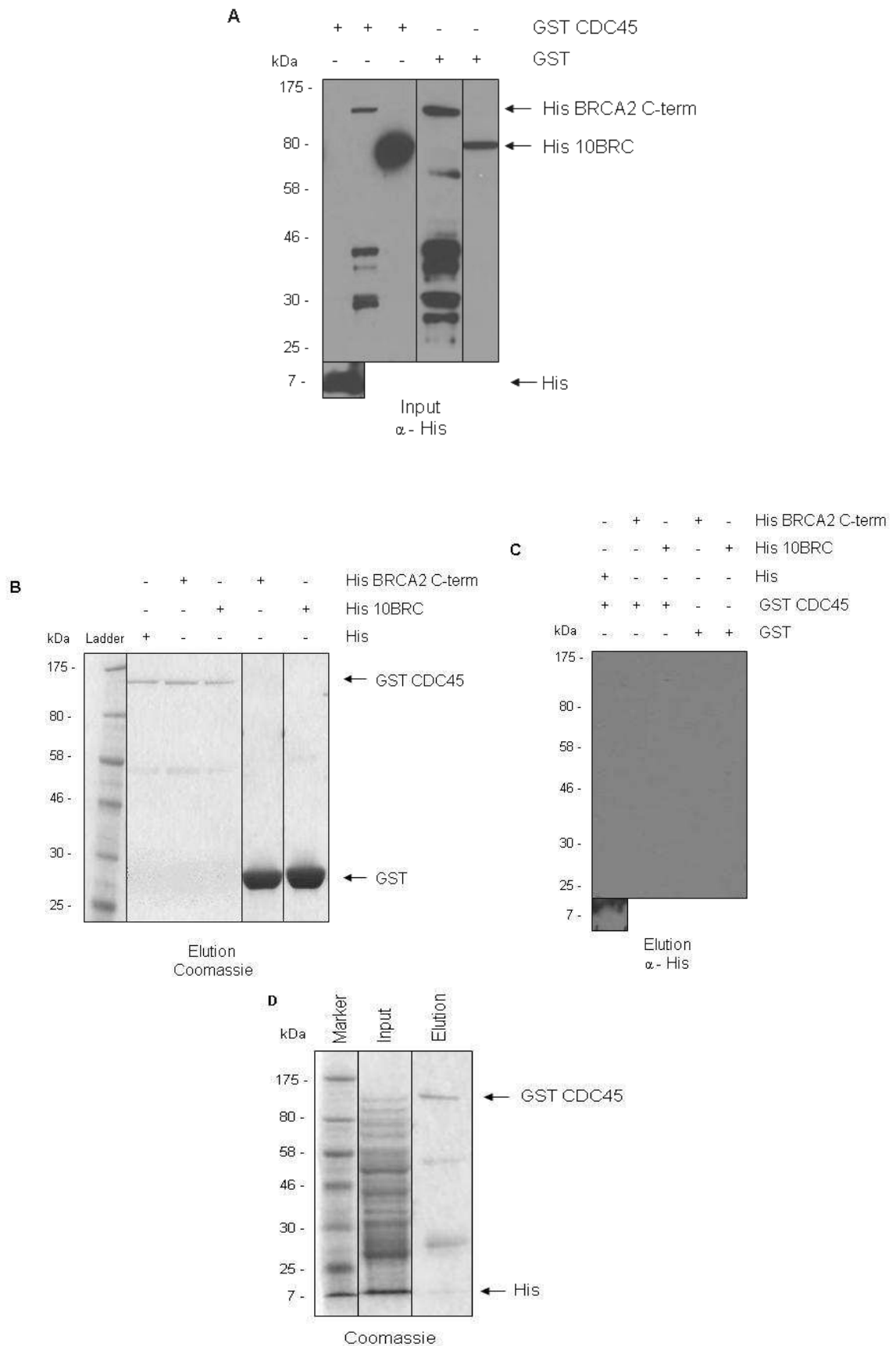


Figure 6-16 GST pull-down analysis of the interactions between CDC45 and BRCA2. (A) A western blot of the separated input samples probed with anti-His antiserum (1:750 dilution). His-tagged proteins are indicated (black arrows), and the GST-tagged proteins that were co-expressed are indicated (top). (B) A coomassie stained gel of the separated elution samples showing GST CDC45 and the GST tag (black arrows). His-tagged proteins that were co-expressed are indicated (top). (C) A western blot of the separated elution samples probed with anti-His antiserum (1:750 dilution). GST-tagged proteins immunoprecipitated

are indicated as are the co-expressed His-tagged proteins (top). (D) A coomassie stained gel of the separated input and elution samples from GST CDC45 co-expressed with the His tag (black arrows). In each panel size markers are shown (kDa).

6.4 Summary

The aim of this chapter was to test the reported interaction between the C-terminus of *T. brucei* BRCA2 and CDC45 (Oyola, Bringaud, and Melville, 2009), with the longer term goal of investigating the potential mechanism this provided for the observed replication phenotype in BSF *brca2*^{-/-} mutants that was also localised to the C-terminus of BRCA2 (Claire Hartley, PhD Thesis, 2008). *In vivo* co-immunoprecipitation was carried out using endogenous C- and N- terminally epitope tagged CDC45 and BRCA2. The robust interaction between *T. brucei* BRCA2 and RAD51 was used to ensure that epitope tagging of BRCA2 did not impair its ability to functionally interact with RAD51 and subsequent co-immunoprecipitation between BRCA2 and RAD51 was reliably detected. In contrast, no such interaction was observed between BRCA2 and CDC45. The induction of DNA damage prior to harvesting cells for co-immunoprecipitation was carried out in order to try and increase the probability of detecting an interaction between BRCA2 and CDC45, with the assumption that such an interaction may only occur in this context. Again, no interaction was found *in vivo* by immunoprecipitation. Next, *in vitro* GST pull-down was employed using full length CDC45 and the C-terminal ‘half’ of BRCA2 expressed in *E. coli*. Again, no interaction was detected.

Why might the above experiments and those reported by Oyola *et al.*, (2009) be in disagreement? It is clearly possible that BRCA2 and CDC45 do, indeed, interact in *T. brucei* and that this interaction is either transient and the *in vivo* approaches therefore too insensitive, or these approaches are disrupted by the tagging strategies employed. It is less clear why the GST pull-down approach should not reveal an interaction, given that the BRCA2 variants used are clearly functional in this context for interaction with RAD51 (Chapter 5). Of course, we cannot rule out that the CDC45 expressed in this setting is non-functional, but it is in the 2-hybrid approach used by Oyola *et al.*, (2009). Nevertheless, the experiments employed by Oyola *et al.*, (2009) expressed only a fragment of CDC45, and this was demonstrated to bind to the C-terminus of BRCA2. No experiments were performed with full length CDC45, as attempted here. It is

clearly possible that this fragment of CDC45 may have folded anomalously, and led to a non-physiological and artefactual interaction between BRCA2 and CDC45. Nonetheless, immunoprecipitation of *T. brucei* BRCA2 from cell extracts and mass spectrometry identification of interacting proteins could be used to test this further. Indeed, this approach may find novel factors that interact with BRCA2, some of which may be components of the replication machinery and could provide an understanding of the replication phenotype observed in BSF *brca2*^{-/-} mutants.

Chapter 7: Discussion

7.1 Introduction

The initial aim of this thesis was to further investigate the role of BRCA2 in the regulation of genome stability in *T. brucei*, extending previous work by Hartley and McCulloch (2008). This was achieved by generation of *brca2*^{-/-} mutants in the PCF life cycle stage in both TREU 927 and Lister 427 strains of *T. brucei* and subsequent phenotypic analyses. Investigation of genomic stability in these *brca2*^{-/-} mutant cell lines was performed after prolonged passaging, looking for evidence for genome rearrangements by Southern blotting and pulsed field agarose gel electrophoresis. Neither of these approaches revealed evidence for putative gross chromosomal rearrangements as previously observed in the BSF *brca2*^{-/-} mutants in the Lister 427 strain (Hartley and McCulloch, 2008), which meant that genetic dissection of these rearrangements at the sequence level was unable to be carried out. Nonetheless, the generation of these mutants allowed, for the first time in any organism, the function of multiple BRC repeats in a BRCA2 orthologue to be examined by the systematic generation and expression of variants of BRCA2 with reduced numbers of BRC repeats. This approach was possible due to the unusual BRC repeat expansion present in *T. brucei* BRCA2, where the RAD51-binding repeats are found in a tandem array organisation. BRC repeat number variants of *T. brucei* BRCA2 were examined in both the PCF and BSF life cycle stages, in order to try and understand the contribution this BRC repeat expansion makes to growth, DNA repair and RAD51 foci formation, since a function in VSG switching had been previously ruled out by the observation that a BRCA2 variant with a single BRC repeat could support this process (Hartley and McCulloch, 2008).

A further aim of this thesis was to define the interactions *T. brucei* BRCA2 makes with some key further factors. Interaction between BRCA2 and RAD51, which is considered the central function of BRCA2 orthologues (Holloman, 2011), was analysed by *in vitro* GST pull-down, *in vivo* immunoprecipitation and immunolocalisation of the two proteins. This revealed a surprising level of complexity in the interplay between these two HR proteins in *T. brucei*, both in terms of the extent of BRCA2 domains that mediate physical interaction with RAD51 and also the dynamics of detectable co-localisation. By related approaches, the final chapter of this thesis investigated a putative function for *T. brucei* BRCA2 in DNA replication by attempting to validate a proposed

interaction with CDC45 (Oyola, Bringaud, and Melville, 2009). Such a putative protein:protein interaction was tested both *in vivo* and *in vitro*, however we were unable to demonstrate the validity of this interaction.

7.2 *T. brucei* BRCA2 functions in the maintenance of genome stability in the bloodstream form only.

Analysis of the growth and DNA repair phenotypes of the PCF TREU 927 and PCF Lister 427 *brca2*^{-/-} mutants, and comparison to the relatively severe phenotype of the BSF Lister 427 *brca2*^{-/-} mutants (Hartley and McCulloch, 2008; Claire Hartley, PhD thesis, 2008), revealed a striking difference in the consequences of the removal of BRCA2 between the two life cycle stages. PCF *brca2*^{-/-} mutant cells, in both parasite strains, were found to be growth impaired and to display increased sensitivity to exogenous DNA damage (MMS or phleomycin). However, the extent of each of these phenotypes was less severe than when observed in BSF *brca2*^{-/-} mutants (Hartley and McCulloch, 2008).

A number of reasons can be considered for these life cycle stage differences. It is possible that the differences simply result from aspects of growth that impact on the assays used. For instance, the underlying growth rate of BSF cells is higher than PCF cells in culture (8 hrs relative to 10 hrs, respectively), which may result in greater apparent levels of death in the BSF relative to the PCF when the mutants are exposed to damage. A number of studies have also suggested that cell cycle checkpoints differ between BSF and PCF cells (Hammarton *et al.*, 2003; Hammarton, 2007). Though very little is known regarding DNA damage checkpoints, if PCF cells did not cease growth after MMS or phleomycin treatment to the same extent as BSF cells, this would be manifest as lesser apparent killing in the Alamar blue assay employed here. The alternative is that the differences reflect variation in genome maintenance functions between PCF and BSF cells. It seems unlikely that PCF and BSF cells are naturally exposed to differing levels of general DNA damage, which might have selected for increased BRCA2-mediated repair activity in the BSF. The only potential exception to this may be increased oxidative damage, as the greater mitochondrial metabolism in PCF cells relative to BSF cells (Bienen *et al.*, 1991; Hajduk *et al.*, 1992; Fang and Beattie, 2003) is likely to yield higher levels

of reactive oxygen species (ROS), which can damage DNA (Kryston *et al.*, 2011). Perhaps, then, some undefined repair activity is upregulated in PCF cells to deal with this, and can also contribute to greater repair of MMS- and phleomycin-induced damage and reduce the impact of BRCA2 loss. BRCA2 has also been suggested to play a key role in ensuring the efficient progression of DNA replication (Michel *et al.*, 2004; Nagaraju and Scully, 2007; Constanzo, 2011). However, as for DNA repair, it seems unlikely that this fundamental mechanism could differ substantially between PCF and BSF cells. A final possible explanation is that BRCA2 acts in an additional, as yet undefined, function beyond general repair and replication maintenance. If such a function assumed greater importance in the BSF life cycle stage, more of the available pool of BRCA2 may be directed to that function, and less then might be available to tackle the increased DNA damage imposed by exogenous MMS or phleomycin. The difference in growth rates of PCF and BSF *brca2*^{-/-} mutants in the absence of induced damage is less easy to explain in this scenario, but it may be that such a putative role has a significant impact on the general health of BSF cells. Below, I consider whether the broader phenotypes detailed in this thesis might offer support for any of the above suggestions. In particular, the discussion will focus on that proposed role of BRCA2 in the maintenance of genome stability, which is only apparent in the BSF, the DNA replication phenotypes observed in *brca2*^{-/-} mutants, and the contribution of BRCA2 to RAD51 subnuclear dynamics, as revealed by analysis of the BRC repeat variants and co-localisation.

brca2^{-/-} mutants in BSF Lister 427 *T. brucei* display an accumulation of putative gross chromosomal rearrangements after prolonged passaging (~ 290 generations; Hartley and McCulloch, 2008). Work presented here demonstrates that these genome rearrangements occur at an earlier time point than previously analysed (~ 150 generations). Even more strikingly, this work shows that *brca2*^{-/-} mutants in PCF cells of both TREU 927 and Lister 427 strains do not display detectable genome rearrangements, even after passaging (~ 380 and ~ 230 generations, respectively) to an extent at least equivalent to that in the BSF mutants. This work also provides further evidence to suggest that the putative GCRs observed in BSF *brca2*^{-/-} mutants may be specifically targeted to VSGs located in the megabase chromosome, although genetic dissection of the genome rearrangements is required to confirm this. It was previously reported

that detectable GCRs in BSF mutants were only seen in the megabase chromosomes, which harbour *VSG* subtelomere arrays, and not in intermediate- and mini-chromosomes, which carry only telomeric *VSGs* (Hartley and McCulloch, 2008). Here, probing of the BSF *brca2*^{-/-} mutants with *ingi* sequences revealed complex banding patterns in Southern blots that showed no variation between clones, in contrast to the changes in *VSG121* copy number that is observed. These data are consistent with *ingi* being widespread in the *T. brucei* genome (Bringaud *et al.*, 2004; Berriman *et al.*, 2005; Bringaud *et al.*, 2008), but demonstrate that *ingi* are not detectably rearranged during the rearrangements that cause visible changes in the subtelomeres of the megabase chromosomes of the BSF *brca2*^{-/-} mutants.

Is it possible that the above data point to a BSF-specific function for BRCA2 in the maintenance of the subtelomeric *VSG* arrays? If so, quite why the functions of BRCA2 in this role would differ between the BSF and PCF life cycle stages so dramatically is not known. An obvious explanation could be a requirement for antigenic variation in the BSF, which may be inactivated in the PCF. Most *VSG* switching is driven by gene conversion, which means that sequence changes normally focus on the recipient DNA molecule, which would be the *VSG* ES (Robinson *et al.*, 1999; Glover, Jun, and Horn, 2011). However, perhaps during the process of *VSG* switching homology searching scans the subtelomeric *VSGs* to a significant extent, and in the absence of BRCA2 this reaction is undermined, leading to broad destabilisation of the *VSGs*. Alternatively, it may be that there is a greater level of background, silent *VSG* gene conversion occurring in the subtelomeres than has been appreciated, which is again undermined by the absence of BRCA2 and leads to GCRs. This could perhaps explain the extensive chromosome size variations observed in *T. brucei*, which have been localised to the *VSGs* (Callejas *et al.*, 2006). In this regard, it is interesting to consider the process of mosaic *VSG* formation (Thon *et al.*, 1990; Barbet and Kamper, 1993; Marcello and Barry, 2007), which is not well understood mechanistically, and may rely on a novel function for BRCA2 in the BSF.

7.3 The BRC repeat expansion is critical for RAD51 subnuclear dynamics.

Analysis of variants of *T. brucei* BRCA2 with 1, 4, 7, 10 and 12 BRC repeats *in vivo* has allowed us to ask why HR in some organisms, such as mammals, plants and *T. brucei*, functions with a BRCA2 protein containing multiple BRC repeats, while others, such as *C. elegans* and *U. maydis*, utilises an orthologue with a single BRC repeat. A similar study by Carreira and Kowalczykowski (2011), relied upon *in vitro* interaction analyses, and suggested that eight BRC repeats of human BRCA2 fall into two classes with differing affinities for Rad51 monomers and nucleoprotein filaments which co-operate to bring about Rad51 nucleation onto ssDNA and filament propagation thereby stimulating DNA strand exchange (Carreira and Kowalczykowski, 2011). The question of the need for multiple BRC repeats in *T. brucei* is especially compelling because bioinformatic analysis suggest that the BRC repeat expansion is not found in closely related species, notably *T. vivax* and *T. congolense*, where BRCA2 is predicted to have 1 and 3 BRC repeats, respectively (Lo *et al.*, 2003).

This work reveals that the purpose of the BRC repeat expansion in *T. brucei* is more subtle than might have been predicted. Hartley and McCulloch (2008) examined *T. brucei* BSF cells expressing BRCA2 containing only the single, most C-terminal BRC repeat and found that they were impaired in the following processes: repair of MMS and phleomycin damage, HR and the formation of subnuclear RAD51 foci after damage. This thesis shows that those findings paint only part of the picture. In both life cycle stages, cells expressing BRCA2 variants with 3 or more BRC repeats were capable of repairing MMS and phleomycin damage with the same efficiency as wild-type cells. In addition, every BRC variant analysed supported growth at wild-type rates. This indicates that the BRC repeat expansion is largely dispensable for normal growth and DNA repair. Notably, PCF cell lines expressing BRCA2 containing only the most C-terminal 'degenerate' BRC repeat repaired DNA damage as well as wild-type cells, showing that even a single BRC repeat can operate in DNA repair. The impairment in DNA repair observed by Hartley and McCulloch (2008) is, in fact, limited to BSF 1BRC cells, which is the only BRC variant cell line analysed where repair of DNA damage is impaired relative to wild-type cells. These data indicate, first, that the putatively degenerate C-terminal BRC repeat is

functional. Second, they illustrate again that the function of BRCA2 differs between PCF and BSF cells. Finally, they suggest that the BRC repeat expansion evolved to serve another purpose than general DNA repair, which would make sense as it is hard to imagine what aspect of the biology of *T. brucei* would require greater general repair than a close relative such as *T. vivax*.

The most striking data on the BRC repeat expansion was obtained when analysing the ability of the BRCA2 BRC variant cell lines to form subnuclear RAD51 foci after the induction of DNA damage. In both life cycle stages a BRC repeat number-dependent increase in the ability to form RAD51 foci was observed, with both the number of cells that display detectable RAD51 foci and the number of RAD51 foci observed per cell increasing with increasing BRC repeat number. This was found for both the PCF cells and BSF cells. However, again, life cycle stage differences were found. In the PCF cells, BRCA2 with 1 BRC repeat was found to be sufficient for RAD51 foci formation to be detectably improved relative to *brca2*^{-/-} cells, though still impaired relative to wild-type cells. In contrast, in BSF cells, BRCA2 with 1 BRC repeat was virtually indistinguishable from *brca2*^{-/-} mutant cells, consistent with the findings of Hartley and McCulloch (2008), and 3 BRC repeats were required to begin to complement the RAD51 foci formation defect in *brca2*^{-/-} mutant cells. For both life cycle stages, it was also apparent that multiple BRC repeats were needed to reach the levels of RAD51 foci formation seen in wild-type cells (minimally 10 BRC repeats and 12 BRC repeats in PCF and BSF, respectively). These data indicate a function for the BRC repeat expansion in the regulation of RAD51 foci formation and, hence, in RAD51 subnuclear dynamics.

The above data provide a quantitative link between BRC repeat number and BRCA2 function, and suggest that the number of repeats present in the array is important. However, it remains unclear why *T. brucei* BRCA2 possesses this unusual BRC repeat expansion, and the disconnection between DNA repair efficiency and RAD51 foci formation observed here is perplexing. The composition of DNA repair foci is unknown (Lisby and Rothstein, 2009; Bekker-Jensen and Mailand, 2010), however, they have been shown to contain multiple copies of HR proteins including Rad51, BRCA1 and BRCA2, and are thought to be repair factories where the high local concentration of repair factors facilitates efficient DSB repair (Lisby and Rothstein, 2009; Bekker-Jensen and Mailand,

2010). After the induction of DNA damage in mammalian cells, *Drosophila* and *C. elegans* multiple repair foci are observed microscopically (Mizuta *et al.*, 1997; Tarsounas, Davies, and West, 2003; Martin *et al.*, 2005; Brough *et al.*, 2008). However, it is important to consider that a focus indicates an attempt to repair DNA damage, that may not necessarily be successful and also that the repair reaction may occur faster than detection can allow (Lisby and Rothstein, 2009). The available data rule out that the BRC repeat expansion is needed for the normal requirements of DNA repair or for the activation of intact VSGs during VSG switching, as a single BRC repeat is sufficient for these functions (Hartley and McCulloch, 2008). This work has shown that the ability to form RAD51 foci is proportionally linked to the number of BRC repeats present in BRCA2, but further work will be needed to understand this. For instance, it would be interesting to determine if the BRC repeat number was also related to the extent of GCRs observed in the BSF, as this would suggest it has evolved for the maintenance of genome stability in BSF cells (section 7.2). It would also be interesting to measure the number of lesions induced by damage and see how this relates to the number of foci, or whether a single lesion is a site for accumulation of increasing amounts of RAD51. Finally, it would be useful to detail if the unique tandem repeat organisation of the BRC repeats in *T. brucei* BRCA2 is important, or whether multiple BRC repeats in a dispersed arrangement would suffice (section 7.4). Is it possible that these data are consistent with the dual function of BRCA2 proposed in section 7.2? For instance, is the purpose of the BRC repeat expansion in *T. brucei* BRCA2 to allow the efficient localisation of RAD51 or BRCA2, or both, from a non-repair function to sites of damage when they arise? This would assume that RAD51 or BRCA2 are present in excess to accommodate this, and that the non-physiological levels of damage generated in these experiments are rapidly repaired, but result in concentrating the proteins at damage sites, visible as foci. This is consistent with the absence of evidence for an upregulation of RAD51 after DNA damage in *T. brucei*, as observed in *T. cruzi* and *L. major* (McKean *et al.*, 2001; Regis-da-Silva *et al.*, 2006).

7.4 Interactions between *T. brucei* BRCA2 and RAD51 are unusually extensive.

Mammalian BRCA2 interacts with Rad51 at two well-defined locations: through the conserved eight BRC repeat motifs, which function to promote strand

exchange (Wong *et al.*, 1997;Chen *et al.*, 1998;Carreira and Kowalczykowski, 2011), and also through a distinct C-terminal Rad51-binding domain that is regulated by cell cycle dependent phosphorylation and may function in DNA replication (Esashi *et al.*, 2005;Esashi *et al.*, 2007;Ayoub *et al.*, 2009;Schlacher *et al.*, 2011). The data presented here indicate that the interactions between *T. brucei* BRCA2 and RAD51 are more extensive than those observed in mammals, and may differ in their details. *In vitro* GST pull-down analysis indicates that 10 BRC repeats are required for detectable binding of *T. brucei* BRCA2 to RAD51, which would be consistent with the general picture that BRC repeat number is critical for RAD51 interaction (section 7.3). However, the physiological significance of this is unclear, as we do not know if the BRC repeat binding observed was to RAD51 monomers or to protein filaments (perhaps even nucleoprotein filaments). Thus, these experiments do not reveal the function for the unusual tandem repeat organisation of the BRC repeats. Nonetheless, this requirement for 10 BRC repeats to detect RAD51 binding is in contrast to other systems: a single BRC repeat motif isolated from mammalian BRCA2, or the naturally occurring single BRC repeat from *C. elegans* CeBRC-2 or *U. maydis* Brh2, is sufficient for binding to Rad51 *in vitro* (Wong *et al.*, 1997;Chen *et al.*, 1998;Kojic *et al.*, 2002;Martin *et al.*, 2005;Petalcorin *et al.*, 2006).

Analysis of the interaction between the C-terminal ‘half’ of *T. brucei* BRCA2 and RAD51 indicates that a RAD51-binding site exists in the non-conserved C-tail region downstream of the DNA/DSS1-binding domain, and that this interaction is not regulated by phosphorylation of Serine1523. Thus, though it appears that binding between RAD51 and BRCA2 via a C-terminal motif is positionally conserved between *T. brucei* and mammals, the sequence requirements for this interaction are not (Esashi *et al.*, 2005;Esashi *et al.*, 2007). Further work will be needed to localise this binding site in *T. brucei* BRCA2 in order to dissect its function.

RAD51 binding was found to occur at a yet further location in *T. brucei* BRCA2, which has not been described in any other organism. This was between the BRC repeats and the C-tail and, if it is assumed to result from a single domain, it is proposed that the interaction would either localise within the DNA/DSS1-binding domain or in the region of BRCA2 between a putatively conserved DMC1 interaction motif (PhePP) and the start of the DNA/DSS1-binding domain. Again,

further work is required to fine map this site of interaction and to understand its function. Purification of *T. brucei* RAD51 and BRCA2, with the aim to set up *in vitro* DNA recombination assays, was attempted during this work but was hampered by insolubility of BRCA2 in the bacterial expression systems adopted. However, were this to be pursued, especially in the light of the recent successful purification of the much larger human BRCA2 protein (Jensen, Carreira, and Kowalczykowski, 2010), this would allow biochemical analyses to be conducted that might detail how the above interactions influence the mechanism of RAD51 regulation in HR by BRCA2.

Immunolocalisation of BRCA2 in *T. brucei* suggests a complex picture of BRCA2 subnuclear localisation, with peripheral nuclear ‘rings’ observed in some cells, while in others BRCA2 was found in more discrete focal accumulations. Possibly the most surprising finding was that overlap between BRCA2 and RAD51 signals was observed relatively rarely. In cells without induced DNA damage, RAD51 is essentially undetectable by immunofluorescence, whereas BRCA2 signal is detectable in > 70% of cells, primarily as ‘foci’ in the nucleus and rings of ‘foci’ around the nuclear periphery. After damage, RAD51 foci can be seen and BRCA2 nuclear peripheral rings were more common, but these signals were found not to overlap. RAD51 and BRCA2 were seen only to overlap when each was seen as foci, and even here this was only in ~ 50% of cells and in a single focus amongst many BRCA2 foci. This appears to contrast with mammals and *Drosophila* where almost complete co-localisation between BRCA2 and Rad51 is observed after damage in multiple foci (Mizuta *et al.*, 1997; Tarsounas, Davies, and West, 2003; Brough *et al.*, 2008). Why the subnuclear localisation between *T. brucei* BRCA2 and RAD51 appears more complex than in any other organism to date, remains elusive, and it is not clear if this relates to the apparently greater physical interactions between the proteins. Nonetheless, it is intriguing that BRCA2 appears to be more readily localised in the *T. brucei* nucleus than RAD51, and that the putative mediator does not always co-localise at sites of RAD51 foci. It is possible that this is consistent with BRCA2 not simply acting in DNA repair, and therefore supporting the proposal that it may have dual roles in the biology of *T. brucei*.

7.5 *T. brucei* BRCA2 does not bind CDC45.

The report of a putative interaction between the C-terminus of BRCA2 and CDC45 in *T. brucei* (Oyola, Bringaud, and Melville, 2009), coupled with the finding that the impaired replication seen in BSF *brca2*^{-/-} mutants cells could be localised to the C-terminus of BRCA2 (Claire Hartley, PhD Thesis, 2008), presented a possible novel mechanism for the involvement of BRCA2 in DNA replication. *brca2*^{-/-} mutants in BSF Lister 427 and PCF TREU 927 display defects in replication, albeit with differences. BSF *brca2*^{-/-} mutants display a defect which is manifest as an accumulation of cells with either raised kDNA or raised nDNA content (Claire Hartley, PhD Thesis, 2008; Oyola, Bringaud, and Melville, 2009). The PCF TREU 927 *brca2*^{-/-} mutants analysed here display a predominant accumulation of zoids (anucleate cells) which may be due to the lack of a mitosis to cytokinesis checkpoint in this life cycle stage (Hammarton, 2007), allowing cells that have not completed their nuclear DNA replication to proceed through cytokinesis generating zoids. Many approaches were taken in order to validate the putative interaction between BRCA2 and CDC45, but none were successful. Though it remains possible that the interaction is real, it must be sufficiently transient or infrequent to escape detection in the experiments performed here. In addition, this meant that the precise mechanism of involvement of BRCA2 in DNA replication in *T. brucei* could not be elucidated, and distinct approaches will be needed.

Very recently, evidence has been published to suggest that in mammalian cells the C-terminal Rad51-binding motif of BRCA2 acts to stabilise Rad51 filaments on nascent DNA at a stalled replication fork and so prevent degradation of this DNA by Mre11 (Hashimoto *et al.*, 2010; Schlacher *et al.*, 2011). It would clearly be interesting to investigate if this action is conserved in trypanosomatids, especially in light of the extensive interactions between the C-terminus of BRCA2 and RAD51 found here (section 7.4). A striking similarity is seen between the BRCA2 ‘rings’ observed after immunolocalisation in *T. brucei* and the localisation of the replication origin recognition complex protein (*orc1/cdc6*) in *Trypanosoma cruzi* (Elias *et al.*, 2002; Calderano *et al.*, 2011). This may suggest that BRCA2 does indeed play a role in replication, and in fact this could be the non-repair function that has been proposed. However, if correct, it is not clear how this could lead to GCRs in BSF cells and not in PCF cells, unless the

connection is specific to some aspects of the genome, such as the *VSG* subtelomeres. Exploration of this may reveal a novel mechanism for the function of BRCA2 in DNA replication.

Appendices

Appendix 1: *BRCA2* gene sequence



 CCGGCGTGCAGGTGAATGGACGAGATCAAGTGGCCCCGCGGTTGCTGCAAAATTTGCGCAATCATTGGAGCAGGTGGATCATCCCCATGAACCGCGAA

 GGCGCCACGTCCACTTACCTGCTCTAGTTCACCGGGGACGCCAACGACGTTTATAACGCGTTAGTAAACCCTCGTCCACCTAGTAGGGGTACTTGGCGCTT

CATTACCGATTGCAGCCAAGTGCGGTCAGGGAGGTGTGCTTGCATTCCTGACGGATGTTGATGATGATGTTAGGCGTCGTACCGGAGCTTCGGAGTGCAT

 GTAATGGCTAACGTCCGTTACGCCAGTCCCTCCACACGAACGTAAGGACTGCCTACAACACTACTACAATCCGCAGCATGGCTCGAAGCCTCACGTA

CACGGCGTGTGTCGGTGGACTTGTGTTAGATATGATTGAGCAGTGTGCACTCTGCTGTTCCCTTCTCGAAAGAGAGGGGGTCATTAATATGGCCGCT

 GTGCCGCACGACAGCACCTGAACACAATCTATACTAACTCGTCACGACGTGAGACGACAAGGAAAGAAGCTTCTCTCCGCCAGTAATATACCGGCGA

GTTCAGCGTGAAGCGTGTGTTGCGCGTGGCGTAGGAAACGCCGACGGGGGATCAGGGGAAACGACAGAAGAACTGCTATAGGTGAGACGGACA

 CAAGTCGCACTTTTTCGCACACCAACGCGCACCGCATCCCTTTCGGGCTGCCGCCCTAGTCCCCTTTGCTGTCTTTGACGATATCCACTCTGCCTGT

ATTCGACGCGCAAGTGTGCTGCTGCTATTACCAATGGAGTACCTTCTCCGTTTGTGTTGGCACTTCCGCTCTGCTTGCGCATTATGATAAATAGGTGG

 TAAGCGTCGCGTTTACACGACGACATAATGGTAACCTCATGGAAGAGGCAACAAACACCGTGAAGGCAGAGACGACGCGTAACTACTATTTAATCCACC

GTCTACGATGCCGGTGCCTTTAAGCAGCCCCTCTGGAATTATGTGAATGCCGTTCTCGATATCATGAAGGACATGACATTTCTTGACCCATCGGAATAC


 CAGATGCTACGGCCGACGCAAAATTCGTCCGGGAGACCTTAATACACTTACGGCAAGAGCTATAGTACTTCTGTACTGTAAGAAGAACTGGGTAGCCTTATG



ATACCCCTCCGATAACAAGAAAGGTGGGCATCTGTTAGGGCCCTTTTCCCCCTTCTGCGGTAAGTGTGCTGTGCGGAAGCGAAATATTCACATCTGCG

 TATGGGAGGCTATTGTTCTTCCACCCGTAGACAAATCCCGGGAAAAGGGGAAAGACGCCATGACAAACGACAGCGCTTCGCTTATAAGTGTAGACGC





 CTTGTTGATACTGAGTATACATAAGTGTATACCGTGTGTTGCCGGTGCCTTTCACCCGACGTTTCTGCTCGCTCATTCTCACCACTCCACCTC

 GAACAACTATGACTCATATGTATTCACATATGGCAACAACAGGGCCACGACGGGAAACGTTGGCTGCAAAGACGAGCGAGTAAAGTGGTGGAGGTGGAG



 CACACGCGTGCATTTGAATGCCTTTTAGTACTTTGTTGCACTACATTCGGTCCCTTTTCTTCTTTTTCGGCTCCTCCTCCTCCTCTCTTTTCTT

 GTGTGCGCACGTTAACTTACGGAAAATCATGAAACAAACGTGATGTAAGGCCAGGGGAAAAGAAGAAAAGCCGAGGAGGAGGAGGAGGAAAAGAA

CCATCCTGAAATCCCGTGTGTTGTTAATTAATCTGCTCGGAAGTCAAATTCGATTATATGAGCCACAAAAAGGAAGACAAGGCAGCAACTCTGG

 GGTAGGACTTTAAGGGGCACACAACAAATTAATTAGACGAGCCTTCAGTTTAAAGACTAATAATACTCGGTGTTTTTCTTCTGTTCCGTCGTTGAGACC





93, 112
BRCA2 ORF

115, 153

M S H K K G R Q G S N S G

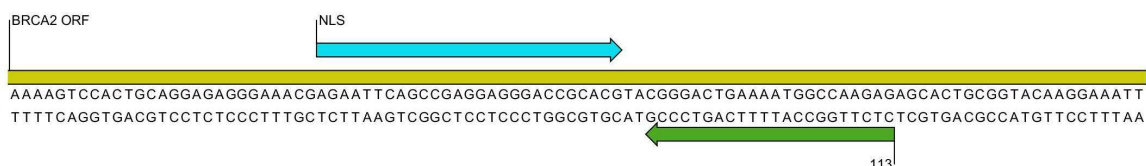
BRCA2 ORF



 AGCGCGCAAAATTCGATACGCCGCAACGGAACCGTACGAAAGTCCGCTCCGATGCCCCCAAGAGACAACGCAGTCGGTCTGGAGAAAGTGTACAAGGA

 TCGCGCGGTTTTAAGGCTATGCGGCGTTGCCCTTGCCATGCTTACCGGCGAGGCTACGGGGTTCTCTGTTGCGTCAGCCAGACCTCTTTCACATGTTCTCT

A R Q N S D T P Q R N R T K C R S D A P K R Q R S R S G E S V Q G



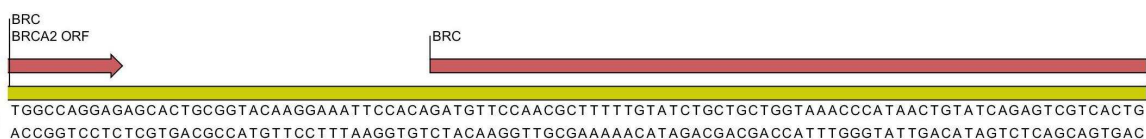
AAAAGTCCACTGCAGGAGAGGGAAACGAGAATTCAAGCCGAGGAGGGACCGCACGTACGGGACTGAAAAATGGCCAAAGAGAGCACTGCGGTACAAGGAAATT
TTTTCAGGTGACGTCTCTCCCTTTGCTCTTAAGTCGGCTCCTCCCTGGCGTGCATGCCCTGACTTTTACCAGTTCTCTCGTGACGCCATGTTCTCTTAA

K S P L Q E R E T R I Q P R R D R T Y G T E N G Q E S T A V Q G N



CCACAGATGTTCCAACGCTTTTTGTATCTGCTGCTGGTAAACCCATAACTGTATCAGAGTCGTCAGTCAAGTAGCAAGGGCACGAATGAATACTGAAAA
GGTGCTACAAGGTTGCGAAAAACATAGACGACGACCATTGGGTATTGACATAGTCTCAGCAGTGACGTTTCATCGTTCCCGTGCTTACTTATGACTTTT

S T D V P T L F V S A A G K P I T V S E S S L Q V A R A R M N T E N



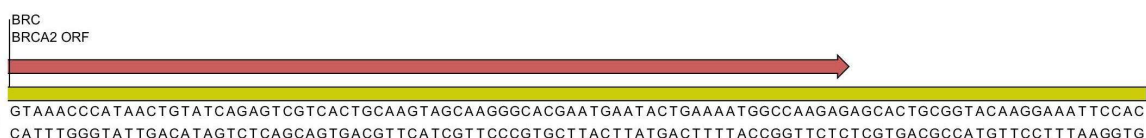
TGGCCAGGAGAGCACTGCGGTACAAGGAAATCCACAGATGTTCCAACGCTTTTTGTATCTGCTGCTGGTAAACCCATAACTGTATCAGAGTCGTCAGT
ACCGGTCTCTCGTGACGCCATGTTCTTTAAGGTGTCTACAAGTTGCGAAAAACATAGACGACGACCATTGGGTATTGACATAGTCTCAGCAGTGAC

G Q E S T A V Q G N S T D V P T L F V S A A G K P I T V S E S S L



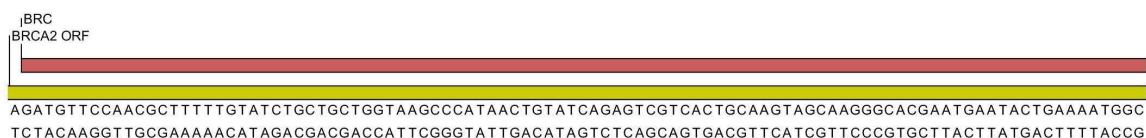
CAAGTAGCAAGGGCACGAATGAATACTGAAAAATGGCCAGGAGAGCACTGCGGTACAAGGAAATCCACAGATGTTCCAACGCTTTTTGTATCTGCCGCTG
GTTTCATCGTTCCCGTGCTTACTTATGACTTTTACCAGTCTCTCGTGACGCCATGTTCTTTAAGGTGTCTACAAGTTGCGAAAAACATAGACGGCGAC

Q V A R A R M N T E N G Q E S T A V Q G N S T D V P T L F V S A A



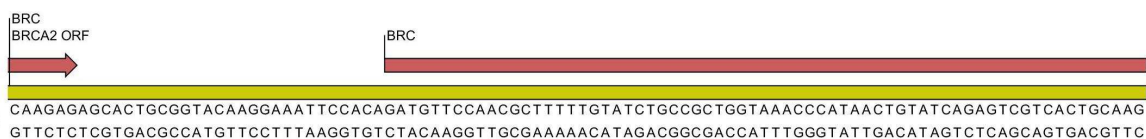
GTAACCCATAACTGTATCAGAGTCGTCAGTCAAGTAGCAAGGGCACGAATGAATACTGAAAAATGGCCAAAGAGAGCACTGCGGTACAAGGAAATCCAC
CATTGGGTATTGACATAGTCTCAGCAGTGACGTTTCATCGTTCCCGTGCTTACTTATGACTTTTACCAGTCTCTCGTGACGCCATGTTCTTTAAGGTG

G K P I T V S E S S L Q V A R A R M N T E N G Q E S T A V Q G N S T



AGATGTTCCAACGCTTTTTGTATCTGCTGCTGGTAAAGCCATAACTGTATCAGAGTCGTCAGTCAAGTAGCAAGGGCACGAATGAATACTGAAAAATGGC
TCTACAAGTTGCGAAAAACATAGACGACGACCATTGGGTATTGACATAGTCTCAGCAGTGACGTTTCATCGTTCCCGTGCTTACTTATGACTTTTACC

D V P T L F V S A A G K P I T V S E S S L Q V A R A R M N T E N G



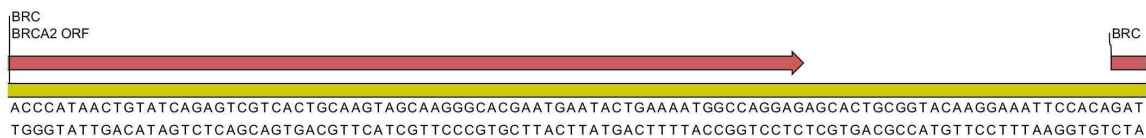
CAAGAGAGCACTGCGGTACAAGGAAATCCACAGATGTTCCAACGCTTTTTGTATCTGCCGCTGGTAAACCCATAACTGTATCAGAGTCGTCAGTCAAG
GTTCTCTCGTGACGCCATGTTCTTTAAGGTGTCTACAAGTTGCGAAAAACATAGACGGCGACCATTGGGTATTGACATAGTCTCAGCAGTGACGTTT

Q E S T A V Q G N S T D V P T L F V S A A G K P I T V S E S S L Q



TAGCAAGGGCACGAATGAATACTGAAAAATGGCCAAAGAGAGCACTGCGGTACAAGGAAATCCACAGATGTTCCAACGCTTTTTGTATCTGCCGCTGGTAA
ATCGTTCCCGTGCTTACTTATGACTTTTACCAGTCTCTCGTGACGCCATGTTCTTTAAGGTGTCTACAAGTTGCGAAAAACATAGACGGCGACCATT


V A R A R M N T E N G Q E S T A V Q G N S T D V P T L F V S A A G K



ACCCATAACTGTATCAGAGTCGTCAGTCAAGTAGCAAGGGCACGAATGAATACTGAAAAATGGCCAGGAGAGCACTGCGGTACAAGGAAATCCACAGAT
TGGGTATTGACATAGTCTCAGCAGTGACGTTTCATCGTTCCCGTGCTTACTTATGACTTTTACCAGTCTCTCGTGACGCCATGTTCTTTAAGGTGTCTA

P I T V S E S S L Q V A R A R M N T E N G Q E S T A V Q G N S T D


BRC
BRCA2 ORF



GTTCCAACGCTTTTGTATCTGCTGCTGGTAAACCCATAACTGTATCAGAGTCGTCACCTGCAAGTAGCAAGGGCACGAATGAATACTGAAAAATGGCCAGG
CAAGGTTGCGAAAAACATAGACGACGACCATTTGGGTATTGACATAGTCTCAGCAGTGACGTTTCATCGTCCCGTGCTTACTTATGACTTTTACCGGTTCC

V P T L F V S A A G K P I T V S E S S L Q V A R A R M N T E N G Q

BRC
BRCA2 ORF



AGAGCACTGCGGTACAAGGAAATTCACAGATGTTCCAACGCTTTTGTATCTGCTGCTGGTAAACCCATAACTGTATCAGAGTCGTCACCTGCAAGTAGC
TCTCGTGACGCCATGTTCCCTTAAAGGTGTCTACAAGGTTGCGAAAAACATAGACGACGACCATTTGGGTATTGACATAGTCTCAGCAGTGACGTTTCATCG

E S T A V Q G N S T D V P T L F V S A A G K P I T V S E S S L Q V A


BRC
BRCA2 ORF



AAGGGCACGAATGAATACTGAAAAATGGCCAAGAGAGCACTGCGGTACAAGGAAATTCACAGATGTTCCAACGCTTTTGTATCTGCGGCTGGTAAACCC
TTCCCGTGCTTACTTATGACTTTTACCGGTTCTCTCGTGACGCCATGTTCCCTTAAAGGTGTCTACAAGGTTGCGAAAAACATAGACGGGACCATTTGGG

R A R M N T E N G Q E S T A V Q G N S T D V P T L F V S A A G K P


BRC
BRCA2 ORF



ATAACTGTATCAGAGTCGTCACCTGCAAGTAGCAAGGGCACGAATGAATACTGAAAAATGGCCAAGAGAGCACTGCGGTACAAGGAAATTCACAGATGTTCC
TATTGACATAGTCTCAGCAGTGACGTTTCATCGTCCCGTGCTTACTTATGACTTTTACCGGTTCTCTCGTGACGCCATGTTCCCTTAAAGGTGTCTACAAG

I T V S E S S L Q V A R A R M N T E N G Q E S T A V Q G N S T D V


BRC
BRCA2 ORF



CAACGCTTTTGTATCTGCGGCTGGTAAACCCATAACTGTATCAGAGTCGTCACCTGCAAGTAGCAAGGGCACGAATGAATACTGAAAAATGGCCAAGAGAG
GTTGCGAAAAACATAGACGGGACCATTTGGGTATTGACATAGTCTCAGCAGTGACGTTTCATCGTCCCGTGCTTACTTATGACTTTTACCGGTTCTCTC

P T L F V S A A G K P I T V S E S S L Q V A R A R M N T E N G Q E S

BRCA2 ORF



CACTGCGGTACAAGGAAATTCACAGATGTTCCAACGCTTTTGTATCTGCTGCTGGTAAACCCATAACTGTATCAGAGTCGTCACCTGCAAGTAGCAAGG
GTGACGCCATGTTCCCTTAAAGGTGTCTACAAGGTTGCGAAAAACATAGACGACGACCATTTGGGTATTGACATAGTCTCAGCAGTGACGTTTCATCGTTCC

T A V Q G N S T D V P T L F V S A A G K P I T V S E S S L Q V A R


BRC
BRCA2 ORF



GCACGAATGAATACTGAAAAATGGCCAGGAGAGCACTGCGGTACAAGGAAATTCACAGATGTTCCAACGCTTTTGTATCTGCTGCTGGTAAACCCATAA
CGTGCTTACTTATGACTTTTACCGGTTCTCTCGTGACGCCATGTTCCCTTAAAGGTGTCTACAAGGTTGCGAAAAACATAGACGACGACCATTTGGGTATT

A R M N T E N G Q E S T A V Q G N S T D V P T L F V S A A G K P I

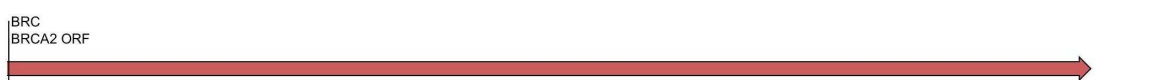
BRC
BRCA2 ORF



CTGTATCAGAGTCGTCACCTGCAAGTAGCAAGGGCACGAATGAATACTGAAAAATGGCCAAGAGAGCACTGCGGTACAAGGAAATTCACAGATGTTCCAAC
GACATAGTCTCAGCAGTGACGTTTCATCGTCCCGTGCTTACTTATGACTTTTACCGGTTCTCTCGTGACGCCATGTTCCCTTAAAGGTGTCTACAAGGTTG

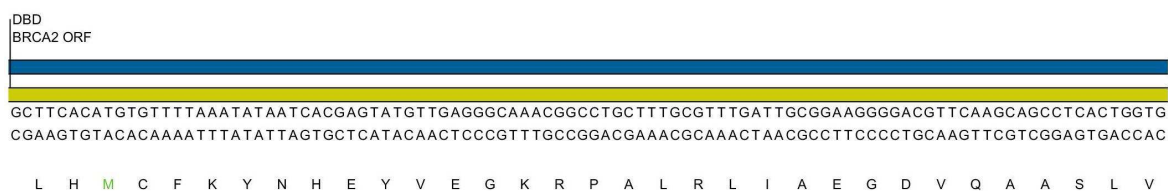
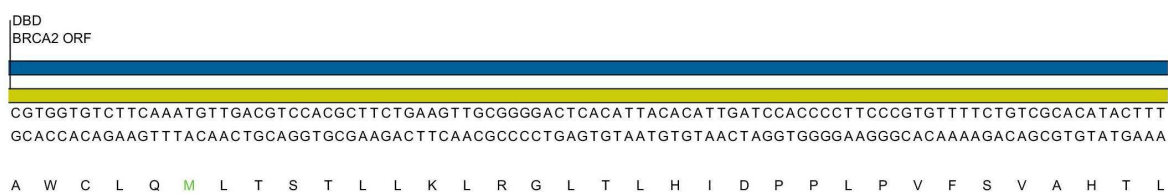
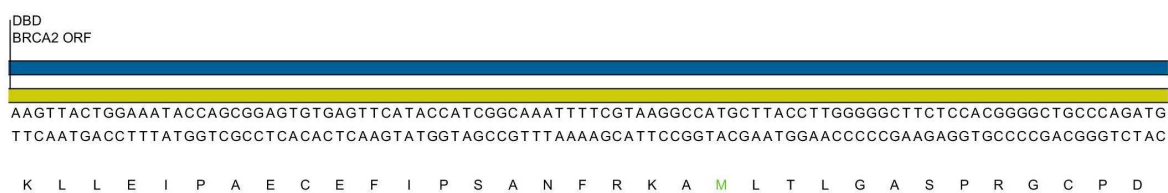
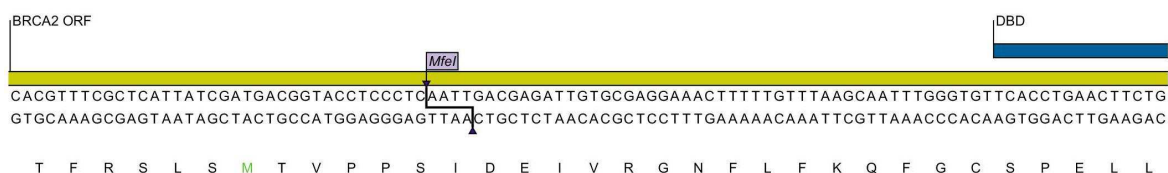
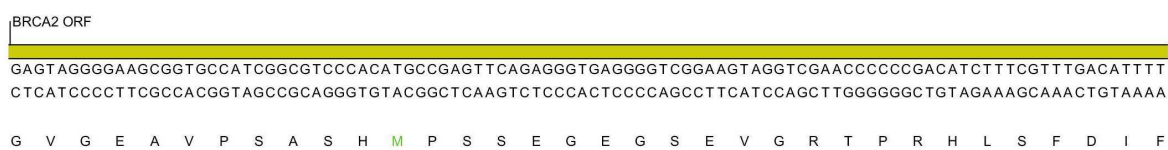
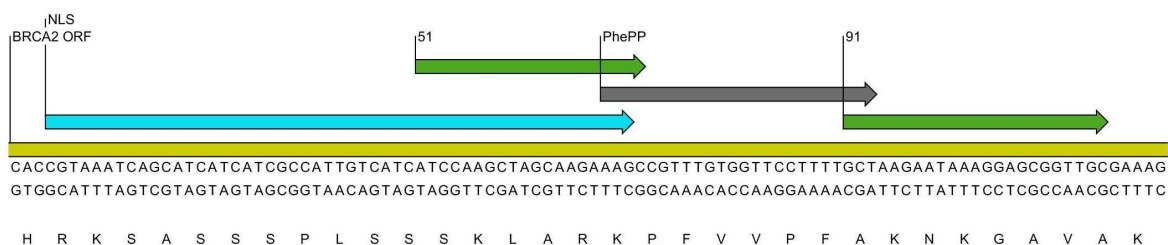
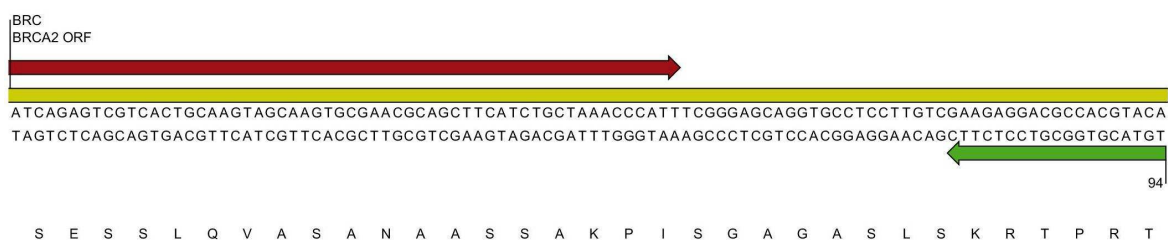
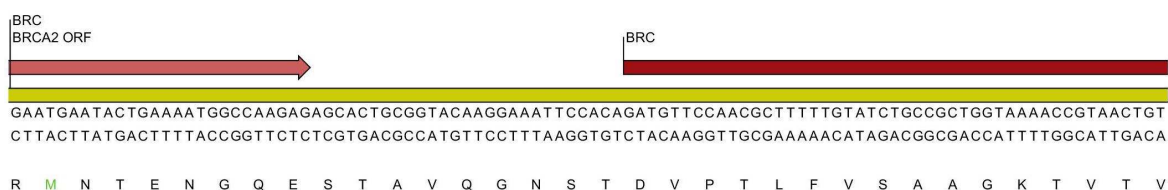
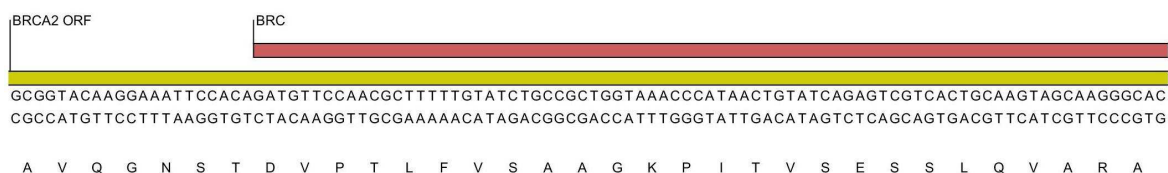
T V S E S S L Q V A R A R M N T E N G Q E S T A V Q G N S T D V P T

BRC
BRCA2 ORF



GCTTTTGTATCTGCGGCTGGTAAACCCATAACTGTATCAGAGTCGTCACCTGCAAGTAGCAAGGGCACGAATGAATACTGAAAAATGGCCAAGAGAGCACT
CGAAAAACATAGACGGGACCATTTGGGTATTGACATAGTCTCAGCAGTGACGTTTCATCGTCCCGTGCTTACTTATGACTTTTACCGGTTCTCTCGTGA

L F V S A A G K P I T V S E S S L Q V A R A R M N T E N G Q E S T



DBD
BRCA2 ORF

GTAGTCTGGGTAGTGTCCGGTATCTTTTGAGGAGCGCCTTACTCCTCACACCTGCACGGCAGTGGTTCCGATGGGTTTACCACGTTAAAGTGTCTCTTG
CATCAGACCCATCACAGCCATAGAAAACCTCTCGCGGAATGAGGAGTGTGGACGTGCCGTACCAAAGGCTACCCAAAATGGTGAATTTACACAGAGAAC

V V W V V S V S F E E R L T P H T C T A V V S D G F Y H V K V S L

DBD
BRCA2 ORF

ATATTCCATTAACGAACTTAGTTCGTAATGGAACCCTGCGGTGTGGTCAGAAGATTGTTACTTGCAGTGCAGGATGCTGAGGAGAGACTGTGTTCTCC
TATAAGGTAATTGCTTGAATCAAGCATTACCTTGGGACGCCACACCAGTCTTCTAAACAATGAACGCCACGCTCCTACGACTCCTCTCTGACAACAAGAGG

D I P L T N L V R N G T L R C G Q K I V T C G A R M L R R D C C S P

DBD
BRCA2 ORF

48

ACTAGAATGCAAAGATGAAGTGTCCCTCTCCATTAAC TACAAC TGCACACAACCTGTGGACCTTCTCACCTCTAGGTCTCTATCATACTTGTTCGCCG
TGATCTTACGTTTCTACTTACGAGGAGAGGTAATTGATGTTGACGTGTGTTGGACACCCTGGAAGGAGTGGAGATCCAGAGATAGTATGAACAAAACGGC

L E C K D E V L L S I N Y N C T Q P V G P S S P L G L Y H T C L P

48
DBD
BRCA2 ORF

138

ACACTGCTGCCTTCCGCTATGGATATGCTTGGTGGTTTGGTACCTTGTGTTGAAAGGCGAGTGGAGCGCGTGCTTCCGCCCTTTTCTTGAGAAAACAT
TGTGACGACGGAAGGCGATACCTATACGAACCACCAAACCATGGAAACAACTTTCGCGTCCACTCGCGCACGAAGGGGGAAAAAGGAACCTTTTGTGA

139

T L L P S A M D M L G G L V P C L K G R V E R V L P P F F L E K T

DBD
BRCA2 ORF

TTAAGGGTGCAGCAACTGGCGACACAAGAGGCAGCACAGGTGGTGCCTGAAAATTGTGAGGAGTTTATTGGCGCAGCTAAGTTTCCAGGAATGTATGGC
AATCCCACGCGCTTGACCCTGTGTTCTCCGTGCTGCCACACGCAACTTTAACACTCCTCAAATAACCGGCTCGATTCAAAGGTCCTTACATACCG

F K G A R T G D T R G S T G G A L K I V R S L L A Q L S F Q E C M A

DBD
BRCA2 ORF

ACGCGGAGCTGTGCTCCGTTTGAAGGAAAAAGTGACCGACAACCTTTCACGCTGTGACATCGTTTTTGTGCTTGTGAGCGACAGGGGACGTCCTCTTG
TGCGCTCGACAACGAGGCAAACTTCTTTTCACTGGCTGTGAAAAGTGCAGACTGTAGCAAAAACAACAGAACACTCGCTGTCCCCTGCAGGAGAAC

R G A V A P F E G K S D R Q L S R L T S F L L S C E R Q G D V L L

DBD
BRCA2 ORF

CAAAATATGGGATGATTGCGGTGCCAACTGTCCGGCGGGGATTTGGAGGAACATTGCGTGTGATTTTCCACCGGAGGGAGCTGAGATTGTCGTTTTCTCCG
GTTTATACCTACTAACGCCACGGTTGACAGGCCGCCCTAAACCTCCTTGTAAAGCACAATAAAAGGTGGCCTCCCTCGACTCTAACAGCAAAAAGAGGC

Q I W D D C G A N C P A G D L E E H S C D F P P E G A E I V V F S

DBD
BRCA2 ORF

TAACCCCTTCACGCTTCCGACCTGGTCACCCCTTCCAGCGGACGACAGTTTTGACTCTCGGAGCCCTCTTCCGATATAGCATAGTCTCACGCCCGGTAA
ATTGGGGAAGTGCAGGCTGGACCAGTGGGGAAGGTGCCTGCTGTCAAAACATGAGAGCCTCGGGAGAAGCCATATCGTATCAGAGTGGCGGCGCATT

V T P S R F R P G H P F Q R T T V L Y S R S P L R Y S I V S P P R K

DBD
BRCA2 ORF

GGGGTTTGTGAGGCAACCTTTGCGCTCAGCTGAAGATGTGTCCCAAAAACAGAGACAGGTGATGCCATCGATTTTGTGGCTTGTTCGTCGGCACCAAG
CCCCAAACACTCCGTTGGAACGCGAGTTCGACTTCTACACAGGGGTTTTGTCTCTGTCCACTACGGTAGCTAAAACGACCGAACAAGCAGCCGTGGTTT

G F V R Q P L R S A E D V S P K T E T G D A I D F A G L F V G T K

DBD
BRCA2 ORF

AGTGTGGACACGGTCAACTCACATATTATCGTGGCCTTAAATGACGGATGGAACCTGGATGTGTTCCGGCTTCTACTTTATGATTGATGTCCACATG
TCACACCTGTGCCAGTTGAGTGTATAATAGCACCGGAATTTACTGCCTACCTTTGGACCTACACAAGGCCGAAGGATGAAATACCTAACACAGGGTGTAC

S V D T V N S H I I V A L N D G W K P G C V P A S Y F M I D V P H

DBD
BRCA2 ORF

CCACGGGCTCAAAGAGATTGTGCTTGTCTTGGCATCAATACCATTACACCTGTTATTGTGCAGAAATGCTTCTTTTATACGTTGCGCGGAGGACTTGGG
GGTGCCCGAGTTTTCTCTAACACGAACGAAACGGTAGTTATGGTAAAGTGTGGACAATAACACGCTTACGAAAGAAAATATGCAACGCGCCTCCTGAACCC

A T G S K E I V L A L P S I P F T P V I V Q N A S F I R C A E D L G

DBD
BRCA2 ORF

ACCCGATTGCATACACGTAAGTGGCGAATGAGTACACGAAGTTTTACAGCCGCTCCTGCTGAGCCGCTCCTTCGCGGTGTTGTTGAGTCACTTGGGAAAAAT
TGGGCTAACGTATGTGCATGACCGCTTACTCATGTGCTTCCAAAATGTGCGCAGGACGACTCGGCGAGGAAGCGCCACAACAACCTCAGTGAACCCCTTTAA

P D C I H V L A N E Y T K V Y S R P A E P L L R G V V E S L G K I

DBD
BRCA2 ORF

CGTGGGATGGCGAAGTCAAGTAGGCCTATTATTGCCCGTTCTGAGGAGCTGCTACGAATGCGGACGTTGAGTGAGGAAGCTCGGGCCGATATATGTGCAC
GCACCCCTACCGCTTCAAGTTCATCCGGATAATAACGGGCAAGACTCCTCGACGATGCTTACGCTGCAACTCACTCCTTCGAGCCCGGCTATATACAGCTG

R G M A K S S R P I I A R S E E L L R M R T L S E E A R A D I C R

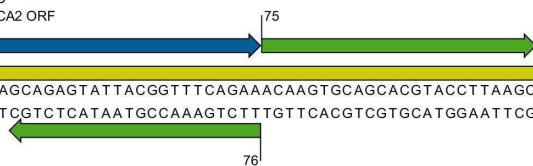
DBD
BRCA2 ORF

TGTGAGAGAAGTGGTGGAGGGGATGAGTTACCTAATCCTGCAGCCACAGCGCAGCCGCTCCACGGTATCAATTACGCCAGGAAGCATACCCCTGT
ACAGCTCTCTTGACCAACCTCCCTACTCAATGGATTAGGACGTGGTGTGCGGTGGCAGAGGTGCCATAGTTAATGCGGTCCCTTCGTAGATGGGGACA

L S R E L V G G D E L P N P A A T A Q P S P R Y Q L R Q E A S T P V

DBD
BRCA2 ORF

TGAGCAGAGTATTACGGTTTCAGAAAACAAGTGCAGCACGTACCTTAAAGCAGTGAAGAAGAACAGGTAGAGGATTTAAGGTCCCTCGAATGTCAAGGCTAGC
ACTCGTCTCATAATGCCAAAGCTTTGTTTACAGTCGTGCATGGAATTCGTCACTTCTTCTTGTCCATCTCCTAAATCCAGGAGCTTACAGTTCGGATCG



E Q S I T V S E T S A A R T L S S E E E Q V E D L R S S N V K A S

BRCA2 ORF

CCACGGCGTCATGATTTGGCAACATTGTGGGATTTCCGGCTTCTCAAAGTCCAGGGCTCTGACAAAACCGAATGCATTGAGATTTGGGTGGCCGTCCTCA
GGTGCCGACGATACATAAACCGTTGTAACACCCATAAGCCGAAGAGTTCAGGTCGCGAGACTGTTTGGGCTTACGTAACCTAAAACCCACCGCAGGGT

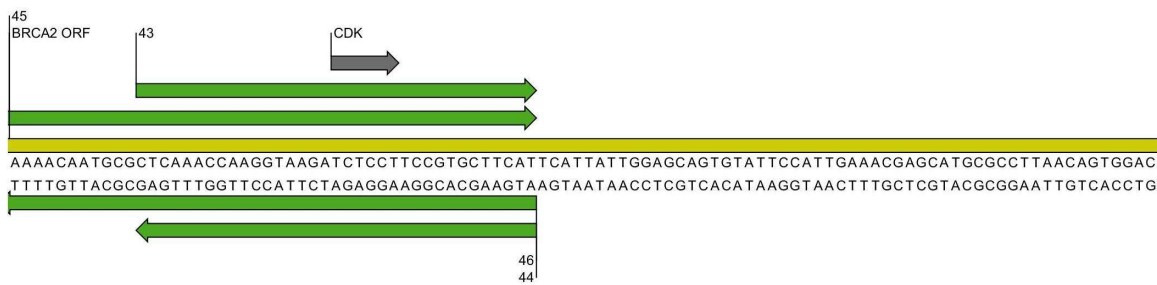
P R R H V F G N I V G F R L L K C Q G S D K P E C I E I L G G R P

BRCA2 ORF

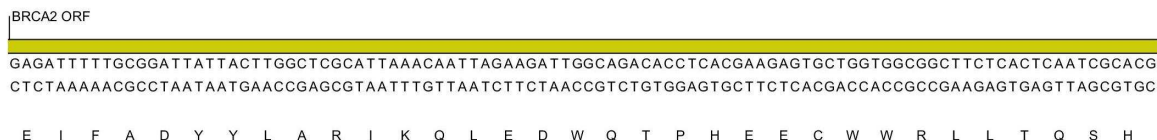
GCACCTCTGCTCTGGAAGTGGAAAGTTTGTAGTGTCCCCCTCGGACTTTTCTCAGAGCCTTGTGACTTTGAGGCTGATATCAATTTGGTGCCACCGC
CGTGAGAGCAGAGACCTTACCTTTCAAACATCACAGGGGAGCCTGAAAAGAGTCTCGGAACACATGAAACTCCGACTATAAGTTAAACCCAGGTGGCG

S T L V S G S G K F V V S P S D F S Q S L V Y F E A D I Q F G A T A

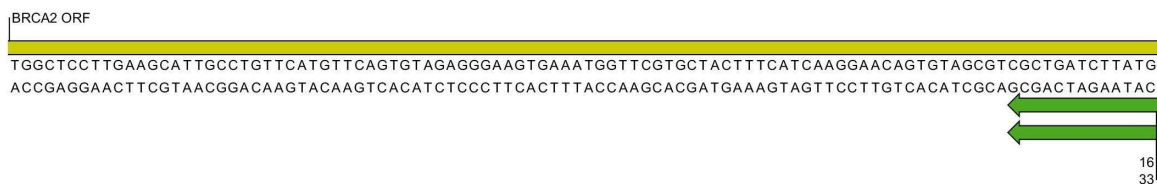
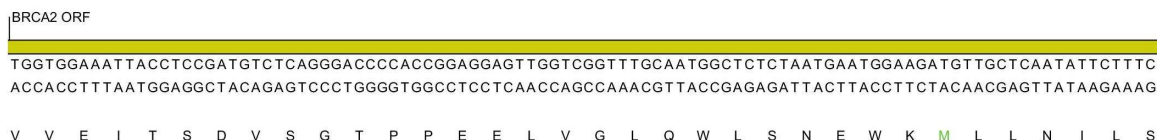
46



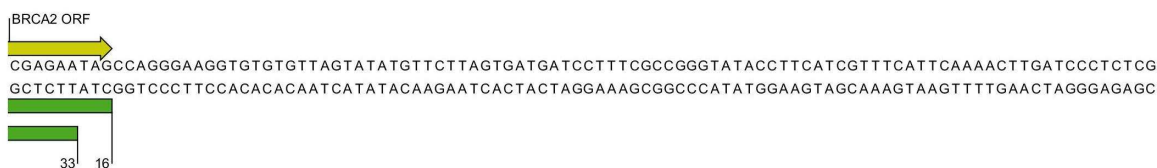
K Q C A Q T K V R S P S V L H S L L E Q C I P L K R A C A L T V D



E I F A D Y Y L A R I K Q L E D W Q T P H E E C W W R L L T Q S H



G S L K H C L F M F S V E G S E M V R A T F I K E Q C S V A D L M



R E *

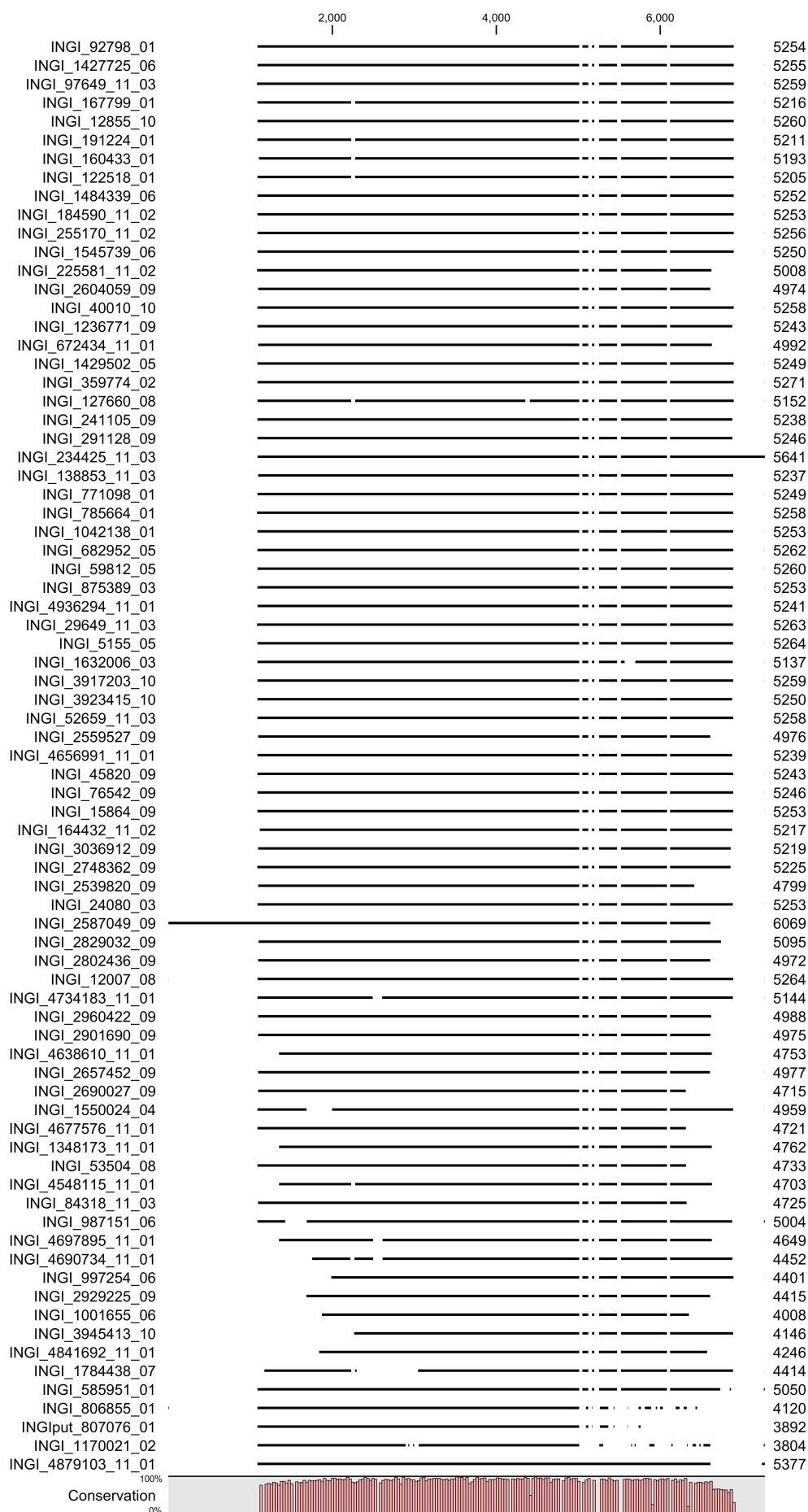
CATTGTCTAACTCTCATTGTCAATATTTGGTTTCGTACTCTGCGTTCGGACAAGGTTCTCTCAAGAGTCTGGTCTTTTTTTTTTCCGCTCCTCTGGTTGTAACAGTATTGAGAGTAACAGTTATAAAACCAAGCATGAGACGCAAGCCTGTTCCAAGAGAGTTCAGACCAAGAAAAAAGGCGAGGAGACCAA



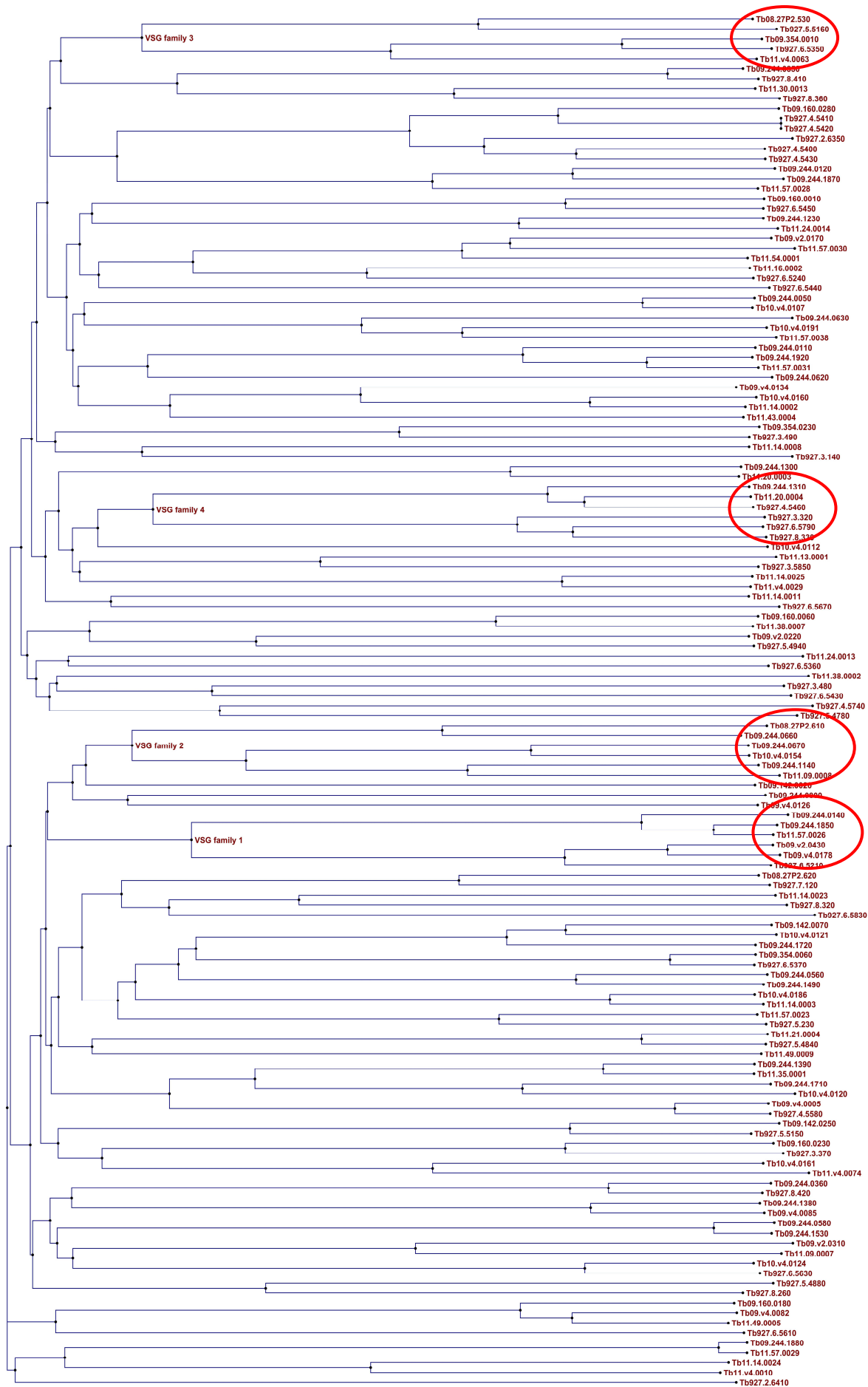
CACTTCCCTTTTTTTTTTTTTTGCACCTTTCATTTTCAGCCAAGAAAAACGAAAGAACTGAGGGAAGGACGTGGTAGTAGTGTGCACATTCGTCAGTACGGTAAGGGAAAAAAGGCGGTAAGGTAAGTAAAGTCGGTCTTTTTTGTCTTCTTGACTCCCTTCTGCACCATCATACAACGTGTAAGCAGTCATGC

GCAGTACTTAAGGACATACTCGGCTGTGCGCGCCCAA
CGTCATGAATTCCTGTATGAGCCGACAGCGCGGGTT

Appendix 2: Alignment of *ingi* retrotransposons in TREU 927.

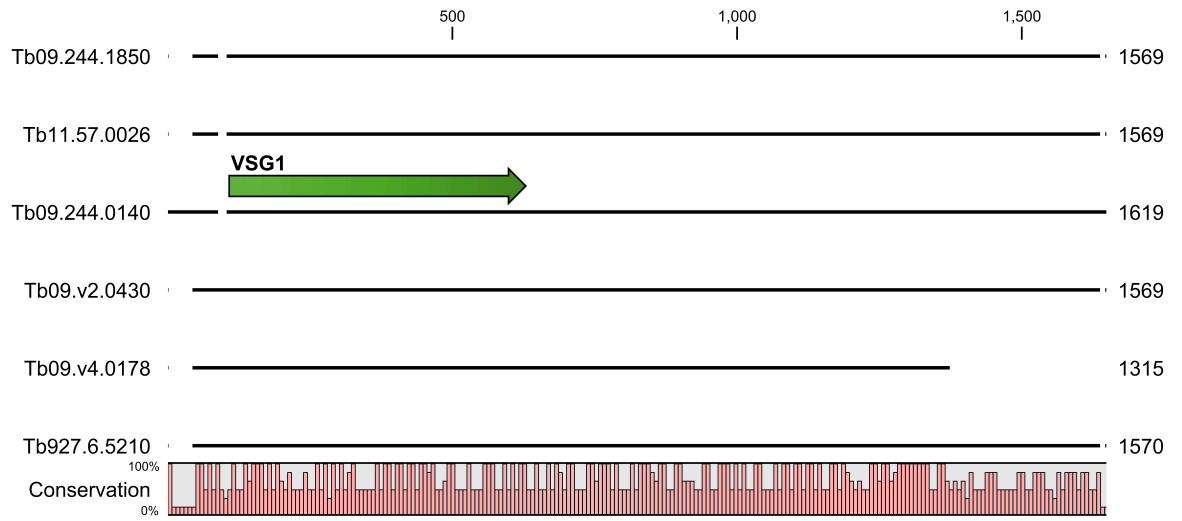


Appendix 3: Tree of TREU 927 VSGs

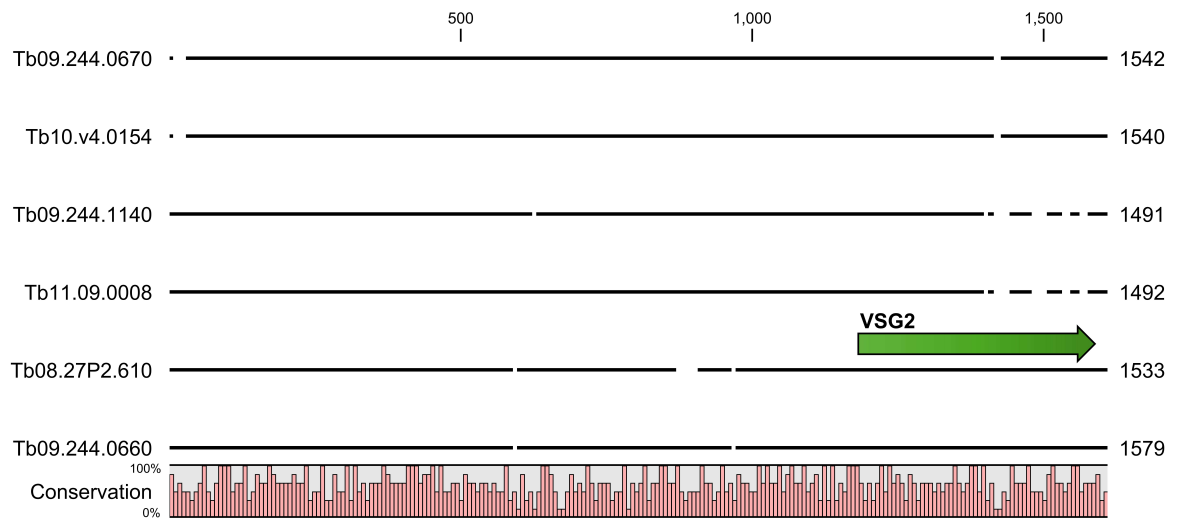


Appendix 4: Alignment of TREU 927 VSG family members

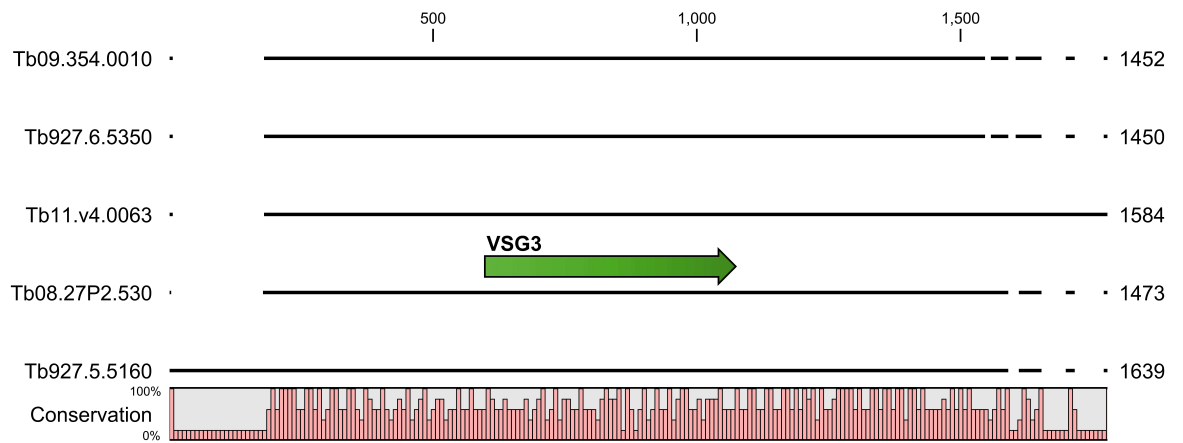
VSG family 1



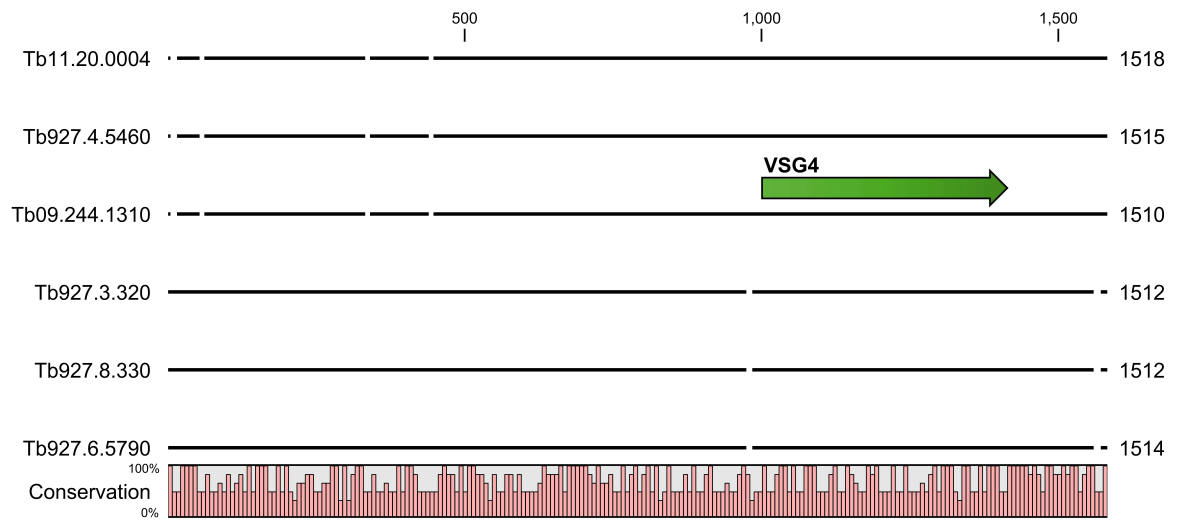
VSG family 2



VSG family 3



VSG family 4



List of references

- Abbott,D.W., Freeman,M.L., and Holt,J.T. (1998) Double-strand break repair deficiency and radiation sensitivity in BRCA2 mutant cancer cells *Journal of the National Cancer Institute* **90**: 978-985.
- Adl,S.M., Simpson,A.G., Farmer,M.A., Andersen,R.A., Anderson,O.R., Barta,J.R., Bowser,S.S., Brugerolle,G., Fensome,R.A., Fredericq,S., James,T.Y., Karpov,S., Kugrens,P., Krug,J., Lane,C.E., Lewis,L.A., Lodge,J., Lynn,D.H., Mann,D.G., McCourt,R.M., Mendoza,L., Moestrup,O., Mozley-Standridge,S.E., Nerad,T.A., Shearer,C.A., Smirnov,A.V., Spiegel,F.W., and Taylor,M.F. (2005) The new higher level classification of eukaryotes with emphasis on the taxonomy of protists *J.Eukaryot.Microbiol.* **52**: 399-451.
- Alsford,N.S., Navarro,M., Jamnadass,H.R., Dunbar,H., Ackroyd,M., Murphy,N.B., Gull,K., and Ersfeld,K. (2003) The identification of circular extrachromosomal DNA in the nuclear genome of *Trypanosoma brucei* *Mol.Microbiol.* **47**: 277-289.
- Alsford,S., Horn,D. (2008) Single-locus targeting constructs for reliable regulated RNAi and transgene expression in *Trypanosoma brucei* *Mol.Biochem.Parasitol.* **161**: 76-79.
- Amitani,I., Baskin,R.J., and Kowalczykowski,S.C. (2006) Visualization of Rad54, a chromatin remodeling protein, translocating on single DNA molecules *Mol.Cell* **23**: 143-148.
- Aparicio,O.M., Weinstein,D.M., and Bell,S.P. (1997) Components and dynamics of DNA replication complexes in *S-cerevisiae*: Redistribution of MCM proteins and Cdc45p during S phase *Cell* **91**: 59-69.
- Aparicio,T., Guillou,E., Coloma,J., Montoya,G., and Mendez,J. (2009) The human GINS complex associates with Cdc45 and MCM and is essential for DNA replication *Nucl.Acids.Res.* **37**: 2087-2095.
- Aparicio,T., Ibarra,A., and Mendez,J. (2006) Cdc45-MCM-GINS, a new power player for DNA replication *Cell Div.* **1**: 18.
- Arata,H., Dupont,A., Mine-Hattab,J., Disseau,L., Renodon-Corniere,A., Takahashi,M., Viovy,J.L., and Cappello,G. (2009) Direct observation of twisting steps during Rad51 polymerization on DNA *Proceedings of the National Academy of Sciences of the United States of America* **106**: 19239-19244.
- Ayoub,N., Rajendra,E., Su,X., Jeyasekharan,A.D., Mahen,R., and Venkitaraman,A.R. (2009) The Carboxyl Terminus of Brca2 Links the Disassembly of Rad51 Complexes to Mitotic Entry *Curr.Biol.*
- Badie,S., Escandell,J.M., Bouwman,P., Carlos,A.R., Thanasoula,M., Gallardo,M.M., Suram,A., Jaco,I., Benitez,J., Herbig,U., Blasco,M.A., Jonkers,J., and Tarsounas,M. (2010) BRCA2 acts as a RAD51 loader to facilitate telomere replication and capping *Nature Structural & Molecular Biology* **17**: 1461-1U93.

- Bangs, J.D., Crain, P.F., Hashizume, T., McCloskey, J.A., and Boothroyd, J.C. (1992) Mass-Spectrometry of Messenger-Rna Cap-4 from Trypanosomatids Reveals 2 Novel Nucleosides *Journal of Biological Chemistry* **267**: 9805-9815.
- Barbet, A.F., Kamper, S.M. (1993) The importance of mosaic genes to trypanosome survival *Parasitol.Today* **9**: 63-66.
- Barbour, A.G., Restrepo, B.I. (2000) Antigenic variation in vector-borne pathogens *Emerging Infectious Diseases* **6**: 449-457.
- Barrett, M.P., Boykin, D.W., Brun, R., and Tidwell, R.R. (2007) Human African trypanosomiasis: pharmacological re-engagement with a neglected disease *British Journal of Pharmacology* **152**: 1155-1171.
- Barrett, M.P., Burchmore, R.J., Stich, A., Lazzari, J.O., Frasch, A.C., Cazzulo, J.J., and Krishna, S. (2003) The trypanosomiasis *Lancet* **362**: 1469-1480.
- Barry, J.D. (1997) The relative significance of mechanisms of antigenic variation in African trypanosomes *Parasitol.Today* **13**: 212-218.
- Barry, J.D., Ginger, M.L., Burton, P., and McCulloch, R. (2003) Why are parasite contingency genes often associated with telomeres? *Int.J.Parasitol.* **33**: 29-45.
- Barry, J.D., Marcello, L., Morrison, L.J., Read, A.F., Lythgoe, K., Jones, N., Carrington, M., Blandin, G., Bohme, U., Caler, E., Hertz-Fowler, C., Renault, H., El Sayed, N., and Berriman, M. (2005) What the genome sequence is revealing about trypanosome antigenic variation *Biochem.Soc.Trans.* **33**: 986-989.
- Barry, J.D., McCulloch, R. (2001) Antigenic variation in trypanosomes: enhanced phenotypic variation in a eukaryotic parasite *Adv.Parasitol.* **49**: 1-70.
- Baumann, P., West, S.C. (1997) The human Rad51 protein: polarity of strand transfer and stimulation by hRP-A *Embo Journal* **16**: 5198-5206.
- Becker, M., Aitcheson, N., Byles, E., Wickstead, B., Louis, E., and Rudenko, G. (2004) Isolation of the repertoire of VSG expression site containing telomeres of *Trypanosoma brucei* 427 using transformation-associated recombination in yeast *Genome Res.* **14**: 2319-2329.
- Bekker-Jensen, S., Mailand, N. (2010) Assembly and function of DNA double-strand break repair foci in mammalian cells *Dna Repair* **9**: 1219-1228.
- Bennett, R.L., Holloman, W.K. (2001) A RecA homologue in *Ustilago maydis* that is distinct and evolutionarily distant from Rad51 actively promotes DNA pairing reactions in the absence of auxiliary factors *Biochemistry* **40**: 2942-2953.
- Benson, F.E., Baumann, P., and West, S.C. (1998) Synergistic actions of Rad51 and Rad52 in recombination and DNA repair *Nature* **391**: 401-404.
- Benson, F.E., Stasiak, A., and West, S.C. (1994) Purification and Characterization of the Human Rad51 Protein, An Analog of *Escherichia-Coli* RecA *Embo Journal* **13**: 5764-5771.
- Beranek, D.T. (1990) Distribution of Methyl and Ethyl Adducts Following Alkylation with Monofunctional Alkylating-Agents *Mutation Research* **231**: 11-30.

Berriman, M., Ghedin, E., Hertz-Fowler, C., Blandin, G., Renaud, H., Bartholomeu, D.C., Lennard, N.J., Caler, E., Hamlin, N.E., Haas, B., Bohme, U., Hannick, L., Aslett, M.A., Shallom, J., Marcello, L., Hou, L., Wickstead, B., Alsmark, U.C., Arrowsmith, C., Atkin, R.J., Barron, A.J., Bringaud, F., Brooks, K., Carrington, M., Cherevach, I., Chillingworth, T.J., Churcher, C., Clark, L.N., Corton, C.H., Cronin, A., Davies, R.M., Doggett, J., Djikeng, A., Feldblyum, T., Field, M.C., Fraser, A., Goodhead, I., Hance, Z., Harper, D., Harris, B.R., Hauser, H., Hostetler, J., Ivens, A., Jagels, K., Johnson, D., Johnson, J., Jones, K., Kerhornou, A.X., Koo, H., Larke, N., Landfear, S., Larkin, C., Leech, V., Line, A., Lord, A., MacLeod, A., Mooney, P.J., Moule, S., Martin, D.M., Morgan, G.W., Mungall, K., Norbertczak, H., Ormond, D., Pai, G., Peacock, C.S., Peterson, J., Quail, M.A., Rabinowitsch, E., Rajandream, M.A., Reitter, C., Salzberg, S.L., Sanders, M., Schobel, S., Sharp, S., Simmonds, M., Simpson, A.J., Tallon, L., Turner, C.M., Tait, A., Tivey, A.R., Van Aken, S., Walker, D., Wanless, D., Wang, S., White, B., White, O., Whitehead, S., Woodward, J., Wortman, J., Adams, M.D., Embley, T.M., Gull, K., Ullu, E., Barry, J.D., Fairlamb, A.H., Opperdoes, F., Barrell, B.G., Donelson, J.E., Hall, N., Fraser, C.M., Melville, S.E., and El Sayed, N.M. (2005) The genome of the African trypanosome *Trypanosoma brucei* *Science* **309**: 416-422.

Berriman, M., Hall, N., Shearer, K., Bringaud, F., Tiwari, B., Isobe, T., Bowman, S., Corton, C., Clark, L., Cross, G.A., Hoek, M., Zanders, T., Berberof, M., Borst, P., and Rudenko, G. (2002) The architecture of variant surface glycoprotein gene expression sites in *Trypanosoma brucei* *Mol. Biochem. Parasitol.* **122**: 131-140.

Berriman, M., Harris, M. (2004) Annotation of parasite genomes *Methods Mol. Biol.* **270**: 17-44.

Bertwistle, D., Swift, S., Marston, N.J., Jackson, L.E., Crossland, S., Crompton, M.R., Marshall, C.J., and Ashworth, A. (1997) Nuclear location and cell cycle regulation of the BRCA2 protein *Cancer Res.* **57**: 5485-5488.

Bienen, E.J., Saric, M., Pollakis, G., Grady, R.W., and Clarkson, A.B. (1991) Mitochondrial Development in *Trypanosoma-Brucei-Brucei* Transitional Blood-Stream Forms *Molecular and Biochemical Parasitology* **45**: 185-192.

Bignell, G., Micklem, G., Stratton, M.R., Ashworth, A., and Wooster, R. (1997) The BRC repeats are conserved in mammalian BRCA2 proteins *Hum. Mol. Genet.* **6**: 53-58.

Bishop, D.K. (1994) RecA homologs Dmc1 and Rad51 interact to form multiple nuclear complexes prior to meiotic chromosome synapsis *Cell* **79**: 1081-1092.

Bishop, D.K., Park, D., Xu, L., and Kleckner, N. (1992) DMC1: a meiosis-specific yeast homolog of *E. coli* recA required for recombination, synaptonemal complex formation, and cell cycle progression *Cell* **69**: 439-456.

Blum, M.L., Down, J.A., Gurnett, A.M., Carrington, M., Turner, M.J., and Wiley, D.C. (1993) A structural motif in the variant surface glycoproteins of *Trypanosoma brucei* *Nature* **362**: 603-609.

Boothroyd, C.E., Dreesen, O., Leonova, T., Ly, K.I., Figueiredo, L.M., Cross, G.A., and Papavasiliou, F.N. (2009) A yeast-endonuclease-generated DNA break induces antigenic switching in *Trypanosoma brucei* *Nature* **459**: 278-281.

Boothroyd, J.C., Paynter, C.A., Coleman, S.L., and Cross, G.A.M. (1982) Complete Nucleotide-Sequence of Complementary-Dna Coding for A Variant Surface Glycoprotein from *Trypanosoma-Brucei* *Journal of Molecular Biology* **157**: 547-556.

Bork, P., Blomberg, N., and Nilges, M. (1996) Internal repeats in the BRCA2 protein sequence *Nat.Genet.* **13**: 22-23.

Borst, P. (1986) Discontinuous Transcription and Antigenic Variation in Trypanosomes *Annual Review of Biochemistry* **55**: 701-732.

Borst, P. (2002) Antigenic Variation in Eukaryotic Parasites. In *Mobile DNA II*. Craig, N.L., Berg, D.E. (eds). Washington: ASM Press, pp. 953-971.

Branzei, D., Foiani, M. (2010) Maintaining genome stability at the replication fork *Nature Reviews Molecular Cell Biology* **11**: 208-219.

Brayton, K.A., Palmer, G.H., Lundgren, A., Yi, J., and Barbet, A.F. (2002) Antigenic variation of *Anaplasma marginale* msp2 occurs by combinatorial gene conversion *Mol.Microbiol.* **43**: 1151-1159.

Bringaud, F., Biteau, N., Zuiderwijk, E., Berriman, M., El Sayed, N.M., Ghedin, E., Melville, S.E., Hall, N., and Baltz, T. (2004) The ingi and RIME non-LTR retrotransposons are not randomly distributed in the genome of *Trypanosoma brucei* *Mol.Biol.Evol.* **21**: 520-528.

Bringaud, F., Ghedin, E., El Sayed, N.M.A., and Papadopoulou, B. (2008) Role of transposable elements in trypanosomatids *Microbes and Infection* **10**: 575-581.

Bringaud, F., Muller, M., Cerqueira, G.C., Smith, M., Rochette, A., El Sayed, N.M., Papadopoulou, B., and Ghedin, E. (2007) Members of a large retroposon family are determinants of post-transcriptional gene expression in *Leishmania* *PLoS.Pathog.* **3**: 1291-1307.

Brookes, P., Lawley, P.D. (1961) Reaction of Mono- and Di-Functional Alkylating Agents with Nucleic Acids *Biochemical Journal* **80**: 496-501.

Brough, R., Wei, D., Leulier, S., Lord, C.J., Rong, Y.S., and Ashworth, A. (2008) Functional analysis of *Drosophila melanogaster* BRCA2 in DNA repair *DNA Repair (Amst)* **7**: 10-19.

Brun, R., Schonenberger (1979) Cultivation and in vitro cloning or procyclic culture forms of *Trypanosoma brucei* in a semi-defined medium. Short communication *Acta Trop.* **36**: 289-292.

Budzowska, M., Kanaar, R. (2009) Mechanisms of Dealing with DNA Damage-Induced Replication Problems *Cell Biochemistry and Biophysics* **53**: 17-31.

Bugreev, D.V., Mazin, A.V. (2004) Ca²⁺ activates human homologous recombination protein Rad51 by modulating its ATPase activity *Proceedings of the National Academy of Sciences of the United States of America* **101**: 9988-9993.

Burri,M., Schlimme,W., Betschart,B., and Hecker,H. (1994) Characterization of the Histones of Trypanosoma-Brucei-Brucei Blood-Stream Forms *Acta Tropica* **58**: 291-305.

Burton,P., McBride,D.J., Wilkes,J.M., Barry,J.D., and McCulloch,R. (2007) Ku Heterodimer-Independent End Joining in Trypanosoma brucei Cell Extracts Relies upon Sequence Microhomology *Eukaryot. Cell* **6**: 1773-1781.

Calderano,S.G., de Melo Godoy,P.D., Motta,M.C., Mortara,R.A., Schenkman,S., and Elias,M.C. (2011) Trypanosoma cruzi DNA replication includes the sequential recruitment of pre-replication and replication machineries close to nuclear periphery *Nucleus*. **2**: 136-45.

Callejas,S., Leech,V., Reitter,C., and Melville,S. (2006) Hemizygous subtelomeres of an African trypanosome chromosome may account for over 75% of chromosome length *Genome Res.* **16**: 1109-1118.

Capbern,A., Giroud,C., Baltz,T., and Mattern,P. (1977) [Trypanosoma equiperdum: antigenic variations in experimental trypanosomiasis of rabbits] *Exp.Parasitol.* **42**: 6-13.

Capewell,P., Veitch,N.J., Turner,C.M., Raper,J., Berriman,M., Hajduk,S.L., and MacLeod,A. (2011) Differences between *Trypanosoma brucei gambiense* groups 1 and 2 in their resistance to killing by trypanolytic factor 1. *PLoS Negl. Trop. Dis.* **5**: e1287.

Carreira,A., Hilario,J., Amitani,I., Baskin,R.J., Shivji,M.K., Venkitaraman,A.R., and Kowalczykowski,S.C. (2009) The BRC repeats of BRCA2 modulate the DNA-binding selectivity of RAD51 *Cell* **136**: 1032-1043.

Carreira,A., Kowalczykowski,S.C. (2009) BRCA2: Shining light on the regulation of DNA-binding selectivity by RAD51 *Cell Cycle* **8**.

Carreira,A., Kowalczykowski,S.C. (2011) Two classes of BRC repeats in BRCA2 promote RAD51 nucleoprotein filament function by distinct mechanisms *Proceedings of the National Academy of Sciences of the United States of America* **108**: 10448-10453.

Carrington,M., Miller,N., Blum,M., Roditi,I., Wiley,D., and Turner,M. (1991) Variant specific glycoprotein of Trypanosoma brucei consists of two domains each having an independently conserved pattern of cysteine residues *J.Mol.Biol.* **221**: 823-835.

Chaves,I., Zomerdijk,J., Dirks-Mulder,A., Dirks,R.W., Raap,A.K., and Borst,P. (1998) Subnuclear localization of the active variant surface glycoprotein gene expression site in Trypanosoma brucei *Proc.Natl.Acad.Sci.U.S.A* **95**: 12328-12333.

Chen,C., Kolodner,R.D. (1999) Gross chromosomal rearrangements in Saccharomyces cerevisiae replication and recombination defective mutants *Nat.Genet.* **23**: 81-85.

Chen,C.F., Chen,P.L., Zhong,Q., Sharp,Z.D., and Lee,W.H. (1999) Expression of BRC repeats in breast cancer cells disrupts the BRCA2-Rad51 complex and leads

- to radiation hypersensitivity and loss of G(2)/M checkpoint control *J.Biol.Chem.* **274**: 32931-32935.
- Chen, J.M., Cooper, D.N., Chuzhanova, N., Ferec, C., and Patrinos, G.P. (2007) Gene conversion: mechanisms, evolution and human disease *Nature Reviews Genetics* **8**: 762-775.
- Chen, P.L., Chen, C.F., Chen, Y., Xiao, J., Sharp, Z.D., and Lee, W.H. (1998) The BRC repeats in BRCA2 are critical for RAD51 binding and resistance to methyl methanesulfonate treatment *Proc.Natl.Acad.Sci.U.S.A* **95**: 5287-5292.
- Chi, P., Van Komen, S., Sehorn, M.G., Sigurdsson, S., and Sung, P. (2006) Roles of ATP binding and ATP hydrolysis in human Rad51 recombinase function *DNA Repair (Amst)* **5**: 381-391.
- Chowdhury, A.R., Zhao, Z., and Englund, P.T. (2008) Effect of hydroxyurea on procyclic *Trypanosoma brucei*: an unconventional mechanism for achieving synchronous growth *Eukaryot.Cell* **7**: 425-428.
- Chung, H.M.M., Shea, C., Fields, S., Taub, R.N., and Vanderploeg, L.H.T. (1990) Architectural Organization in the Interphase Nucleus of the Protozoan *Trypanosoma-Brucei* - Location of Telomeres and Minichromosomes *Embo Journal* **9**: 2611-2619.
- Chung, W.L., Carrington, M., and Field, M.C. (2004) Cytoplasmic targeting signals in transmembrane invariant surface glycoproteins of trypanosomes *Journal of Biological Chemistry* **279**: 54887-54895.
- Clayton, C.E. (2002) Life without transcriptional control? From fly to man and back again *EMBO J.* **21**: 1881-1888.
- Constanzo, V. (2011) Brca2, Rad51 and Mre11: performing balancing acts on replication forks *DNA repair (Amst)*. **10**: 1060-5.
- Connor, F., Bertwistle, D., Mee, P.J., Ross, G.M., Swift, S., Grigorieva, E., Tybulewicz, V.L.J., and Ashworth, A. (1997) Tumorigenesis and a DNA repair defect in mice with a truncating Brca2 mutation *Nature Genetics* **17**: 423-430.
- Conway, C., McCulloch, R., Ginger, M.L., Robinson, N.P., Browitt, A., and Barry, J.D. (2002a) Ku is important for telomere maintenance, but not for differential expression of telomeric VSG genes, in African trypanosomes *J.Biol.Chem.* **277**: 21269-21277.
- Conway, C., Proudfoot, C., Burton, P., Barry, J.D., and McCulloch, R. (2002b) Two pathways of homologous recombination in *Trypanosoma brucei* *Mol.Microbiol.* **45**: 1687-1700.
- Costa, A., Ilves, I., Tamberg, N., Petojevic, T., Nogales, E., Botchan, M.R., and Berger, J.M. (2011) The structural basis for MCM2-7 helicase activation by GINS and Cdc45 *Nature Structural & Molecular Biology* **18**: 471-U110.
- Crackower, M.A., Scherer, S.W., Rommens, J.M., Hui, C.C., Poorkaj, P., Soder, S., Cobben, J.M., Hudgins, L., Evans, J.P., and Tsui, L.C. (1996) Characterization of the split hand split foot malformation locus SHFM1 at 7q21.3-q22.1 and analysis

- of a candidate gene for its expression during limb development *Human Molecular Genetics* **5**: 571-579.
- Cramer,P. (2002) Multisubunit RNA polymerases *Current Opinion in Structural Biology* **12**: 89-97.
- Critchlow,S.E., Jackson,S.P. (1998) DNA end-joining: from yeast to man *Trends Biochem.Sci.* **23**: 394-398.
- Cromie,G.A., Connelly,J.C., and Leach,D.R. (2001) Recombination at double-strand breaks and DNA ends: conserved mechanisms from phage to humans *Mol.Cell* **8**: 1163-1174.
- Cross,G.A. (1975) Identification, purification and properties of clone-specific glycoprotein antigens constituting the surface coat of *Trypanosoma brucei* *Parasitology* **71**: 393-417.
- Cross,G.A. (2001) African trypanosomes in the 21st century: what is their future in science and in health? *Int.J.Parasitol.* **31**: 427-433.
- D'Andrea,A.D. (2010) Mechanisms of Disease Susceptibility Pathways in Fanconi'S Anemia and Breast Cancer *New England Journal of Medicine* **362**: 1909-1919.
- D'Andrea,A.D., Grompe,M. (2003) The Fanconi anaemia BRCA pathway *Nature Reviews Cancer* **3**: 23-34.
- Daboussi,F., Courbet,S., Benhamou,S., Kannouche,P., Zdzienicka,M.Z., Debatisse,M., and Lopez,B.S. (2008) A homologous recombination defect affects replication-fork progression in mammalian cells *J.Cell Sci.* **121**: 162-166.
- Dacks,J.B., Walker,G., and Field,M.C. (2008) Implications of the new eukaryotic systematics for parasitologists *Parasitology International* **57**: 97-104.
- Dai,Q., Restrepo,B.I., Porcella,S.F., Raffel,S.J., Schwan,T.G., and Barbour,A.G. (2006) Antigenic variation by *Borrelia hermsii* occurs through recombination between extragenic repetitive elements on linear plasmids *Mol.Microbiol.* **60**: 1329-1343.
- Dang,H.Q., Li,Z.Y. (2011) The Cdc45.Mcm2-7.GINS Protein Complex in Trypanosomes Regulates DNA Replication and Interacts with Two Orc1-like Proteins in the Origin Recognition Complex *Journal of Biological Chemistry* **286**: 32424-32435.
- Daniels,M.J., Wang,Y., Lee,M., and Venkitaraman,A.R. (2004) Abnormal cytokinesis in cells deficient in the breast cancer susceptibility protein BRCA2 *Science* **306**: 876-879.
- Davies,A.A., Masson,J.Y., McIlwraith,M.J., Stasiak,A.Z., Stasiak,A., Venkitaraman,A.R., and West,S.C. (2001) Role of BRCA2 in control of the RAD51 recombination and DNA repair protein *Mol.Cell* **7**: 273-282.
- Davies,O.R., Pellegrini,L. (2007) Interaction with the BRCA2 C terminus protects RAD51-DNA filaments from disassembly by BRC repeats *Nat.Struct.Mol.Biol.* **14**: 475-483.

- Davis, A.P., Symington, L.S. (2004) RAD51-dependent break-induced replication in yeast *Mol. Cell Biol.* **24**: 2344-2351.
- Decottignies, A. (2007) Microhomology-mediated end-joining in fission yeast is repressed by Pku70 and relies on genes involved in homologous recombination *Genetics*.
- Devaux, S., Lecordier, L., Uzureau, P., Walgraffe, D., Dierick, J.F., Poelvoorde, P., Pays, E., and Vanhamme, L. (2006) Characterization of RNA polymerase II subunits of *Trypanosoma brucei* *Molecular and Biochemical Parasitology* **148**: 60-68.
- Dobbs, T.A., Tainer, J.A., and Lees-Miller, S.P. (2010) A structural model for regulation of NHEJ by DNA-PKcs autophosphorylation *Dna Repair* **9**: 1307-1314.
- Dobson, R., Stockdale, C., Lapsley, C., Wilkes, J., and McCulloch, R. (2011) Interactions among *Trypanosoma brucei* RAD51 paralogues in DNA repair and antigenic variation *Molecular Microbiology* **81**: 434-456.
- Donoho, G., Brenneman, M.A., Cui, T.X., Donoviel, D., Vogel, H., Goodwin, E.H., Chen, D.J., and Hasty, P. (2003) Deletion of Brca2 exon 27 causes hypersensitivity to DNA crosslinks, chromosomal instability, and reduced life span in mice *Genes Chromosomes & Cancer* **36**: 317-331.
- Edwards, S.L., Brough, R., Lord, C.J., Natrajan, R., Vatcheva, R., Levine, D.A., Boyd, J., Reis, J.S., and Ashworth, A. (2008) Resistance to therapy caused by intragenic deletion in BRCA2 *Nature* **451**: 1111-1118.
- Ehmsen, K. and Heyer, W.-D. (2008) Biochemistry of Meiotic Recombination: Formation, Processing, and Resolution of Recombination Intermediates. In Egel, R. and Lanckenau, D.-H. (eds.), *Genome Dynamics & Stability - Recombination and Meiosis*. Springer Berlin Heidelberg, **3**: 91-164.
- Elias, Q.B., Faria, M., Mortara, R.A., Motta, M.C.M., de Souza, W., Thiry, M., and Schenkman, S. (2002) Chromosome localization changes in the *Trypanosoma cruzi* nucleus *Eukaryotic Cell* **1**: 944-953.
- El Sayed, N.M., Ghedin, E., Song, J., MacLeod, A., Bringaud, F., Larkin, C., Wanless, D., Peterson, J., Hou, L., Taylor, S., Tweedie, A., Biteau, N., Khalak, H.G., Lin, X., Mason, T., Hannick, L., Caler, E., Blandin, G., Bartholomeu, D., Simpson, A.J., Kaul, S., Zhao, H., Pai, G., Van Aken, S., Utterback, T., Haas, B., Koo, H.L., Umayam, L., Suh, B., Gerrard, C., Leech, V., Qi, R., Zhou, S., Schwartz, D., Feldblyum, T., Salzberg, S., Tait, A., Turner, C.M., Ullu, E., White, O., Melville, S., Adams, M.D., Fraser, C.M., and Donelson, J.E. (2003) The sequence and analysis of *Trypanosoma brucei* chromosome II *Nucleic Acids Res.* **31**: 4856-4863.
- El Sayed, N.M., Hegde, P., Quackenbush, J., Melville, S.E., and Donelson, J.E. (2000) The African trypanosome genome *Int. J. Parasitol.* **30**: 329-345.
- El Sayed, N.M., Myler, P.J., Bartholomeu, D.C., Nilsson, D., Aggarwal, G., Tran, A.N., Ghedin, E., Worthey, E.A., Delcher, A.L., Blandin, G., Westenberger, S.J., Caler, E., Cerqueira, G.C., Branche, C., Haas, B., Anupama, A., Arner, E., Aslund, L., Attipoe, P., Bontempi, E., Bringaud, F., Burton, P., Cadag, E., Campbell, D.A., Carrington, M., Crabtree, J., Darban, H., da Silveira, J.F., de

- Jong, P., Edwards, K., Englund, P.T., Fazelina, G., Feldblyum, T., Ferella, M., Frasc, A.C., Gull, K., Horn, D., Hou, L., Huang, Y., Kindlund, E., Klingbeil, M., Kluge, S., Koo, H., Lacerda, D., Levin, M.J., Lorenzi, H., Louie, T., Machado, C.R., McCulloch, R., McKenna, A., Mizuno, Y., Mottram, J.C., Nelson, S., Ochaya, S., Osoegawa, K., Pai, G., Parsons, M., Pentony, M., Pettersson, U., Pop, M., Ramirez, J.L., Rinta, J., Robertson, L., Salzberg, S.L., Sanchez, D.O., Seyler, A., Sharma, R., Shetty, J., Simpson, A.J., Sisk, E., Tammi, M.T., Tarleton, R., Teixeira, S., Van Aken, S., Vogt, C., Ward, P.N., Wickstead, B., Wortman, J., White, O., Fraser, C.M., Stuart, K.D., and Andersson, B. (2005) The genome sequence of *Trypanosoma cruzi*, etiologic agent of Chagas disease *Science* **309**: 409-415.
- Engstler, M., Pfohl, T., Herminghaus, S., Boshart, M., Wiegertjes, G., Heddergott, N., and Overath, P. (2007) Hydrodynamic flow-mediated protein sorting on the cell surface of trypanosomes *Cell* **131**: 505-515.
- Esashi, F., Christ, N., Gannon, J., Liu, Y., Hunt, T., Jasin, M., and West, S.C. (2005) CDK-dependent phosphorylation of BRCA2 as a regulatory mechanism for recombinational repair *Nature* **434**: 598-604.
- Esashi, F., Galkin, V.E., Yu, X., Egelman, E.H., and West, S.C. (2007) Stabilization of RAD51 nucleoprotein filaments by the C-terminal region of BRCA2 *Nat. Struct. Mol. Biol.* **14**: 468-474.
- Esposito, M.S. (1978) Evidence That Spontaneous Mitotic Recombination Occurs at 2-Strand Stage *Proceedings of the National Academy of Sciences of the United States of America* **75**: 4436-4440.
- Essers, J., Houtsmuller, A.B., van Veelen, L., Paulusma, C., Nigg, A.L., Pastink, A., Vermeulen, W., Hoeijmakers, J.H., and Kanaar, R. (2002) Nuclear dynamics of RAD52 group homologous recombination proteins in response to DNA damage *EMBO J.* **21**: 2030-2037.
- Falaschi, A., Kornberg, A. (1964) Antimetabolites Affecting Protein Or Nucleic Acid Synthesis - Phleomycin Inhibitor of Dna Polymerase *Federation Proceedings* **23**: 940-941.
- Fang, J., Beattie, D.S. (2003) Alternative oxidase present in procyclic *Trypanosoma brucei* may act to lower the mitochondrial production of superoxide *Archives of Biochemistry and Biophysics* **414**: 294-302.
- Featherstone, C., Jackson, S.P. (1999) Ku, a DNA repair protein with multiple cellular functions? *Mutat. Res.* **434**: 3-15.
- Feng, Z.H., Scott, S.P., Bussen, W., Sharma, G.G., Guo, G.S., Pandita, T.K., and Powell, S.N. (2011) Rad52 inactivation is synthetically lethal with BRCA2 deficiency *Proceedings of the National Academy of Sciences of the United States of America* **108**: 686-691.
- Fenn, K., Matthews, K.R. (2007) The cell biology of *Trypanosoma brucei* differentiation *Current Opinion in Microbiology* **10**: 539-546.

Ferguson,D.O., Holloman,W.K. (1996) Recombinational repair of gaps in DNA is asymmetric in *Ustilago maydis* and can be explained by a migrating D-loop model *Proc.Natl.Acad.Sci.U.S.A* **93**: 5419-5424.

Ferguson,D.O., Rice,M.C., Rendi,M.H., Kotani,H., Kmiec,E.B., and Holloman,W.K. (1997) Interaction between *Ustilago maydis* REC2 and RAD51 genes in DNA repair and mitotic recombination *Genetics* **145**: 243-251.

Ferguson,M.A. (1999) The structure, biosynthesis and functions of glycosylphosphatidylinositol anchors, and the contributions of trypanosome research *J.Cell Sci.* **112** (Pt 17): 2799-2809.

Figueiredo,L.M., Cross,G.A., and Janzen,C.J. (2009) Epigenetic regulation in African trypanosomes: a new kid on the block *Nat.Rev.Microbiol.* **7**: 504-513.

Figueiredo,L.M., Cross,G.A.M. (2010) Nucleosomes Are Depleted at the VSG Expression Site Transcribed by RNA Polymerase I in African Trypanosomes *Eukaryotic Cell* **9**: 148-154.

Figueiredo,L.M., Janzen,C.J., and Cross,G.A. (2008) A histone methyltransferase modulates antigenic variation in African trypanosomes *PLoS Biol.* **6**: e161.

Forsythe,G.R., McCulloch,R., and Hammarton,T.C. (2009) Hydroxyurea-induced synchronisation of bloodstream stage *Trypanosoma brucei* *Mol.Biochem.Parasitol.* **164**: 131-136.

Frederiks,F., van Welsem,T., Oudgenoeg,G., Heck,A.J.R., Janzen,C.J., and van Leeuwen,F. (2010) Heterologous expression reveals distinct enzymatic activities of two DOT1 histone methyltransferases of *Trypanosoma brucei* *Journal of Cell Science* **123**: 4019-4023.

Galkin,V.E., Esashi,F., Yu,X., Yang,S., West,S.C., and Egelman,E.H. (2005) BRCA2 BRC motifs bind RAD51-DNA filaments *Proc.Natl.Acad.Sci.U.S.A* **102**: 8537-8542.

Galletto,R., Amitani,I., Baskin,R.J., and Kowalczykowski,S.C. (2006) Direct observation of individual RecA filaments assembling on single DNA molecules *Nature* **443**: 875-878.

Garcia-Higuera,I., Taniguchi,T., Ganesan,S., Meyn,M.S., Timmers,C., Hejna,J., Grompe,M., and D'Andrea,A.D. (2001) Interaction of the fanconi anemia proteins and BRCA1 in a common pathway *Molecular Cell* **7**: 249-262.

Gayther,S.A., Mangion,J., Russell,P., Seal,S., Barfoot,R., Ponder,B.A.J., Stratton,M.R., and Easton,D. (1997) Variation of risks of breast and ovarian cancer associated with different germline mutations of the BRCA2 gene *Nature Genetics* **15**: 103-105.

Ghedin,E., Bringaud,F., Peterson,J., Myler,P., Berriman,M., Ivens,A., Andersson,B., Bontempi,E., Eisen,J., Angiuoli,S., Wanless,D., Von Arx,A., Murphy,L., Lennard,N., Salzberg,S., Adams,M.D., White,O., Hall,N., Stuart,K., Fraser,C.M., and El Sayed,N.M. (2004) Gene synteny and evolution of genome architecture in trypanosomatids *Mol.Biochem.Parasitol.* **134**: 183-191.

- Gibson,W., Peacock,L., Ferris,V., Williams,K., and Bailey,M. (2008) The use of yellow fluorescent hybrids to indicate mating in *Trypanosoma brucei* *Parasit.Vectors.* **1**: 4.
- Gibson,W., Stevens,J. (1999) Genetic exchange in the trypanosomatidae *Adv.Parasitol.* **43**: 1-46.
- Gildemeister,O.S., Sage,J.M., and Knight,K.L. (2009) Cellular redistribution of Rad51 in response to DNA damage: A novel role for Rad51C *J.Biol.Chem.*
- Glover,L., Jun,J., and Horn,D. (2011) Microhomology-mediated deletion and gene conversion in African trypanosomes *Nucl.Acids.Res.* **39**: 1372-1380.
- Glover,L., McCulloch,R., and Horn,D. (2008) Sequence homology and microhomology dominate chromosomal double-strand break repair in African trypanosomes *Nucleic Acids Res.* **36**: 2608-2618.
- Goggins,M., Schutte,M., Lu,J., Moskaluk,C.A., Weinstein,C.L., Petersen,G.M., Yeo,C.J., Jackson,C.E., Lynch,H.T., Hruban,R.H., and Kern,S.E. (1996) Germline BRCA2 gene mutations in patients with apparently sporadic pancreatic carcinomas *Cancer Research* **56**: 5360-5364.
- Greaves,D.R., Borst,P. (1987) *Trypanosoma brucei* variant-specific glycoprotein gene chromatin is sensitive to single-strand-specific endonuclease digestion *J.Mol.Biol.* **197**: 471-483.
- Grompe,M., D'Andrea,A. (2001) Fanconi anemia and DNA repair *Human Molecular Genetics* **10**: 2253-2259.
- Gudmundsdottir,K., Lord,C.J., Witt,E., Tutt,A.N., and Ashworth,A. (2004) DSS1 is required for RAD51 focus formation and genomic stability in mammalian cells *EMBO Rep.* **5**: 989-993.
- Gunzl,A. (2010) The Pre-mRNA Splicing Machinery of Trypanosomes: Complex or Simplified? *Eukaryotic Cell* **9**: 1159-1170.
- Gunzl,A., Bruderer,T., Laufer,G., Schimanski,B., Tu,L.C., Chung,H.M., Lee,P.T., and Lee,M.G. (2003) RNA polymerase I transcribes procyclin genes and variant surface glycoprotein gene expression sites in *Trypanosoma brucei* *Eukaryot.Cell* **2**: 542-551.
- Haaf,T., Golub,E.I., Reddy,G., Radding,C.M., and Ward,D.C. (1995) Nuclear foci of mammalian Rad51 recombination protein in somatic cells after DNA damage and its localization in synaptonemal complexes *Proc.Natl.Acad.Sci.U.S.A* **92**: 2298-2302.
- Haber,J.E., Hearn,M. (1985) Rad52-Independent Mitotic Gene Conversion in *Saccharomyces-Cerevisiae* Frequently Results in Chromosomal Loss *Genetics* **111**: 7-22.
- Haber,J.E., Ira,G., Malkova,A., and Sugawara,N. (2004) Repairing a double-strand chromosome break by homologous recombination: revisiting Robin Holliday's model *Philos.Trans.R.Soc.Lond B Biol.Sci.* **359**: 79-86.

Hajduk,S., Adler,B., Bertrand,K., Fearon,K., Hager,K., Hancock,K., Harris,M., Leblanc,A., Moore,R., Pollard,V., Priest,J., and Wood,Z. (1992) Molecular-Biology of African Trypanosomes - Development of New Strategies to Combat An Old Disease *American Journal of the Medical Sciences* **303**: 258-270.

Hall,J.M., Lee,M.K., Newman,B., Morrow,J.E., Anderson,L.A., Huey,B., and King,M.C. (1990) Linkage of Early-Onset Familial Breast-Cancer to Chromosome-17Q21 *Science* **250**: 1684-1689.

Hall,M., Misra,S., Chaudhuri,M., and Chaudhuri,G. (2011) Peptide aptamer mimicking RAD51-binding domain of BRCA2 inhibits DNA damage repair and survival in *Trypanosoma brucei* *Microbial Pathogenesis* **50**: 252-262.

Hamatake,R.K., Dykstra,C.C., and Sugino,A. (1989) Presynapsis and synapsis of DNA promoted by the STP alpha and single-stranded DNA-binding proteins from *Saccharomyces cerevisiae* *J.Biol.Chem.* **264**: 13336-13342.

Hammarton,T.C. (2007) Cell cycle regulation in *Trypanosoma brucei* *Molecular and Biochemical Parasitology* **153**: 1-8.

Hammarton,T.C., Clark,J., Douglas,F., Boshart,M., and Mottram,J.C. (2003) Stage-specific differences in cell cycle control in *Trypanosoma brucei* revealed by RNA interference of a mitotic cyclin *J.Biol.Chem.* **278**: 22877-22886.

Hampl,V., Hug,L., Leigh,J.W., Dacks,J.B., Lang,B.F., Simpson,A.G.B., and Roger,A.J. (2009) Phylogenomic analyses support the monophyly of Excavata and resolve relationships among eukaryotic "supergroups" *Proceedings of the National Academy of Sciences of the United States of America* **106**: 3859-3864.

Hamrick,T.S., Dempsey,J.A., Cohen,M.S., and Cannon,J.G. (2001) Antigenic variation of gonococcal pilin expression in vivo: analysis of the strain FA1090 pilin repertoire and identification of the pilS gene copies recombining with pilE during experimental human infection *Microbiology* **147**: 839-849.

Hardy,C.F.J. (1997) Identification of Cdc45p, an essential factor required for DNA replication *Gene* **187**: 239-246.

Hartley,C.L., McCulloch,R. (2008) *Trypanosoma brucei* BRCA2 acts in antigenic variation and has undergone a recent expansion in BRC repeat number that is important during homologous recombination *Mol.Microbiol.* **68**: 1237-1251.

Hashimoto,Y., Chaudhuri,A.R., Lopes,M., and Costanzo,V. (2010) Rad51 protects nascent DNA from Mre11-dependent degradation and promotes continuous DNA synthesis *Nature Structural & Molecular Biology* **17**: 1305-U268.

Hays,S.L., Firmenich,A.A., and Berg,P. (1995) Complex formation in yeast double-strand break repair: participation of Rad51, Rad52, Rad55, and Rad57 proteins *Proc.Natl.Acad.Sci.U.S.A* **92**: 6925-6929.

Helleday,T. (2011) The underlying mechanism for the PARP and BRCA synthetic lethality: Clearing up the misunderstandings *Molecular Oncology* **5**: 387-393.

Hendriks,E., van Deursen,F.J., Wilson,J., Sarkar,M., Timms,M., and Matthews,K.R. (2000) Life-cycle differentiation in *Trypanosoma brucei*: molecules and mutants *Biochem.Soc.Trans.* **28**: 531-536.

Henriksson,J., Porcel,B., Rydaker,M., Ruiz,A., Sabaj,V., Galanti,N., Cazzulo,J.J., Frasch,A.C.C., and Pettersson,U. (1995) Chromosome-Specific Markers Reveal Conserved Linkage Groups in Spite of Extensive Chromosomal Size Variation in *Trypanosoma-Cruzi* *Molecular and Biochemical Parasitology* **73**: 63-74.

Hertz-Fowler,C., Figueiredo,L.M., Quail,M.A., Becker,M., Jackson,A., Bason,N., Brooks,K., Churcher,C., Fahkro,S., Goodhead,I., Heath,P., Kartvelishvili,M., Mungall,K., Harris,D., Hauser,H., Sanders,M., Saunders,D., Seeger,K., Sharp,S., Taylor,J.E., Walker,D., White,B., Young,R., Cross,G.A., Rudenko,G., Barry,J.D., Louis,E.J., and Berriman,M. (2008) Telomeric expression sites are highly conserved in *Trypanosoma brucei* *PLoS ONE.* **3**: e3527.

Hertz-Fowler, C., Renauld, H. & Berriman, M. (2007). The genome of *Trypanosoma brucei*. In *Trypanosomes: After the Genome*, pp. 5-48. Edited by D. Barry, R. McCulloch, J. C. Mottram & A. Acosta-Serrano. Norfolk, UK: Horizon Bioscience.

Heyer,W.D., Li,X., Rolfsmeier,M., and Zhang,X.P. (2006) Rad54: the Swiss Army knife of homologous recombination? *Nucl.Acids.Res.* **34**: 4115-4125.

Hilario,J., Amitani,I., Baskin,R.J., and Kowalczykowski,S.C. (2009) Direct imaging of human Rad51 nucleoprotein dynamics on individual DNA molecules *Proceedings of the National Academy of Sciences of the United States of America* **106**: 361-368.

Hirumi,H., Hirumi,K. (1989) Continuous cultivation of *Trypanosoma brucei* blood stream forms in a medium containing a low concentration of serum protein without feeder cell layers *J.Parasitol.* **75**: 985-989.

Hoare,C.A. (1973) *Trypanosoma brucei* subgroup *Transactions of the Royal Society of Tropical Medicine and Hygiene* **67**: 421-422.

Hofer,A., Schmidt,P.P., Graslund,A., and Thelander,L. (1997) Cloning and characterization of the R1 and R2 subunits of ribonucleotide reductase from *Trypanosoma brucei* *Proceedings of the National Academy of Sciences of the United States of America* **94**: 6959-6964.

Holliday,R. (1964) A mechanism for gene conversion in fungi *Genet.Res.* **5**: 282-304.

Holliday,R., Halliwell,R.E., Rowell,V., and Evans,M.W. (1971) Genetic Instability in A Radiation Sensitive, Recombination Deficient Mutant of *Ustilago Maydis* *Heredity* **27**: 484-&.

Holloman,W.K. (2011) Unraveling the mechanism of BRCA2 in homologous recombination *Nature Structural & Molecular Biology* **18**: 748-754.

Holmes,A.M., Haber,J.E. (1999) Double-strand break repair in yeast requires both leading and lagging strand DNA polymerases *Cell* **96**: 415-424.

Holthausen, J.T., Wyman, C., and Kanaar, R. (2010) Regulation of DNA strand exchange in homologous recombination *Dna Repair* **9**: 1264-1272.

Hopwood, B., Dalton, S. (1996) Cdc45p assembles into a complex with Cdc46p/Mcm5p, is required for minichromosome maintenance, and is essential for chromosomal DNA replication *Proceedings of the National Academy of Sciences of the United States of America* **93**: 12309-12314.

Horn, D., McCulloch, R. (2010) Molecular mechanisms underlying the control of antigenic variation in African trypanosomes *Current Opinion in Microbiology* **13**: 700-705.

Howlett, N.G., Taniguchi, T., Olson, S., Cox, B., Waisfisz, Q., Die-Smulders, C., Persky, N., Grompe, M., Joenje, H., Pals, G., Ikeda, H., Fox, E.A., and D'Andrea, A.D. (2002) Biallelic inactivation of BRCA2 in Fanconi anemia *Science* **297**: 606-609.

Hughes, K., Wand, M., Foulston, L., Young, R., Harley, K., Terry, S., Ersfeld, K., and Rudenko, G. (2007) A novel ISWI is involved in VSG expression site downregulation in African trypanosomes *EMBO J.* **26**: 2400-2410.

Hussain, S., Wilson, J.B., Medhurst, A.L., Hejna, J., Witt, E., Ananth, S., Davies, A., Masson, J.Y., Moses, R., West, S.C., de Winter, J.P., Ashworth, A., Jones, N.J., and Mathew, C.G. (2004) Direct interaction of FANCD2 with BRCA2 in DNA damage response pathways *Human Molecular Genetics* **13**: 1241-1248.

Hussain, S., Witt, E., Huber, P.A.J., Medhurst, A.L., Ashworth, A., and Mathew, C.G. (2003) Direct interaction of the Fanconi anaemia protein FANCG with BRCA2/FANCD1 *Human Molecular Genetics* **12**: 2503-2510.

Ilves, I., Petojevic, T., Pesavento, J.J., and Botchan, M.R. (2010) Activation of the MCM2-7 Helicase by Association with Cdc45 and GINS Proteins *Molecular Cell* **37**: 247-258.

Ip, S.C., Rass, U., Blanco, M.G., Flynn, H.R., Skehel, J.M., and West, S.C. (2008) Identification of Holliday junction resolvases from humans and yeast *Nature* **456**: 357-361.

Ira, G., Satory, D., and Haber, J.E. (2006) Conservative inheritance of newly synthesized DNA in double-strand break-induced gene conversion *Molecular and Cellular Biology* **26**: 9424-9429.

Ivens, A.C., Peacock, C.S., Worthey, E.A., Murphy, L., Aggarwal, G., Berriman, M., Sisk, E., Rajandream, M.A., Adlem, E., Aert, R., Anupama, A., Apostolou, Z., Attipoe, P., Bason, N., Bauser, C., Beck, A., Beverley, S.M., Bianchetti, G., Borzym, K., Bothe, G., Bruschi, C.V., Collins, M., Cadag, E., Ciarloni, L., Clayton, C., Coulson, R.M., Cronin, A., Cruz, A.K., Davies, R.M., De Gaudenzi, J., Dobson, D.E., Duesterhoeft, A., Fazelina, G., Fosker, N., Frasch, A.C., Fraser, A., Fuchs, M., Gabel, C., Goble, A., Goffeau, A., Harris, D., Hertz-Fowler, C., Hilbert, H., Horn, D., Huang, Y., Klages, S., Knights, A., Kube, M., Larke, N., Litvin, L., Lord, A., Louie, T., Marra, M., Masuy, D., Matthews, K., Michaeli, S., Mottram, J.C., Muller-Auer, S., Munden, H., Nelson, S., Norbertczak, H., Oliver, K., O'neil, S., Pentony, M., Pohl, T.M., Price, C., Purnelle, B., Quail, M.A., Rabinowitsch, E., Reinhardt, R., Rieger, M., Rinta, J., Robben, J., Robertson, L., Ruiz, J.C., Rutter, S., Saunders, D., Schafer, M., Schein, J., Schwartz, D.C., Seeger, K., Seyler, A., Sharp, S., Shin, H.,

Sivam,D., Squares,R., Squares,S., Tosato,V., Vogt,C., Volckaert,G., Wambutt,R., Warren,T., Wedler,H., Woodward,J., Zhou,S., Zimmermann,W., Smith,D.F., Blackwell,J.M., Stuart,K.D., Barrell,B., and Myler,P.J. (2005) The genome of the kinetoplastid parasite, *Leishmania major* *Science* **309**: 436-442.

Janion,C. (2008) Inducible SOS Response System of DNA Repair and Mutagenesis in *Escherichia coli* *International Journal of Biological Sciences* **4**: 338-344.

Janse,C.J. (1993) Chromosome Size Polymorphism and Dna Rearrangements in *Plasmodium* *Parasitology Today* **9**: 19-22.

Janzen,C.J., Lander,F., Dreesen,O., and Cross,G.A. (2004) Telomere length regulation and transcriptional silencing in KU80-deficient *Trypanosoma brucei* *Nucleic Acids Res.* **32**: 6575-6584.

Jensen,R.B., Carreira,A., and Kowalczykowski,S.C. (2010) Purified human BRCA2 stimulates RAD51-mediated recombination *Nature* **467**: 678-U62.

Joenje,H., Patel,K.J. (2001) The emerging genetic and molecular basis of Fanconi anaemia *Nature Reviews Genetics* **2**: 446-457.

Jonsdottir,A.B., Vreeswijk,M.P.G., Wolterbeek,R., Devilee,P., Tanke,H.J., Eyfjord,J.E., and Szuhai,K. (2009) BRCA2 heterozygosity delays cytokinesis in primary human fibroblasts *Cellular Oncology* **31**: 191-201.

Kass,E.M., Jasin,M. (2010) Collaboration and competition between DNA double-strand break repair pathways *FEBS Lett.* **584**: 3703-3708.

Keely,S.P., Renauld,H., Wakefield,A.E., Cushion,M.T., Smulian,A.G., Fosker,N., Fraser,A., Harris,D., Murphy,L., Price,C., Quail,M.A., Seeger,K., Sharp,S., Tindal,C.J., Warren,T., Zuiderwijk,E., Barrell,B.G., Stringer,J.R., and Hall,N. (2005) Gene arrays at *Pneumocystis carinii* telomeres *Genetics* **170**: 1589-1600.

Kelly,S., Reed,J., Kramer,S., Ellis,L., Webb,H., Sunter,J., Salje,J., Marinsek,N., Gull,K., Wickstead,B., and Carrington,M. (2007) Functional genomics in *Trypanosoma brucei*: A collection of vectors for the expression of tagged proteins from endogenous and ectopic gene loci *Molecular and Biochemical Parasitology* **154**: 103-109.

Kennedy,P.G. (2004) Human African trypanosomiasis of the CNS: current issues and challenges *J.Clin.Invest* **113**: 496-504.

Khanna,K.K., Jackson,S.P. (2001) DNA double-strand breaks: signaling, repair and the cancer connection *Nat.Genet.* **27**: 247-254.

Kieft,R., Capewell,P., Turner,C.M.R., Veitch,N.J., MacLeod,A., and Hajduk,S. (2010) Mechanism of *Trypanosoma brucei gambiense* (group 1) resistance to human trypanosome lytic factor *Proceedings of the National Academy of Sciences of the United States of America* **107**: 16137-16141.

Kim,H.S., Cross,G.A.M. (2010) TOPO3 alpha Influences Antigenic Variation by Monitoring Expression-Site-Associated VSG Switching in *Trypanosoma brucei* *Plos Pathogens* **6**.

- Kimmel,B.E., Olemoiyoi,O.K., and Young,J.R. (1987) Ingi, A 5.2-Kb Dispersed Sequence Element from Trypanosoma-Brucei That Carries Half of A Smaller Mobile Element at Either End and Has Homology with Mammalian Lines *Molecular and Cellular Biology* **7**: 1465-1475.
- Ko,E., Lee,J., and Lee,H. (2008) Essential Role of brc-2 in Chromosome Integrity of Germ Cells in *C. elegans* *Molecules and Cells* **26**: 590-594.
- Kojic,M., Kostrub,C.F., Buchman,A.R., and Holloman,W.K. (2002) BRCA2 homolog required for proficiency in DNA repair, recombination, and genome stability in *Ustilago maydis* *Mol.Cell* **10**: 683-691.
- Kojic,M., Mao,N., Zhou,Q., Lisby,M., and Holloman,W.K. (2008) Compensatory role for Rad52 during recombinational repair in *Ustilago maydis* *Mol.Microbiol.* **67**: 1156-1168.
- Kojic,M., Thompson,C.W., and Holloman,W.K. (2001) Disruptions of the *Ustilago maydis* REC2 gene identify a protein domain important in directing recombinational repair of DNA *Mol.Microbiol.* **40**: 1415-1426.
- Kojic,M., Yang,H., Kostrub,C.F., Pavletich,N.P., and Holloman,W.K. (2003) The BRCA2-interacting protein DSS1 is vital for DNA repair, recombination, and genome stability in *Ustilago maydis* *Mol.Cell* **12**: 1043-1049.
- Kojic,M., Zhou,Q., Lisby,M., and Holloman,W.K. (2005) Brh2-Dss1 interplay enables properly controlled recombination in *Ustilago maydis* *Mol.Cell Biol.* **25**: 2547-2557.
- Kojic,M., Zhou,Q., Lisby,M., and Holloman,W.K. (2006) Rec2 interplay with both Brh2 and Rad51 balances recombinational repair in *Ustilago maydis* *Mol.Cell Biol.* **26**: 678-688.
- Kojic,M., Zhou,Q.W., Fan,J., and Holloman,W.K. (2011) Mutational analysis of Brh2 reveals requirements for compensating mediator functions *Molecular Microbiology* **79**: 180-191.
- Kooter,J.M., Van der Spek,H.J., Wagter,R., d'Oliveira,C.E., Van der Heijden,H.F., Johnson,P.J., and Borst,P. (1987) The anatomy and transcription of a telomeric expression site for variant-specific surface antigens in *T. brucei* *Cell* **51**: 261-272.
- Kryston,T.B., Georgiev,A.B., Pissis,P., and Georgakilas,A.G. (2011) Role of oxidative stress and DNA damage in human carcinogenesis *Mutation Research-Fundamental and Molecular Mechanisms of Mutagenesis* **711**: 193-201.
- Kulakova,L., Singer,S.M., Conrad,J., and Nash,T.E. (2006) Epigenetic mechanisms are involved in the control of *Giardia lamblia* antigenic variation *Mol.Microbiol.* **61**: 1533-1542.
- Kupiec,M., Petes,T.D. (1988) Meiotic Recombination Between Repeated Transposable Elements in *Saccharomyces-Cerevisiae* *Molecular and Cellular Biology* **8**: 2942-2954.

- Kuzminov,A. (1995) A Mechanism for Induction of the Sos Response in Escherichia-Coli - Insights Into the Regulation of Reversible Protein Polymerization In-Vivo *Journal of Theoretical Biology* **177**: 29-43.
- Lambert,S., Mizuno,K., Blaisonneau,J., Martineau,S., Chanet,R., Freon,K., Murray,J.M., Carr,A.M., and Baldacci,G. (2010) Homologous Recombination Restarts Blocked Replication Forks at the Expense of Genome Rearrangements by Template Exchange *Molecular Cell* **39**: 346-359.
- Lambert,S., Watson,A., Sheedy,D.M., Martin,B., and Carr,A.M. (2005) Gross chromosomal rearrangements and elevated recombination at an inducible site-specific replication fork barrier *Cell* **121**: 689-702.
- Lamont,G.S., Tucker,R.S., and Cross,G.A. (1986) Analysis of antigen switching rates in Trypanosoma brucei *Parasitology* **92 (Pt 2)**: 355-367.
- Landeira,D., Bart,J.M., Van Tyne,D., and Navarro,M. (2009) Cohesin regulates VSG monoallelic expression in trypanosomes *J.Cell Biol.* **186**: 243-254.
- Lee,M., Daniels,M.J., Garnett,M.J., and Venkitaraman,A.R. (2011) A mitotic function for the high-mobility group protein HMG20b regulated by its interaction with the BRC repeats of the BRCA2 tumor suppressor *Oncogene* **30**: 3360-3369.
- Lee,M.G., Van der Ploeg,L.H. (1987) Frequent independent duplicative transpositions activate a single VSG gene *Mol.Cell Biol.* **7**: 357-364.
- Lee,S.A., Roques,C., Magwood,A.C., Masson,J.Y., and Baker,M.D. (2009) Recovery of deficient homologous recombination in Brca2-depleted mouse cells by wild-type Rad51 expression *DNA Repair (Amst)* **8**: 170-181.
- Lekomtsev,S., Guizetti,J., Pozniakovsky,A., Gerlich,D.W., and Petronczki,M. (2010) Evidence that the tumor-suppressor protein BRCA2 does not regulate cytokinesis in human cells *Journal of Cell Science* **123**: 1395-1400.
- Leppert,B.J., Mansfield,J.M., and Paulnock,D.M. (2007) The soluble variant surface glycoprotein of African trypanosomes is recognized by a macrophage scavenger receptor and induces I kappa B alpha degradation independently of TRAF6-mediated TLR signaling *Journal of Immunology* **179**: 548-556.
- Levitus,M., Joenje,H., and de Winter,J.P. (2006) The Fanconi anemia pathway of genomic maintenance *Cellular Oncology* **28**: 3-29.
- Li,X., Zhang,X.P., Solinger,J.A., Kiianitsa,K., Yu,X., Egelman,E.H., and Heyer,W.D. (2007) Rad51 and Rad54 ATPase activities are both required to modulate Rad51-dsDNA filament dynamics *Nucleic Acids Research* **35**: 4124-4140.
- Liang,F., Han,M., Romanienko,P.J., and Jasin,M. (1998) Homology-directed repair is a major double-strand break repair pathway in mammalian cells *Proc.Natl.Acad.Sci.U.S.A* **95**: 5172-5177.
- Lieber,M.R. (2010) The mechanism of double-strand DNA break repair by the nonhomologous DNA end-joining pathway *Annu.Rev.Biochem.* **79**: 181-211.
- Lieber,M.R., Lu,H., Gu,J., and Schwarz,K. (2008) Flexibility in the order of action and in the enzymology of the nuclease, polymerases, and ligase of

vertebrate nonhomologous DNA end joining: relevance to cancer, aging, and the immune system *Cell Research* **18**: 125-133.

Lin,Z., Kong,H., Nei,M., and Ma,H. (2006) Origins and evolution of the recA/RAD51 gene family: evidence for ancient gene duplication and endosymbiotic gene transfer *Proc.Natl.Acad.Sci.U.S.A* **103**: 10328-10333.

Lisby,M., Rothstein,R. (2009) Choreography of recombination proteins during the DNA damage response *DNA Repair (Amst)* **8**: 1068-1076.

Little,J.W., Mount,D.W. (1982) The SOS regulatory system of Escherichia coli *Cell* **29**: 11-22.

Liu,A.Y., Van der Ploeg,L.H., Rijsewijk,F.A., and Borst,P. (1983) The transposition unit of variant surface glycoprotein gene 118 of Trypanosoma brucei. Presence of repeated elements at its border and absence of promoter-associated sequences *J.Mol.Biol.* **167**: 57-75.

Liu,J., Doty,T., Gibson,B., and Heyer,W.D. (2010) Human BRCA2 protein promotes RAD51 filament formation on RPA-covered single-stranded DNA *Nat.Struct.Mol.Biol.* **17**: 1260-1262.

Liu,J., Heyer,W.D. (2011) Who's who in human recombination: BRCA2 and RAD52 *Proceedings of the National Academy of Sciences of the United States of America* **108**: 441-442.

Liveris,D., Mulay,V., Sandigursky,S., and Schwartz,I. (2008) Borrelia burgdorferi vlsE antigenic variation is not mediated by RecA *Infect.Immun.* **76**: 4009-4018.

Llorente,B., Smith,C.E., and Symington,L.S. (2008) Break-induced replication: what is it and what is it for? *Cell Cycle* **7**: 859-864.

Lo,T., Pellegrini,L., Venkitaraman,A.R., and Blundell,T.L. (2003) Sequence fingerprints in BRCA2 and RAD51: implications for DNA repair and cancer *DNA Repair (Amst)* **2**: 1015-1028.

Lomonosov,M., Anand,S., Sangrithi,M., Davies,R., and Venkitaraman,A.R. (2003) Stabilization of stalled DNA replication forks by the BRCA2 breast cancer susceptibility protein *Genes Dev.* **17**: 3017-3022.

Longhese,M.P., Bonetti,D., Manfrini,N., and Clerici,M. (2010) Mechanisms and regulation of DNA end resection *Embo Journal* **29**: 2864-2874.

Lord,C.J., Ashworth,A. (2007) RAD51, BRCA2 and DNA repair: a partial resolution *Nat.Struct.Mol.Biol.* **14**: 461-462.

Ludwig,T., Chapman,D.L., Papaioannou,V.E., and Efstratiadis,A. (1997) Targeted mutations of breast cancer susceptibility gene homologs in mice: lethal phenotypes of Brca1, Brca2, Brca1/Brca2, Brca1/p53, and Brca2/p53 nullizygous embryos *Genes & Development* **11**: 1226-1241.

Lukes,J., Guilbride,D.L., Votypka,J., Zikova,A., Benne,R., and Englund,P.T. (2002) Kinetoplast DNA network: Evolution of an improbable structure *Eukaryotic Cell* **1**: 495-502.

MacGregor,P., Savill,N.J., Hall,D., and Matthews,K.R. (2011) Transmission Stages Dominate Trypanosome Within-Host Dynamics during Chronic Infections *Cell Host & Microbe* **9**: 310-318.

Malkova,A., Naylor,M.L., Yamaguchi,M., Ira,G., and Haber,J.E. (2005) RAD51-dependent break-induced replication differs in kinetics and checkpoint responses from RAD51-mediated gene conversion *Mol.Cell Biol.* **25**: 933-944.

Marcello,L., Barry,J.D. (2007) Analysis of the VSG gene silent archive in *Trypanosoma brucei* reveals that mosaic gene expression is prominent in antigenic variation and is favored by archive substructure *Genome Res.* **17**: 1344-1352.

Marmorstein,L.Y., Kinev,A.V., Chan,G.K., Bochar,D.A., Beniya,H., Epstein,J.A., Yen,T.J., and Shiekhattar,R. (2001) A human BRCA2 complex containing a structural DNA binding component influences cell cycle progression *Cell* **104**: 247-257.

Marmorstein,L.Y., Ouchi,T., and Aaronson,S.A. (1998) The BRCA2 gene product functionally interacts with p53 and RAD51 *Proc.Natl.Acad.Sci.U.S.A* **95**: 13869-13874.

Marston,N.J., Richards,W.J., Hughes,D., Bertwistle,D., Marshall,C.J., and Ashworth,A. (1999) Interaction between the product of the breast cancer susceptibility gene BRCA2 and DSS1, a protein functionally conserved from yeast to mammals *Mol.Cell Biol.* **19**: 4633-4642.

Martin,J.S., Winkelmann,N., Petalcorin,M.I., McIlwraith,M.J., and Boulton,S.J. (2005) RAD-51-Dependent and -Independent Roles of a *Caenorhabditis elegans* BRCA2-Related Protein during DNA Double-Strand Break Repair *Mol.Cell Biol.* **25**: 3127-3139.

Masson,J.Y., West,S.C. (2001) The Rad51 and Dmc1 recombinases: a non-identical twin relationship *Trends Biochem.Sci.* **26**: 131-136.

Matthews,K.R., Ellis,J.R., and Paterou,A. (2004) Molecular regulation of the life cycle of African trypanosomes *Trends Parasitol.* **20**: 40-47.

Matthews,K.R., Gull,K. (1994) Evidence for an interplay between cell cycle progression and the initiation of differentiation between life cycle forms of African trypanosomes *J.Cell Biol.* **125**: 1147-1156.

Matthews,K.R., Gull,K. (1997) Commitment to differentiation and cell cycle re-entry are coincident but separable events in the transformation of African trypanosomes from their bloodstream to their insect form *J.Cell Sci.* **110 (Pt 20)**: 2609-2618.

Matthews,K.R., Shiels,P.G., Graham,S.V., Cowan,C., and Barry,J.D. (1990) Duplicative activation mechanisms of two trypanosome telomeric VSG genes with structurally simple 5' flanks *Nucleic Acids Res.* **18**: 7219-7227.

Mazin,A.V., Mazina,O.M., Bugreev,D.V., and Rossi,M.J. (2010) Rad54, the motor of homologous recombination *DNA Repair (Amst)* **9**: 286-302.

- Mazloum, N., Holloman, W.K. (2009) Brh2 Promotes a Template-Switching Reaction Enabling Recombinational Bypass of Lesions during DNA Synthesis *Molecular Cell* **36**: 620-630.
- Mazloum, N., Zhou, Q., and Holloman, W.K. (2007) DNA Binding, Annealing, and Strand Exchange Activities of Brh2 Protein from *Ustilago maydis* *Biochemistry*.
- Mazloum, N., Zhou, Q., and Holloman, W.K. (2008) D-loop formation by Brh2 protein of *Ustilago maydis* *Proc.Natl.Acad.Sci.U.S.A.*
- McAllister, K.A., Bennett, L.M., Houle, C.D., Ward, T., Malphurs, J., Collins, N.K., Cachafeiro, C., Haseman, J., Goulding, E.H., Bunch, D., Eddy, E.M., Davis, B.J., and Wiseman, R.W. (2002) Cancer susceptibility of mice with a homozygous deletion in the COOH-terminal domain of the Brca2 gene *Cancer Research* **62**: 990-994.
- McAllister, K.A., HaugenStrano, A., Hagevik, S., Brownlee, H.A., Collins, N.K., Futreal, P.A., Bennett, L.M., and Wiseman, R.W. (1997) Characterization of the rat and mouse homologues of the BRCA2 breast cancer susceptibility gene *Cancer Research* **57**: 3121-3125.
- McCulloch, R. (2004) Antigenic variation in African trypanosomes: monitoring progress *Trends Parasitol.* **20**: 117-121.
- McCulloch, R., Barry, J.D. (1999) A role for RAD51 and homologous recombination in *Trypanosoma brucei* antigenic variation *Genes Dev.* **13**: 2875-2888.
- McCulloch, R., Rudenko, G., and Borst, P. (1997) Gene conversions mediating antigenic variation in *Trypanosoma brucei* can occur in variant surface glycoprotein expression sites lacking 70- base-pair repeat sequences *Mol.Cell Biol.* **17**: 833-843.
- McEachern, M.J., Haber, J.E. (2006) Break-induced replication and recombinational telomere elongation in yeast *Annu.Rev.Biochem.* **75**: 111-135.
- McIlwraith, M.J., Van Dyck, E., Masson, J.Y., Stasiak, A.Z., Stasiak, A., and West, S.C. (2000) Reconstitution of the strand invasion step of double-strand break repair using human Rad51 Rad52 and RPA proteins *Journal of Molecular Biology* **304**: 151-164.
- McKean, P.G. (2003) Coordination of cell cycle and cytokinesis in *Trypanosoma brucei* *Curr.Opin.Microbiol.* **6**: 600-607.
- McKean, P.G., Keen, J.K., Smith, D.F., and Benson, F.E. (2001) Identification and characterisation of a RAD51 gene from *Leishmania major* *Mol.Biochem.Parasitol.* **115**: 209-216.
- McVey, M., Lee, S.E. (2008) MMEJ repair of double-strand breaks (director's cut): deleted sequences and alternative endings *Trends Genet.* **24**: 529-538.
- Meetei, A.R., Medhurst, A.L., Ling, C., Xue, Y.T., Singh, T.R., Bier, P., Steltenpool, J., Stone, S., Dokal, I., Mathew, C.G., Hoatlin, M., Joenje, H., de Winter, J.P., and Wang, W.D. (2005) A human ortholog of archaeal DNA repair protein Hef is defective in Fanconi anemia complementation group M *Nature Genetics* **37**: 958-963.

- Melville, S.E., Gerrard, C.S., and Blackwell, J.M. (1999) Multiple causes of size variation in the diploid megabase chromosomes of African trypanosomes *Chromosome. Res.* **7**: 191-203.
- Melville, S.E., Leech, V., Gerrard, C.S., Tait, A., and Blackwell, J.M. (1998) The molecular karyotype of the megabase chromosomes of *Trypanosoma brucei* and the assignment of chromosome markers *Mol. Biochem. Parasitol.* **94**: 155-173.
- Melville, S.E., Leech, V., Navarro, M., and Cross, G.A. (2000) The molecular karyotype of the megabase chromosomes of *Trypanosoma brucei* stock 427 *Mol. Biochem. Parasitol.* **111**: 261-273.
- Michel, B. (2005) After 30 years of study, the bacterial SOS response still surprises us *Plos Biology* **3**: 1174-1176.
- Michel, B., Boubakri, H., Baharoglu, Z., LeMasson, M., and Lestini, R. (2007) Recombination proteins and rescue of arrested replication forks *DNA Repair (Amst)* **6**: 967-980.
- Michel, B., Ehrlich, S.D., and Uzest, M. (1997) DNA double-strand breaks caused by replication arrest *Embo Journal* **16**: 430-438.
- Michel, B., Flores, M.J., Viguera, E., Grompone, G., Seigneur, M., and Bidnenko, V. (2001) Rescue of arrested replication forks by homologous recombination *Proc. Natl. Acad. Sci. U.S.A* **98**: 8181-8188.
- Michel, B., Grompone, G., Flores, M.J., and Bidnenko, V. (2004) Multiple pathways process stalled replication forks *Proc. Natl. Acad. Sci. U.S.A* **101**: 12783-12788.
- Michels, P.A., Liu, A.Y., Bernards, A., Sloof, P., Van der Bijl, M.M., Schinkel, A.H., Menke, H.H., Borst, P., Veeneman, G.H., Tromp, M.C., and van Boom, J.H. (1983) Activation of the genes for variant surface glycoproteins 117 and 118 in *Trypanosoma brucei* *J. Mol. Biol.* **166**: 537-556.
- Mimura, S., Takisawa, H. (1998) *Xenopus* Cdc45-dependent loading of DNA polymerase alpha onto chromatin under the control of S-phase cdk *Embo Journal* **17**: 5699-5707.
- Min, J., Park, P.G., Ko, E., Choi, E., and Lee, H. (2007) Identification of Rad51 regulation by BRCA2 using *Caenorhabditis elegans* BRCA2 and bimolecular fluorescence complementation analysis *Biochem. Biophys. Res. Commun.* **362**: 958-964.
- Mine, J., Disseau, L., Takahashi, M., Cappello, G., Dutreix, M., and Viovy, J.L. (2007) Real-time measurements of the nucleation, growth and dissociation of single Rad51-DNA nucleoprotein filaments *Nucl. Acids. Res.* **35**: 7171-7187.
- Mizuta, R., LaSalle, J.M., Cheng, H.L., Shinohara, A., Ogawa, H., Copeland, N., Jenkins, N.A., Lalande, M., and Alt, F.W. (1997) RAB22 and RAB163/mouse BRCA2: proteins that specifically interact with the RAD51 protein *Proc. Natl. Acad. Sci. U.S.A* **94**: 6927-6932.
- Morrison, L.J., Majiwa, P., Read, A.F., and Barry, J.D. (2005) Probabilistic order in antigenic variation of *Trypanosoma brucei* *Int. J. Parasitol.* **35**: 961-972.

- Morrison,L.J., Marcello,L., and McCulloch,R. (2009) Antigenic variation in the African trypanosome: molecular mechanisms and phenotypic complexity *Cell Microbiol.* **11**: 1724-1734.
- Mowatt,M.R., Aggarwal,A., and Nash,T.E. (1991) Carboxy-terminal sequence conservation among variant-specific surface proteins of *Giardia lamblia* *Mol.Biochem.Parasitol.* **49**: 215-227.
- Moynahan,M.E., Chiu,J.W., Koller,B.H., and Jasin,M. (1999) Brca1 controls homology-directed DNA repair *Molecular Cell* **4**: 511-518.
- Moynahan,M.E., Pierce,A.J., and Jasin,M. (2001) BRCA2 is required for homology-directed repair of chromosomal breaks *Molecular Cell* **7**: 263-272.
- Munday,J.C., McLuskey,K., Brown,E., Coombs,G.H., and Mottram,J.C. (2011) Oligopeptidase B deficient mutants of *Leishmania major* *Molecular and Biochemical Parasitology* **175**: 49-57.
- Murphy,N.B., Pays,A., Tebabi,P., Coquelet,H., Guyaux,M., Steinert,M., and Pays,E. (1987) Trypanosoma-Brucei Repeated Element with Unusual Structural and Transcriptional Properties *Journal of Molecular Biology* **195**: 855-871.
- Nagaraju,G., Scully,R. (2007) Minding the gap: The underground functions of BRCA1 and BRCA2 at stalled replication forks *DNA Repair (Amst)*.
- Nassif,N., Penney,J., Pal,S., Engels,W.R., and Gloor,G.B. (1994) Efficient copying of nonhomologous sequences from ectopic sites via P- element-induced gap repair *Mol.Cell Biol.* **14**: 1613-1625.
- Nathanson,K.N., Wooster,R., and Weber,B.L. (2001) Breast cancer genetics: What we know and what we need *Nature Medicine* **7**: 552-556.
- Navarro,M., Gull,K. (2001) A pol I transcriptional body associated with VSG mono-allelic expression in *Trypanosoma brucei* *Nature* **414**: 759-763.
- Nomme,J., Takizawa,Y., Martinez,S.F., Renodon-Corniere,A., Fleury,F., Weigel,P., Yamamoto,K., Kurumizaka,H., and Takahashi,M. (2008) Inhibition of filament formation of human Rad51 protein by a small peptide derived from the BRC-motif of the BRCA2 protein *Genes to Cells* **13**: 471-481.
- Nussenzweig,A., Nussenzweig,M.C. (2007) A backup DNA repair pathway moves to the forefront *Cell* **131**: 223-225.
- O'Brien,J., Wilson,I., Orton,T., and Pognan,F. (2000) Investigation of the Alamar Blue (resazurin) fluorescent dye for the assessment of mammalian cell cytotoxicity *Eur.J.Biochem.* **267**: 5421-5426.
- O'Donovan,P.J., Livingston,D.M. (2010) BRCA1 and BRCA2: breast/ovarian cancer susceptibility gene products and participants in DNA double-strand break repair *Carcinogenesis* **31**: 961-967.
- Ochiai,K., Yoshikawa,Y., Yoshimatsu,K., Oonuma,T., Tomioka,Y., Takeda,E., Arikawa,J., Mominoki,K., Omi,T., Hashizume,K., and Morimatsu,M. (2011) Valine 1532 of human BRC repeat 4 plays an important role in the interaction between BRCA2 and RAD51 *Febs Letters* **585**: 1771-1777.

- Ogawa,T., Yu,X., Shinohara,A., and Egelman,E.H. (1993) Similarity of the yeast RAD51 filament to the bacterial RecA filament *Science* **259**: 1896-1899.
- Oli,M.W., Cotlin,L.F., Shiflett,A.M., and Hajduk,S.L. (2006) Serum resistance-associated protein blocks lysosomal targeting of trypanosome lytic factor in *Trypanosoma brucei* *Eukaryotic Cell* **5**: 132-139.
- Olivares,M., Alonso,C., and Lopez,M.C. (1997) The open reading frame 1 of the L1Tc retrotransposon of *Trypanosoma cruzi* codes for a protein with apurinic-aprimidinic nuclease activity *J.Biol.Chem.* **272**: 25224-25228.
- Onyango,J.D., Burri,C., and Brun,R. (2000) An automated biological assay to determine levels of the trypanocidal drug melarsoprol in biological fluids *Acta Trop.* **74**: 95-100.
- Orelli,B.J., Bishop,D.K. (2001) BRCA2 and homologous recombination *Breast Cancer Research* **3**: 294-298.
- Oyola,S.O., Bringaud,F., and Melville,S.E. (2009) A kinetoplastid BRCA2 interacts with DNA replication protein CDC45 *Int.J.Parasitol.* **39**: 59-69.
- Palmer,G.H., Brayton,K.A. (2007) Gene conversion is a convergent strategy for pathogen antigenic variation *Trends Parasitol.* **23**: 408-413.
- Paques,F., Haber,J.E. (1999) Multiple pathways of recombination induced by double-strand breaks in *Saccharomyces cerevisiae* *Microbiol.Mol.Biol.Rev.* **63**: 349-404.
- Park,J.H., Jensen,B.C., Kifer,C.T., and Parsons,M. (2001) A novel nucleolar G-protein conserved in eukaryotes *Journal of Cell Science* **114**: 173-185.
- Parsons,M., Worthey,E.A., Ward,P.N., and Mottram,J.C. (2005) Comparative analysis of the kinomes of three pathogenic trypanosomatids: *Leishmania major*, *Trypanosoma brucei* and *Trypanosoma cruzi* *BMC.Genomics* **6**: 127.
- Patel,K.J., Yu,V.P., Lee,H., Corcoran,A., Thistlethwaite,F.C., Evans,M.J., Colledge,W.H., Friedman,L.S., Ponder,B.A., and Venkitaraman,A.R. (1998) Involvement of Brca2 in DNA repair *Mol.Cell* **1**: 347-357.
- Paull,T.T. (2010) Making the best of the loose ends: Mre11/Rad50 complexes and Sae2 promote DNA double-strand break resection *Dna Repair* **9**: 1283-1291.
- Paulnock,D.M., Freeman,B.E., and Mansfield,J.M. (2010) Modulation of innate immunity by African Trypanosomes *Parasitology* **137**: 2051-2063.
- Pays,E., Guyaux,M., Aerts,D., Van Meirvenne,N., and Steinert,M. (1985) Telomeric reciprocal recombination as a possible mechanism for antigenic variation in trypanosomes *Nature* **316**: 562-564.
- Pays,E., Lips,S., Nolan,D., Vanhamme,L., and Perez-Morga,D. (2001) The VSG expression sites of *Trypanosoma brucei*: multipurpose tools for the adaptation of the parasite to mammalian hosts *Mol.Biochem.Parasitol.* **114**: 1-16.

- Pays, E., Vanhollebeke, B., Vanhamme, L., Paturiaux-Hanocq, F., Nolan, D.P., and Perez-Morga, D. (2006) The trypanolytic factor of human serum *Nat.Rev.Microbiol.* **4**: 477-486.
- Peacock, L., Ferris, V., Sharma, R., Sunter, J., Bailey, M., Carrington, M., and Gibson, W. (2011) Identification of the meiotic life cycle stage of *Trypanosoma brucei* in the tsetse fly *Proceedings of the National Academy of Sciences of the United States of America* **108**: 3671-3676.
- Pellegrini, L., Venkitaraman, A. (2004) Emerging functions of BRCA2 in DNA recombination *Trends Biochem.Sci.* **29**: 310-316.
- Pellegrini, L., Yu, D.S., Lo, T., Anand, S., Lee, M., Blundell, T.L., and Venkitaraman, A.R. (2002) Insights into DNA recombination from the structure of a RAD51-BRCA2 complex *Nature* **420**: 287-293.
- Petalcorin, M.I., Galkin, V.E., Yu, X., Egelman, E.H., and Boulton, S.J. (2007) Stabilization of RAD-51-DNA filaments via an interaction domain in *Caenorhabditis elegans* BRCA2 *Proc.Natl.Acad.Sci.U.S.A* **104**: 8299-8304.
- Petalcorin, M.I., Sandall, J., Wigley, D.B., and Boulton, S.J. (2006) CeBRC-2 stimulates D-loop formation by RAD-51 and promotes DNA single-strand annealing *J.Mol.Biol.* **361**: 231-242.
- Petermann, E., Helleday, T. (2010) Pathways of mammalian replication fork restart *Nat.Rev.Mol.Cell Biol.*
- Prakash, S., Johnson, R.E., and Prakash, L. (2005) Eukaryotic Translesion Synthesis DNA Polymerases: Specificity of Structure and Function *Annu.Rev.Biochem.* **74**: 317-353.
- Proudfoot, C., McCulloch, R. (2005) Distinct roles for two RAD51-related genes in *Trypanosoma brucei* antigenic variation *Nucleic Acids Res.* **33**: 6906-6919.
- Proudfoot, C., McCulloch, R. (2006) *Trypanosoma brucei* DMC1 does not act in DNA recombination, repair or antigenic variation in bloodstream stage cells *Mol.Biochem.Parasitol.* **145**: 245-253.
- Putnam, C.D., Jaehnig, E.J., and Kolodner, R.D. (2009) Perspectives on the DNA damage and replication checkpoint responses in *Saccharomyces cerevisiae* *Dna Repair* **8**: 974-982.
- Radding, C.M. (1991) Helical interactions in homologous pairing and strand exchange driven by RecA protein *J.Biol.Chem.* **266**: 5355-5358.
- Rajendra, E., Venkitaraman, A.R. (2010) Two modules in the BRC repeats of BRCA2 mediate structural and functional interactions with the RAD51 recombinase *Nucleic Acids Res.* **38**: 82-96.
- Rass, U., Compton, S.A., Matos, J., Singleton, M.R., Ip, S.C.Y., Blanco, M.G., Griffith, J.D., and West, S.C. (2010) Mechanism of Holliday junction resolution by the human GEN1 protein *Genes & Development* **24**: 1559-1569.

Raz,B., Iten,M., Grether-Buhler,Y., Kaminsky,R., and Brun,R. (1997) The Alamar Blue assay to determine drug sensitivity of African trypanosomes (T.b. rhodesiense and T.b. gambiense) in vitro *Acta Trop.* **68**: 139-147.

Regis-da-Silva,C.G., Freitas,J.M., Passos-Silva,D.G., Furtado,C., Augusto-Pinto,L., Pereira,M.T., DaRocha,W.D., Franco,G.R., Macedo,A.M., Hoffmann,J.S., Cazaux,C., Pena,S.D., Teixeira,S.M., and Machado,C.R. (2006) Characterization of the Trypanosoma cruzi Rad51 gene and its role in recombination events associated with the parasite resistance to ionizing radiation *Mol.Biochem.Parasitol.* **149**: 191-200.

Reid,S., Schindler,D., Hanenberg,H., Barker,K., Hanks,S., Kalb,R., Neveling,K., Kelly,P., Seal,S., Freund,M., Wurm,M., Batish,S.D., Lach,F.P., Yetgin,S., Neitzel,H., Ariffin,H., Tischkowitz,M., Mathew,C.G., Auerbach,D., and Rahman,N. (2007) Biallelic mutations in PALB2 cause Fanconi anemia subtype FA-N and predispose to childhood cancer *Nature Genetics* **39**: 162-164.

Reiter,H., Kelley,P., and Milewski.M. (1972) Mode of Action of Phleomycin on Bacillus-Subtilis *Journal of Bacteriology* **111**: 586-5.

Reiter,H., Strauss,B., Robbins,M., and Marone,R. (1967) Nature of Repair of Methyl Methanesulfonate-Induced Damage in Bacillus Subtilis *Journal of Bacteriology* **93**: 1056-5.

Resnick,M.A. (1978) Repair of Ionizing-Radiation Damage in Fungi *Journal of Supramolecular Structure*: 32.

Robinson,N.P., Burman,N., Melville,S.E., and Barry,J.D. (1999) Predominance of duplicative VSG gene conversion in antigenic variation in African trypanosomes *Mol.Cell Biol.* **19**: 5839-5846.

Robinson,N.P., McCulloch,R., Conway,C., Browitt,A., and Barry,J.D. (2002) Inactivation of Mre11 Does Not Affect VSG Gene Duplication Mediated by Homologous Recombination in Trypanosoma brucei *J.Biol.Chem.* **277**: 26185-26193.

Roditi,I., Liniger,M. (2002) Dressed for success: the surface coats of insect-borne protozoan parasites *Trends Microbiol.* **10**: 128-134.

Rowley,M., Ohashi,A., Mondal,G., Mills,L., Yang,L., Zhang,L.Z., Sundsbak,R., Shapiro,V., Muders,M.H., Smyrk,T., and Couch,F.J. (2011) Inactivation of Brca2 Promotes Trp53-Associated but Inhibits KrasG12D-Dependent Pancreatic Cancer Development in Mice *Gastroenterology* **140**: 1303-+.

Rubin,B.P., Ferguson,D.O., and Holloman,W.K. (1994) Structure of REC2, a recombinational repair gene of Ustilago maydis, and its function in homologous recombination between plasmid and chromosomal sequences *Mol.Cell Biol.* **14**: 6287-6296.

Rudenko,G. (2010) Epigenetics and transcriptional control in African trypanosomes *Essays in Biochemistry: Epigenetics, Disease and Behaviour* **48**: 201-219.

- Rudenko,G., McCulloch,R., Dirks-Mulder,A., and Borst,P. (1996) Telomere exchange can be an important mechanism of variant surface glycoprotein gene switching in *Trypanosoma brucei* *Mol.Biochem.Parasitol.* **80**: 65-75.
- Rutter W Jr, Valenzuela P, Bell G E, Holland M, Hager G L, Degennaro L J, and Bishop R J (1976) The role of DNA-dependent RNA polymerase in transcriptive specificity. In *The Organization and Expression of the Eukaryotic Genome*. Bradbury,E.M., and Javeherian K (eds). New York: Academic Press, pp. 279-293.
- Saeki,H., Siaud,N., Christ,N., Wiegant,W.W., van Buul,P.P., Han,M., Zdzienicka,M.Z., Stark,J.M., and Jasin,M. (2006) Suppression of the DNA repair defects of BRCA2-deficient cells with heterologous protein fusions *Proc.Natl.Acad.Sci.U.S.A* **103**: 8768-8773.
- Sambrook,J., Fritsch,E.F., and Maniatis,T. (1989) *Molecular cloning: a laboratory manual* N.Y.: Cold Spring Harbor.
- San Filippo,J., Chi,P., Sehorn,M.G., Etchin,J., Krejci,L., and Sung,P. (2006) Recombination mediator and RAD51 targeting activities of a human BRCA2 polypeptide *J.Biol.Chem.*
- San Filippo,J., Sung,P., and Klein,H. (2008) Mechanism of eukaryotic homologous recombination *Annu.Rev.Biochem.* **77**: 229-257.
- Schell,D., Evers,R., Preis,D., Ziegelbauer,K., Kiefer,H., Lottspeich,F., Cornelissen,A.W., and Overath,P. (1991) A transferrin-binding protein of *Trypanosoma brucei* is encoded by one of the genes in the variant surface glycoprotein gene expression site *EMBO J.* **10**: 1061-1066.
- Scherf,A., Figueiredo,L.M., and Freitas-Junior,L.H. (2001) Plasmodium telomeres: a pathogen's perspective *Curr.Opin.Microbiol.* **4**: 409-414.
- Schimanski,B., Nguyen,T.N., and Gunzl,A. (2005) Highly efficient tandem affinity purification of trypanosome protein complexes based on a novel epitope combination *Eukaryot.Cell* **4**: 1942-1950.
- Schlacher,K., Christ,N., Siaud,N., Egashira,A., Wu,H., and Jasin,M. (2011) Double-Strand Break Repair-Independent Role for BRCA2 in Blocking Stalled Replication Fork Degradation by MRE11 *Cell* **145**: 529-542.
- Schlimme,W., Burri,M., Bender,K., Betschart,B., and Hecker,H. (1993) *Trypanosoma-Brucei-Brucei* - Differences in the Nuclear Chromatin of Blood-Stream Forms and Procyclic Culture Forms *Parasitology* **107**: 237-247.
- Schwede,A., Jones,N., Engstler,M., and Carrington,M. (2011) The VSG C-terminal domain is inaccessible to antibodies on live trypanosomes *Molecular and Biochemical Parasitology* **175**: 201-204.
- Scully,R., Chen,J.J., Ochs,R.L., Keegan,K., Hoekstra,M., Feunteun,J., and Livingston,D.M. (1997) Dynamic changes of BRCA1 subnuclear location and phosphorylation state are initiated by DNA damage *Cell* **90**: 425-435.
- Scully,R., Puget,N., and Vlasakova,K. (2000) DNA polymerase stalling, sister chromatid recombination and the BRCA genes *Oncogene* **19**: 6176-6183.

- Sedgwick, B. (2004) Repairing DNA-methylation damage *Nat. Rev. Mol. Cell Biol.* **5**: 148-157.
- Seigneur, M., Bidnenko, V., Ehrlich, S.D., and Michel, B. (1998) RuvAB acts at arrested replication forks *Cell* **95**: 419-430.
- Sharan, S.K., Morimatsu, M., Albrecht, U., Lim, D.S., Regel, E., Dinh, C., Sands, A., Eichele, G., Hasty, P., and Bradley, A. (1997) Embryonic lethality and radiation hypersensitivity mediated by Rad51 in mice lacking Brca2 *Nature* **386**: 804-810.
- Shea, C., Glass, D.J., Parangi, S., and Van der Ploeg, L.H. (1986) Variant surface glycoprotein gene expression site switches in *Trypanosoma brucei* *J. Biol. Chem.* **261**: 6056-6063.
- Shin, D.S., Pellegrini, L., Daniels, D.S., Yelent, B., Craig, L., Bates, D., Yu, D.S., Shivji, M.K., Hitomi, C., Arvai, A.S., Volkmann, N., Tsuruta, H., Blundell, T.L., Venkitaraman, A.R., and Tainer, J.A. (2003) Full-length archaeal Rad51 structure and mutants: mechanisms for RAD51 assembly and control by BRCA2 *EMBO J.* **22**: 4566-4576.
- Shinohara, A., Ogawa, H., and Ogawa, T. (1992) Rad51 protein involved in repair and recombination in *S. cerevisiae* is a RecA-like protein *Cell* **69**: 457-470.
- Shivji, M.K., Mukund, S.R., Rajendra, E., Chen, S., Short, J.M., Savill, J., Klenerman, D., and Venkitaraman, A.R. (2009) The BRC repeats of human BRCA2 differentially regulate RAD51 binding on single- versus double-stranded DNA to stimulate strand exchange *Proc. Natl. Acad. Sci. U.S.A* **106**: 13254-13259.
- Sibanda, B.L., Critchlow, S.E., Begun, J., Pei, X.Y., Jackson, S.P., Blundell, T.L., and Pellegrini, L. (2001) Crystal structure of an Xrcc4-DNA ligase IV complex *Nat. Struct. Biol.* **8**: 1015-1019.
- Sibley, L.D. (2004) Intracellular parasite invasion strategies *Science* **304**: 248-253.
- Simpson, A.G., Stevens, J.R., and Lukes, J. (2006) The evolution and diversity of kinetoplastid flagellates *Trends Parasitol.* **22**: 168-174.
- Smith, G.C., Jackson, S.P. (1999) The DNA-dependent protein kinase *Genes Dev.* **13**: 916-934.
- Smogorzewska, A., Matsuoka, S., Vinciguerra, P., McDonald, E.R., Hurov, K.E., Luo, J., Ballif, B.A., Gygi, S.P., Hofmann, K., D'Andrea, A.D., and Elledge, S.J. (2007) Identification of the FANCI protein, a monoubiquitinated FANCD2 paralog required for DNA repair *Cell* **129**: 289-301.
- Spain, B.H., Larson, C.J., Shihabuddin, L.S., Gage, F.H., and Verma, I.M. (1999) Truncated BRCA2 is cytoplasmic: Implications for cancer-linked mutations *Proceedings of the National Academy of Sciences of the United States of America* **96**: 13920-13925.
- Stanne, T.M., Rudenko, G. (2010) Active VSG Expression Sites in *Trypanosoma brucei* Are Depleted of Nucleosomes *Eukaryotic Cell* **9**: 136-147.

- Sternberg, J.M. (2004) Human African trypanosomiasis: clinical presentation and immune response *Parasite Immunol.* **26**: 469-476.
- Steverding, D. (2008) The history of African trypanosomiasis *Parasites & Vectors* **1**.
- Su, X., Bernal, J.A., and Venkitaraman, A.R. (2008) Cell-cycle coordination between DNA replication and recombination revealed by a vertebrate N-end rule degraon-Rad51 *Nat. Struct. Mol. Biol.* **15**: 1049-1058.
- Sugiyama, T., New, J.H., and Kowalczykowski, S.C. (1998) DNA annealing by Rad52 Protein is stimulated by specific interaction with the complex of replication protein A and single-stranded DNA *Proceedings of the National Academy of Sciences of the United States of America* **95**: 6049-6054.
- Sugiyama, T., Zaitseva, E.M., and Kowalczykowski, S.C. (1997) A single-stranded DNA-binding protein is needed for efficient presynaptic complex formation by the *Saccharomyces cerevisiae* Rad51 protein *J. Biol. Chem.* **272**: 7940-7945.
- Sumoy, L., Carim, L., Escarceller, M., Nadal, M., Gratacos, M., Pujana, M.A., Estivill, X., and Peral, B. (2000) HMG20A and HMG20B map to human chromosomes 15q24 and 19p13.3 and constitute a distinct class of HMG-box genes with ubiquitous expression *Cytogenetics and Cell Genetics* **88**: 62-67.
- Sun, H., Treco, D., and Szostak, J.W. (1991) Extensive 3'-overhanging, single-stranded DNA associated with the meiosis-specific double-strand breaks at the ARG4 recombination initiation site *Cell* **64**: 1155-1161.
- Sung, P. (1994) Catalysis of ATP-dependent homologous DNA pairing and strand exchange by yeast RAD51 protein *Science* **265**: 1241-1243.
- Sung, P. (1997a) Function of yeast Rad52 protein as a mediator between replication protein A and the Rad51 recombinase *J. Biol. Chem.* **272**: 28194-28197.
- Sung, P. (1997b) Yeast Rad55 and Rad57 proteins form a heterodimer that functions with replication protein A to promote DNA strand exchange by Rad51 recombinase *Genes Dev.* **11**: 1111-1121.
- Sung, P., Roberson, D.L. (1995) DNA strand exchange mediated by a RAD51-ssDNA nucleoprotein filament with polarity opposite to that of RecA *Cell* **82**: 453-461.
- Suwaki, N., Klare, K., and Tarsounas, M. (2011) RAD51 paralogs: Roles in DNA damage signalling, recombinational repair and tumorigenesis *Semin. Cell Dev. Biol.* 2011 [epub ahead of print].
- Suzuki, A., de la Pompa, J.L., Hakem, R., Elia, A., Yoshida, R., Mo, R., Nishina, H., Chuang, T., Wakeham, A., Itie, A., Koo, W., Billia, P., Ho, A., Fukumoto, M., Hui, C.C., and Mak, T.W. (1997) Brca2 is required for embryonic cellular proliferation in the mouse *Genes & Development* **11**: 1242-1252.

- Symington,L.S. (2002) Role of RAD52 epistasis group genes in homologous recombination and double-strand break repair *Microbiol.Mol.Biol.Rev.* **66**: 630-70, table.
- Symington,L.S., Gautier,J (2011) Double-Strand Break End Resection and Repair Pathway Choice *Annu.Rev.Genet.* **45**; 247-271.
- Tait,A., Turner,C.M. (1990) Genetic exchange in *Trypanosoma brucei* *Parasitol.Today* **6**: 70-75.
- Tal,A., Arbel-Goren,R., and Stavans,J. (2009) Cancer-Associated Mutations in BRC Domains of BRCA2 Affect Homologous Recombination Induced by Rad51 *Journal of Molecular Biology* **393**: 1007-1012.
- Tamura,T.A., Konishi,Y., Makino,Y., and Mikoshiba,K. (1996) Mechanisms of transcriptional regulation and neural gene expression *Neurochemistry International* **29**: 573-581.
- Tan,K.S., Leal,S.T., and Cross,G.A. (2002) *Trypanosoma brucei* MRE11 is non-essential but influences growth, homologous recombination and DNA double-strand break repair *Mol.Biochem.Parasitol.* **125**: 11-21.
- Taniguchi,T., D'Andrea,A.D. (2006) Molecular pathogenesis of Fanconi anemia: recent progress *Blood* **107**: 4223-4233.
- Tarsounas,M., Davies,A.A., and West,S.C. (2004) RAD51 localization and activation following DNA damage *Philos.Trans.R.Soc.Lond B Biol.Sci.* **359**: 87-93.
- Tarsounas,M., Davies,D., and West,S.C. (2003) BRCA2-dependent and independent formation of RAD51 nuclear foci *Oncogene* **22**: 1115-1123.
- Tarsounas,M., Morita,T., Pearlman,R.E., and Moens,P.B. (1999) RAD51 and DMC1 form mixed complexes associated with mouse meiotic chromosome cores and synaptonemal complexes *J.Cell Biol.* **147**: 207-220.
- Tashiro,S., Kotomura,N., Shinohara,A., Tanaka,K., Ueda,K., and Kamada,N. (1996) S phase specific formation of the human Rad51 protein nuclear foci in lymphocytes *Oncogene* **12**: 2165-2170.
- Tercero,J.A., Labib,K., and Diffley,J.F.X. (2000) DNA synthesis at individual replication forks requires the essential initiation factor Cdc45p *Embo Journal* **19**: 2082-2093.
- Tetley,L., Turner,C.M.R., Barry,J.D., Crowe,J.S., and Vickerman,K. (1987) Onset of Expression of the Variant Surface Glycoproteins of *Trypanosoma-Brucei* in the Tsetse-Fly Studied Using Immunoelectron Microscopy *Journal of Cell Science* **87**: 363-372.
- Thacker,J. (2005) The RAD51 gene family, genetic instability and cancer *Cancer Lett.* **219**: 125-135.
- Thon,G., Baltz,T., Giroud,C., and Eisen,H. (1990) Trypanosome variable surface glycoproteins: composite genes and order of expression *Genes Dev.* **4**: 1374-1383.

Thorslund,T., Esashi,F., and West,S.C. (2007) Interactions between human BRCA2 protein and the meiosis-specific recombinase DMC1 *EMBO J.*

Thorslund,T., McIlwraith,M.J., Compton,S.A., Lekomtsev,S., Petronczki,M., Griffith,J.D., and West,S.C. (2010) The breast cancer tumor suppressor BRCA2 promotes the specific targeting of RAD51 to single-stranded DNA *Nat.Struct.Mol.Biol.*

Timmers,H.T., de Lange,T., Kooter,J.M., and Borst,P. (1987) Coincident multiple activations of the same surface antigen gene in *Trypanosoma brucei* *J.Mol.Biol.* **194**: 81-90.

Turner,C.M. (1997) The rate of antigenic variation in fly-transmitted and syringe-passaged infections of *Trypanosoma brucei* *FEMS Microbiol.Lett.* **153**: 227-231.

Turner,C.M., Barry,J.D. (1989) High frequency of antigenic variation in *Trypanosoma brucei rhodesiense* infections *Parasitology* **99 Pt 1**: 67-75.

Turner,C.M., Sternberg,J., Buchanan,N., Smith,E., Hide,G., and Tait,A. (1990) Evidence that the mechanism of gene exchange in *Trypanosoma brucei* involves meiosis and syngamy *Parasitology* **101 Pt 3**: 377-386.

Turner,C.M.R., McLellan,S., Lindergard,L.A.G., Bisoni,L., Tait,A., and MacLeod,A. (2004) Human infectivity trait in *Trypanosoma brucei*: stability, heritability and relationship to sra expression *Parasitology* **129**: 445-454.

Van den Abbeele,J., Claes,Y., van Bockstaele,D., Le Ray,D., and Coosemans,M. (1999) *Trypanosoma brucei* spp. development in the tsetse fly: characterization of the post-mesocyclic stages in the foregut and proboscis *Parasitology* **118 (5)**: 469-478.

Van der Ploeg,L.H., Liu,A.Y., and Borst,P. (1984) Structure of the growing telomeres of *Trypanosomes* *Cell* **36**: 459-468.

Van der Heijden,H.T., Seidel,R., Modesti,M., Kanaar,R., Wyman,C., and Dekker,C. (2007) Real-time assembly and disassembly of human RAD51 filaments on individual DNA molecules *Nucleic Acids Res.* **35**: 5646-5657.

Van Deursen,F.J., Shahi,S.K., Turner,C.M.R., Hartmann,C., Guerra-Giraldez,C., Matthews,K.R., and Clayton,C.E. (2001) Characterisation of the growth and differentiation in vivo and in vitro-of bloodstream-form *Trypanosoma brucei* strain TREU 927 *Molecular and Biochemical Parasitology* **112**: 163-171.

Vandenberg,C.J., Gergely,F., Ong,C.Y., Pace,P., Mallery,D.L., Hiom,K., and Patel,K.J. (2003) BRCA1-independent ubiquitination of FANCD2 *Molecular Cell* **12**: 247-254.

Vassella,E., Reuner,B., Yutzy,B., and Boshart,M. (1997) Differentiation of African trypanosomes is controlled by a density sensing mechanism which signals cell cycle arrest via the cAMP pathway *J.Cell Sci.* **110 (Pt 21)**: 2661-2671.

Venkitaraman,A.R. (2002) Cancer susceptibility and the functions of BRCA1 and BRCA2 *Cell* **108**: 171-182.

Vickerman,K. (1978) Antigenic Variation in *Trypanosomes* *Nature* **273**: 613-617.

- Vickerman, K. (1985) Developmental Cycles and Biology of Pathogenic Trypanosomes *British Medical Bulletin* **41**: 105-114.
- Vinciguerra, P., Godinho, S.A., Parmar, K., Pellman, D., and D'Andrea, A.D. (2010) Cytokinesis failure occurs in Fanconi anemia pathway-deficient murine and human bone marrow hematopoietic cells *Journal of Clinical Investigation* **120**: 3834-3842.
- Walker, G.C. (1984) Mutagenesis and inducible responses to deoxyribonucleic acid damage in *Escherichia coli* *Microbiol.Rev.* **48**: 60-93.
- Walker, J.E., Saraste, M., Runswick, M.J., and Gay, N.J. (1982) Distantly related sequences in the alpha- and beta-subunits of ATP synthase, myosin, kinases and other ATP-requiring enzymes and a common nucleotide binding fold *EMBO J.* **1**: 945-951.
- Wang, W.D., Chi, T.H., Xue, Y.T., Zhou, S., Kuo, A., and Crabtree, G.R. (1998) Architectural DNA binding by a high-mobility-group/kinesin-like subunit in mammalian SWI/SNF-related complexes *Proceedings of the National Academy of Sciences of the United States of America* **95**: 492-498.
- Wang, X.Z., Andreassen, P.R., and D'Andrea, A.D. (2004) Functional interaction of monoubiquitinated FANCD2 and BRCA2/FANCD1 in chromatin *Molecular and Cellular Biology* **24**: 5850-5862.
- Weiden, M., Osheim, Y.N., Beyer, A.L., and Van der Ploeg, L.H. (1991) Chromosome structure: DNA nucleotide sequence elements of a subset of the minichromosomes of the protozoan *Trypanosoma brucei* *Mol. Cell Biol.* **11**: 3823-3834.
- West, S.C. (2003) Molecular views of recombination proteins and their control *Nat.Rev.Mol.Cell Biol.* **4**: 435-445.
- White, C.I., Haber, J.E. (1990) Intermediates of recombination during mating type switching in *Saccharomyces cerevisiae* *EMBO J.* **9**: 663-673.
- WHO (1995) <http://www.who.int/en/>
- WHO (2009) <http://www.who.int/en/>
- Wickstead, B., Ersfeld, K., and Gull, K. (2004) The small chromosomes of *Trypanosoma brucei* involved in antigenic variation are constructed around repetitive palindromes *Genome Res.* **14**: 1014-1024.
- Wickstead, B., Ersfeld, K., and Gull, K. (2003) The frequency of gene targeting in *Trypanosoma brucei* is independent of target site copy number *Nucl.Acids.Res.* **31**: 3993.
- Wijers, D.J., Willett, K.C. (1960) Factors that may influence the infection rate of *Glossina palpalis* with *Trypanosoma gambiense*. II. The number and morphology of the trypanosomes present in the blood of the host at the time of the infected feed. *Ann Trop Med Parasitol* **54**: 341-350.
- Williams, R.O., Young, J.R., and Majiwa, P.A.O. (1982) Genomic Environment of T-Brucei Vsg Genes - Presence of A Minichromosome *Nature* **299**: 417-421.

Wincker,P., Ravel,C., Blaineau,C., Pages,M., Jauffret,Y., Dedet,J.P., and Bastien,P. (1996) The Leishmania genome comprises 36 chromosomes conserved across widely divergent human pathogenic species *Nucleic Acids Research* **24**: 1688-1694.

Wong,A.K., Pero,R., Ormonde,P.A., Tavtigian,S.V., and Bartel,P.L. (1997) RAD51 interacts with the evolutionarily conserved BRC motifs in the human breast cancer susceptibility gene brca2 *J.Biol.Chem.* **272**: 31941-31944.

Woodward,R., Gull,K. (1990) Timing of nuclear and kinetoplast DNA replication and early morphological events in the cell cycle of *Trypanosoma brucei* *J.Cell Sci.* **95 (Pt 1)**: 49-57.

Wooster,R., Bignell,G., Lancaster,J., Swift,S., Seal,S., Mangion,J., Collins,N., Gregory,S., Gumbs,C., Micklem,G., Barfoot,R., Hamoudi,R., Patel,S., Rice,C., Biggs,P., Hashim,Y., Smith,A., Connor,F., Arason,A., Gudmundsson,J., Ficenech,D., Kessel,D., Ford,D., Tonin,P., Bishop,D.T., Spurr,N.K., Ponder,B.A.J., Eeles,R., Peto,J., Devilee,P., Cornelisse,C., Lynch,H., Narod,S., Lenoir,G., Egilsson,V., Barkadottir,R.B., Easton,D.F., Bentley,D.R., Futreal,P.A., Ashworth,A., and Stratton,M.R. (1995) Identification of the Breast-Cancer Susceptibility Gene Brca2 *Nature* **378**: 789-792.

Wooster,R., Neuhausen,S.L., Mangion,J., Quirk,Y., Ford,D., Collins,N., Nguyen,K., Seal,S., Tran,T., Averill,D., Fields,P., Marshall,G., Narod,S., Lenoir,G.M., Lynch,H., Feunteun,J., Devilee,P., Cornelisse,C.J., Menko,F.H., Daly,P.A., Ormiston,W., Mcmanus,R., Pye,C., Lewis,C.M., Cannonalbright,L.A., Peto,J., Ponder,B.A.J., Skolnick,M.H., Easton,D.F., Goldgar,D.E., and Stratton,M.R. (1994) Localization of A Breast-Cancer Susceptibility Gene, Brca2, to Chromosome 13Q12-13 *Science* **265**: 2088-2090.

Xia,B., Dorsman,J.C., Ameziane,N., de Vries,Y., Rooimans,M.A., Sheng,Q., Pals,G., Errami,A., Gluckman,E., Llera,J., Wang,W., Livingston,D.M., Joenje,H., and de Winter,J.P. (2007) Fanconi anemia is associated with a defect in the BRCA2 partner PALB2 *Nature Genetics* **39**: 159-161.

Xia,B., Sheng,Q., Nakanishi,K., Ohashi,A., Wu,J., Christ,N., Liu,X., Jasin,M., Couch,F.J., and Livingston,D.M. (2006) Control of BRCA2 Cellular and Clinical Functions by a Nuclear Partner, PALB2 *Mol.Cell* **22**: 719-729.

Xia,F., Taghian,D.G., DeFrank,J.S., Zeng,Z.C., Willers,H., Iliakis,G., and Powell,S.N. (2001) Deficiency of human BRCA2 leads to impaired homologous recombination but maintains normal nonhomologous end joining *Proceedings of the National Academy of Sciences of the United States of America* **98**: 8644-8649.

Xong,H.V., Vanhamme,L., Chamekh,M., Chimfwembe,C.E., Van den,A.J., Pays,A., Van Meirvenne,N., Hamers,R., De Baetselier,P., and Pays,E. (1998) A VSG expression site-associated gene confers resistance to human serum in *Trypanosoma rhodesiense* *Cell* **95**: 839-846.

Xu,Y., Price,B.D. (2011) Chromatin dynamics and the repair of DNA double strand breaks *Cell Cycle* **10**: 261-267.

- Xu,Z., Fulop,Z., Zhong,Y., Evinger,A.J., III, Zan,H., and Casali,P. (2005) DNA lesions and repair in immunoglobulin class switch recombination and somatic hypermutation *Ann.N.Y.Acad.Sci.* **1050**: 146-162.
- Yan,C.T., Boboila,C., Souza,E.K., Franco,S., Hickernell,T.R., Murphy,M., Gumaste,S., Geyer,M., Zarrin,A.A., Manis,J.P., Rajewsky,K., and Alt,F.W. (2007) IgH class switching and translocations use a robust non-classical end-joining pathway *Nature* **449**: 478-482.
- Yang,H., Jeffrey,P.D., Miller,J., Kinnucan,E., Sun,Y., Thoma,N.H., Zheng,N., Chen,P.L., Lee,W.H., and Pavletich,N.P. (2002) BRCA2 function in DNA binding and recombination from a BRCA2-DSS1-ssDNA structure *Science* **297**: 1837-1848.
- Yang,H., Li,Q., Fan,J., Holloman,W.K., and Pavletich,N.P. (2005) The BRCA2 homologue Brh2 nucleates RAD51 filament formation at a dsDNA-ssDNA junction *Nature* **433**: 653-657.
- Young,R., Taylor,J.E., Kurioka,A., Becker,M., Louis,E.J., and Rudenko,G. (2008) Isolation and analysis of the genetic diversity of repertoires of VSG expression site containing telomeres from *Trypanosoma brucei gambiense*, *T. b. brucei* and *T. equiperdum* *BMC.Genomics* **9**: 385.
- Yu,D.S., Sonoda,E., Takeda,S., Huang,C.L., Pellegrini,L., Blundell,T.L., and Venkitaraman,A.R. (2003) Dynamic control of Rad51 recombinase by self-association and interaction with BRCA2 *Mol.Cell* **12**: 1029-1041.
- Yu,V.P., Koehler,M., Steinlein,C., Schmid,M., Hanakahi,L.A., van Gool,A.J., West,S.C., and Venkitaraman,A.R. (2000) Gross chromosomal rearrangements and genetic exchange between nonhomologous chromosomes following BRCA2 inactivation *Genes Dev.* **14**: 1400-1406.
- Yuan,S.S.F., Lee,S.Y., Chen,G., Song,M.H., Tomlinson,G.E., and Lee,E.Y.H.P. (1999) BRCA2 is required for ionizing radiation-induced assembly of rad51 complex in vivo *Cancer Research* **59**: 3547-3551.
- Zambrano-Villa,S., Rosales-Borjas,D., Carrero,J.C., and Ortiz-Ortiz,L. (2002) How protozoan parasites evade the immune response *Trends Parasitol.* **18**: 272-278.
- Zeiner,G.M., Sturm,N.R., and Campbell,D.A. (2003) Exportin 1 mediates nuclear export of the kinetoplastid spliced leader RNA *Eukaryot.Cell* **2**: 222-230.
- Zhang,J.R., Hardham,J.M., Barbour,A.G., and Norris,S.J. (1997) Antigenic variation in Lyme disease borreliae by promiscuous recombination of VMP-like sequence cassettes *Cell* **89**: 275-285.
- Zhang,J.R., Norris,S.J. (1998) Genetic variation of the *Borrelia burgdorferi* gene *vlsE* involves cassette-specific, segmental gene conversion *Infect.Immun.* **66**: 3698-3704.
- Zhou,Q.W., Kojic,M., and Holloman,W.K. (2009) DNA-binding Domain within the Brh2 N Terminus Is the Primary Interaction Site for Association with DNA *Journal of Biological Chemistry* **284**: 8265-8273.

Zhu,C., Mills,K.D., Ferguson,D.O., Lee,C., Manis,J., Fleming,J., Gao,Y., Morton,C.C., and Alt,F.W. (2002) Unrepaired DNA breaks in p53-deficient cells lead to oncogenic gene amplification subsequent to translocations *Cell* **109**: 811-821.

Ziegelbauer,K., Overath,P. (1993) Organization of 2 Invariant Surface Glycoproteins in the Surface-Coat of Trypanosoma-Brucei *Infection and Immunity* **61**: 4540-4545.

Zou,L., Mitchell,J., and Stillman,B. (1997) CDC45, a novel yeast gene that functions with the origin recognition complex and MCM proteins in initiation of DNA replication *Molecular and Cellular Biology* **17**: 553-563.